the ENERGY lab

Office of Fossil Energy
Advanced Turbine Program

2010 Annual Report

Turbines for Coal Based Power Systems that Capture Carbon

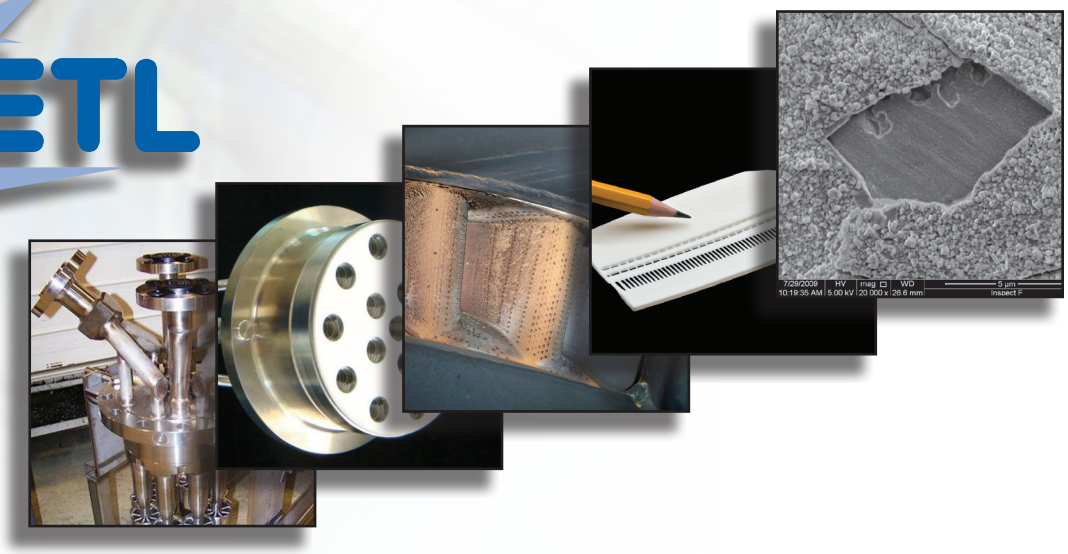

U.S. DEPARTMENT OF ENERGY

DOE/NETL-2010/1437

OFFICE OF FOSSIL ENERGY ADVANCED TURBINE PROGRAM 2010 ANNUAL REPORT

October 2010

Disclaimer

This report was prepared as an account of work sponsored by an agency of the United States Government. Neither the United States Government nor any agency thereof, nor any of their employees, makes any warranty, express or implied, or assumes any legal liability or responsibility for the accuracy, completeness, or usefulness of any information, apparatus, product, or process disclosed, or represents that its use would not infringe privately owned rights. Reference therein to any specific commercial product, process, or service by trade name, trademark, manufacturer, or otherwise does not necessarily constitute or imply its endorsement, recommendation, or favoring by the United States Government or any agency thereof. The views and opinions of authors expressed therein do not necessarily state or reflect those of the United States Government or any agency thereof.

Table of Contents

I. INTRODUCTION . . . 1

II. HYDROGEN TURBINES FOR NEAR-ZERO EMISSION SYSTEMS . . . 19

1 GE Energy: DOE Advanced IGCC/H_2 Gas Turbine Development . . . 21

2 Siemens Energy, Inc.: Advanced Hydrogen Turbine Development . . . 25

III. ADVANCED RESEARCH . . . 29

A. AERO-HEAT TRANSFER . . . 29

1 Purdue University: Analysis of Gas Turbine Performance . . . 31

2 National Energy Technology Laboratory: Materials and Component Development for Advanced Turbine Systems – Airfoil Life Prediction Modeling and Heat Transfer Enhancement . . . 34

B. COMBUSTION . . . 43

1 Clean Energy Systems, Inc.: Coal-Based Oxy-Fuel System Evaluation and Combustor Development . . . 45

2 Georgia Institute of Technology: Prediction of Combustion Stability and Flashback in Turbines with High-Hydrogen Fuel . . . 50

3 Lawrence Berkeley National Laboratory: Low-Swirl Injectors for Hydrogen Gas Turbines in Near-Zero Emissions Clean Coal Power Plants . . . 54

4 National Energy Technology Laboratory: Aerothermal and Fundamental H_2 Studies and CO_2 Recycle Effects. . . . 58

5 National Institute of Standards and Technology: Develop Data for Thermophysical Properties of Humid Gases in Power Cycles . . . 63

6 Parker Hannifin: Micro-Mixing Lean-Premix System for Ultra-Low Emission Hydrogen/Syngas Combustion . . . 67

7 Precision Combustion, Inc.: Compact and Streamlined Oxy-Syngas Reheat Combustor . . . 72

8 Precision Combustion, Inc.: Catalytic Combustion for Ultra-Low NOx Hydrogen Turbines . . . 75

9 Princeton University: Reduced and Validated Kinetic Mechanisms for Hydrogen-CO-Air Combustion in Gas Turbines. . . . 78

C. MATERIALS . . . 83

1 National Energy Technology Laboratory: Materials Performance in High CO_2 + Steam Environments . . . 85

2 National Energy Technology Laboratory: Stress-Environment Synergies in Advanced Combustion Systems: Hydrogen & Oxy-Fuel Turbines . . . 88

3 National Energy Technology Laboratory: Materials and Component Development for Advanced Turbine Systems – Advanced Coating Development . . . 92

4 National Energy Technology Laboratory: Materials and Component Development for Advanced Turbine Systems – Non-Destructive Evaluation. . . . 99

5 Oak Ridge National Laboratory: Materials Issues in Coal-Derived Synthesis Gas/Hydrogen-Fired Turbines . . . 105

6 Siemens Energy, Inc.: Zero Emissions Coal Syngas-Oxygen Turbo Machinery . . . 110

IV. UNIVERSITY TURBINE SYSTEMS RESEARCH . . . 115

A. AERO-HEAT TRANSFER . . . 115

1 The Ohio State University: Designing Turbine Endwalls for Deposition Resistance with 1,400°C Combustor Exit Temperatures and Syngas Water Vapor Levels . . . 117

IV. UNIVERSITY TURBINE SYSTEMS RESEARCH (CONTINUED)

A. AERO-HEAT TRANSFER (CONTINUED)

2 Texas A&M University: Aerodynamics and Heat Transfer Studies of Parameters Specific to the IGCC Requirements: Endwall Contouring, Leading Edge Filleting and Blade Tip Ejection under Rotating Turbine Conditions . . . 121

3 University of Texas at Austin: Simulating Particle Deposition and Mitigating Deposition Degradation Effects in Film-Cooled Turbine Sections . . . 126

4 Virginia Polytechnic Institute and State University: Syngas Particulate Deposition and Erosion at the Leading Edge of a Turbine Blade with Film Cooling . . . 131

B. COMBUSTION . . . 135

1 Georgia Institute of Technology: Turbulent Flame Speed Measurements and Modeling of Syngas Fuels . . . 137

2 The Pennsylvania State University: An Experimental and Chemical Kinetics Study of the Combustion of Syngas and High Hydrogen Content Fuels . . . 140

3 The Pennsylvania State University: Combustion Dynamics in Multi-Nozzle Combustors Operating on High-Hydrogen Fuels . . . 144

4 University of California, Irvine: Numerical and Experimental Study of Mixing Processes Associated with Hydrogen and High Hydrogen Content Fuels . . . 148

5 University of Colorado at Boulder: High Pressure Kinetics of Syngas and Nearly Pure Hydrogen Fuels . . . 152

C. MATERIALS . . . 157

1 The Ohio State University: Degradation of Thermal Barrier Coatings from Deposits and Its Mitigation . . . 159

2 University of California, Santa Barbara: Evaluating Coatings for Current and Future Service . . . 163

3 University of Pittsburgh: Materials for Oxy-Fuel Turbomachine Conditions . . . 168

4 University of Texas at El Paso: Hafnia-Based Nanostructured Thermal Barrier Coatings for Application in Advanced Turbine Technology . . . 172

V. SMALL BUSINESS INNOVATION RESEARCH . . . 175

A. ALLOYS . . . 175

1 QuesTek Innovations LLC: Computational Design of Oxidation and Creep-Resistant Niobium Superalloys for High Temperature Turbine Applications . . . 177

B. INNOVATIVE COOLING CONCEPTS . . . 181

1 Aerodyne Research, Inc.: Vaporization Cooling for IGCC Turbines . . . 183

2 Florida Turbine Technologies, Inc.: High Temperature Capability and Innovative Cooling with a Spar and Shell Turbine Blade . . . 187

3 Florida Turbine Technologies, Inc.: Development of Innovative Cooling Approaches for Robust Design . . . 191

4 Mikro Systems, Inc.: Industrial Gas Turbine Cores Produced with Advanced Cooling Features . . . 194

5 Ultramet: Transpiration-Cooled Turbine Components for High Temperature IGCC Turbines . . . 197

C. MANUFACTURING . . . 201

1 Florida Turbine Technologies, Inc.: Application of Advanced Refractory Metals in Revolutionary Turbine Airfoils . . . 203

V. SMALL BUSINESS INNOVATION RESEARCH (CONTINUED)

C. MANUFACTURING (CONTINUED)

2 Florida Turbine Technologies, Inc.: Spar-Shell Cooling Technology Verification and Manufacturing Development. 207

3 Physical Sciences Inc.: Advanced Laser Machining Techniques for Cooling Holes in Gas Turbines 212

D. THERMAL BARRIER COATINGS. 215

1 Directed Vapor Technologies: Novel Coating Methods for Unique TBC/Bond Coat Architectures for Elevated Temperature Operation 217

2 Faraday Technology, Inc.: FARADAYIC ElectroPhoretic Deposition of YSZ for Use in Thermal Barrier Coatings 221

3 Modumetal, Inc.: Functionally Graded Laminated Metal-Ceramic Thermal Barrier Systems by Low-Cost Electrochemical Processing. 225

4 NanoSonic, Inc.: Ultra High Temperature Environmentally Robust Nanocomposite Thermal Barrier Coatings for Nickel Super Alloy IGCC Turbine Components 229

5 Plasma Processes, Inc.: High Temperature Bond and Thermal Barrier Coatings 234

6 Plasma Technology Inc.: Novel Thermally-Sprayed Architectures for High Temperature Thermal Barrier Coating Systems. 237

VI. ACRONYMS AND ABBREVIATIONS 241

VII. PRIMARY CONTACT INDEX. 247

VIII. ORGANIZATION INDEX 249

IX. CONTRACT NUMBER INDEX. 251

I. INTRODUCTION

I. Introduction

On behalf of the Office of Fossil Energy (FE), the Advanced Turbine Program is pleased to present the Fiscal Year (FY) 2010 Advanced Turbine Program Annual Report. This report summarizes current progress towards developing turbines that help to meet the goal of power production from coal that is clean, efficient, less costly, and minimizes carbon dioxide emissions (CO_2).

Background and Technology Status

Turbines are a proven technology for power generation, which is typified by the shear number of turbines in use today. Turbines find use in a wide range of applications: turbines for propulsion in the aviation industry, steam turbines in pulverized coal combustion boilers, megawatt (MW)-scale turbines for shaft work and electric power, compressors, micro-turbines and turbines fueled with natural gas in simple and combined cycle (CC) applications (combined cycle applications couple a natural gas turbine with a steam turbine). Turbine technology is responsible for the vast majority of power production in the U.S. and the world. For the past 25 years, increases in power generation, in terms of added capacity, have been dominated by natural gas turbines in the CC configuration. This growth in natural gas CC applications is due to unprecedented performance in terms of cost, efficiency, emissions and power density when compared to other utility-scale power generation systems.

Gas turbine technology for electric power generation continues to advance in response to ever more demanding performance requirements. This advancement has been achieved in part because of cost-shared research and development (R&D) partnerships between industry and the government. These partnerships strive to advance turbine technology and performance beyond what the industry is expected to achieve on its own in terms of efficiency, emissions, cost and time-to-market. This advanced performance with accelerated availability to the marketplace has direct and tangible benefits to the public: lower cost of electricity and reduced emissions of criteria pollutants.

The U.S. Department of Energy (DOE) is committed to using coal in ways that are cleaner and more efficient. The technological progress of recent years has created a new opportunity for coal. Aggressive goals have been developed to lead the industry to a new, affordable breed of coal plant – a low-emissions plant that generates power with minimal impact on the environment.

Using integrated gasification combined cycle (IGCC) technology, an essential component of which is an advanced gas turbine, these new power plants will produce electricity from coal while capturing and sequestering the produced CO_2. In these plants, the IGCC synthesis gas is "shifted" to produce a fuel stream of hydrogen and CO_2. The CO_2 is then separated for capture, leaving a pure stream of hydrogen available as a gas turbine fuel. IGCC plants with pre-combustion CO_2 capture offer the most efficient form of coal-based power generation with carbon capture and the potential for the lowest cost of electricity (COE). To realize the full potential of these coal plants in meeting the nation's energy goals, progress must be made on hydrogen-fueled turbine performance to increase efficiency, reduce emissions, and reduce cost.

There are significant scientific and engineering challenges associated with meeting increasing demands on turbine technology when using hydrogen fuels derived from coal. Examples of technical approaches being undertaken within the Advanced Turbine Program to address these challenges include the following:

- **Combustor Design** – Design and develop the combustion portion of the turbine to leverage the best current and advanced technologies to meet strategic system-level goals of an advanced syngas- or hydrogen-fueled gas turbine. Efforts are focused on the measurement and assessment of the fundamental properties of hydrogen combustion and the use of these properties to design and develop low-NOx (oxides of nitrogen) combustion systems. Several combustion technologies are under evaluation, including high- and low-swirl pre-mixed, diffusion, hybrid forms of pre-mixed and diffusion, axial staging, rich-lean catalytic, and others.
- **Thermal Barrier Coatings (TBCs)** – Assess and develop TBCs that can provide the performance and durability required for use in syngas- and hydrogen-fueled advanced gas turbines. Efforts

are focused on identifying candidate TBC architectures and material compositions with the proper thermal, mechanical, and chemical properties for use in reducing heat flux to combustor transition pieces, stationary nozzles, and rotating airfoils. Advanced TBC and bond coat architectures are being developed to improve durability and thermal performance in the harsh environment found in the IGCC gas turbine.

- **Aero-Thermo-Mechanical Design** – Assess the unique aero-thermo-mechanical operational conditions associated with hydrogen turbines, and investigate design improvements for addressing these unique design spaces. Efforts are focused on reducing cooling flows, reducing sealing and leakage flow rates, reducing rotating blade count, increasing expansion stage areas and increasing airfoil length. The goal of these efforts is to develop machines that are more efficient with a higher power output.

Resolving the scientific and engineering design challenges using the approaches outlined above will allow advanced hydrogen-fueled turbines to be used in IGCC power systems with carbon capture and storage (CCS).

Office of Fossil Energy and Advanced Turbine Program Goals

The DOE's Office of FE manages a portfolio of research programs directed to demonstrate advanced coal-based electric power generation with near-zero emissions. Programs managed by the Office of FE's Office of Clean Coal are depicted in the figure below. These programs are designed to provide low-cost technological solutions to high-level Presidential initiatives.

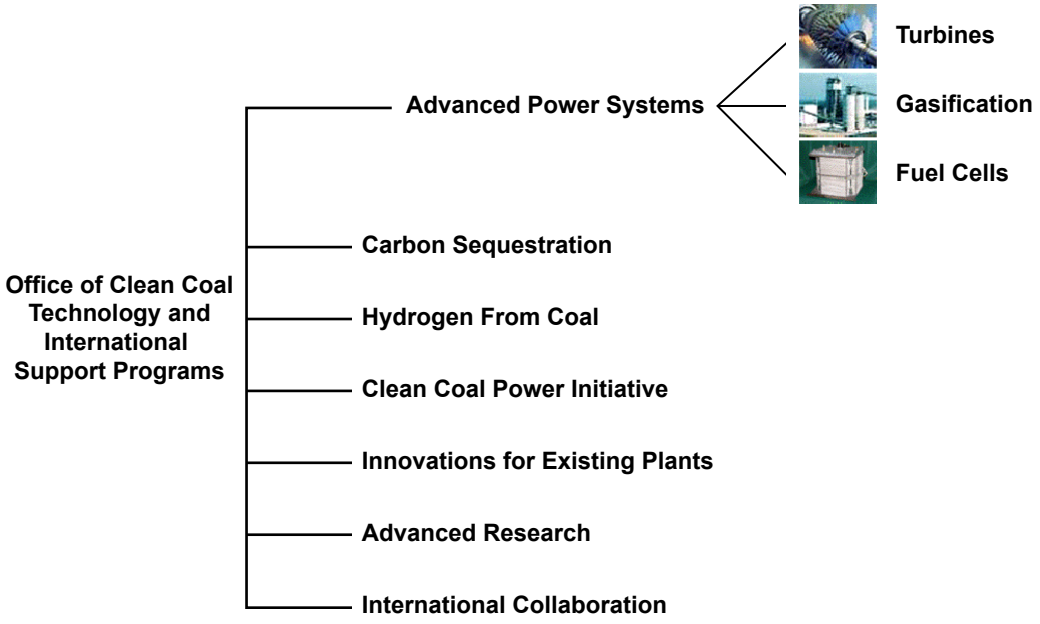

One of these Presidential initiatives establishes a greenhouse gas reduction target of >80% from 1990 levels by 2050. In response to this target and other drivers, the FE program is focused on:

- Research, development and demonstration to enable CCS deployment in the post-2020 timeframe.
- Sufficient demonstrations of first-generation CCS and power plant technologies to provide confidence that these technologies can be safely and reliably integrated into power plant and industrial plant operations.

- Development and demonstration of new, advanced second-generation CCS and power plant technologies for deployment in the post-2020 timeframe.

To realize this initiative and provide program area priorities, the following best practice performance targets have been established:

- <10% increase in COE with CCS (pre-combustion for IGCC)
- <35% increase in COE with CCS (post- and oxy-combustion for pulverized coal power plants)
- <$700/kW fuel cell power blocks (2007$)
- 50% plant efficiency, up to 60% with fuel cells
- 90% CO_2 capture
- 99% CO_2 storage permanence
- +/- 30% storage capacity resolution

Advanced Turbine Program's Objectives

The Advanced Turbine Program is organized into three areas: hydrogen-fueled turbines for IGCC applications with CCS, advanced research, and the University Turbine Systems Research Program. The program is augmented by a portfolio of Small Business Innovation Research (SBIR) projects. This annual report presents the status of projects addressing these topic areas and progress towards the performance targets and best practices outlined above.

The Advanced Turbine Program will contribute to these performance targets and best practices by meeting the following objectives:

By 2010, demonstrate:

- Efficiency improvement of 2–3 percentage points above the baseline[1] for CC performance for an IGCC syngas-fueled system.
- Cost reduction of 20–30 percent (below the baseline) in CC capital cost, plus enhanced value for lower COE.
- Emissions reduction to 2 ppm NOx from the power plant exhaust and single-digit NOx emissions in the simple cycle exhaust (at 15 percent O_2).

System studies indicate that the 2010 objectives described above have been met through the R&D sponsored by the program to date (see 2010 Annual Accomplishments). The achievement of the objectives will be demonstrated by incorporating the latest technological advances in a gas turbine power plant. It is envisioned that this turbine could be installed with a pre-planned technology improvement philosophy. This approach would allow the machine to be optimized in the field for combustion, firing temperature and other performance-enhancing components or subsystems. This approach would also allow for a machine fueled with 100 percent hydrogen to operate with the highest efficiency and lowest NOx emissions.

Having achieved the 2010 objectives, the Advanced Turbine Program is now focused on further advancements to turbine technology to attain the ultimate performance targets for IGCC power plants with CCS. Thus, by 2015, the program plans to demonstrate:

- Hydrogen-fueled turbines with 3-5 percentage points improvement in CC efficiency (total above baseline).
- Competitive cost of electricity for near-zero emission systems.
- Hydrogen-fueled IGCC with 2 ppm NOx at the power plant exhaust.

[1] Baseline efficiency is defined in "Development of Baseline Performance Values for Turbines in Existing IGCC Applications," Richard A. Dennis, Walter W. Shelton, and Patrick Le, Proceedings of GT2007, May, 2007.

2010 Annual Accomplishments

System Studies Confirm That Goals Can Be Achieved. At the inception of the Advanced Turbine Program, system studies were used to baseline turbine and IGCC performance. Power plants with advanced turbines have since been modeled by hydrogen turbine developers General Electric and Siemens Energy, holding the balance of plant constant between the baseline plant and the advanced plant unless there was an obvious change required to make the balance of plant compatible with the advanced turbine. The results of these studies have been substantiated with system studies conducted by the National Energy Technology Laboratory (NETL), and they show that the Program's efficiency and cost goals are attainable, assuming that the R&D pathways (combustion, materials, aerodynamics, heat transfer, and systems) being pursued by the Program are successfully implemented. The project highlights below and 2010 accomplishments outlined in the body of this report present the key results accomplished along these R&D pathways.

SBIR and American Recovery and Reinvestment Act Projects Awarded. In FY 2009, Advanced Turbine Program topics–namely alloys, cooling materials, and TBC–were included in DOE SBIR and American Recovery and Reinvestment Act funding opportunity announcements (FOAs) for basic research. Thirteen projects were awarded for Phase I R&D up to 12 months. These projects are detailed in Section 3 (along with three older SBIR projects). In FY 2010, there was a continuation solicitation for the 13 projects, and there was another DOE SBIR Phase I solicitation that selected three new projects:

- UES, Inc., *"High Temperature Unique Low Thermal Conductivity Thermal Barrier Coating (TBC) Architectures"*
- Technology Assessment and Transfer, Inc., *"Rapid Prototyping and Manufacturing of Cast Turbine Components"*
- Innovative Science Engineering and Management LLC, *"A Novel Micro Circuit Based Film Cooling Design for a Ceramic Combustor Liner"*

New University Turbine Systems Research (UTSR) Grants Launched. The UTSR Program addresses scientific research to develop and transition advanced turbines and turbine-based systems that will operate cleanly and efficiently when fueled with coal-derived synthesis gas (syngas) and hydrogen fuels. This research focuses on the areas of combustion, aerodynamics/heat transfer, and materials, in support of the DOE Office of FE's Advanced Turbine Program goals.

In FY 2010, the Advanced Turbine Program issued an FOA for university-based research. This FOA was designed to solicit applied research for high-hydrogen content (HHC) fuel turbine applications that could be integrated with coal-based IGCC with carbon capture. Research proposals were sought in three topic areas: 1) Combustion Kinetics Modeling, 2) Aerodynamics & Heat Transfer, and 3) Materials. Through a merit-based selection process, the seven projects listed below were selected for award.

- Texas A&M University, *Turbulent Flame Speeds and NOx Kinetics of HHC Fuels with Contaminants and High Dilution Levels*
- Georgia Institute of Technology, *Turbulent Flame Propagation Characteristics of High Hydrogen Content Fuels*
- University of Texas at Austin, *Improving Durability of Turbine Components through Trenched Film Cooling and Contoured Endwalls*
- University of North Dakota, *Environmental Considerations and Cooling Strategies for Vane Leading Edges in Syngas Environments*
- University of California, Irvine, *Mechanisms Underpinning Degradation of Protective Oxides and Thermal Barrier Coatings in High Hydrogen Content (HHC) – Fueled Turbines*
- Louisiana State University and A&M College, *Computational Design and Experimental Validation of New Thermal Barrier Systems*
- Stony Brook University, *Advanced Thermal Barrier Coatings for Operation in High Hydrogen Content Fueled Gas Turbines*

The NETL-Regional University Alliance Advances Technology Development Critical to Manufacturer Efforts for Achieving DOE FE's Advanced Turbine Program Goals. During FY 2010, NETL, the University of Pittsburgh, West Virginia University, and Virginia Polytechnic Institute and State University (Virginia Tech) collaboratively developed advanced turbine material systems, demonstrated significant internal double wall or skin cooling enhancement through the use of novel pin-fin arrays as well as enhanced external airfoil film cooling effectiveness, and developed early failure non-destructive evaluation (NDE) prediction techniques for application in DOE FE's future land-based gas turbine engines.

Working in conjunction with commercial metal and coating suppliers, the team demonstrated the stability, insulating capability, and cyclic operating life of a high-purity, low-density TBC that exceeded bench-scale performance of conventional state-of-the-art TBC coatings. The feasibility of diffusion barrier coatings to reduce elemental interdiffusion while retaining high-temperature oxidation resistance of nickel-based superalloys was additionally shown. Excellent high-temperature life as compared with commercial state-of-the-art bond coat systems was demonstrated for NETL's modified, reduced-cost, diffusion bond coat system, and thicknesses and compositions of extreme-temperature overlayer coatings were projected for use in advanced land-based engines where turbine inlet operating temperatures exceed 1,400ºC.

Addressing DOE FE's performance goal requirements for future land-based turbines where the airfoil coolant supply and availability will need to be substantially reduced in comparison to natural gas-fired engines, the team designed and bench-scale tested novel internal cooling channel pin-fin vortex generator arrays, demonstrating an ~4.3x heat transfer enhancement over a wide range of Reynolds numbers, which is a record high achievement for single-phase forced convection enhancement. The use of coolant jet impingement with a 90-degree inlet flow turn was also shown to significantly increase the overall heat transfer in cooling passages as compared to the use of conventional straight coolant injection inlets. The incorporation of side blockages within the coolant channel, and uniquely positioned pin-fin arrays within the airfoil's tip turn region, provided additional internal heat transfer enhancement. Coolant impingement under high Coriolis force rotating conditions using angled cooling holes resulted in higher heat transfer along the corner of side and bottom channel walls in comparison to traditional multi-row impingement cooling. The team initiated laboratory testing using superheated steam as an internal coolant with next-generation pin-fin array configurations that were developed in consultation with turbine original equipment manufacturers (OEMs). Using a low-speed wind tunnel, a reduced number of tripod film cooling holes generated a higher external cooling effectiveness than rows of cylindrical holes typically used in current engine configurations.

With respect to projecting advanced turbine operating life, three-dimensional finite element and damage mechanics-based models for creep and fatigue, and creep-fatigue interactions, were refined and applied to model airfoil geometries, simulating operation under advanced turbine inlet conditions. Validation of the computational models was initiated in conjunction with OEM support, and incorporation of TBC layer damage mechanisms using continuum micromechanics and fracture mechanics was undertaken to predict the initiation and growth of cracks within the TBC layers. To support the team's computational life prediction modeling effort, experimental testing was conducted which demonstrated that 1,100ºC, uniaxially-applied compressive stress did not enhance thermally grown oxide formation along the surface of nickel-based single crystal substrate materials, micro-crack formation, or TBC debonding and/or spallation.

Among the significant accomplishments achieved with respect to NDE efforts conducted during FY 2010, the team demonstrated that variation in average surface stiffness measured by micro-indentation, as well as wave reflection amplitude and travel time observed by pulse-echo NDE techniques, identified the early onset of internal TBC debonding in bench-scale laboratory testing, prior to visually observing external crack formation, spallation, and loss of the TBC coating. The success of the team's acousto-ultrasonic NDE efforts attracted a field-service supplier to provide an in-service full combustor liner for identification of potential subsurface TBC debonding areas where refurbishment would be needed.

2010 UTSR Workshop to Be Held at Pennsylvania State University in State College, Pennsylvania. The UTSR program will hold its annual workshop October 19-21, 2010, at Pennsylvania State University in State College, Pennsylvania. The workshop, co-organized by NETL and

Pennsylvania State University, is open to the public and will bring together experts from academia, industry and government to present and discuss ongoing turbine research in the areas of combustion, materials, and aerodynamics/heat transfer, with a focus on advanced syngas and hydrogen turbine systems. The agenda will include invited talks, technical presentations, panel discussions, poster presentations, and laboratory tours. Principal Investigators of DOE-funded projects will present their latest results. The findings and recommendations will be used by DOE to guide future work and to make programmatic and funding decisions for the upcoming fiscal years. The 2010 workshop proceedings will be posted on the NETL Web site; 2009 proceedings are at http://www.netl.doe.gov/publications/proceedings/09/UTSR/index.html.

Innovative Micro-Mixing Fuel Injectors Demonstrate Superior Operability and Ultra-Low Emissions Combustion When Operating on Hydrogen Fuel. Parker Hannifin has completed the development of prototype micro-mixing lean-premix fuel injection technologies for hydrogen/syngas combustion. Building on Parker's proven Macrolamination technology for liquid fuels, Parker developed scalable high-performing multi-point injectors that utilize multiple, small mixing cups in place of a single conventional large-scale premixer. The small size enables fuel and air to mix rapidly within the cups, thereby providing well-premixed reactants to the flame front, which minimizes NOx emissions. The Macrolaminate fuel injectors are made from metal layers that are diffusion bonded to generate monolithic structures. This manufacturing process also enables flexibility in the design, yielding injectors with superior mixing and combustion capabilities. The 1.3 MW full-scale injectors tested in the final phase of this DOE-sponsored project have demonstrated superior NOx emissions and enhanced flame stability without flashback over a wide range of operating pressures using high-hydrogen fuels, supporting the DOE goals of increased energy diversity and reduced greenhouse gases. The injectors that were developed are scalable to all engine sizes, are very economical, and are able to burn a wide range of fuels from natural gas to syngas to high-hydrogen content fuels. Combustion tests at an OEM facility have demonstrated the technology to operating pressures as high as 13 atm., typical of medium-size gas turbine engines. Excellent part-load operability was demonstrated for high-hydrogen fuels, and emissions were shown to be insensitive to operating pressure. The injector operated without flashback on fuel mixtures ranging from 100% natural gas to 100% hydrogen, and emissions were shown to be insensitive to combustor pressure. The project goal for MW-scale combustor development of 3 ppm NOx emissions was met at a flame temperature of 1,750 K (2,690°F) when operating on a fuel mixture containing 50% hydrogen and 50% natural gas by volume with 40% nitrogen dilution; furthermore, 1.5 ppm NOx was achieved at a flame temperature of 1,680 K (2,564°F) using only 10% nitrogen dilution. The excellent emissions and operability results that were obtained demonstrate the viability of the micro-mixing fuel injectors for the challenging high-hydrogen content fuels. Parker maintains that the newly developed technology is easily adaptable to large-scale engines, and future work is planned to integrate this technology into engines in the tens of megawatts range. Now that the basic building block for this technology has been fully validated, new combustor concepts can be designed to take advantage of Macrolamination technology for a wide range of engines and combustion systems from annular to can-annular combustion systems.

Project Highlights

Hydrogen Turbines for Near-Zero Emission Systems

Advanced Combustor Demonstrates Low NOx Emissions on Hydrogen Fuel. At GE Energy in Greenville, South Carolina, a novel combustion concept was tested extensively in a full can configuration. Testing was conducted with pure hydrogen, natural gas, and hydrogen-nitrogen fuels, along with a more traditional syngas blend containing higher levels of carbon. During the year, DOE 2012 targets were realized, as the system was operated on high-hydrogen fuel in excess of F-Class conditions with single-digit NOx emissions. A level of reliability and durability on H_2 fuel was also demonstrated with over 60 hours of fired test time, including several instances of full-load operation for more than 6 hours. During the rest of Phase II of the project, the main focus will be on 1) expanding demonstrated performance to the DOE 2015 conditions; 2) further reducing NOx emissions; 3) addressing requirements such as reliability, manufacturability, and durability; and 4) further increasing the size of the demonstration tests.

New Thermal Barrier Coating Achieves Higher Operating Temperature. Siemens Energy Inc. is developing high-temperature TBCs for industrial gas turbines which operate on coal-based fuels. Through extensive testing in calibrated rigs, a near-term target to increase allowable surface temperature by over 10% was demonstrated. TBCs are a critical component to achieving high efficiency, facilitating higher engine operating temperature, and lowering cooling consumption. By achieving this intermediate goal, Siemens is building confidence towards reaching its long-term temperature target and providing a system which can be adapted to benefit near-term applications. Such applications include the existing service fleet of engines where improved coatings can potentially improve parts durability while validating the long-term performance of the system in a relevant environment.

Advanced Research

Oxy-Fuel Reheat Combustor Boosts Power Plant Efficiency. Clean Energy Systems, Inc. (CES) has completed hot-fire testing of a prototype oxy-fuel (O-F) reheat combustor. The O-F reheater confirms the feasibility of increasing power plant efficiency by reheating the drive gas (primarily steam and CO_2) between the high and intermediate pressure turbines (HPT/IPT) in a turbine "train." Studies have shown that O-F plant efficiency can be increased by 10 percentage points by increasing the temperature of the drive gas exhausting from HPT to optimal inlet temperature for the following IPT. This takes advantage of the higher operating temperature capabilities of modern IPTs. CES used a single "can" from a J79 GE turbine, instrumented and modified by Florida Turbine Technologies, Inc. (FTT), to develop operating parameters, confirm combustion patterns, and demonstrate material compatibilities. The J79 combustor demonstrated its ability to heat the inlet steam/CO_2 mixture from 600°F to 1,700°F, to maintain stable combustion while throttling up and down, and to operate smoothly during test runs lasting up to one hour. The engineering data gathered during this test will be used to develop advanced O-F reheat combustors for 2nd-generation O-F IPTs.

Second-Generation Oxy-Fuel Intermediate Pressure Turbine Reaches Preliminary Design Review. CES and FTT have completed the preliminary design review for the first utility-scale O-F IPT. Leveraging an existing Siemens gas turbine design and previous CES development work on a first-generation O-F IPT (based on a J79), the CES/FTT team is redesigning the SGT-900 to serve as a 150 MW_e O-F IPT (OFT-900). This second-generation, O-F advanced turbine will be used to improve plant efficiency by 10 percentage points in the zero-emission CES-cycle. The OFT-900 obtains this efficiency boost by the use of advanced O-F reheat combustors to boost the inlet temperature of the steam/CO_2 drive gas to optimal turbine inlet conditions. This means reheating the 600°F steam/CO_2 coming from an upstream high-pressure turbine to the 1,976°F capability of the OFT-900. FTT expects to complete engineering redesign of the OFT-900 in the fall of 2010. OFT-900 remanufacture from an existing SGT-900 is planned for 2011 to enable the OFT-900 to be ready for deployment and commissioning in mid-2012. The OFT-900 is a critical development step towards achieving the long-term DOE goals of advanced oxy-turbines operating at temperatures of up to 3,200°F in utility-scale, 600 MW_e power plants.

Modeling and Analysis Expand Understanding of Combustion Physics. Georgia Tech Research Corporation is improving the state-of-the-art in understanding and modeling combustion instabilities, one of the most critical problems associated with burning high-hydrogen fuels in low-emissions turbines. "Combustion instabilities" refers to damaging pressure oscillations excited by the combustion process. During the past year, a detailed analysis of key physics controlling heat release response for flames during high-frequency instabilities was completed. In addition, a variety of data quantifying the flame response to velocity and fuel/air ratio fluctuations, needed for both understanding of key controlling physics as well as model validation, was obtained. Finally, Georgia Tech Research Corporation worked closely with industrial partners to facilitate transition of models and understanding into design processes for next-generation gas turbines.

Low-Swirl Injector Optimized for H_2 Operation. A low-swirl injector (LSI) being developed at the Lawrence Berkeley National Laboratory for the gas turbine in IGCC power plants has been optimized for burning of high-hydrogen fuel (HHF). The modification enables the LSI to burn a HHF of 90% H_2/10% CH_4 at the same adiabatic flame temperatures as natural gas without inciting flashback

or significant flame instabilities. The new flared-shape LSI exit nozzle shields the HHF flame from being influenced by the outer shear layer and the corner recirculation zone. Its development is an outcome of basic studies on the effects of changing fuel and combustor geometry on the LSI flame. Laboratory measurements and analysis of the LSI flow fields and flame acoustics have shown that the high diffusivity and reactivity of HHF promote burning in the unstable outer shear layer. A feasibility study of an LSI-based fuel-flexible combustion system for IGCC has been carried out. Using a typical F-frame gas turbine combustor geometry as a baseline, the study shows that multi-fuel LSI operation is feasible by the use of dual parallel fuel circuits. A number of issues and potential challenges have been identified that will need further attention as design development efforts continue.

New Aero-Thermal Rig Completes Construction and Shakedown. Through a collaborative effort between researchers at the NETL and the University of Pittsburgh, an existing NETL pressurized combustion rig has been modified to include an aero-thermal test section. This new capability will be used to assess film cooling concepts and TBCs that can increase the efficiency of gas turbine systems. Initially, the testing will focus on flat coupons (both with and without TBCs). At least three different film cooling approaches have been identified for study. Shakedown testing of the upgraded facility has been performed at atmospheric pressure, and additional testing at higher pressure will soon commence.

Optical Temperature Method Tested for Aerothermal Rig. Researchers at NETL and the University of Pittsburgh are collaborating to develop an aerothermal test facility to examine innovative cooling concepts for application in advanced, land-based gas turbine systems. Preliminary shakedown of the optical temperature measurement technique to be used for the heat transfer measurements has now been completed. The method utilizes an emissivity-compensated pyrometer to measure the emissivity of the coupon surface at a particular wavelength. A charged-couple device camera with an optical filter at the same wavelength provides a way to determine the temperature across the coupon surface. The initial test coupon was impingement cooled with coupon temperatures in excess of 800°C (1,470°F) at very lean conditions. Gas temperatures were in excess of 1,200°C (2,190°F). This test also provided an opportunity to do some preliminary testing of a temperature probe developed by Sporian Microsystems for the advanced research sub-program. Testing had to be terminated early due to failure of a ceramic liner in the test section, but useful data were obtained for NETL's optical temperature method as well as for the Sporian probe.

New Data Obtained for Advanced Power Cycle Design. The development of innovative power cycles such as IGCC and oxy-fuel is hindered by the lack of validated data for thermodynamic and transport properties of the gaseous mixtures in the turbines and other parts of these cycles. Approaches such as ideal-gas thermodynamics are inaccurate for such systems, primarily due to the presence of water. Research at the National Institute of Standards and Technology is developing alternative modeling approaches, supplemented by selected high-temperature experimental measurements. First-principles molecular modeling has been used to provide accurate thermodynamic properties, with the key water-CO_2 interaction being added in FY 2010. One-of-a-kind apparatus have been designed and constructed for high-temperature measurements of density and thermal conductivity for mixtures of water with CO_2 and with nitrogen. These data have been successfully obtained at temperatures up to approximately 470°C for the thermal conductivity and 350°C for the density.

Ultra-Low NOx Catalytic Combustors for MW-Scale Hydrogen Turbines Demonstrated. Precision Combustion, Inc. (PCI), in collaboration with Solar Turbines, Incorporated, is developing a combustion system for MW class turbines having the capability to burn hydrogen as fuel while maintaining or improving current levels of cycle efficiency, reducing NOx to less than 2 ppm, reducing diluent requirements, and eliminating emissions of carbon dioxide. Subscale testing at 10 atm. at PCI demonstrated low single digit NOx emissions (<2 ppm) corrected to 15% O_2 with stable operation at equivalent IGCC base-load combustor conditions. A full-scale single injector hydrogen module has been fabricated based on the subscale results. This module has undergone atmospheric flow testing to validate performance parameters at PCI. Full-scale single injector testing of hydrogen-nitrogen fuel mixtures at high pressure (16 atm.) simulated engine conditions is scheduled to be performed at Solar Turbines, Incorporated during July 2010.

Syngas Chemical Model Updated to Predict High-Pressure Flames Accurately. Princeton University expanded the experimental data set of flame speeds and burning rates for high-pressure, low-flame-temperature syngas flames to cover *lean* mixtures of more direct interest to typical syngas turbine conditions, employing a parametric approach by individually varying pressure from 1 to 25 atm., flame temperature from 1,400 to 1,800 K, and equivalence ratio from 0.3 to 1.0. These measurements mapped the pressure dependence of H_2 burning rates, indicating the existence of *negative pressure dependence* in the burning rate at high-pressure, low-flame-temperature conditions. Significant deficiencies in current state-of-the-art kinetic models in predicting relevant syngas flame behavior were identified. In order to improve model performance, the key kinetic pathways and causes of the modeling difficulties under these conditions were analyzed. The H_2 kinetic model was updated to incorporate better elementary reaction information from a number of recent studies. The updated model is demonstrated to yield improved agreement against the more recent high-pressure, low-flame-temperature flame targets as well as reproduce previous validation targets. Additionally, strategies that reduce computational time in combustion calculations by over an order of magnitude were formulated and validated.

Performance of Nickel and Cobalt Alloys in Oxy-Fuel Conditions Explored. Materials performance of nickel-base and cobalt-base alloys and alloy/coating systems are being evaluated at NETL in the oxy-fuel turbine environment to qualify them for use. Ni-base alloys, at 748°C and below, exhibited low corrosion rates with protective parabolic behavior. Rates at 821°C were higher, but remained parabolic. In terms of effective metal loss, internal oxidation was the primary factor for the nickel-base alloys. Co-base alloys were more of a concern, with a tendency towards oxide spallation. Coated materials (a bond coat and a TBC) experienced only a modest amount of growth of the thermally grown oxide and loss of aluminum from the bond coat. Low cycle fatigue (LCF) testing resulted in some detriment to life as a result of exposure to the oxy-fuel turbine steam-CO_2-oxygen environment. Depending on the alloy, LCF capability was less than that for fatigue coupons tested in dry air at same test temperature. In some instances the decrease in LCF capability was within the scatter of the dry air tested specimens while in other instances it felt clearly outside the data scatter. Examination of the surfaces of the fractured LCF specimens revealed mixed mode failure with areas of intergranular fracture along with regions of transgranular fracture.

Platinum Diffusion Bond Coatings Show Excellent Lifetimes in Laboratory Testing. A coating evaluation project at Oak Ridge National Laboratory has been studying the processing and performance of a new class of bond coatings to protect Ni-base superalloys at high temperature in the first stage of a gas turbine. These Pt diffusion coatings hold the promise of improved performance in coal-derived synthesis gas- or H_2-fired turbines where the environment is expected to degrade conventional coating performance, resulting in shorter coating lifetimes or lower turbine peak operating temperatures. In accelerated laboratory furnace cycle testing at 1,150°C, Pt diffusion bond coatings with a commercial ceramic overlayer typical of TBC systems showed >50% increase in the durability relative to conventional aluminide and Pt-modified aluminide coatings. The study also showed that the composition of the superalloy substrate was critical to the coating performance. Substrate composition effects will be further investigated in the next phase of this study, where current MCrAlY-type coating compositions are included.

Turbine Materials Compatibility Evaluation with Oxy-Fuel Working Fluid Initiated. At Siemens Energy, one of the goals of the turbine development project for oxy-fuel conditions is to quantify the life of superalloy/TBC systems in an environment of steam and CO_2. This is important because originally, these systems were designed for operation in a regular gas turbine with products of combustion of natural gas in air. Siemens made significant progress towards understanding the material behavior in steam/CO_2 atmosphere. Baseline TBC spallation data from thermal cycling were generated. The oxidation effects of the environment on the microstructure underneath the TBC were studied. Further, machined LCF specimens were exposed to steam/CO_2 atmosphere in order to prepare these specimens for tests and quantify the effects of the exposure on low cycle fatigue properties. When completed, this work will allow an estimation of the expected life of blades and vanes in the selected Siemens SGT-900 turbine modified for oxy-fuel combustion conditions.

NETL's University Turbine Systems Research

Particle Deposition Simulations Verified as Representative of Operating Turbine. A key goal for the University of Texas (UT) at Austin is to simulate depositions that occur on turbine components of a gas turbine engine when operated with coal-derived syngas fuels. By successfully simulating this deposition process in a laboratory test section, improved film cooling designs that reduce the depositions on turbine section surfaces and/or maintain effective film cooling performance can be investigated. Recognizing that the essential physical process for these depositions is the solidification of molten contaminant particles on cooled turbine surfaces, UT developed a process whereby molten wax particles of the appropriate size and temperature are used to simulate contaminants in the laboratory test facility. These particles were sized so that the Stokes number and a thermal scaling parameter (developed in this project) were matched to engine conditions. Simulations of depositions to model vanes and endwalls were verified by industry partners to be representative of those found in actual engine operations. Experiments were conducted to determine how these depositions affected film cooling performance. Results showed that deposition reduced endwall adiabatic effectiveness by as much as 30%, but further tests on a blade leading edge model showed that the overall cooling of the blade improved because of the insulating effect of the depositions.

Syngas Ash Deposition Simulated in a Film-Cooled Leading Edge of a Turbine Vane. At Virginia Polytechnic Institute and State University, syngas ash deposition dynamics were investigated in a three-row film-cooled leading edge with blowing ratios ranging from 0.5 to 2.0 and ash particle sizes of 5 and 7 microns (Stokes numbers 0.25, 0.49, respectively) using large-eddy simulations. It was demonstrated that stagnation row cooling is quite effective in protecting the blade surface from deposition locally by blowing away as well as cooling ash particles. However, it was also demonstrated that at higher Stokes numbers, the blowing ratio did not have any significant effect on preventing deposition at the leading edge. Detailed deposition profiles were obtained from these studies. A surface ash deposition model was developed as a function of ash composition and particle softening temperature. This model was validated with experimental data and is the first such comprehensive model of its type which can be used for calculating ash deposition. Complementing the modeling effort, experiments using polyvinyl chloride particles were also conducted at the leading edge of a film-cooled vane. These experiments measured the capture efficiency at different blowing ratios and different free stream temperatures.

Physics-Based Correlation Model Developed for Predicting Turbulent Flame Speeds. Georgia Institute of Technology has obtained turbulent flame speed data of high-hydrogen fuel blends over a range of conditions of interest, including fuel composition, velocity, turbulence intensity, preheat temperature, and pressure. The strong effects of hydrogen fuel composition upon turbulent flame speeds were demonstrated at gas turbine realistic velocities, turbulence intensities, and combustor inlet temperatures. In addition, a physics-based correlation model was developed based on flame strain and differential diffusion to predict turbulent flame speeds. These data and models are being used to develop low-emission gas turbine combustion technology capable of operation with high H_2 levels.

Prototype Combustor Demonstrates Ultra-Low NOx with Syngas. An integrated and collaborative effort involving Pennsylvania State University and Princeton University composed of experiments and complementary chemical kinetic modeling is investigating the effects of major species (H_2O and CO_2) and minor species (CH_4, C_2H_6, etc.) on the ignition and combustion of HHC fuels that are characteristic of syngas. Mass burning rates have recently been measured for $H_2/O_2/He$ and H_2/fuel-additive/O_2/diluent mixtures at pressures up to 25 atm. at selected temperatures (1,400 and 1,600 K) and equivalence ratios (0.3 and 0.7). The mass burning rate is observed to increase and then decrease as pressure is varied from 1 to 25 atm. Comparisons with the current chemical kinetics models indicate differences in the predicted mass burning rate of up to a factor of 4. Of particular interest is the lack of agreement with the "GRI mech" model that is widely used in the research community. An updated chemical kinetics model was formulated to address the difficulties observed in modeling recent high-pressure flame data. Emphasis was placed on assessing the current state of knowledge of relevant elementary processes and the approach needed to achieve a rigorous solution that yields quantitative predictive capability across a wide range of conditions. Overall, the updated

model predicts flame speed spanning a wide range of equivalence ratios, pressures, diluents, and flame temperatures to within 20%.

Chemical Kinetics of Syngas and Hydrogen Fuels Studied in Tubular Flow Reactor. At the University of Colorado at Boulder, a high-temperature (hyperthermal) miniature tubular flow reactor has been designed and fabricated to explore the chemical kinetics of syngas and nearly pure hydrogen fuels at conditions of interest in gas turbine combustion. The reactor has been used to explore the role of surface reactions in pre-ignition events that take place in the inlet region. It has been shown that current gas phase reaction mechanisms do a poor job of predicting combustion characteristics at the high pressures and low temperatures typical of gas turbine inlets, especially ignition delay, where predictions and experiments differ by three orders of magnitude. This has serious consequences for the reliability and survivability of premixed injectors. Thus, heterogeneous catalytic reactions between the reactant gas and the inlet surface material may cause the observed behavior. The experimental set-up includes temperature control of the tubular reactor and matrix isolation/infrared spectroscopy diagnostics. Nickel, Inconel and stainless steel have been tested, and hydrogen oxidation has been observed on both nickel and Inconel. For nickel, the results are in rough agreement with an existing surface reaction mechanism.

New Thermal Barrier Coatings Are Resistant to Molten Fly Ash Deposits. Over the past year, significant progress has been made in the understanding of the interaction between molten fly ash and TBCs. The fly ash was found to completely destroy the conventional 7 wt% yttria-stabilized zirconia (7YSZ) TBCs by penetration and exfoliation of the grains. An alternative TBC material, gadolinium zirconate or $Gd_2Zr_2O_7$, has been selected, which is found to mitigate the effects of molten ash on the TBC. Comprehensive testing is underway to determine how well this top-coat will perform in-service by employing both isothermal testing and thermal gradient testing, as well as furthering the understanding of the mechanism(s) of mitigation.

Small Business Innovation Research

Niobium Superalloys Demonstrate Oxidation Resistance and High-Temperature Capability. QuesTek Innovations LLC successfully designed a concept niobium (Nb)-based alloy that achieved significantly higher-temperature capability than Ni-based superalloys (>1,200°C), enhanced oxidation resistance (nearly an order of magnitude slower rate compared to commercial Nb-based alloys) trending towards commercial Ni-base superalloys, and a microstructure that was almost 100% body-centered cubic (critical in achieving enhanced ductility). Turbines operating at higher temperatures, enabled by new niobium-based superalloys, could operate at higher efficiency and thus reduce electricity-generation costs and CO_2 emissions. The breakthrough high-temperature capability of those new alloys would also allow hydrogen-fueled turbines and ultra-high-temperature steam turbines to be developed, thus making the vision of zero-emission fossil-fuel power plants possible.

Advanced Cooling Technology Has Potential for Major Efficiency Increase. Turbine component cooling using internal vaporization – condensation heat transfer has been explored by Aerodyne Research, Inc. for application to IGCC power systems. This cooling technology forces cooled components to be essentially isothermal and enables operation in much higher temperature environments than those allowed by conventional cooling. Unlike conventional heat pipes, this cooling approach is fully functional at very high acceleration, as required for use in rotating turbine components. A fully cooled engine, operating at higher pressure ratio and peak gas temperature than is possible with conventional technologies, can achieve a 20-percent efficiency improvement, with corresponding decrease in fuel consumption and emissions. This is highly attractive for IGCC power systems as well as natural gas-fired power plants. Previous research focused on turbine blade cooling, as a critical component for increased cycle efficiency. This project has identified compressor and turbine discs, and turbine nozzles and stators, as high-payoff components for initial IGCC application. Conceptual designs have been developed. Detailed thermal and stress analysis of the disc design showed stresses to be fully acceptable, and on average lower than for a conventional disc.

Spar-Shell Turbine Component Development Enables a Disruptive Leap in Gas Turbine Performance. At Florida Turbine Technologies, engineers are developing Spar-Shell gas turbine components to provide significant efficiency improvements in existing and advanced power systems,

including proposed turbomachinery using high-hydrogen and alternative synthetic fuels. Feasibility of the technology has been demonstrated through conceptual design studies, and detailed design of equipment is in progress. Spar-Shell airfoil technology can be retrofit into existing power plants worldwide to create up to 15% more power from the same plants, one-third of which will be completely carbon-free and require no additional fuel.

Industrial Gas Turbine Cores Produced with Advanced Cooling Features. Mikro Systems has demonstrated that their proprietary Tomo-Lithographic-Molding process can lead to revolutionary new turbine cooling designs, which can be developed faster and at significantly lower cost than current techniques allow. During this Phase I project, three new industrial-scale cores (trailing edges only) were designed by turbine industry experts and produced by Mikro Systems. These cores embodied cooling features that cannot be produced using current techniques. Small lots of cores for two of the three designs were successfully cast, fired, and sintered using a ceramic material that is fully compatible with directional solidification (DS) (or single crystal) foundry casting. Optical and mechanical inspection methods were used to characterize the cores. Mikro then demonstrated the manufacturability of these advanced designs at the foundry level, that is, Mikro developed two foundry-test core designs with the revolutionary cooling features used in the trailing edge cores above. Eight cores (four of each design) were successfully cast, fired, and sintered, and coupons were produced using the DS casting process and 247LC alloy. The cast parts were evaluated by X-ray inspection, boroscope, physical inspection (after sectioning), and coordinate measuring machine. The evaluation demonstrated that the cores are compatible with the foundry process and provided initial feedback on the capabilities and limitations of the casting process for casting these advanced cooling features.

Transpiration-Cooled Turbine Components Demonstrated for High-Temperature IGCC Turbines. Practical application of efficient and cost-effective IGCC turbines requires the development of gas turbines with higher firing temperatures and pressure ratios than those currently in use. Ultramet developed a transpiration-cooled high-temperature first-stage nozzle vane with a core formed using structural open-cell foam that defines the interior cooling path, adds structural stiffness and strength, and functions as a template for application of an outer skin with fine, uniform porosity for flow of the transpiration coolant. The demonstrated vane processing provides a low-cost and short-lead-time method for producing high-temperature transpiration-cooled turbine components. A subscale vane was designed based on a current turbine engine selected by Pratt & Whitney Rocketdyne, and a transpiration cooling model was developed based on the use of a metal foam core with a porous and integrally attached outer skin. Component specimens were fabricated using a molybdenum foam core with a porous molybdenum skin, and pressure drop data generated by flowing gas through the foam and porous skin were consistent with model predictions. Initial modeling suggested a significant increase in vane cooling efficiency, and overall efficiency of IGCC engines may be realized through use of this transpiration-cooled foam core vane design.

Water Guided Laser Drilling Demonstrated for Gas Turbine Alloys. Physical Sciences Inc. (PSI) demonstrated water guided laser drilling of 0.018-inch cooling holes in Inconel 718 alloy. The water guided laser drilling process has the potential for producing cooling holes in gas turbine components at speeds comparable to current gas-assisted laser drilling processes with quality comparable to electro-discharge machining processes. The water guided laser drilling process developed by PSI adapts beam delivery hardware to a commercial laser cutting head. The diameter of a drilled hole is controlled by the diameter of the high-pressure (up to 200 psi) water stream used to guide the drilling laser. Holes were drilled through 0.050-inch Inconel 718 at rates exceeding 3 sec/hole using a pulsed Nd:YaG laser delivering pulses with power densities of 8×10^5 W/cm^2. Pin gauging shows that the holes drilled using the water guided process have diameters 0.018±0.0005 inches.

Advanced Thermal Barrier Coating System Exhibits Enhanced Performance. At Directed Vapor Technologies International, the feasibility of effectively depositing advanced TBC systems needed for use in high-temperature IGCC environments has been demonstrated during a Phase I SBIR project. The high-temperature TBC systems are enabled by the use of the novel coating materials, coating architectures, and advanced processing approaches. Coatings in this work were deposited using a high-rate Directed Vapor Deposition (DVD) approach. The developed system consisted of a DVD-deposited, γ/γ'-based bond coat layer and a bi-layered 7YSZ/multi-component hafnia top coat. The system was successful tested for 2,000 cycles in a jet engine thermal shock gradient test (surface temperature

= 1,400°C) and a 500-hour cyclic exposure at 1,150°C without any failure. Thermal conductivity testing of the DVD-deposited multi-component hafnia top coat in a laser-based testing rig at the National Aeronautics and Space Administration (NASA) (collaboration: Dongming Zhu at NASA) has demonstrated a low TBC thermal conductivity of 0.8 W/m-K.

Electrophoretic Deposition Process Deposits Thermal Barrier Coatings for Turbine Applications. Researchers at Faraday Technology Inc. are developing a pulse/pulse reverse electrophoretic deposition (EPD) process for the application of TBCs to hot section components of gas turbines. The new manufacturing process utilizes pulsed electric fields to induce migration of charged particles in suspension to uniformly deposit the TBCs. After binder burnout and sintering processing steps, a porous ceramic coating is formed on the turbine component. The non-line-of-sight nature of the process makes it suitable for coating complex shaped components, such as turbine vanes and blades that are difficult to uniformly coat using the industrially practiced techniques of plasma spray or electron beam physical vapor deposition. The pulse/pulse reverse EPD process is applicable to conventional and newly developed low-conductivity TBCs that will enable higher temperatures in natural gas and synthesis gas environments. Recent experiments at Faraday Technology have shown that the TBCs deposited by the pulse/pulse reverse EPD process exhibit decreased roughness and enhanced uniformity when compared with TBCs deposited by conventional EPD, and exhibit favorable results in preliminary and long-term thermal cycling tests. In addition to the technical benefits, the enabling manufacturing process equipment will be affordable and relatively simple to operate.

Low-Cost Electrochemical Methods Demonstrated for Producing Functionally Graded and Laminated Thermal Barrier Coating Systems. Modumetal has produced laminated and functionally graded TBCs using low-cost electrochemical synthesis routes. Microlaminated and functionally graded top coats of YSZ/Al_2O_3, as well as nanolaminated Ni/NiAl bond coats, were produced and microstructurally characterized. The effects of process variables on coating microstructure and composition were determined. Project highlights include a) the demonstrated ability to impart desirable vertical segmentation cracks in composite ceramic top coats, b) the ability to grow NiAl coatings with tailorable porosities ranging from fully dense to ~60% porosity, and c) the ability to deposit NiAl-ceramic composite alloys ranging from 0 to 90% nickel. The resulting coatings are anticipated to improve cyclic oxidation life and reduce thermal conductivity.

Ultra-High-Temperature Environmentally Robust Nanocomposite Thermal Barrier Coatings Developed for Nickel Superalloy Integrated Gasification Combined Cycle Turbine Components. NanoSonic has successfully demonstrated the thermal durability of its spray-deposited polymer-derived nanocomposite TBC technology up to the thermal limit of modern nickel superalloys of 1,200°C. To that end, researchers molecularly engineered over 100 coating formulations to identify a synergy of copolymer – nanoparticle compositions that anneal to high-durability TBC nanocomposites that retain their desirable adhesive, impact, thermomechanical, and abrasion durability after repeated cycling from room temperature to 1,200°C. NanoSonic's polymer-derived nanocomposite coatings may be spray-deposited under ambient conditions using low-cost, conventional spray equipment and converted to mechanically robust, thermally insulative TBCs on a production basis with significantly reduced material and labor cost, as well as without hidden uncoated areas inherent to line-of-sight deposition techniques. In fact, it has been demonstrated that after twenty heating cycles from room temperature to 1,200°C for 1 hour, Inconel substrates coated with optimized polymer-derived nanocomposite formulations retain the following performance metrics:

- Adhesive rating of 5A per ASTM D3359
- Impact durability per ASTM D5628-07
- Exceptional abrasion resistance (less than 0.05 weight percent loss after 1,000 wear cycles with a 250 g load)
- No coating spallation, cracking or delamination
- Less than 0.1 weight percent loss after soaking at 1,200°C for 12 hours
- Rapid spray deposition onto planar and curved 2-inch by 2-inch nickel alloy substrates using commonly employed facile high-volume low-pressure painting techniques used for aerospace topcoats

Novel Multilayer Multicomponent Thermal Barrier Coatings Successfully Developed. IGCC future generation energy systems demand higher operating temperatures, as well as more complex interactions among the corrosive coal gases and turbine materials. Coatings are the most efficient, flexible and cost-effective solution to meet present and future needs of these IGCC systems. Thermal spray coatings offer a pragmatic and cost-effective solution to a wide range of requirements in power turbines. During a collaborative SBIR project between Plasma Technology Inc., the Center for Thermal Spray Research at Stony Brook University, Prof. Carlos Levi of University of California, Santa Barbara, and Dr. Robert Vassen of Julich Research Center, novel multilayer and multicomponent co-doped TBC architectures based on gadolinium and lanthanum zirconate materials in combination with YSZ coatings were successfully developed and evaluated. Incorporation of co-doped YSZ with rare earth oxides (Gd+Yb+YSZ) and pyrochlore-type zirconate ($La_2Zr_2O_7$, $Gd_2Zr_2O_7$) materials into thermally-sprayed coatings has led to further decreases in thermal conductivity, greater thermal protection at high temperatures (better than YSZ at 1,300-1,400°C), better sinter and erosion resistance, enhanced toughness for withstanding cyclic thermal stresses, and overall improved ability to sustain aggressive IGCC corrosive environment.

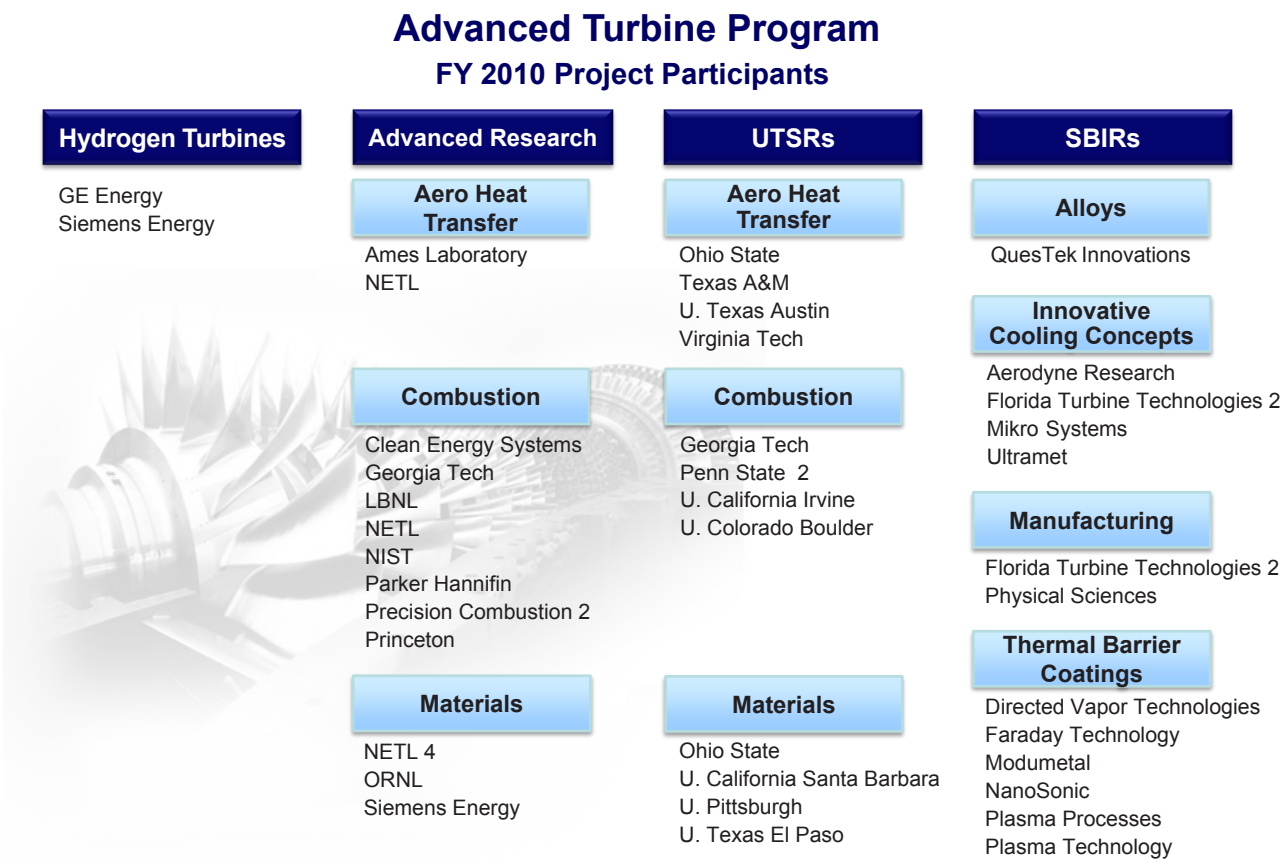

Summary

In response to the Nation's increasing power supply challenges, NETL is researching next-generation turbine technology with the goal of producing reliable, affordable, diverse, and environmentally friendly energy supplies. With the Advanced Turbine Program, NETL is leading the research, development, and demonstration of these technologies to achieve power production from coal that is clean, efficient, and cost-effective, minimizes carbon dioxide emissions, and will help maintain the Nation's leadership in the export of electric power equipment.

Critical technologies must be modeled and developed for future gas turbine engines in advanced IGCC systems running on high-hydrogen content fuels. Either new materials must be developed or coatings with novel chemistries must be engineered to protect engine components and allow further increases in engine temperatures to achieve higher efficiency. The development is limited, in part, by the available materials and manufacturing abilities.

The DOE's Advanced Turbine Program is striving to show that the U.S. can operate on coal-based hydrogen fuel power, increase combined cycle efficiency by three to five percentage points over the baseline, and reduce carbon dioxide and other toxic emissions by 2015. Program and project emphasis is on understanding the underlying factors affecting combustion, aero/heat transfer, and materials for current IGCC syngas turbines and using that knowledge to design and conduct the research needed to transition to nearly pure hydrogen fuels.

Following is a summary status for each project managed through the Advanced Turbine Program. The scope, objectives, status and accomplishments are reported for each project. The Advanced Turbine Program is encouraged by the technical progress made this year and the prospects for continued advancements in the coming year are good, paving the way to achievement of the goals.

II. HYDROGEN TURBINES FOR NEAR-ZERO EMISSION SYSTEMS

II.1 DOE Advanced IGCC/H_2 Gas Turbine Development

Reed Anderson
GE Energy
1 River Road, 55-211
Schenectady, NY 12345
Phone: (518) 385-5689; Fax: (518) 385-8796
E-mail: reed.anderson@ge.com

DOE Project Manager: Robin Ames
Phone: (304) 285-0978
E-mail: Robin.Ames@netl.doe.gov

Subcontractors:
- GE Global Research Center, Niskayuna, NY
- GE Aviation, Cincinnati, OH

Contract Number: 42643

Start Date: October 1, 2005
End Date: September 30, 2012

FY 2010 Objectives

Develop technology advancements necessary for an advanced integrated gasification combined cycle (IGCC), fuel-flexible (coal-derived hydrogen and syngas), gas turbine to meet the DOE program goals of:

- Improve IGCC efficiency (+3-5 pts combined cycle efficiency).
- Reduce NOx emissions to 2 ppm NOx at 15% O_2.
- Contribute to capital cost reductions.

Accomplishments

- Continued excellent progress in the development of pre-mixed combustion technology for syngas and hydrogen by conducting extensive megawatt-scale, full head end testing on leading concept – achieved single digit NOx emissions at target 2012 cycle conditions (in excess of F-Class).
- Completed rig test validation of optimized transition piece to stage one nozzle (TP-S1N) seal design – demonstrated targeted leakage flow reduction.
- Completed cooling effectiveness characterization for first generation advanced cooling design concept – demonstrated that targeted performance achievements are possible.
- Conducted initial phase of turbine aerodynamic validation rig testing.
- Completed second iteration component coating composition down selection (thermal barrier coatings and bond coats) in preparation for the process refinement stage and comprehensive performance evaluations/validation tests.

Introduction

Coal is this nation's most abundant domestic energy resource and is used to produce about 50% of the nation's electricity needs. Its continued use is an important part of realizing an "energy secure" United States. The challenge is to produce electricity in a cleaner and more efficient manner while significantly reducing carbon emissions. The goal of this project is to advance gas turbine technologies so that future coal-based IGCC power generation plants, including CO_2 capture, can be accomplished with higher efficiency, lower cost, and reduced emissions. The gas turbine has a significant influence on the performance of the IGCC power plant. The inherent performance penalties associated with CO_2 capture are driving a renewed focus on gas turbine technology advancement as a means to minimize the penalty.

In an IGCC power plant, syngas produced from the coal is cleanly burned in a heavy-duty gas turbine. With pre-combustion CO_2 capture, the resulting fuel burned in the gas turbine is hydrogen. GE's advanced gas turbine technology program addresses key technology developments required to achieve specific DOE performance goals relative to emissions, efficiency, and capital cost. The project is comprised of two phases. Phase I, which ran from October 2005 to September 2007, was focused on conceptual design and technology identification. The output of Phase I was a down selection of key technologies that are currently being further applied and developed in Phase II. The Phase II effort started in October 2007 and is focused on technology development and validation at a component level.

Approach

This gas turbine technology advancement project is comprised of three main technology areas (combustion, turbine/aero, and materials) plus a systems-level activity.

- The combustion element of the project is focused on improving combustion technology to achieve the emissions target of 2 ppm NOx at the higher temperatures necessary to achieve the targeted efficiency improvement. Work in this area addresses the challenges of developing a combustion system that can burn both syngas and

high hydrogen fuels to produce extremely low NOx emissions while avoiding flameholding, flashback, and dynamics issues.

- The turbine/aero element of the project drives technology improvements to address the efficiency targets. Examples include improved aerodynamic characteristics and better flow management.
- The materials portion of the project is focused on applying materials technology to enable the turbine to operate reliably at higher firing temperatures in the harsher IGCC environment. This includes evaluation of advanced coatings, along with targeted use of ceramic matrix composites with environmental barrier coatings.
- The systems level approach translates the integration of technology improvements into plant performance and investigates the various system trade-offs and their impact on overall plant performance.

In summary, this comprehensive project addresses the technology development needs for advanced gas turbines for IGCC applications while targeting the specific goals identified by the DOE relative to emissions, efficiency, and capital cost.

Results

Fiscal Year 2010 was the third year of Phase II of the project, and as such, advanced analysis tools and rig testing continued to be used extensively in the process of developing and characterizing performance improvements from each technology area.

The leading combustion concept was tested extensively in a full can arrangement. Testing was conducted with pure hydrogen, natural gas, and hydrogen-nitrogen fuels, along with a more traditional syngas blend including carbon. A picture of testing in progress is shown in Figure 1. During the year, DOE 2012 targets were realized, as the system was operated on high hydrogen fuel in excess of F-Class conditions with single digit NOx emissions. System pressure drop and dynamic responses were favorable. A level of reliability and durability on H_2 fuel was demonstrated with over 60 hours of fired test time, including several instances of full load operation for more than 6 hours. During the rest of Phase II, the main focus will be on 1) expanding demonstrated performance at the full can level to the 2015 conditions, 2) further reducing NOx emissions, 3) addressing requirements such as reliability, manufacturability, and durability, and 4) further increasing the size of the demonstration tests.

The first suite of tests to investigate the performance and behavior of a new advanced cooling design concept were conducted. The tests were conducted in an experimental rig utilizing

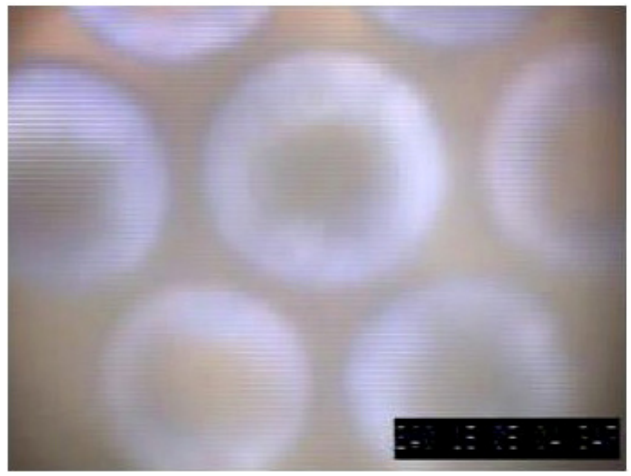

FIGURE 1. Full Head End Combustion Test on High Hydrogen Fuel

a symmetric airfoil with contoured outer walls to provide a representative static pressure distribution on the airfoil. Film effectiveness measurements were made for different versions of the advanced concept currently under investigation. Figure 2 provides results from the testing, and shows the level of improvement achieved relative to the baseline. Measurements of hole discharge coefficients were also made. While full data analysis was still ongoing at the time of writing, initial observations indicate that targeted performance achievements are possible, and new configurations are being created for a subsequent round of testing to further optimize the concept and increase capability.

An optimized TP-S1N seal design was tested in a rig that simulates first stage nozzles and one transition piece plus short segments of the two neighboring transition pieces. Using this rig, shown in Figure 3, the targeted leakage flow reduction was achieved.

Turbine aerodynamics were tested in a specially designed multi-stage validation test rig. A photograph

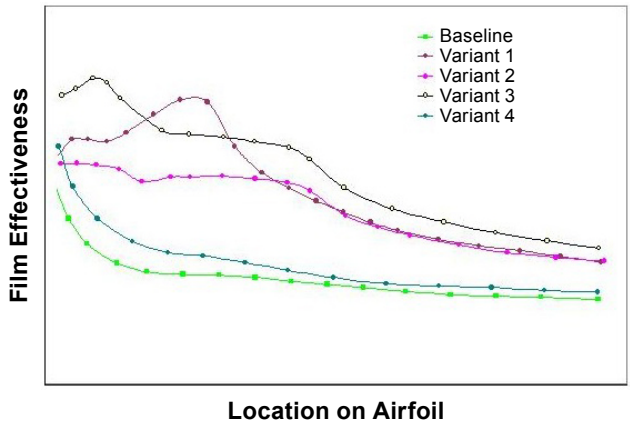

FIGURE 2. Film Effectiveness Measurements for Advanced Cooling Concept

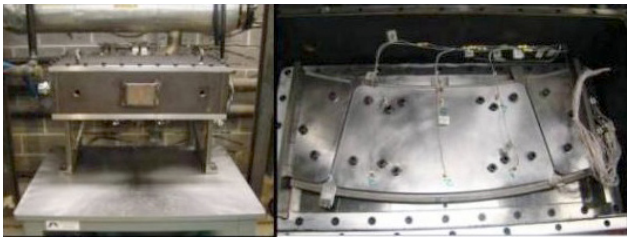

FIGURE 3. Transition Piece to Stage 1 Nozzle (TP/S1N) Test Rig

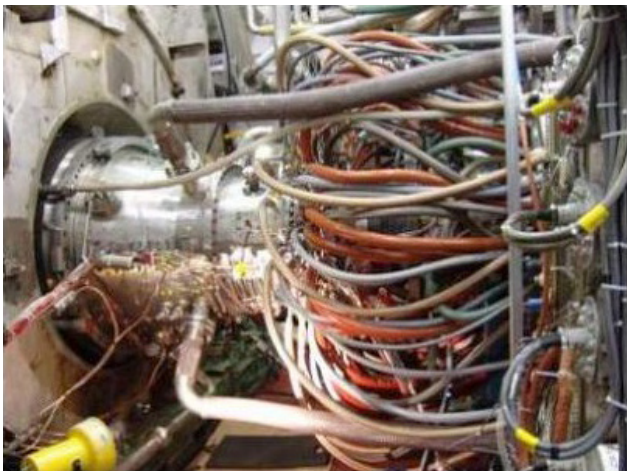

FIGURE 4. Fully Assembled Aerodynamic Validation Test Rig

of the fully assembled test rig is shown in Figure 4. Detailed performance characterizations where conducted over a wide range of flow rates. Derivatives on tip clearance and purge flows were also obtained. Preliminary analysis of the test data supports the initially projected improvement potential. Subsequent testing will evaluate and validate advanced technology concepts that are currently being designed based on findings from the initial testing.

A series of tests were conducted on second iteration TBCs and bond coats (BCs) to assess their performance relative to baseline coatings. For BCs, Type I hot corrosion behavior and oxidation resistance were characterized along with strain tolerance and low cycle fatigue life. For TBCs, relative phase and dimensional stability, along with erosion/impact/spallation resistance was characterized. Based on the results of these tests, a down-selection was made to two TBCs and two BCs that will be further evaluated later in 2010 in a rig test that will characterize performance of the integrated TBC/BC system.

The systems function continues to perform studies necessary to quantify the plant level performance and cost impact of the various technology development efforts, as well as guide component design decisions.

Conclusions and Future Directions

Phase II (technology development and validation) of this project is a continuation from Phase I (technology identification and conceptual design) which was completed on time, within budget, and with all major milestones achieved. In FY 2010 the third year of the Phase II project was completed. Results to date in Phase II have been positive and continued to indicate that project progress is on track relative to available funding. Building on work performed in FY 2010, future years will continue unfinished efforts from this year and initiate remaining areas of the program. Looking ahead, some of the specific technology areas are:

- Combustion technology will continue to be matured, as the project moves through the technology transition phase. In this phase there will be an increased focus on alternate construction/geometry to make the technology more reliable, affordable, easier to manufacture/service, and/or better integrated with other components/systems.
- Optimized designs for several more sealing locations will be completed and their improvement levels validated through rig testing. Results from cooling and aero tests will be used for qualification of advanced design tools and optimization of next generation component designs.
- Integrated testing of the selected TBC and BC system will be completed and a final down selection will be made. This will be followed by the process refinement stage and comprehensive performance evaluations/validation tests.

Special Recognitions & Awards/Patents Issued

1. Sixty-seven U.S. patent filings have occurred, with another 14 in various stages of the filing process.

2. To date one patent has been awarded (P/N: 7578130, Axial Staggering of Fuel Vane Pack For Combustion Dynamics Reduction Associated with Rayleigh Gain).

FY 2010 Publications/Presentations

1. Harry Jaeger, "Advanced H_2 Turbine for Meeting Future Power Generation Challenge," Gas Turbine World, May-June 2009.

2. Roger Schonewald, "Turbine and System Developments for Syngas/Hydrogen Gas Turbine Technology," ICEPAG 2010, February 2010.

3. Reed Anderson, "Combustion Developments for Syngas/Hydrogen Gas Turbine Technology," ICEPAG 2010, February 2010.

4. Joe Citeno, "The Pathway Forward: Future Gas Turbine Products and Their Enabling Technologies," ASME Turbo Expo 2010, June 2010.

5. Ron Bunker and Nuo Sheng, "Investigation of Augmented Angel Wing Sealing through the Use of Surface Concavity Arrays," ASME Turbo Expo 2010, June 2010.

II.2 Advanced Hydrogen Turbine Development

Joseph Fadok (Primary Contact), Tim Bradley
Siemens Energy, Inc.
4400 Alafaya Trail
Orlando, FL 32826
Phone: (407) 736-2361; Fax: (407) 736-5633
E-mail: joseph.fadok@siemens.com
tim.bradley@siemens.com

DOE Project Manager: Robin Ames
Phone: (304) 285-0978
E-mail: Robin.Ames@netl.doe.gov

Subcontractors:

- Florida Turbine Technologies, Jupiter, FL
- Agillis, Jupiter, FL
- Florida Institute of Technology, Melbourne, FL
- University of Florida, Gainesville, FL
- Georgia Institute of Technology, Atlanta, GA
- Purdue University, West Lafayette, IN
- Virginia Polytechnic Institute and State University, Blacksburg, VA

Contract Number: 42644

Start Date: October 1, 2005
End Date: September 30, 2012

FY 2010 Objectives

- Demonstrate through subscale testing, simulations, and systems studies that the 2010 DOE goals are achievable.
- Further refine the concepts necessary to meet the 2015 objectives and advance the technology readiness.
- Complete initial validation of the low conductivity thermal barrier coatings to demonstrate increased temperature capability over the baseline.
- Continue to improve the premix design and verify the results through high pressure combustion rig testing with syngas and high hydrogen.
- Down-select the optimized bond coat composition for high temperature, environmental resistance, and mechanical integrity.
- Complete aerodynamic rig testing of highly loaded turbine airfoils.

Accomplishments

- Materials verification testing was completed for thermal barrier coatings that demonstrated a significant increase in temperature capability.
- Several bond coat compositions were also tested to support down selection and full characterization. Figure 1 shows high temperature testing at the Siemens test facility.
- The Siemens premixed combustion design shown in Figure 2 has been tested at H-class engine conditions on syngas fuels demonstrating stable operation and low emissions.
- Extensive systems studies show that the DOE 2010 goals are exceeded with technologies developed to date. Figure 3 shows that over 50% of the penalty for carbon capture and sequestration can be recovered with the 2015 advanced hydrogen turbine technology.
- Multiple airfoil configurations have been tested in support of turbine component design with high stage loading (see Figure 4). These results are validating computer simulation results predicted with computational fluid dynamics (CFD) methods.
- Improved selective catalytic reduction formulations are showing over 30% improvement in catalyst durability. This novel emissions reduction system is also consistently showing high performance even in the presence of harsh integrated gasification combined cycle (IGCC) turbine exhaust conditions [1].

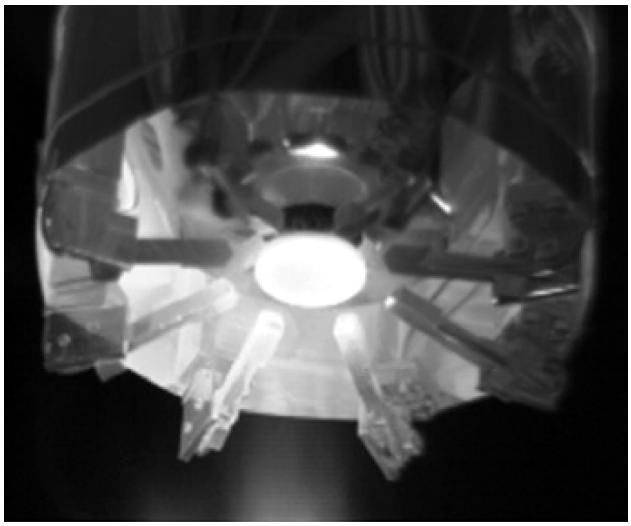

FIGURE 1. High Temperature Materials Testing at the Siemens Test Facility

FIGURE 2. Premix Syngas Combustor Nozzle

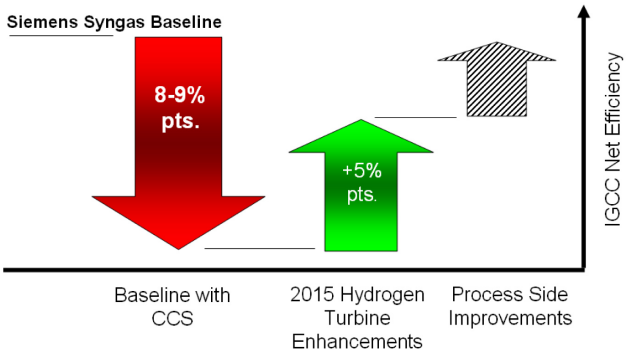

FIGURE 3. Recovering the Efficiency Penalty from Carbon Capture and Sequestration

Introduction

Siemens Energy, Inc. was awarded a contract by the U.S. Department of Energy (DOE) for Phases 1 and 2 of the Advanced Hydrogen Turbine Development Program in October, 2005. The DOE Advanced Power Systems overall goal is to conduct research and development necessary to produce CO_2 sequestration-ready coal-based IGCC power systems with high efficiency, near zero emissions and competitive capital cost.

Fiscal Year 2010 activities focused on the detailed evaluation of component level technologies and systems to demonstrate the 2010 goals and verify the 2015 project objectives can be achieved. Technologies were verified in subscale tests and design tools were updated with fundamental data obtained through laboratory tests at universities. Additionally, near-term targets for combustor performance and materials improvements were attained.

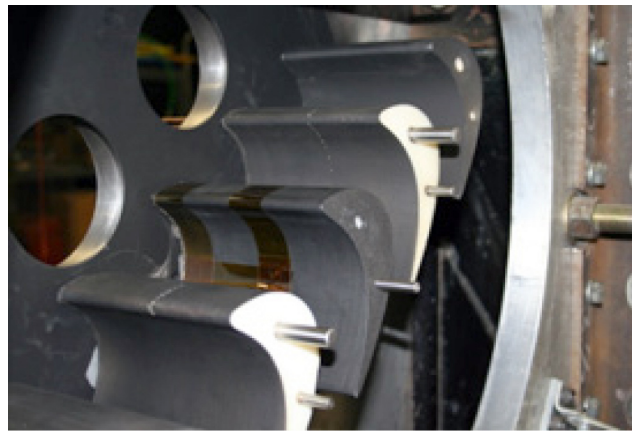

FIGURE 4. Turbine Blade Test Rig

Approach

Siemens has developed an overall project strategy that supports the DOE program goals and future commercialization. The path forward is a stepped approach which ensures the DOE intermediate (2010) and long-term (2015) goals are addressed. Phase 2 includes advanced technologies development, down-selection and validation, as well as basic component designs. In Phase 3, if awarded, the final product manufacturing specifications will be completed and the engine will be manufactured and installed in an IGCC plant for validation testing to demonstrate the project's commercial viability and that the DOE program goals have been achieved.

Results

Significant progress has been made in characterization of materials needed for the advanced hydrogen turbine. By meeting the 2010 goal for increasing temperature capability, Siemens coatings development is already producing systems for adaption to near-term applications. With the down-selection of bond coat compositions this year, the coatings system needed for the 2015 goals are being further defined. These high temperature thermal barrier coating systems are being testing at the Siemens test facility to quantify the material capability and fully characterize the system for design use. Coupled with the success of the modified superalloys project, the combined system will offer superior performance to the baseline materials system.

System studies have concluded that by increasing power output and efficiency, a substantial reduction in power block cost can be realized on a $/kW basis. Furthermore, the enhancements which are being developed under this project can also recover over 50% of the efficiency penalty resulting from capture and sequestration of CO_2 and greatly improve the cost of electricity. To the largest extent, the power block is flexible to future process side enhancements which could also have a positive effect on plant efficiency and economics.

Exceeding the 2010 performance goals was necessitated by the successful operation of the premix syngas combustor at the targeted elevated temperature. The operation on 100% syngas was also complimented by operation with increased hydrogen concentration. From the successful syngas demonstration, further enhancements were made that enabled operation with almost twice the hydrogen concentration compared to prior testing campaigns.

Several iterations of high turning airfoils were tested in the cascade rig and experimental results for blade loadings at 20%, mid-span, and 80% span at various mach numbers and inlet angles were obtained. A good correlation to CFD predictions has increased the confidence that the targeted stage loadings can be achieved.

Conclusions and Future Directions

The development effort continues to focus on key enabling technologies such as low emissions, high temperature fuel flexible combustor, novel turbine component concepts that improve aerodynamic and cooling efficiency. Material and coating technologies are being developed to enable increased operating temperature and mechanical integrity. The progress made in coatings technology is a key to producing a turbine with the lowest possible cooling flow at elevated temperature. Through advanced manufacturing processes and modular component technology, the feasibility of producing these novel turbine component concepts is made possible. Results from rig testing show that a high temperature premix combustor can operate on syngas at the elevated temperatures and low emissions to meet the DOE goals. By incorporating these advanced technologies, this gas turbine can significantly improve the efficiency, lower the capital cost, and improve the cost of electricity for IGCC plants with carbon capture.

By following a stepped approach, Siemens is addressing the specific goals for 2010 and 2015. Down-selected technologies will continue to undergo rigorous testing to fully characterize all design parameters. Improvements to the premix combustor design will be tested at high hydrogen concentrations to verify performance with carbon capture fuels. Early adaptation of technologies to near-term applications is planned to accelerate validation and ultimately reduce risk. The technology roadmap to meet the 2015 project objectives is established, and future work will continue towards executing the defined validation plans.

Special Recognitions & Awards/Patents Issued

1. More than 65 patent disclosures have been submitted on the new technologies being investigated in this project.

FY 2010 Publications/Presentations

1. DOE 10Q1 Quarterly Review Presentation, February 2010.

2. ICEPAG Conference Presentation, February 2010.

3. DOE Turbine Program Peer Review, April 2010.

4. DOE 10Q1 Quarterly Review Presentation, June 2010.

References

1. A. Sobolevskiy and J. Rossin, “Development of Novel Multifunctional Selective Catalytic Reduction Systems for IGCC Plants,” Pittsburgh Coal Conference, 2009.

III. ADVANCED RESEARCH

A. Aero-Heat Transfer

III.A.1 Analysis of Gas Turbine Performance

Tom I-P. Shih (Primary Contact), Kyle Chi, Kenny Hu, K. Minking Chyu, and Mark Bryden
Purdue University
West Lafayette, IN 47907
Phone: (765) 494-5118; Fax: (765) 494-0307
E-mail: tomshih@purdue.edu

DOE Project Manager: Robin Ames
Phone: (304) 285-0978
E-mail: Robin.Ames@netl.doe.gov

Contract Number: AL05205018

Start Date: October 1, 2009
End Date: September 30, 2014

FY 2010 Objectives

- Develop and evaluate computational fluid dynamics (CFD) analysis tools that can be used to study heat transfer issues in the design of turbine components to support the development of turbine technologies for advanced near-zero emission, coal-based power systems.
- Apply CFD analysis tools to explore and study heat transfer issues in turbine components to support the development of turbine technologies for advanced near-zero emission, coal-based power systems.

Accomplishments

- Performed a steady Reynolds-averaged Navier-Stokes (RANS) study of the flow and heat transfer in a U-duct with smooth walls and with walls lined with pin fins under rotating (3,600 rpm) and non-rotating conditions as a function of duct aspect ratio (H=W and H = 0.25W).
- Performed a steady RANS study of pedestals and its height and arrangement in enhancing surface heat transfer in a straight duct with high aspect ratio under non-rotating conditions.
- Developed and evaluated models for the "residual" in the discrete error transport equation (DETE) to estimate grid-induced errors in time-accurate CFD solutions.

Introduction

Developing turbine technologies to operate on coal-derived synthesis gas (syngas), hydrogen fuels, and oxyfuels is critical to the development of advanced power generation technologies such as integrated gasification combined cycle and the deployment of near-zero emission type power plants that can lead to the capture and separation of carbon dioxide (CO_2). Whether the fuel burned is natural gas (the predominant fuel used in current electric power generation gas turbines), syngas, a hydrogen mixture, or an oxyfuel, the efficiency and service life of the gas turbine engine are strongly affected by the turbine component, where the thermal energy contained in the high-pressure and high-temperature gas is converted into mechanical energy to drive the compressor and the electric generator. The most effective way to increase the efficiency of the turbine component is to raise the temperature of the gas entering the turbine component, which can be as high as the adiabatic flame temperature from the combustion of fuel and oxidizer. Although the temperatures sought today, up to 1,755 K, is still considerably lower than the adiabatic flame temperature (indicating that there is still room to increase efficiency by increasing inlet temperature), 1,755 K already far exceeds the maximum temperature the best super alloys and thermal barrier coatings (TBCs) can withstand and still maintain structural integrity and reliable operation, which are 1,320 to 1,475 K for super alloys without TBCs and 1,475 to 1,625 K with TBCs. Thus, cooling - such as internal, film, and impingement - is essential for all parts of the turbine whose surfaces come in contact with the hot gases if a reasonable service life is to be achieved.

Since cooling requires work input (e.g., pressure of cooling flow must be raised high enough to enter the turbine to cool it), effective cooling (i.e., ensure material temperatures to never exceeds maximum allowable material temperature) must be accomplished efficiently. This issue deserves increasing attention because of three major reasons. The first is that today's turbines are already designed to operate very close to the material's maximum allowable temperature based on existing design experience so that there is little room for mistakes. The second is that industry's current goal is to reduce the cooling flow by 50% to further increase efficiency when it is already extremely difficult to cool effectively with the existing flow rates. This indicates the need for new cooling strategies that can

only come about with in depth understanding of how fluid mechanics affects heat transfer and how external heat transfer with and without film cooling on the hot-gas side is coupled to the internal heat transfer on the cooling side through the super alloy and the TBC. The third is that when the fuel burned is syngas, a hydrogen fuel, or an oxyfuel, the heat transfer characteristics in the turbine on the hot gas side can increase because of increase in water vapor content, because of increase in erosion and deposition tendencies, and because of increase in the hot gas mass flow rate, which could make cooling even more difficult. Thus, there is very little room for mistakes in the design of cooling strategies. For example, a 10 to 20 K beyond the maximum allowable temperature will lead to material degradation, which will reduce service life.

The objective of this project is two-fold. The first is to develop and evaluate CFD-based analysis tools that can be used to study heat-transfer issues in the design of the turbine component and to develop guidelines and best practices on their usage. The second is to apply those analysis tools to support the development of turbine technologies for advanced near-zero emission type coal-based power systems. The analysis tools of interest are those that can properly account for the steady and unsteady three-dimensional heat transfer from the hot gas in the turbine blade/vane passages through the turbine material – the TBC system and the super alloy – to the internal cooling passages as a function of the cooling strategy as well as a function of the hot gas and coolant compositions, the mass flow rates, and the temperature of the hot gas and the coolant.

Approach

Analysis tools used to design gas turbine cooling strategies are typically based on quasi-dimensional methods. These analysis tools require inputs on the details of the fluid-flow and heat transfer processes such as pressure loss coefficients as well as regional or laterally-averaged heat transfer coefficients. There are two ways to generate the information needed, and they are experimental measurements and CFD simulations. Here, CFD is used, and it is based on the conservation/balance equations of species, continuity, momentum, and energy that govern the three-dimensional flow and heat transfer processes. Depending on the nature of the problem, the effects of turbulence may be modeled by steady RANS, unsteady RANS, detached eddy simulation, or large-eddy simulation.

Results

To improve turbine efficiency, in addition to the aggressive goals on the turbine inlet temperature, industry wants to reduce the cooling flow rate by 50%. One region, where cooling is an issue is the tip region of blades and vanes, especially with the markedly reduced coolant flow rates. The issue in the cooling design is how to place heat transfer enhancement devices inside internal cooling passages so that cooling in turn regions of U-shaped ducts is nearly uniform with minimal pressure loss. Figure 1 shows results from a CFD simulation of a U-duct, where the heat transfer enhancement device is the pin fin. Results obtained show that in the absence of pin

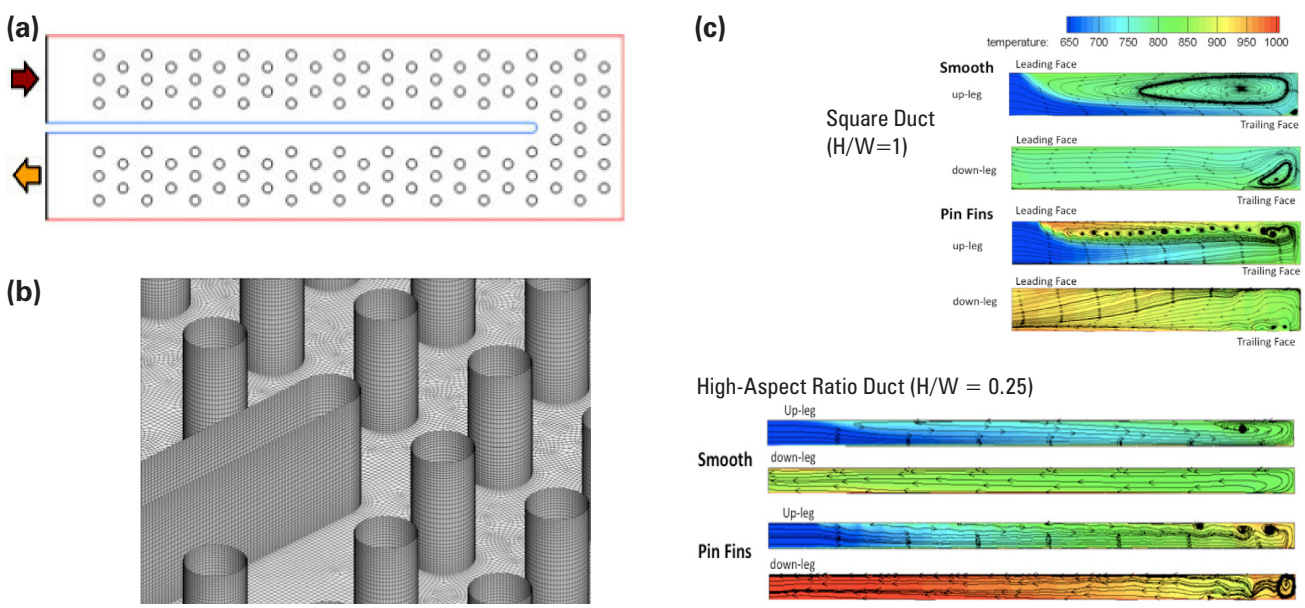

FIGURE 1. Flow and temperature distribution in a U-duct. (a) Schematic of U-duct lined with pin fins. (b) Grid near the tip-turn region of the U-duct. (c) Predicted flow pattern colored by temperature in mid plane to show effects of centrifugal buoyancy.

fins, centrifugal buoyancy can induce a large separated region next to the leading face of a square duct (H=W), greatly reducing the heat transfer on that surface. With pin fins, that separated region is greatly reduced. For a high aspect ratio duct (H/W=0.25), the centrifugal buoyancy induced flow separation is much smaller for both the smooth duct and a duct with pin fins. However, by adding pin fins, heat transfer is greatly increased as can be seen by the higher temperature in the coolant as it exits the U-duct.

Conclusions and Future Directions

Study of the flow and heat transfer in the U-duct lined with pin fins under rotating and non-rotating conditions showed a need to resolve the horseshoe vortex that wraps around each pin fin at the base of the pin fin and the wake behind each circular cylinder. Other issues involve turbulence modeling for flows with strong streamline curvature, rotation, and numerous stagnation regions.

The DETE method was found to be a promising method for estimating errors induced by the grid and in providing an error bound on computed CFD solutions if the flow is steady. If the flow is unsteady and the unsteadiness changes with grid resolutions (e.g., the time and point of separation changes as the grid is refined), then the models developed so far for the residual was found to not work. Thus, a new modeling approach is needed.

FY 2010 Publications/Presentations

1. B. Williams and T.I-P. Shih, "Estimating Grid-Induced Errors in Unsteady CFD Solutions Using a Discrete Error Transport Equation," AIAA Paper 2010, Orlando, Florida, January 2010.

2. P. Ganmol, S.C. Siw, M.K. Chyu, M.A. Alvin, X. Chi, and T.I-P. Shih, "Effect of 90 Degree Jet Inlet on Heat Transfer from Staggered Pin Fin Arrays," ASME-ATI-UIT 2010 Conference on Thermal and Environmental, Sorrento, Italy, May 16–19, 2010.

3. S.C. Siw, M.K. Chyu, T.I-P. Shih, and M.A. Alvin, "Effects of Pin Detached Space on Heat Transfer in Fin Arrays," ASME Paper GT2010-23227, Glasgow, Scotland, June 14–18, 2010.

III.A.2 Materials and Component Development for Advanced Turbine Systems – Airfoil Life Prediction Modeling and Heat Transfer Enhancement

Mary Anne Alvin
U.S. Department of Energy (DOE)
National Energy Technology Laboratory (NETL)
626 Cochrans Mill Road
Pittsburgh, PA 15236-0940
Phone: (412) 386-5498; Fax: (412) 386-4806
E-mail: Maryanne.Alvin@netl.doe.gov

NETL – Regional University Alliance (RUA):
- NETL - Mary Anne Alvin
- University of Pittsburgh, Pittsburgh, PA – Dr. Minking Chyu, Mr. Sean Siw, Mr. Pavin Ganmol, Dr. Tom Shih (Purdue University), Dr. Will Slaughter, Dr. Ventzi Karaivanov, and Mr. Hassan Mohamed
- Virginia Polytechnic Institute and State University (Virginia Tech), Blacksburg, VA – Dr. Srinath Ekkad, Mr. Justin Lamont, Mr. Preston Stoakes, Dr. Diganta Narzary, and Mr. Chris Leblanc

Contract Number: 0004000.5.610.243.001

Start Date: October 1, 2009
End Date: September 30, 2010

FY 2010 Objectives

- Develop a three-dimensional finite element analysis (FEA) and damage mechanics model for predicting the life of hydrogen-fired and oxy-fuel turbine airfoils.
- Develop and assess the performance of innovative airfoil internal cooling concepts that lead to significant reduction in external cooling.
- Assess the impact of airfoil rotation on internal cooling heat transfer.
- Develop and assess the performance of innovative film cooling hole concepts.
- Develop and assess the performance of novel internal cooling concepts that utilize steam and/or CO_2 as the working fluid.
- Assist in test campaigns conducted at NETL's turbine aerothermal test facility in Morgantown, West Virginia.

Accomplishments

- Damage mechanics-based models for creep and fatigue were successfully implemented into a commercial FEA code (ANSYS), and applied to model airfoil geometries simulating operation under advanced turbine inlet conditions (i.e., turbine inlet temperatures [TITs] and combustor exhaust gas compositions).
- An increase in the densification rate of as-manufactured, porous, MCrAlY (M = Ni, Co) bond coatings was identified at 1,100°C when uniaxial compressive stress was applied to thermal barrier-coated single crystal coupons. Differences with respect to the thermally grown oxide (TGO) growth rate, micro-cracking, or yttria-stabilized zirconia (YSZ) debonding and/or spallation were not observed in stress vs. unstressed materials.
- Bench-scale testing identified a heat transfer enhancement of ~4.3 over a wide range of Reynolds numbers using detached pin-fin arrays for airfoil internal channel cooling.
- Jet impingement with a 90-degree inlet across a staggered pin-fin array was shown to significantly increase the overall heat transfer coefficient in the cooling passage as compared to the conventional straight coolant inlets. Additional side blockages which direct more coolant flow through the core section of pin-fin array further increased heat transfer in the cooling channel.
- Under strong rotating conditions (i.e., high Coriolis forces), tangential velocity assists in impingement of angled cooling jets along the corner of the side wall and bottom walls which resulted in much higher heat transfer than that obtained for traditional multi-row impingement cooling.
- Experimental testing in a low-speed wind tunnel indicted that even with a reduced number of tripod holes, a higher cooling effectiveness was obtained in comparison to tight cylindrical hole rows that are typical of current engine configurations.
- Heat transfer studies were performed with pin-fins in a staggered array using superheated steam. In consultation with original equipment manufacturers (OEMs), next generation array configurations were identified.
- Initial testing was conducted in NETL's high-temperature, pressurized, aerothermal facility using flat Hayne 230 test coupons with holes simulating film cooling. These results will be used as a benchmark reference for comparison of film cooling effectives generated for plates with various film cooling hole geometries and thermal barrier coated surfaces.

Introduction

As industry addresses extended operability and performance of advanced hydrogen-fired and oxy-fuel turbines (Table 1), heat transfer enhancement and airfoil cooling effectiveness are considered to be critical design requirements with respect to land-based engine technology development. The following sections summarize the accomplishments of eight university projects that were conducted at the University of Pittsburgh and Virginia Tech during Fiscal Year 2010 in the areas *Airfoil Life Prediction Modeling and Heat Transfer Enhancement*. Innovative internal airfoil cooling concepts that could potentially lead to significant reduction in external airfoil cooling were addressed. These included novel double wall cooling designs, and 90-degree inlet jet impingement and tip-turn region heat transfer enhancement concepts. The impact of turbine rotation on angled coolant jet inlet heat transfer, as well as novel tripod film cooling hole architectures was additionally assessed. Heat transfer studies using superheated steam as the working fluid, and initial heat transfer testing in NETL's high-temperature, pressurized aerothermal test facility in Morgantown, West Virginia, were undertaken.

TABLE 1. Advanced Turbine Operating Conditions

	Syngas Turbine 2010	Hydrogen-Fired Turbine 2015	Oxy-Fuel Turbine 2010	Oxy-Fuel Turbine 2015
Combustor Exhaust Temp., °C	~1,480	~1,480		
Turbine Inlet Temp., °C	~1,370	~1,425	~620	~760 (HP) ~1760 (IP)
Turbine Exhaust Temp., °C	~595	~595		
Turbine Inlet Pressure, psig	~265	~300	~450	~1,500 (HP) ~625 (IP)
Combustor Exhaust Composition	72.8% N_2 9.27% CO_2 8.6% O_2 8.5% H_2O 0.8% Ar	72.2% N_2 17.3% H_2O 8.2% O_2 1.4% CO_2 0.9% Ar	82% H_2O 17% CO_2 1.1% N_2 1% Ar 0.1% O_2	75-90% H_2O 10-25% CO_2 1.7% O_2-N_2-Ar

HP – high pressure
IP – intermediate pressure

Approach and Results

Airfoil Life Prediction

Based on three-dimensional FEA and damage mechanics, a computational model was developed during FY 2008-09 for predicting the evolution of creep and fatigue in hydrogen-fired and oxy-fuel first row blades. In conjunction with this modeling effort, bench-scale furnace testing was undertaken to begin validation of the underlying damage mechanics concepts for the evolution of thermal barrier coating (TBC) damage. This effort focused on the impact of uniaxial in-plane stress on nickel-based single crystal René N5 coupons that were coated with a low-pressure plasma spray MCrAlY bond coat, and an external air plasma sprayed (APS) YSZ TBC. Mechanical properties were developed and correlated with microstructural changes within the single crystal René N5 substrate and TBC after conduct of 100-1,000 hours of unstressed and stress-induced, isothermal, testing at 900°C and 1,100°C.

René N5/MCrAlY/APS YSZ coupons were placed in a slotted Hexoloy®SA holder, and subsequently tested in a high-temperature bench-scale furnace. The difference in the thermal coefficient of expansion for the holder and the coupon, and the size of the gap between the coupon and the slot in the fixture were used to introduce thermally induced compressive stress within the thermal barrier coated coupons (i.e., 235 MPa at 900°C; 250 MPa at 1,100°C). Rigid alumina paper strips were cut, compressed and placed between the coupon and the holder to mitigate elemental interdiffusion reactions of the single crystal matrix and the silicon carbide fixture. Significant stress relaxation was expected to occur during the first hour of high-temperature testing, with constant stress levels of 50 MPa and 88 MPa maintained throughout the remainder of each test campaign. An additional thermal barrier coated coupon was placed on the surface of the holder to serve as an unstressed control coupon.

Post-test naterial characterization was conducted using scanning electron microscopy and energy dispersive X-ray analysis to identify the morphology and qualitative elemental composition at five cross-sectional locations in the as-manufactured and bench-scale exposed coupons (Figure 1). Mechanical properties as Young's modulus and hardness were additionally determined at each of these locations using a Hysitron Tribo Nano-Indenter that was fitted with a two-dimensional (2D), three-plate capacitive force/displacement transducer and a three-faced pyramid Berkovich indenter. Nano-indentation was performed in a 4 x 3 indentation pattern, with three indentations at each location. Within the René N5 substrate and MCrAlY bond coat, indentations were 10 µm apart. Due to porosity and observed phase multiplicity, indentations were performed 5 µm apart during characterization of the YSZ top coat, bond coat interface (i.e., adjacent to the TGO), and substrate interdiffusion interface.

The uniaxial in-plane stress was initially considered to impact the rate of diffusion and densification of the bond coat, and subsequently

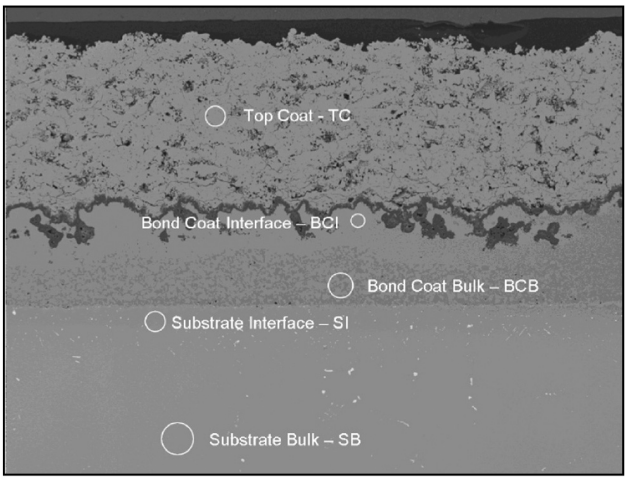

FIGURE 1. Scanning Electron Micrograph Illustrating Nano-Indentation Locations

the rate of TGO growth and crack formation, and ultimately the TBC time-to-failure. The only effect that was observed for substrate deformation was an increase in the rate of densification of the initially porous MCrAlY bond coat at 1,100°C with applied stress. No other differences were observed between stress and unstressed coupons with regard to the rate of TGO growth (Table 2), micro-cracking, YSZ debonding or spallation. However, it was observed that after isothermal exposure at 1,100°C, the elastic modulus and hardness within the bond coat were higher near the interface with a TGO layer than elsewhere. This is counter to what is expected given β-phase (NiAl) depletion and a predominance of γ-phase (Ni_3Al) within the bond coat with continued exposure to high temperature, and may be responsible for the initiation and growth of cracks with the YSZ TBC.

A significant decrease in the Young's modulus and hardness of the YSZ top coat resulted with continued exposure at 900°C for both stressed (i.e., ~257 GPa → ~200 GPa) and unstressed conditions (i.e., ~17.3 GPa → ~14.5 GPa). In contrast an apparent slight increase in Young's modulus (i.e., ~257 GPa → ~267 GPa) and hardness (i.e., ~17.3 GPa → ~18 GPa) resulted in the top coat after initial 1,100°C conditioning of the APS YSZ. Rapid annealing with slight densification of the René N5 matrix was reflected in the hardness measurements with extended exposure time for both the stressed and unstressed, 900°C and 1,100°C coupons.

When coupled with similar information generated during high temperature tensile testing, further insight into TBC failure mechanisms will be available for incorporation into the computationally-based airfoil predictive life assessment models.

Advanced Airfoil Cooling Concepts

In order to develop innovative internal airfoil cooling concepts that could lead to significant reduction in external airfoil cooling, efforts in FY 2010 addressed novel double wall cooling designs, and 90-degree inlet jet impingement and tip-turn region heat transfer enhancement concepts. The impact of turbine rotation on angled coolant jet inlet heat transfer, as well as novel tripod film cooling hole architectures were additionally assessed.

Double Wall Cooling

The ultimate goal of the double wall cooling effort is to achieve heat transfer enhancements that are ~5 times greater than that of smooth internal cooling passages through the use of pin-fin-based designs. In FY 2010, efforts addressed

- The effects of detached pin clearance on the heat transfer and pressure characteristics of circular pin-fin arrays.
- The impact of pin-fins with fully-expanded and broken ribs with various detached pin-tip spacing.

A rectangular test section was constructed of 2.54 cm thick Plexiglas with an overall channel geometry (Width: 10.16 cm; Height: 2.54 cm) simulating a wide aspect ratio gas turbine airfoil internal cooling passage (Figure 2). Inline and staggered arrays of aluminum pin-fins were installed in the channel. Using a given pin diameter (i.e., D = 6.35 mm = ¼H), three different pin-fin height-to-diameter ratios (i.e., H/D = 4, 3, and 2) were evaluated. Each of these three pin-fin arrays corresponded to a specific pin array geometry detachment spacing (C) between the pin-tip and one of the endwalls (i.e., C/D = 0, 1, 2, respectively). A thermochromic

TABLE 2. TGO Thickness, μm

Total Isothermal Exposure Time, Hrs	100		300		600		1,000	
Stress Condition	Unstressed	Stressed	Unstressed	Stressed	Unstressed	Stressed	Unstressed	Stressed
900°C (a)	~2	~2	~4	~4			~5.6	~5
1,100°C (b)	~5	~6	~9	~8.5	~11.5	~11.5		

(a) All six coupons were intact at test completion.
(b) Five coupons were intact at test completion. One coupon experienced TBC delamination after ~600 hrs of isothermal exposure.

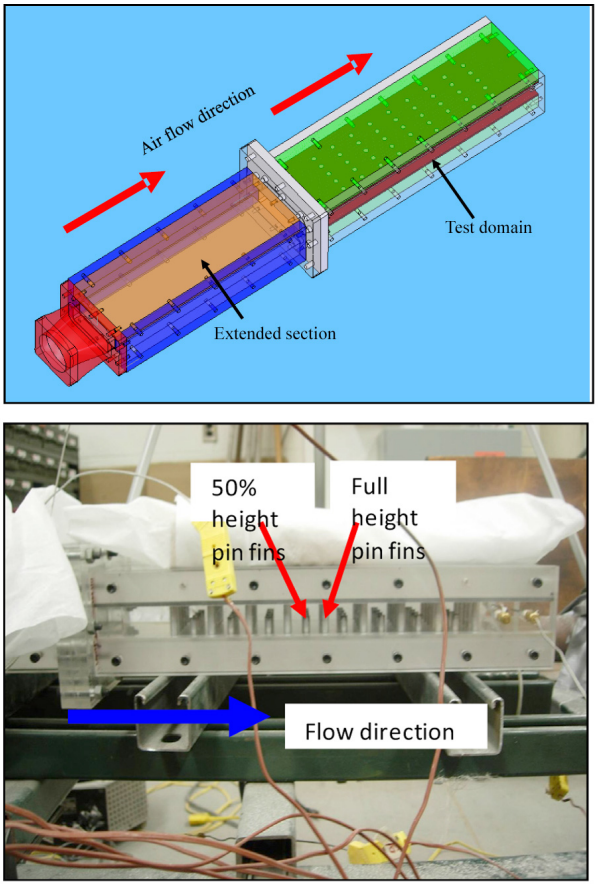

FIGURE 2. Design Model and Fabricated Plexiglas Test Section with Mounted Aluminum Pins

liquid crystal spray and a thin layer of black paint were applied to all pins and endwalls of the internal channel passage in order to obtain local heat transfer coefficient distributions when the unit was tested with 60°C flowing air. The Reynolds number, based on the hydraulic diameter of the unobstructed cross-section and the mean bulk velocity, ranged from 10,000 to 25,000.

Experimental results indicated that the presence of a detached space between the pin-tip and the endwall has a significant effect on the convective heat transfer and pressure loss in the channel. The presence of pin-to-endwall spacing promoted wall-flow interaction, generated additional separated shear layers, and augmented turbulent transport. In general, an increase in detached spacing, or C/D led to lower heat transfer enhancement and pressure drop. Heat transfer enhancement of ~4.3 over a wide range of Reynolds numbers was obtained.

Efforts additionally addressed the level of heat transfer enhancement induced by fully-expanded and broken ribs with various detached pin-tip spacing. The ribs contribute somewhat limitedly to the overall heat transfer enhancement. Based on the averaged row-resolved results normalized by the baseline designs without ribs, ribs were identified to further augment the heat transfer coefficient of the endwall, but reduced the heat transfer coefficient from the pins.

90-Degree Inlet Jet Impingement

The primary objective of this effort was to address the heat transfer characteristics of a pin-fin array with a 90-degree coolant jet inlet. The 90-degree inlet was designed to promote more turbulent mixing and heat transfer with the effect of jet impingement. This configuration is relevant to the *double wall cooling* or *skin cooling* technology, representing industry's current trend of internal cooling. Detailed heat transfer coefficients on both the endwalls and all pin-fin surfaces were obtained using the previously described liquid crystal thermography technique. The experimental study indicated that jet impingement with a 90-degree inlet across a staggered pin-fin array significantly increased the overall heat transfer coefficient by ~5-7 fold in the cooling passage as compared to the conventional straight coolant inlet. Additional side blockages which direct more coolant flow through the core section of pin-fin array further increased heat transfer in the cooling channel, achieving an additional 15-30% enhancement.

The pressure drop associated with the 90-degree jet inlet across a pin-fin array is ~50-80 times higher than that of the corresponding straight through-flow design. While this is a substantial pressure loss, the cooling performance index which is a measurement of heat transfer enhancement per pressure loss was comparable to that of a through-flow channel. This suggested that the 90-degree jet inlet configuration in conjunction with a staggered pin-fin array is a viable approach for enhancing heat transfer in an internal cooling channel provided that the coolant is effectively dispersed across the lateral span of the pin-fin array.

Complementary computational fluid dynamics (CFD) simulations predicted the flow field and general heat transfer distribution trends reasonably well (Figure 3). However, quantitative comparison with the experimental data (i.e., surface heat transfer coefficient, etc.) was seen to deviate by as much as 50% which was attributed to a combination of limitations in the CFD turbulence model with respect to resolving impingement and separated heat transfer, and inconsistent thermal boundary conditions.

Tip-Turn Region Heat Transfer Enhancement

This effort addressed the heat transfer characteristics in the turning region of serpentine internal cooling passages with 180-degree sharp turns. Technical insights and advancements could lead to

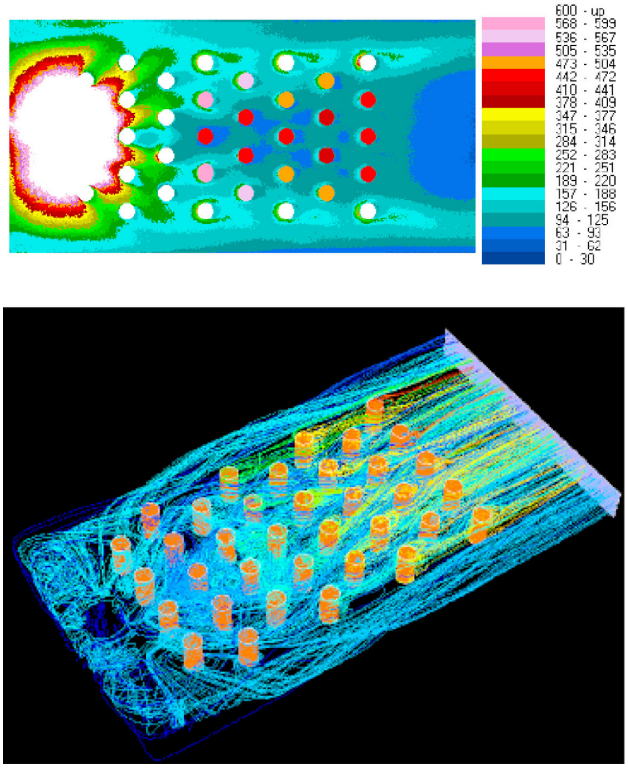

FIGURE 3. Local Heat Transfer Coefficient (W/m^2-K) and CFD Simulated Streak Lines in a Double Wall Cooling Channel (Reynolds Number = 8,000)

more effective internal cooling strategies over the tip region, and subsequently reduce the level of reliance on external cooling in this region. While the transport phenomena associated with the sharp-turn geometry can be very complex, virtually no study has previously been pursued. Seven tip-turn designs were initially evaluated, and four designs were down-selected for further analysis. Detailed heat transfer enhancement and flow characteristic of the channel with different pin-fin configurations in the turning region were investigated by using liquid crystal thermography.

Rotational Impact on Double Wall Cooling

Several patented double wall cooling designs were evaluated in terms of viability and performance, as well as applicability for rotating blades. To determine viability, manufacturing and cost constraints and design requirements were established for double wall cooling schemes, and were compared to those for traditional ribbed airfoil configurations. Design correlations which included non-dimensionalized calculations predicting heat transfer boundary conditions for various double wall impingement cooling designs were developed. To address performance in terms of overall cooling, heat transfer was experimentally measured and computationally predicted for ribbed channel baseline configurations in order to address optimization of the patented double wall cooling configurations. An optimization routine was developed to provide a design for double wall cooling that generated the highest heat transfer. To determine the applicability of the double wall cooling scheme for rotating blades, heat transfer was measured experimentally using a rotating test rig. The heat transfer performance of the baseline double wall cooling configurations was then compared to the performance of rotating traditional ribbed channel airfoils.

Rotation changes the heat transfer distributions inside blade channels due to the effect of Coriolis forces resulting in mal-distribution of the coolant, and thus differential heat transfer rates on the pressure and suction sides of the cooling channels. Rotational effects on impinging cooling jets were evaluated. Design concepts are being developed to counter rotational effects, reducing coolant mal-distribution and associated uneven heat transfer rates.

Heat transfer coefficients for baseline cases as ribbed channels and simple impingement designs indicate that jet impingement is greatly affected by a small jet height to diameter ratio. Preliminary results show that the jet impingement design with angled jets can sustain itself under strong rotating conditions. The angle design for the jet imparts a strong tangential component to the jet velocity resulting in stronger impingement than straight jets under rotating conditions. The tangential velocity also assists in impingement of the jets along the corner of the side wall and bottom walls resulting in much higher heat transfer than obtained for traditional multi-row impingement cooling.

Advanced Film Cooling Hole Designs

Airfoil cooling is governed by various parameters such as cooling hole geometry, location, airfoil pressure distribution, Mach number, Reynolds number, flow turning angle, inlet boundary layer thickness, free-stream turbulence intensity, wake passing frequency, etc. Film cooling has a significant effect on the overall engine performance. Discrete holes are drilled at several locations on the blade's exterior surface to permit a portion of the internal cooling air to be ejected, forming a protective cooling film on the surface. For low-temperature operations, simple angle holes, which are angled only along the flow direction, are used and are sufficient.

Film cooling hole designs have been limited by manufacturing capabilities. Typically cylindrical holes embedded in trenches and craters have been studied on flat plate test sections. During FY 2010, a Design of Experiments (DoE) method was employed to obtain the optimum width and depth of the trench and crater

to embed the coolant hole. Tripod hole designs which have one entrance and three exit holes for cooling (Figure 4), provide higher cooling effectiveness using lower coolant flow, and reduce the number of hole inlets from the internal cooling side while maintaining coverage on the outside surface of the airfoil.

In order to address the overall reduction in coolant usage, a flat acrylonitrile butadiene styrene plastic plate was fabricated with a row of tripod holes (Figure 5). Experimental testing in a low-speed wind tunnel under low-temperature conditions indicted that the sparse tripod hole array (i.e., reduced number of holes), provided as much if not higher cooling effectiveness than a tight row of cylindrical holes that is typical of current engine configurations. Additionally, trenching was shown to provide a more 2-D type coolant structure producing a sheet of cooler air along the surface of the plate, resulting in better cooling effectiveness.

New Concepts for Enhanced Cooling with Superheated Steam

In order to address the use of steam and/or CO_2 as the internal cooling fluid, as well as to develop effective novel concepts for heat transfer enhancement, a test rig was designed and constructed in FY 2008-09. In order to benchmark the test facility's performance, baseline heat transfer experiments, such as turbulent flow over a flat plate with Dittus-Boetler correlation,

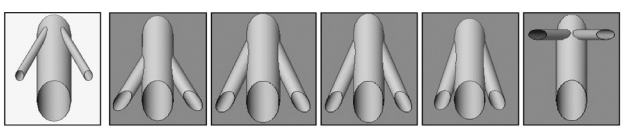

FIGURE 4. Tripod Hole Configurations

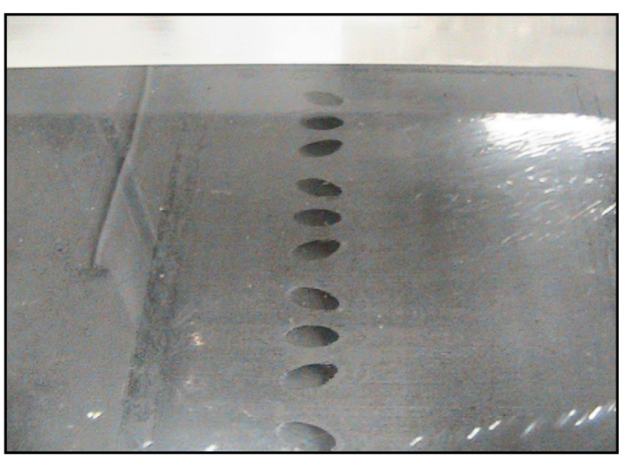

FIGURE 5. Tripod Hole Array on a Flat Plate

were conducted. The baseline tests were followed by more complex testing with staggered pin-fin arrays, and the results based on steam as a working fluid were compared with the corresponding data using air as the internal coolant. The results indicate a favorable agreement using Prandtl number transformation between steam and air.

Efforts were additionally focused on development of advanced concepts using superheated steam for cooling the turbine trailing edge. Enhanced cooling may be achieved by implementing the concept similar to *mesh cooling*. Newer and more effective designs are being developed for more uniform cooling with lower coolant requirements. Two test plates with cubic-element meshes were designed, and are being fabricated.

Pressurized, High-Temperature, Test Facility for Assessment of Aerothermal Cooling Concepts

In order to address airfoil heat transfer at near turbine operating conditions, the combustion test facility at NETL in Morgantown, West Virginia, was modified to include an aerothermal test module section. Pressurized combustion gases flow over nickel-based superalloy Haynes 230 coupons at temperatures of ~1,000°C, with back-side cooling of the coupons with ~400°C air. The Haynes 230 coupons are designed with various film cooling hole configurations (Figure 6), and are either uncoated or coated with an MCrAlY bond coat and an APS YSZ TBC. CFD simulations were additionally performed to characterize the flow field and heat transfer near the coupon test section.

Heat transfer results obtained during an initial test campaign using flat coupons with film cooling holes (Figure 7) will be used as a baseline reference for comparison with future planned tests that address the impact of film cooling hole geometry and TBC surface roughness.

Future Directions

Airfoil Life Prediction

Extension of the life prediction modeling effort includes incorporation of TBC layer damage mechanisms to predict TBC failure (e.g., spallation). Continuum micromechanics and fracture mechanics are planned to be used to predict the initiation and growth of cracks within the TBC layers. The results of this analysis will then be used to construct TBC damage evolution relationships that will be incorporated into the existing three-dimensional finite element-based airfoil life prediction model.

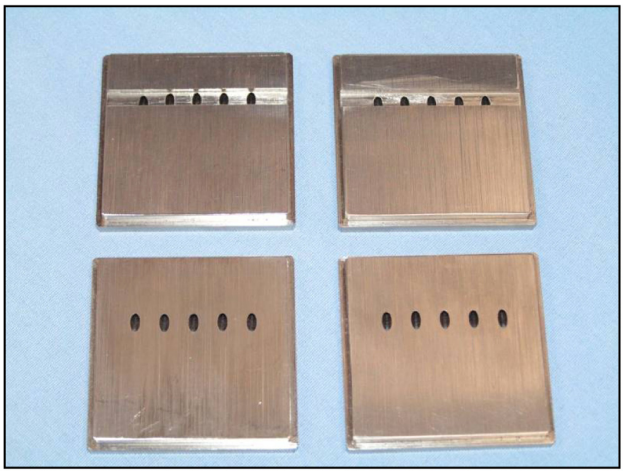

FIGURE 6. Haynes 230 Test Coupons with Film Cooling Holes

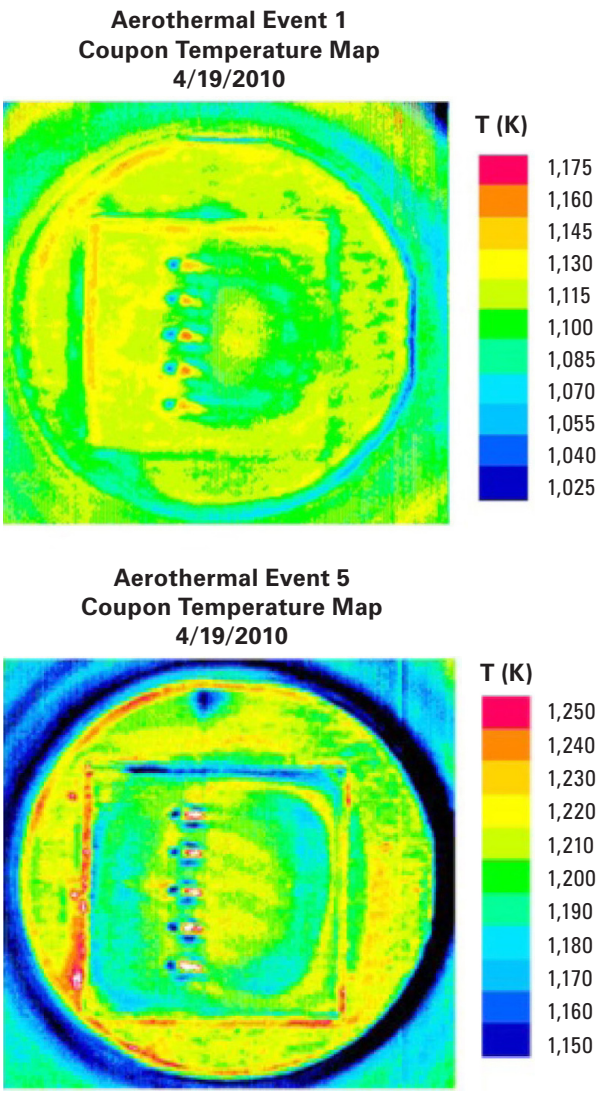

FIGURE 7. Surface Temperature Distribution of the Haynes 230 Test Coupons with Film Cooling Holes Generated for Two Test Conditions

Advanced Airfoil Cooling Concepts

Double Wall Cooling

Efforts will continue to be focused on innovative cooling concepts with an ultimate goal of achieving an enhancement factor of 5 based on only passive methods. Experimental testing will be performed on a refined *partial detachment* approach using microcircuits (i.e., small pin elements) and surface heat transfer augmentation features.

90-Degree Inlet Jet Impingement

Efforts are planned to continue innovative vortex generator development using various jet inlet configurations in internal airfoil cooling channels.

Tip-Turn Region Heat Transfer Enhancement

Efforts will be focused on completing the detailed heat transfer study at the tip-turn region with selected pin-fin configurations. Numerical simulations will be performed, and when combined with experimental results, significant insight can be realized with respect to localized coolant distributions over the entire turning domain.

Rotational Impact on Double Wall Cooling

Variation in internal surface architectures and channel geometries will be addressed using a DoE approach. Complex double wall, lexan test model airfoil geometries will be fabricated and tested using transient liquid crystal techniques, providing high resolution local heat transfer measurements within experimentally and CFD optimized cooling channel designs.

Advanced Film Cooling Hole Designs

A low-speed cascade with turbulence generated from an upstream array of combustor swirlers will be used to evaluate the impact of film cooling on a GE E^3 vane. Heat transfer characteristics of optimized tripod hole configurations in the vane will be assessed in terms of lower coolant usage and projected lower operating temperatures for hot gas path components.

New Concepts for Enhanced Cooling with Superheated Steam

Effort is planned to further address innovative internal heat transfer enhancement concepts based on closed-loop steam cooling. This will be achieved through close consultation with OEMs, developing ideal configurations and a representative test matrix. Additionally, an external cooling study will be conducted using superheated steam as a film cooling

injectant. Issues associated with conjugate cooling (i.e., combined internal-external cooling) will be addressed, and CFD simulations will be performed.

Pressurized, High-Temperature, Test Facility for Assessment of Aerothermal Cooling Concepts

Efforts will be focused on completing the detailed heat transfer study for external cooling of test coupons with film cooling holes in NETL's aerothermal test facility in Morgantown, West Virginia. The effects of TBC (i.e., surface roughness) on film cooling performance and trailing edge cooling will be explored.

FY 2010 Publications/Presentations

1. M. Chyu and M.A. Alvin, "Turbine Airfoil Aerothermal Characteristics in Future Coal-Gas Based Power Generation Systems," International Symposium on Heat Transfer in Gas Turbine Systems, Antalya, Turkey, August 9–14, 2009.

2. M.A. Alvin, "Materials and Component Development for Advanced Turbine Systems," Presentation at the UTSR Workshop VII, Orlando, Florida, October 27–29, 2009.

3. P. Ganmol, M. Chyu, X. Chi, T. Shih, and M.A. Alvin, "Effects of 90-Degree Jet Inlet on Heat Transfer from Staggered Pin Fin Arrays," ASME-ATI-UIT 2010 Conference on Thermal and Environmental Issues in Energy Systems, Sorrento, Italy, May 16–19, 2010.

4. V. Karaivanov, W. Slaughter, S. Siw, M. Chyu, and M.A. Alvin, "Compressive Creep Testing of Thermal Barrier Coated Nickel-Based Superalloys," ASME Turbo Expo 2010, Glasgow, Scotland, June 14–18, 2010. Accepted for publication in the ASME Journal of Engineering for Gas Turbines and Power.

5. M. Chyu, M.A. Alvin, S. Siw, and T. Shih, "Effects of Pin Detached Space on Heat Transfer and From Pin Fin Arrays," ASME Turbo Expo 2010, Glasgow, Scotland, June 14–18, 2010.

6. M.A. Alvin, "Materials and Component Development for Advanced Turbine Systems – Project Summary," ASME Turbo Expo 2010, Glasgow, Scotland, June 14-18, 2010.

7. P. Ganmol, M. Chyu, and M.A. Alvin, "Heat Transfer in Tip-Turn Region of Two-Pass Channel with a 180-Degree Turn," 2010 ASME International Mechanical Engineering Congress and Exposition, Vancouver, British Columbia, Canada, November 12–18, 2010 (submitted).

8. C. Leblanc, D. Narzary, and S. Ekkad, "Film Cooling with Sister Hole Design on a Flat Plate," 2011 AJTEC, Hawaii, March 2011 (submitted).

9. P. Stoakes and S. Ekkad, "An Optimized Impingement Cooling Configuration for Double Wall Cooling Designs," 2011 AJTEC, Hawaii, March 2011 (submitted).

10. J. Lamont, D. Narzary, and S. Ekkad, "Effect of Rotation on Heat Transfer in Mini Channels Fed by Impinging Flows," 2011 AJTEC, Hawaii, March 2011 (submitted).

11. C. Leblanc, D. Narzary, and S. Ekkad, "Film Cooling with Sister Hole Design on a Pressure Surface of a First Stage Vane," ASME IGTI 2011, Vancouver, June 2011 (submitted).

12. J. Lamont and S.V. Ekkad, "Double Wall Impingement Cooling Configurations for Rotating Blades," ASME IGTI 2011, Vancouver, June 2011 (submitted).

13. P. Stoakes and S. Ekkad, "An Optimized Double Wall Cooling Geometry for Turbine Airfoil Cooling," ASME IGTI 2011, Vancouver, June 2011 (submitted).

14. D. Narzary and S. Ekkad, "Impingement Cooling Study with High Jet Diameter to Channel Height Ratio for Double Wall Cooling Applications: Correlation," ASME IGTI 2011, Vancouver, June 2011 (submitted).

15. J. Lamont and S. Ekkad, "Rotational Effects on Ribbed Internal Cooling Channels Using a Transient Liquid Crystal Technique," ISTP-21, Taiwan, November 2010 (submitted).

III. ADVANCED RESEARCH

B. Combustion

III.B.1 Coal-Based Oxy-Fuel System Evaluation and Combustor Development

Ronald Bischoff
Clean Energy Systems, Inc. (CES)
3035 Prospect Park Drive, Suite 150
Rancho Cordova, CA 95670-6071
Phone: (916) 638-7967; Fax: (916) 638-0167
E-mail: rwbischoff@cleanenergysystems.com

DOE Project Manager: Robin Ames
Phone: (304) 285-0978
E-mail: Robin.Ames@netl.doe.gov

Subcontractor:
Florida Turbine Technologies, Inc. (FTT), Jupiter, FL

Contract Number: 42645

Start Date: October 1, 2005
End Date: September 30, 2010 (extension expected to December 2013 with additional scope and funding)

FY 2010 Objectives

- Evaluate and test use of a modified gas turbine combustor for suitability as an oxy-fuel reheat (O-F RH) combustor. Hot-fire the O-F RH combustor at CES's Kimberlina Power Plant (KPP) and analyze results. Provide test results to OFT-900 design team.
- Perform detailed engineering redesign of an existing gas turbine (SGT-900) to make it suitable for use as an O-F intermediate pressure turbine (IPT). The new turbine, designated OFT-900, will utilize the steam/CO_2 drive gases in the CES cycle and use O-F RH combustors to increase drive gas temperature, improving cycle efficiency by 10 percentage points.
- Prepare Validation Test Plan to support testing the 100 MW_t oxy-syngas combustor (Phase III).
- NEW: Provide Phase III Project Scope and Budget required to begin hot-fire testing both the O-F combustor and an O-F IPT by December 2012. Scope to include objectives, tasks, and schedule.

Accomplishments

- **O-F RH Combustor** – Completed hot-fire testing of two versions of O-F RH combustors derived from modified J79 air-fuel combustors. Test results have been applied to RH development for the OFT-900 O-F IPT.
- **OFT-900 Design** – Established contract with Florida Turbine Technologies, Inc. (FTT) to redesign existing Siemens SGT-900 gas turbine as an O-F IPT (OFT-900). FTT is approximately 50% through their redesign. Completion targeted for November.
- **Test Plan** – Novel test approach devised to significantly shorten (by 8-10 years) O-F turbine development. This significant project acceleration is made possible by dual-phase testing – initial testing conducted with natural gas (NG), followed by testing with syngas. Expected completion is August 2010.
- **Phase III Tasks, Schedule, and Budget** (not yet funded) – Developed two-stage test approach to significantly reduce Phase III equipment lead-time, test site preparation time, and initial capital costs to commission and begin hot-fire testing of both the CES O-F combustor and Siemens O-F IPT. Draft objectives, tasks, budget, and schedule have been completed. Expected completion is August 2010.

Introduction

CES has developed a novel O-F power generation concept that uses proven aerospace technology to enable near-zero emission power generation from fossil fuels. The core of the technology is a high-pressure oxy-combustor that burns gaseous fuels with oxygen (O_2) in the presence of water to produce a steam/carbon dioxide (CO_2) working fluid for steam turbines or modified gas turbines. The CES oxy-combustor has been demonstrated with both NG and (simulated) synthetic fuel at CES's 20 MW_t KPP outside Bakersfield, California, where it was used to produce electricity for export to the grid.

CES is also developing an O-F RH combustor ("reheater") which burns fuel with O_2 (no additional water) to increase the temperature of the drive gas (steam/CO_2) as it enters a high-temperature IPT. Such a reheater increases power cycle efficiency and overall plant performance by taking advantage of the higher inlet temperature capabilities inherent in aero-derivative IPTs. The key difference between the reheater and the oxy-combustor is that the reheater requires no water injection. The RH combustor is closely integrated with the gas turbine expander (O-F combustor).

Under DOE award DE-FC26-05NT42645, CES is developing its oxy-combustion technology for coal-

based power plants that utilize synthesis gas for fuel. It supports DOE award DE-FC26-05NT42646 to Siemens Energy to develop high-temperature turbines powered by steam/CO_2 from the CES oxy-combustor. These technologies offer highly efficient, zero emissions coal-based systems that can capture and sequester CO_2 and meet the DOE goal of enabling high-efficiency, coal-based power generation with >99% CO_2 capture by 2015.

Approach

Phase I: In Phase I of the project (Fiscal Year 2006), CES conducted systems studies of long-term oxy-syngas power plants deployable by 2015 to select the most promising approaches. CES also confirmed the operability of its existing oxy-combustor on syngas by fabricating a pilot-scale oxy-syngas injector, installing it in CES's KPP, and successfully operating it with both simulated syngas and simulated hydrogen-depleted syngas.

Phase II: During the first portion of Phase II (FY 2007-2008), CES completed a detailed design for a near-zero emission, 100 MW_t oxy-syngas combustor, its control system, and most associated piping and instrumentation. In FY 2009, CES proposed to improve O-F cycle efficiency by incorporating O-F RH combustors into an IPT. CES tested this concept by modifying an existing gas turbine combustor (from a J79) to serve as a "first generation" O-F RH combustor. This O-F reheater was fabricated and hot-fire tested in 2009-2010 to confirm RH modeling assumptions. A more powerful RH combustor is being designed for incorporation into a redesigned turbine expander (Siemens SGT-900), which will become the first "second generation" O-F IPT.

At the end of FY 2009, CES awarded a contract to FTT to redesign an existing Siemens gas turbine (SGT-900) to utilize the steam/CO_2 drive gas in the CES-cycle and incorporate O-F RH combustors to improve CES-cycle efficiency (by 10 percentage points). This O-F IPT (designated the OFT-900) is approximately 50% through the redesign process. Use of derivative turbine expanders as O-F IPTs offers an accelerated and cost-efficient approach to significantly improve near-term cycle efficiencies of oxy-coal-syngas power systems.

Results

J79 O-F RH Reheat Combustor: In September 2009, CES began testing instrumented, first generation O-F RH combustors. These combustors were fabricated from modified J79 combustor "cans." Following preliminary cold-flow testing, CES conducted three months of hot-fire testing on the RH combustors (Figure 1). While cold-flow results

FIGURE 1. J79 RH Combustor Test Rig

closely followed model predictions, the modified O-F combustor had sporadic ignition results. Investigations revealed a mixing problem, which limited ignition to a narrow range of fuel and O_2 pressure and flow rate conditions instead of the wide range predicted. Reliable ignition was achieved for subsequent tests by supplying the igniter with a small stream of methane (main constituent in NG) during light-off. Once light-off was achieved, the combustor successfully re-heated the steam/CO_2 drive gas mixture from 600°F to the desired 1,700°F. The combustor maintained stable combustion during throttling and operated smoothly during test runs lasting up to 1 hour. The RH also demonstrated a good turn-down factor. Analysis of instrumentation and emissions data, however, showed further development was needed to reduce the RH's tendency to create a "hot core" in the drive gas and to reduce the fuel-O_2 ratio needed for a stable burn. Both problems were attributed to poor front-end mixing.

CES made an interim modification to the O_2 injection system to direct more O_2 to the combustor's front-end to attenuate the RH's hot core temperature and reduce the amount of excess O_2 necessary for a stable burn. Though partially successful, tests revealed that core exhaust temperatures were still higher than desired and that excess O_2 was still necessary for stable combustion. In addition, the O_2 distribution change made system light-offs more difficult. These results were analyzed and the lessons learned are being used for igniter development for the OFT-900 O-F RH combustors.

OFT-900 Design: The concept of accelerating O-F turbine development by leveraging the capabilities of existing aero turbines received its impetus in March 2008, when FTT, under contract to CES, completed an engineering feasibility study on the use of a

modified Siemens SGT-900 gas turbine as a high-temperature IPT for CES-cycle (zero emission) power plants. Favorable study results led CES to propose, and the National Energy Technology Laboratory to approve, funding for detailed engineering redesign of the SGT-900 to an O-F turbine system. In September 2009, CES issued a subcontract to FTT to perform a detailed engineering redesign of the Siemens gas turbine. Under this contract, FTT will conduct rotor dynamics, thermal, and structural analyses, create a design for an O-F IPT, and prepare detailed engineering (manufacturing) drawings. The reconfigured engine has been designated the OFT-900 (Oxy-Fuel Turbine-900, see Figure 2).

Project scope was divided into six main tasks, each addressing changes determined during the initial feasibility study. Main work tasks include analysis and redesign of the turbine rotor system, turbine casing, turbine gas path, casing/exhaust frame, and development of an effective and efficient O-F reheat combustor system. Overall system design and component integration will be provided by systems engineering and project management.

Siemens Energy is providing reference drawings and engineering data on the SGT-900. FTT has utilized this information to create computer-aided design drawings of the engine assembly layout, analyze primary (aerodynamic) and secondary (cooling and leakage) flows, and conduct risk assessments.

The most challenging task is design of the O-F RH combustor system. Multiple O-F burner concepts were analyzed prior to a down-select to the two most promising designs. FTT is focusing on a premix design where O_2 is introduced into the steam/CO_2 working fluid prior to the O-F combustion chamber. In parallel, CES is designing a duct-style O-F burner, a variation on their proven injector concepts. Both designs emphasize use of existing SGT-900 components where practical.

FTT has utilized extensive turbine system modeling, including loading the existing SGT-900 configuration to confirm model accuracy. The redesign effort is 50 percent complete with final engineering manufacturing drawings due October 2010.

In May 2010, CES received approval add no-cost scope to its existing OFT-900 work task and begin development of controls integration between O-F combustor and turbines. CES will use an existing CES NG-fired O-F combustor and a CES-developed J79 O-F turbine (Figures 3 and 4) as "mules" to test controls integration. They will provide an opportunity to develop, integrate, and test control algorithms for both the combustor and turbine well before the OFT-900 has been fabricated. Controls system performance verification, in conjunction with combustor-turbine

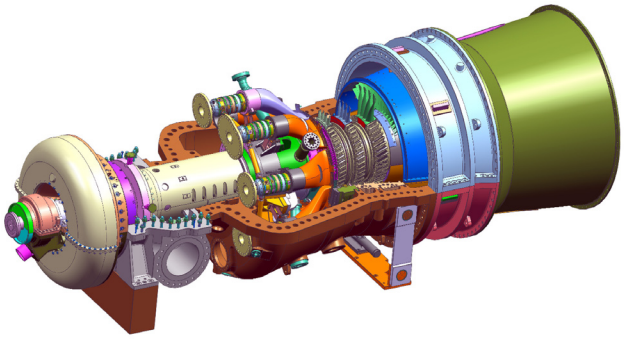

FIGURE 2. OFT-900 Oxy-Fuel IPT

FIGURE 3. 10 MW Generator/Gearbox Enclosure

FIGURE 4. O-F J79 Turbine

testing, is expected to begin in the August-September 2010 timeframe.

Validation Test Plan: CES altered the focus of the Validation Test Plan in early February from a stand-alone, synthesis gas test of the 100 MW_t O-F CES combustor to a *combined* combustor/IPT test concept. Progress on the detailed design of a second generation O-F IPT and added Phase II funding created an opportunity to accelerate fielding of both the O-F combustor and O-F IPT. "Out-of-the-box" thinking for cost reduction options led to a novel test approach which significantly shortens (by 8-10 years) O-F turbine development and reduces short-term test costs for the O-F combustor and O-F IPT. This significant project acceleration is made possible by dual-phase testing – conducting initial and duration testing with NG, followed by syngas testing for verification of performance with lower Btu fuels.

During Phase I studies and analyses, CES conducted hot-fire testing of an existing CES O-F combustor utilizing simulated synthesis gas. CES discovered that the performance of its O-F combustor on synthesis gas was very similar to empirical test data of operations with NG. To accelerate equipment fabrication and test, CES will perform equipment commissioning and initial life-cycle testing for both the O-F combustor and O-F IPT using NG. Once these goals have been achieved, CES will switch to synthesis gas. This approach enables significant cost and lead-time reductions as NG is both cheaper and more readily available than syngas from a coal-gasification unit. Coupled NG testing of the O-F combustor and Siemens OFT-900 will build empirical test data on both units, data which will be compiled years earlier than otherwise available on a utility-scale O-F turbine. While this revised approach still requires funding to enter the fabrication and test phase, it provides an opportunity to begin commissioning both the O-F combustor and the OFT-900 by the end of 2012 and at significantly reduced test costs through FY 2013. The test plan will make provision for follow-on testing with synthesis gas, as funding permits.

Follow-On Equipment Fabrication and Test: (not yet funded) CES is proposing to streamline O-F combustor and turbine testing by implementing initial testing with NG and adding *coupled* testing of the CES O-F combustor and the Siemens O-F IPT.

Prior to fabricating the OFT-900, its O-F RH combustors must be tested to confirm their performance meets modeling and design expectations. Competing RH combustor designs from CES and FTT will be hot-fired at CES's KPP facility and a down-select made for the most effective design. This RH test information will be used to update the detailed engineering design of the OFT-900.

The next step will be to fabricate both the O-F combustor and OFT-900. The latter will require acquisition of a used SGT-900 (W251), its overhaul to "like-new" condition, and then remanufacture to the OFT-900 baseline design. In parallel, CES will document test facility equipment requirements, procure required equipment, and construct a test facility able to meet O-F test requirements. Following facility commissioning, both the O-F combustor and O-F IPT will be installed.

To reduce equipment lead-times and significantly reduce test costs, initial combustor/IPT testing will be accomplished with NG versus synthesis gas. The inherent fuel flexibility of O-F combustor permits equipment commissioning and initial life testing with lower-cost NG with virtually no loss in test fidelity. Use of NG instead of synthesis gas dramatically shortens facility preparation time and significantly reduces capital expense. Following a satisfactory period of test operations on NG, a coal-gasification system can be installed and testing transitioned to synthesis gas.

The O-F combustor will be the first article commissioned as combustor performance must be verified before being coupled to the IPT. Following demonstration of satisfactory combustor performance, CES will proceed with commissioning and coupled test of the O-F IPT.

Conclusions and Future Directions

CES has developed a detailed design for a functional, 100 MW_t oxy-syngas combustor which is ready for fabrication and test. In collaboration with FTT and Siemens, CES is also developing an O-F IPT as a derivative of the Siemens SGT-900. Use of NG for initial equipment commissioning and coupled life-testing will permit deployment of an O-F combustor and turbine up to a decade earlier than otherwise feasible. The CES oxy-syngas combustor coupled with a redesigned aero-derivative turbine (Siemens OFT-900) as an O-F IPT offers the next step towards deploying a zero emission powertrain in the 2012-2013 timeframe.

Patent Applications

1. Utility Application No. 12/660,780 for "Method of Direct Steam Generation Using an Oxyfuel Combustor"

2. International Application No. PCT/US2010/000664 for "Method of Direct Steam Generation Using an Oxyfuel Combustor"

3. International Application No. PCT/US2010/000476 for "Method and System for Enhancing Power Output for Renewable Thermal Cycle Power Plants"

4. Utility Application No. 12/660,779 for "Methods of Oxy-Combustion Power Generation Using Low Heating Value Fuel"

Foreign Patents Issued

1. Canadian Patent No. 2,409,700 for "Semi-Closed Brayton Cycle Gas Turbine Power Systems"

2. Australian Patent No. 2003295610 for "Low Pollution Power Generation System with Ion Transfer Membrane Air Separation"

FY 2010 Publications/Presentations

1. R. Anderson, F. Viteri, R. Hollis, A. Keating, J. Shipper, G. Merrill, C. Schillig, S. Shinde, J. Downs, D. Davies, and M. Harris, "Oxy-Fuel Gas Turbine, Gas Generator and Reheat Combustor Technology Development and Demonstration," ASME Paper No. GT2010-23001, 2010.

2. A. Keating, "Alternative Synthetic Fuels Injector Tests," EISG Report on Project EISG 04-10, California Energy Commission Grant #54085A, July 2007 (published 2010).

III.B.2 Prediction of Combustion Stability and Flashback in Turbines with High-Hydrogen Fuel

Tim Lieuwen (Primary Contact),
Dom Santavicca, and Vigor Yang
School of Aerospace Engineering
Georgia Institute of Technology
Atlanta, GA 30332
Phone: (404) 894-3041
E-mail: tim.lieuwen@ae.gatech.edu

DOE Project Manager: Mark Freeman
Phone: (412) 386-6094
E-mail: Mark.Freeman@netl.doe.gov

Contract Number: 43069

Start Date: April 1, 2007
End Date: March 31, 2010

FY 2010 Objectives

- Remove critical barriers to usage of high-hydrogen fuels in low-emissions turbines by developing predictive capabilities for combustion instability.
- Develop computational simulation capabilities to predict the conditions under which combustion instabilities occur.
- Perform validating experiments of instability conditions.
- Distill knowledge gained from simulations and experiments into a reduced order model which can be used as a design tool.

Accomplishments

- Performed detailed analysis of key physics controlling heat release response for flames during high-frequency instabilities.
- Developed model predicting flame response to transverse acoustic instabilities, such as are encountered in annular combustors.
- Investigated the responses of a lean premixed flame to three different forcing mechanisms: velocity oscillations, equivalence ratio oscillations, and the combination of velocity and equivalence ratio oscillations.
- Analyzed important physical mechanisms controlling the response of a partially premixed flame to inlet velocity and equivalence ratio oscillations.
- Worked closely with industrial partners to facilitate transition of models and understanding into design processes for next generation gas turbines.

Introduction

The objective of this project is to improve the state-of-the-art in understanding and modeling combustion instabilities, one of the most critical problems associated with burning high-hydrogen fuels in low-emissions turbines. "Combustion instabilities" refers to damaging pressure oscillations excited by the combustion process. The damage due to these oscillations causes significant damage in low-emissions turbines every year, through forced outages and broken parts.

Approach

This project is investigating these problems with a three pronged approach: experiments, computational kinetic calculations, and analytic modeling. It consists of a collaborative effort involving two universities, both with strong expertise in dynamical combustion phenomena, and gas turbine manufacturers. In addition, the proposed research is structured to provide significant student involvement (including high school teachers, undergraduate students, and graduate students) and therefore will make an important contribution to the future science and technology base of our nation. Its focus upon high fidelity simulations, coupled with validating measurements, and development of reduced order models will significantly improve understanding of these phenomena and capabilities for predicting their occurrence.

Results

Analysis: Analytical work has continued on the development of engineering prediction models that can be used to predict flame characteristics. The basic modeling framework developed by the authors utilizes a level-set approach to quantitatively describe the flame dynamics. This approach eliminates phenomenological or heuristic descriptions of the flame dynamics. This facilitates in breaking down the much larger problem of combustion instability into a more fundamental problem at the flame. The investigated geometries are illustrated schematically in Figure 1. The

instantaneous location of the flame surface $\zeta(r, \theta, t)$ is given by the flame-front tracking equation,

$$\frac{\partial \xi}{\partial t} + u_r \frac{\partial \xi}{\partial r} + \frac{u_\theta}{r}\frac{\partial \xi}{\partial \theta} + s_L \left[\left(\frac{\partial \xi}{\partial r}\right)^2 + \frac{1}{r^2}\left(\frac{\partial \xi}{\partial \theta}\right)^2 + 1 \right]^{1/2} = u_z$$

Our focus has been the understanding of quantitative and qualitative characteristics of solutions of this nonlinear, partial differential equation. These solutions are first of their kind. For example, typical results illustrating the flame response to fuel/air ratio oscillations are shown in Figure 2. In addition, Figure 3 illustrates the effect of including high frequency corrections to the flame response, important for capturing screeching flame instability characteristics.

Extensive theoretical development and calculations have also been performed to understand the flame response to transverse oscillations. Figure 4 shows

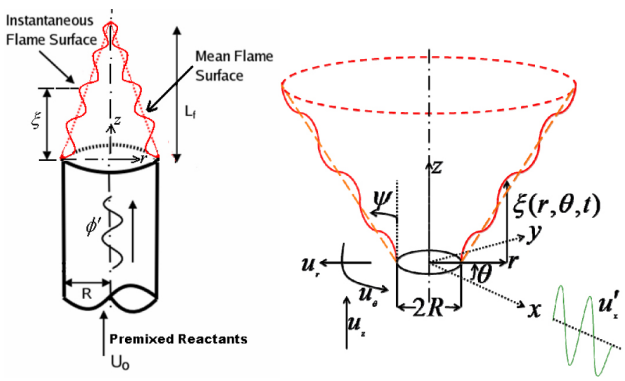

FIGURE 1. (left) Schematic of geometry for the fuel/air ratio and pressure forcing investigation of a conical flame. The flow is from bottom to top. (right) Schematic of geometry for effect of swirl on a velocity-forced center-body stabilized flame. Flow component directions are as shown.

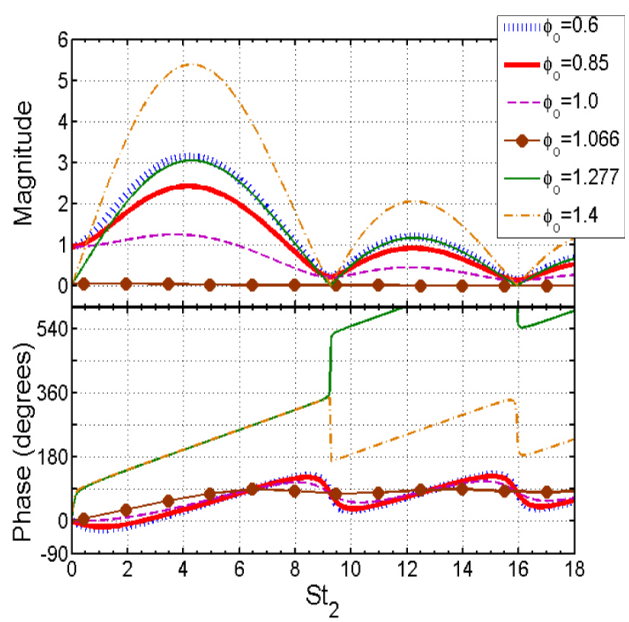

FIGURE 2. Variation of the linear transfer function with St_2 for different values of equivalence ratio. β=4.

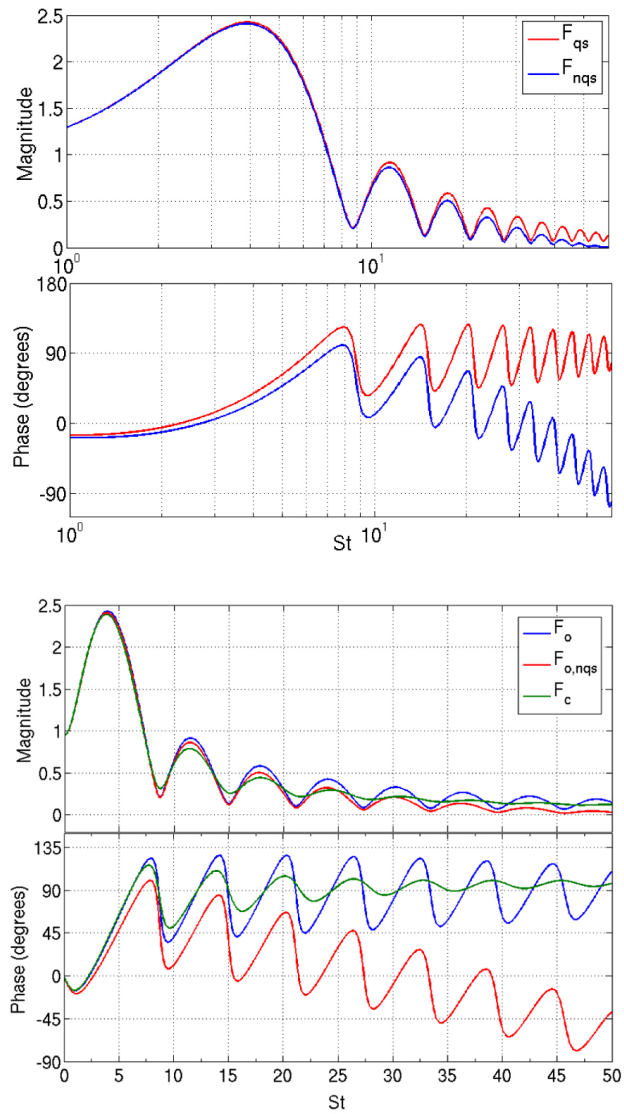

FIGURE 3. (Top) Differences between quasi-steady and non-quasi-steady effects. (Bottom) Differences between stretched and un-stretched flame response.

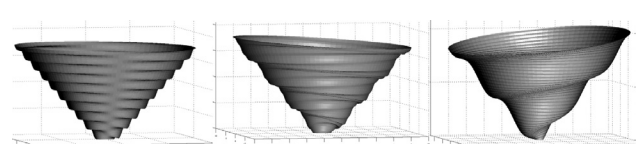

FIGURE 4. Typical flame shapes for characteristic swirl numbers of 0.0, 0.6 and 1.1, respectively.

typical instantaneous flame shapes for swirling flames responding to transverse oscillations. This figure clearly shows that the amount of swirl in the flow has a very important influence on the flame characteristics in the transverse forced case.

Experiments: The purpose of the present work is to investigate a superposition/decomposition method of analyzing the heat release response of a partially premixed flame by using a vector summation method. The decomposition of the partially premixed flame response into two sub-component vectors provides useful insight into the underlying phenomena, and consequently suggests potential passive control methodologies to suppress combustion instabilities.

The heat release response of a partially premixed flame can be mathematically expressed as the following equation (two-input one-output model):

$$\frac{Q'}{\overline{Q}} = H_V(\omega)\frac{V'}{\overline{V}} + H_\Phi(\omega)\frac{\Phi'}{\overline{\Phi}}$$

where H_V and H_Φ denote the flame transfer functions for independent oscillations of the inlet velocity and the equivalence ratio. Physically, the equation means that the response of a partially premixed flame can be linearly superposed from two independent responses. Each term in the equation is a complex quantity. Therefore, the response of the partially premixed flame can be reconstructed by a vector summation. In Figure 5, the two vectors, Q_V and Q_Φ, denote the heat release response to velocity oscillations and equivalence ratio oscillations, respectively. They were measured separately. The phase of the individual heat release response, which is represented by the angle between the vector and the X-axis and is equal to the phase of the corresponding oscillation, i.e., V' or Φ'. The resulting summation vector, $Q_{V+\Phi}$, gives the predicted heat release response of the partially premixed flame with the indicated inlet velocity and equivalence ratio oscillations. Also shown in Figure 5 is a symbol (■) which represents the actual flame response of a partially premixed flame at the inlet conditions.

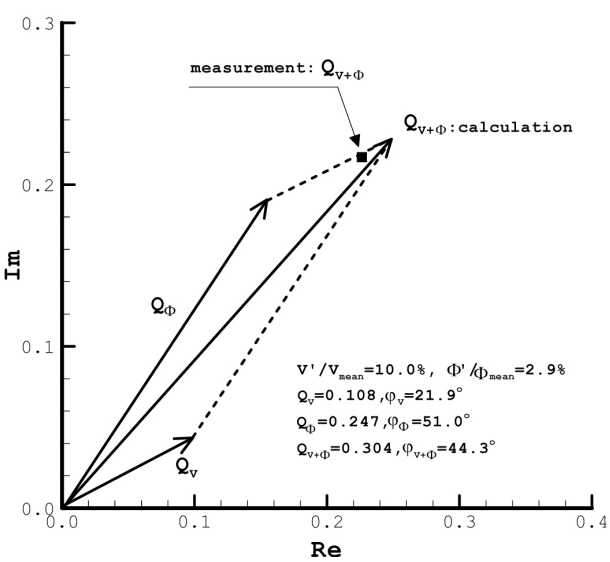

FIGURE 5. Prediction of the normalized heat release response of a partially premixed flame at a modulation frequency of 100 Hz and amplitude of V'/V_{mean} = 10.0 %, Φ'/Φ_{mean} = 2.9 %. Inlet conditions: T_{in} = 200°C, V_{mean} = 60 m/s, Φ_{mean} = 0.60, and X_{H2} = 0.00.

First of all, this analysis demonstrates that the heat release response of a partially premixed flame can be effectively reconstructed using independent measurements of the flame's response to velocity and equivalence ratio fluctuations. Second, the contribution of equivalence ratio oscillation to the global heat release rate oscillation of the partially premixed flame exceeds that of the velocity fluctuation by a factor of 2. Third, the phase difference between the heat release and equivalence ratio oscillations is larger than the phase difference between heat release and inlet velocity oscillations, by a factor of approximately two. This result indicates that the heat release response of a partially premixed flame is chemical kinetics-controlled in terms of the response time scales. The vector plots further suggest that depending on the phase difference between the velocity and equivalence ratio oscillations, the response of a partially premixed flame can be reconstructed constructively and destructively.

The effect of the in-phase and out-of-phase interference between the velocity and equivalence ratio oscillations on the flame dynamics is shown in Figure 6. It is evident at the phase angle of 330° (A) that the flame starts to divide into two regions, as the upstream part of the flame moves in the direction of increasing flame angle. In the middle of the projected reaction zone, a thin local region with weak CH* chemiluminescence intensity is observed; the reaction zone appears to be divided in two. At a phase-angle of 60°, a continuous reaction region is not sustained, and consequently unsteady local extinction occurs. The in-phase interaction of the two inlet disturbances results in the unsteady destruction of flame surface area, leading to the nonlinear response of the partially premixed flame. On the other hand, significant differences are observed when the phase difference is close to 120°, as shown in Figure 6 (B). Localized flame extinction is not seen. CH* chemiluminescence intensity does not vary significantly during an oscillation cycle, since reactants with high equivalence ratio enter the combustion chamber with low velocity and reactants with low equivalence ratio reach the flame front with high inlet velocity. As a result, the

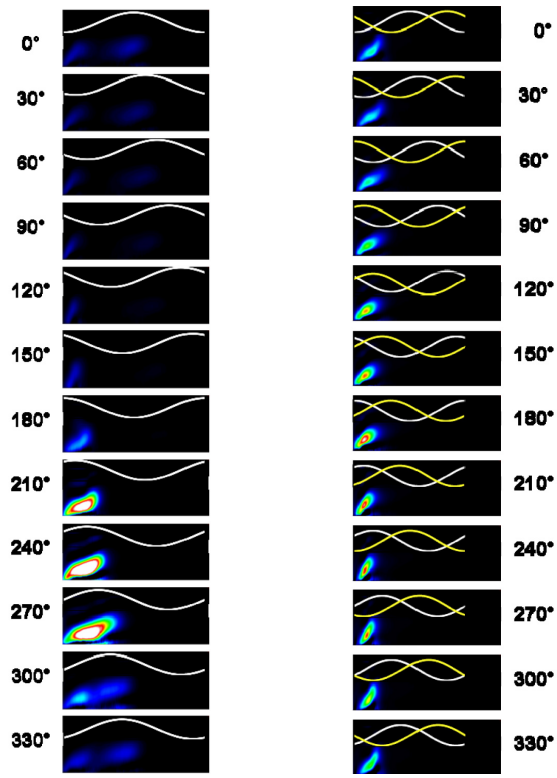

(A) In-phase interference (B) Out-of-phase interference

FIGURE 6. Phase-synchronized CH* chemiluminescence images at a modulation frequency of 200 Hz. (A) in-phase interference, (B) out-of-phase interference. Inlet conditions: T_{in} = 200°C, V_{mean} = 60 m/s, Φ_{mean} = 0.60, X_{H2} = 0.60, f = 200 Hz, and V'/V_{mean} = 42%.

flame "meets" almost the same amount of fuel per unit time.

Conclusions and Future Directions

Work to date has made important progress in modeling and measuring flame responses to flow perturbations. Such capabilities are absolutely essential in developing robust, ultra-clean engines capable of operation with a range of fuels. Future work will continue toward obtaining quantitative measurements and predictions of flame response to flow and fuel/air ratio perturbations. In addition, future work will focus on continuing transition of these results to conditions encountered in practical systems.

FY 2010 Publications/Presentations

1. K.T. Kim, J.G. Lee, H.J. Lee, B.D. Quay, and D.A. Santavicca, "Characterization of Forced Flame Response of Swirl-Stabilized Turbulent Lean-Premixed Flames in a Gas Turbine Combustor," *Journal of Engineering for Gas Turbines and Power*, Vol. 132, 2010, 04.

2. K.T. Kim, J.G. Lee, B.D. Quay, and D.A. Santavicca, "Spatially Distributed Flame Transfer Functions for Predicting Combustion Dynamics in Lean Premixed Gas Turbine Combustors," *Combustion and Flame*, 2010, doi:10.1016/j.combustflame.2010.04.016.

3. K.T. Kim, J.G. Lee, B.D. Quay, and D.A. Santavicca, "Response of Partially Premixed Flames to Acoustic Velocity and Equivalence Ratio Perturbations," *Combustion and Flame*, 2010, doi:10.1016/j.combustflame.2010.04.006.

4. K.T. Kim, J.G. Lee, B.D. Quay, and D.A. Santavicca, "Reconstruction of the Heat Release Response of Partially Premixed Flames," *Combustion Science and Technology*, 2010, In Press.

5. K.T. Kim, J.G. Lee, B.D. Quay, and D.A. Santavicca, "Experimental Investigation of the Nonlinear Response of Swirl Stabilized Flames to Equivalence Ratio Oscillations," *Journal of Engineering for Gas Turbines and Power*, 2010, In Press.

6. Shreekrishna and T. Lieuwen, "High Frequency Premixed Flame Response to Acoustic Perturbations," Presented at 15th AIAA/CEAS Aeroacoustics Conference, Miami, Florida, 2009, AIAA#2009-3261.

7. Shreekrishna, H. Santosh, and T. Lieuwen, "Premixed Flame Response to Equivalence Ratio Perturbations," Submitted to Combustion Theory and Modeling, 2010.

8. S.A. Vishal, Shreekrishna, D.H. Shin, and T. Lieuwen, "Response of Premixed Swirling Flames to Transverse Excitation," Proceedings of the 2009 Fall Technical Meeting of the Eastern States Section of the Combustion Institute, 2009.

III.B.3 Low-Swirl Injectors for Hydrogen Gas Turbines in Near-Zero Emissions Clean Coal Power Plants

Robert K. Cheng (Primary Contact) and David Littlejohn
Lawrence Berkeley National Laboratory (LBNL)
MS 70-108B, 1 Cyclotron Road
Berkeley, CA 94720
Phone: (510) 486-5438; Fax: (510) 486-7303
E-mail: RKCheng@lbl.gov

DOE Project Manager: Robin Ames
Phone: (304) 285-0978
E-mail: Robin.Ames@netl.doe.gov

Subcontractors:
- United Technologies Research Center, East Hartford, CT
- University of Iowa, Iowa City, IA
- University of California, Irvine, CA

Contract Number: 678403

Start Date: October 1, 2009
End Date: September 31, 2010

FY 2010 Objectives

- Develop a conceptual fuel injection scheme for the low-swirl injector (LSI) to operate with natural gas, syngas and high hydrogen fuels (3-fuel operation).
- Modify LSI exit nozzle for operation with high-hydrogen fuel (HHF).
- Design a reduced scale LSI prototype for evaluation with HHF at simulated gas turbine conditions.
- Characterize LSI flame acoustics and oscillations.
- Analyze lean premixed turbulent CH_4 and H_2 flames to support turbulent modeling development.

Accomplishments

- An analysis of the fuel delivery and injection requirement showed that a 3-fuel LSI gas turbine is feasible with dual parallel fuel circuits.
- Laboratory experiments at atmospheric conditions demonstrated that a LSI with a modified flared nozzle extends its operability with HHF to an adiabatic flame temperature T_{ad} of 1,700 K without inciting flame flashback.
- Measurements of the acoustic signatures and flowfield structures of CH_4 and HHF flames showed a direct link between the flame oscillations in the outer shear region of the LSI with the acoustics frequencies.

Introduction

This goal of this project is to develop a cost-effective and robust combustion system for the gas turbines in near-zero emissions integrated gasification combined cycle (IGCC) coal power plants that burn HHF (80%+) and syngas derived from coal gasification. The DOE Fossil Energy Advanced Turbine Program (ATP) sets a very aggressive emissions goal of less than 2 ppm NOx for these turbines. Current dry low NOx (DLN) combustion technologies developed for natural gas may not be readily adaptable to accommodate the highly reactive and dynamic characteristics of the HHF flames. Some gas turbine original equipment manufacturers (OEMs) are re-evaluating the option of using conventional and more polluting combustion methods for operating with HHF and treating the exhaust stream with expensive "tailpipe" catalytic cleanup methods to reduce NOx to the targeted level.

All contemporary DLN gas turbines employ lean premixed combustion as their operating principle to mitigate NOx emissions by burning of highly diluted lean fuel/air mixtures. Lean turbulent premixed flames are dynamic in nature and behave as self-propelling waves. They burn faster or slower according to the fluid mechanical, chemical, and thermodynamic properties of the system. These include fuel type, initial temperature and pressure, flow velocities, and turbulence intensities. The complex coupling of the flame with turbulence dictates its dynamic behaviors and is the crux of the challenges in designing and engineering of DLN combustion systems for gas turbines. The conventional DLN approach is to hold the dynamic premixed turbulent flames within the recirculation zones of intensely swirling flows. The LSI concept takes an opposite approach. It enables the premixed flame to propagate freely and burn in a divergent flow generated at the core of a weakly swirling flow.

Approach

The LSI concept was originally conceived at LBNL for basic research. Laboratory studies and analysis have provided the scientific foundation to facilitate the

transfer of this combustion method to gas turbines. To adapt the LSI for the large-frame 200 MW+ hydrogen fueled engines, the strategy is to optimize the basic LSI nozzle developed for a 7 MW natural gas engine to burn hydrogen, and collaborate with a gas turbine manufacturer to scale the design to larger sizes. The heart of the LSI is a patented swirler engineered to produce a turbulent divergent flow. It is capable of supporting stable turbulent lean premixed flames under a wide range of operating conditions. A characteristic signature of the LSI is a lifted flame that does not touch any part of the nozzle. The LSI swirler can be adjusted to accommodate the changes in the combustion properties of various fuels. This is done by reconfiguring the swirler components to change the swirl intensity.

The development of an LSI for IGCC gas turbines started with laboratory studies to optimize the configuration for burning of lean hydrogen flames whose NOx emissions are below 2 ppm. The experiments also provided turbulent flame speed data and quantitative information on the LSI flowfield to support the development of an analytical model that can be used to guide the design of LSI hardware for gas turbines. Testing of the LSI at simulated gas turbine conditions had shown its potential to meet the DOE ATP NOx emissions goals. In collaboration with researchers from national laboratories and universities, laboratory and computational research are being pursued to assist in the development of combustion models and computational design tools for scaling of the LSI to large capacities and adaptation to different engine configurations. The developments of the LSI for HHF gas engines are pursued in collaboration with the OEMs. Prototype hardware will be developed to meet specific engine and system operation requirements and to address issues on combustion intensity, dynamics, emissions, flashback, blowoff and auto-ignition.

Results

The variations in the compositions of natural gas, syngases and HHF create significant engineering challenges to the gas turbine combustor design and its control. Differences in the energy contents of these fuels require a flexible injection system that can handle a large range of throughputs for each specific fuel type. The gas turbine is the "starter" of the IGCC power plant that provides the energy to start the other plant components such as the gasifier and the air separation unit. Therefore, natural gas is required to start the gas turbine before the engine transitions to operate on HHF. Ideally, during IGCC startup the gas turbine would switch from natural gas to syngas and then to HHF. However, due to the low energy content of the syngases, maintaining combustion stability during the operation on these fuels can be problematic. The power plant operators may prefer a more practical approach by side-stepping the syngas operation phase. This would mean that the syngases produced during the start-up cycle will be released into the atmosphere. This is a highly undesirable and an environmentally unacceptable scenario.

To gain some insight on the fuel delivery and injection issue, we conducted a feasibility study of the requirements for a "3-fuel" capable LSI. The three fuels are defined as natural gas, a medium hydrogen syngas of 30% H_2 and 56% CO and a high hydrogen syngas of up to 81% H_2. Using a typical F-frame combustion system as the design platform, the analysis shows that a 3-fuel LSI gas turbine is feasible with dual parallel fuel circuits. One circuit is dedicated to natural gas and the other one is for the medium hydrogen and high hydrogen syngases (Figure 1). The diameters of the fuel lines and fuel injection orifices for the two circuits are sized to accommodate the differences in the fuel mass flow rates of the three fuels. The dual circuits should provide for full range of turbine operation in a configuration consistent with low pollutant emissions. Implementation of dual fuel circuit concept can be further refined once a candidate gas turbine has been selected for prototype development. Our study also identified a number of issues and potential challenges as design development efforts continue. These include combustor and first stage cooling, fuel injector length, fuel spoke design, combustor volume, acoustic oscillations, and large fuel mass flow, fuel circuit transition. The results of this investigation are reported in a paper presented at the Turbo-Expo 2010.

Our study of HHF flames at simulated gas turbine conditions have shown that the outer shear layer and the recirculation zone at the corner of the combustor inlet have significant influence on the HHF flame stabilization mechanism. To mitigate these effects, the exit nozzle of the LSI has been modified to include a flared nozzle (Figure 2). As shown, the flared conical

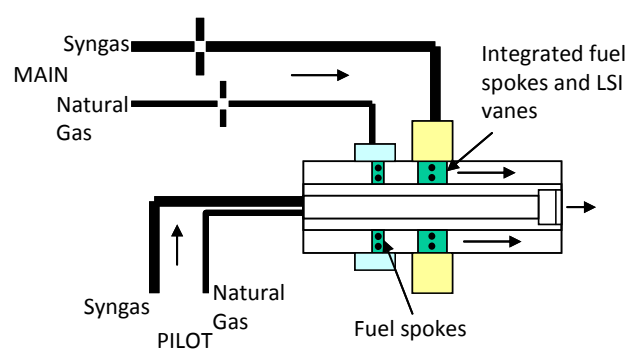

FIGURE 1. Schematics of the Dual-Fuel Circuit for a Typical F-Frame Gas Turbine Injector to Operate with Natural Gas, Syngas and High-Hydrogen Fuels

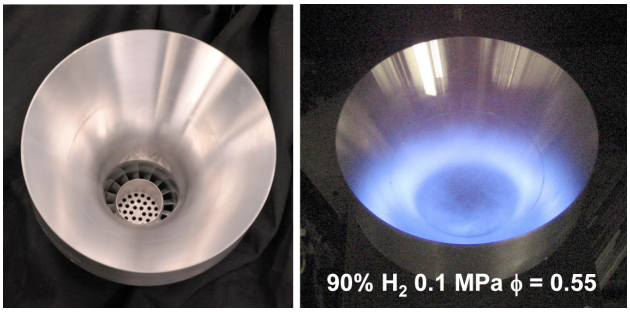

FIGURE 2. An LSI with a Modified Flared Nozzle Can Extend the Flash Back Limit for HHF Operation Because It Isolates the Flame from Being Influenced by the Outer Shear Layer

section extends to the wall of the combustor (full-cone). To study the effect of the length of the flared section on flashback, flame noise, and flame stability, the top half of the nozzle is removable so that it extends to half the diameter of the combustor (half-cone).

The full-cone and half-cone flared nozzles have been tested in the open and also in a quartz combustor. The results show that the flared nozzles are effective in extending the operating limit of the HHF flames. In the open, (Figure 2, right), the full-cone nozzle supports a 90% H_2/0.1 CH_4 flame of $\phi = 0.55$ at $U_0 = 10$ m/s. Without the cone, the highest ϕ accessible is 0.4. When the flared nozzles were tested inside the quartz liner, the full-cone nozzle was found to be less effective than the half-cone nozzle. This seems to be a consequence of the geometric constraint imposed by the full-cone nozzle and the combustor wall. Based on these observations, the half-cone nozzle geometry has been selected as a design criterion of the HHF LSI.

The acoustic signatures of the LSI were studied in collaboration with Siemens Energy Inc. To obtain some insights into the oscillation characteristics of the LSI system, this study includes experimental measurements and also modeling analysis of the fuel effects and influences of combustor inlet geometry.

Figure 3 compares the pressure spectral distributions obtained for CH_4 and 0.9 H_2/0.1 CH_4 flames with and without a conical nozzle. Without the conical nozzles, the flames excite acoustic frequencies between 300 to 400 Hz corresponding to the first longitudinal resonance frequency of the LSI experimental system. The fluctuating pressures measured in the 90% H_2–10% CH_4 flames are significantly higher than in the CH_4 despite the fact that the power outputs of the 90% H_2–10% CH_4 flames are lower. For both fuels, the use of the conical nozzle reduces the fluctuating pressures in the combustion chamber by up to a factor of 7. The velocity results show this to be a consequence of the conical nozzle mitigating the formation of large vortices in the outer shear layer. A laser beam defection method was also

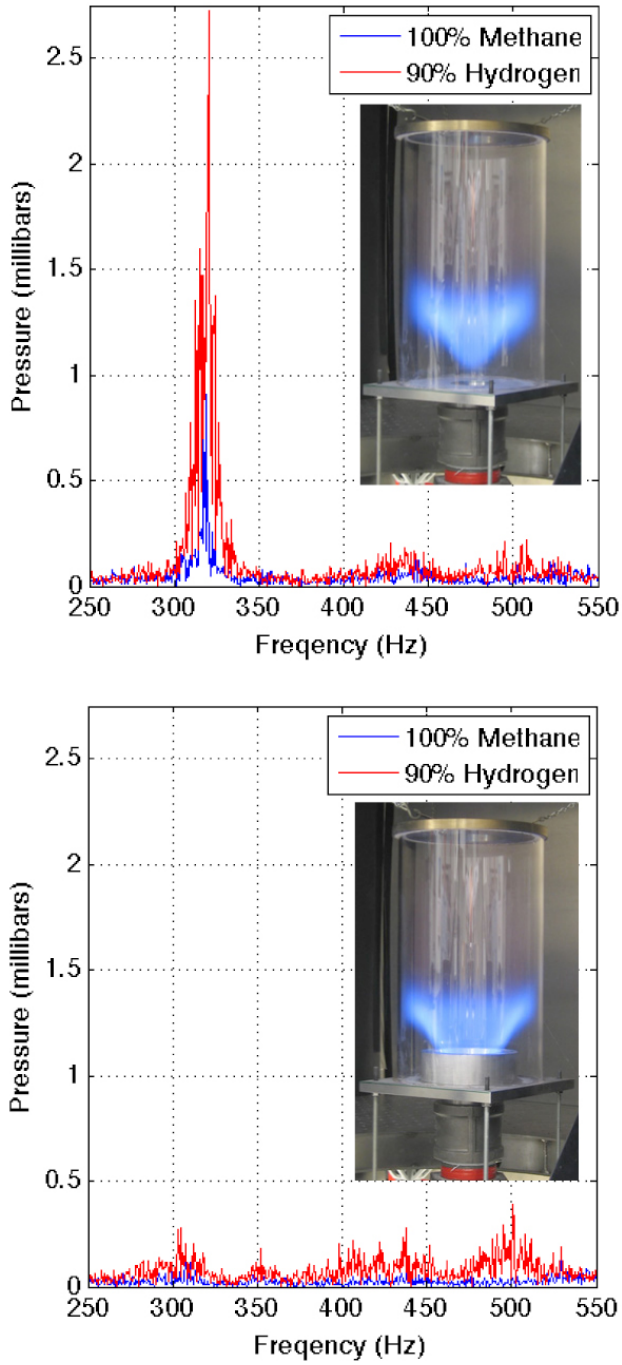

FIGURE 3. Pressure Frequency Spectra Show that the Use of a Conical Nozzle at the Combustor Inlet is Effective in Reducing Noise Generated by a CH_4/Air Flame at $\phi = 0.7$ and a 0.9 H_2/0.1 CH_4 Air Flame at $\phi = 0.35$, Both at U_0=15 m/s

used to quantify the frequency of flame fluctuations. For the cases without the conical nozzle, the data for CH_4 and 0.90 H_2/0.1 CH_4 flames confirm that the flame oscillation frequencies are consistent with the acoustics frequencies. This provides the experimental evidence to show a direct link between flame oscillations and the acoustics.

A general instability model (GIM) was also developed to predict dominant acoustic frequencies generated by the LSI and to conduct a stability analysis on two baseline flames without the conical nozzle. The results show that the GIM is able to model the self-excited combustion instabilities and confirms that the LSI triggers the first longitudinal mode of the system. The analysis also suggests that first longitudinal mode is triggered due to the presence of an acoustic pressure node along the swirler. Otherwise the second longitudinal mode would have been triggered because of a higher predicted instability growth rate.

Conclusions and Future Directions

Laboratory experiments and analysis have been conducted to address the basic and engineering issues for adapting the LSI to HHF gas turbines. These include an analysis of the fuel circuit requirements and modification of the nozzle to reduce HHF flame dynamics and flashback. The results are being used in designing a reduced scale HHF LSI that will be evaluated in Fiscal Year 2010 at gas turbine conditions.

Future work will be focused on the evaluation of the reduced-scale LSI prototypes. The results will be used to develop a research plan and roadmap for deployment of the LSI technology in utility size HHF gas turbines.

- Evaluate the performance of a reduced scale fully function LSI with HHF at gas turbine conditions.
- Determine the operability of the flare nozzle with HHF at gas turbine conditions.
- Continue the development of LSI for heavy-frame gas turbines operating on natural gas.
- Gain more insights into the fuel effects on the oscillation characteristics of the LSI.

FY 2010 Publications/Presentations

1. R.K. Cheng, D. Littlejohn, D.R. Noble, and T. Lieuwen, "Laboratory Investigations of Low-Swirl Injectors Operating with Syngases," J. Eng. Gas Turbine and Power v. 132 1, p. 011502-011510 (2010).

2. R.K. Cheng, "Turbulent Combustion Properties of Premixed Syngas," in Synthesis Gas Combustion – Fundamentals and Applications, p. 129-168, CRC Press (2009).

3. K.O. Smith, P.L. Therkelsen, D. Littlejohn, S. Ali, and R.K. Cheng, "Conceptual Study of a Fuel-Flexible Low-Swirl Combustion System in Clean-Coal Power Plant," ASME paper GT2010-23506.

4. P.L. Therkelsen, D. Littlejohn, R.K. Cheng, J. Enrique Portillo, and S.M. Martin, "Effects of Combustor Inlet Geometry on Acoustic Signature and Flow Field Behaviour of the Low-Swirl Injector," ASME paper GT2010-23498.

5. K-J Nogenmyr, C.K. Chan, C.W. Leung, and R.K. Cheng, "LES and Experimental Studies of Confinement Effects on Premixed Turbulent Swirling Flame," in preparation for submission to Comb. and Flame.

6. R.K. Cheng, "Combustion and Carbon Cycle 2,0," LBNL Carbon Cycle 2.0 Symposium, February 3, 2010, http://carboncycle2.lbl.gov/categories/Combustion.html.

III.B.4 Aerothermal and Fundamental H_2 Studies and CO_2 Recycle Effects

Dr. Kent Casleton (Primary Contact),
Doug Straub, Dr. Pete Strakey,
Dr. Don Ferguson
U.S. Department of Energy
National Energy Technology Laboratory (NETL)
3610 Collins Ferry Rd., P.O. Box 880
Morgantown, WV 26507-0880
Phone: (304) 285-4573; Fax: (304) 285-0903
E-mail: Kent.Casleton@netl.doe.gov

Subcontractors:
- RDS, LLC, Morgantown, WV
- URS Corporation, Washington Division, Morgantown, WV and Pittsburgh, PA

Contract Number: This is a component of Project 10220623 6926

Start Date: October 1, 2009
End Date: September 30, 2010

FY 2010 Objectives

- Test impingement cooling and one film cooling design for baseline aerothermal test coupons and report results.
- Test an array-style injector for dilute diffusion concept, measuring NOx and unburned H_2 as a function of pressure and flow rate.
- Measure the effect of CO_2 and N_2 dilution on the combustion dynamics for methane and methane/H_2 fuel mixes and document results.

Accomplishments

- Completed shakedown testing with impingement-cooled coupons, and demonstrated optical temperature measurement methodology on the hot side. Initiated study with film-cooled test coupons. A report of these results is being prepared.
- Developed NOx scaling relationships to account for effects of injector geometry, fuel jet velocity, and coaxial jet velocity in dilute diffusion concepts.
- Designed and fabricated an array-style injector to assess NOx performance of the dilute diffusion concept at high pressure.
- Measured the combustion stability of various blends of H_2 and CH_4 fuels with CO_2 and N_2 dilution to simulate the impact of exhaust gas recycle (EGR) on combustion dynamics. Generally, dilution reduces the occurrence on instability due to the lengthening of the flame.

Introduction

The Department of Energy's Turbine Program is developing advanced turbine technology that is capable of efficiently utilizing coal-derived gases, including hydrogen, for the production of electricity. This approach addresses the need to control carbon emissions while offering a means to continue to utilize the nation's abundant coal resources.

This project, "Aerothermal and fundamental H_2 studies and CO_2 recycle effects," supports the NETL turbine program and addresses these critical needs in the following tasks by:

- Collaborating with the University of Pittsburgh to design, fabricate and begin testing of a high-pressure test rig for aerothermal heat transfer studies appropriate for hydrogen and oxy-combustion turbines. Success in this activity will help identify improved cooling approaches that will result in improvements in overall turbine operating efficiency.
- Investigating an innovative diffusion combustion concept for high-hydrogen fueled turbines to assess combustor stability and NOx emission limits. Success in this activity will identify the suitability in this approach to achieve DOE's emission goal of less than 2 ppmv NOx at target turbine inlet temperatures.
- Examining the impact of turbine EGR on combustion phenomena such as combustion dynamics. Success in this activity will identify operating regimes where EGR could potentially offer an option for improved efficiency of CO_2 post-combustion removal for natural gas-fired engines.

Approach

In order to explore aerothermal cooling of airfoils for use in advanced, land-based, turbine applications, an experimental aero-thermal test facility has been developed at NETL. This development, done in collaboration with the University of Pittsburgh, utilizes the high-pressure combustion expertise and facilities at NETL. Figure 1 illustrates the layout of the pressurized combustor and aerothermal test section.

Several different laboratory-scale, atmospheric pressure bench-scale [1,2], and high-pressure larger-scale test rigs [3] are available at NETL to study a variety of possible combustion alternatives and combustion phenomena for hydrogen turbine applications. These facilities are used to evaluate

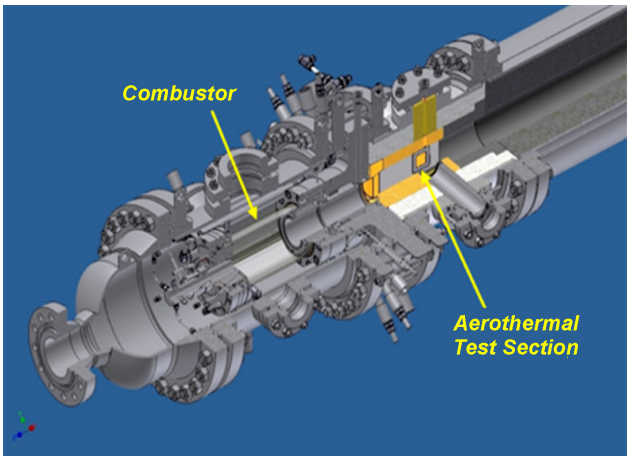

FIGURE 1. Pressurized Combustor and Aerothermal Test Section

and test novel combustor designs for use with high-hydrogen fuels to assess their applicability for low NOx operation and to map combustion dynamics phenomena.

Results

Aerothermal Heat Transfer Studies

Achieving DOE's efficiency goals for land-based gas turbines will require increasing the engine firing temperatures above current state-of-the-art. This increase in operating temperature will put significant demands on materials and cooling methodologies. This project seeks to collect aerothermal heat-transfer data at elevated pressure and at simulated gas turbine conditions. These validation datasets will be useful for improving aero-thermal cooling effectiveness, reducing NOx emissions, and increasing turbine efficiencies. Data will be collected on a baseline fuel and a fuel representative of the hydrogen turbine environment.

This project leverages the aerothermal heat transfer expertise of the University of Pittsburgh with NETL's extensive background in and experimental facilities for high-pressure combustion appropriate to gas turbine combustion systems. The main objective of this project is to systematically explore the issues of aerothermal cooling pertinent to high-hydrogen and oxy-fuel turbine systems. Different cooling strategies, including backside impingement and film cooling for bare coupons as well as coupons with thermal barrier coatings are being investigated.

The primary focus of activities to date has included:

- Completing all safety related requirements associated with installing a new optically-accessible pressure vessel component into the existing combustion test rig.
- Completing the shakedown of the aerothermal rig and associated test modules.
- Developing and implementing techniques to measure the hot-side surface temperature of the test coupon.
- Working with an external partner (Apogee Scientific) to implement a multi-spectral optical imaging approach to determine test coupon surface temperature distributions. The initial application would be for measurement of temperatures on the coupon back-side surface.
- Initial testing has been done for both flat coupons with back-side impingement cooling as well as film cooled coupons.

Modifications and shakedown testing have been completed. Based on these preliminary tests, the following items have been highlighted:

- The new safety instrumented system performed well.
- An approach for optically measuring the hot side surface temperature was successfully demonstrated (see Figure 2).
- The target gas temperatures (greater than 1,200°C) and surface temperatures (800-1,000°C) are easily achieved.

The preliminary testing also identified the following areas for improvement:

- The smooth wall liner that was rated for operation at 1,650°C failed on two occasions at operating temperatures near 1,200°C. This required a redesign of this component. Further testing showed that performance of this component is still not adequate and additional redesign will be required. As a result, the schedule has suffered.

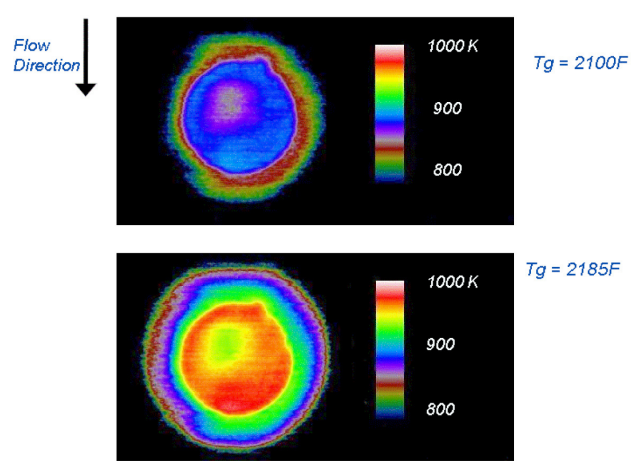

FIGURE 2. Impingement-Cooled Coupon Real-Time Surface Temperature Contours

- There were some issues with rust particles in the air lines. These particulates deposited on the back-side of the test coupon and also caused some issues with the optical viewports. A portion of the air piping has been replaced and filters have been installed.

Hydrogen Dilute Diffusion Combustion Studies

Existing lean premixed gas turbines operating on natural gas are susceptible to a number of problems including flame flashback and combustion instabilities when operating on fuels containing large amounts of hydrogen. Combustion strategies for syngas and hydrogen that utilize diffusion flames, where the fuel and air are not premixed prior to combustion, are much less prone to combustion instabilities. The challenge is to design a diffusion combustor that operates at high turbine inlet temperatures but still meets DOE's aggressive NOx goals.

NETL's approach to this challenge involves highly strained dilute hydrogen diffusion flames. Nitrogen, an available byproduct in an oxygen-blown integrated gasification combined cycle power plant, is used to dilute the hydrogen fuel. This reduces peak flame temperature, increases mixing to reduce the flame size, and improves static flame stability. The diluted fuel injector uses very high injection velocities and small fuel injectors to reduce NOx production significantly. This project combines small-scale laboratory experiments, larger scale, high-pressure experiments, and computational modeling to explore the use of flame strain to reduce NOx emissions, characterize NOx formation in highly strained, dilute diffusion hydrogen flames, and determine if this is a viable approach for a hydrogen combustor.

Recent accomplishments:

- Investigated geometry and scalability issues involved in the design of a multi-point, array-style injector for achieving DOE's NOx emissions goals. The flame holding stability of a 3-lobed injector design was evaluated and appears to be superior to an annular air injector and a star-shaped injector design, while providing comparable NOx emissions and lower pressure drop.
- Computational fluid dynamics (CFD) simulations were performed to model the flame. These were validated against experimental results and then used to refine NOx scaling laws and identify improved injector designs for better performance.
- Completed a detailed mechanical design and fabrication of an array-style injector for high-pressure testing in NETL's Simulation-Validation (SimVal) test facility at representative gas turbine conditions. (See Figure 3.)

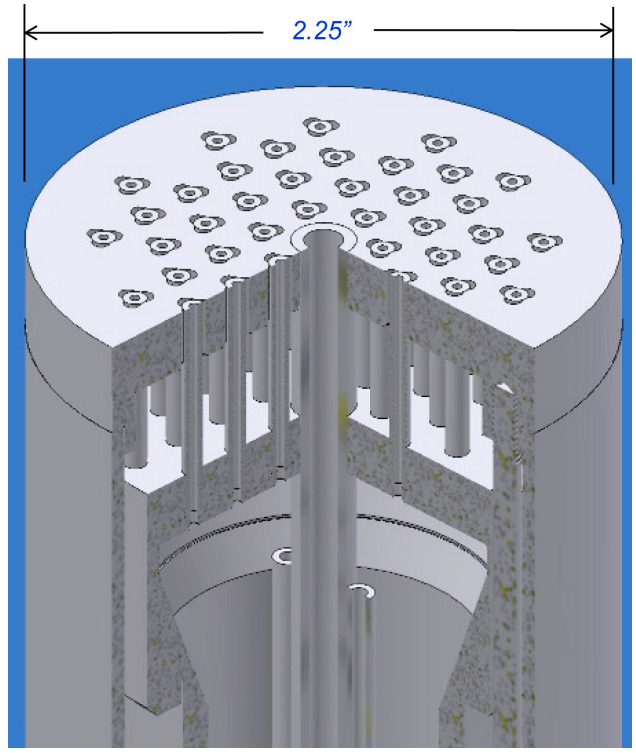

FIGURE 3. Array-Style Injector Design

- Determined effects of combustion product recirculation, array spacing, and adiabatic combustion environment on NOx emissions and flame holding stability for a dump-plane style injector.

CO_2 Recycle Effects

EGR is being considered as a possible option in advanced gas turbine systems as a way to concentrate CO_2 in the exhaust. This would improve the efficiency of CO_2 post-combustion removal processes and reduce the volume of flue gas to be processed. This could ultimately lead to a significant decrease in the cost of carbon removal. However, these changes to the overall combustion environment could affect the combustion process and potentially affect the combustion stability and emissions. The goal of this research is to examine the impact of EGR on combustion phenomena such as combustion dynamics.

Experimental studies were conducted to assess the impact of EGR on flame dynamics and thermoacoustic instabilities. Mapping of instabilities with respect to dilution level and operating condition was performed in a fully premixed atmospheric pressure, laboratory-scale burner with both low- and high-swirl injector designs. For the high-swirl configuration, the unstable pressure amplitude in the combustor was found to depend on Strouhal number, implying a well-known link between

convective time delay and instabilities still occurs in the presence of dilution. Further characterization of the convective time delay was conducted for the low-swirl injector via phase-locked imaging of the flame chemiluminescence. It was found that rate at which disturbances were swept through the flame could be approximated as the mean flow velocity at the exit of the injector.

The combustor was modeled using CFD to validate and test the effectiveness of existing techniques at predicting flame characteristics under EGR conditions. A three-dimensional Reynolds Averaged Navier-Stokes (RANS)-based model was used to determine the flow-field and was reduced to two-dimensions for coupling with a substantially reduced (nine species) chemistry model. The ability of this model to predict overall exhaust composition was compared with experimental measurements made in the laboratory. The results showed that the model was able to show qualitative trends, but failed to correctly predict absolute values for the exhaust composition, possibly indicating the necessity of more detailed chemistry models.

Conclusions and Future Directions

Aerothermal Studies

- Initial testing has been done for both flat coupons with back-side impingement cooling as well as film cooled coupons.
- Failure of the high purity alumina liner in the aerothermal test module will require further modification to the liner design.

H_2 Dilute Diffusion Flames

- Acceptable NOx performance appears to be feasible. Design of the SimVal array-style injector was completed and testing at high pressures will be performed to assess this potential.

Turbine EGR

- Experimental studies and CFD and chemical reactor network simulations of turbine EGR applications are in progress.

FY 2010 Publications/Presentations

1. N.T. Weiland, T.G. Sidwell, and P.A. Strakey, "Effect of Pressure and Air Preheating on Dilute Hydrogen Jet Diffusion Flames with Coaxial Air Injection," 2010 Spring Technical Meeting, Central States Section/Combustion Institute, Champaign, Illinois, March 21–23, 2010.

2. N.T. Weiland and P.A. Strakey, "Flame Structure and NOx Scaling of Confined Dilute Hydrogen Diffusion Flames," 2010 Spring Technical Meeting, Central States Section/ Combustion Institute, Champaign, Illinois, March 21–23, 2010.

3. P. Strakey and N. Weiland, "Effects of Coaxial Air on Nitrogen-Diluted Hydrogen Jet Diffusion Flame Length and NOx Emission," 33rd International Symposium on Combustion, Beijing, China, August 1–6, 2010, Accepted for publication.

4. N.T. Weiland and P.A. Strakey, "NOx Reduction by Air-Side vs. Fuel-Side Dilution in Hydrogen Diffusion Flame Combustors," ASME Paper: GT2009-60128, Presented at ASME Turbo Expo, Orlando, Florida, June 8–12, 2009, and accepted for publication in *Journal of Engineering for Gas Turbines and Power*.

5. N.T. Weiland and P.A. Strakey, "Stability Characteristics of Turbulent Hydrogen Dilute Diffusion Flames," *Combustion Science and Technology*, (181): 756-781, 2009.

6. J.A. Ranalli, D. Ferguson, and J. Escobar, "On Use of OH* and CO_2* Chemiluminescence for Heat Release Rate Measurement in Diluted Flames," Proceedings of the 2010 Technical Meeting of the Eastern States Section/ Combustion Institute, College Park, Maryland, October 18–21, 2009.

7. J. Escobar, D. Ferguson, J. Ranalli, J. Nanduri, and I. Celik, "An Experimental and Computational Study of Emissions from a Swirl Stabilized Burner under EGR Conditions," Proceedings of the 2010 Technical Meeting of the Central States Section of The Combustion Institute, Champaign, Illinois, March 21–23, 2010.

8. J.A. Ranalli and D. Ferguson, "Convective Wave Motion during Combustion Instability in a Low-Swirl Burner Flame," Proceedings of the 2010 Technical Meeting of the Central States Section of The Combustion Institute, Boulder, Colorado, March 21–23, 2010.

9. D. Ferguson, J.A. Ranalli, and P. Strakey, "Influence of Exhaust Gas Recirculation on Combustion Instabilities in CH_4 and H_2/CH_4 Fuel Mixtures," Paper GT2010-23642, Proceedings of the 2010 ASME Turbo-Expo, Glasgow, United Kingdom, June 14–18, 2010.

10. J.A. Ranalli and D. Ferguson, "Convective Wave Motion during Combustion Instability in a Low-Swirl Burner Flame," Western States Section Meeting of the Combustion Institute, University of Colorado, Boulder, Colorado, March 22–23, 2010.

11. Peter Strakey and Gilles Eggenspieler, "Development and Validation of a Thickened Flame Modeling Approach for Large Eddy Simulation of Premixed Combustion," GT2009-60077, Proceedings of the ASME Turbo Expo 2009, Orlando, Florida, June 8–12, 2009. (Also accepted for publication in the *Journal of Engineering for Gas Turbines and Power*.)

12. R.K. Cheng, D. Littlejohn, P.A. Strakey, and T. Sidwell, "Laboratory Investigations of a Low-Swirl Injector with H_2 and CH_4 at Gas Turbine Conditions," *Proceedings of the Combustion Institute*, 32 (2009), 3001-3009.

13. J.R. Nanduri, D.R. Parsons, I.B. Celik, and P.A. Strakey, "Predictions of Emissions Using RANS: Simulation of Lean Premixed Methane Air Flames in Swirl Stabilized Combustor," 2009 Fall Technical Meeting, Eastern States Section/Combustion Institute, University of Maryland, October 18–21, 2009.

References

1. N. Weiland and P. Strakey, "Global NOx Measurements in Turbulent Nitrogen-Diluted Hydrogen Jet Flames," Paper B22, 5th U.S. Combustion Meeting, San Diego, California, March 25–28, 2007.

2. D. Ferguson, "Experimental Investigation of Oscillatory Heat Release Mechanisms and Stability Margin Analysis in Lean-Premixed Combustion," Ph.D. Dissertation, West Virginia University, https://eidr.wvu.edu/etd/documentdata.eTD?documentid=3854, 2005.

3. T. Sidwell, G. Richards, K. Casleton, D. Straub, D. Maloney, P. Strakey, D. Ferguson, S. Beer, and S. Woodruff, "Optically Accessible Pressurized Research Combustor for CFD Model Validation," AIAA Journal, 44(3), pp. 434-443, 2006.

III.B.5 Develop Data for Thermophysical Properties of Humid Gases in Power Cycles

Dr. Allan H. Harvey
Thermophysical Properties Division
National Institute of Standards and Technology
325 Broadway, MS 838.08
Boulder, CO 80305
Phone: (303) 497-3555; Fax: (303) 497-5044
E-mail: aharvey@boulder.nist.gov

DOE Project Manager: Mark Freeman
Phone: (412) 386-6094
E-mail: Mark.Freeman@netl.doe.gov

Contract Number: 42957

Start Date: August 1, 2006
End Date: May 31, 2010

FY 2010 Objectives

- Use results of first-principles quantum mechanics to develop description of thermodynamics of humid gases in power cycles.
- Validate thermodynamic description by high-accuracy density measurements at high temperatures.
- Measure thermal conductivity of key water/gas mixtures at conditions relevant to power cycles.

Accomplishments

- Completed first-principles molecular analysis of H_2O/CO_2 system and implemented resulting parameters in software for calculation of thermodynamic properties of humid gases containing H_2O with Ar, O_2, N_2, CH_4, CO, and CO_2.
- Completed gas-phase density measurements and preliminary data analysis for mixtures of N_2 with H_2O and CO_2 with H_2O at temperatures from 500 K to 620 K, finding agreement with molecular modeling results.
- Completed thermal conductivity measurements of pure N_2, CO_2, H_2O, and mixtures of N_2 with H_2O and CO_2 with H_2O at temperatures from 500 K to 740 K.

Introduction

Innovative power cycles (such as integrated gasification combined cycle and oxyfuel) are being developed for production of electric power with higher efficiency and reduced environmental impact, including the possibility of CO_2 capture and sequestration. For optimizing the design of these systems, it is important to have accurate values of the thermophysical properties (density, heat capacity, thermal conductivity, etc.) of the fluid mixtures in the turbines and other parts of these cycles. These mixtures have a large H_2O content, along with other gases such as nitrogen and CO_2; they are at high temperatures where thermodynamic data are scarce, but the pressures are only moderately high. Typical approaches such as ideal-gas thermodynamics or common engineering equations of state are inaccurate for such systems, primarily due to the presence of water. Therefore, it is necessary to develop alternative modeling approaches, supplemented by selected high-temperature experimental measurements.

Approach

The description of the thermodynamic properties is developed at the level of the second virial coefficient, which is the first-order correction to the ideal-gas law. The key parameters are the "cross" second virial coefficients representing interactions between one water molecule and one gas molecule. Our approach is to use computational quantum mechanics to develop accurate surfaces describing the potential energy between the molecules, from which the virial coefficients can be calculated with high accuracy.

In order to validate our theoretical results, we perform high-accuracy density measurements on the key H_2O-N_2 and H_2O-CO_2 binary systems at high temperatures. The high temperatures are necessary because adsorption renders the measurements nearly impossible below about 500 K, but few laboratories have the capability for precision densimetry at high temperatures. We have developed such capability in conjunction with this work. The instrument is known as a "single-sinker magnetic-suspension densimeter." It operates on the Archimedes or buoyancy principle. By knowing the sinker volume and comparing the apparent weight while it is immersed in the gas mixture to the known mass of the sinker, the density is determined. This is an absolute method, meaning that

no calibration fluids are required. The key elements of the instrument are the sinker (which is the actual sensing element), a magnetic suspension coupling which transmits the weight of the sinker to the balance and isolates the balance from the extreme conditions of the fluid, and the balance (which provides the quantitative measurement).

We have developed parallel capability for measuring the thermal conductivities of these mixtures at high temperatures; in this case, the measurements are essential because no good theoretical approach is available for this property. The measurements use the transient hot-wire method, which has become the method of choice for high-accuracy thermal conductivity measurements. Because water's electrical conductivity is problematic for the traditional direct current implementation of this technique, an alternating current (AC) version of the apparatus has been developed.

Results

As a preliminary to this work (not funded by this project), we produced potential-energy surfaces for the H_2O-N_2 and H_2O-O_2 molecular pairs and used them to calculate second virial coefficients in a large temperature range with uncertainties better than all but the most precise experimental data. The H_2O-CO_2 pair, which is the central theoretical work in this project, is now completed and second virial coefficients for this cross virial coefficient have been calculated. Figure 1 shows the calculated second virial coefficients and their uncertainty, along with the limited (and sometimes inconsistent) experimental data from the literature. It is noteworthy that the theoretical results are valid to roughly 2,000 K, much higher than the limited temperature range of experimental data shown in Figure 1.

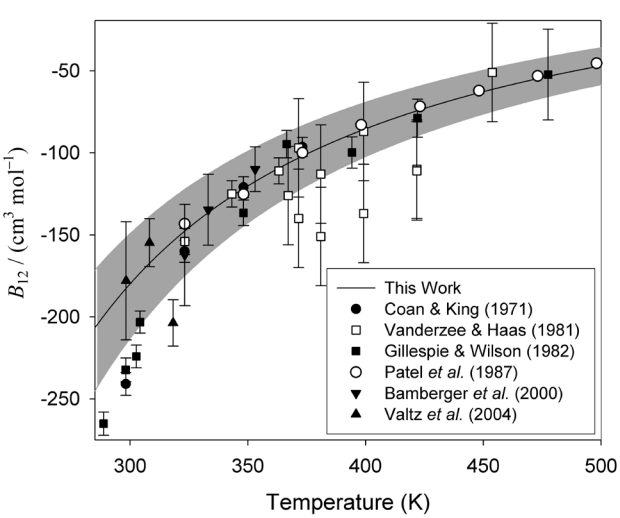

FIGURE 1. Cross second virial coefficients for the H_2O/CO_2 mixture. The solid line and shading represent the molecular modeling results with their expanded (k=2) uncertainty, and the points represent experimental data from the literature with their expanded uncertainties where reported.

All these data have been incorporated into software for accurate calculation of thermodynamic properties of humid gases containing H_2O with Ar, O_2, N_2, CH_4, CO, and CO_2 at any composition. The software is a spreadsheet plug-in based on the National Institute of Standards and Technology's (NIST's) REFPROP program [1] which provides reference-quality thermophysical properties for (among other things) nonaqueous gas mixtures such as natural gas and air.

Accurate measurements of the density and thermal conductivity of the H_2O-N_2 and H_2O-CO_2 mixtures require samples with well-known compositions. Because of the very large volatility difference of H_2O compared to N_2 or CO_2, it is not possible to prepare mixtures outside the measurement system at room temperature. Thus, the mixture samples for this work are prepared in situ in each measurement apparatus, with compositions determined from difference weighings of separate gas-charge (nitrogen or CO_2) and smaller water cylinders. The two are connected in series for charging the sample into the apparatus, with the high pressure gas sample pushing the water sample into the measuring cell. Differences in the mass of each cylinder, before and after charging each apparatus, give the quantity of sample charged and allow the mixture composition in the apparatus to be determined with high accuracy.

A new high-temperature densimetry apparatus has been constructed by NIST (not using project funds) for use in this project. The key parts include the measuring cell/pressure vessel, the density measuring system, a multi-layer thermostat for temperature control with stability and uncertainty in temperature of a few mK, a vacuum chamber (for thermal isolation) and vacuum pumping system, a sample-handling system, and pressure instrumentation. Figure 2 is a photograph of the apparatus. The densimeter "kernel," which was contracted to Rubotherm, GmbH, Bochum, Germany, is positioned in the center of the thermostat. The system is built around a custom version of the Rubotherm high-temperature, high-pressure magnetic suspension coupling. The major custom items are a silicon sinker and a high resolution mass-comparator balance. The density-sensing system comprises the silicon sinker together with the balance and magnetic suspension coupling. The thermal expansion of silicon is known to very high accuracy, and thus the volume of the sinker as a function of temperature can be computed accurately. The measuring cell is designed for pressures up to 50 MPa.

FIGURE 2. Photo showing the high-temperature densimeter. From left-to-right the major components are: vacuum system; main part of densimeter with the mass-comparator balance at the top and the vacuum chamber containing the measuring cell at the bottom; instrument rack; and display for the control computer.

Density measurements have been completed on H_2O/N_2 and H_2O/CO_2 mixtures at 500, 560, and 620 K. Two or three compositions were measured for each mixture at each temperature. Preliminary analysis of the isotherms indicates that the experimental results for the cross second virial coefficient are consistent with the theoretical predictions for both systems; final data analysis, including uncertainty analysis, is in progress.

The density measurements, when extrapolated to zero density, also yield the average molar mass for the mixture, which for these binary systems is equivalent to knowing the composition. These results are consistent with the compositions derived from the weighing procedure in the sample charging system, verifying that our procedure for making mixtures is reliable.

The new AC hot-wire thermal conductivity cell is enclosed in an electrical furnace that provides temperature control from ambient to over 750 K. The temperature is measured with a reference platinum resistance thermometer with an uncertainty of 5 mK, while the pressure is measured with a pressure transducer (0 to 70 MPa) with an uncertainty of 0.007 MPa. The filling manifold and pressure transducer have small volumes and are water-filled to reduce uncertainty in the composition of the sample that would result from condensation of water from the mixture in these colder regions of the pressure system.

After testing and calibration, thermal conductivity measurements of mixtures of N_2 with H_2O have been completed for two compositions each at temperatures of 500, 560, 620, 680 and 740 K. The dilute-gas thermal conductivity (low-density limiting value) of the mixtures is larger than that of either pure N_2 or H_2O at the lower temperatures. This behavior has been reported for a few limited measurements of thermal conductivity for mixtures of polar with nonpolar gases but is not understood at a fundamental level. The density dependence of the mixture thermal conductivity falls between those of the pure components at a fixed temperature. Figure 3 shows this behavior at temperatures near 500 K; this figure also shows the good agreement of the present data with the accepted values for pure N_2 and H_2O in the NIST REFPROP database [1]. Thermal conductivity measurements of mixtures of CO_2 with H_2O have been also been completed for two compositions each at temperatures of 500, 560, 620, 680 and 740 K. Figure 4 shows the thermal conductivity at temperatures near 680 K. Again the dilute-gas thermal conductivity (low-density limiting value) of the mixtures is larger than that of either pure CO_2 or H_2O at this temperature.

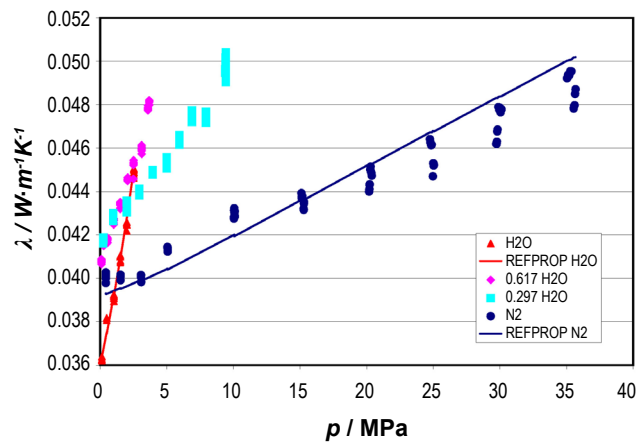

FIGURE 3. Thermal conductivity of mixtures of N_2 with H_2O at temperatures near 500 K. The upper pressure and density for pure H_2O and the mixtures is limited by condensation of liquid.

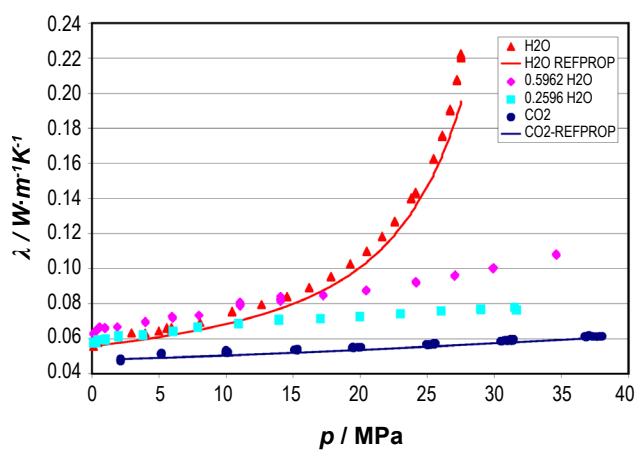

FIGURE 4. Thermal conductivity of mixtures of CO_2 with H_2O at temperatures near 680 K with pressures up to 40 MPa.

Conclusions and Future Directions

For the modeling part of the work, we have now incorporated our molecular modeling results to produce a complete description of the gas-phase thermodynamics of the main components of combustion gases. These results have been integrated into a mixture equation-of-state model.

On the experimental side, density measurements have been performed for the H_2O/N_2 and H_2O/CO_2 systems at 500, 560, and 620 K. The results are consistent with the modeling work. Measurements of the thermal conductivity of pure H_2O, N_2 and CO_2 and the binary H_2O/N_2 and H_2O/CO_2 mixtures have been completed at temperatures of 500, 560, 620, 680, and 740 K with pressures up to 40 MPa.

While this completes the present project, there are related areas of need that could be considered as extensions to this work. These would include:

- Extension of the thermodynamic framework to allow prediction of condensation of water and of vapor-liquid equilibria more generally.
- Experimental measurements of the sound speed and/or the viscosity for gaseous H_2O/N_2 and H_2O/CO_2 mixtures.
- Experimental measurements for saturated vapor composition for the H_2O/CO_2 mixture at low temperatures (where the uncertainty of our theoretical results becomes larger) in order to provide data for separation and sequestration of CO_2 from combustion gases.

FY 2010 Publications/Presentations

1. R.J. Wheatley and A.H. Harvey, "Intermolecular potential energy surface and second virial coefficients for the water-CO_2 dimer," *J. Chem. Phys.*, to be submitted.

References

1. E.W. Lemmon, M.L. Huber, and M.O. McLinden, *REFPROP: Reference Fluid Thermodynamic and Transport Properties*, NIST Standard Reference Database 23, Version 8.0 (National Institute of Standards and Technology, Gaithersburg, Maryland, 2007).

III.B.6 Micro-Mixing Lean-Premix System for Ultra-Low Emission Hydrogen/Syngas Combustion

Dr. Adel Mansour (Primary Contact),
Dr. Erlendur Steinthorsson, Brian Hollon
Parker Hannifin
8490 Tyler Blvd.
Mentor, OH 44060
Phone: (440) 266-2300; Fax: (440) 266-2311
E-mail: amansour@parker.com

DOE Project Manager: Robin Ames
Phone: (304) 285-5436
E-mail: Robin.Ames@netl.doe.gov

Subcontractor:
University of California, Irvine, Irvine, CA

Contract Number: 42648

Start Date: October 1, 2008
End Date: June 30, 2010

FY 2010 Objectives

Fabricate and test a full-scale, 1 MW_{th} micro-mixing fuel injector and demonstrate stable operation and 3 ppm NOx at an adiabatic flame temperature of 1,750 K when operating on hydrogen and syngas fuels (Phase III emissions target, 2 ppm stretch goal).

Accomplishments

- Fabricated a full-scale 16-cup injector rated at 1.3 MW_{th} when operating on natural gas at 12.4 bar combustor pressure, 3.5% pressure drop and equivalence ratio of 0.5.
- Demonstrated operation of the full-scale injector without flashback at pressures ranging from 6.9 bar (100 psi) to 12.4 bar (180 psi) and adiabatic flame temperatures up to 2,000 K (2,940°F) using hydrogen-natural gas fuel mixtures ranging from 100% natural gas to 100% hydrogen, and using from 0% to 40% nitrogen or carbon dioxide dilution.
- Demonstrated emissions performance that, at most conditions, is nearly independent of operating pressure, an indication of a well-premixed flame.
- Demonstrated 3 ppm NOx emissions at a flame temperature of 1, 750 K (2,690°F) operating with a fuel mixture containing 50% hydrogen and 50% natural gas combined with 40% nitrogen dilution (180 psi combustor pressure, 4% pressure drop, 755 K (900°F) inlet-air temperature).
- Demonstrated ultra-low NOx emissions of 1.5 ppm at a flame temperature of 1,677 K (2,560°F) when operating on a fuel mixture containing 50% hydrogen and 50% natural gas with only 10% nitrogen dilution.
- Demonstrated NOx emissions of 3.5 ppm at a flame temperature of 1,730 K (2,650°F) when operating on a fuel mixture containing 50% hydrogen and 50% natural gas with only 10% carbon dioxide dilution.
- Demonstrated NOx emissions of 3.6 ppm at a flame temperature of 1,600 K (2,420°F) when operating on 100% hydrogen with 30% carbon dioxide dilution.

Introduction

The focus of this project was to develop the next generation of fuel injection technologies for environmentally friendly, hydrogen syngas combustion in gas turbine engines that satisfy DOE's objectives of reducing NOx emissions to 3 ppm. Building on Parker Hannifin's proven Macrolamination technology for liquid fuels, Parker developed a scalable high-performing multi-point injector that utilizes multiple, small mixing cups in place of a single conventional large-scale premixer. Due to the small size, fuel and air mix rapidly within the cups, providing a well-premixed fuel-air mixture at the cup exit in a short time such that risks of auto-ignition are eliminated. Scalability is achieved by integrating multiple small mixing cups into a single larger injector.

Detailed studies and experimentation with the micro-mixing injectors were conducted to elucidate the effects of various injector design attributes and operating conditions on combustion efficiency, lean stability and emissions. Through our university partner, data on flame and stability characteristics, turbulent flame propagation, and impact of the anchoring mechanism, burning conditions and syngas composition were collected experimentally. Computational analyses, corroborated with diagnostics, were used to determine the role of chemistry, transport and fluid mechanics on combustion. Strategies were developed to mitigate the impact of flashback. In the earlier phases of the project, the experimental studies focused on single-cup injectors and small multi-cup injectors, taking advantage of the modularity of the multi-cup approach to minimize cost of development

and testing. In the final phase of the project, a full-scale 1.3 MW_{th} multi-cup injector was built and tested.

Approach

Utilizing Parker Hannifin's Macrolamination technology, the general approach was to adapt Macrolaminated designs and concepts to hydrogen/syngas combustion and hydrogen-enriched combustion. With Macrolamination technology, elegant and sophisticated multipoint lean-premix nozzles and burners were developed, incorporating complex geometry with exceptional affordability. The modularity of our approach afforded us the flexibility to build multiple scales of these injectors from a basic building block (a single mixing-cup) affordably and expeditiously. We proposed to develop, build and test a large number of burners spanning a wide range of scales from small-scale single-cup premixers to 1 MW_{th} size premixers.

Lean conditions, coupled with multiple point injection for fast and efficient mixing were our primary vehicle for achieving low NOx emissions. In order to further reduce NOx levels, consideration was given to operability at ultra-lean conditions, where flame stability can become a concern. Stability augmentation was achieved through optimization of swirl and other aerodynamic features. Zone staging was also used to enhance lean operability for multi-cup, full-scale injectors.

Results

Building on micro-mixing cup designs that were demonstrated in Phase II to operate without flashback on 100% hydrogen at pressures up to 8 atm and temperatures up to 2,000 K, Parker developed and fabricated a 16-cup 1.3 MW_{th} multi-cup injector that was then used in the final full-scale combustion tests in Phase III. The injector is shown in Figure 1 along with an image of a single-cup injector module and a schematic showing the mixing cup design. The injector has four fuel feeds that supply fuel to a central pilot cup and two concentric mixing-cup zones that enable staging of the fuel flow during operation and independent control of the fuel-air ratio of the pilot. The injector was fabricated out of multiple layers of etched metal plates that are diffusion bonded to form a single monolithic metal injector with all manifolds that distribute fuel to the individual cups incorporated internal to the structure. Two variants of the full-scale injector were produced, differing only in the injector mounts. One of the injectors was used in atmospheric combustion tests at the University of California, Irvine while the other was used in high pressure full-scale testing at an original equipment manufacturer (OEM) facility.

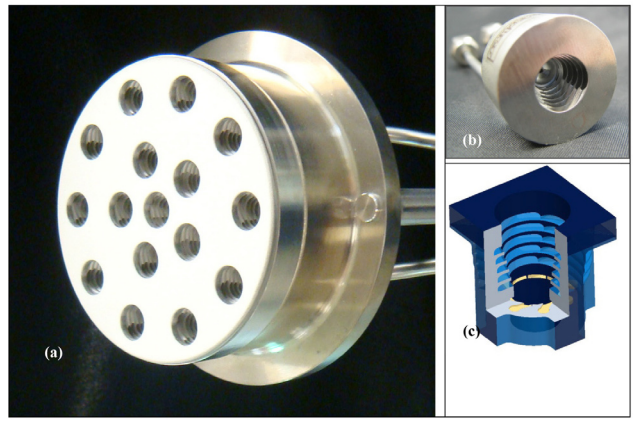

FIGURE 1. A 16-cup 1.3 MW_{th} micro-mixing (a) four-cup injector modules, (b) a single cup injector module used in development testing, and (c) a schematic showing the air circuit design.

The atmospheric tests focused on detailed measurements of fuel-air mixing in the individual mixing cups, and flame imaging and emissions testing when operating on 100% hydrogen with and without nitrogen dilution. The atmospheric tests were conducted in a staged mode with only the pilot cup or the center six cups of the injector fueled. Sample results from the fuel-air mixing studies are shown in Figure 2. For undiluted hydrogen fuel at an overall equivalence ratio of 0.5 - a fuel-air ratio typical of full-load operating conditions - the measurements showed a well distributed mixture over the cup exit area but with some islands of low fuel concentration that correspond to the location of nearby, up-stream air slots (Figure 2a). When 25% nitrogen dilution was added to the fuel, increased penetration of the hydrogen-nitrogen mixture to the core of the flow resulted in lower concentration near the cup walls and higher concentration in the core (Figure 2b). These results suggest that further optimization of the mixing cup design is possible to maximize the impact of diluents.

The full-scale tests focused on emissions and operability over a wide range of operating conditions and fuel mixtures of hydrogen and natural gas. The injector was operated at combustor pressures from 6.9 bar (100 psi) to 12.4 bar (180 psi) and inlet air temperatures from 615 K to 750 K (about 650°F to about 900°F), using mixtures ranging from 100% natural gas to 100% hydrogen with nitrogen or carbon dioxide as diluent. Excellent flashback resistance was demonstrated over the entire range of conditions and fuel mixtures that were tested, including in tests of 100% hydrogen fuel with 30% carbon dioxide dilution at operating pressure of 8.4 bar and flame temperature above 1,600 K. At the same time, superior part-load operability was also demonstrated for the hydrogen-natural gas fuel mixtures, with stable combustion achieved at flame temperatures as low as

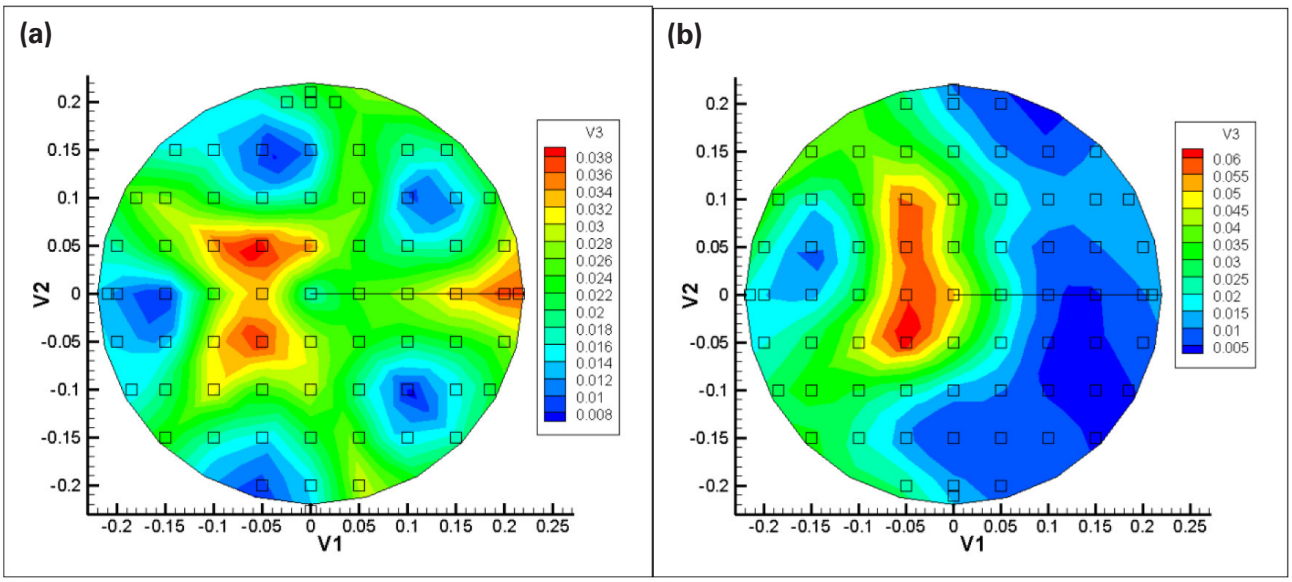

FIGURE 2. Mass fraction of hydrogen in a cross-section near cup exit measured at atmospheric conditions, 3.5% pressure drop and equivalence ratio of 0.5 (a) 100% hydrogen without dilution, (b) 75% hydrogen with 25% nitrogen.

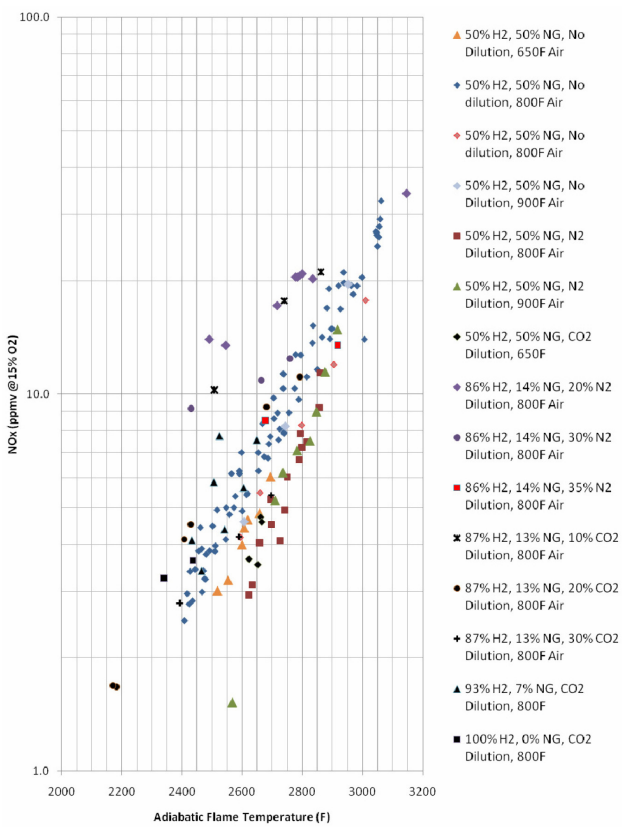

FIGURE 3. OEM full-scale test results for 1.3 MW_{th} hydrogen/syngas injector: NOx emissions (ppmv at 15% O_2) as a function of adiabatic flame temperature (°F) for 6.9 bar-12.4 bar operating pressure, 3.2%-4% pressure drop, and 650°F-900°F inlet air temperature) demonstrating ultra-low emissions (less than 3 ppmv) at multiple conditions at flame temperatures above 2,400°F and single-digit emissions up to temperatures of 2,900°F (1,860K).

1,590 K (2,402°F) for fuel mixture containing 50% hydrogen and as low as 1,425 K (2,105°F) on a fuel mixture containing 86% hydrogen. Carbon monoxide emissions remained well within 1 ppm at all conditions except when blow-off was immediately imminent. Part-load operation of the injector on 100% natural gas was more challenging when operating on all sixteen cups. However, operation in staged mode (e.g., on the center six cups of the injector) was not tested. For many conditions, the part-load operability was achieved without sacrifice of emissions. For instance, for a fuel mixture containing 87% hydrogen and 13% natural gas combined with 20% carbon dioxide dilution, the injector could be operated on all 16 cups at temperatures below 1,470 K (below 2,200°F) without the use of an enriched pilot, achieving NOx emissions well below 2 ppm.

Figure 3 summarizes the bulk of emissions data that was obtained at operating pressures of 6.9 bar (100 psi), 8.4 bar (120 psi) and 12.4 bar (180 psi) using various blends of hydrogen and natural gas. Figure 4 shows a reduced set of emissions data for clarity. Overall, the data shows excellent emissions results over a wide range of operating conditions and fuel mixtures. Air inlet temperature was shown to have only a minor impact on emissions (less than 1 ppm difference when raising the temperature from 615 K to 755 K (about 650°F to 900°F) and the emissions results were shown to be insensitive to operating pressure for the range tested. For fuel mixtures containing 50% hydrogen and 50% natural gas by volume, very consistent emissions trends were observed with emissions dropping steadily with increasing diluent content. Operating with this mixture without the use of dilution, NOx emissions of

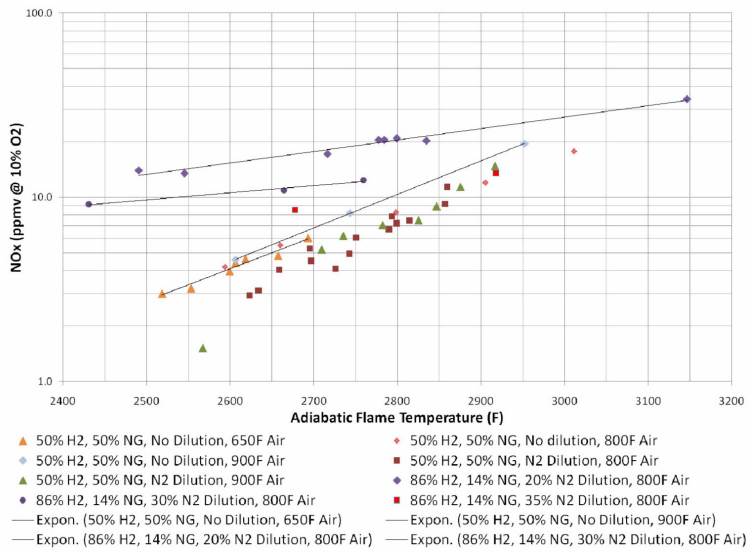

(a)

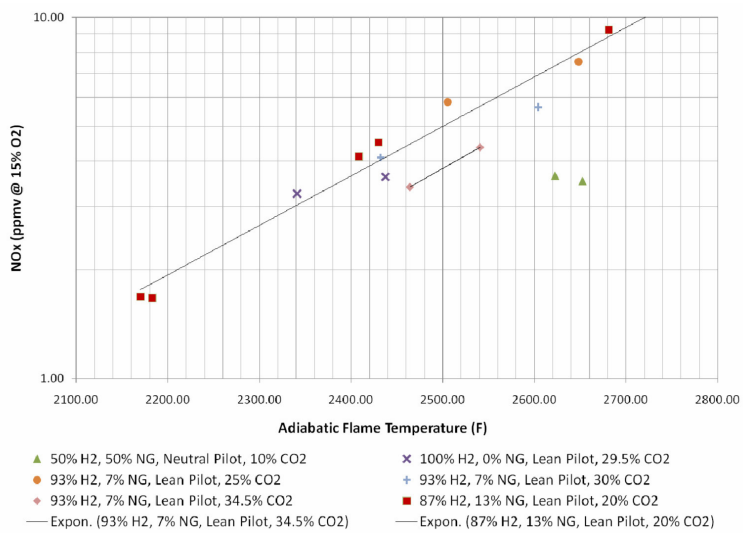

(b)

FIGURE 4. Subsets of emissions results for the 16-cup micro-mixing fuel injector operating on mixtures of hydrogen and natural gas; (a) data obtained without dilution and with nitrogen dilution (up to 40%), (b) data obtained with carbon dioxide dilution (up to 35%).

6 ppm were achieved at a flame temperature of 1,750 K (2,690°F) and ultra-low NOx emissions of 3 ppm were achieved when the amount of nitrogen dilution was increased to 40%. Using the same fuel mixture, 1.5 ppm NOx was achieved at a flame temperature of 1,680 K (2,564°F) with only 10% nitrogen dilution. For higher hydrogen content in the fuel (86% and higher), emissions remained close to 20 ppmv at the target flame temperature of 1,750 K (2,690°F) when small amounts of nitrogen dilution were used. Increasing the amount of nitrogen dilution to 35% reduced the emissions to 9 ppm at 1,750 K. Greater reduction in emissions was obtained using carbon dioxide as a diluent than was obtained using nitrogen. NOx emissions of 3.5 ppm were achieved at a flame temperature of 1,730 K (2,650°F) with only 10% carbon dioxide dilution. Also, using 100% hydrogen with 30% carbon dioxide dilution, 3.6 ppm NOx emissions were demonstrated at a flame temperature over 1,600 K (2,420°F). It is noted here that further testing on 100% hydrogen fuel was planned, pushing the flame temperature towards 1,900 K (2,960°F) and the operating pressure to 12.4 bar. However, the testing was cut short near the end of the test campaign due to a malfunctioning back-pressure valve in the test rig.

Conclusions and Future Directions

Parker has made substantial progress on developing scalable injectors for gas turbines. The full-scale injectors tested during this fiscal year have demonstrated superior NOx emissions, enhanced flame stability and no flashback at a wide range of operating pressures using high-hydrogen fuels. Excellent part-load operability was also demonstrated for high-hydrogen fuels, and emissions were shown to be insensitive to operating pressure. Program goals of 3 ppm NOx emissions were met at an adiabatic flame temperature of 1,750 K for a fuel mixture containing 50% hydrogen and 1.5 ppm NOx was demonstrated at a flame temperature of 1,680 K.

The excellent emissions and operability results obtained demonstrate the viability of the micro-mixing fuel injector concept for the challenging high-hydrogen content fuels. Parker maintains that the technology is easily adaptable to large-scale engines and future work will include developing larger-scale injectors in the tens of megawatt range. Now that the basic building block for this technology has been fully validated, new combustor concepts can be designed to take advantage of Macrolamination technology for a wide range of engines and combustion systems from annular to can-annular combustion systems. Further optimization work can include additional exploration of part-load operability for low-hydrogen fuels and natural gas. This can be accomplished through innovative cup arrangement and more elaborate fuel staging. Also,

further development of the mixing cup is anticipated to yield significant reduction in diluents use for high-hydrogen fuels, thereby reducing cost of operation while improving operability.

FY 2010 Publications/Presentations

1. "Micro-Mixing Lean Premix System for Ultra-Low Emission Hydrogen/Syngas Combustion," Presentation at the International Conference on Environmentally Preferred Advanced Generation (ICEPAG), Costa Mesa, California, February 9–11, 2010.

III.B.7 Compact and Streamlined Oxy-Syngas Reheat Combustor

Shahrokh Etemad (Primary Contact), Sandeep Alavandi, Benjamin Baird, and William C. Pfefferle
Precision Combustion, Inc. (PCI)
410 Sackett Point Rd.
North Haven, CT 06473
Phone: (203) 287-3700 x217; Fax: (203) 287-3710
E-mail: setemad@precision-combustion.com

DOE Project Manager: Mark Freeman
Phone: (412) 386-6094
E-mail: Mark.Freeman@netl.doe.gov

Contract Number: 85015

Start Date: June 30, 2008
End Date: August 13, 2011

FY 2010 Objectives

- Design and develop reheat injector for intermediate pressure turbine for oxygen, steam and syngas streams.
- Fabricate injector hardware and test performance at simulated engine conditions.
- Demonstrate no NOx emissions and equilibrium CO emissions within a short distance from the exit plane of the injector.
- Demonstrate injector capability to handle similar or lower pressure drop with low acoustics.

Accomplishments

- Analytical studies provided successful demonstration of the oxy-syngas injector:
  - Non-combusting mixing studies indicated mixing occurred within short distance – 2 inches from the exit of the injector with low unmixedness (<5%).
  - Combustion studies showed stable flame characteristics with high diluents.
  - Near equilibrium CO levels were reached within 3 inches from the injector exit.
  - No quenching of CO occurred and fast kinetics lead to reduced emissions.
- Kinetic studies for various steam/oxygen ratios for equilibrium CO levels with oxy-syngas mixtures were conducted using chemical kinetics software (Cantera).
- A poster was presented at the University Turbine Systems Research (UTSR) meeting in October, 2009 showing the key results of the oxy-fuel injector.
- Designing of steam/oxygen premixer for the oxy-fuel application is currently in progress.

Introduction

Concerns about global climate change due to CO_2 emissions from power generation (in particular coal) have led to significant interest in innovative power plant cycles [1]. Three CO_2 capture cycles currently under study are pre-combustion, post-combustion and oxy-fuel. Pre-combustion CO_2 capture is done by an upstream water-gas shift catalyst and a CO_2 absorber. In this the carbon-based fuel is converted to hydrogen for combustion. This demands a chemical plant for CO_2 removal that needs to be regenerated. Also, after CO_2 capture, there are issues of downstream H_2 combustion. Post-combustion CO_2 capture is done downstream of the plant using a scrubber removing CO_2 from the flue gases. This needs multiple components to be integrated on the downstream end, leading to efficiency penalties [2]. The third cycle is oxy-fuel combustion that removes the nitrogen component from the air and combusts the fuel (natural gas or syngas) directly with oxygen using steam as diluent producing steam and CO_2 as working fluid. This cycle has significant advantages compared to the other two technologies for CO_2 capture. Firstly, use of oxygen, fuel, and steam for combustion produces an exhaust stream consisting of primarily CO_2 and H_2O that makes sequestration simple through condensing the water out. This eliminates the need to use expensive CO_2 separation units. This is in contrast to conventional combustors using air as the oxidant having product gases with a high nitrogen concentration and low CO_2 concentration leading to efficiency penalties due to N_2 separation. Secondly, using pure oxygen has the binary benefit of near zero NOx emissions. Thirdly, since no emissions are generated hence no expensive exhaust stack clean-up is required, leading to further cost savings [3-6]. In summary, oxy-fuel power plants have the potential to re-define the power production industry.

Oxy-fuel combustion technology offers both the benefits of zero-emission power generation coupled with economical carbon capture and storage effectively. However, in order to boost cycle efficiency levels equal to or greater than other fossil fuel power generating cycles, the reheat combustor is a critical component that needs to be integrated. A robust reheat combustor capable of driving the working fluid temperature

necessitates innovative injector/combustor design and advanced liner cooling techniques and material. Currently there is no existing re-heat combustor design that can operate in the harsh steam/CO_2 environment expected in the cycle. PCI's unique design approach addresses and resolves these key challenges.

Approach

PCI's novel injector for oxy-syngas reheat combustion provides fast and efficient steam/O_2/syngas mixing and complete CO burnout using its distinctive mixing and flame zone design. This system can effectively mix the fluid streams (the steam-rich high-pressure turbine exhaust, O_2 and syngas) in a unique design delivering ultra-low unmixedness and establishing a stable flame zone. This novel design enhances combustion, avoids excess O_2, reduces CO quenching, avoids high local primary zone temperatures, and reduces combustion acoustics. This technology offers the potential to be simple, robust and cost-effective as a reheat combustor for the high temperature working fluid of an intermediate-pressure steam/CO_2 turbine thus enabling higher cycle efficiencies.

Results

Analytical Results

Analytical studies provided successful demonstration of the oxy-syngas injector:

a) The analysis confirmed that the reactants become perfectly mixed (less than 5% unmixedness) within two inches from the exit of the mixing plane corresponding to 2 milliseconds residence times respectively demonstrating rapid mixing of the design.

b) Reacting flow simulations showed a flame strongly attached to the end of the injector exit plane for two different reaction models. This gave confidence that the flame will show stability and robustness in actual operation.

c) Computational fluid dyanmics analysis was conducted and low mole fractions of CO were achieved within a short distance (3 inches) from the injector exit plane.

Technical Poster Presentation

Based on the successful results obtained from the Phase I analytical studies, a poster was presented at the UTSR meeting in October, 2009. Results showing low unmixedness (<5%) and equilibrium CO emissions close to the injector exit and stable flame characteristics with high diluents were presented at the meeting. The poster presentation was well received.

Evaluation of Test Conditions and Injector

PCI is in the process of down-selecting the injector dimensions and design for fabrication of the injector for testing. The injector design with minimum pressure drop and enhanced mixing characteristics will be fabricated based on the analytical results. The oxygen/steam premixer designs are being reviewed and evaluated.

Test Facility for Subscale testing

PCI has contacted DOE/National Aeronautics and Space Administration (NASA) for test facility availability. Also, other technical inputs were obtained for the subscale testing from these agencies for testing at the NASA Plum Brook facility. Based on these discussions it was concluded that testing at NASA facility may not be a viable option.

PCI is currently in contact with Clean Energy Systems (CES) for availability of the reheat test facility. A few meetings have been held discussing the feasibility and the cost estimate for testing PCI's reheat injector at CES' test facility.

Conclusions and Future Directions

PCI will expand on the success of Phase I work by demonstrating the performance of the novel injector system in subscale testing. A module will be fabricated and tested to demonstrate stable combustion and low emission performance. At the conclusion of Phase II, an optimized single injector module will be fabricated for testing at a high pressure/temperature test facility at simulated engine conditions in a Phase III project. The work plan is designed to demonstrate high pressure full-scale simulated engine testing readiness by addressing the key technical challenges of aerodynamics, mechanical robustness, emissions, and reliability with stable system performance.

Special Recognitions & Awards/Patents Issued

1. One patent application has been submitted.

FY 2010 Publications/Presentations

1. S. Etemad, S. Alavandi, B. Baird, and W.C. Pfefferle, "Compact Streamlined Oxy-Syngas Reheat Combustor," Poster presentation at UTSR-2009, Orlando, Florida, October 2009.

References

1. K. Zanganeh, A. Shafeen, M. Gupta, E. Ogedengbe, and M. Mitrovic, "Gas Turbine Integrated High Efficiency Oxy-Fuel Combustion Process with CO_2 Capture," ASME GT2008-51456.

2. Jordan, Haywood, "Oxy-Fuel Combustion Cycle for CO_2 Capture," A&WMA Florida Section Annual Conference, Deerfield Beach, Florida, October 2007.

3. B. Buhre, L. Elliott, C. Sheng, R. Gupta, and T. Wall, "Oxy-Fuel Combustion Technology for Coal Fired Power Generation," Progress In Energy and Combustion Science, vol. 31, 2005, pp. 283-307.

4. R. Anderson, S. Macadam, F. Viteri, D. Dvies, J. Downs, and A. Paliszewski, "Adapting Gas Turbines for Zero Emission Oxy-Fuel Power Plants," ASME GT2008-51377.

5. R. Anderson, S. Doyle, and K. Pronske, "Demonstration and Commercialization of Zero Emission Power Plant," 29th International Technical Conference on Coal Utilization and Fuel Systems, Florida, USA.

6. J. Martinez-Frias, S. Aceves, J. Smith, and H. Brandt, "A Coal Fired Power Plant with Zero Atmospheric Emissions," 2003 ASME International Mechanical Engineering Congress and RD&D Expo, Washington D.C., 2003.

III.B.8 Catalytic Combustion for Ultra-Low NOx Hydrogen Turbines

Shahrokh Etemad (Primary Contact), Benjamin Baird, Sandeep Alavandi, and William C. Pfefferle
Precision Combustion, Inc. (PCI)
410 Sackett Point Rd.
North Haven, CT 06473
Phone: (203) 287-3700; Fax: (203) 287-3710
E-mail: setemad@precision-combustion.com

DOE Project Manager: Robin Ames
Phone: (304) 285-0978
E-mail: Robin.Ames@netl.doe.gov

Subcontractor:
Leonel O. Arellano and Ram Srinivasan
Solar Turbines, Inc., San Diego, CA

Contract Number: 42647

Start Date: October 1, 2005
End Date: June 31, 2011 (extension requested)

FY 2010 Objectives

- Demonstrate NOx < 2 ppm, for megawatt-scale hydrogen gas turbine application.
- Same or lower pressure drop (4%) than existing gas turbine.
- Focus on hydrogen with fuel flexible capability: natural gas, syngas.
- New and retrofit machines (sized to fit existing combustor envelope).
- Meet 24,000-hour life requirement.
- Allowance for single injector fabrication and testing by utility original equipment manufacturers (OEMs).

Accomplishments

Accomplishments for the Fiscal Year 2010 are as follows:

- Atmospheric flow testing of the performance parameters of the full-scale Rich Catalytic Hydrogen (RCH) module was completed at PCI. Based on this testing, modifications to the next generation (Gen III) hardware have been identified and will be implemented.
- Solar Turbines, Inc. has identified leaks in its H_2-diluent mixing test facility and are completing the repair. Upon fixing the leaks and shakedown of the test facility, hydrogen combustion testing is being conducted. Targeted date for testing the RCH module is July-August 2010.
- Presented results of the sub-scale RCH module and initial atmospheric testing of the full-scale RCH module at the International Colloquium on Environmentally Preferred Advanced Power Generation (ICEPAG) 2010 conference. The presentation was well received.
- A project design review with DOE staff was held during January 2010. Discussed project status and technical progress. Identified issues with the current RCH build and discussed improvements and solutions.

Introduction

The project is progressing towards a full-scale, high-pressure, single-injector demonstration of an ultra-low-NOx rich-catalytic system for fuel-flexible hydrogen combustors in megawatt-scale turbines. This is being achieved by developing PCI's rich catalytic combustion technology for fuel-flexible hydrogen applications, in collaboration with Solar Turbines, Inc. This technology, in a previous DOE project, demonstrated sub-scale ultra-low NOx emissions with syngas and with fuel mixtures comprised of hydrogen diluted with nitrogen (sub-scale tests at PCI demonstrated low single-digit NOx - corrected to 15% O_2) with operation at integrated gasification combined cycle (IGCC) baseload combustor temperatures and 10 atm rig pressure). The successful achievement of the project objectives will lead to combustors capable of delivering near-zero NOx without costly post-combustion controls and without added requirements for sulfur control. This advances DOE's objectives for achievement of low single-digit NOx emissions, improvement in efficiency versus post-combustion controls, fuel flexibility, a significant net reduction in IGCC system net capital and operating costs, and a route to commercialization across the power generation field.

The work plan is divided into three phases. Phase I (completed) involved the development of conceptual designs for catalytic combustion technology for hydrogen fuel and the production of a detailed research and development implementation plan. Phase II (ongoing), Detailed Design and Validation Test Program, concentrates on development of full-scale module for validation (high-pressure rig) testing, and the resolution of key performance and durability issues. Phase III will include full-scale testing conducted at an OEM gas turbine company.

Approach

To achieve the project objectives, PCI, in close collaboration with Solar Turbines, Inc., is developing its catalytic combustion system for hydrogen fuel and for fuel-flexible operation in megawatt gas turbines. Conceptually, the efforts centers around three primary system functions: premixing, catalytic reaction, and gas-phase reaction (combustion). These primary systems need to be integrated with each other in a manner that resolves potential issues of flashback, autoignition, flame holding, and flame stabilization. Related scale-up issues must also be considered as the system is integrated into an engine. The overarching goal throughout the project is to achieve ultra-low NOx emissions below 2 ppm with good engine performance and operability using multiple fuels.

Results

For combustion of natural gas, PCI has developed and demonstrated, in an engine (Saturn and Taurus 70), a Rich-Catalytic Lean-burn (RCL®) combustion system capable of delivering low single digit NOx emissions. Similarly, NOx emissions close to 2.5 ppm was demonstrated in a Taurus 70 engine using natural gas at full load with an RCL® system in the injector pilot stream. The RCL® system is based on the concept of stabilizing combustion with catalytically-reacted fuel and air having a temperature below the instantaneous autoignition temperature [1]. The combustion air stream is split into two parts upstream of the catalyst. One part is mixed with all or the majority of the fuel and contacted with the catalyst, while the second part of air is used to backside cool the catalyst. At the exit of the reactor, the catalyzed fuel/air stream and the cooling flow are combined to finalize combustion. Rich catalytic hydrogen combustion has been shown to offer the same low NOx advantage for hydrogen fuel in tests completed at PCI.

Sub-Scale Testing

Sub-scale testing at 10 atm, of a rich catalytic hydrogen reactor design that closely approximated the selected engine hardware design showed good performance achieving low single-digit NOx levels at full load and good combustor stability and turndown. The reactor design has been optimized to produce greater catalytic conversion and has been down-selected and implemented in the full-scale reactor module.

Figure 1 shows the NOx emissions data for hydrogen reactors obtained for two injector configurations in the Gen II design. Both Gen II Injectors (A and B) achieved 2-3 ppm NOx emissions for fuel mixtures of 42 and 52% hydrogen. Injector A achieved a wide turndown (~500°F) with NOx emissions <1 ppm for 42% H_2. A stable downstream flame could be achieved due to increased reaction in the catalyst bed.

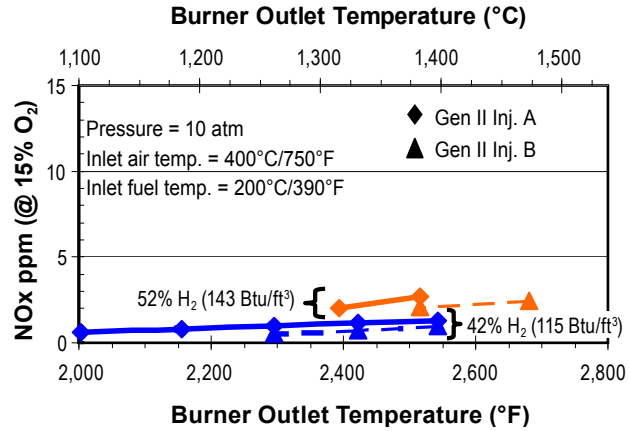

FIGURE 1. Results of Sub-Scale Reactor Showing Low Single Digit NO_x Emissions and Wide Turndown for Gen II Injectors (Tests completed at PCI)

Hardware Fabrication

PCI has completed fabrication of the full-scale catalytic injector hardware after design optimization. The RCH module was designed and fabricated by PCI and the pilot was designed by Solar Turbines, Inc. The complete module was assembled and fabricated by PCI.

Atmospheric Flow Testing of the Full-Scale RCH Module with Pilot

Atmospheric flow testing was conducted for the full-scale module for injector validation at PCI as shown in Figure 2. Unmixedness, effective areas, catalytic temperatures and start-up testing with natural gas was conducted. Effective areas and catalytic operating temperatures were within the expected regime. Pilot stability and start-up was successfully demonstrated with natural gas and the operating regime for the pilot was determined. Atmospheric testing of the full-scale module at PCI showed higher than expected unmixedness. PCI has analyzed these data and modifications/improvements have been identified. In the second round of full-scale module fabrication PCI will implement tighter manufacturing tolerances to improve unmixedness. Also, improvements to the fuel inlet section may also be considered.

Solar Turbines, Inc. High-Pressure Test Facility

Solar Turbines, Inc. conducted preliminary tests to identify potential issues with its high-pressure

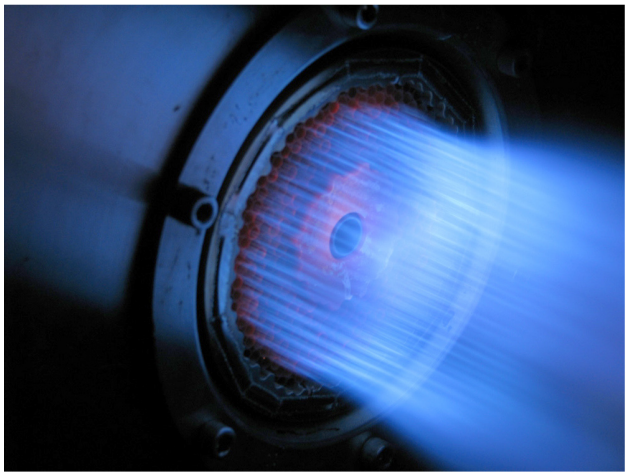

FIGURE 2. Atmospheric RCH Operation

H_2-diluent blending test facility. Based on these tests leaks were found in the blending system. Solar Turbines, Inc. is completing the repair. Upon repairing the leaks H_2-diluent mixture will be run through the test facility to check for safe operation. A shakedown testing will be conducted to ensure reliability of the test facility. After performing shakedown, combustion testing will be conducted with the full-scale RCH module (July-August 2010).

Conclusions and Future Directions

- Successfully demonstrated < 2 ppm NOx emissions with sub-scale testing.
- Full-scale high single injector reactor and pilot fabricated.
- Successful completion of atmospheric flow testing at PCI lead to identification of improvements needed in the next generation full-scale module that will be implemented.
- This full-scale injector will be installed at Solar Turbines, Inc. high-pressure rig and performance will be demonstrated, including transition from methane startup to full hydrogen-mix fuel operation.
- High-pressure single-injector testing will be conducted at Solar Turbines, Inc. upgraded test facility.

FY 2010 Publications/Presentations

1. Presented "Rich Catalytic Combustion for Ultra-Low NOx Hydrogen Turbines," February 9-11, 2010, Costa Mesa, California, ICEPAG2010.

2. DOE Program Progress Review, January 29, 2010.

References

1. L.L. Smith, H. Karim, M.J. Castaldi, S. Etemad, W.C. Pfefferle, V. Khanna, and K.O. Smith (2005), "Rich-Catalytic Lean-Burn Combustion for Low-Single-Digit NOx Gas Turbines," Journal of Engineering for Gas Turbines and Power, vol. 127, pp. 27-35.

III.B.9 Reduced and Validated Kinetic Mechanisms for Hydrogen-CO-Air Combustion in Gas Turbines

Professor Yiguang Ju (Primary Contact),
Professor Frederick L. Dryer, Michael P. Burke
Princeton University
D115 Equad, Olden Street
Princeton, NJ 08544
Phone: (609) 258-5644; Fax: (609) 258-6233
E-mail: yju@princeton.edu

DOE Project Manager: Mark Freeman
Phone: (412) 386-6094
E-mail: Mark.Freeman@netl.doe.gov

Contract Number: 42716

Start Date: January 1, 2006
End Date: December 31, 2009

FY 2010 Objectives

- Measure flame speed and burning rate data of $H_2/CO/CO_2$ mixtures at high pressure and low flame temperature conditions characteristic of gas turbine engines.
- Develop and validate chemical models for $H_2/CO/CO_2$ combustion for use in the numerical design of low-emission syngas turbine combustion systems.
- Construct new methodologies to reduce computational time for combustion calculations to make detailed engine simulations feasible.

Accomplishments

- Extended experimental data set for high pressure, low flame temperature syngas flames to cover *lean* mixtures of more direct interest to typical syngas turbine conditions, employing a parametric approach by individually varying:
  - Pressure: 1 to 25 atm
  - Flame temperature: 1,400 to 1,800 K
  - Equivalence ratio: 0.3 to 1.0
- Experimental measured and numerically simulated the pressure dependence of H_2 burning rates experimentally and numerically and identified the existence of *negative pressure dependence* in the measured burning rates at high pressure, low flame temperature conditions for lean mixtures.
- Demonstrated significant deficiencies in current state-of-the-art kinetic models in predicting relevant syngas flame behavior.
- Identified key kinetic pathways in high pressure, low flame temperature flames, potential for previously unconsidered pathways, and possible areas for improvement in kinetic modeling.
- Conducted efforts to improve model performance have been conducted with our collaborators in the elementary reaction kinetics field. Preliminary model results show improved agreement with high-pressure flame predictions; continuing efforts are underway to enhance extendibility to more general conditions.
- Formulated and tested strategies that reduce computational time in combustion calculations by over an order of magnitude.

Introduction

Although renewable energy sources will have a growing share in the energy market, we will still need to rely on fossils fuels as a major energy source for many years. With more stringent environmental standards and climate change concerns, coal-based integrated gasification combined cycle systems for generation of syngas, hydrogen, and electricity offer opportunities to control air pollutant emissions, achieve high energy conversion efficiencies, and sequester carbon. In gas turbine engines, low flame temperatures are utilized to reduce the NO_x emissions, which are formed more readily at higher temperatures.

A successful design of reliable and efficient gas turbine engines operating on high hydrogen content sygnas fuels strongly depends on the knowledge of the combustion properties of syngas at actual gas turbine conditions and on the availability of reliable chemical kinetic models for numerical modeling. Unfortunately, very limited experimental data of syngas and hydrogen burning properties such as flame speeds and burning rates at typical gas turbine pressures are currently available. Most available high pressure data do not focus on low flame temperature conditions. Consequently, no kinetic model for syngas and hydrogen combustion has been validated against flame speeds and burning rates for low flame temperatures over an extensive range of conditions. Therefore, there exists a great need for more experimental data and validated models for high pressure, low flame

temperature conditions. Additionally, methods to reduce computational time using these validated syngas models are necessary to facilitate utilization of engine simulations in the design process.

Approach

Experiments are conducted in a high pressure, dual-chambered cylindrical bomb developed in our lab [1]. Mixtures of H_2, O_2, and other diluents are prepared using the partial pressure method. Outwardly propagating spherical flames are initiated by a spark across two electrodes at the center of the chamber. Evolution of the flames is filmed using high-speed Schlieren photography. The radius of the flame front as a function of time is measured from the images, such that the flame speed and mass burning rate can be extracted from the experiments using improved methodologies developed in the course of this study [2].

Experimental values for flame speed and burning rate are obtained from the experiment over a variety of conditions. Conclusions are drawn from the trends in the experimental data. The measured values are compared with the predicted values by available chemical models. If agreement is acceptable, the model is considered validated for use at those conditions. If agreement is poor, the model must be revised to yield acceptable agreement at those conditions.

In order to reduce computational time for combustion calculations, a dynamic multi-scale (DMS) kinetic reduction method has been developed which solves for each species with a time step appropriate for its characteristic time scale. In such a way, "fast" species are calculated with smaller time steps and "slow" species are calculated with larger time steps. Consequently, the number of time steps for which all species is calculated is reduced.

Results

The experimental data for flame speeds and burning rates was significantly extended to cover a wide range of *lean* mixtures: pressures from 1 to 25 atm, equivalence ratios from 0.3 to 1.0, and flame temperatures from 1,400 to 1,800 K. Figure 1 shows experimentally measured burning rates for $H_2/O_2/He$ flames of various equivalence ratios with the diluent varied for each case to achieve flame temperatures near 1,400 K. The results demonstrate a pressure-dependent trend with equivalence ratio when dilution is varied to maintain the same flame temperature – at low pressures the burning rate increases with equivalence ratio and at higher pressures the burning rate decreases with equivalence ratio. None of the state-of-the-art kinetic models for syngas combustion predict the observed trends.

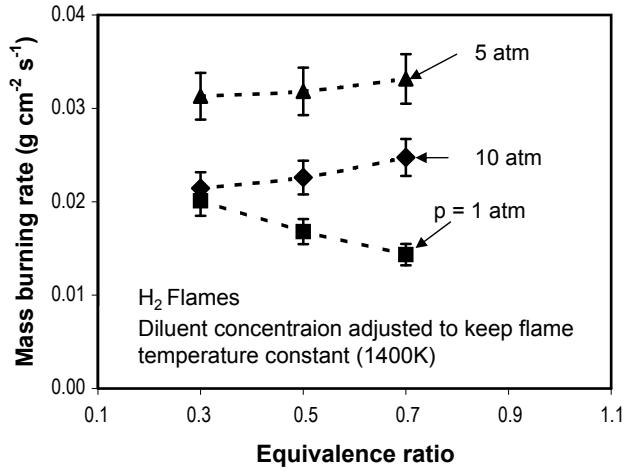

FIGURE 1. Mass Burning Rates for H_2 Mixtures at Various Equivalence Ratios and Pressures with Dilution Varied to Maintain the Same Flame Temperature (1,400 K)

Figure 2 presents the mass burning rates for an equivalence ratio 0.3 with sufficient diluent to achieve a flame temperature near 1,400K. The data indicate that *negative reaction orders* are present for the dependence with pressure. While the burning rate increases with pressure up to ~5 atm, the burning rate decreases with pressure increase thereafter. Non-monotonic pressure dependences for the mass burning rate are somewhat unusual.

Measured mass burning rates are compared to predictions using two recently published, extensively validated kinetic models [3-4] in Figure 2. The two models demonstrate reasonable agreement with the experimental data 1 atm. For higher pressures, however, there exist large disparities between the measured and predicted burning rates. In fact, at 10 atm, the disagreement between experimental data and kinetic models reach a factor of two.

Numerical analysis of the sensitivity of predicted burning rates to elementary reaction rates was conducted in order to identify the key reaction pathways and the likely sources of disagreement. Sensitivity coefficients are plotted in Figure 3. The results indicate high importance of competition between $H+O_2(+M)=HO_2(+M)$ and HO_2+H/O/OH/HO_2 with the main branching reactions. Further analyses show that high pressure, low flame temperature flames of relevance to gas turbine combustion emphasize different temperature and pressure regions of elementary reaction rates than typically used for kinetic model validation. In particular, large uncertainties remain in the pressure and bath gas dependence of $H+O_2(+M)=HO_2(+M)$ and the temperature dependence of HO_2+ H/O/OH/HO_2 reactions.

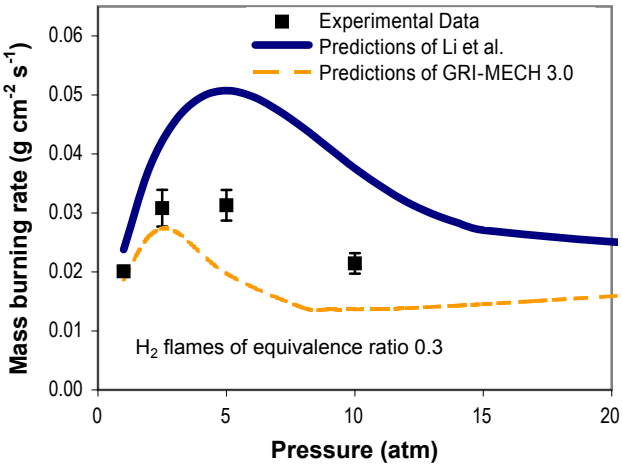

FIGURE 2. Mass Burning Rates for Lean H_2 Mixtures at High Pressures and Low Flame Temperatures

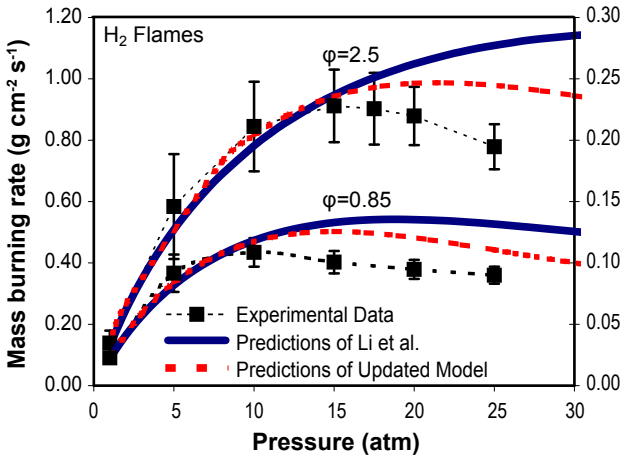

FIGURE 4. Exemplar Performance of the Updated Kinetic Model Against High Pressure, Low Flame Temperature Flame Targets

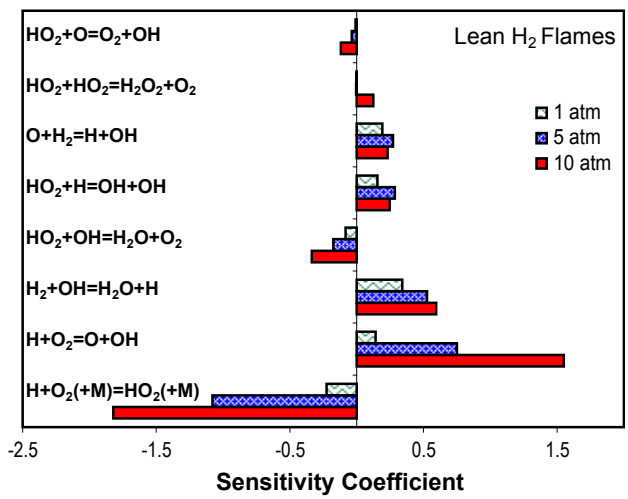

FIGURE 3. Sensitivity of Model Predictions for Burning Rate to Elementary Reaction Rate Constants

The kinetic model of Li et al. [3] was updated to incorporate improved rate constants for several key reactions, including $H+HO_2=H_2+O_2$ and $H+OH+M=H_2O+M$. The updated model reproduces the homogeneous validation targets used in Li et al., flame speed validation targets used in Li et al. within ~10%, and the recent dilute high-pressure burning rate measurements conducted during the course of this project [5] within ~25%. Exemplar improvements to high pressure, low flame temperature syngas flames are shown in Figure 4. Continuing efforts are underway to enhance extendibility to more general conditions that encompass ignition delays and a greater range of parameter space for flames. We are working to improve the representation of $H+O_2(+M)=HO_2(+M)$ in multi-component bath gases, incorporate more accurate expressions for HO_2+H/O/OH/HO_2, and include better descriptions of H atom diffusion coefficients.

The dynamic multi-scale modeling technique was implemented and validated for hydrogen ignition computations. The technique reduces the computational time by an order of magnitude.

Conclusions and Future Directions

The experimental dataset for flame speeds and burning rates was significantly extended to encompass a wider range of *lean* mixtures of more direct interest to syngas combustion in gas turbine engines: pressures from 1 to 25 atm, flame temperatures from 1,400 to 1,800 K, equivalence ratios from 0.3 to 1.0. *Negative pressure dependence* was observed for burning rates in H_2 flames at high pressure, low flame temperature conditions. Predictions using kinetic models available in the literature for the flame speed and burning rate exhibit good agreement with the measured data at atmospheric pressure, though demonstrate significant deficiencies at high-pressure, low-flame-temperature conditions. Key kinetic pathways in high pressure, low flame temperature flames, potential for previously unconsidered pathways, and possible areas for improvement in kinetic modeling were identified. An updated kinetic model was constructed to improve representation of the key elementary reactions based on recent fundamental kinetic studies. The updated model was validated against all of the previous targets for homogenous kinetics used in Li et al., and shows improve agreement against high-pressure flame targets, particularly at low flame temperatures. Continuing efforts are underway to enhance extendibility to more general conditions that encompass ignition delays and a greater range of parameter space for flames.

A DMS modeling approach was developed, validated, and demonstrated to reduce computation time for hydrogen ignition calculations by an order of magnitude.

Selected FY 2010 Publications/Presentations

1. M.P. Burke, M. Chaos, F.L. Dryer, and Y. Ju, "Negative pressure dependence of mass burning rates of $H_2/CO/O_2$/diluent flames at low flame temperatures," *Combustion and Flame* 157 (2010) 618–631.

2. M.P. Burke, F.L. Dryer, and Y. Ju, "Assessment of kinetic modeling for lean $H_2/CH_4/O_2$/diluent flames at high pressures," *Proceedings of the Combustion Institute* (2010) accepted for publication.

3. M.P. Burke, M. Chaos, Y. Ju, and F.L. Dryer, "An updated model and discussion of modeling challenges in high-pressure H_2/O_2 flames," Spring Technical Meeting of the Combustion Institute, Boulder, Colorado, March 2010.

4. M.P. Burke, F.L. Dryer, and Y. Ju, "Negative pressure dependence of high pressure burning rates of H_2/O_2 flames at lean conditions," 48th AIAA Aerospace Sciences Meeting and Exhibit, Orlando, Florida, January 2010.

5. M. Chaos, M.P. Burke, Y. Ju, and F.L. Dryer, "Syngas chemical kinetics and reaction mechanisms," Synthesis Gas Combustion: Fundamentals and Applications. Ed. T.C. Lieuwen, V. Yang, R.A. Yetter. Taylor & Francis (2009), p. 29-70.

6. M.P. Burke, M. Chaos, F.L. Dryer, and Y. Ju, "Development and validation of chemical kinetic mechanisms for synthetic gas combustion in gas turbines," 2nd International Forum on Multidisciplinary Education & Research for Energy Science, Okinawa, Japan, December 2009.

References

1. X. Qin, Y. Ju, *Proceedings of the Combustion Institute* 30 (2005) 233-240.

2. M.P. Burke, Z. Chen, Y. Ju, and F.L. Dryer, *Combustion and Flame* 156 (2009) 771-779.

3. J. Li, A. Kazakov, Z. Zhao, M. Chaos, F.L. Dryer, and J.J. Scire, *International Journal of Chemical Kinetics* 39 (2007) 109-136.

4. G.P. Smith, D.M. Golden, M. Frenklach, N.W. Moriarty, B. Eiteneer, M. Goldenberg, C.T. Bowman, R.K. Hanson, S. Song, W.C. Gardiner Jr., V.V. Lissianski, and Z. Qin, GRI-MECH 3.0. Available at: <http://www.me.berkeley.edu/gri_mech/>.

5. M.P. Burke, M. Chaos, F.L. Dryer, and Y. Ju, *Combustion and Flame* 157 (2010) 618–631.

III. ADVANCED RESEARCH

C. Materials

III.C.1 Materials Performance in High CO_2 + Steam Environments

Gordon R. Holcomb
National Energy Technology Laboratory (NETL)
1450 Queen Ave. SW
Albany, OR 97321
Phone: (541) 967-5874; Fax: (541) 918-4494
E-mail: Gordon.Holcomb@netl.doe.gov

Contract Number: FY10.MSE.1610243.682

Start Date: October 1, 2009
End Date: September 30, 2010

FY 2010 Objectives

- Determine how oxidation mechanisms differ in the mixed oxidant oxy-combustion environments on alloys of interest for oxy-fuel turbine systems.
- Focus on oxygen activity in the mixed oxidant environment as to how it influences the role of CO_2 and H_2O on oxidation.

Accomplishments

- Analyzed the prior year's exposure test samples and determined that the Ni-base alloys, especially at 748°C and below, exhibit low corrosion rates with parabolic behavior. In terms of effective metal loss, internal oxidation is the primary factor for the nickel-base alloys.
- The cobalt-base alloys are more of a concern, with a tendency towards oxide spallation.
- Coated materials (a bond coat and a thermal barrier coating [TBC]) experienced only a modest amount of growth of the thermally grown oxide (TGO) and loss of Al from the bond coat.
- Carburization was not observed for these alloys. The chromia and alumina scales that form have such low permeabilities for CO_2 and CO that the activity of carbon at the oxide/metal interface was not sufficient to form carbides.

Introduction

The goal of the overall turbine research at NETL is to develop oxy-fuel turbine and combustor technologies for highly efficient (50-60 percent), near zero emissions, coal-based power systems. Oxy-fuel combustion, which burns fuel in oxygen rather than in air, has a distinct advantage of generating combustion gas with a much higher percentage of CO_2 than conventional systems. This higher percentage of CO_2 allows for easier and more efficient carbon capture. Further development of this technology will push the temperatures higher. Conventional steam turbines are proposed for use as the high-pressure turbine (HPT) and low-pressure turbine (LPT).

Materials issues related to higher efficiency power plants, like hydrogen or oxy-fuel fired gas turbines, require materials with higher temperature capability than the current generation of turbines. Research to extend the usable critical temperature of nickel superalloys has been focused maintaining the strength and integrity of grain boundaries and the interface between the grain boundary phases (carbide and/or topologically close-packed) and the matrix, as well as improving the long-term stability of fine strengthening precipitates at the use temperature. Concurrent with achieving these goals is to understand how temperature, stress, and environment affect grain boundary, matrix and surface/coating interface stability as a consequence of exposure to the gas turbine environment.

Approach

This project continues the research from Fiscal Year 2009 to examine and understand the behavior of alloys used in the SGT-900 in oxy-fuel environments to qualify its use as the intermediate pressure turbine in one of the proposed oxy-fuel systems [1]. Analysis of oxidation coupon specimens is also continued.

The understanding of environment-material interactions occurring in oxy-fuel turbine environments will be broadened by examining the role of oxygen in multiple oxidant environments. Additional oxidation coupons and low cycle fatigue (LCF) specimens will be exposed in steam with 10% CO_2 and three oxygen activities. The test matrix (Table 1) shows seven alloys (two Co-base superalloys ECY 768 and X45, three Ni-base superalloys IN 738, IN 939, and U520, and two ferritic steels T91 and T92) with three types of samples (LCF, bare oxidation coupons, and oxidation coupons coated with a bond coat and TBC).

Results

The set of exposures for FY 2010 are to commence in July, 2010. The analyses of the FY 2009 oxidation coupons (both bare and coated) form the basis of the efforts thus far in FY 2010. The FY 2009 exposures were in the medium oxygen activity (H_2O-10%CO_2-0.2%O_2) at temperatures ranging from

630°C to 821°C. The alloys are the two Co-base and three Ni-base alloys as shown in Table 1.

In general, the amount of oxidation on these alloys is relatively low. Bare Ni-base alloys, especially at 748°C and below, exhibit low corrosion rates with parabolic behavior. At 821°C, the Ni-base alloys showed significantly higher oxidation rates, but still with protective parabolic kinetics. Internal oxidation of the Ni-base alloys was more extensive, in terms of effective metal loss, than the direct surface oxidation. Figure 1 is a back-scatter election (BSE) scanning electron microscopy (SEM) image of IN 939 after exposure in H_2O + 10% CO_2 + 0.2% O_2 at 821°C for 1,000 hr. Images with BSE show atomic weight contrast–lighter elements appear darker and heavier elements appear brighter. Figure 1 shows the external Cr_2O_3 scale, internal Al_2O_3 oxidation, and an advancing front of Al depletion below the internal oxidation.

The Co-base alloys are more of a concern, with a tendency towards oxide spallation. Figure 2 shows a spall location, where the Cr_2O_3 surface oxide is cracked and a section has detached. Unlike the Ni-base alloys, the Co-base alloys do not have significant amounts of Al and so showed little internal oxidation.

The coated specimens showed only a modest amount of growth of alumina at the bond coat and TBC interface–termed a thermally grown oxide. This is illustrated in Figure 3. There were only modest amounts of Al losses from the bond coat.

TABLE 1. FY 2010 Test Matrix for 1,000-Hour Exposures in Three Oxygen Activity Levels: Low (L) H_2O-10%CO_2-2%(N_2+4%H_2), Medium (M) H_2O-10%CO_2-0.2%O_2, and High (H) H_2O-10%CO_2-2%O_2

		ECY 768			X45			IN 738			IN 939			U520			T91			T92		
	O_2	L	M	H	L	M	H	L	M	H	L	M	H	L	M	H	L	M	H	L	M	H
630°C	LCF														14							
	Ox Bare	2	2	2	2	2	2	2	2	2	2	2	2	2	2	2	2	2	2	2	2	2
	Ox TBC	2	2	2	2	2	2	2	2	2	2	2	2	2	2	2						
750°C	LCF					14																
	Ox Bare	2	2	2	2	2	2	2	2	2	2	2	2	2	2	2	2	2	2	2	2	2
	Ox TBC	2	2	2	2	2	2	2	2	2	2	2	2	2	2	2						

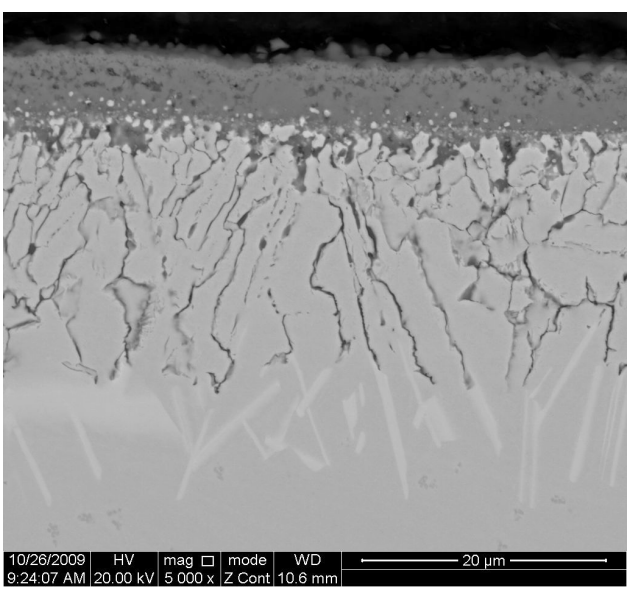

FIGURE 1. Cross-section BSE SEM image of uncoated IN 939 after exposure in H_2O + 10% CO_2 + 0.2% O_2 at 821°C for 1,000 hr.

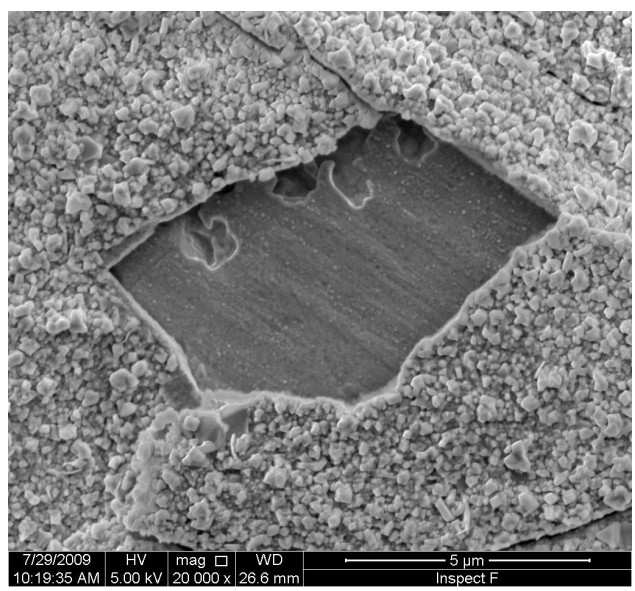

FIGURE 2. Surface image at a spall location of X-45 after 500 hr exposure in H_2O + 10% CO_2 + 0.2% O_2 at 693°C.

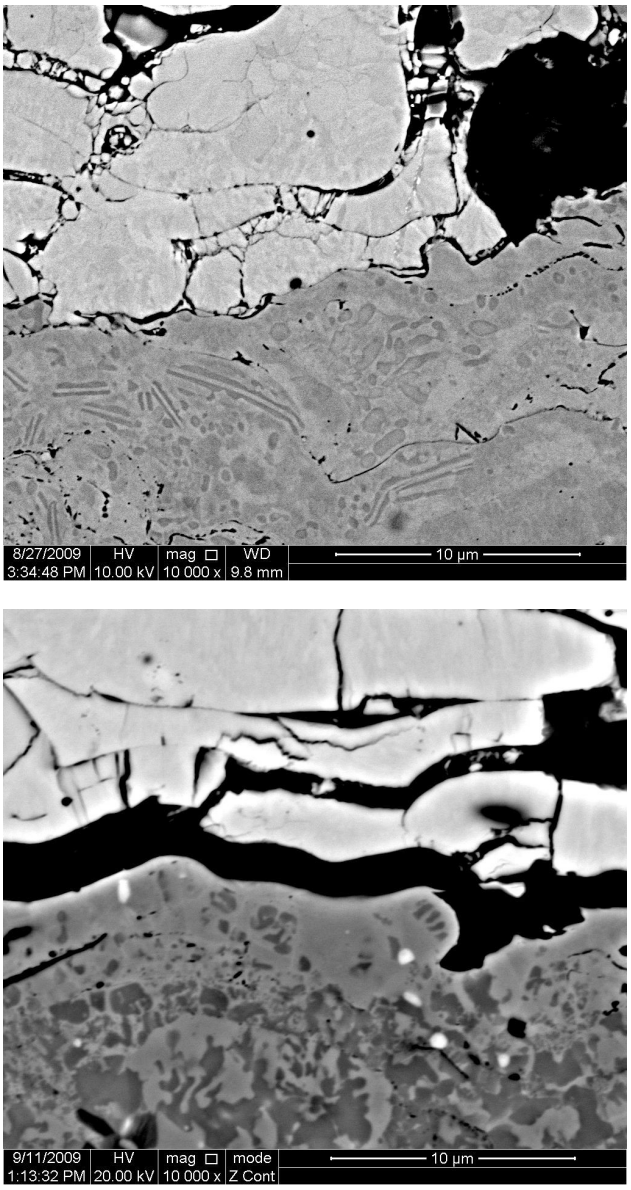

FIGURE 3. Cross-section BSE SEM images of coated ECY-768 showing the growth in the TGO, which is the dark region between the bond coat (lower half the images) and the TBC (upper half of the images). On the top is the as-received material, on the bottom is after 1,000 hrs at 821°C in H_2O + 10% CO_2 + 0.2% O_2.

Carburization was not observed for these alloys. The chromia and alumina scales that formed had such low permeability for CO_2 and CO that the activity of carbon at the oxide/metal interface was not sufficient to form carbides.

Conclusions and Future Directions

Ni-base alloys, at 748°C and below, exhibit low corrosion rates with parabolic behavior. In terms of effective metal loss, internal oxidation is the primary factor for the nickel-base alloys.

Co-base alloys are more of a concern, with a tendency towards oxide spallation.

Coated materials (a bond coat and a TBC) experienced only a modest amount of growth of the TGO and loss of Al from the bond coat.

Beyond this year's work, several issues remain to be examined:

- Some alloys, such as T91 and T92 [2] show much greater oxidation rates in steam-CO_2-O_2 than they do in steam, steam-CO_2, moist air, or Ar-CO_2 environments. Understanding the agressive nature of the steam-CO_2-O_2 environement could allow better alloy selection (in terms of effectiveness and cost) in oxy-fuel turbine and combustion systems.
- Impurities from the fuel in the gas phase may result in additional corrosion issues, both in terms of metal oxidation and in TBC phase transformations from destabilizing the favorable zircona phase.

FY 2010 Publications/Presentations

1. G.R. Holcomb and P. Wang, "Materials Performance of Oxyfuel Turbine Alloys," 6th International Conference on Advances in Materials Technology for Fossil Power Plants, EPRI , Santa Fe, New Mexico, August 31 – September 3, 2010.

References

1. R.E. Anderson, S. MacAdam, F. Viteri , D.O. Davies, J.P. Downs, and A. Paliszewski, "Adapting Gas Turbines to Zero Emission Oxy-fuel Power Plants," Proceedings of ASME Turbo Expo 2008: Power for Land, Sea and Air, GT 2008, Berlin, Germany, June 9–13, GT2008-51377.

2. G.R. Holcomb, "Oxidation in Environments with Elevated CO_2 Levels," 23rd Annual Conference on Fossil Energy Materials, Pittsburgh, Pennsylvania, May 12–14, 2009.

III.C.2 Stress-Environment Synergies in Advanced Combustion Systems: Hydrogen & Oxy-Fuel Turbines

Jeffrey A. Hawk
National Energy Technology Laboratory
1450 Queen Ave. SW
Albany, OR 97321
Phone: (541) 918-4404; Fax: (541) 967-5845
E-mail: Jeffrey.Hawk@netl.doe.gov

Contract Number: FY10.MSE.1610243.683

Start Date: October 1, 2009
End Date: September 30, 2010

FY 2010 Objectives

- Determine how oxidation in the mixed oxidant oxy-combustion environment affects microstructural features within the Ni-base and Co-base alloys of interest under oxy-fuel firing conditions.
- Determine how the mixed oxidant oxy-combustion environment affects mechanical behavior of the Ni-base and Co-base alloys of interest, in particular low cycle fatigue.

Accomplishments

- The prior year's exposure test samples were analyzed and it was determined that the Ni-base alloys, especially at 748°C and below, exhibited low corrosion rates with parabolic behavior. In terms of effective metal loss, internal oxidation is the primary factor for the Ni-base alloys, especially along grain boundaries. This could affect fatigue behavior by providing preferential sites for fatigue crack initiation (and indeed it was noted that fatigue crack initiation occurred at the periphery of the sample, in the region most affected by oxidation).
- The Co-base alloys showed a tendency towards oxide spallation.
- The fracture surfaces of the Ni-base and Co-base alloys, fatigue tested under low cycle conditions and exposed in the mixed oxidant oxy-combustion environments, were examined. Aspects on intergranular and transgranular failure were evident in all fractured surfaces to some degree.
- In comparison with baseline fatigue data at temperature and in dry air, Ni-base and Co-base alloys exposed to the mixed oxidant oxy-combustion environments showed less fatigue capability.

Introduction

The goal of the overall turbine research at NETL is to develop oxy-fuel turbine and combustor technologies for highly efficient (50-60 percent), near-zero emissions, coal-based power systems. Oxy-fuel combustion, which burns fuel in oxygen rather than in air, has a distinct advantage of generating combustion gas with a much higher percentage of CO_2 than conventional systems. This higher percentage of CO_2 allows for easier and more efficient carbon capture. Further development of this technology will push the temperatures higher. Conventional steam turbines are proposed for use as the high pressure turbine and low pressure turbine.

Materials issues related to higher efficiency power plants, like hydrogen or oxy-fuel fired gas turbines, require materials with higher temperature capability than the current generation of turbines. Research to extend the usable critical temperature of nickel superalloys has been focused maintaining the strength and integrity of grain boundaries and the interface between the grain boundary phases (carbide and/or topologically close packed) and the matrix, as well as improving the long-term stability of fine strengthening precipitates at the use temperature. Concurrent with achieving these goals is to understand how temperature, stress, and environment affect grain boundary, matrix and surface/coating interface stability as a consequence of exposure to the gas turbine environment.

Approach

Previous research in the companion project *Materials Performance in High CO_2 + Steam + O_2 Environments*, Gordon Holcomb, principal investigator, looked at the exposure effect of different CO_2 levels on oxidation and how exposure to this environment subsequently affected fatigue performance on a variety of nickel superalloys used as gas turbine airfoils. In collaboration with Siemens Power Systems, low cycle fatigue (LCF) and oxidation samples of five alloys and alloy/coating systems were exposed for 1,000 hours in H_2O-10%CO_2-0.2%O_2 environments at temperatures representative of various sections in the SGT-900 gas

turbine [1]. Mass change measurements showed that Co-base alloys exhibited significantly less mass gain at 748°C than Ni-base alloys. Mass gains for all the alloys were low and very similar to each other at 630°C.

Research initiated in Fiscal Year 2009 was continued in FY 2010 in that specimens used in the SGT-900 were exposed and subsequently tested under LCF conditions. These LCF tested specimens were returned to NETL and examined in order to understand the fracture behavior of alloys as a consequence of exposure in oxy-fuel environments. Additionally, material sectioned from unexposed alloy, alloy exposed only to the environment and alloy exposed to the environment and deformed to failure under LCF conditions have been extracted from untested, untested and exposed, and tested and exposed sections of Ni-base and Co-base alloys. Fracture surfaces from LCF tested samples were examined in the scanning electron microscope to assess fracture morphology and crack initiation location. Also, sections as indicated have been prepared for examination in the transmission electron microscope (TEM).

In FY 2010 the project scope was broadened such that understanding the mechanisms of environment-material interactions occurring in oxy-fuel turbine environments could be further refined by examining the role of oxygen in multiple oxidant environments. Additional oxidation coupons and LCF specimens were exposed in steam with 10% CO_2 and three oxygen activities. The alloys to be exposed and tested include two Co-base superalloys ECY 768 and X45, and three Ni-base superalloys IN 738, IN 939, and U520. In addition, the following additional alloys were provided by Siemens Power Systems for exposure and mechanical behavior analysis: CM247LC and PWA1483SX. Material sufficient to make miniature LCF specimens was provided by Siemens Power Systems. Alloys and chemistries are shown in Table 1.

Results

The set of exposures for FY 2010 commenced in July 2010. The analyses of the FY 2009 oxidation coupons (both bare and coated), specimens tested under LCF conditions, and unexposed material formed the basis of research efforts thus far in FY 2010. The FY 2009 exposures were in the medium oxygen activity (H_2O-10%CO_2-0.2%O_2) at temperatures ranging from 630°C to 821°C. The alloys exposed during FY 2009 are the two Co-base (ECY 768 and X45) and three Ni-base (IN 738, IN 939, and U520) alloys as shown in Table 1.

In general, the amount of oxidation on these alloys is relatively low. Bare Ni-base alloys, especially at 748°C and below, exhibit low corrosion rates with parabolic behavior. At 821°C, the Ni-base alloys showed significantly higher oxidation rates, but still with protective parabolic kinetics. Internal oxidation of the Ni-base alloys was more extensive, in terms of effective metal loss, than the direct surface oxidation.

The Co-base alloys are more of a concern, with a tendency towards oxide spallation. Unlike the Ni-base alloys, the Co-base alloys do not have significant amounts of Al and so showed little internal oxidation. The coated specimens showed only a modest amount of growth of alumina at the bond coat and thermally grown oxide interface - termed a thermally grown oxide. There were only modest amounts of Al losses from the bond coat. Carburization was not observed for these alloys. The chromia and alumina scales that formed had such low permeability for CO_2 and CO that the activity of carbon at the oxide/metal interface was not sufficient to form carbides.

TABLE 1. Alloys for Testing and Evaluation; Values in wt%

Alloy	Ni	Co	Cr	Al	Ti	Ta+Nb	W	Fe	Mo	C	B	Other
X-45	10.1	bal	24.8				7.8	1.0		0.25	0.010	0.6Mn
ECY768	9.7	bal	23.8	0.1	0.2	3.5	7.0	0.2		0.59		
IN738	bal	8.5	15.8	3.5	3.3	1.7	2.5		1.7	0.12	0.010	
IN939	bal	18.9	22.5	1.9	3.8	2.4	2.0			0.14	0.010	
U520	bal	19.0	2.0	3.0		1.2		6.3	0.06		0.007	
CM247LC	bal	9.0	8.0	5.6	0.7	3.2	10.0		0.5	0.07	0.015	1.4Hf
PWA1483SX	bal	9.0	12.8	3.6	4.0	4.0	3.8		1.9			
Bond Coat	bal		17.0	10.0								***
TBC	ZrO_2	Y_2O_3	HfO_2									
TBC	89.0	10.0	1.0									

*** Bond coat contains 1.5 Re and 0.3 Y.
TBC – thermal barrier coating

In assessing microstructural characteristics that could alter mechanical behavior, the first step was to do a comprehensive investigation of oxide scale morphology, oxygen penetration along the grain boundaries, element consumption via transport to oxide, and any other changes that affect γ′ precipitates. Figure 1 shows one such example. U520 was sectioned such that the plane perpendicular to the surface was investigated. The figure shows U520 exposed at 821°C in H_2O + 10% CO_2 + 0.2% O_2. Note the extensive oxidative attack along the grain boundaries with many grains attacked on all sides. This type of oxidative attack was characteristic to one degree or another for all of the samples and especially true for those exposed at 821°C. For materials not coated this could be a problem in that the oxide penetrated boundaries would be easy crack initiation sites during fatigue.

In Figure 2, U520 was exposed at 630°C in H_2O + 10% CO_2 + 0.2% O_2 for 1,000 hours and then tested under LCF conditions in dry air at 630°C. The applied strain in this particular test was 1.2%. The specimen lasted for 202 cycles before crack initiation leading to subsequent failure. Note the intergranular nature of the fracture and the secondary cracks.

Figure 3 shows one example of LCF test results for U520 exposed at 630°C in H_2O + 10% CO_2 + 0.2% O_2 for 1,000 hours and then tested under LCF conditions in dry air at 630°C. Although it would be more appropriate to test under the environmental conditions of interest, testing facilities to do so are not available. The design curves for these materials tested in air at the appropriate temperature are available but are proprietary. Suffice to say that in all instances,

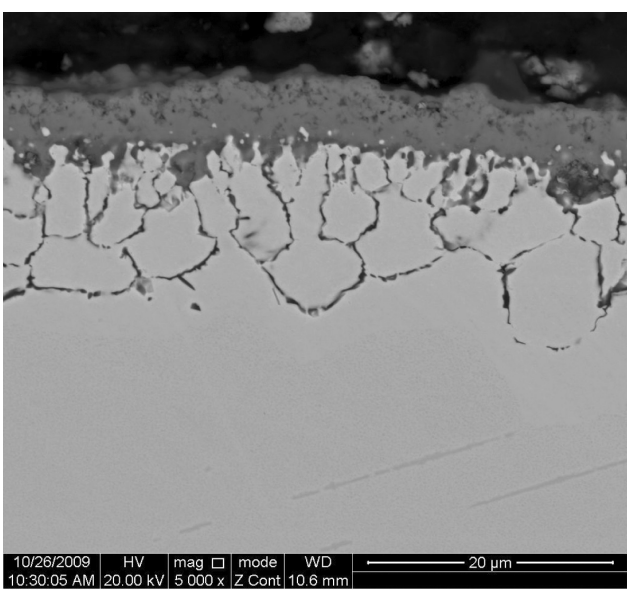

FIGURE 1. U520 exposed at 821°C in H_2O + 10% CO_2 + 0.2% O_2. Note the extensive oxidative attack along the grain boundaries.

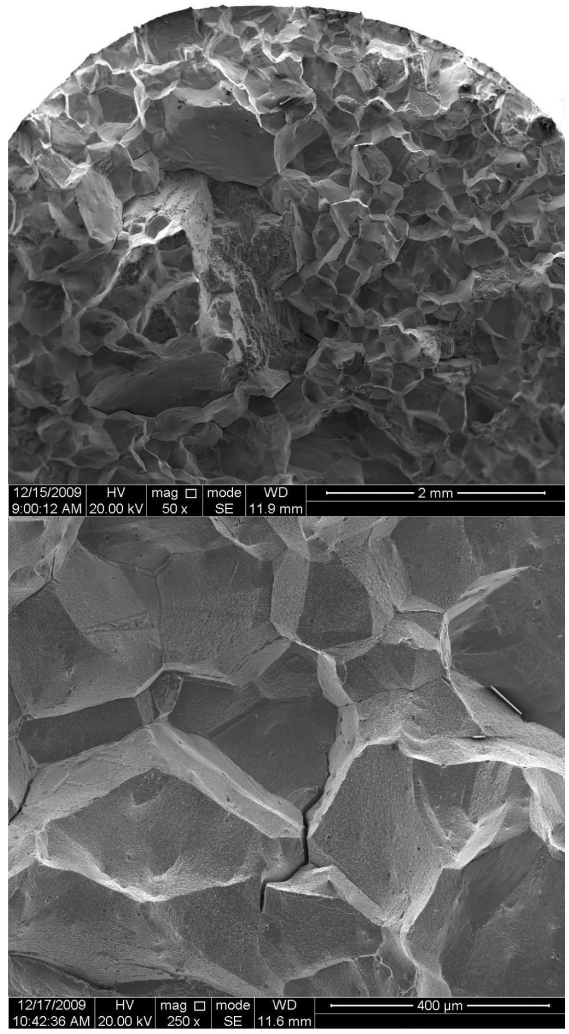

FIGURE 2. U520 exposed at 630°C in H_2O + 10% CO_2 + 0.2% O_2 and then tested under LCF conditions in dry air at 630°C and 1.2% strain; 202 cycles to crack initiation. Note the intergranular nature of the fracture and the secondary cracks.

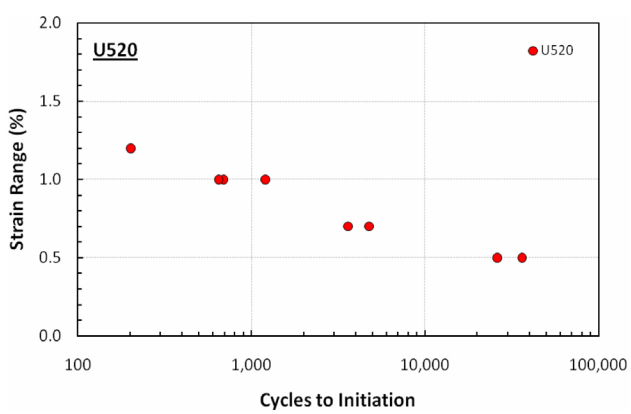

FIGURE 3. LCF test results for U520 exposed at 630°C in H_2O + 10% CO_2 + 0.2% O_2 and then tested under LCF conditions in dry air at 630°C.

the exposed fatigue specimens exhibited strain-life behavior lower than those samples not exposed to the H_2O + 10% CO_2 + 0.2% O_2 environment. In some instances the strain-life behavior was within the scatter design scatter while in other instances the decrease in strain-life was significant. However, care should be exercised at this point since only a few tests were performed. Additional LCF specimen exposures are underway in FY 2010 in order to improve the quality of LCF strain-life data.

Conclusions and Future Directions

Summary of Oxidation Exposure:

- Ni-base alloys, at 748°C and below, exhibited low corrosion rates with parabolic behavior. In terms of effective metal loss, internal oxidation is the primary factor for the Ni-base alloys.
- Co-base alloys are more of a concern, with a tendency towards oxide spallation.
- Coated materials (a bond coat and a TBC) experienced only a modest amount of growth of the thermally grown oxide and loss of Al from the bond coat.

Beyond this year's work, several issues remain to be examined:

- Some alloys show much greater oxidation rates in steam-CO_2-O_2 than they do in steam, steam-CO_2, moist air, or Ar-CO_2 environments. Understanding the aggressive nature of the steam-CO_2-O_2 environment could allow better alloy selection (in terms of effectiveness and cost) in oxy-fuel turbine and combustion systems.
- Impurities from the fuel in the gas phase may result in additional corrosion issues, both in terms of metal oxidation and in TBC phase transformations from destabilizing the favorable zircona phase.

Summary of Microstructural Investigations of Exposed LCF Specimens:

Exposure to the simulated oxy-combustion H_2O + 10% CO_2 + 0.2% O_2 environment at temperatures from 630-821°C caused various degrees of oxidative damage to the Ni-base and Co-base alloys. The degree of damage has been noted (see above Summary of Oxidation Exposure and in companion report *Materials Performance in High CO_2 + Steam Environments*, Gordon R. Holcomb), and mechanical behavior is affected.

Beyond this year's work, several issues remain to be examined:

- It is not clear if the percent intergranular/transgranular fracture is due exclusively to the simulated oxy-combustion H_2O + 10% CO_2 + 0.2% O_2 environment, or is partly due to the oxygen in the atmosphere during elevated temperature testing. In order to determine the extent of this effect, fatigue specimens have been prepared so that testing can be done at the same test conditions but for exposed and unexposed samples.
- Sufficient fatigue specimens have been prepared so that the effect of time at exposure temperature in the simulated oxy-combustion H_2O + 10% CO_2 + 0.2% O_2 environment can be evaluated. In FY 2009 exposures up to 1,000 hours were carried out. However, gas turbines operate for much longer times. Consequently, the potential effect of time at exposure temperature in the simulated oxy-combustion H_2O + 10% CO_2 + 0.2% O_2 environment must be ascertained.
- Microstructural examination in the TEM will be continued, documenting features well away from the surface that are affected by temperature and environment and contribute to mechanical behavior. In addition, examination of the grain boundary regions in the oxidation affected zone will be extended to assess changes that could possibly enhance environmental sensitivity of the alloy to the simulated oxy-combustion H_2O + 10% CO_2 + 0.2% O_2 environment.

References

1. R.E. Anderson, S. MacAdam, F. Viteri , D.O. Davies, J.P. Downs, and A. Paliszewski, "Adapting Gas Turbines to Zero Emission Oxy-fuel Power Plants," Proceedings of ASME Turbo Expo 2008: Power for Land, Sea and Air, GT 2008, June 9–13, Berlin, Germany GT2008-51377.

III.C.3 Materials and Component Development for Advanced Turbine Systems – Advanced Coating Development

Mary Anne Alvin
U.S. Department of Energy (DOE)
National Energy Technology Laboratory (NETL)
626 Cochrans Mill Road
Pittsburgh, PA 15236-0940
Phone: (412) 386-5498; Fax: (412) 386-4806
E-mail: Maryanne.Alvin@netl.doe.gov

NETL – Regional University Alliance (RUA)

- NETL – Mary Anne Alvin
- University of Pittsburgh, Pittsburgh, PA – Dr. Brian Gleeson, Dr. Gerald Meier, Dr. Meltem Yanar, Mr. Michael Helminiak, Dr. Scott Mao, and Dr. Bruce Warnes

Subcontractor:

- Mr. Kevin Klotz, Coatings for Industry, Souderton, PA

Contract Number: 0004000.5.610.243.001

Start Date: October 1, 2009
End Date: September 30, 2010

FY 2010 Objectives

Develop enhanced oxidation resistant, thermal barrier coatings (TBCs) for nickel-based superalloys and single crystal substrate materials for use in advanced hydrogen-fired and oxy-fuel turbine applications. Efforts were directed to the development of diffusion barrier coatings (DBCs), reduced cost bond coat systems, high purity, low density yttria-stabilized zirconia (YSZ) TBCs, and extreme temperature ceramic overlayer material systems.

Accomplishments

- *DBC Development:* Mechanically milled and heat treated σ-phase Re-Ni-Cr powder was air plasma sprayed (APS) onto Ni-18Al-10Cr-based superalloy coupons to form a DBC. Microstructural and elemental characterization of the coupons after exposure to temperatures up to ~1,200°C indicated minimal interdiffusion between the DBC and the superalloy substrate, identifying DBC concept feasibility.
- *Bond Coat Development:* A commercially-modified, wet spray, aluminum-based, diffusion bond coating was shown to have excellent bench-scale, 1,100°C, cyclic thermal oxidation life as compared to the performance of state-of-the-art (SOTA) diffusion bond coat systems.
- *APS YSZ TBC Development:* The properties of APS YSZ TBCs with controlled thickness and density and bond coat optimization for TBC durability were investigated. High-purity, low-density (HP-LD) APS TBCs on NiCoCrAlY bond coats were shown to be highly resistant to sintering and phase transformation, with as-manufactured thermal conductivities identified at <1 W/mK. When thermally cycled, the 750 µm thick HP-LD APS coating had a cyclic life greater than that of a conventional 100 µm thick electron beam physical vapor deposition (EBPVD) coating. The failure times and mechanisms were observed to depend on HP-LD APS thickness, the nature of the thermal exposure, and the coefficient of thermal expansion (CTE) of the metallic substrate.
- *Extreme Temperature Ceramic Overlayer Development:* For use at extreme temperatures (i.e., >1,300°C), bi-layer ceramic systems were fabricated consisting of APS YSZ and $La_2Zr_2O_7$. Cyclic fatigue testing at 1,100°C identified early failure of thick overlayer coatings that were thermally sprayed onto commercially applied YSZ TBC surfaces. Preliminary testing was conducted in a steam-containing environment to address phase stability of $La_2Zr_2O_7$, and parametric calculations were conducted to address the thickness criteria of the bi-layer architecture as a function of turbine inlet temperature (TIT).

Introduction

Future hydrogen-fired or oxy-fuel turbines will likely experience an enormous level of thermal and mechanical loading, as TITs approach ~1,425-1,760°C (~2,600-3,200°F) with pressures of ~300-625 psig, respectively. Maintaining the structural integrity of future turbine components under these extreme conditions will require: (1) durable TBCs, (2) high-temperature creep-resistant metal substrates, and (3) effective cooling techniques. While advances in substrate materials have been limited for the past decades, thermal protection of turbine airfoils in future hydrogen-fired and oxy-fuel turbines will rely primarily on collective TBC and aerothermal cooling advancements.

With respect to durable TBC systems, surface protection of structural metal substrates via the use of oxidation-resistant coatings is a necessity, and it will be critically important to maintain the stability of these coatings for extended service life (i.e., 8,000-30,000 hrs). This means that there needs to be minimal interdiffusion between the structural metal substrate and the surface-modified region. A viable engineering solution would be to utilize a metallic alumina-scale forming surface coating with an intermediate diffusion barrier that will essentially preclude coating-substrate interdiffusion, and therefore sustain the protective properties of the coating.

As commercially applied diffusion or overlay bond coat systems are subjected to high temperature for extended periods of time, oxidation (i.e., formation of thick thermally grown oxides [TGOs]) and rumpling of the bond coat surface result, which induce stress and spallation of the insulating APS or EBPVD YSZ TBC – ultimately leading to reduced turbine operating life. Mitigating not only bond coat oxidation, but also surface rumpling are essential for extending the operating lifetime of TBC systems.

As advanced turbine inlet design temperatures are projected to exceed 1,300ºC, significant sintering of current SOTA YSZ TBCs will likely occur, leading to microstructural changes and a reduction of strain tolerance of the YSZ in combination with an increase in Young's modulus. Higher stresses originating in the YSZ TBC coating, will ultimately lead to a reduced service operating life, particularly during cyclic load conditions. Through the development of HP-LD APS YSZ TBC systems, negligible sintering and phase transformations have been demonstrated up to temperatures of 1,400°C. The HP-LD YSZ is currently viewed as a candidate material for extending turbine service life.

As TIT design temperatures exceed 1,400°C, and possibly reach ~1,760°C for oxy-fuel applications, additional thermal protection of turbine superalloy and single crystal structural materials will be required. For this reason extreme temperature overlayer architectures are being developed as either single, bi-layer, or multi-layer structures.

Efforts that have been conducted at the National Energy Technology Laboratory (NETL) and at the University of Pittsburgh in each of these areas during Fiscal Year 2010 are presented in the following sections.

Approach and Results

Diffusion Barrier Coating Development

Alloys for high-temperature turbine applications are often protected from surface degradation by either overlay MCrAlY (M = Ni and/or Co) or Al-diffusion coatings of β-NiAl, β-Ni(Pt)Al, or γ'-$(Ni,Pt)_3Al$. Loss of Al from the coatings occurs by exfoliation of the thermally grown Al_2O_3 scale as a result of thermal cycling and also by interdiffusion between the coating and substrate. In addition to loss of Al to the substrate, it would also be preferred to suppress the ingress of Ni and other alloying elements such as S, Ti, Mo and Ta from the substrate into the coating. To achieve this, a great number of barrier compounds such as TiN, AlN, SiC, AlON, ZrO_2, Al_2O_3, Ir, Re and W have been investigated. However, overall, almost all diffusion barrier layers proposed lose their protective ability after relatively short exposures because of destabilization of the barrier layer.

Recent research indicates that Re-Cr-Ni-based compositions can act as highly effective diffusion-barrier layers between the heat-resistant alloy and an Al-reservoir layer, to form and maintain a protective, long-lasting Al_2O_3 scale. Coatings deposited by multiple electrodeposition/heat treatment cycles, generating a two-layer structure comprised of an inner, Re-based alloy layer and an outer β-NiAl layer, have been successfully formed on single-crystal nickel-base superalloys (e.g., second-generation CMSX-4, and the third-generation TMS-82+). Results have additionally demonstrated that the Cr-Re-Ni σ-phase can act as an effective diffusion barrier at high-temperatures.

Development of a viable and cost-effective process for the deposition of oxidation resistant DBC systems onto nickel-base superalloys for long-tem, high-temperature applications was the focus of the FY 2010 efforts in this project. DBCs were prepared by mechanically milling powders of pure Re, Ni and Cr in amount corresponding to 40Re-40Cr-20Ni (atomic %) for 120 hours, followed by heat treatment for 6 hours at 1,200°C. The resulting homogenous powders were deposited by APS, leading to an ~200 µm thick coating along the surface of nickel-based superalloys as Haynes 214 (Figure 1). Microstructural characterization and electron microprobe analysis of the coupons after static air exposure at temperatures of 1,200°C for 2 hours, followed by 50 hours at 1,150°C, identified minimal Al diffusion from the metal substrate into the APS DBC layer, while limited diffusion of Cr occurred from the coating into the underlying metal substrate. No apparent reaction product formation was evident in the interdiffusion zone, reflecting compatibility of the DBC with the nickel-base superalloy. Efforts in FY 2010 have also been focused on preparation of the σ-phase Re-Cr and lower cost W-Cr powders using a high-energy mill and depositing the DBCs using low-pressure plasma spraying or high velocity oxy-fuel techniques. Bench-scale cyclic oxidation testing and characterization of these materials are planned.

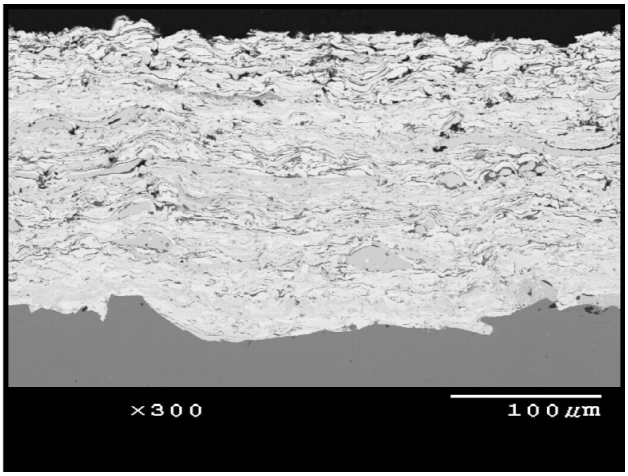

FIGURE 1. Scanning Electron Micrograph of the Cross-Sectioned, As-Deposited, 40Re-40Cr-20Ni (at%) APS Coating on Haynes 214

Bond Coat Development

SOTA TBCs typically consist of two layers: (1) β-phase intermetallic diffusion coatings and/or MCrAlY overlays as bond coat systems that are applied to the surface of alloy, superalloy or single crystal substrates, and (2) a YSZ layer that is applied to the external surface of the bond coat. The metallic bond coat provides oxidation resistance to the underlying metal substrate generally through the formation of a TGO alumina-enriched scale, and serves to improve bonding of the thermally insulating ceramic YSZ top coat to the underlying structural metal substrate.

For extended service operating life, the advanced turbine systems will require high-temperature material stability, and adherence/retention of the ceramic TBC along underlying metal substrates. When diffusion or overlay bond coats are commercially applied to metal substrates and then exposed at high temperature for extended periods of time, oxidation (i.e., TGO formation) and rumpling of the bond coat surface occur which induce stress and lead to spallation of the APS or EBPVD YSZ TBC – ultimately leading to reduced turbine operating life. Additionally at high temperature, interdiffusion of the SOTA β(Ni,Pt)Al, as well as Pt+Hf Mod γ+γ'(PtAl G2P) bond coats occurs, leading to external surface depletion of alumina and subsequently reduction in the protective oxidation resistance of the bond coat, as well as the formation of an internal, mechanical strength reduced, secondary reaction zone (SRZ).

In developing a reduced-cost, high-temperature, oxidation resistant bond coat system that potentially limits TGO and SRZ formation, NETL has collaboratively worked with Coating for Industry, modifying the commercial-based Alseal product line. The modified β-NiAl diffusion bond coating was wet-sprayed onto nickel-based superalloy or single crystal coupons, and subjected to bench-scale cyclic oxidation testing at 1,100°C. Bond coat stability and performance were monitored through mass change data as a function of time, as well as cross-sectional scanning electron microscopy (SEM) analyses. Comparison of these results was made with comparably tested commercially available diffusion and overlay bond coat systems.

The modified β-NiAl bond coat was shown to significantly enhance the oxidation life of René N5 (i.e., from 850 cycles to 2,120 cycles), and exceed the oxidative stability of SOTA β(Ni,Pt)Al diffusion coatings, as well as Pt-Hf Mod γ + γ' G2P coatings (i.e., ~1,600 and ~1,100 cycles, respectively). Post-test characterization indicated that a thin TGO scale formed (i.e., ~3-5 μm after 260 cycles, in contrast to ~12-20 μm after 200 cycles on NiCoCrAlY at 1,100°C) along the relatively smooth external surface of the modified β-NiAl bond coat (i.e., limiting rumpling and YSZ top coat spallation), and that a detrimental SRZ was not formed after extended cyclic fatigue testing.

APS YSZ TBC Development

Future advanced power plants that are being designed to operate at extreme TITs will require TBCs with increased thermal insulating capabilities. The insulating effectiveness of a TBC may be expressed in terms of a thermal resistance,

$$R_{therm} = \frac{h_{topcoat}}{\kappa_{topcoat}} \quad (\mathrm{m^2K/W})$$

where h is the thickness and κ is the thermal conductivity of the coating. Thus, maximizing thickness and minimizing thermal conductivity will produce the largest thermal resistance. Increasing thickness also increases the driving force for coating delamination, which requires material selection and microstructural control to reduce the stored elastic energy and increase the fracture toughness of the coating.

Decreasing thermal conductivity can be achieved by choosing a top coat material with a very low thermal conductivity. While there has been some progress in identifying oxides with lower thermal conductivities than conventionally used YSZ, they do not have the balance of properties necessary for advanced systems. An alternative approach is to improve the durability of APS YSZ TBCs so that they can be used at larger thicknesses and control the microstructure (e.g., high porosity) to minimize thermal conductivity. Efforts continue to be focused on developing a fundamental understanding that facilitates fabrication of APS YSZ TBCs with controlled thickness and density combinations, bond coat optimization for maximum

thermal resistance, and TBC durability. This has included development of insights with respect to the degradation mechanisms of plasma-sprayed TBCs, and expansion of the knowledge-base with respect to processing-microstructure-properties interrelationships for APS TBCs (e.g., definition of methods for controlling density, pore morphology, and crack morphology to optimize properties).

Working in conjunction with Praxair Surface Technologies, APS YSZ TBC top coats were fabricated with controlled thickness and density combinations, as well as variation of the yttrium content and surface roughness of NiCoCrAlY bond coats deposited by argon shrouded plasma spraying. The thicknesses of the high purity, 85% dense YSZ (HP-LD) APS TBCs deposited onto iron- and cobalt-based alloys and nickel-based single crystal substrate coupons were typically 375 µm, 700 µm, and 1,125 µm. The coupons were evaluated using cyclic oxidation and jet engine thermal shock (JETS) testing, and were characterized with respect to APS resistance to sintering and phase transformation, thermal conductivity, fracture toughness and modulus of elasticity. Notably as the severity of bench-scale testing was increased (i.e., rapid thermal ramp rate for the JETS test vs. furnace cycle testing), the apparent lifetime of the TBC was reduced.

Sintering and Phase Transformation: In order to demonstrate sintering and phase transformation resistance of the HP-LD APS YSZ, free-standing 1,125 µm coatings were prepared and exposed for 100 hours at temperatures of 1,200°C, 1,300°C, 1,400°C, and 1,500°C. Negligible increase in YSZ density was observed at 1,200°C and 1,300°C, while small increases in density resulted at the higher temperatures. Surface connected porosity decreased slowly and systematically up to 1,400°C, but dropped sharply at 1,500°C. The high resistance to sintering exhibited by these TBCs was attributed to the very high purity YSZ powder used in this effort. Negligible transformation of the metastable tetragonal structure to the monoclinic structure resulted within the HP-LD TBCs during 100 hours of exposure up to temperatures of 1,400°C. Although speculative, the absence of silicon in the HP-LD APS YSZ, was considered to limit diffusion of yttrium at the grain boundaries, providing phase stability to the matrix.

Thermal Conductivity: The thermal conductivity of the as-manufactured HP-LD APS YSZ was measured at temperatures up to 1,000°C in 100°C increments. Measured at <1 W/mK, the HP-LD YSZ thermal is less than the thermal conductivity of high density YSZ coatings (i.e., 1.5 W/mK), and is expected to provide increased thermal resistance in comparison to current commercial TBC systems.

Effect of Superalloy Substrates: As shown in Figure 2, longer thermal cyclic life is associated with

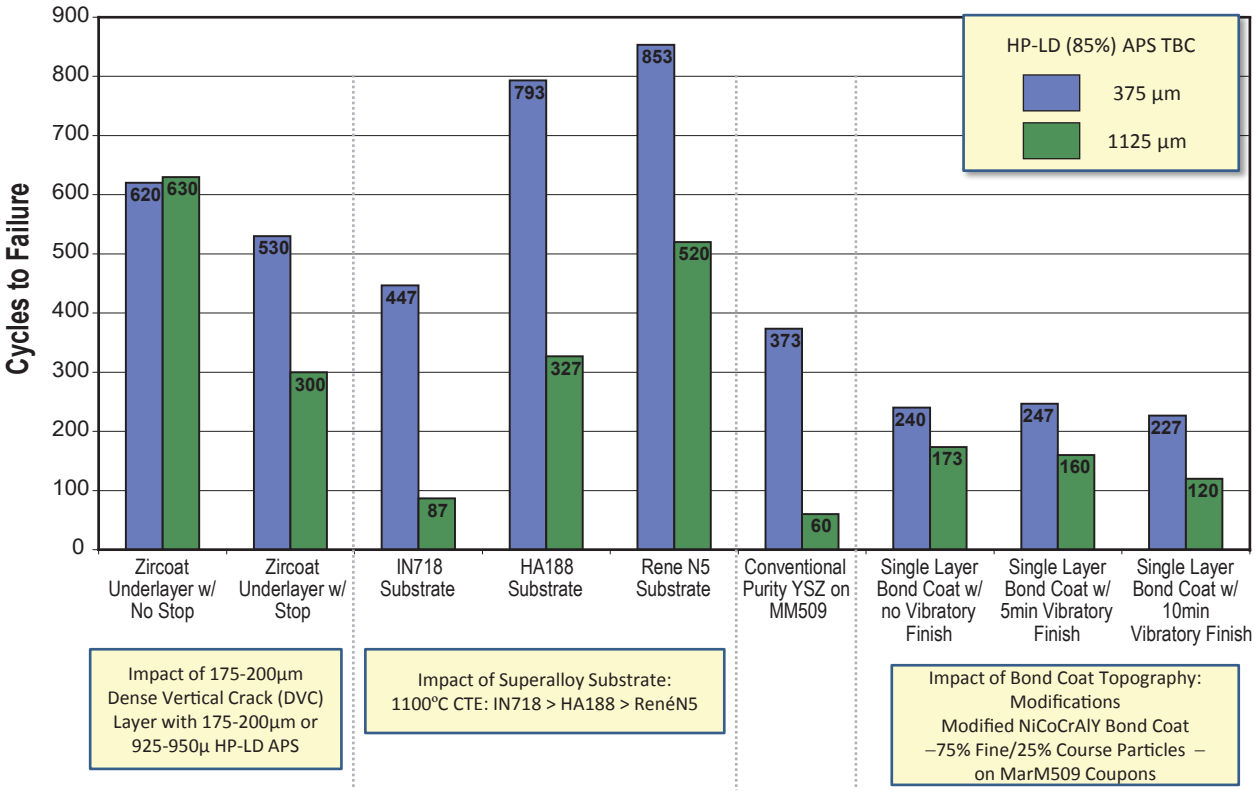

FIGURE 2. 1,100°C Cycle to Failure Lifetimes for High-Purity, Low-Density APS YSZ TBCs

thinner APS coatings. In order to address the effect of superalloy substrate composition on APS TBC life, 375 µm and 1,125 µm HP-LD coatings were applied to the NiCoCrAlY bond coat surfaces that were deposited on iron-based IN718, cobalt-based HA188, and nickel-based René N5 coupons. As the CTE at 1,100ºC for these materials increases (~16.2 x 10^{-6}/ºC René N5; ~17 x 10^{-6}/ºC HA188; ~17.4 x 10^{-6}/ºC IN718), cyclic oxidation life of the HP-LD APS TBCs decreases. Post-test SEM characterization identified failure to have occurred within the 1,125 µm HP-LD APS TBC on the IN718 coupon. In contrast, bond coat oxidation and thermal cyclic fatigue led to crack formations and delamination occurring at the TGO-TBC interface for the HA188 and René N5-coated coupons.

APS TBC Purity: Efforts were also conducted to address the 1,100ºC thermal cycle life of conventional APS YSZ TBCs on cobalt-based MarM509. Both 375 µm and 1,125 µm APS thickness were applied to dual layer NiCoCrAlY bond coats. The dual layer bond coat consisted of a dense inner layer of fine plasma sprayed particles, and a less dense outer layer of coarser plasma sprayed particles, in order to generate a rougher outer surface for application and physical adherence of the APS YSZ layer.

Although the CTE at 1,100°C for MarM509 (~15.5 x 10^{-6}/°C) is lower than the CTE for IN718, HA188, or René N5, when conventional APS YSZs were applied to NiCoCrAlY-coated MarM509 coupons, cyclic oxidation failure occurred earlier than for the HP-LD-coated IN718, HA188, and René N5 coupons. Failure of the MarM509-APS coating was attributed to the numerous SiO_2-Al_2O_3-particles that were observed to be dispersed near the APS YSZ-bond coat interface. These particles increase the rate of densification in the TBC which is undesirable, as sintering increases strength, but decreases toughness, making the coating more susceptible to fracture. Sintering and densification near this interface can lead to void formations that can then serve as crack nucleation sites.

Modification of the Bond Coat Topography: MarM509 substrates were coated with a single layer of NiCoCrAlY that was argon shrouded plasma sprayed from a blend of 75% fine particles and 25% coarse particles. Once sprayed, several of the coupons were then sprayed with a top coat while others were vibratory finished for five and ten minutes, and subsequently the HP-LD YSZ top coat was applied. The R_a values for the roughness of the unmodified, 5-minute, and 10-minute vibratory finished bond coats were 10.7 µm, 9.8 µm, and 8.6 µm, respectively. As shown in Figure 2, bond coat surface finish did not seem to have a substantial effect on the lifetime of the APS YSZ.

Dense Vertically Cracked Top Coat Inner Layers: The purpose of dense vertically cracked (DVC) TBCs is to provide strain relief during heating and cooling periods when thermal strain occurs. These coatings usually have a higher thermal conductivity than the low density coatings because the spraying parameters used to achieve the segmented structure also produce a dense YSZ structure, which subsequently increases thermal conductivity. To minimize thermal conductivity while still providing strain relief, coatings were prepared with a 175-200 µm high purity DVC inner layer, and an outer layer of either 175-200 µm or 925-950 µm HP-LD YSZ APS.

Two coating processes were utilized to produce the DVC coatings. In the first process, the DVC layer was sprayed, deposition was stopped and the spray parameters were adjusted, prior to applying the HP-LD APS coating. In the second process, the DVC layer was sprayed and subsequently during deposition the spray parameters were adjusted to achieve the low density YSZ structure. A definitive difference was observed in the microstructure of the two layers (Figure 3). The lower DVC layer contained denser YSZ with vertical cracks (as well as horizontal cracks) scattered throughout the layer extending from the bond coat-YSZ interface, while the upper layer was much less dense. After ~200 thermal cycles at 1,100°C, a 1-3 mm ring of YSZ spalled from along the outer edge of the coupons. After initial spallation of the outer ring, further cracking or localized spallation of the coating was not observed until complete spallation of the entire YSZ coating occurred at the time of failure.

Extreme Temperature Ceramic Overlayer Development

YSZ TBCs are currently used in engine applications as high-temperature (i.e., ~1,200-1,300°C) insulating top coat systems. At higher temperatures, as 1,400-1,760°C for the hydrogen-fired and oxy-fuel TITs, YSZ undergoes two detrimental changes. Significant sintering leads to microstructural changes and a reduction of the strain tolerance in combination

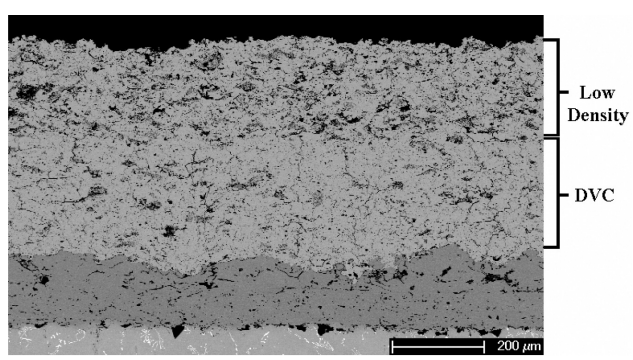

FIGURE 3. Scanning Electron Micrograph of the 375 µm DVC Layer beneath the HP-LD APS YSZ Layer

with an increase of Young's modulus. Additionally phase transformations occur, leading to the formation of tetragonal and cubic phases. Upon cooling, the tetragonal phase further undergoes transformation to the monoclinic phase which is accompanied by a volume change, leading to spallation of the coating. As a result, efforts have been directed to development of new TBC systems for use at extreme temperature conditions.

Among the extreme temperature TBC candidates are those materials with pyrochlore structures and high melting points as $La_2Zr_2O_7$, $La_2Hf_2O_7$, $Gd_2Zr_2O_7$, or $Nd_2Zr_2O_7$. Previous research has shown that these materials have excellent physical properties (i.e., thermal conductivity lower than YSZ and high thermal stability). However, their thermal expansion coefficient is typically lower (9-10 x 10^{-6}/K) than that of YSZ (10-11 x 10^{-6}/K), which leads to higher thermal stress in the TBC system if applied directly to the bond coat system. Additionally, relatively low toughness values are observed in the pyrochlore materials.

Recently research efforts have been focused on developing double ceramic or bi-layer coating systems using 8YSZ and a pyrochlore overlayer. In the bi-layer, the outermost ceramic layer needs to have low thermal conductivity and high phase stability, with thermal insulating properties that maintain the overlayer/YSZ interface temperature at ~1,300°C. To achieve effective thermal protection of nickel-based superalloys or single crystal substrates at advanced TITs, determination of the YSZ and overlayer thicknesses, as well as optimal porosity and deposition techniques are required. Additionally, the influence of the high steam-containing environment on the phase stability of the overlayer needs to be addressed.

Lanthanum zirconate ($La_2Zr_2O_7$) powder purchased from Praxair Specialty Ceramics was air-plasma sprayed at Stony Brook to thicknesses ranging from 50 to 350 µm onto APS YSZ TBC/MCrAlY/René N5 coupons. The bi-layer coupons were subsequently subjected to 1,100°C thermal cycle testing. Complete spallation of the overlayer/YSZ occurred (Figure 4) within the first 24 hours of testing on all coupons with the exception of the 50 µm $La_2Zr_2O_7$/250 µm YSZ coupon. Debonding and spallation were considered to result from residual stress induced during direct application of the $La_2Zr_2O_7$ layer onto the initially commercially manufactured APS YSZ surface.

In contrast to thermal cycle testing in air where smaller cracks resulted along the intact adherent $La_2Zr_2O_7$ surface, crack formations were observed along the 50 µm $La_2Zr_2O_7$/YSZ interface when coupons were subjected to 1,100°C static exposure for 24 hours in a ~20% moisture-containing environment. This led to localized debonding/spallation of the

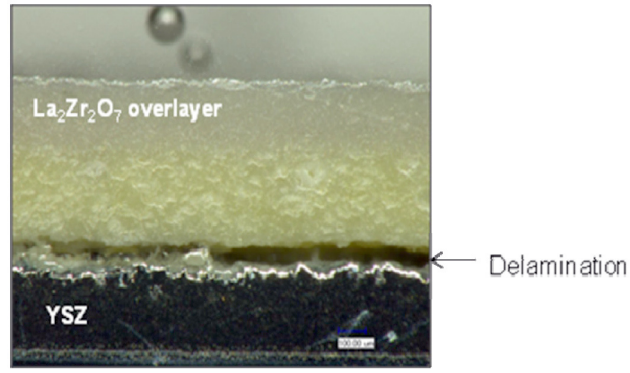

FIGURE 4. Cross-Sectional Scanning Electron Micrograph Illustrating Delamination of the 200 μm Overlayer Coating along the YSZ Surface after Twenty 1,100°C Thermal Cycles

overlayer from the YSZ surface. Larger cracks, without coating debonding/spallation, were observed along the surface of the 350 µm $La_2Zr_2O_7$/YSZ coated coupon after exposure to the 1,100°C, ~20% moisture-containing environment. Irrespective of the observed crack formations, phase stability (i.e., absence of phase transformations) was demonstrated for $La_2Zr_2O_7$ and YSZ during the initial 24 hours of exposure at 1,100°C in the steam-containing environment.

Parametric calculations were conducted to establish the thickness of both the YSZ and $La_2Zr_2O_7$ coating layers for use in 1,600°C and 1,760°C applications. In order to maintain temperatures of 1,300°C within a 200 µm YSZ top coat, and a maximum bond coat/YSZ interface temperature of <1,050-1,100°C, a 100 µm and 200 µm $La_2Zr_2O_7$ coating thickness, respectively, was projected to be required for use at these extreme TIT conditions (Figure 5).

Future Directions

In the area of diffusion barrier coating development, two interrelated paths are being considered which include: (1) optimization of the Re-Cr and/or W-Cr σ-phase DBC compositions and deposition process, and (2) exploiting known benefits of reactive element (RE) additions as Hf, Y and/or Si, forming a graded reservoir at the DBC/β-NiAl interface. The RE reservoir would serve to greatly improve the scaling behavior of Al reservoir.

Regarding bond coat development, efforts are planned to further enhance the high-temperature oxidative performance of the modified β-NiAl bond coat system through compositional co-doping.

Efforts are planned to extend the fundamental study of sintering and phase transformations in YSZ TBCs, addressing the effects of reactive elements

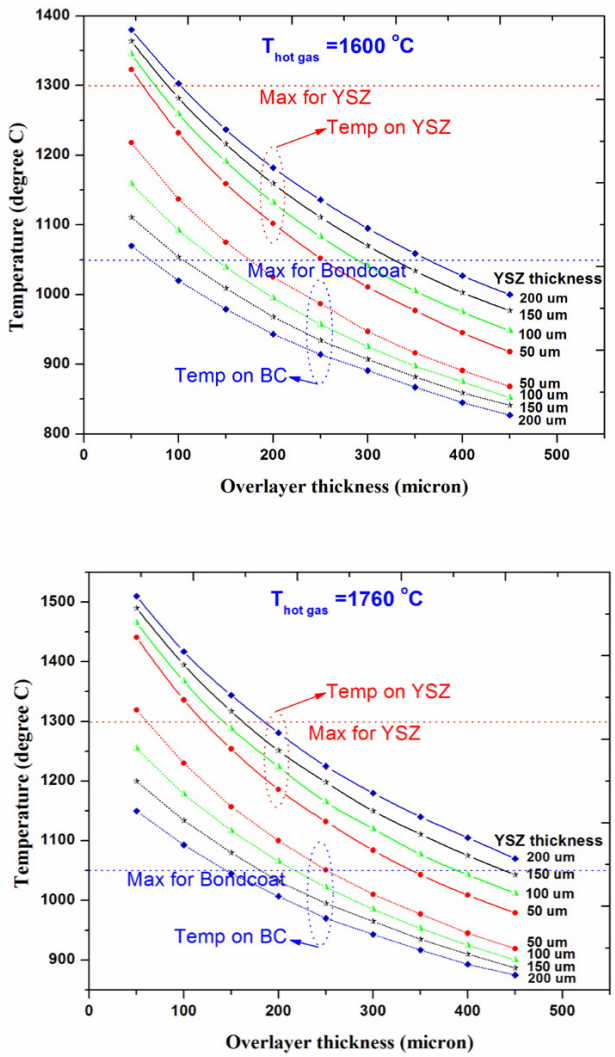

FIGURE 5. Bi-Layer Coating Thicknesses for Extreme Temperature Operations

and engineering of bond coat topography via micro-machining with the aim of optimizing TBC processing, resulting properties, and ultimately durability. Additionally, efforts are planned to assess the effects of moisture and CO_2 on the degradation of EBPVD and APS TBCs, including the high-purity, low-density TBCs. Coating of blades, vanes, and combustion liners for engine testing is being considered. Assessment of the HP-LD APS YSZ TBC erosion characteristics needs to be addressed in view of the coating's porosity and mechanical strength relative to commercial APS YSZ TBC systems.

Fabrication of APZ YSZ/overlayer systems is planned, addressing overlayer powder particle size and composition (i.e., $La_2Zr_2O_7$ and Gd-doped zirconates), and thermal spray deposition rates. Mechanical properties of the as-manufactured and 1,100°C thermally cycled bi-layers will be assessed, and coating interfacial fracture toughness properties will be determined using micro- and nano-indentation.

Future efforts will additionally be focused on addressing the performance feasibility of a full TBC architecture for advanced TIT applications in extreme temperature operations such as the ~1,425°C (~2,600°F) hydrogen-fired and ~1,760°C (~3,200°F) oxy-fuel systems. Integrated TBC architectures will be developed to include superalloy and/or single crystal substrates with diffusion barrier coatings, reduced cost bond coat systems, APS YSZ TBC architectures, and extreme temperature ceramic overlayer systems. High temperature thermal flux testing of these materials will be performed at NASA Glenn Research Center (GRC) and at the Westinghouse Plasma Corporation (WPC), followed by materials characterization.

FY 2010 Publications/Presentations

1. M.A. Alvin, "Materials and Component Development for Advanced Turbine Systems," Presentation at the UTSR Workshop VII, Orlando, Florida, October 27-29, 2009.

2. M.A. Helminiak, N.M. Yanar, F.S. Pettit, T.A. Taylor, and G.H. Meier, "The Behavior of High Purity, Low Density Air Plasma Sprayed Thermal Barrier Coatings," Surface & Coatings Technology, 204, 793 (2009).

3. G.H. Meier, "High-Purity Low-Density TBCs," Presentation at the American Ceramics Society Conference on *Advanced Composites and Ceramics*, Daytona Beach, Florida, January 27, 2010.

4. M.A. Helminiak, "Factors Affecting the Lifetime of Air Plasma Sprayed Thermal Barrier Coatings," M.S. Thesis, University of Pittsburgh, April 2010.

5. M.A. Helminiak, "Thick High-Purity Low Density APS Thermal Barrier Coatings," Poster Presentation at the ECI Conference on *Surface Stability of Materials in High-Temperature Aggressive Environments*, Vail, Colorado, May 17, 2010.

6. M.A. Alvin and J. Klotz, "TBC Bond Coat Systems," NETL Patent Disclosure, May 25, 2010.

7. M.A. Alvin, "Materials and Component Development for Advanced Turbine Systems," ASME Turbo Expo, Glasgow, United Kingdom, June 18, 2010.

8. G.H. Meier, "Factors Affecting the Microstructural Stability and Durability of Thermal Barrier Coatings Fabricated by Air Plasma Spraying," Presentation at the Materials Engineering: Building on the Legacy of Tony Evans, a Memorial Conference at UCSB, September 8, 2010.

III.C.4 Materials and Component Development for Advanced Turbine Systems — Non-Destructive Evaluation

Mary Anne Alvin
U.S. Department of Energy (DOE)
National Energy Technology Laboratory (NETL)
626 Cochrans Mill Road
Pittsburgh, PA 15236-0940
Phone: (412) 386-5498; Fax: (412) 386-4806
E-mail: Maryanne.Alvin@netl.doe.gov

NETL – Regional University Alliance (RUA):

- NETL — Mary Anne Alvin
- West Virginia University, Morgantown, WV — Dr. Bruce Kang, Mr. Jared Tannenbaum, Dr. Roger Chen, Mr. Binwei Zhang

Contract Number: 0004000.5.610.243.001

Start Date: October 1, 2009
End Date: September 30, 2010

FY 2010 Objectives

- Develop ultrasonic micro-indentation and pulse-echo non-destructive evaluation (NDE) techniques to detect material property changes that occur in thermal barrier coatings (TBCs) during extended, bench-scale, isothermal and cyclic oxidation testing.
- Develop NDE techniques to provide advanced warning of internal yttria-stabilized zirconia (YSZ)/bond coat interfacial debonding prior to visually observing TBC delamination or spallation.

Accomplishments

- In comparison to the surrounding TBC matrix, areas with higher average surface stiffness measurements as determined by micro-indentation testing were considered as locations where internal YSZ debonding was occurring during bench-scale isothermal and cyclic oxidation testing. As predicted, these areas were locations where debonding and spallation of the TBC were initially visually observed.
- Variations in wave reflection amplitude and travel time observed by pulse-echo techniques addressed the onset of internal YSZ TBC debonding during isothermal and cyclic oxidation testing of thermal barrier coated coupons.
- Both NDE techniques were utilized to address TBC thickness variations on an as-manufactured thermal barrier coated first row turbine blade.
- Pulse-echo NDE was successfully used to identify localized TBC delamination on a field-serviced combustor liner.

Introduction

State-of-the-art TBCs consist of metallic bond coat and YSZ systems that are deposited along the surface of superalloys or single crystal substrate materials. Coating failure, such as YSZ delamination and spallation during high temperature engine operation, leads to localized heating of the turbine airfoil or combustor structural support metal, and service downtime with required maintenance. Failures are usually caused by internal residual stress, originating from differences in thermal properties of the various coating layers in the TBC system. As residual stress increases, microcracks can be formed and cause damage accumulation. When the accumulated damage produces a critical crack size, the YSZ top coat could buckle locally and spall. NDE techniques that detect early internal surface debonding or delamination of the YSZ layer prior to spallation from metal surfaces potentially address remaining service life or the need for refurbishment of coated components during scheduled power plant maintenance intervals.

The following sections describe the Fiscal Year 2010 efforts conducted at West Virginia University with respect to the development of bench-scale micro-indentation and acousto-ultrasonic NDE techniques as predictive TBC life assessment tools.

Approach and Results

Micro-Indentation Testing

With the evolution of nano-technologies, micro- and nano-indentation testing techniques have become prevalent. The load and depth relationship developed through these techniques provide insight with respect to a material's mechanical properties such as elastic modulus and hardness. Load and depth relationships acquired during indentation are found to be both elastic and plastic, and as a result, analysis of the unloading portion of an indentation load displacement curve is used to establish a material's elastic modulus.

A multiple-partial unloading (MPU) micro-indentation technique was developed for mechanical property evaluation of commercial TBC systems.

The MPU technique eliminates the need for precise indentation depth measurements required by current nano- and micro-indentation methods. The MPU technique led to the development of several load-depth sensing indentation systems (Figure 1) capable of determining the elastic modulus of metallic alloys with flat, tubular, or curved architectures. Additionally, portable, highly maneuverable, and high-temperature units were developed that identified stiffness properties of TBCs, and predicted the location of TBC debonding and spallation on bench-scale laboratory test coupons.

Each of the micro-indentation systems shown in Figure 1 consists of a rigid loading frame, a 100 lb load cell, a 30-120 µm piezoelectric actuator, and a spherical tungsten or sapphire 750 µm radius indenter. Due to the limited travel range of piezoelectric actuators (40-180 µm), each system initially determines the contact position between the indenter and the test sample using a relatively small load (<0.1 N). An automated LabVIEW™ software program controls the performance of the micro-indentation tests using a predefined multiple-partial unloading test procedure. Following test completion, data are processed for the multiple unloading slope measurements, and the elastic modulus is calculated. Excellent agreement was demonstrated for the elastic modulus values generated for O1Tool Steel, Aluminum 6061, and Bronze 932 by micro-indentation testing and modulus values reported in the literature (Table 1).

A load-based micro-indentation technique was additionally developed for evaluating the mechanical properties of materials at elevated temperatures (i.e., ≤1,250°C). Tests conducted on a H13 Tool Steel coupon from 22°C to 500°C generated modulus values that were in excellent agreement with reported literature values. Additionally, the elastic modulus of Hayne 230 at 1,000°C was accurately identified (i.e., literature: 150 GPa; micro-indentation: 148.7±3 GPa).

TABLE 1. Elastic Modulus

Flat Coupons			
	O1 Tool Steel	**Aluminum 6061**	**Bronze 932**
Literature, GPa	193-214	69-79	103-124
Micro-Indent, GPa	208.8±2.6[(a)]	68.8±1.0	111.9±2.0
Cylindrical Tubes			
	O1 Tool Steel (0.75 inch Diameter)	**O1 Tool Steel (1.0 inch Diameter)**	**Bronze 932 (0.75 inch Diameter)**
Literature, GPa	193-214	193-214	103-124
Micro-Indent, GPa	203±5.9	207.9±5.1	107.3±5.5

(a) 1σ standard deviation for five test coupons.

In contrast to metals, air plasma sprayed (APS) or electron beam physical vapor deposited (EBPVD) YSZ TBCs are relatively porous, have multiple interface surfaces, and have a relatively rough outer surface topography. Therefore instead of modulus values being determined by micro-indentation for TBC systems, surface stiffness response measurements are obtained. When compared to areas along the TBC surface that had not been subjected to micro-indentation testing, scanning electron microscopy (SEM) surface and cross-sectional analyses indicated that *indentation-induced* TBC microcracks were not

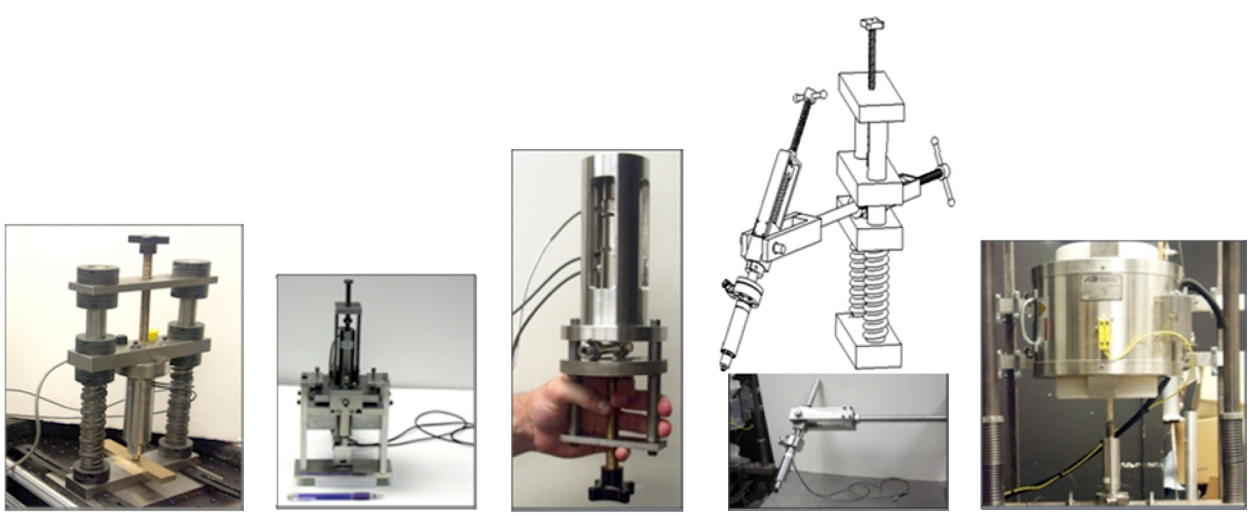

(a) (b) (c) (d) (e)

FIGURE 1. Micro-Indentation Load-Depth Sensing Systems: (a) Table-Top Model; (b) Portable Table-Top Model; (c) Hand-Held Model; (d) Maneuverable Table-Top Model; (e) High-Temperature System

evident after micro-indentation testing was conducted with an applied indentation load of <90 N. Similarly, testing of TBCs to spallation failure occurred at comparable times with/without micro-indentation testing, indicating that micro-indentation does not cause detectable cumulative surface damage or TBC degradation.

A series of seven isothermal and cyclic oxidation tests with René N5/MCrAlY/APS YSZ or EBPVD YSZ coupons was conducted at 1,100°C in a bench-scale tube furnace until TBC debonding or spallation was visually observed. Periodically the coupons were removed from the furnace and subjected to micro-indentation testing at 20 locations along the TBC surface (Figure 2; 4 x 5 evenly distributed locations, 4 mm from the edge of the coupon). A finite element interpolation routine was developed to generate TBC stiffness contour maps (Figure 3), where blue was indicative of locations with lower average surface stiffness response, and red was indicative of locations having higher average stiffness response. Surface stiffness along the edges of the coupons was extrapolated.

With continued high-temperature testing, TBC debonding was visually observed along areas of the coupon where higher average surface stiffness response measurements were initially obtained. For example, increased near-edge stiffness responses were identified after ~185 hours of isothermal testing for the René N5/MCrAlY/APS YSZ coupon shown in Figure 3, while debonding of the YSZ at these locations was only visually observed after 500 hours of isothermal testing. Similar early failure location predictions were accurately identified for the alternate six coupons. Through finite element analyses (FEA), the higher average surface stiffness regions were linked to an increase in out-of-plane residual stress at the YSZ/thermally grown oxide (TGO) interface, which was considered to ultimately be responsible for initiating debonding and TBC spallation.

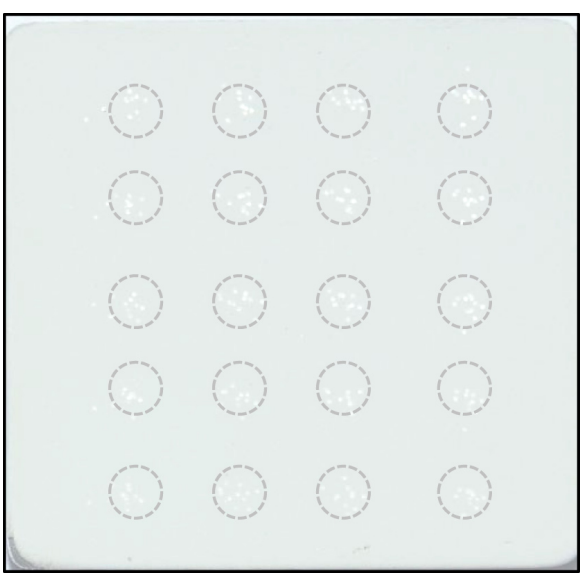

FIGURE 2. Micro-Indented Areas along the Surface of a 25.4 mm x 25.4 mm Thermal Barrier Coated Coupon

Acousto-Ultrasonic Testing

Various NDE techniques have been utilized to address TBC thickness, material properties, and performance integrity during high-temperature bench-scale testing. These techniques include pulse-echo, water immersed pulse-echo, electrochemical impedance spectroscopy, thermal tomography, and implementation of laser excitation response waveforms. During FY 2010, pulse-echo techniques continued to be developed to provide rapid NDE of the YSZ/bond coat interface, as well as identification of YSZ material property changes that occur during extended isothermal or cyclic oxidation bench-scale testing. Waveform diagnostics indicated that damaged materials show a greater attenuation, and that early detection of interface degradation can be observed.

Ultrasonic testing was performed using gel contact piezoelectric sensors along the surface of as-manufactured, and 1,100°C isothermally and cyclic oxidation tested René N5/MCrAlY/APS-coated coupons. During FY 2009 pitch/catch surface acoustic waves and pulse-echo through-thickness techniques were evaluated. With pitch/catch, two Pico sensors (5 mm diameter x 4 mm) were utilized, where one sensor acted as a transmitter, and the other sensor served as a receiver. Both sensors were attached to an acrylic block, and were separated by 3 mm.

Using pulse-echo testing, a pulse is generated and as it traveled through the thickness of the coupon, reflections are returned at each TBC material interface (i.e., YSZ/bond coat interface; bond coat/metal substrate interface). A 20 MHz sensor with a delay-line tip was utilized to acquire reflections through a pulser-receiver unit, with the signal recorded by a digital oscilloscope. Multiple reflections were identified due to the wave traveling back and forth inside the coupon. Because of the attenuation properties of the various materials, energy loss caused an amplitude drop after the first reflection. Time measured between reflections indicated how long the wave traveled inside a particular medium. The measured time resolution was obtained in the nano-second range.

The total pulse-echo travel time through-thickness results are shown in Figure 4 for an 1,100°C isothermally tested René N5/MCrAlY/APS YSZ TBC coupon. The total wave travel time through the thickness of the coupon, as well as through the

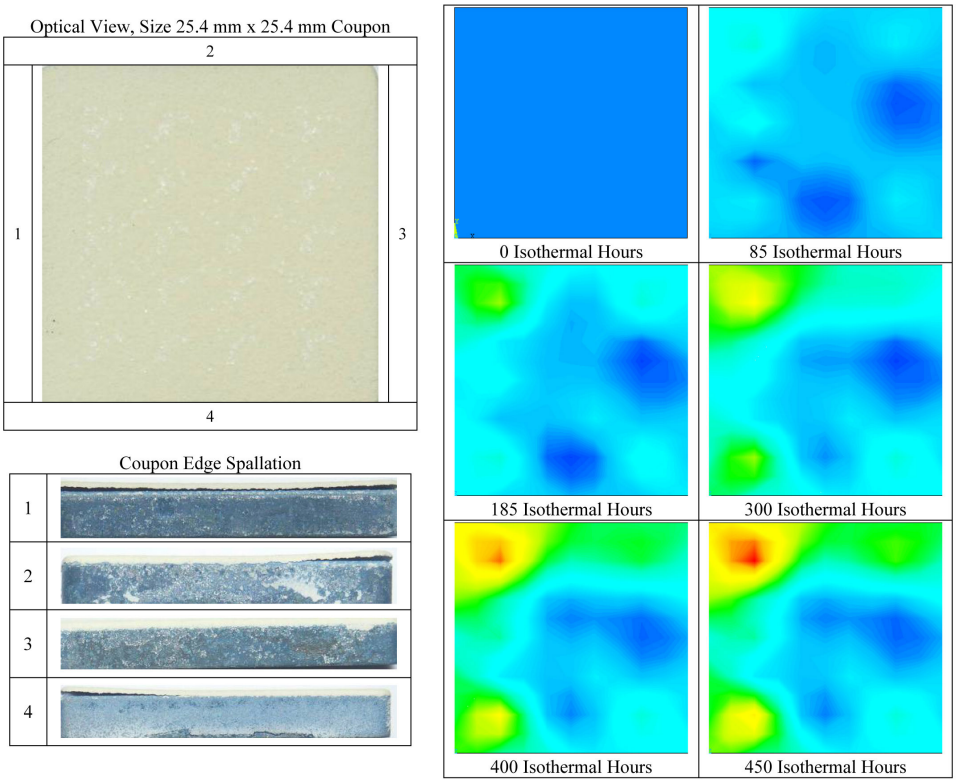

FIGURE 3. Surface and Edge Photographs of a René N5/MCrAlY/APS YSZ Thermal Barrier Coated Coupon after 500 Hours of 1,100°C Isothermal Testing, and Corresponding Average Surface Stiffness Response Color Maps as a Function of Isothermal Exposure Time

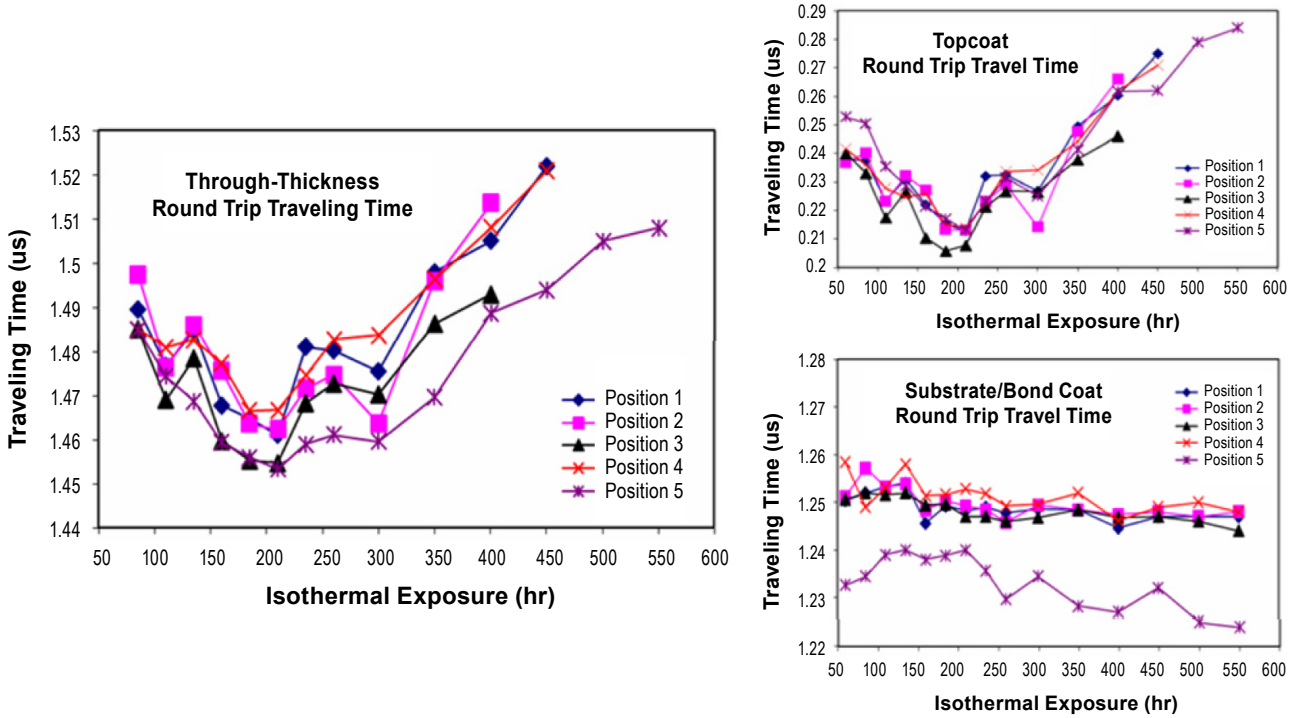

FIGURE 4. Ultrasonic Wave Travel Time through the Isothermally Tested APS YSZ TBC Coupon

APS YSZ top coat continued to decrease during the initial ~210 hours of bench-scale testing. After ~210 hours, wave travel time increased with continued high temperature exposure. In contrast, the wave travel time in the substrate/bond coat remained nearly constant throughout the entire isothermal test exposure. These results implied that changes in the material properties of the APS YSZ occurred (i.e., reduction in Young's modulus; sintering), and that early detection of internal delamination resulting from generation of a critical crack size along the YSZ/bond coat interface was observed (i.e., >400 hours when sensor reflections could no longer be detected). Notably initiation of YSZ APS TBC detachment (debonding) was visually evident only along one corner of the coated coupon after 400 hours of high temperature isothermal exposure (Figure 5). In contrast, clear separation of the APS YSZ TBC from the underlying metal substrate was observed after 550 hours of isothermal testing.

Pulse-echo NDE characterization along the YSZ TBC surface of additional 1,100°C isothermal and cyclic oxidation tested coupons identified a diminishing metal/air waveform reflection amplitude, and a change in sign of the top coat/TGO interface reflection when delamination was predicted to have occurred (Figure 6). When pulsed along the metal substrate surface, the top coat/TGO interface reflections were strengthened with continued thermal exposure. The amplitude sign change was considered to be a clear indication of the time when internal delamination was initiated.

Variations in wave reflection amplitude and travel time as observed by pulse-echo techniques addressed the onset of internal YSZ TBC debonding during isothermal and cyclic oxidation testing of thermal barrier coated coupons. FEA models were additionally developed using ABAQUS to simulate the wave propagation through the various TBC layers, to establish a better understanding of the defect detection phenomenon, and to estimate the material properties such as the Young's Modulus and mass density of each TBC layer.

An industrial combustor liner and an as-manufactured first row turbine blade were examined

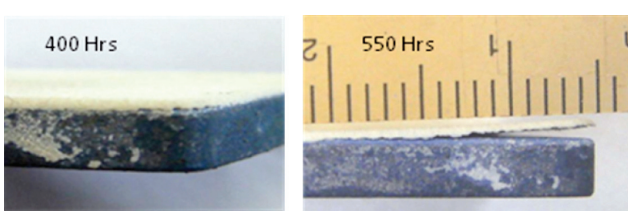

FIGURE 5. Photographs Illustrate Detachment of the YSZ Top Coat during Bench-Scale 1,100°C Isothermal Testing of a René N5/MCrAlY/APS YSZ TBC Coupon

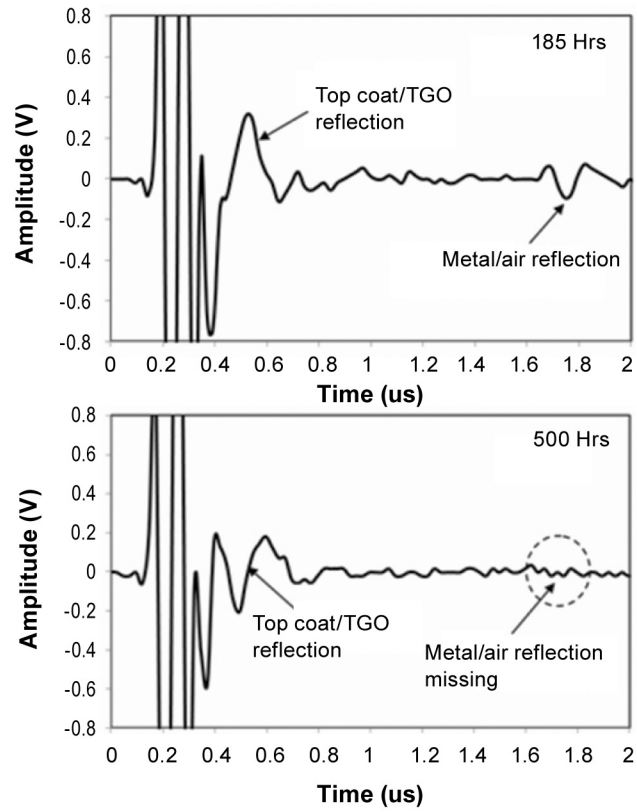

FIGURE 6. Pulse-Echo Waveforms for an 1,100°C Isothermally Tested René N5/MCrAlY/APS YSZ TBC Coupon

using the pulse-echo ultrasonic technique. The results from NDE characterization of these industrial components show successful detection of internal delamination on the combustor liner, and the thickness of the top coat and metal of both the liner and the turbine airfoil.

Future Directions

Micro-Indentation Testing

Micro-indentation testing of thermal barrier coated coupons is planned to be conducted at temperatures up to 1,200°C in ≥50% moisture-containing environments. Color contour maps will be utilized to predict TBC failure locations, and SEM characterization will be attempted to validate internal crack formation and/or debonding at the TGO/YSZ interface or within the YSZ coating.

Acousto-Ultrasonic Testing

A small thermal barrier coated turbine blade was obtained from Directed Vapor Technologies International for as-manufactured and 1,100°C

thermally cycled acousto-ultrasonic characterization. Bench-scale testing will continue with six additional TBC coupons focusing on validating early detection of internal YSZ delamination (i.e., detecting the formation of the TGO and identifying critical crack size) and changes in material properties, and comparison of the experimental observations and NDE results with the FEA models.

FY 2010 Publications/Presentations

1. M.A. Alvin, "Materials and Component Development for Advanced Turbine Systems," Presentation at the UTSR Workshop VII, Orlando, Florida, October 27–29, 2009.

2. J. Tannenbaum, B. Kang, and M.A. Alvin, "A Load-Based Depth-Sensing Micro-Indentation Technique for Spallation Detection of Thermal Barrier Coatings," TMS Conference, Seattle, Washington, February 14, 2010.

3. J. Tannenbaum, B. Corklin, B. Kang, and M.A. Alvin, "Development of as High Temperature Micro-Indentation Technique for Material Mechanical Property Evaluation up to 1200°C," TMS Conference, Seattle, Washington, February 14, 2010.

4. M.A. Alvin, "Materials and Component Development for Advanced Turbine Systems," ASME Turbo Expo, Glasgow, United Kingdom, June 18, 2010.

5. J. Tannenbaum, B. Kang, and M.A. Alvin, "Non-Destructive TBC Spallation Detection by a Micro-Indentation Method," ASME Turbo Expo 2010, Glasgow, Scotland, June 14–18, 2010.

6. C. Feng, J. Tannenbaum, B. Kang, and M.A. Alvin, "A Load-Based Multiple-Partial Unloading Micro-Indentation Technique for Mechanical Property Evaluation," Experimental Mechanics, Vol. 50, Issue 6 (2010), p. 737-743 (DOI 10.1007/s11340-009-9271-4).

7. B. Zhang, "Non-Destructive Evaluation of Thermal Barrier Coating Systems Using Ultrasonic Techniques," Master's Thesis, West Virginia University, May 4, 2010.

8. R. Chen, B. Zhang, and M.A. Alvin, "Ultrasonic Detection of Delamination and Material Characterization of Thermal Barrier Coatings," Manuscript being prepared for Journal submission.

9. J. Tannenbaum, K. Lee, B. Kang, and M.A. Alvin, "Non-Destructive Spallation Prediction of Thermal Barrier Coatings by a Load-Based Micro-Indentation Technique," Materials Science and Technology 2010, Houston, Texas, October 17–21, 2010 (submitted).

10. J. Tannenbaum, C. Chou, B. Kang, and M.A. Alvin, "A Portable Load-Based Micro-Indentation Technique for On-Site Mechanical Property Evaluation of Structural Components," Materials Science and Technology 2010, Houston, Texas, October 17–21, 2010 (submitted).

11. J. Tannenbaum, K. Lee, B. Kang, and M.A. Alvin, "Non-Destructive Thermal Barrier Coating Spallation Prediction by a Load-Based Micro-Indentation Technique," 2010 ASME International Mechanical Engineering Congress and Exposition, Vancouver, British Columbia, Canada, November 12–18, 2010 (submitted).

12. K. Lee, J. Tannenbaum, B. Kang, and M.A. Alvin, "A Load-Based Depth-Sensing Indentation Technique for Elastic-Plastic Material Mechanical Property Evaluation," 2010 ASME International Mechanical Engineering Congress and Exposition, Vancouver, British Columbia, Canada, November 12–18, 2010 (submitted).

13. J.M. Tannenbaum, K. Lee, B.S.-J. Kang, and M.A. Alvin, "An Indentation-Based Non-Destructive Evaluation Technique for Thermal Barrier Coating Spallation Prediction," 35th International Conference and Exposition on Advanced Ceramics and Composites (ICACC2011), Daytona Beach, Florida, January 23–28, 2011 (submitted).

14. J.M. Tannenbaum, K. Lee, B.S.-J. Kang, and M.A. Alvin, "Material Performance of TBCs in High Temperature Moisture-Containing Environments Using a Load-based Micro-indentation Technique," TMS Annual Meeting & Exhibition, San Diego, California, February 27 – March 3, 2011 (submitted).

15. J.M. Tannenbaum, B.S.-J. Kang, and M.A. Alvin, "The Development of a Non-Destructive Multiple Partial Unloading Micro-Indentation Technique for Thermal Barrier Coating Spallation Prediction," TMS Annual Meeting & Exhibition, San Diego, California, February 27 – March 3, 2011 (submitted).

III.C.5 Materials Issues in Coal-Derived Synthesis Gas/Hydrogen-Fired Turbines

Bruce Pint
Oak Ridge National Laboratory (ORNL)
1 Bethel Valley Rd.
Oak Ridge, TN 37831-6156
Phone: (865) 576-2897
E-mail: pintba@ornl.gov

DOE Project Manager: Briggs White
Phone: (304) 285-5437
E-mail: Briggs.White@netl.doe.gov

Contract Number: FEAA070

Start Date: December 1, 2009
End Date: September 30, 2010

FY 2010 Objectives

- Maximize the service lifetime of bond coatings in thermal barrier coatings (TBCs) by applying mechanistic understanding of the factors that contribute to their degradation in the environments expected in syngas/hydrogen-fired turbines.
- Complete characterization of failed TBC specimens from the 2009 study of the effect of superalloy composition and bond coating type on TBC lifetime in furnace cyclic testing.
- Obtain MCrAlY coatings on various doped superalloys and begin characterization and initial oxidation assessment of their oxidation behavior at 1,050°-1,150°C.
- Explore the effect of water vapor on TBC lifetime by: 1) constructing a new cyclic oxidation rig for mixed gases with water vapor; 2) obtaining standard TBC specimens for testing with well-characterized diffusion bond coatings; and 3) performing an initial test matrix on these specimens in air with three levels of water vapor (10, 50 and 90 vol%).

Accomplishments

- Demonstrated that the TBC lifetime with Pt diffusion bond coatings was >50% higher compared to that observed with Pt-modified aluminide coatings and significantly less rumpling was observed on the Pt diffusion coatings, ~10X reduction in the rate of surface rumpling without a ceramic top coating.
- Obtained high velocity oxygen fuel (HVOF) sprayed MCrAlYHfSi coatings on three versions of CMSX4 with different dopant levels (Y and La).
- Completed construction of a thermal cycling furnace rig capable of testing with air or bottled gases and water vapor concentrations from 5-90 vol%.
- Completed characterization of the thermally-grown scale formed on LPPS (low-pressure plasma-sprayed) MCrAlYHfSi on a commercial Ni-base superalloy after three isothermal laboratory exposures at 1,050°-1,100°C and observed the ionic segregation of Y and Hf to the alumina scale grain boundaries in each case.

Introduction

Using gas synthesized from coal (i.e., syngas) or hydrogen to fuel land-based gas turbines represents several operational and materials concerns compared to burning natural gas. These fuels require different combustion conditions and generate more water vapor in the exhaust gas entering the turbine hot section [1]. Also, during the synthesis process, upset conditions in the gas cleanup process can allow sulfur and other contaminants to periodically enter the turbine. Thus, compared to the normally clean natural gas fuel, these synthetic fuels will likely require more robust materials in the turbine hot section in order to achieve the same performance. To maintain turbine availability with current materials, the turbine inlet temperature may be reduced thereby reducing the turbine efficiency.

Superalloy turbine blades and vanes in the hot section typically are protected by oxidation-resistant coatings including a TBC to reduce the metal temperature in service. There are dozens of different commercial MCrAlYX (M=Ni,Co; X=Hf, Si, Re, etc.) coatings, therefore, the likelihood of developing a new bond coating is limited. All TBC systems rely on the formation of a slow-growing, adherent alumina scale between the metallic bond coating and the ceramic yttria-stabilized zirconia (YSZ) top coating. The overall goals of this project are to: 1) study strategies to make the alumina more adherent or slower growing; 2) quantify how the syn-gas/H_2 environment is more aggressive than a conventional natural gas-fired turbine; and 3) use advanced characterization techniques (e.g., high resolution transmission electron microscopy) to better understand the underlying mechanisms involved in each case.

Approach

The oxidation resistance of the bond coating is a critical weak link determining TBC lifetime because spallation of the thermally grown alumina scale formed on the bond coating will ultimately result in loss of the outer ceramic thermal protection layer. The strategy adopted here is to identify issues that could have a strong near-term impact on coating performance and generate data that could be easily transferred to turbine manufacturers and users. Rather than developing a new coating composition or process, an unresolved issue is quantifying the benefit of dopants to the superalloy on coating performance. Commercially available Y- and La-doped alloy CMSX4 has limited experimental evidence showing improvements in TBC lifetime [2]. The strategy adopted here is to coat three different variations of CMSX4 with one bond coating and then to conduct controlled oxidation experiments to determine the effect of the dopants on the scale growth rate and adhesion. In future work, similar specimens will be coated with a YSZ top coat to determine the effect of dopants on the YSZ lifetime in furnace cycling tests.

For understanding the syn-gas/H_2 environment, it seems clear that these environments will have higher water vapor contents either due to combustion or the use of steam diluents [1]. Therefore, a clear understanding of how higher water vapor contents affect TBC lifetime appears to be necessary to develop improved coatings as well as to design proper experiments. Controlled laboratory experiments with different water vapor contents will yield initial information about the effect of increasing water vapor on TBC lifetime. Rather than initially studying MCrAlY coatings for this task, well-characterized Pt diffusion ($\gamma+\gamma'$ phase) and Pt-modified aluminide (β phase) coatings will first be studied as these coatings have baseline TBC lifetime in dry O_2 (Figure 1).

In both cases, characterizing the alumina scale microstructure and microchemistry is essential to understanding the role of dopants and water vapor. Since the scale is typically 1-10 µm thick, it is difficult to gain understanding using conventional scanning electron microscopy (SEM) or electron microprobe analysis (EPMA). Therefore, analytical transmission electron microscopy (TEM) characterization is needed to gain a better mechanistic understanding of these effects.

Results

To conclude work begun in FY 2009, Figure 1 shows the final TBC lifetime for various superalloy/bond coating combinations. Three bond coatings were evaluated on substrate N5 and the 7 µm Pt diffusion coating was evaluated on three different commercial

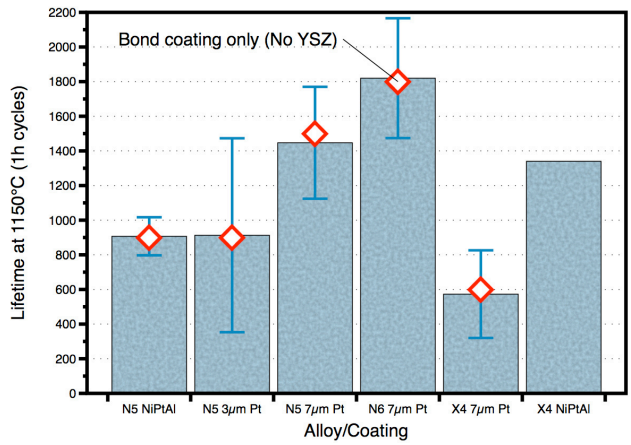

FIGURE 1. Lifetimes for EB-PVD YSZ-coated specimens for various alloys and coatings exposed in 1 h cycles at 1,150°C in dry O_2. The bars note the standard deviation for three specimens, the diamonds are where the exposure of the specimen without a YSZ coating was stopped for characterization.

superalloys (N5, N6 (high Re) and CMSX4). All of the substrates had the same YSZ top coating of ~125 µm deposited by electron beam-physical vapor deposition (EB-PVD) through a cooperation with General Electric. A Pt-modified aluminide (β) coating made at ORNL by low activity chemical vapor deposition [3] was used as a baseline coating on alloy N5 and had an average lifetime of 900 1-h thermal cycles at 1,150°C. The bars in Figure 1 show the relatively low standard deviation of the three specimens evaluated. To study the effect of Pt content on Pt diffusion ($\gamma+\gamma'$) coatings [4], both 3 µm and 7 µm Pt were deposited on the same N5 superalloy substrates and diffused into the substrate by vacuum annealing for 2 h at 1,100° and 1,175°C, respectively. The average lifetime for the 3 µm Pt diffusion coating was similar to the baseline β coatings but with a much larger standard deviation, not an attractive feature for turbine designers. The 7 µm Pt diffusion coatings on N5 showed a >50% higher lifetime than the β coatings. This increase in lifetime was attributed to the significant reduction in rumpling or roughening [5] of the bond coating surface during exposure, Figure 2. The roughness was measured on the specimens without a YSZ coating that were exposed for a similar number of cycles as the average lifetime (diamonds in Figure 1). However, in cross-sections of the failed YSZ-coated specimens, the rumpling was less on the YSZ-coated side of the specimen compared to the uncoated side, suggesting that rumpling may be inhibited by the YSZ coating and measurements of uncoated surfaces less relevant to actual TBC performance.

The same 7 µm Pt diffusion coating was evaluated on three different superalloys, Figure 1. The high Re N6 substrate showed the highest average TBC lifetime,

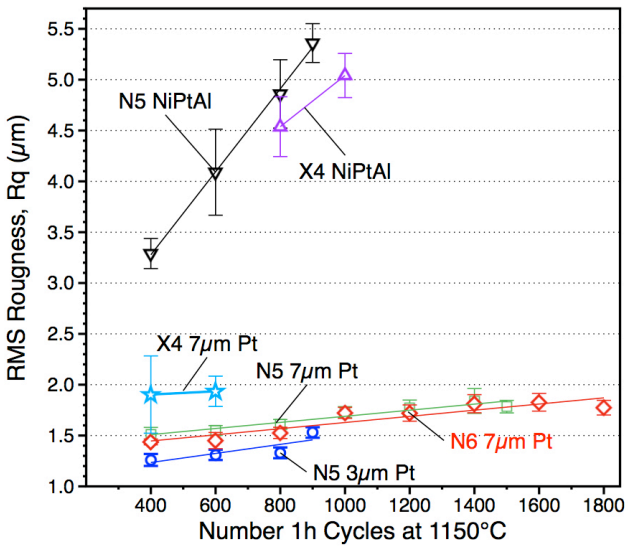

FIGURE 2. Root mean square (RMS) roughness (Rq) for the specimens without a YSZ coating as a function of 1 h cycles at 1,150°C. As expected, the Pt-modified aluminide coatings have a higher roughness than the Pt diffusion coatings.

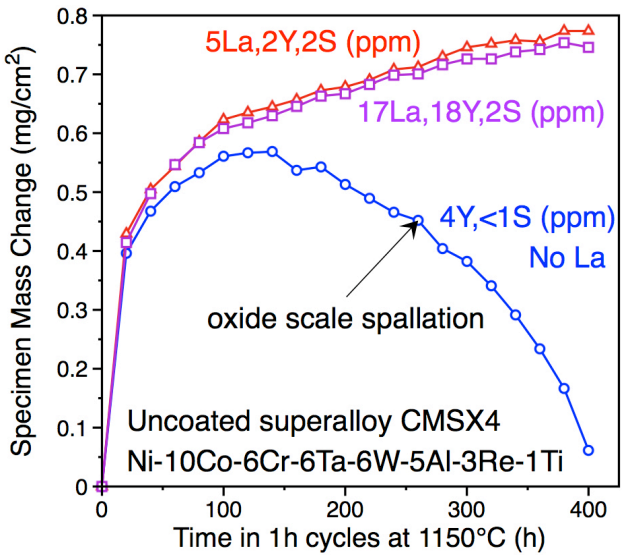

FIGURE 3. Specimen mass gain for uncoated CMSX4 specimens exposed in 1 h cycles at 1,150°C. The three alloys are identified by their La, Y and S contents. The addition of La prevented mass loss due to scale spallation.

consistent with a prior study [6]. Also consistent with prior work [7,8], the average TBC lifetime on CMSX4 with 7 µm Pt was the lowest. This decrease was attributed to the presence of 1% Ti in the CMSX4 alloy. Characterization by EPMA determined that 2% Ti had replaced Al in the γ+γ'coating. However, a single specimen of CMSX4 with a Pt-modified aluminide (β) coating was included and, with this bond coating, the Ti in CMSX4 did not reduce the TBC lifetime, Figure 1. Therefore, it may be too simplistic to conclude that Ti has a negative effect on coating lifetime in all cases. Nevertheless, Ti is a mobile element and is capable of diffusing through any coating and affecting the alumina scale.

For the FY 2010 work on MCrAlY coatings, substrates were machined from three different versions of CMSX4 with different dopant levels. Substrates were coated with a commercial MCrAlYHfSi coating using HVOF at Stony Brook University and were vacuum annealed at ORNL for 4 h at 1,080°C. The MCrAlYHfSi coating is reported to have superior performance to conventional MCrAlY coatings [9]. Oxidation testing of these coatings at 1,050°, 1,100° and 1,150°C will begin in the last quarter of FY 2010. Prior to coating testing, the uncoated superalloys were cyclicly oxidized at 1,100° and 1,150°C. Figure 3 shows the mass gain for the three uncoated specimens at 1,150°C. At this temperature, the La addition appeared to significantly improve the oxidation resistance of the uncoated alloys. The mass loss for the La-free specimen suggests significant scale spallation, which was visually evident by large spalled regions of the surface oxide.

For the task on water vapor effects, specimens of N5 with a Pt-modified aluminide (β) coating or a Pt diffusion coating have been fabricated and sent for coating by EB-PVD at the same source as the prior study, Figure 1. Evaluations in air with 10, 50 and 90% water vapor are expected to begin in the fourth quarter of FY 2010. The lifetimes on these specimens should be directly comparable to the results in Figure 1. Depending on the coating lifetime, these experiments may be completed in the first quarter of FY 2011. In preparation for this work, a second cyclic rig was constructed at ORNL with the capability for exposures in gases with water vapor. This rig has been completed and will allow testing in more complex environments (e.g. including CO_2) in the future.

The characterization task has focused on the MCrAlYHfSi coating but deposited by LPPS on Ni-base superalloy PWA1484 (coated burner rig bar provided by Pratt & Whitney). One goal of this investigation was to look for the segregation of Y and Hf to the alumina scale grain boundaries after oxidation. It is well known that dopant ions segregate to alumina grain boundaries but a recent review paper found no published segregation observations from commercial MCrAlY bond coatings [10]. The coated specimen was cut into coupons which were isothermally oxidized for 200 h at 1,050°C and 100 and 200 h at 1,100°C. At all three conditions, the coating was investigated by SEM to examine the scale morphology and metallographically cross-sectioned to examine the microstructure and study interdiffusion using EPMA. A TEM cross-section was prepared from each specimen using focused ion beam milling. In each case, Y and Hf were detected

as segregants to the alumina grain boundaries, an example is given in Figure 4. To better understand the role of these dopants, the long-term goal is to quantify the segregation as a function of time and temperature. This segregation information provides a baseline for evaluating the coated CMSX4 specimens where the goal is to locate La and Ti from the superalloy substrate in the scale or coating.

Conclusions and Future Directions

The TBC lifetime tests of the Pt diffusion coatings concluded the multi-year evaluation of that class of coatings. It was demonstrated that these coatings were more durable than Pt-modified aluminide coatings in furnace cycling tests and exhibited less surface rumpling during these exposures. Due to the Pt in the $\gamma+\gamma'$coating, it was shown that the Al content actually increased during exposure. However, these coatings appear to be more sensitive than other compositions to the underlying superalloy composition. Because of a lack of current interest by land-based turbine manufacturers in diffusion coatings, the ORNL project has shifted to evaluating MCrAlY-type coatings.

The evaluation of MCrAlYHfSi coatings on La- and Y-doped superalloys is just beginning with initial cyclic oxidation exposures planned for the fourth quarter. Likewise, the water vapor effect study on TBC lifetime is just starting with specimens prepared with diffusion bond coatings and awaiting commercial YSZ deposition. This testing also should begin in the fourth quarter.

Future work on this project will include:

- Determining the effect of Y- and La-doping on alumina scale adhesion and growth rate.
- Coating coupons with air plasma sprayed (APS) YSZ to determine the effect of Y- and La-doping on the lifetime of the ceramic layer in furnace testing.
- Evaluating the effect of water vapor (10-90%) on furnace cycle TBC lifetime, initially on diffusion bond coatings with EB-PVD YSZ, then on APS YSZ with MCrAlYHfSi bond coatings.
- Characterizing the alumina scale microstructure and microchemistry using high-resolution TEM and other characterization techniques to gain a better mechanistic understanding of the role of dopants and water vapor.

FY 2010 Publications/Presentations

1. B.A. Pint, J.A. Haynes, and Y. Zhang, "Effect of Superalloy Substrate and Bond Coating on TBC Lifetime," in press and presentation at the International Conference on Metallic Coatings and Thin Films, San Diego, California, April 2010.

2. K.A. Unocic and B.A. Pint, "Characterization of the Alumina Scale Formed on a Commercial MCrAlYHfSi Coating," in press and presentation at the International Conference on Metallic Coatings and Thin Films, San Diego, California, April 2010.

3. B.A. Pint, "Materials Issues in Coal-Derived Synthesis Gas/Hydrogen-Fired Turbines," presentation at the 2009 University Turbine Systems Research Workshop, Orlando, Florida, October 2009.

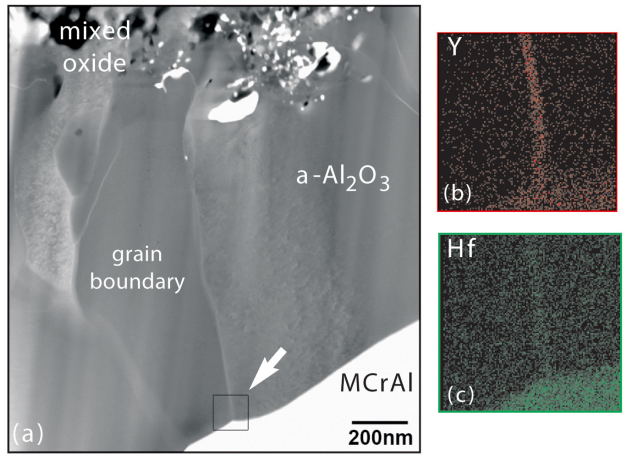

FIGURE 4. Alumina scale formed on LPPS MCrAlYHfSi coated 1484 oxidized for 100 h at 1,100°C in dry O_2 (a) shows a TEM annular dark field image of the columnar section of the scale and X-ray maps (b) Y and (c) Hf show grain boundary segregation in box in (a), see arrow.

References

1. P. Chiesa, G. Lozza, and L. Mazzocchi, "Using Hydrogen as Gas Turbine Fuel," J. Eng. Gas Turbines & Power, 127 (2005) 73-80.

2. K. Harris and J.B. Wahl, "Improved Single Crystal Superalloys. CMSX-4®(SLS)[La+Y] and CMSX-486®," in K.A. Green, T.M. Pollock, H. Harada, T.E. Howson, R.C. Reed, J. Schirra and S. Walston eds., Superalloys 2004, TMS, Warrendale, Pennsylvania, 2004, p. 45-52.

3. Y. Zhang, W.Y. Lee, J.A. Haynes, I.G. Wright, B.A. Pint, K.M. Cooley, and P.K. Liaw, "Synthesis and Cyclic Oxidation Behavior of a (Ni,Pt)Al Coating on a Desulfurized Ni-base Superalloy," Met. Trans. A, 30 (1999) 2679-2687.

4. B.A. Pint, J.A. Haynes, K.L. More, J.H. Schneibel, Y. Zhang, and I.G. Wright, "The Performance of Pt-modified Alumina-Forming Coatings and Model Alloys," in R.C. Reed, et al. eds., Superalloys 2008, TMS, Warrendale, Pennsylvania, 2008, p. 641-650.

5. P. Deb, D.H. Boone, and T.F. Manley, "Surface Instability of Platinum Modified Aluminide Coatings During 1100°C Cyclic Testing," J. Vac. Sci. Technol. A, 5 (1987) 3366-3372.

6. K. Bouhanek, O.A. Adesanya, F.H. Stott, P. Skeldon, D.G. Lees, and G.C. Wood, "High Temperature Oxidation of Thermal Barrier Coating Systems on RR3000 Substrates: Pt Aluminide Bond Coats," Mater. Sci. Forum, 369-72 (2001) 615-22.

7. H.M. Tawancy, A.I. Mohamed, N.M. Abbas, R.E. Jones, and D.S. Rickerby, "Effect of Superalloy Substrate Composition on the Performance of a Thermal Barrier Coating System," J. Mater. Sci., 38 (2003) 3797-3807.

8. R.T. Wu, K. Kawagishi, H. Harada and R.C. Reed, "The Retention of Thermal Barrier Coating Systems on Single-Crystal Superalloys: Effects of Substrate Composition," Acta Mater. 56 (2008) 3622-3639.

9. D.K. Gupta and D.S. Duvall, "A Silicon and Hafnium Modified Plasma Sprayed MCrAlY Coating for Single Crystal Superalloys," in Superalloys 1984, M. Gell, et al. eds., p. 711-20, TMS, Warrendale, Pennsylvania (1984).

10. B.A. Pint and K.L. More, "Characterization of Alumina Interfaces in TBC Systems," J. Mater. Sci. 44 (2009) 1676-86.

III.C.6 Zero Emissions Coal Syngas-Oxygen Turbo Machinery

Dennis Horazak
Siemens Energy, Inc.
4400 Alafaya Trail
Orlando, FL 32826
Phone: (407)736-5131; Fax: (407) 736-5014
E-mail: Dennis.Horazak@siemens.com

DOE Project Manager: Robin Ames
Phone: (304) 285-0978
E-mail: Robin.Ames@netl.doe.gov

Contract Number: 42646

Start Date: October 1, 2005
End Date: September 30, 2010

FY 2010 Objectives

- Determine basic oxidation/corrosion behavior and characterize it under defined steam/CO_2 conditions for the alloys in SGT-900 hot gas path.
- Quantify the low cycle fatigue (LCF) life of select SGT-900 turbine alloys after exposure to steam/CO_2 environment for comparison with baseline (atmospheric) data.
- Conduct modeling of plant cycles with an OFT-900 oxy-fuel turbine as the intermediate pressure (IP) turbine under two different fuel scenarios – natural gas and syngas produced by the Siemens Fuel Gasifier. The OFT-900 design is based on the design of the SGT-900 industrial gas turbine, but using a steam/CO_2 mixture as its working fluid instead of air, and without an air compressor.

Accomplishments

- Exposure of coated and uncoated buttons of SGT-900 turbine alloys has been completed under steam/CO_2 atmosphere up to 500 hours. Beta-phase depletion measurements to assess the oxidation resistance are complete. On completion of the studies a comparison of the depletion curves can be made between the two environments – products of natural gas combustion and steam/CO_2. Results show accelerated oxidation in steam/CO_2 environment due to increase in formation of transient oxides.
- LCF was determined to be the most important mechanical property to quantify the effects of environmental exposure in steam/CO_2. Exposures of LCF specimens were completed at two temperatures and are complete. The results show that for nickel alloys tested that there is no effect on life due to steam/CO_2 environment. For cobalt alloys, there is a life debit at high strain levels on uncoated alloys. However, it was also determined that there is no debit on cobalt alloys utilizing thermal barrier coatings (TBCs) for protection.
- Modeling of the selected near-term oxy-fuel cycle with CO_2 capture has been completed with two fuels – natural gas and coal syngas. The cycle utilized a high pressure (HP) turbine with a combustor and an OFT-900 (modified SGT-900 Siemens gas turbine) with a reheater as an IP turbine.

Introduction

Advanced power systems that utilize nearly pure oxygen as the oxidant and coal-derived gaseous fuels are an attractive approach to highly efficient zero emissions systems that capture and sequester carbon dioxide. In these systems, the oxidant and fuel are combusted to create a working fluid composed mostly of steam and CO_2. This working fluid can be utilized in a Rankine cycle turbine to generate power while CO_2 can be captured after condensation of the drive gas mixture. In order to achieve high cycle efficiency, it is necessary to use the drive gas at temperatures comparable to or higher than those of today's gas turbines. Turbines using such a drive gas at high temperatures (1,750°C or higher) have not been developed. Power generation using the oxy-fuel combustion process has been demonstrated by Clean Energy Systems, Inc. of Rancho Cordova, California, albeit on a small scale. The advantages of developing turbines that are large enough for commercial power generation are as follows:

- Use of coal – the least expensive and most abundant domestic fuel.
- Mitigation of NOx emissions since the oxidizer is pure oxygen instead of air.
- Greater than 99.5% of CO_2 captured.
- Materials and coatings development will benefit gas turbines used in combined cycle or peaking power generation applications.
- Steam cooling and other design technologies such as rim cavity sealing will also benefit gas turbine products.
- Technology will also apply to oxy-fuel turbines using natural gas (since the drive gas is the same) for near-term applications such as peaking power generation with enhanced oil recovery.

Approach

The project approaches the development of turbo machinery to use the working fluid produced by syngas-oxygen combustion products in a pragmatic way by evaluating the technology promise in the short-term as well as in the long-term. Siemens Energy, Inc. and Clean Energy Systems, Inc. have jointly arrived at an arrangement of combustors, re-heaters and turbines that provides competitive plant cycle efficiency. In order to achieve high efficiency, it is necessary to use the drive gas at a very high temperature. For the long-term, the target value of the drive gas (steam, CO_2 mixture) in this project is 1,760°C (3,200°F) for the IP turbine and 760°C (1,400°F) for the HP turbine. These temperatures are significantly higher than those utilized in current day industrial gas turbines or steam turbines.

Just as in Fiscal Year 2008 and FY 2009 during FY 2010 the project approach was re-focused on near-term application of existing turbines (rather than developing a very high-temperature turbine) to an oxy-fuel power generation demonstration project. Such an approach was seen to be necessary to understand the material behavior in steam/CO_2 environments and also to validate turbine performance assumptions since a turbine typically used as a 'gas' turbine is to be employed for expanding steam/CO_2 drive gas mixtures.

Results

1. Beta-phase depletion studies under steam/ CO_2 atmosphere: These studies are important because they provide additional safety margin if the protection from the TBC is lost due to thermal spallation or foreign object damage (FOD). In such an event the ability of the bond coat to resist oxidation becomes critical to avoid a component failure. Tests were run in order to assess the oxidation resistance of the bond coat when exposed to the actual turbine atmosphere (approximately 90% steam, 10% CO_2). The materials selected were the cobalt-based alloy ECY768 used in row 1 vane and nickel-based alloy IN738 used in row 1 blade. (These rows experience the highest fluid temperatures in the turbine.)

The specimens were exposed at temperatures relevant to the OFT-900 oxy-fuel calculated hot gas path. Every 100 hours a specimen was pulled for microstructural assessment and measurement of the depleted beta phase zone. (Atmospheres included products of natural gas combustion as well as steam/CO_2 for comparison.) Figure 1 shows the microstructure of one of the alloys, IN738, with bondcoat and TBC from which beta phase depletion measurements were made. Depletion vs. time curves (as shown in Figure 2) have been generated for ECY768 and IN738. Figure 3 shows a comparison of

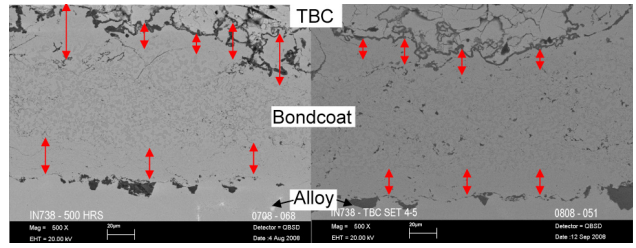

FIGURE 1. Example of microstructure of IN738 with bondcoat and TBC after exposure in steam/CO_2 (left) and natural gas (right). Red arrows indicate the beta phase depletion regions.

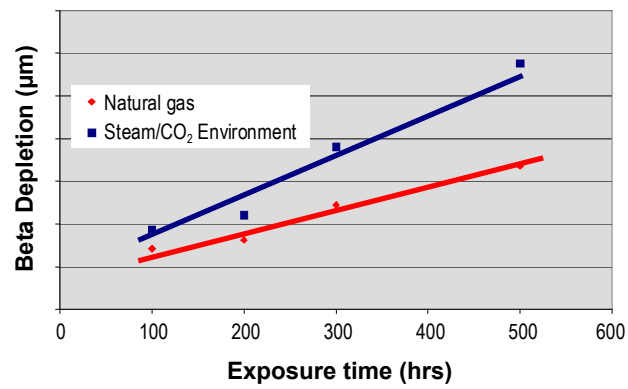

FIGURE 2. Depletion vs. time curve for ECY768 with bondcoat and TBC in steam/CO_2 and natural gas. (IN738 shows a similar trend.)

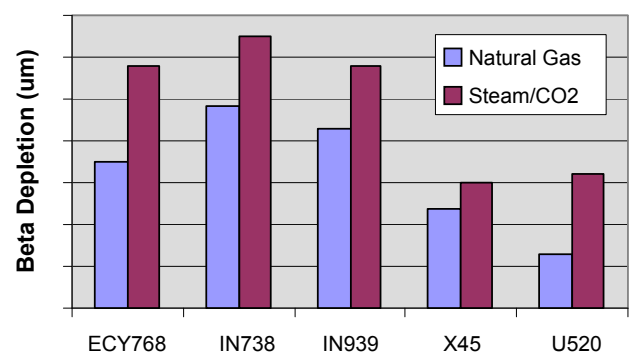

FIGURE 3. Comparison of depletion of system after 500 hours in steam/CO_2 and natural gas environments for hot gas path alloys.

the depletion after 500 hours in steam/CO_2 and natural gas for all SGT-900 alloys with bondcoat. In all cases, it was found that steam/CO_2 atmosphere was more aggressive in depleting the bondcoat beta phase when compared to a natural gas environment. In addition, modification of the protective oxides formed was observed in the steam/CO_2 atmosphere on bare alloys (as shown in Figure 4).

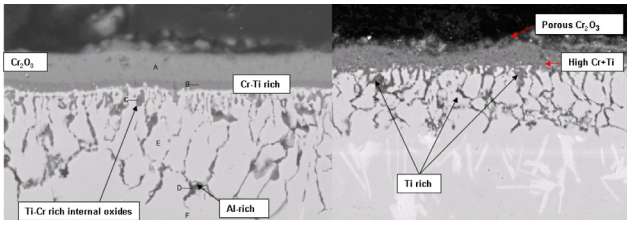

FIGURE 4. Comparison of oxide scales after exposure in simulated gas turbine environment (left) and steam/CO_2 environment (right).

2. Low cycle fatigue testing on steam/CO_2 exposed specimens: In addition to the outside surfaces of the turbine airfoils getting exposed to the steam/CO_2 fluid, the airfoils that are cooled internally (vanes and blades in the first two stages) can also be degraded by the oxidizing nature of the coolant. The coolant temperature is lower than that of the working fluid; therefore steam/CO_2 exposure tests on LCF specimens were performed at different temperatures on non-coated and coated specimens to mimic the effect of steam/CO_2 on the cooling passages and on the alloys in the hot gas path. The lower temperature exposure was performed by Cranfield University (United Kingdom) and the higher temperature exposure was performed by National Energy Technology Laboratory-Albany (Albany, Oregon). Subsequent LCF tests were completed at the expected operational metal temperature. Results show oxy-fuel exposure had little effect on the strain-life relationship in hot gas path conditions on either coated (rows 1 and 2) or uncoated (row 3) alloy samples, as shown in Figure 5. Also, different effects were found on different uncoated alloys at low temperatures. Nickel-based alloys showed minor effects from the oxy-fuel exposure to the strain-life properties, similar to the trend shown in Figure 5, whereas uncoated cobalt alloys showed a noticeable debit to strain-life properties at high strain ranges, as shown in Figure 6.

3. Zero CO_2 emission plant cycle modeling: This work was subcontracted to The Advanced Power & Energy Programs group of the University of California, Irvine. The objective was to model the Zero Emission Power Plant cycle with conditions suitable for the OFT-900 IP turbine. Both natural gas and coal syngas were considered for fuel since the first plant is expected to use natural gas as fuel, with syngas being used in the later years with more operating experience. The cycle utilizes an HP combustor, an HP turbine, a reheater and an OFT-900 (modified SGT-900) turbine as the IP turbine. Both turbines work on steam/CO_2 mixtures and heat recovery and a low-pressure turbine are utilized downstream. (The IP turbine is assumed to run with an inlet temperature of only 1,080°C in the near term case.) For the natural gas case, the model includes a separate air separation unit (ASU) to supply pure oxygen. The cycle efficiency, including all

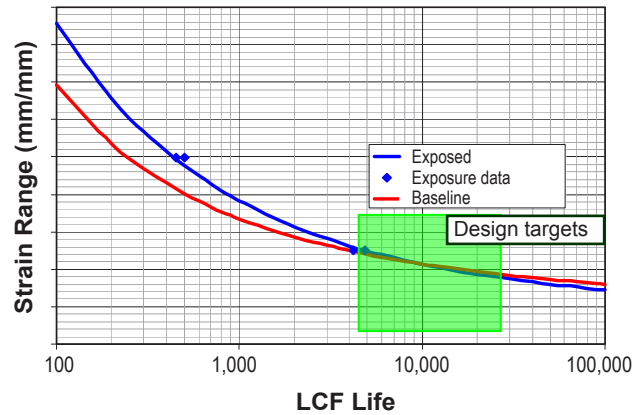

FIGURE 5. Strain-life LCF plot of steam/CO_2 exposed cobalt alloy (with overlay coating) at high temperature versus baseline cobalt alloy. Coated and uncoated nickel alloys show similar trends, with negligible effects at target OFT design conditions.

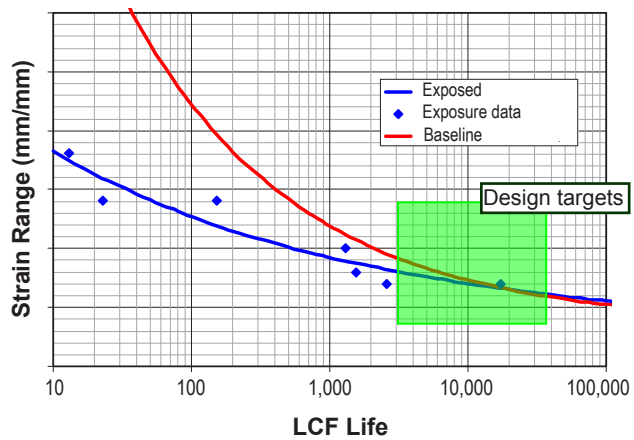

FIGURE 6. Strain-life LCF plot of steam/CO_2 exposed cobalt alloy (no coating) at low temperature versus baseline cobalt alloy; note the negligible effects at target OFT design conditions.

parasitic loads was calculated as 33.9% (lower heating value [LHV] basis). The coal syngas case, in addition to utilizing the ASU, employs a Siemens engineered coal gasifier. The resulting efficiency (LHV basis) is 25.8%, again including all parasitic loads.

Conclusions and Future Directions

The work performed during FY 2010 has focused on a near-term application of an existing Siemens turbine while keeping the development effort linked to the needs of the far-term syngas oxy-fuel cycle. The materials testing and analytical work undertaken is the first step towards adapting the Siemens SGT-900 IP turbine to perform with steam/CO_2 as its fluid. The principles applied here will work equally well whether the fuel is natural gas or coal-derived syngas since the

resulting fluid in both cases is a mixture of steam and CO_2. While they still need to be consolidated, some preliminary conclusions about the material behavior can be stated as follows:

- Initial assessment showed that beta phase retention was adversely affected by steam/CO_2 atmospheres when compared to a natural gas baseline. (This could affect the oxidation resistance once the TBC is lost.) Work is continuing to attempt to quantify this into an effect on lifetime.
- The oxidation products observed after steam/CO_2 exposure indicated a more aggressive and unstable scale formation when compared to natural gas, which will negatively impact life. Increased spinel formation was observed in the steam/CO_2 environment, and this has been shown to disrupt the formation of protective oxides.
- The generation of low cycle fatigue data after exposure in steam/CO_2 will provide a preliminary assessment of any debit for both hot gas path and cooling flow design.
- Modeling of the plant cycle has been completed with both natural gas and coal syngas as the fuels. Expected efficiencies for the plant are 33.9% and 25.8% respectively (LHV) with only a moderate temperature (1,080°C) utilized for the IP turbine inlet.

In the future, this project will focus on the near-term natural gas application that requires an inlet temperature in the range of 1,080°C to 1,180°C (1,976°F to 2,156°F) for the SGT-900 IP turbine. The project will continue materials evaluation work to adapt the turbine to a plant cycle that uses the IP turbine by itself in a simple cycle or in conjunction with a HP steam/CO_2 turbine and a low-pressure steam turbine as in a "combined" cycle. Further, it will seek opportunities to refurbish and deliver the IP turbine to a zero CO_2 emission power plant for demonstration and testing.

FY 2010 Publications/Presentations

1. R. Anderson, V. Viteri, R. Hollis, A. Keating, J. Shipper, G. Merrill, C, Shilling, S. Shinde, J. Downs, D. Davies, M. Harris, "Oxy-Fuel Gas Turbine, Gas Generator and Reheat Combustor Technology Development and Demonstration," ASME Turbo Expo 2010, paper GT2010-23001.

IV. UNIVERSITY TURBINE SYSTEMS RESEARCH

A. Aero-Heat Transfer

IV.A.1 Designing Turbine Endwalls for Deposition Resistance with 1,400°C Combustor Exit Temperatures and Syngas Water Vapor Levels

Jeffrey P. Bons (Primary Contact), Ali Ameri
Department of Aerospace Engineering
The Ohio State University (OSU)
2300 West Case Rd.
Columbus, OH 43235
Phone: (614) 247-8414
E-mail: bons.2@osu.edu

DOE Project Manager: Mark Freeman
Phone: (412) 386-6094
E-mail: Mark.Freeman@netl.doe.gov

Subcontractor:
Thomas H. Fletcher
Brigham Young University (BYU), Provo, UT

Contract Number: NT0005055

Start Date: October 1, 2008
End Date: September 30, 2011

FY 2010 Objectives

- Perform Turbine Accelerated Deposition Facility (TADF) test series varying gas temperature and fuel type.
- Analyze TADF coupon deposition and thermal barrier coating (TBC) degradation.
- Obtain second vane sector hardware from industry.
- Perform deposition sensitivity study on second vane sector.
- Compare model predictions to OSU Turbine Reacting Flow Rig (TuRFR) results.
- Perform design of leading edge/endwall geometry optimization relative to deposition.

Accomplishments

- Fluent was selected as the computational fluid dynamics (CFD) test bed for deposition studies and a particle deposition model was developed and validated using comparisons to experimental deposition data from BYU's TADF facility.
- New silicon carbide components for BYU TADF successfully demonstrated operation up to 1,400°C. This will allow investigation of the temperature dependency of deposition, beyond the previous facility limit of 1,200°C. The higher operating temperature is necessary to simulate the operating environment of modern H-class power turbines.
- OSU TuRFR assembly completed. This unique facility simulates the flowfield at the inlet to a modern nozzle guide vane, with gas temperatures up to 1,100°C and Mach numbers approaching 0.1. The facility also includes the capability to cool from both the hub and casing endwalls.
- Deposition studies commenced with two nozzle guide vane (NGV) doublets donated from General Electric (GE). The combustor was seeded with 10 micron diameter bituminous coal ash particles. Initial tests show a strong sensitivity to gas temperature between 1,000°C and 1,050°C. This is very near the transition temperature reported in other deposition studies. Deposits are primarily found in the leading edge and pressure surface region. The suction surface is relatively untouched by the deposits. Maximum deposit thicknesses in the leading edge region can exceed 3 mm.
- Film cooling at up to 12% of the mainflow was shown to substantially reduce deposition in TuRFR, though cooling holes become sites for deposit initiation.
- Discussions are underway for additional hardware commitments from Pratt & Whitney, Siemens, and Solar Turbines.
- Computational deposition model was successfully implemented in three dimensional (3D) vane geometry. The geometry used is the GE/National Aeronautics and Space Administration (NASA) Energy Efficient Engine (EEE) design. Though this is not the same as the CFM56 geometry employed in the TuRFR experiments, the two vanes share many similarities.
- Simulations predict increased deposition with increasing particulate size and gas temperature, consistent with experimental observations.

Introduction

Turbine inlet temperatures for large power generation gas turbines have been steadily increasing over the last several decades due to significant advances in materials and cooling technologies. At the same time, political and economic pressures are pushing utilities to consider fuel flexibility using synfuels that have higher concentrations of trace elements and ash compared to "clean" burning natural gas. Current plans to transition from current syngas to high hydrogen fuels produced from coal syngas and

oxy-fuels will only exacerbate these challenges with high water vapor levels. The combination of increased engine operating temperatures and synfuel integration warrant a reevaluation of current hot gas path design to consider the potential impact of deposition. In the first stage high pressure turbine vane (nozzle), the majority of material system failures occur at the junction of the vane and the passage endwall. Secondary flows in this region create unique challenges for thermal management and efficient cooling design. Recent initiatives of passage endwall contouring and vane leading edge modifications have been developed for use with natural gas fired turbines and thus their compatibility with ash-bearing and/or high steam content synfuels at elevated operating temperatures has yet to be assessed. Clearly, there is a critical need to explore innovative endwall designs that could both increase turbine durability and mitigate the adverse effects of deposition in the endwall.

Approach

This research effort addresses this critical turbine operability and maintainability issue in three distinct phases.

- **Phase 1** – Modeling and Experimental Validation: A deposition model will be developed and incorporated in an existing CFD code capable of handling modern turbine geometries. Validation of this new model will be performed using both the OSU and BYU accelerated deposition facilities. The BYU TADF facility will be modified to accommodate higher firing temperatures (up to H-class engine temperatures 1,400°C) and the addition of water vapor. The OSU facility will be used to investigate deposition patterns around real film-cooled turbine hardware at engine relevant conditions. Hardware will be donated from GE, Siemens, and Pratt through collaborative agreements.
- **Phase 2** – CFD and Experimental Endwall Design Study: Various endwall design modifications will be evaluated, both experimentally and computationally, to determine their influence on deposition. The objective will be to evaluate each of the design modifications for deposition resistance as well as aerodynamic and heat transfer performance. BYU will perform gas temperature and fuel type test series to determine high temperature extension of deposition data.
- **Phase 3** – CFD Design Study with Cooling and Experiments with Water Vapor: BYU will explore the effect of water vapor on turbine deposition. Experiments will be conducted with various TBC material systems with water vapor levels up to 15% to simulate levels anticipated with high hydrogen combustion. The effect of film cooling on deposition will also be studied, both at BYU and OSU. Deposition models will be used to determine optimum film flow location to mitigate endwall deposition and improve material system survivability.

Thus, with this aggressive research project, DOE and industry will gain valuable insights into factors affecting the safe, efficient operation of modern industrial turbines with alternative fuels as well as new, innovative endwall designs that are tailored for this more adverse operating environment.

Results

Experimental Facility at BYU:

The TADF went through a major redesign during the first year of this effort. The objective was to allow high temperature operation up to 1,400°C. Silicon carbide was chosen as the candidate material for the new hot section. These modified components were designed, manufactured and installed successfully. The new range of testing parameters is shown in Figure 1. Testing with the modified facility has been very promising. During the second year, a number of facility maintenance issues were resolved that will allow safe, efficient testing for years to come. In addition, new test coupons were received from GE and Siemens. These are being modified to conform to the coupon holder and some are being fitted with film cooling holes to then be returned to the provider for the TBC.

Experimental Facility at OSU:

The fabrication and initial performance testing of the now fully-assembled OSU TuRFR was completed during the first year of this effort (Figure 2). Following those initial tests, the facility was taken off-line for several system upgrades including: new flameholders,

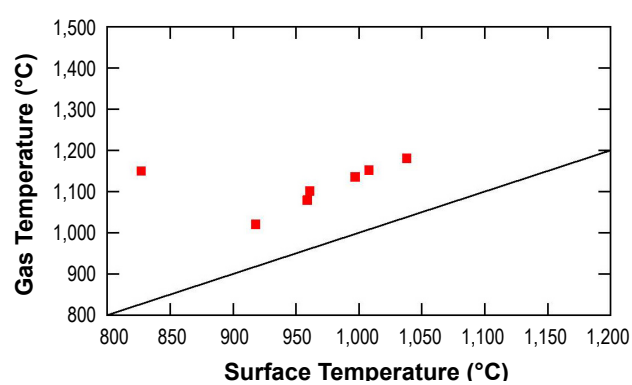

FIGURE 1. Operating Range of Redesigned TADF at BYU

FIGURE 2. Digital Image of OSU TuRFR Showing Upper and Lower Sections Assembled

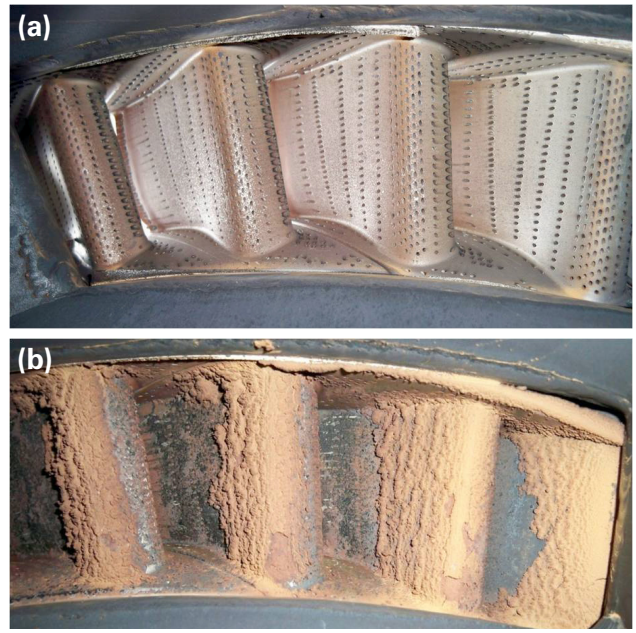

FIGURE 3. 1-hr Accelerated Deposition Test with 10 Micron Bituminous Coal Particulate on GE CFM56 Vane: Inlet Mach Number = 0.09, Exit Reynolds Number = 400,000, Gas Temperature (a) 1,850°F and (b) 1,950°F

improved particulate feed system, and new gaskets. To avoid further gasket failures the facility has been derated to a lower inlet Mach number and exit Reynolds number (0.08 and 350,000 respectively). Several new deposition tests were then conducted at gas temperatures of 1,800°F. Wake loss measurements taken before and after deposition over a range of flow Reynolds numbers from 0.25 to 1.5 million indicate a reduction in total pressure loss with the deposit layer. This indicates the possibility that the deposit roughness produces a premature boundary layer transition at this Reynolds number. Further testing will be conducted to verify this result. The gas temperature was then raised from 1,800°F to 1,950°F to determine the effect of temperature on deposition. A dramatic increase in deposit thickness and character was noted around 1,900°F for the bituminous coal fly ash used in the present study (Figures 3a and 3b). When film cooling was added at 1,900°F, the deposition levels were reduced dramatically. Video footage revealed that the film cooling holes near the leading edge actually became sites for deposition. Deposition also accumulated near the casing endwall at the leading edge fillet. This is an area of particular concern that will be a subject of future investigation during the third year. Communications continue with Siemens to identify future hardware donations.

Computational Methods at OSU:

An initial literature survey covering research efforts centered on alternative (syngas) fuels deposition on turbine blades with film cooling was completed. After consulting the literature a methodology for particle tracking and deposition was selected where an Eulerian-Lagrangian approach is to be followed: the Eulerian approach for the continuous phase and the Lagrangian approach for the discrete phase. After considering various options, it was decided that the particle-tracking and deposition models would be developed and implemented with the use of a commercial CFD code, FLUENT. The FLUENT-based deposition model was successfully validated against both the TADF deposition data and a previous study at Von Karman Institute during the first year of the grant. During the second year, the team exercised the deposition model in an actual 3D vane geometry with the NASA/GE EEE design. This architecture is particularly interesting since it actually has derivatives that currently operate in industrial gas turbines. Preliminary simulations indicate significant deposition on the pressure surface and in the leading edge region (Figure 4), similar to the TuRFR results with the CFM56 vane. Results also show dependency on surface temperature and particle size.

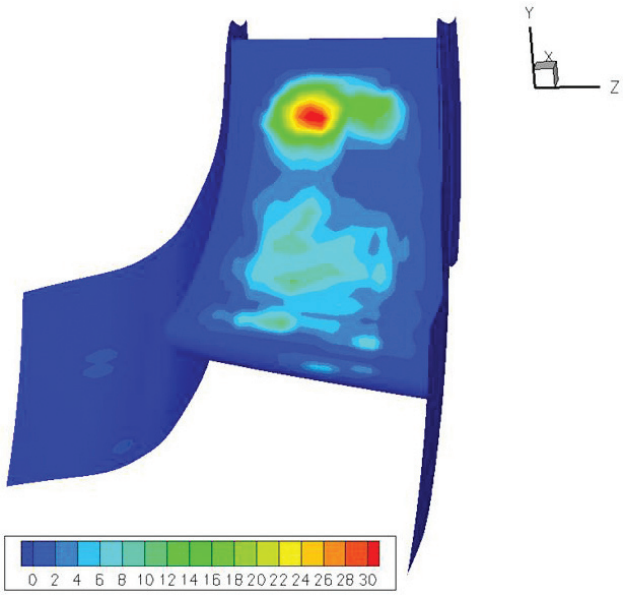

FIGURE 4. Prediction of Deposition for 10 Micron Particulate for Conditions Similar to Figure 3, Using GE EEE Vane Design

Conclusions and Future Directions

In summary, the project is going strong with healthy progress during the first six quarters. Both the BYU TADF and the OSU TuRFR facilities have been redesigned and are operational. During the remainder of the second year, the test coupons will be finished so that a series of deposition tests at higher gas temperatures can be conducted. Following this, tests will be conducted with film cooling holes. For the OSU facility, testing will continue with the CFM56 nozzle hardware. The intent is to further explore the dependency of deposition on flow temperature, velocity, and film cooling level. We will also continue to explore the effect of deposition on aerodynamic losses over a wider range of Reynolds numbers. We are hopeful that Siemens will become the second hardware donor for this facility. We are exploring all avenues to obtain the computational geometry for CFD simulations and validation of Dr. Ameri's deposition code. We have also secured the capability to make detailed surface scans of the deposit topology. Finally, significant progress has been made with the computational model development. The commercial CFD code, FLUENT, has been exercised and the required "User Defined Functions" for particle deposition have been developed. Preliminary comparisons with previous studies at BYU appear to be promising. Deposition testing with the BYU and OSU facilities is well underway. An alternative deposition model based on constituent viscosities is being explored. This model has been successfully used by Sreedharan and Tafti [1] in modeling similar turbine deposition. Comparisons with the El Batch and Haselbacher [2] model will be conducted during the next quarter. We also hope to have the actual CFM56 geometry modeled in FLUENT shortly. The deposition models will be used to guide the endwall redesign work planned for Phase 2 and 3 of the project.

FY 2010 Publications/Presentations

1. C. Smith, B. Barker, C. Clum, and J.P. Bons, "Deposition in a Turbine Cascade with Combusting Flow," Presented at the ASME Turbo Expo 2010, June 14–18 in Glasgow, United Kingdom (GT-2010-22855).

References

1. S.S. Sreedharan and D.K. Tafti, 2009, "Effect of blowing ratio on syngas fly ash particle deposition on a three row leading edge film cooling geometry using large eddy simulations," ASME Paper No. GT2009-59326.

2. H. El-Batsh and H. Haselbacher, "Numerical investigation of the effect of ash particle deposition on the flow field through turbine cascades," IGTI, 2002, Amsterdam, Netherlands, GT-2002-30600.

IV.A.2 Aerodynamics and Heat Transfer Studies of Parameters Specific to the IGCC Requirements: Endwall Contouring, Leading Edge Filleting and Blade Tip Ejection under Rotating Turbine Conditions

Dr. Meinhard T. Schobeiri (Primary Contact),
Dr. Je-Chin Han
TPFL, the Turbomachinery Performance and
Flow Research Laboratory
Mechanical Engineering
Texas A&M University
College Station, TX 77843-3123
Phone: (979)845-0819; Fax: (979) 845-0812
E-mail: tschobeiri@mengr.tamu.edu

DOE Project Manager: Robin Ames
Phone: (304) 285-5436
E-mail: Robin.Ames@netl.doe.gov

Contract Number: FE0000753

Start Date: October 1, 2009
End Date: September 30, 2012

FY 2010 Objectives

The objective of the proposed research is to provide the engine designer with a set of quantitative aerodynamics and film cooling effectiveness data that are essential for understanding the basic physics of the complex secondary flow, its influence on the efficiency and performance of gas turbines, and the impact of film cooling ejection arrangements on suppressing the detrimental effect of secondary flows. Proposed endwall aerodynamics, film cooling experimental and the complementary numerical investigations will be performed exclusively under rotating conditions. The highly advanced three-stage turbine designed by Dr. Schobeiri for the past DOE-Univeristy Turbine Systems Research (UTSR) project, will serve as the experimental platform. Using the baseline configuration, axisymmetric and non-axisymmetric endwall segments will be attached successively to the rotor hub for endwall contouring. Subsequent attachment of the leading edge fillets will determine their additional effects on the secondary flow losses. Interstage measurement will be performed for proposed configurations by traversing the entire flow field from hub to tip and in circumferential direction over three spacings. Static, absolute and relative total pressure, velocity components distributions, as well as pitch and yaw angle distributions delivered by the traverse will be analyzed to obtain loss distributions from hub to tip for stator as well as rotor row. The stator and rotor loss coefficient distributions of the contoured endwall case will then be compared with the loss coefficient distributions of the non-contoured endwall of the baseline configuration. This comparison will provide a definitive quantitative answer to the question about the improving effect of the endwall contouring and filleting under rotating conditions. The proposed blade tip ejection rotating rig experiments to counteract the tip clearance vortex is intended to: (a) reduce the induced drag force by the tip clearance vortex; and (b) to reduce the tip clearance leakage, thus, improving the efficiency and simultaneously reducing the potential for corrosion, erosion, and deposition on the blade tip. Detailed interstage aerodynamics measurements coupled with heat transfer experiments and accompanied by numerical investigations, will provide a full understanding of tip clearance secondary flow physics and its impact on gas turbine design. Although the topic of this research defined by UTSR is specific to gas turbines operating with hydrogen/syngas fuels, the proposed research results will be also applicable to gas turbines operating with conventional fuels. Understanding the impact of secondary flow on turbine performance, particularly the formation of depositions due to fuel impurities, requires quantifying the secondary flow physics in a rotating environment. By controlling the secondary flow on the blade platform, there is less potential for the impurities to be entrained by the vortices and deposited on the blade platform.

Accomplishments

- Fabricated 12 thermocouple implanted sensor blades with J-type thermal sensor.
- Assembled three reference turbine stator rings with four sensor blades spaced 90 degrees in circumferential direction in each.
- Two types of non-axisymmetric endwall contouring and a large leading edge filleting have been designed and evaluated via computation fluid dynamics (CFD) simulations. Certain positive improvement, such as reduction of vorticity and elimination of horseshoe vortex, has been verified by numerical calculations, which contributes nearly 0.2% increase in rotor efficiency.

Introduction

The reference turbine contains three stator and rotor stages. In order to take temperature data of the flow field at the inlet of stator 1, stator 2 and stator 3, we installed in each stator ring four blades instrumented with thermocouples. Additionally, two different three-dimensional endwall contouring and one leading edge filleting were designed for the rotors in the turbine. A set of CFD simulations has been systematically performed with the commercial CFD software CFX. Comprehensive analysis and comparison have been completed for three different designs.

Approach

We installed thermocouples (TT-J-30-SLE, OMEGA Engineering) into five openings that were evenly distributed (10.5 mm apart) on the stagnation line of stator blades. For the sake of data acquisition quality, and system reliability, aside from configuration angle, sensor wiring was the second issue attracted our focus. Two measures were taken to constrain and secure the thermocouple wirings from the sensor blades to the data acquisition system. Flexible fiber glass tubes were used at where the thermocouple wired out sensor blade tip; the main concern of applying this material is to avoid the fragile wiring to break because of the sharp turn on the stator ring inner shard. Accounted in system working temperature and hardware configuration, we employed nylon spirally-cut cable warp band into our thermocouple wiring after the fiber glass tube as well. Since all the properly wired thermal sensor warps share the same exit at 9 o'clock, and a certain off-machine length to avoid both unnecessary tension and torsion was crucial, thermocouple length at various positions must be taken into account. In our design, the length of thermal sensors at 3 o'clock, 6/12 o'clock, and 9 o'clock were 210 cm, 155 cm, and 100 cm, respectively.

A system of four-digit sensor numbering strategy was developed for marking all connect ends of thermocouples. The first digit indicates the number of the stator stage, while the second and third digits combined to provide information for the position on the stator stage. The forth digit demonstrated the sensor position on each blades, and the numbering increased progressively from hub to tip as 1 to 5. For example, a four-digit sequence '3 12 3' was decoded as following information: the thermocouple was located on stage three, 12 o'clock, and the third sensor counted for the hub side.

For the CFD part, the contouring design methods and numerical simulation methodology would be introduced, respectively. The contouring design is based on several different polynomial functions, which are able to approximate smooth curves. The main idea is that the streamwise contouring shape is defined by polynomial functions and then the filleting-like surface is generated which is tangent to both blade and hub. Considering the controllable of the polynomial functions, the 5th order polynomial was selected as the shape function. With six boundary conditions (height at starting point and ending point, maximum height and its location, slope at these three positions) fixed, the 5th order shape function is eventually determined uniquely. According to the preliminary investigations, the maximum height of the contouring was chosen as 13 mm which is 20% span height. Additionally, the location of maximum height is adjusted too. Eventually two different locations were set along the streamwise direction-the one is at 15% C_{ax} while the other one is at 30% C_{ax} for comparison. At the same time, leading edge filleting is also considered since large leading edge filleting is able to significantly reduce the horseshoe vortex which has been discussed in References 1-3. According to geometric information in these references, the height of the filleting is set to 10% of span height and the length was 20%. In addition, the outer profile of the filleting is restricted by the elliptical curve and the height of the filleting varies linearly. Finally, four cases corresponding to four different models were performed. The reference case which has no modifications to the endwall is noted as the reference case, as shown in Figure 1(a). The case with large leading edge filleting attached to the second rotor is signed as leading edge (LE)-filleting (Figure 1(b)). The two contoured cases with maximum height at 15% C_{ax} and 30% C_{ax} are called 13mm-15 C_{ax} (Figure 1(c)) and 13mm-30C_{ax} (Figure 1(d)), respectively. The last two cases only have the second rotor contoured.

Actually, both 13mm-15C_{ax} and 13mm-30C_{ax} were calculated before and the results were exhibited in the first quarter of 2010. The preliminary evaluation with an acceptable grid density showed a nearly 0.5% increase in efficiency for the three-stage turbine for only the second rotor being contoured. This improvement seemed quite promising at the preliminary stage of calculation. However, after carefully examining the mesh sensitivity, we found that for simulating the endwall contouring an extraordinary dense grid must be applied that penetrates far into the laminar sub-layer with y+ <2. According to the geometric features of the contouring, the mesh used for preliminary calculations was too coarse that the y^+ on the wall was larger than unity. As a result, the shear stress near the wall would be largely underestimated and thus the performance of the turbine could be overestimated. Therefore, mesh refinement has to

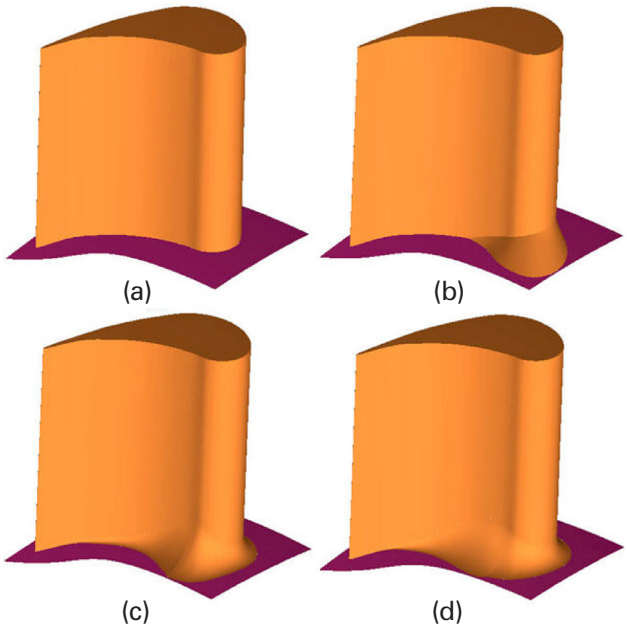

FIGURE 1. Profiles of second rotor in four cases: (a) reference case; (b) LE-filleting case with large LE-filleting; (c) 13mm-15C_{ax} – contoured case with maximum height of 13 mm at 15% C_{ax}; (d) 13mm-30C_{ax} - contoured case with maximum height of 13 mm at 30% C_{ax}.

be performed to acquire accurate results. Since the stator is not the primary part we are concerned with, a relative fine mesh (nearly 1 million elements) is used in stator domains. Meanwhile, a set of meshes with different elements were generated for rotor. Eventually, four meshes that have 0.5 million, 1 million, 2 million and 3 million elements, respectively were applied for mesh sensitivity investigation. The test results revealed that the change of the rotor efficiency became quite small when 2 million elements were used. However, the mesh with 3 million could not help the CFD-solver converge. Therefore, the mesh with 2 million elements was chosen to be the standard mesh for our CFD simulations. Accordingly, the mesh used for the CFD computations is a fully structured hexagonal mesh consisting of around 9 million elements for the entire three-stage turbine. The cells are given a geometric distribution in order to increase the density within the boundary layer region near the endwall. The y^+ for the domain is in the order of unity. Total pressure and total temperature were given at the inlet while the back pressure was set at the exit of the turbine, which specified the boundary conditions for the calculations. Additionally, the turbulence model SST k-ω was implemented in CFX-12.0.

Results

The thermocouples implanted into the stator sensor blades passed the electrical tests. Together with the three five-hole probes we calibrated in the first quarter, our facility is now capable in both thermal and fluid dynamic data acquisition. At the same time, CFD results showed certain positive predictions about the endwall modifications. Except for the reference case, only the second rotor is configured with contouring or filleting. The numerical simulations showed that LE-filleting and 13mm-15C_{ax} contributed some benefit to rotor efficiency, compared with the reference case, while 13mm-30C_{ax} has a negative influence on rotor performance. As shown in Figure 2, rotor efficiency is increased 0.17% in the LE-filleting case and 0.11% in 13mm-15C_{ax}, but it is slightly decreased in 13mm-30C_{ax}. After all the three rotors are contoured (noted as LE-filleting-3rows, 13mm-15 C_{ax}-3rows and 13mm-30 C_{ax}-3rows), the former two cases achieved an increase of 0.16% and 0.05% in efficiency for the entire machine, respectively. This is lower than the rotor efficiency because neither contouring nor filleting is implemented on stators. Consistently, the case 13mm-30 C_{ax}-3rows shows a reduction of 0.03% on global performance. Therefore, the contouring profile implemented in 13mm-30 C_{ax} is apparently not the design in need.

One of the major secondary loss sources is the horseshoe vortex. Its formation mechanism is quite complicated. Simply speaking, the rolling up of the inlet boundary layer begins to generate the horseshoe vortex as it is moving downstream. After colliding on the LE of the blade, the horseshoe vortex separates into two legs. The pressure side leg crosses the passage (as shown along the arrow) and then interacts with the suction side leg from adjacent blade and also the passage crossflow, which would generate great secondary losses and vorticities. As a result, the passage vortex is formed during the process and a

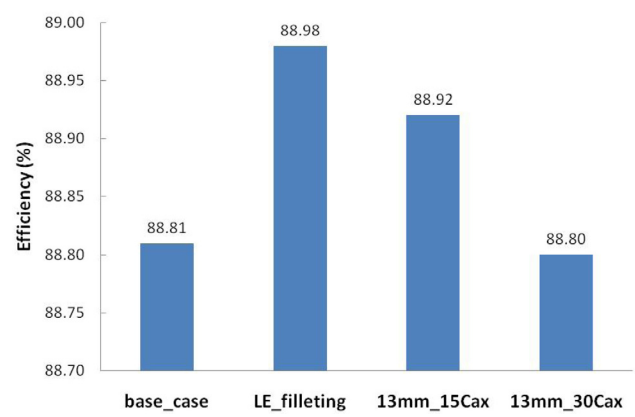

FIGURE 2. Efficiency of second rotor in four cases: base_case – reference case; LE-filleting – case with large leading edge filleting; 13mm-15C_{ax} – contoured case with maximum height of 13 mm at 15% C_{ax}; 13mm-30C_{ax} - contoured case with maximum height of 13 mm at 30% C_{ax}.

small vortex system, corner vortex, is also generated in the corner of blade and hub. This is the essential mechanism of secondary flow near endwall.

Figure 3 shows the vorticity distribution at 0.5% span for all cases. In Figure 3(a), areas with high vorticity indicate the activity of horseshoe vortex. It is clearly seen that the horseshoe is generated in front of the LE and then separates into two legs. Similar phenomena can be observed in Figure 3(c) and (d), indicating that neither 13mm-15 C_{ax} nor 13mm-30 C_{ax} has an obvious positive effect on the reduction of the horseshoe vortex. However, the filleting shows a difference. It is noticeable that the suction side leg of horseshoe vortex has been significantly weakened and the pressure side leg is to some extent suppressed too. Therefore, the addition of the LE filleting is able to reduce the strength of the horseshoe vortex, or even avoid the generation of horseshoe vortex.

The vorticity distribution at 1% span in Figure 4 further demonstrates the conclusion above. As marked in Figure 4(a), the generation and separation of the horseshoe vortex creates a large area with high vorticity and thus high loss and dissipation. As the filleting almost eliminates the horseshoe vortex, the intensity of vorticity has been largely reduced, especially in front of the leading edge, compared with the same area in the reference case. However, the high vorticity area located at about 50% C_{ax} has no obvious reduction. This is consistent with the profile of streamlines in that region. Additionally, neither 13mm-15 C_{ax} nor 13mm-30 C_{ax} has brought great changes to the flow field according to Figure 4.

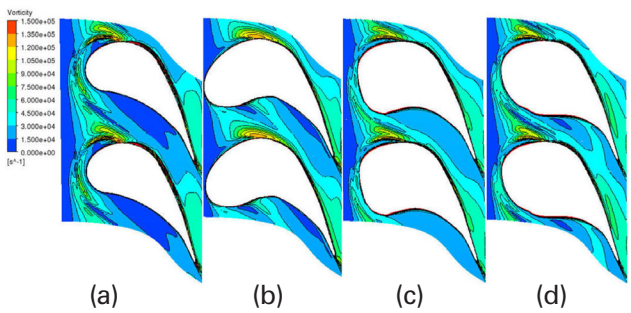

FIGURE 3. Vorticity distributioin at 0.5% span in second rotor passage: (a) reference case; (b) LE-filleting – case with large leading edge filleting; (c) 13mm-15C_{ax} – contoured case with maximum height of 13 mm at 15% C_{ax}; (d) 13mm-30C_{ax} – contoured case with maximum height of 13 mm at 30% C_{ax}.

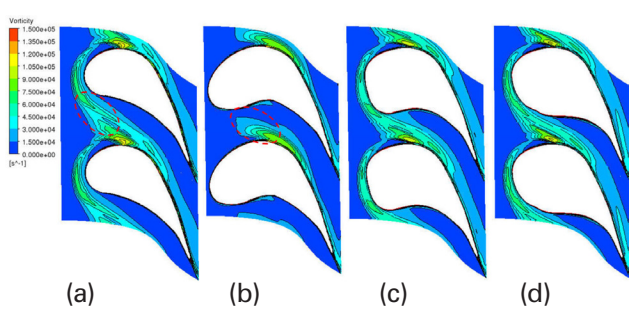

FIGURE 4. Vorticity distributioin at 1% span in second rotor passage: (a) reference case; (b) LE-filleting – case with large leading edge filleting; (c) 13mm-15C_{ax} – contoured case with maximum height of 13 mm at 15% C_{ax}; (d) 13mm-30C_{ax} – contoured case with maximum height of 13 mm at 30% C_{ax}.

The pitchwise-averaged relative total pressure loss coefficient is calculated with Eq. (1) and exhibited in Figure 5.

$$C_{P_{tr}} = \frac{\overline{P}_{tr,in} - \overline{P}_{tr,out}}{\frac{1}{2}\rho U_{ref}^2} \quad (1)$$

It is apparent that the loss coefficient is much smaller from about 16% to nearly 29% span, when LE-filleting is compared with other cases. A smaller loss coefficient implies lower total pressure loss. Therefore, the addition of the filleting to some extent reduces the total pressure loss at certain areas. This positive improvement is attributed to the reduction on the intensity of the passage vortex due to the suppression to the horseshoe vortex. 13 mm-15 C_{ax} has a similar effect too but not as large as LE-filleting does. This can well explain why these two cases give higher rotor efficiency than the other two cases. However, relatively poor performance is shown at the region beneath 10% span. This is possible because the thickness of the downstream boundary layer at the endwall is increased or the corner vortex is to some extent strengthened. Unfortunately the exact mechanism is not completely clear yet. Therefore, further investigation must be done in order to achieve more improvement on performance.

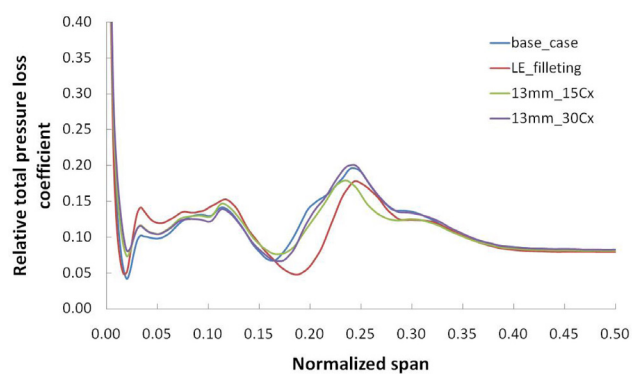

FIGURE 5. The distribution of pitchwise-averaged relative total pressure loss coefficient along second rotor spanwise: base_case – reference case; LE_filleting – case with large leading edge filleting; 13mm-15C_{ax} – contoured case with maximum height of 13 mm at 15% C_{ax}; 13mm-30C_{ax} – contoured case with maximum height of 13 mm at 30% C_{ax}.

Conclusions and Future Directions

Turbine Rig: We will finish assembly and test run the reference turbine before the last week of July. Efficiency and performance tests will be conducted and completed as scheduled. The final filler and contoured design delivered by the CFD investigations will be designed and given for manufacturing.

CFD calculations have shown that the endwall modifications do have some benefit to turbine global performance. Currently our existing cases indicate near a 0.2% increase on rotor efficiency, which is contributed by the reduction of the vortex system in the turbine, especially the horseshoe vortex and the passage vortex. However, further research will be focusing on modification and verification of non-axisymmetric endwall contouring. It seems that it is quite promising to combine both large LE-filleting and endwall contouring.

FY 2010 Publications/Presentations

1. M.T. Schobeiri, Je-Chin Han, S. Yang, K. Lu, "Quarterly Report TPFL-Q-1-2010: Aerodynamics and Heat Transfer Studies of Parameters Specific to the IGCC-Requirements: Endwall Contouring, Leading Edge Filleting and Blade Tip Ejection under Rotating Turbine Conditions," 2010.

References

1. G.A. Zess and K.A. Thole, "Computational Design and Experimental Evaluation of Using A Leading Edge Fillet on A Gas Turbine Vane," *ASME EXPO 2001,* 2001-GT-0404.

2. S. Becz and M.S. Majewski, "Leading Edge Modification Effects on Turbine Cascade Endwall Loss," *ASME TURBO EXPO 2003*, GT2003-38898.

3. A.K. Saha, G.I. Mahmood, and S. Acharya, "The Role of Leading-Edge Contouring on End-Wall Flow and Heat Transfer: Computations and Experiments," *ASME TURBO EXPO*, GT2006-91318.

IV.A.3 Simulating Particle Deposition and Mitigating Deposition Degradation Effects in Film-Cooled Turbine Sections

David G. Bogard (Primary Contact) and
Jason E. Albert
University of Texas at Austin (UT)
Department of Mechanical Engineering
1 University Station C2200
Austin, TX 78712
Phone: (512) 471-3128; Fax: (512) 471-8727
E-mail: dbogard@mail.utexas.edu

DOE Project Manager: Mark Freeman
Phone: (412) 386-6094
E-mail: Mark.Freeman@netl.doe.gov

UTSR Manager of Research: Richard Wenglarz
Phone: (864) 656-2267
E-mail: RWNGLRZ@exchange.clemson.edu

Subcontractors:
Karen A. Thole and Seth A. Lawson
Pennsylvania State University (Penn State)
Department of Mechanical and Nuclear Engineering
136 Reber Building
University Park, PA 16802-1412
Phone: (814) 865-2519; Fax: (814) 865-1280
E-mail: kthole@psu.edu

Contract Number: 41431/UTSR 07-01-SR127

Start Date: August 1, 2007
End Date: September 30, 2010

FY 2010 Objectives

- Develop an experimental methodology to actively simulate the deposition of syngas contaminant particles on film-cooled turbine surfaces, using large-scale turbine vane cascade models.
- Investigate and quantify the effects of deposition on the film cooling of turbine airfoils and endwalls.
- Identify and develop features that reduce depositions and/or limit the adverse effects of depositions on film-cooling.

Accomplishments

- At UT, large-scale models of a turbine vane were designed and constructed. These models incorporate removable hatches to quickly change film cooling configurations between tests. One model was constructed of a low thermal conductivity material (polyurethane foam) so that film cooling performance parameters can be measured independent of the internal cooling configuration. The other model was constructed of a moderate thermal conductivity material (Corian) that was selected so that the Biot number of the model matched that of an actual turbine airfoil. Consequently the nondimensional temperatures of the model (scaled with mainstream and coolant temperatures) match those of the actual turbine airfoil.
- A series of experiments were performed at UT that measured the adiabatic film effectiveness of various combinations of film cooling rows on the vane model suction side. These experiments show how film cooling performance changes when different rows of holes are activated, which will be useful when assessing deposition results in later experiments. These experiments also served to further develop the experimental facility and methodology used in the deposition simulations experiments.
- Experimental simulations of contaminant depositions have been performed at UT using a spray of molten wax droplets impinging on a cooled vane model. Only a non-film cooled vane airfoil model has been tested so far, but a film-cooled version of this model will be tested shortly. These tests reveal a significant influence of surface temperature on the amount of deposition forming on the surface, with lower surface temperatures suppressing deposition thickness.
- At Penn State an improved deposition methodology was developed to dynamically simulate deposition in a large-scale turbine cascade with endwall film cooling. A Stokes analysis showed that wax particles between 1 and 100 µm in the large-scale facility would match the trajectories of fly ash particles between 0.1 and 10 µm in an engine.
- A thermal scaling parameter (TSP) was developed at Penn State to scale the phase change process of particles immersed in the hot gas path. The TSP is the solidification time of a particle scaled by the time it takes the particle to travel from the combustor to the surface of interest.
- Results from experiments conducted in the large-scale turbine cascade at Penn State showed that cooling effectiveness reduction approached an equilibrium state as deposition developed. Results showed that deposition reduced endwall cooling effectiveness by as much as 30% and was dependent on thermal scaling parameter, momentum flux ratio, and the location of cooling holes on the endwall.

Introduction

A major concern for the next generation of power generation gas turbines is the capability to operate with greater efficiency while using new coal-derived high hydrogen fuels. A major factor when using these fuels is the effects of contaminants on engine operation, particularly the hot section of the gas turbine. In general, contaminants in the main flow can affect the turbine section by causing erosion, corrosion, or deposition to turbine airfoil and endwall surfaces. For higher temperature operation, which is the goal of future designs, the primary degradation effect of contaminants occurs from deposition on turbine surfaces. This deposition results in much rougher surfaces and partial blockage of film cooling holes that seriously degrade the cooling performance. Performing full engine tests to determine where these contaminants deposit and how to mitigate that deposition is cost prohibitive and often results in a lack of detailed information needed to understand the underlying physics of the deposition process. Methods need to be developed whereby accurate deposition simulations can take place in a facility that allows for the underlying physical effects on airfoil heat transfer and aerodynamics to be understood. A major objective of our proposed work is to determine a reliable methodology for simulating contaminant deposition in a low speed wind tunnel facility where testing is considerably less costly.

This project is aimed at developing new cooling designs for turbine components that will minimize the effect of the depositions of contaminant particles on turbine components and maintain good film-cooling performance even when surface conditions deteriorate. Moreover, a methodology will be established that allows controlled laboratory experiments to simulate relevant deposition mechanisms for gas turbines using coal-derived fuels. New film cooling designs for turbine airfoils and endwalls and new endwall contouring designs will result. Reliable and improved film cooling performance for turbine vanes will lead to reduced costs for the user as a result of longer component life.

Approach

Facilities have been constructed at Penn State and UT to develop deposition simulation methodologies. Deposition can be simulated dynamically by dispersing wax particles into the flowfield simulating the hot mainstream flow through a turbine vane cascade. The inertial behavior of particles that exist in engine conditions can be simulated using the appropriate particle size distribution of wax particles. The use of wax also allows for the simulation of the liquid-to-solid phase change that is essential to the primary deposition mechanism.

The performance of shallow trench film cooling configurations for various positions on the suction and pressure sides of a simulated vane with active deposition is being investigated at UT. At Penn State the effect of active deposition on various endwall cooling configurations is being investigated. Preliminary results showed that deposition could be simulated dynamically using wax and that the effects of deposition could be quantified using infrared thermography. New endwall and vane surface film-cooling configurations will be developed to minimize deposition and maximize cooling performance under contaminated conditions.

Results

At UT, two new large-scale models of turbine vane airfoils have been constructed for use in this study. Both models have removable hatches at four locations around the airfoil surface so that film cooling configurations can be quickly changed and tested. One model is constructed of a low thermal conductivity polyurethane foam material; this model isolates the heat transfer due to the internal flows so that the adiabatic film effectiveness (η) of a film cooling configuration can be measured. The second model is geometrically identical to the first, but it is constructed of a moderate thermal conductivity Corian material that was selected so that the Biot number of this model in the wind tunnel test section matches that of an actual turbine vane in and engine. Consequently, the scaled, nondimensional, external surface temperatures of this conducting model will closely match those of an actual turbine vane.

A series of experiments were performed with the low conductivity model at UT that measured the adiabatic film effectiveness on the suction side of the airfoil for several different combinations of film cooling rows. In these experiments, the film cooling holes were relatively simple designs, with more advanced designs (e.g. “trench” film cooling) to be tested later. A representative summary of these experimental results is shown in Figure 1, which compares the laterally averaged η distribution on the suction side surface for the following film configurations: only showerhead active, only row SS1 active, showerhead and row SS1 active, and showerhead and rows SS1 and SS2 active. In all data sets in Figure 1, the showerhead blowing ratio was approximately $M_{shd} = 2$ and the body film holes blowing ratio was approximately M_{SS1} ~M_{SS2} ~1, as applicable. Also shown in Figure 1 is an analytical estimate of the combined effectiveness of the showerhead and SS1 rows, using a common

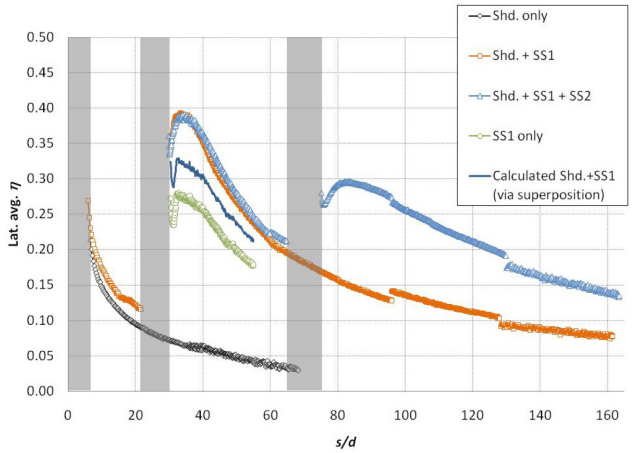

FIGURE 1. Laterally-Averaged Adiabatic Film Effectiveness Measurements on Vane Model Suction Side for Various Combinations of Showerhead and Suction Side Film Cooling Rows ($M_{shd} \sim 2$ and $M_{SS1} \sim M_{SS2} \sim 1$)

method to superimpose film effectiveness values for separate rows: $\eta_{combined} = \eta_{shd} + \eta_{SS1}(1\text{-}\eta_{shd})$. Note that the measured values of the combined film effectiveness is significantly higher than the analytical estimate. This improved performance may be due to changes in the approach flow induced by the showerhead blowing that causes the SS1 coolant jets to remain closer to the surface. These data also provide a baseline standard with which the performance of advanced film cooling designs can be evaluated.

Another series of experiments were performed at UT using the matched Biot number model in which the wax spray technique was used to simulate contaminant deposition. For these initial tests the wax spray deposition tests were performed with an internally-cooled model without any film cooling holes. Film cooling flows will be added in later tests. Figure 2 presents photographs of the wax depositions formed on the model with all experimental conditions being equal except for the cooling of the model. Both photos in Figure 2 result from the same type of wax (with a solidification temperature of $T_{solid} = 315$ K), the same wax spray parameters, and the same mainstream flow field (with an approach velocity and temperature of $U_\infty = 5.8$ m/s and $T_\infty = 305$ K). Figure 2(a) shows the deposits that form on an uncooled vane model, with the model surface temperature equal to the mainstream temperature (305 K). Figure 2(b) shows the deposit formed on an internally convectively cooled model with surface temperatures in the range of 265-285 K. Comparing Figures 2(a) and (b), it is evident that the surface temperatures of the model had a significant effect on depositions. Interestingly the cooler surface had the effect of decreasing the deposition thickness. This demonstrates that this experimental

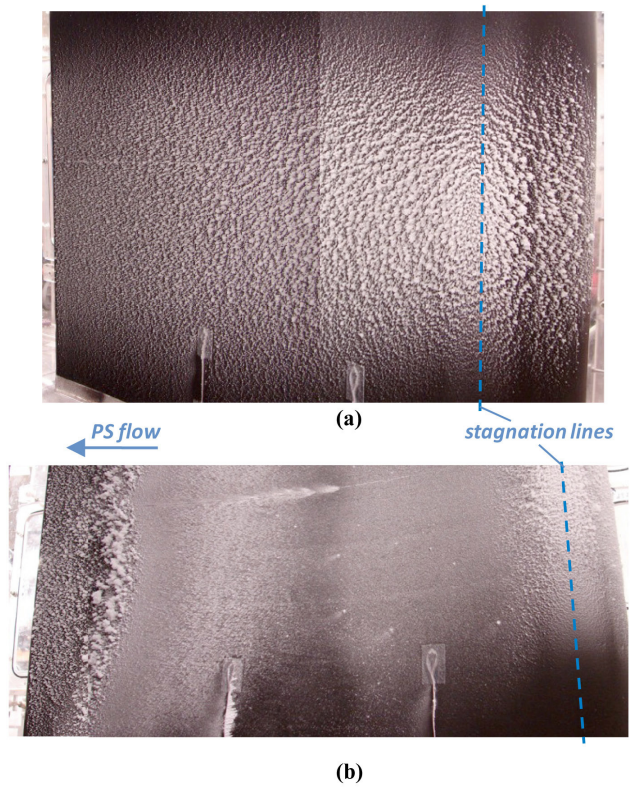

FIGURE 2. Photographs of Simulated Deposits on Vane Models Using the Wax Spray Technique, (a) with the Model Uncooled, and (b) with the Model Internally Cooled

technique captures the influence of the model surface temperature on the formation of deposits, which is consistent with published observations of engine-condition depositions.

To observe the effects of deposition development on cooling effectiveness, three separate tests were conducted with three wax spray durations at $I = 0.23$. Figure 3 shows the effectiveness contours and surface deposition plots for the case with no deposition along with the cases after the injection of 300 g, 600 g, and 900 g of wax. Deposition was densest at the stagnation region of the vane and inside the trailing edge of the upstream slot. As expected, surface deposition increased with an increase in wax deposition with a larger difference between 300 g and 600 g than between 600 g and 900 g [1]. Comparing directly between effectiveness contours and deposition plots, it is evident that the regions with the highest effectiveness (i.e., coldest surface temperatures) had the least deposition. Ai et al. [2] found that deposition capture efficiency decreased with an increase in blowing ratio and Lawson and Thole [3] observed a decrease in coolant wake deposition with an increase in momentum flux ratio. Bons et al. [4] observed trough patterns caused by the lack of deposition in cooling

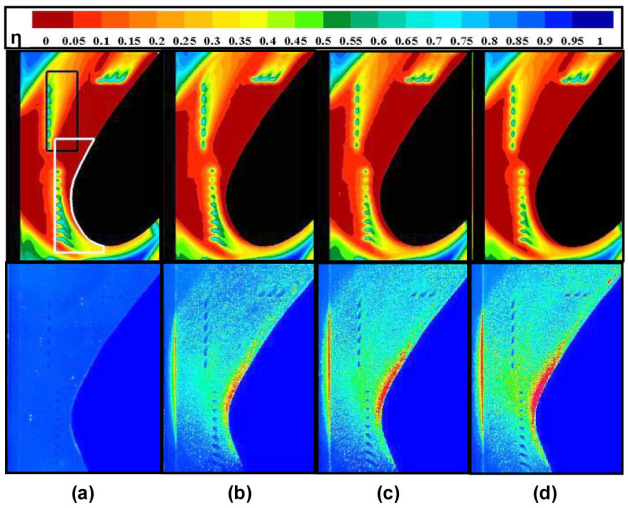

FIGURE 3. Adiabatic Effectiveness Contours and Corresponding Surface Deposition Plots (a) before Deposition, (b) after 300 g, (c) after 600 g, and (d) after 900 g of Wax Injection at I=0.23

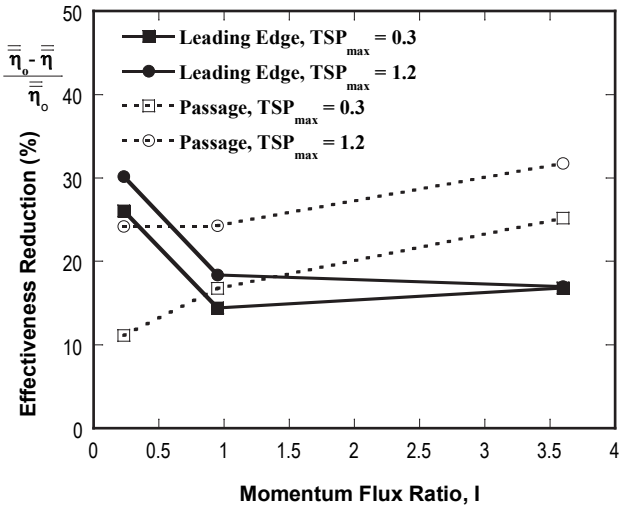

FIGURE 4. Area-Averaged Effectiveness Reduction for Leading Edge and Passage Cooling Holes

hole wakes on actual turbine hardware. The lack of deposition in the wakes of coolant holes on the suction side of the vane leading edge in this case is most likely because of high coolant jet velocities preventing surface impaction of particles.

Not only did the coolant holes have an effect on deposition, but deposition had an effect on the cooling effectiveness of the leading edge row. Deposition has a greater effect on the cooling effectiveness on the suction side of stagnation than on the pressure side. It is interesting to note that cooling effectiveness for 600 g and 900 g cases are practically the same indicating that effectiveness approaches an equilibrium state between 600 g and 900 g of injection. Lawson and Thole [3] also observed that effectiveness reached an equilibrium state with an increase in deposition for a simple flat plate film cooling study. As deposition approaches an equilibrium state, the rate at which particles deposit approaches the rate at which particles are eroded from the surface.

Figure 4 illustrates the effects of momentum flux ratio and TSP on cooling effectiveness reduction for the passage row and leading edge row. Cooling effectiveness for the passage row and leading edge row was averaged across the areas represented by the black and white boxes in Figure 3a, respectively. It was determined that momentum flux ratio and TSP had a different effect on cooling depending on the location of the cooing row relative to the vane row. Cooling effectiveness was reduced by as much as 30% at $TSP_{max} = 1.2$ and $I = 3.6$ for the passage cooling row.

Conclusions and Future Directions

The UT researchers have constructed turbine vane models with film cooling features located on removable hatches, and these models are being used to study contaminant depositions on gas turbine vane airfoils. Measurements of adiabatic film effectiveness were performed for the vane suction side film cooling holes, which provide insight to the film cooling flow fields that influence the contaminant depositions being studied in this project. Experimental simulations of contaminant depositions have been performed that impinge a spray of molten wax droplets on an internally-cooled, conducting (matched-Biot number) airfoil model. These tests revealed a significant influence of the model surface temperature on the thicknesses of the wax depositions that form on it, which is consistent with contaminant depositions at engine conditions.

Future experiments at UT will focus on using the wax spray technique to simulate depositions on a film-cooled turbine vane model. This model will have non-dimensional, scaled temperatures representative of engine hardware (i.e. relative to the hot mainstream and coolant temperatures), so they will capture the effects of contaminant cooling both in the film cooling flows and upon impaction at the model surface. An emphasis for these experiments will be to reveal a detailed understanding of the physics governing the interaction of the contaminant particles, the film cooling flow fields, and the model surface. This will allow for optimized film cooling designs to be developed that are less sensitive to contaminant deposition.

The work conducted at Penn State over the past year has shown that endwall cooling is highly sensitive to deposition. Excess deposition could lead to reduced cooling effectiveness and possibly turbine component failure. It is essential to understand the driving mechanisms behind deposition so that advanced film cooling configurations can be designed to mitigate deposition.

Future experiments at Penn State will be conducted to determine the effects of deposition on film cooling holes embedded in a transverse trench. The literature has shown reason to believe that trenched film cooling geometries may be less susceptible to the negative effects of particle deposition. In addition to trench cooling studies, a separate set of experiments will be conducted to determine the effects of deposition on cooling in a blade passage with non-axisymmetric endwall contouring. Endwall contouring has proven to be a successful method for reducing secondary flow losses; however, it is unknown how deposition will collect on these highly complex endwall geometries. Deposition will be simulated on a previously tested flat and contoured endwall with film cooling to observe the effects of deposition on cooling effectiveness associated with a contoured endwall.

Special Recognitions & Awards/Patents Issued

1. IGTI Heat Transfer Committee Best Paper Award for Lawson and Thole [2009].

2. Seth A. Lawson, Kulakowski Graduate Student Travel Grant to present GT2010-22376.

FY 2010 Publications/Presentations

1. S.A. Lawson and K.A. Thole, 2010, "Simulations of Multi-phase Particle Deposition on Endwall Film-Cooling," ASME Paper GT2010-22376, presented at ASME Turbo Expo, Glasgow, UK and recommended for the *Journal of Turbomachinery*.

2. J.A. Albert, K.J. Keefe, and D.G. Bogard, 2009, "Experimental Simulation of Contaminant Deposition on a Film Cooled Turbine Airfoil Leading Edge," ASME Paper IMECE20090-11582, presented at ASME International Mechanical Engineering Congress and Exposition, Lake Buena Vista, Florida.

References

1. S.A. Lawson and K.A. Thole, 2010, "Simulations of Multi-phase Particle Deposition on Endwall Film-Cooling," ASME Paper GT2010-22376.

2. W. Ai, N. Murray, T.H. Fletcher, S. Harding, S. Lewis, and J.P. Bons, 2008, "Deposition Near Film Cooling Holes on a High Pressure Turbine Vane," GT2008-50901.

3. S.A. Lawson and K.A. Thole, 2009, "The Effects of Simulated Particle Deposition on Film Cooling," GT2009-59109.

4. J.P. Bons, R.P. Taylor, S.T. McClain, and R.B. Rivir, 2001, "The Many Faces of Turbine Surface Roughness," *J. of Turbomachinery*, **123**, pp. 739-748.

IV.A.4 Syngas Particulate Deposition and Erosion at the Leading Edge of a Turbine Blade with Film Cooling

Danesh Tafti (Primary Contact),
Uri Vandsburger, Wing Ng
Virginia Polytechnic Institute and State University
114-I Randolph Hall
Blacksburg, VA 24061
Phone: (540) 231-9975; Fax: (540) 231-9100
E-mail: dtafti@vt.edu

DOE Project Manager: Mark Freeman
Phone: (412) 386-6094
E-mail: Mark.Freeman@netl.doe.gov

UTSR Manager of Research: Richard Wenglarz
Phone: (864) 656-2267
E-mail: RWNGLRZ@exchange.clemson.edu

Contract Number: 41431/UTSR 07-01-SR123

Start Date: August 2007
End Date: July 2010

FY 2010 Objectives

- Develop and validate a surface deposition model based on ash composition and temperature.
- Use low melting point polyvinyl chloride (PVC) particles to experimentally measure capture efficiency in a film-cooled leading edge region as a function of free stream temperature and blowing ratio.

Accomplishments

- Measured the effect of ash particle sizes on deposition in the presence of showerhead film cooling.
- Measured the effect of coolant injection (blowing ratio) on ash particle trajectories and deposition.
- Measured the effect of deposition as a function of ash composition and particle softening temperature.
- Observed the surface topology of the leading edge vane surface due to deposition growth after 100s of operational hours.
- Compared steady flow Reynolds averaged Navier-Stokes computations to time-accurate large eddy simulations (LES).
- Used low melting point PVC particles to experimentally measure capture efficiency in a film cooled leading edge region as a function of free stream temperature and blowing ratio.
- Measured the effect of deposition on the convective heat transfer and film cooling effectiveness at the leading edge.

Introduction

The vision of DOE's Fossil Energy Turbine program is to provide power generation technology essential to the success of advanced fossil energy power systems in the 2008 to 2015 time frame. One of the key capabilities needed to achieve this goal is coal gasification. One of the issues in achieving this goal relates to the durability of turbine components subjected to a harsh high-temperature, high-pressure, and high-velocity environment in the gas path immediately downstream of the combustor.

Coal gasification and combustion can introduce contaminants in the vapor as well as solid or molten state depending on the gas clean-up procedures used, coal composition and operating conditions. These byproducts when combined with high temperatures and high gas stream velocities can cause deposition, erosion, and corrosion (DEC) of turbine components. Some of the common compounds which lead to DEC are trace amounts of sulphates, chlorides, and hydroxides of alkali metals such as calcium, sodium, potassium, and magnesium. Other metallic compounds of antimony, beryllium, chromium, mercury, selenium and vanadium are also threats for DEC. The extent of damage done by DEC in the gas path is directly dependent on the impaction of solid or molten particulates on surfaces, which lead to erosion and deposition. One surface, which is particularly vulnerable, is the leading edge of vanes and blades in the presence of film cooling.

Approach

The proposed project is performed at near engine conditions combining unique computational and experimental equipment and facilities for conditions relevant to the design of systems. A blade with a cylindrical leading edge and a camberless after body in a linear cascade is tested. The work uses the method of time-accurate LES as a theoretical tool for simulating particle dynamics in conjunction with newly developed deposition models and a high-temperature

experimental facility matched to relevant engine conditions. By using carefully derived similarity parameters, the high-temperature experimental facility provides an inexpensive and effective testing environment.

Results

Computational Modeling

We have developed and validated a complete deposition model based on the temperature and composition of flyash particles. The developed deposition model is validated with experiments by Crosby et al. [1] on a flat plate inclined at 45° to an impinging ash laden jet. Particles of size 4 micron in diameter are simulated using the time-accurate LES to study the effects of mainstream temperature and flyash compositions on deposition.

Figure 1 shows an instantaneous snapshot of ash particles impinging on the inclined flat plate. A majority of the ash particles hit the stagnation line located at the bottom of the flat plate and then accelerate straight and parallel to the surface of the flat plate and eventually exit through the outflow. One of the predominant features in Figure 1 is the ash particles getting cooled due to free shear layer mixing between the jet from the pipe and the surrounding stationary fluid.

Figure 2 shows quantitative comparisons of capture efficiency obtained from the model simulations

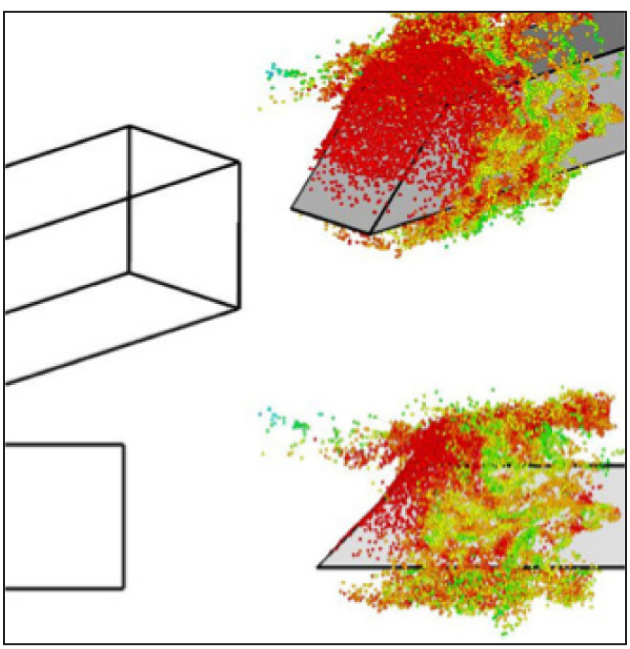

FIGURE 1. Turbulence Dispersion of Particles from Time-Accurate LES (ash particles are colored with temperature)

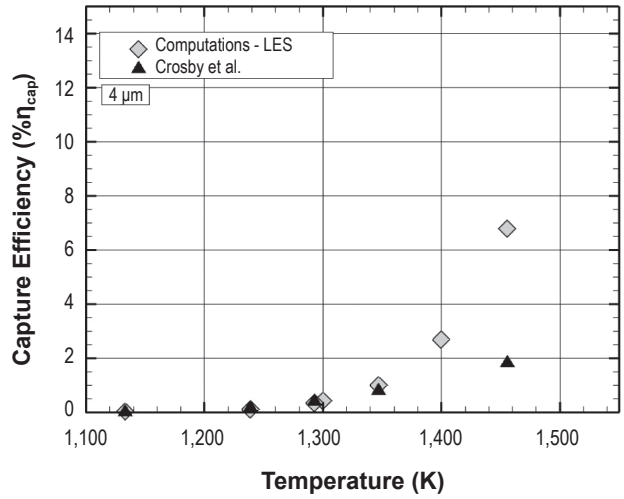

FIGURE 2. Capture Efficiency as a Function of Temperature, Comparisons with Experiments for Particle Size of 4 Micron (T_{soft} = 1,551 K)

to the experiments of Crosby et al. [1] as a function of jet inlet temperature. The deposition trend matches until 1,400 K after which the simulated capture efficiency is higher than the experiments. Crosby et al. mention in their paper that the capture efficiency reported at 1,456 K is lower than that observed by Wenglarz et al.[2]. This low capture efficiency might be due to the flaking of the ash particles that flow away with the mainstream. Other than these differences, the computational model shows the capability of correctly quantifying ash deposition below the softening temperature.

The developed model for ash deposition can be applied to most ash samples with known composition.

Experimental

Experiments on a film-cooled leading edge using PVC particles (~24 microns) have been conducted. Flow conditions were such that the particle momentum Stokes number was 3 and the Reynolds number was about 20,000. The temperature of the free stream was varied near to the melting point of the particles (533 K). Deposition experiments were conducted at three blowing ratios (B.R.=1, 2, and 3). T* is the non-dimensional temperature defined as the ratio of the free stream temperature to the melting point. These results are presented in Figure 3. Capture efficiencies vary between 10 to 25% and increase with an increase in the free-stream temperature. There is a slight decrease in the capture efficiency as the blowing ratio increases to 3.

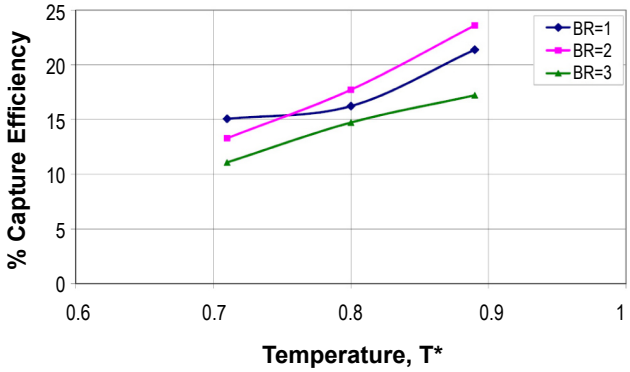

FIGURE 3. Capture Efficiencies of PVC Particles for a Film-Cooled Leading Edge with Different Freestream Temperatures

Conclusions and Future Directions

A deposition model based on ash composition and temperature accurately predicts the deposition observed in experiments. Experiments with PVC particles show capture efficiencies in the range of 10-25%, with a corresponding increase in heat transfer coefficient. Future work will focus on applying the deposition model to a film-cooled leading edge and comparing to experiments.

Special Recognitions & Awards/Patents Issued

Graduate student Sai Shrinivas Sreedharan won the following awards:

1. Third place in Poster Presentation, Paul E. Torgersen Award for Research Excellence.

2. Second Place in Video Presentation, 26th Annual GSA Research Symposium.

FY 2010 Publications/Presentations

1. S.S. Sreedharan and D.K. Tafti, "Composition Dependent Model for the Prediction of Syngas Ash Deposition with Application to a Leading Edge of Turbine Vane," ASME Paper Number GT-2010-23655, 2010.

2. S.S. Sreedharan and D.K. Tafti, "Composition Dependent Model for the Prediction of Syngas Ash Deposition in Turbine Hot Gas Path," Int. J. Heat Fluid Flow, submitted May 2010.

3. E. Wood, U. Vandsburger, W. Ng, and S.D. LePera, "Syngas Ash Deposition Particle Substitution Method for Experimentation," ASME Paper No. GT2010-22445, 2010.

References

1. J.M. Crosby, S. Lewis, J.P. Bons, W. Ai, and T. Fletcher, "Effects of Particle Size, Gas Temperature, and Metal Temperature on High Pressure Turbine Deposition in Land Based Gas Turbines from Various Synfuels," Proceedings of GT2007, ASME Paper No. GT2007-27531, 2007.

2. R.A. Wenglarz, and R.G. Fox, "Physical Aspects of Deposition from Coal-Water Fuels under Gas Turbine Conditions," J. Engineering for Gas Turbines and Power, Vol. 112 (1), pp. 9-15, 1990.

IV. UNIVERSITY TURBINE SYSTEMS RESEARCH

B. Combustion

IV.B.1 Turbulent Flame Speed Measurements and Modeling of Syngas Fuels

Prof. Jerry M. Seitzman (Primary Contact),
Prof. Timothy C. Lieuwen
School of Aerospace Engineering
Georgia Institute of Technology
270 Ferst Drive
Atlanta, GA 30332-0150
Phone: (404) 894-0013; Fax: (404) 894-2760
E-mail: jerry.seitzman@ae.gatech.edu
tim.lieuwen@ae.gatech.edu

DOE Project Manager: Mark Freeman
Phone: (412) 386-6094
E-mail: Mark.Freeman@netl.doe.gov

UTSR Manager of Research: Richard Wenglarz
Phone: (864) 656-2267
E-mail: RWNGLRZ@exchange.clemson.edu

Contract Number: 41431/UTSR 07-01-SR122

Start Date: May 15, 2007
End Date: September 30, 2010

FY 2010 Objectives

- Improve understanding of turbulent flame speeds of synthesis gas (syngas) fuels.
- Measure turbulent flame speeds of syngas fuels at conditions relevant to gas turbine combustors.
- Develop predictive flame speed models that can be used by gas turbine manufacturers to develop syngas combustors.

Accomplishments

- Obtained turbulent flame speed data of high H_2 fuel blends over range of conditions of interest, including fuel compositions, velocity, turbulence intensity, preheat temperature, and pressure.
- Demonstrated strong effects of H_2 fuel composition upon turbulent flame speeds at gas turbine realistic velocities and turbulence intensities.
- Developed physics-based correlation model based upon differential diffusion to predict turbulent flame speeds.

Introduction

The turbulent flame speed, S_T, is a key combustion parameter that impacts the performance of low emissions combustion systems. The turbulent flame speed is a measure of how fast (e.g., at what velocity) the fuel and air is consumed. Unanticipated changes in S_T during operation from the expected (design) conditions can therefore alter gas turbine pollutant emissions and combustor operability. While most current ground power gas turbines operate on natural gas fuel, there is great interest in allowing systems to operate on more available and secure sources, such as fuel gas synthesized from coal. These coal-derived syngas fuels contain varying amounts of H_2, CO and diluents, along with some hydrocarbons. The ability to operate on gases with high H_2 content may also permit reductions in CO_2 emissions.

The technical results obtained from this project have important implications on gas turbine design and operation. First, turbulent flame speed has significant impacts upon many of these parameters, such as thermal load, blowoff limits, flashback limits, and combustion instability. In other words, a thorough understanding of any of these issues necessitates understanding of the turbulent flame speed. Second, essentially no data exist for flame speeds of syngas fuels. The turbulent flame speed has a direct impact on the flame length and its spatial distribution in the combustor. This, in turn impacts the thermal loading distribution on combustor liners, fuel nozzles and other hardware. In the same way, the flame's proclivity to flashback is directly a function of how rapidly the flame propagates into the reactants – again, dependent on the turbulent flame speed. In addition, S_T has important impacts on combustion instability.

Unfortunately, little is known about S_T for syngas fuels, in particular at the temperatures and pressures of interest. The measurements that have been obtained were made primarily at atmospheric conditions and are of extremely limited usefulness for gas turbine operations.

The key end work product will be a model and a validating data set that can be used by industry for calculating the turbulent flame speed of syngas mixtures at temperatures and pressures of practical interest. This will allow gas turbine designers to develop systems sufficiently robust to operate on the range of expected syngas fuel mixtures, and for operators to predict changes that may be required to handle new fuel supplies.

Approach

This effort consists of two basic tasks. First is the measurement task. A facility (Figure 1) was developed to make quantitative turbulent flame speed

measurements. Due to the definition dependency of the turbulent flame speed, the focus is on obtaining the global turbulent consumption speed, $S_{T,GC}$. Measurements of turbulent flame speeds are being acquired over a broad range of temperatures, pressures, and fuel compositions. The range of operating conditions is being determined in close coordination with gas turbine manufacturers. The second part of this project involves development of physics-based correlations of the turbulent flame speed data and models for predicting the flame speed characteristics of other fuels.

Results

During Fiscal Year 2010, significant progress was made in two key areas. First, calculations were performed to determine the sensitivity of the laminar flame speed of the fuel mixtures investigated in Table 1 to the rate of strain in the flame. These calculations are important for determining properties of mixtures such as the Markstein length and the extinction strain rate. The former is a measure of how sensitive the flame speed is to strain and the latter is the point at which the flame will extinguish under high strain.

The fuel mixtures investigated, shown in Figure 2 (legend shown in Table 1), have varying sensitivity to the strain rate as shown in Figure 3. These calculations are important in our research because it is believed that strain sensitivity, through the mechanism of differential diffusion, is an important mechanism affecting the turbulent flame speed. The results of the calculations were also utilized in the development of a model to correlate the flame speed, as discussed next.

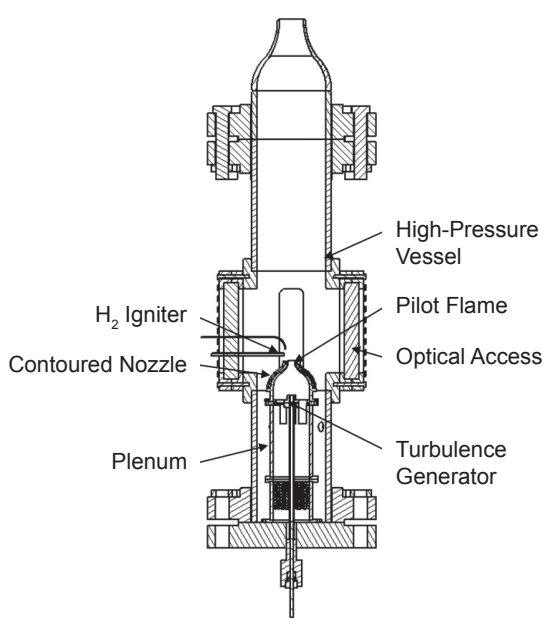

FIGURE 1. High-Pressure, Preheated Test Facility Used for Turbulent Flame Speed Experiments

TABLE 1. Legend Used for Constant $S_{L,0}$ H_2/CO Ratio Sweeps Data

H_2 (%)	Velocity (m/s) 4	10	30	50
30	◇	□	○	×
50	◇	□	○	×
70	◇	□	○	×
90	◇	□	○	×
CH_4	◇	□	○	

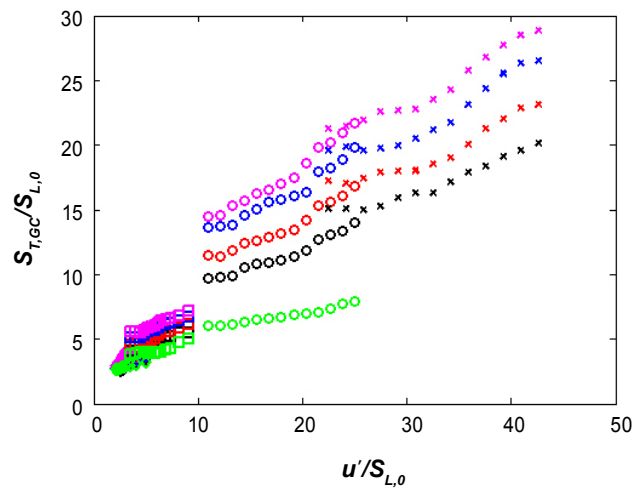

FIGURE 2. Variations of the Turbulent Flame Speed, $S_{T,GC}$, with Turbulence Intensity, u', Normalized by the Laminar Flame Speed $S_{L,0}$ at Various Mean Flow Velocities and H_2/CO Ratios

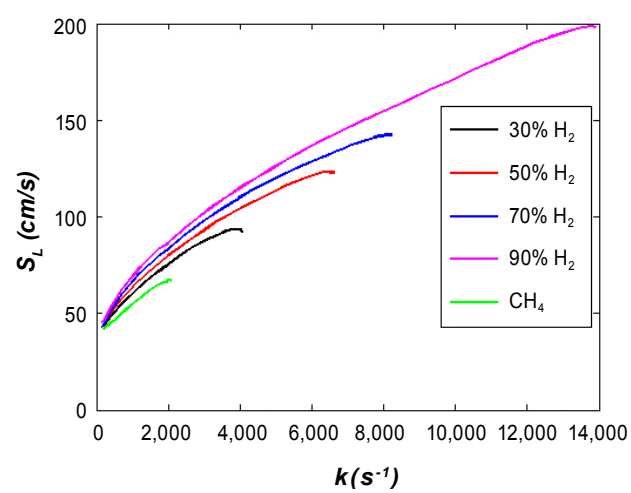

FIGURE 3. Sensitivity of the Laminar Flame Speed, S_L, to the Rate of Strain in the Flame, κ, for Various Fuel Blends

Second, a physics-based model was developed to correlate the flame speed data based on the effects of differential diffusion. The idea behind this model is that the flame surface is pulled along by the points on the surface that propagate the farthest into the unburned reactants, known as the "leading points." These leading points, due to their high strain rate, have enhanced laminar flame speeds, as shown in Figure 3. As these points propagate into the unburned reactants, they increase the flame surface area, thus increasing the fuel consumption rate.

Through theoretical work (not shown here) we have proved that, under steady-state conditions, the flame speed of the leading points will approach the maxima of the curves in Figure 3, which we designate as $S_{L,max}$. Thus, instead of using the unstrained laminar flame speed to normalize the flame speed data as is commonly done, we propose to use the maximum strained laminar flame speed, $S_{L,max}$. The results of this normalization, presented in Figure 4, are promising,

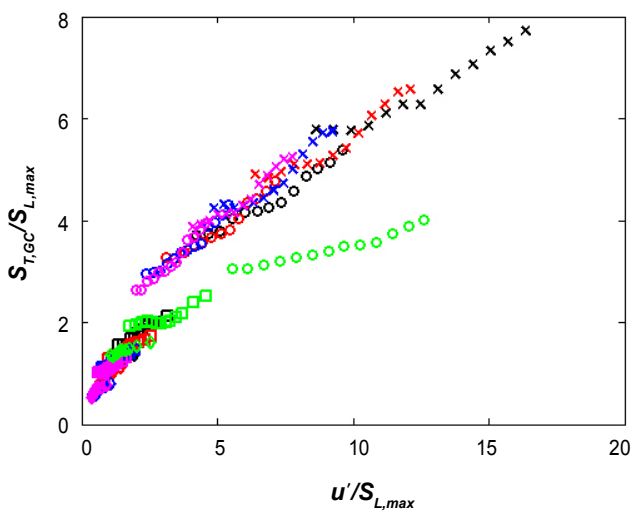

FIGURE 4. Variations in the Turbulent Flame Speed, $S_{T,GC}$, with Turbulence Intensity u', Normalized by the Maximum Strained Laminar Flame Speed, $S_{L,max}$

with variations between the 30% H_2 case and the 90% H_2 case dropping from a factor of 1.5 to a factor of 1.1. The high mean flow velocity methane results do not align well with the rest of the data; however, this is being investigated and is believed to be due to the steady-state assumption employed in the development of this model. Future plans include modifying the model to relax the steady-state assumption.

Conclusions and Future Directions

Data obtained to date have focused upon high nozzle velocities and turbulence intensities that are representative of realistic systems. These data have allowed us to resolve an issue of whether high H_2 influences observed in low intensity burners persist at very high turbulence intensities. Future work will focus on obtaining further data at high pressure and preheat temperatures, in order to explore the parameter space of most interest to future ultra-low emissions energy systems. Modifications will also be made to the model to correlate the flame speed data in order to account for situations in which the assumption of steady-state does not apply.

IV.B.2 An Experimental and Chemical Kinetics Study of the Combustion of Syngas and High Hydrogen Content Fuels

Dr. Robert J. Santoro (Primary Contact),
Dr. Frederick Dryer, Dr. Yiguang Ju
The Pennsylvania State University (Penn State)
240 Research Building East, Bigler Road
University Park, PA 16802-2321
Phone: (814) 863-1285; Fax: (814) 865-3389
E-mail: rjs2@psu.edu

DOE Project Manager: Mark Freeman
Phone: (412) 386-6094
E-mail: Mark.Freeman@netl.doe.gov

Subcontractors:
Drs. Frederick Dryer and Yiguang Li,
Princeton University, Princeton, NJ

Contract Number: NT0000752

Start Date: October 1, 2009
End Date: September 30, 2012

FY 2010 Objectives

- Assess current chemical kinetics models for high hydrogen content fuels (HHC) and develop a validated HHC kinetic mechanism.
- Obtain new experimental data to evaluate the effects of the addition of CO, CO_2 and H_2O as well as small concentrations of CH_4, C_2H_6, etc. in HHC mixtures at high pressures (1-30 atm).
- Incorporate the effects of unaccounted reaction pathways, improved thermochemistry and elementary rate constants into the chemical kinetics models under development for HHC fuels.
- Develop a detailed HHC fuel kinetic mechanism based a multi-time scale modeling algorithm to achieve enhanced computation efficiency for numerical modeling of gas turbine combustion and pollutant emissions.

Accomplishments

- Measured mass burning rate for H_2/O_2/diluent and H_2/O_2/additive/diluents mixtures at high-pressure conditions (1-30 atm).
- Updated model for H_2/O_2 was developed that predicts flame speeds spanning a wide range of equivalence ratios, pressures, diluents, and flame temperatures to within 20%.
- Initiated validation studies using the high-pressure laminar flow reactor (HPLFR) to examine third-body collision effects on the $H+O_2+M$ system.
- Modified high-pressure, high-temperature flow reactor for operation up to 925 K.

Introduction

An integrated and collaborative effort involving Penn State and Princeton University composed of experiments and complementary chemical kinetic modeling is investigating the effects of major species (H_2O and CO_2) and minor species (CH_4, C_2H_6, etc.) on the ignition and combustion of HHC fuels that are characteristic of syngas. The present research effort specifically addresses broadening the experimental database for ignition delay, burning rate and oxidation kinetics at high pressures, and further refinement of chemical kinetic models so as to develop compositional specifications related to the above major species and minor species. The foundation for the chemical kinetic modeling is the well validated mechanism for hydrogen and carbon monoxide developed by Professor Frederick Dryer and his co-workers at Princeton University over the last 25 years. The goal is to further advance the understanding needed to develop practical guidelines for realistic composition limits and operating characteristics for HHC fuels. To achieve this goal a suite of experiments are ongoing which involve a high-pressure laminar flow reactor, a pressure-release type high-pressure combustion chamber and a high-pressure, high-temperature turbulent flow reactor.

The motivation for these studies lies in the recently noted difficulties observed in the ability of existing elementary kinetic models to predict experimental ignition delay, burning rate, and homogenous chemical kinetic oxidation characteristics of hydrogen and hydrogen/carbon monoxide fuels with air and with air diluted with nitrogen and/or carbon dioxide at pressures and compositions in the range of those contemplated for gas turbine applications with low NO_x emissions. This project supports DOE's Advanced Turbine Program, which is striving to show that the U.S. can operate on coal-based hydrogen fuel, increase combined cycle efficiency by two to three percentage points over baseline, and reduce toxic emissions by 2012. The importance of the present project is to further advance the understanding and modeling capabilities needed to develop practical guidelines for realistic composition limits and operating

characteristics for HHC fuels. Results from this project will further research leading to the production of hydrogen and other clean fuels from domestic resources in an effort to reduce reliance on petroleum imports and address environmental concerns, including greenhouse gas emissions.

Approach

A combined experimental and chemical kinetics modeling approach is directed at advancing understanding of combustion of HHC fuels. Three experimental facilities are involved in this effort. The first, which is shown in Figure 1, is the HPLFR that is used principally as a homogenous kinetic reaction system (uncoupled with wall effects) and can be operated at pressures from 10 to 30 atm. Simultaneously, the potential coupling of material surfaces with gas phase kinetic properties will also be addressed. Figure 2 shows a schematic of the second facility, the pressure-release type high-pressure combustion chamber and high-speed Schlieren imaging system, which can operate at pressures from 1 to 30 atm. This apparatus is used to measure flame speeds and burning rate of HHC fuels at high pressures and low flame temperatures as well as to characterize OH and O concentrations near the post flame zone region using laser-based techniques to further constrain chemical kinetic model predictions. The final experimental facility is a high-pressure, high-temperature flow reactor that is used to measure ignition delay for HHC fuels. Similar to the other two facilities, high-pressure operation capabilities allow studies between 1 to 30 atm. The complementary measurements obtained from these experimental facilities will provide benchmark data to be compared with the chemical kinetics models.

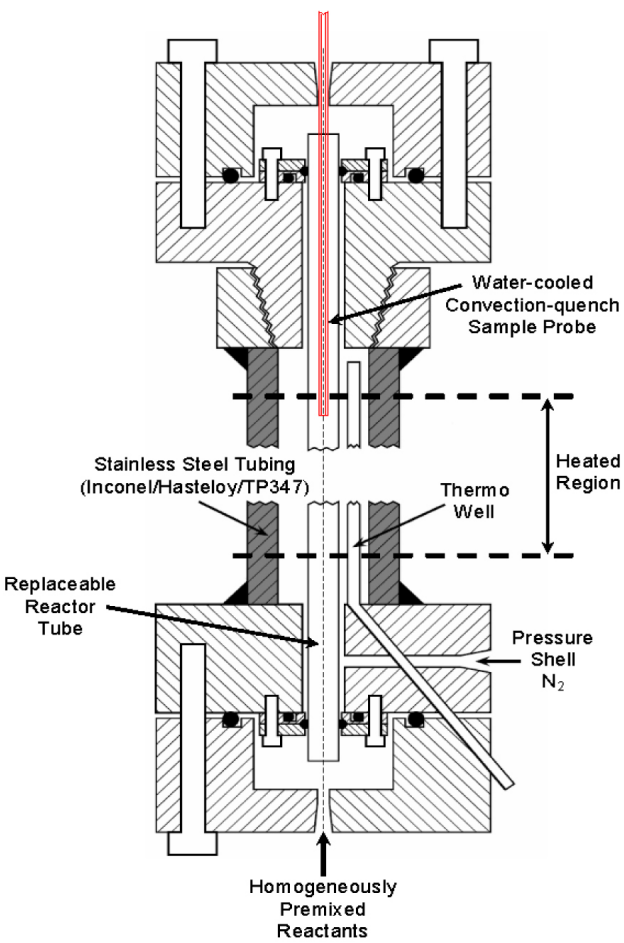

FIGURE 1. Schematic of the high-pressure laminar flow reactor tube assembly. It is noted that the reactor tube extends well beyond the oven-heated region. All parts external to the heating oven are heat traced to prevent condensation.

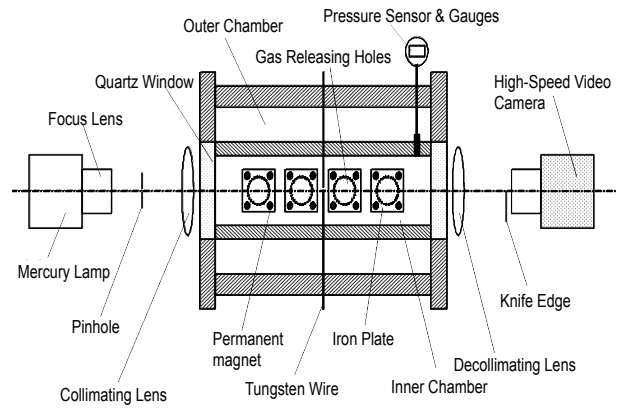

FIGURE 2. Schematic of the present pressure-release type high-pressure combustion chamber and the high-speed schlieren imaging system.

Results

A series of studies have been conducted using the pressure-release type high-pressure combustion chamber (see Figure 3) to measure mass burning rates for $H_2/O_2/He$ and H_2/fuel-additive/O_2/diluent mixtures at selected temperatures (1,400 and 1,600 K) and equivalence ratios (0.3 and 0.7). These results have also been compared to the predictions of several state-of-the-art chemical kinetics models as well as an updated model developed as part of the present work. Figure 3 shows the mass burning rate results as a function of pressure for $H_2/O_2/He$ mixtures at an equivalence ratio of 0.3 at 1,400 K. The mass burning rate is observed to increase and then decrease as pressure is varied from 1 to 25 atm. Comparisons with the models shown in Figure 3 indicate differences in the predicted mass burning rate of up to a factor of 4. Of particular interest is the lack of agreement with the "GRI mech" model that is widely used in the research community.

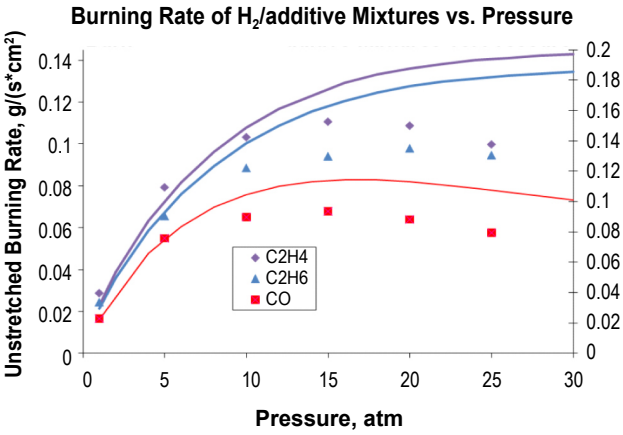

FIGURE 3. Pressure dependence of mass burning rates for H_2/O_2/additive/diluent flames of equivalence ratio 0.70 for H_2/additive=90/10 with diluent concentration adjusted to achieve flame temperatures near 1,600 K. The left axis corresponds to studies with He and Ar as the diluent in the ratio He/Ar=75/25, and the right axis corresponds to studies with He as the diluent. Symbols show experimental data. Lines show predictions from the model considered in this study [1].

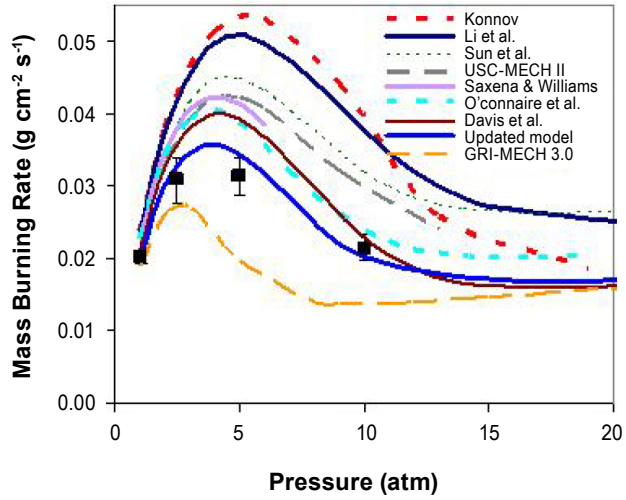

FIGURE 4. Comparison of predictions of the laminar flame mass burning rate of H_2/O_2/He flames of equivalence ratio 0.3 and O_2:He = 1:4.0 ($T_f \sim 1{,}400$ K) for several chemical kinetics models including the recent updated model from the present research effort.

Studies were also conducted to measure the mass burning rate for H_2/fuel-additive/O_2/diluent mixtures. Small concentrations CO, CH_4, C_2H_4, and C_2H_6 at a molar ratio of H_2 to fuel-additive of nine to one are added to characterize fuel-addition effects of species present in syngas mixtures. Figure 4 shows the mass burning rate results as a function of pressure for studies of H_2/O_2/fuel-additive/diluent mixture. The diluent is a mixture of He and Ar in the ratio three to one when the fuel-additive is C_2H_6 or C_2H_4, and when the additive is CO is He. These diluents were used to achieve stable flames in the pressure range of interest. The results shown in Figure 3 were for an equivalence ratio of 0.7 and dilution was adjusted for each mixture to achieve flame temperatures near 1,600 K. Again, the mass burning rate increases and then decreases as pressure is varied from 1 to 25 atm in all cases (see Figure 4). The largest disagreement between model predictions is observed at higher pressures.

An updated chemical kinetics model based on that of Li et al. [2] was formulated to address the difficulties observed in modeling recent high-pressure flame data. Emphasis was placed on assessing the current state of knowledge of relevant elementary processes and the approach needed to achieve a rigorous solution that yields quantitative predictive capability across a wide range of conditions. The primary intent of the updated model is to incorporate a number of rate constant expressions that are more consistent with elementary reaction studies, particular for the reactions most important for high-pressure flame predictions such as $H+O_2(+M)=HO_2(+M)$, HO_2+H/O/OH/HO_2, and $H+OH+M=H_2O+M$. Treatment of a number of additional processes and reactions were considered. Rate constants for the following reactions were revised based on recent proposed expressions: $H+O_2=OH+O$, $O+H_2=OH+H$, $O+H_2O=OH+OH$, $H_2O_2(+M)=OH+OH(+M)$, $OH+H_2O_2=H_2O+HO_2$, and H atom diffusion. Overall, the updated model predicts flame speed spanning a wide range of equivalence ratios, pressures, diluents, and flame temperatures to within 20% (see Figure 4).

Conclusions and Future Directions

Mass burning rate measurements have identified deficiencies in current chemical kinetics model prediction for combustion of H_2/O_2 mixtures at high pressures. These results have motivated a review of current models. An updated model for H_2/O_2 was developed that predicts flame speeds spanning a wide range of equivalence ratios, pressures, diluents, and flame temperatures to within 20%. Future work will focus on high-pressure homogeneous kinetics studies of syngas carried out using the HPLFR and autoignition measurements at high pressures in the high-pressure high-temperature flow reactor.

FY 2010 Publications

1. M.P. Burke, F.L. Dryer, and Y. Ju, "Assessment of Kinetic Modeling for Lean $H_2/CH_4/O_2$/Diluent Flames at High Pressures," *Proceedings of the Combustion Institute* (2011) accepted for publication.

FY 2010 Presentations

1. M.P. Burke, M. Chaos, Y. Ju, and F.L. Dryer, "An Updated Model and Discussion of Modeling Challenges in High-Pressure H_2/O_2 Flames," Spring Technical Meeting of the Combustion Institute, Boulder, Colorado, March 2010.

2. M.P. Burke, Y. Ju, and F.L. Dryer, "Assessment of Kinetic Modeling for Lean $H_2/CH_4/O_2$/Diluent Flames at High Pressures," International Symposium on Combustion, Tsinghua University, Beijing, China, August 2010.

3. M.P. Burke, M. Chaos, Y. Ju, F.L. Dryer, and S.J. Klippenstein, "Updated H_2/O_2 Model to Address High-Pressure Flame Burning Rate Discrepancies," International Symposium on Combustion, Tsinghua University, Beijing, China, August 2010 (poster).

References

1. H. Wang, X. You, A.V. Joshi, S.G. Davis, A. Laskin, F. Egolfopoulos, and C.K. Law, USC Mech Version II. High-Temperature Combustion Reaction Model of H2/CO/C1-C4 Compounds. http://ignis.usc.edu/USC_Mech_II.htm, May 2007.

2. J. Li, Z. Zhao, A. Kazakov, and F.L. Dryer (2004) Int. J. Chem. Kin. 36:566-575.

IV.B.3 Combustion Dynamics in Multi-Nozzle Combustors Operating on High-Hydrogen Fuels

Dom Santavicca
The Pennsylvania State University
Research Bldg. East, Bigler Road
University Park, PA 16802
Phone: (814) 863-1863; Fax: (814) 865-3389
E-mail: das8@psu.edu

DOE Project Manager: Mark Freeman
Phone: (412) 386-6094
E-mail: Mark.Freeman@netl.doe.gov

Subcontractor:
Tim Lieuwen
Georgia Institute of Technology, Atlanta, GA

Contract Number: 05054

Start Date: October 1, 2008
End Date: September 30, 2011

FY 2010 Objectives

- Perform transverse forced response tests in annular combustor test rig.
- Perform longitudinal forced response tests in multi-nozzle can combustor test rig.
- Develop flame response model of transverse forcing in multi-nozzle annular combustor test rig.
- Compare transverse multi-nozzle flame response predictions to measurements.
- Formulate flame response model for longitudinal forcing of multi-nozzle can combustor test rig.
- Initiate comparison of longitudinal multi-nozzle can combustor predictions to measurements.

Accomplishments

- Implementation of high-speed particle image velocimetry (PIV) system on transversely forced combustion system.
- Measurements of transversely forced flow using high-speed PIV and identification of key coupling mechanisms in velocity disturbance field.
- Developed flame response model of transversely forced flame.
- The multi-nozzle can combustor test rig has been completed and successful operation has been demonstrated.
- A preliminary characterization of the air siren capabilities in the multi-nozzle can combustor has been completed.
- A preliminary characterization of the nozzle-to-nozzle variations in mean velocity and velocity modulation in the multi-nozzle can combustor has been completed.
- The first flame response measurements have been made in the multi-nozzle can combustor.

Introduction

Combustion dynamics [1,2] represent one of the major technical challenges in the development of efficient, low emission gas turbines. Current understanding of the underlying phenomenology of combustion dynamics in lean premixed combustors is almost entirely limited to longitudinal mode instabilities in single-nozzle combustors operating on natural gas. In contrast, current combustors employ multi-nozzle can or annular combustor configurations which exhibit both transverse and longitudinal instabilities and are expected to meet operability requirements using a range of gaseous fuels, such a syngas produced by the gasification of coal and biomass.

The goal of this research is to use a synergistic research approach to understand the underlying physics of the coupling mechanisms between catastrophic acoustic resonances and the flame dynamics that fuel them. The use of a multiple-nozzle experimental facility recreates the flow conditions in an actual gas turbine and allows for specific attention to be paid to the complicated interactions between flames that can aggravate the combustion dynamics problem.

Approach

A physics-based, flexible, and synergistic approach is the key to successfully studying the response of a multi-nozzle combustor to longitudinal and transverse acoustic excitation. Two test rigs have been designed and constructed for use on this project, a multi-nozzle can combustor test rig with longitudinal air-forcing and a multi-nozzle annular combustor test rig with transverse air-forcing.
In order to identify and characterize the underlying phenomenology of the flame's response to longitudinal and transverse acoustic oscillations, a number

of measurement techniques are employed. This includes chemiluminescence imaging of the spatial distribution of the flame's heat release rate and PIV measurements of the two-dimensional velocity field. These measurements are phase-synchronized with the acoustic forcing, thereby revealing the periodic phase-averaged flame response and its relationship to the phase-averaged acoustically-forced velocity field. In the later stages of the project, time-resolved PIV measurements will be made in the multi-nozzle annular combustor test rig, which will allow for more detailed inspection of vortex formation, flame movement, and adjacent flame interaction. In addition, a technique will be implemented to characterize the response of a single flame in the multi-nozzle can combustor test rig, in order to isolate and study flame interactions and their effect on the overall flame response.

Results

Details of the complicated velocity coupling mechanism have been measured in the transversely forced rig. These results have been measured using both high-speed PIV and high-speed smoke visualization for a complete picture of the velocity disturbance field. Figure 1 shows an example of the disturbance field measured in the case where a velocity anti-node is present along the centerline of the combustor. In this figure, the flow travels from left to right and several key features are evident. First, vortex formation and downstream convection can be clearly seen in the vorticity isocontours. At 0 degrees, two vortices outlined in red form at the nozzle exit, and by 115 degrees through the cycle have traveled to a downstream position of half of one diameter. Considering the velocity in these shear layers, note that the inner and outer shear layers are oscillating out of phase with each other. In other words, when the inner shear layer velocity field is directed outward, the outer shear layer is directed inward, and vice versa. For example, at 0 degrees, the velocity in the outer shear layer at approximately $x/D=0.5$ has a significant negative axial component, while the corresponding inner shear layer has a significant positive axial component. Finally, the velocity fluctuation transitions from a complex two-dimensional field near the nozzle dump plane to dominantly transverse farther downstream.

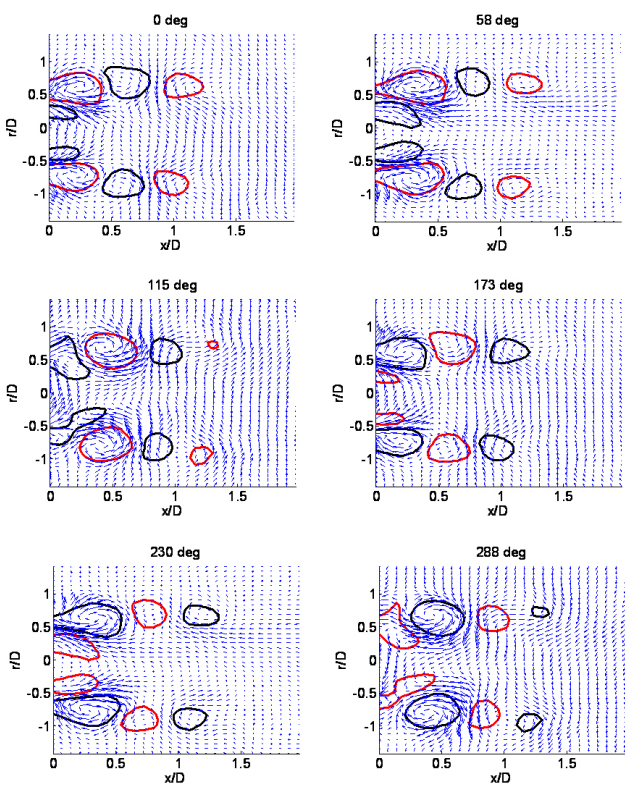

FIGURE 1. Time variation of velocity and vorticity field for f_o=800 Hz out of phase acoustic forcing, non-reacting flow at U_o=40 m/s. Vorticity isocontours correspond to $\omega(r_2-r_1)/U_o$=-0.1 (red) and 0.1 (black).

Additional results from smoke visualization tests have shown the significant effect that transverse acoustic forcing can have on the overall shape of the flow field, which can have significant impact on the flame-flame interaction in a multi-nozzle configuration. Figure 2 shows the shortening of the potential core and the widening of the flow under acoustic forcing, where the potential core can be seen as the dark region between the two smoke-filled shear layers. The shortening of the potential core comes from the forced interaction of the two shear layers, as described above. The fluctuating pressure field, in both the in-phase and out-of-phase forcing cases, causes significant enough transverse velocity to cause the shear layers, particularly the inner shear layer, to flatten, reducing the length of the potential core. This reduction could have a significant effect on flame shape, in configurations where the flame is stabilized in either the inner shear layer or both the inner and outer shear layers. This flattening of the shear layers and the flame could lead to increased flame-flame interactions in the multi-nozzle configuration. The increased interaction of these two flames leads to an increase in flame area destruction, a highly non-linear mechanism that is yet to be understood in the context of combustion dynamics.

The multi-nozzle can combustor test rig has been completed and made operational. Photographs showing the multi-nozzle can combustor test rig and a representative multi-nozzle flame are shown in Figures 3 and 4, respectively. The flame photograph clearly shows regions where adjacent flames interact, as well as evidence of flame-wall interaction.

In multi-nozzle can combustors, nozzle-to-nozzle variations in the air flow rate are expected to be as

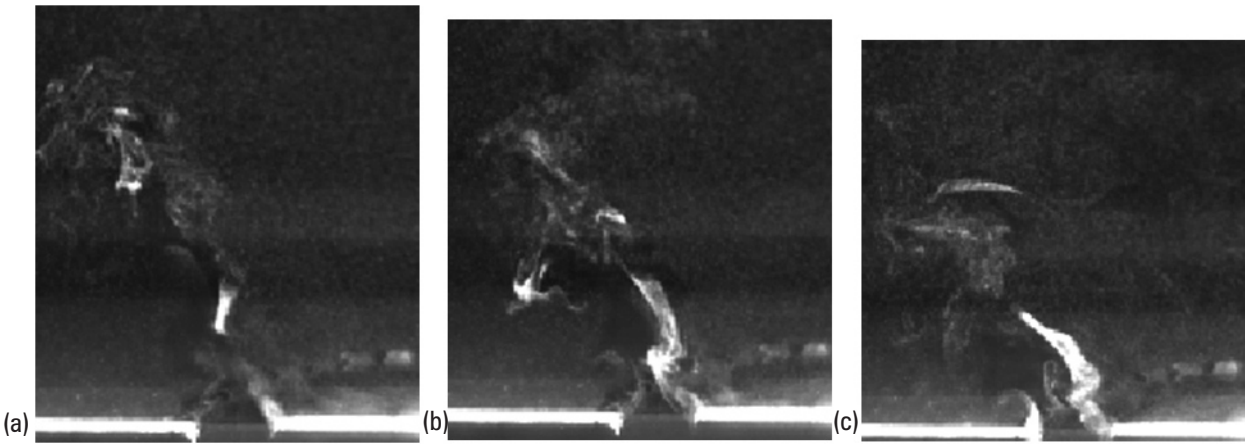

FIGURE 2. Non-reacting smoke visualization showing transverse excitation effects upon interacting shear layers. Shortening of potential core as acoustic forcing amplitude is increased (a-c) for out-of-phase forcing at 400 Hz and a bulk velocity of 10 m/s.

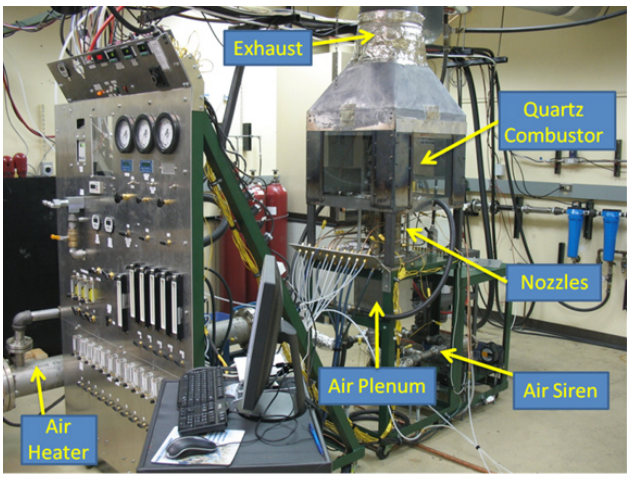

FIGURE 3. Multi-Nozzle Can Combustor Test Rig

FIGURE 4. Photograph of Flame-Flame Interactions in Multi-Nozzle Can Combustor Test Rig

large as 5 to 10%. The effect of such variations on combustion dynamics is of considerable practical interest. In the multi-nozzle can combustor used in this study, the five nozzles are supplied air from a common plenum and only the total air flow rate is metered. To determine the actual flow split between the nozzles, each nozzle has been instrumented with a differential pressure gauge to measure the pressure drop across the swirl vanes. Using calibration curves generated for each nozzle relating the pressure drop to the flow rate, the mean velocity in each nozzle can be measured. Preliminary measurements over a limited range of conditions have shown that the nozzle to nozzle variations in the mean velocity are between 5% and 10%, similar to what is found in actual can combustors. In the current combustor configuration, the fuel supplied to each nozzle is metered such that all nozzles receive the same amount of fuel. Therefore air flow rate variations result in variations in the velocity and the equivalence ratio between nozzles.

For the multi-nozzle flame response measurements it is also important that nozzle-to-nozzle variations in the amplitude and phase of the acoustic velocity oscillations are small. Preliminary measurements using the two-microphone technique show nozzle-to-nozzle variations in the amplitude of the acoustic velocity fluctuations as large as 50%, while variations in the phase of the acoustic velocity fluctuations are less than 10 degrees.

The first flame response measurements have been made in the multi-nozzle can combustor at a forcing frequency of 100 Hz with a velocity fluctuation amplitude of 15%. Figure 5 shows a sequence of phase-averaged chemiluminescence images of the flame recorded every 15 phase-angle degrees. The intensified camera used to record these images is positioned so that the center and two of the outer nozzles are in front

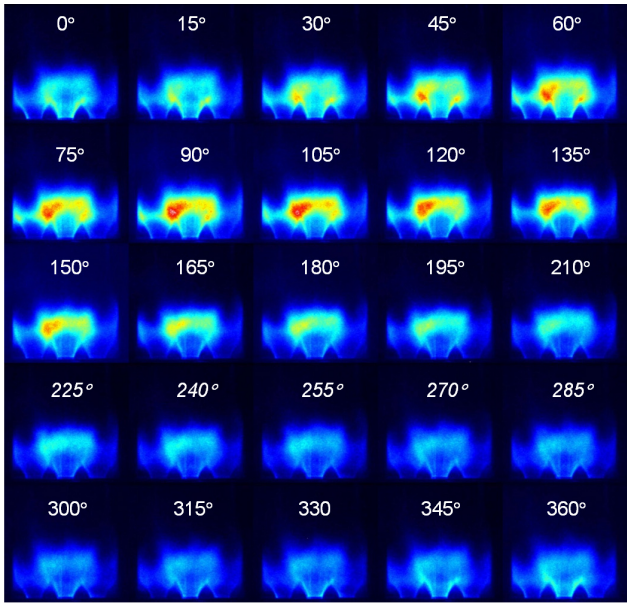

FIGURE 5. Phase-Averaged Images of Forced Flame Response over One Forcing Cycle ($f_{forcing}$ = 100 Hz, V'/V_{mean} = 0.15, V_{mean} = 20 m/s, T_{in} = 150°C, ϕ = 0.55)

of one another, hence the appearance of only three flames with the center flame appearing significantly more intense. The image sequence shows periodic fluctuation in the flame's rate of heat release, and when viewed as a "movie" reveals periodic axial motion of the most intense region of the flame as well as the overall length of the flame. These results, however, cannot be quantified in terms of the rate of heat release because in these tests the fuel was injected through the injection holes in the swirl vanes, and as a result both the velocity and the equivalence ratio were fluctuating.

Conclusions and Future Directions

Much of the key coupling physics between the transverse acoustic field and the flame velocity disturbance field has been measured in the past year. Both quantitative and qualitative descriptions of the flow field and its dynamics have provided the foundation on which to understand the response of the flame to this complex disturbance field. Initial tests have indicated that the transverse forcing configuration can lead to increased flame-flame interactions.

Future work will include additional reacting tests, measuring disturbance field fluctuations using high-speed PIV, and measuring global flame fluctuations using chemiluminescence. These tests will lay the groundwork for forthcoming multi-nozzle measurements of heat release fluctuation from three flames under transverse acoustic excitation.

The multi-nozzle can combustor test rig has been completed and is operational. Preliminary measurements characterizing the nozzle-to-nozzle variations in the mean velocity and in the fluctuation of the mean velocity have been obtained and show that the mean velocity is uniform within 10%, however, the amplitude of the velocity fluctuation varies significantly. Using the current system, the ability to achieve significant flame forcing was demonstrated for the first time.

Two changes are currently being made to the multi-nozzle can combustor which are essential to achieving the project goals. The first is a complete redesign of the inlet plenum that feeds air from the siren to each of the nozzles. The new plenum is designed such that the flow paths from the siren to each of the nozzles are very nearly identical, which is expected to significantly reduce the nozzle-to-nozzle variation in the amplitude of the velocity fluctuation. The second change is to eliminate the equivalence ratio fluctuations by injecting and mixing the fuel and air upstream of a choked orifice which is located upstream of the siren. Once these changes have been completed, the air-forced flame response tests and related measurements will resume.

References

1. S. Ducruix et al., "Combustion Dynamics and Instabilities: Elementary Coupling and Driving Mechanisms," *Journal of Propulsion and Power*, Vol. 19, pp. 722-726, 2003.

2. G. Staffelbach et al., "Large Eddy Simulation of Self Excited Azimuthal Modes in Annular Combustors," *Proceedings of the Combustion Institute*, Vol. 32, No. 2, pp. 2909-2916, 2009.

IV.B.4 Numerical and Experimental Study of Mixing Processes Associated with Hydrogen and High Hydrogen Content Fuels

Vincent G. McDonell (Primary Contact), Amin Akbari, Scott Hill, and Patrick Randall
University of California, Irvine (UCI)
UCI Combustion Laboratory
Irvine, CA 92697-3550
Phone: (949) 824-5950 x121; Fax: (949) 824-7423
E-mail: mcdonell@ucicl.uci.edu

DOE Project Manager: Mark Freeman
Phone: (412) 386-6094
E-mail: Mark.Freeman@netl.doe.gov

Contract Number: NT0006551

Start Date: October 1, 2008
End Date: September 30, 2010

FY 2010 Objectives

- Finalize test matrix.
- Acquire experimental data.
- Complete grids for numerical studies.
- Complete simulations.
- Compare experimental and numerical results.

Accomplishments

- A test matrix involving fuel composition, swirl strength, and radial or axial fuel injection was developed.
- A measurement protocol was established based on use of micro sample probes in conjunction with gas chromatography, hydrogen conductivity, and flame ionization detectors. In addition, pitot-probe and particle image velocimetry (PIV) measurements of the flowfield are currently being obtained.
- Data were acquired for radial and axial fuel injection for non-swirling conditions for both natural gas and hydrogen fuels.
- Grids were generated and refined as needed for each of the geometries of interest. Grid sensitivity studies were carried out to establish suitability of the grids.
- Two and three dimensional (3D) computational fluid dynamics (CFD) simulations were carried out for all the experimental conditions. For the CFD studies, various Reynolds-averaged Navier-Stokes (RANS) turbulence models and values of turbulent Schmidt number were examined. In addition, unsteady RANS (URANS) and large eddy simulations (LES) were carried out for limited cases.
- The results indicate that, for radial fuel injection for the conditions studied, the fuel type has little effect on the overall dispersion and mixing behavior. This was observed despite the higher diffusivity of hydrogen compared to methane.
- The results are most sensitive to turbulence model choice, with Reynolds Stress Model (RSM) providing better overall agreement than the realizable k-epsilon model. While the value of turbulence Schmidt number does affect the simulation results, its impact is not as great as the choice of turbulence model. While LES and URANS tended to provide improved agreement with the measurements, the computational time required rendered them impractical for design screening on the eight-node parallel computing platform used.

Introduction

Efficient design and optimization of combustion hardware requires a combination of engineering experience and skill with effective tools to help evaluate design strategies. The development of lean premixed combustion strategies have resulted in significant advances in low emission, high efficiency gas turbines for operation on natural gas. These advances were been made possible in part by the use of advanced simulation tools like CFD. However, for high hydrogen containing fuels, the applicability of modeling strategies that worked well for natural gas may not be as accurate. As a result, (and as stated by the DOE's funding opportunity notice) research is needed to better characterize, understand, and model the fuel profile and unmixedness using turbine appropriate pre-mixer approaches for operation with low molecular weight, high mass diffusivity fuel mixtures containing high hydrogen levels. The outcomes will: 1) help more efficiently design advanced fuel injection/combustion systems; 2) provide better understanding of the way in which new fuels mix with air/oxygen; and 3) provide a basis for better modeling approaches for the mixing behavior of fuels of interest.

In the present case of hydrogen, detailed measurements of fuel/air mixing for a systematic variation in a generic premixer geometry with

controlled swirl, air side pressure drop, air turbulence levels, fuel injection location, fuel injection momentum, fuel/air density ratios, and fuel type. In addition, the details of the premixer aerodynamic field will be measured and calculated using CFD (LES).

The proposed research is directed at evaluating methods for characterizing fuel profiles and unmixedness and applying these methods to provide detailed fuel concentration profile data that can be used to develop and/or validate modeling approaches for determination of the fuel distribution produced by typical premixing strategies. The objectives of the proposed project are to: 1) establish and apply reliable, accurate measurement methods to establish the instantaneous and time averaged fuel distribution at several locations downstream of the point of injection; and 2) evaluate how CFD software model coefficients and approaches within affect the overall accuracy of the numerical simulations.

Approach

To accomplish the objectives of the project, two major tasks will be carried out. The first task is associated with the experimental study of fuel/air mixing. This task will require minor modifications to existing test hardware to configure it for the experiments planned. This consists of fabricating 12 axi-symmetric parts that will interface with existing hardware. This task will also involve the preparation of the planned diagnostic techniques. This will provide a critical evaluation of the accuracy and ability of each technique to measure the necessary quantities (e.g., time resolved/time averaged concentration of individual fuel species). With the developed hardware and diagnostics, measurements will be made systematically for a number of hardware geometry configurations which will result in detailed data for fuel concentration as a function of swirl, turbulence levels, injection location, injection type (e.g., centerline, radial, from spokes), fuel-to-air density ratio, and fuel type. In addition, the aerodynamic flowfield produced by the test hardware will be delineated using an LES modeling approach coupled with detailed velocity measurements as validation. Using the results obtained, analysis will be carried out to establish physics-based design guides for the fuel/air behavior (e.g., rules for penetration vs. momentum flux ratio, rules for fuel plume spread vs. appropriate non-dimensional groups).

The second major task is the application of different CFD modeling techniques to evaluate their ability to match the measured data over a wide range of conditions. Both RANS and LES will be used. For RANS, sensitivity to different turbulence models and model coefficients (e.g., Schmidt number) will be carried out to determine if a tuned RANS approach can be used. LES will be used as well and the results will establish the required CFD approach for correctly simulating mixing of a wide range of fuel types.

To the extent possible, UCI will work closely with the National Energy Technology Laboroatory and original equipment manufacturer researchers relative to parametric simulations.

Results

Table 1 summarizes the plans for the initial testing/simulation geometries and conditions with a goal of varying the key phenomena associated with mixing processes. Two basic methods, radial and axial fuel injection, are being considered and for both methods a combination of parameters are being considered. For context, Figure 1 shows the test hardware which is based on a combination of existing a new components. Table 2 summarizes the parameters that are being varied for both experimental and numerical studies.

TABLE 1. Experimental Design

Factor	Levels	Comment
Swirl	- 0 (no swirl) - 45 deg axial vanes	
Quarl	- Straight barrel see Figure 1 - Tapered	
Injection Type	Radial jets outward Axial at centerline	
Injection Momentum	Low High	Defined based on jet to crossflow momentum flux ratio
Fuel Type	H_2/CO/methane blends	Could include as a mixture subdesign or select 3-4 discrete fuels

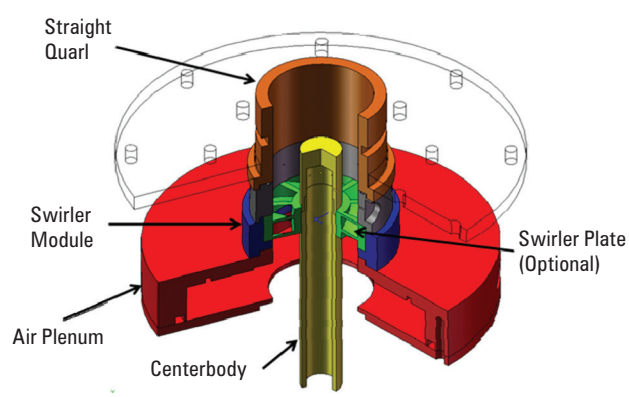

FIGURE 1. Test Hardware Sectioned View

TABLE 2. Summary of Turbulence Models Considered

Turbulence Model	Purported characteristics and applications
Realizable k-epsilon Model	Improved performance for swirling flow and recirculation, as low cost as the standard k-epsilon model.
Standard k-epsilon Model	Common, low cost, good for simple high speed turbulent flows; poor performance in complex 3D, anisotropic turbulence such as swirl, recirculation, flow separation
Renormalization Group Theory (RNG) k-epsilon Model	Use RNG method; add analytic formulation for turbulent Prandtl number, improved performance for swirling flow and recirculation, slightly higher cost and harder to converge than the standard k-epsilon model.
Reynolds Stress model (RSM)	Relatively complex and advanced, in principal can account for non-isotropic turbulent flows with swirl and recirculation

Figure 2 shows the overall measurement locations and strategy to transform the measured values into contours of fuel/air ratio. To date radial and axial fuel injection scenarios have been examined.

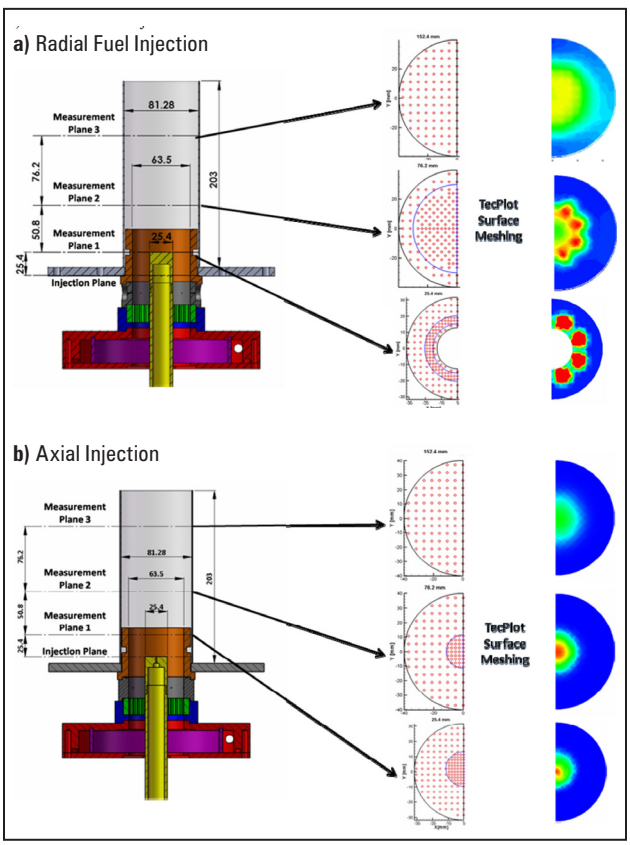

FIGURE 2. Measurement Planes and Example Measured Results

Detailed comparisons with CFD simulations have been carried out for both radial and axial injection cases. For the radial injection, examples of results obtained are shown in Figure 3 and Figure 4 for hydrogen and methane, respectively. The fuel jet to crossflow momentum flux ratio was maintained at 8.9. In these figures, qualitative comparisons are shown for different turbulence models, different turbulent Schmidt numbers, different fuels, and different axial locations.

To help quantify the degree of agreement obtained between the simulation approaches and the measured results, analysis of variance has been carried out. For the analysis of variance, the factors of: 1) fuel; 2) turbulence model; 3) turbulent Schmidt number; and 4) axial plane were considered. The response examined is the average percent difference between the measured and predicted values at all measurement locations over the plane. The "raw" results are shown in Figure 5.

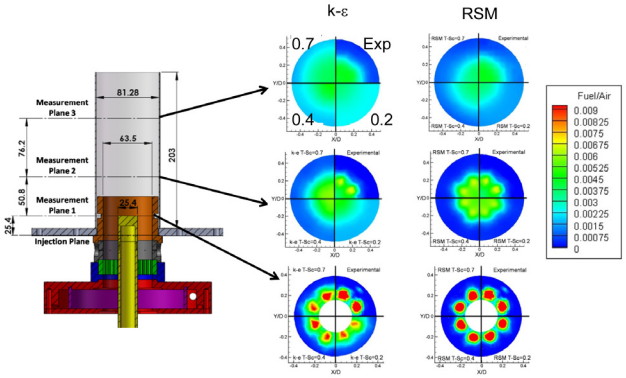

FIGURE 3. Comparison of Measured and Predicted Mixing of Hydrogen into Air for Different Turbulence Models and Turbulent Schmidt Number Values

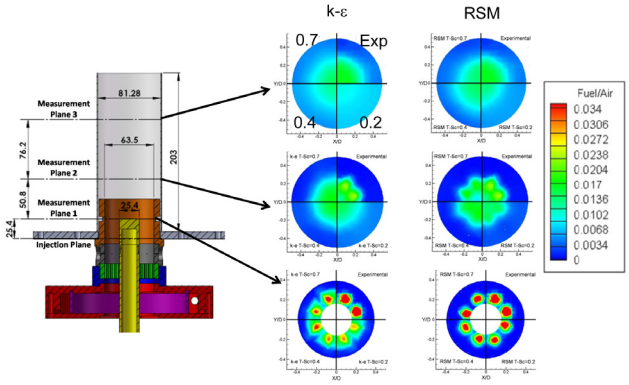

FIGURE 4. Comparison of Measured and Predicted Mixing of Methane into Air for Different Turbulence Models and Turbulent Schmidt Number Values

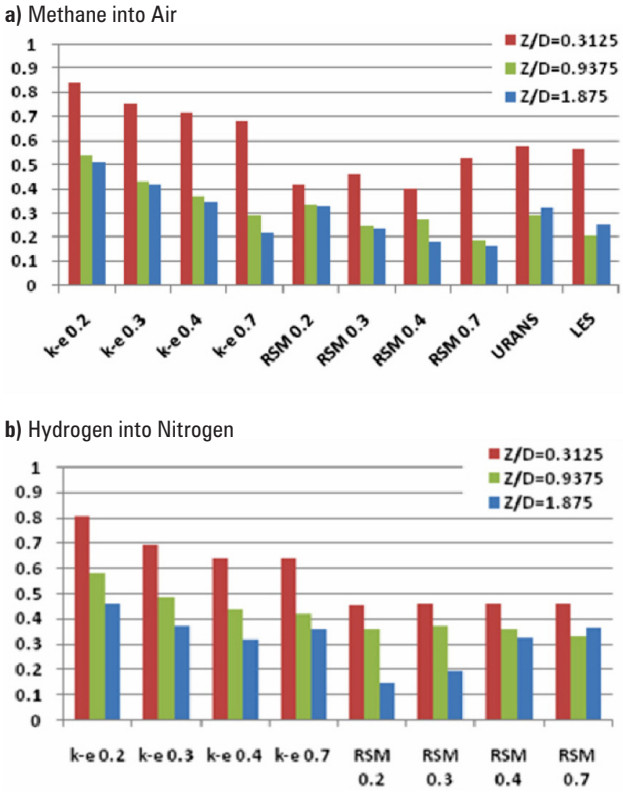

FIGURE 5. Average Percent Difference Between Measured and Predicted Fuel Concentration

The ANOVA results are shown in Table 3. The results indicate that the turbulence model is the most sensitive factor, with the RSM model providing significantly better agreement in general compared with the realizeable k-ε model. The value of turbulent Schmidt number does make a difference as well, although its impact on the agreement is about 16% of the turbulence model. It is evident that the impact of the value of turbulent Schmidt number used also depends on what turbulent model is used. The other observation that is apparent is that the axial plane examined is a strong factor. In this case, it is more difficult to get good agreement at the near plane vs. the far plane.

TABLE 3. Summary of ANOVA

Term	% Contribution
Intercept	
A-Turb Model	28.2
B-Fuel	0.7
C-Plane	50.4
D-T-Sch	4.6
AB	0.3
AC	3.3
AD	4.3
BC	1.7
BD	1.5
CD	0.8
ABC	0.1
ABD	0.5
ACD	0.4
BCD	2.5
ABCD	0.7

Conclusions and Future Directions

Thus far, the radial fuel injection cases are complete as are the axial injection cases. The analysis of the axial injection cases is currently underway. In addition, both axial and radial injection of fuel into a swirling flow is also being investigated both numerically and experimentally. As the results become available, systematic analysis carried out will provide guidance on the best simulation strategy to get the best agreement between predicted and actual fuel concentration for various premixer and fuel injection configurations. Additional conditions will be studied as needed to address questions arising from the systematic studies.

FY 2010 Publications/Presentations

1. Quarterly Progress Report (October-December 2009), January 2010.

2. Quarterly Progress Report (January-March 2010), April 2010.

3. A. Akbari, S. Hill, P. Randall, V. McDonell, and S. Samuelsen, "Numerical and Experimental Study of Mixing of Gaseous Fuels," Paper #09F-70, Presented at the Fall Technical Meeting of the Western States Section of the Combustion Institute, Irvine, California, October 26, 2009.

4. A. Akbari, S. Hill, P. Randall, V. McDonell, and S. Samuelsen, "Numerical and Experimental Study of Mixing of Gaseous Fuels. Numerical and Experimental Study of Mixing Processes Associated with Hydrogen and High Hydrogen Content Fuels," UTSR Program Review, Orlando, Florida, October 28, 2009.

5. A. Akbari, S. Hill, V. McDonell, and S. Samuelsen, "Experimental and Computational Analyses of Methane and Hydrogen Mixing in a Model Premixer," Paper GT2010-23049, Presented at TurboEXPO 2010, Glasgow, Scotland, June 14–18, 2010.

6. A. Akbari, S. Hill, V. McDonell, and S. Samuelsen, "Experimental and Computational Analyses of Methane and Hydrogen Mixing in a Model Premixer," Paper GT2010-23049, Presented at TurboEXPO 2010, Glasgow, Scotland, June 14–18, 2010, accepted for publication in *ASME Journal of Engineering for Gas Turbines and Power.*

IV.B.5 High Pressure Kinetics of Syngas and Nearly Pure Hydrogen Fuels

Professor John W. Daily, Director
Center for Combustion and Environmental Research
Department of Mechanical Engineering
University of Colorado at Boulder (CU)
Boulder, CO 80309-0427
Phone: (303) 492-7110, Fax: (303) 492-3498
E-mail: john.daily@colorado.edu
Web site: http://spot.colorado.edu/~daily

DOE Project Manager: Mark Freeman
Phone: (412) 386-6094
E-mail: Mark.Freeman@netl.doe.gov

UTSR Manager of Research: Richard Wenglarz
Phone: (864) 656-2267
E-mail: RWNGLRZ@exchange.clemson.edu

Contract Number: 41431/UTSR 07-01-SR126

Start Date: May 15, 2007
End Date: September 30, 2010

FY 2010 Objectives

- Develop the necessary chemical kinetics information to understand the combustion of syngas and nearly pure hydrogen fuels at conditions of interest in gas turbine combustion.
- Explore high-pressure kinetics by making detailed composition measurements of combustion intermediates and products in a flow reactor using molecular beam/mass spectrometry (MB/MS) and matrix isolation spectroscopy (MIS).
- Compare experimental data with calculations using existing mechanisms.
- Use theoretical methods to improve the predictability of existing mechanisms.

Accomplishments

Task I. "Select existing reaction mechanisms most likely to form a firm basis for extension to high pressure and carry out sensitivity and rate of production analysis to identify critical reactions and species."

Current chemical kinetic mechanisms do a poor job of predicting important combustion characteristics such as ignition delay at the low temperatures and high pressures found in gas turbine combustor inlets. Discrepancies of nearly three orders of magnitude in ignition delay exist between the theoretical predictions and experimental results at 700 K and 20 bar. Several paths whereby gas phase reactions could explain the observed discrepancy were explored. First, reaction rate uncertainties were examined for several modern mechanisms. Then, a chemometric approach was used to explore whether any important species and/or reactions were overlooked in the mechanisms. In particular, ozone and longer polyoxides were examined to see if they might produce additional chain branching. The possible role of sensitizers, in particular NO and NO_2, were also investigated due to their known ability to induce chain branching reactions at lower pressures. Sensitivity to perturbations in the local thermodynamic state was explored. These gas phase pathways seem extremely unlikely, and other explanations such as catalytic wall effects must be found.

Task II. "Carry out experiments for conditions pertaining to gas turbine operation using both syngas and nearly pure H_2 fuels burned with air and oxygen. Measure species concentrations as a function of temperatures and pressure."

As described in previous reports, this task is being approached with a changed objective. Since gas phase reactions cannot explain discrepancies between experiments and computations for properties such as ignition delay, focus was shifted to catalytic wall reactions. To explore these experimentally, a high temperature micro-nozzle flow reactor assembly was designed and built. The flow reactor is designed to be able to change out reactor wall materials. Many experiments have been completed and more are currently underway.

Task 3. "Compare experimental results with predictions to identify shortcomings in reaction mechanisms. In particular identify, if any, important intermediate species not previously included in existing mechanisms."

A detailed computational fluid dynamics (CFD) analysis of the flow in the micro-nozzle was carried out to support interpretation of the experimental results. It has been shown that nickel and Inconel surfaces are catalytic for H_2 oxidation and that an existing reaction mechanism gives predictions in rough agreement with experiments for nickel.

Introduction

The objective of this project is to develop the necessary chemical kinetics information to understand the combustion of syngas and nearly pure

hydrogen fuels at conditions of interest in gas turbine combustion. Syngas is the product of the gasification of coal and/or biomass. The composition of syngas can vary considerably, but typically contains mostly hydrogen, CO and CO_2 with smaller amounts of CH_4, O_2, N_2, other hydrocarbons and water vapor. With further processing, the hydrogen content can be increased to fairly high levels. Both syngas and nearly pure H_2 mixtures can be oxidized either with air, or with pure oxygen, or any combination thereof. The use of any particular fuel/oxidizer combination in gas turbines will require an ability to predict important combustion properties such as laminar flame speed, autoignition conditions, flammability limits and NOx formation rates.

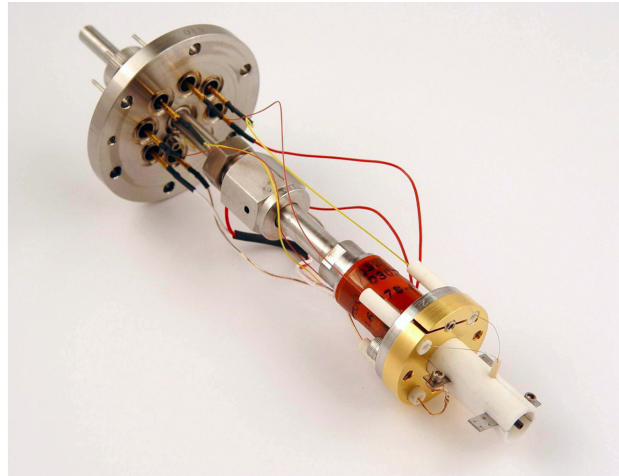

FIGURE 1. Hyperthermal Nozzle Assembly

Approach

Combustion properties depend on the chemical kinetics of the fuel/oxidzer combination. Existing reaction mechanisms do a satisfactory job of predicting these properties at pressures close to atmospheric and below, but are less well tested at higher pressures in the range of 15-20 bar, especially at lower temperatures. The initial approach in this project was to explore the high-pressure kinetics by making detailed composition measurements of combustion intermediates and products in a high-pressure flow reactor using MB/MS and MIS/infrared (IR) spectroscopy. The data would then be compared with calculations using existing mechanisms. However, since concluding that gas phase reactions are not the cause of observed discrepancies between experiments and computation, the focus shifted to catalytic wall reactions. An interesting aspect of wall reactions is that they are sensitive to pressure only through the concentration of gas phase species adjacent to the wall. This is unlike the gas phase, where high pressure amplifies the importance of tri-molecular reactions leading to the unusual explosion limit behavior of H_2/O_2 combustion. Thus, the experiments to explore reaction mechanisms do not need to be carried out at high pressure.

The approach has been to carry out experiments in a specially designed high temperature (hyperthermal) micro nozzle flow reactor who surface material can be changed. (There is extensive experience in using these types of reactors at CU.) The flow reactor is shown in Figure 1. The assembly to the left of the gold flange is a solenoid activated valve. The nozzle/reactor is the small tube seen at the right end of the white insulating shield to the right of the gold flange. The tube can be manufactured using different materials of engineering and scientific interest. Stainless steel, nickel and Inconel have been tested, simulating current gas turbine premixed inlet materials. The tube can be heated electrically to controlled temperatures. The overall reaction sought is surface catalyzed $H_2 + 0.5\ O_2 \rightarrow H_2O$. To avoid problems with water contamination, D_2 has been substituted for H_2, and exhaust gases were examined for D_2O using MIS/IR diagnostics.

The complete experimental configuration (with IR diagnostics) is shown in Figure 2. Cold reactant gases are fed into the reactor where they pass over the heated surface. Both the diagnostics used require that the reactor tube exit into vacuum conditions. There is a practical limit to the mass flow rate that can be handled by the vacuum pumps. Therefore, the reactor is operated in a pulsed mode. In the case of plasma ion mass spectrometry (PIMS) the pulsed operation is also required to match the duty cycle of the pulsed laser ionization light source. The matrix diagnostic could be run continuously except for the pumping limitations just mentioned.

The experiments result in measurements of the compounds exiting the reactor, although all products cannot be detected. When using PIMS, only species whose ionization potential is below 10.8 ev are detectable. This excludes H (D) and O atoms, OH, and H_2O/D_2O. When using IR, only polyatomics and heterogeneous diatomics can be detected. Thus, H_2/D_2 and O_2 cannot be seen, but OD, H_2O/D_2O, CO and CO_2, etc., can be seen easily. Hydrogen-rich syngas is mainly composed of H_2 and CO. The expected products if catalysis is present are OH, H_2O and CO_2 (or in this case OD, D_2O). For this reason, this project has focused on using the IR diagnostic, although experiments at the DOE Advanced Light Source (ALS) are planned to perform PIMS with tunable photons and access all the species of interest.

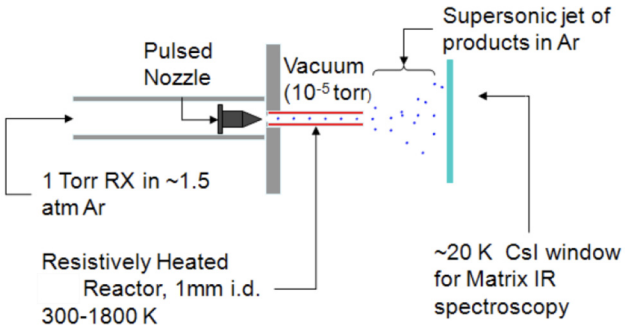

FIGURE 2. Experimental Configuration

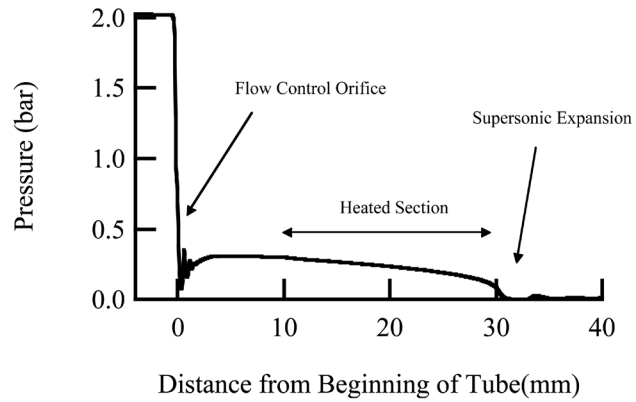

FIGURE 3A. Pressure Distribution through Reaction from CFD Simulation

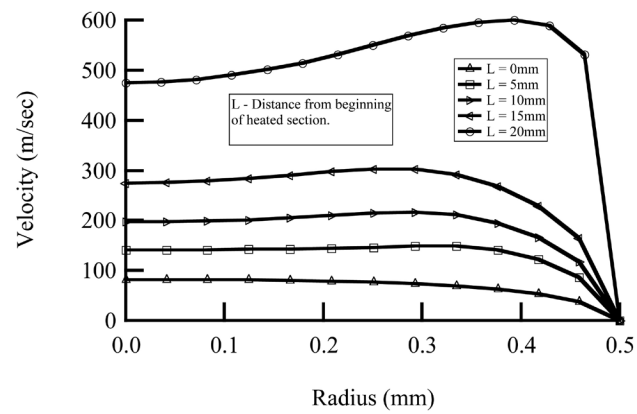

FIGURE 3B. Velocity Profiles in Reactor from CFD Simulation

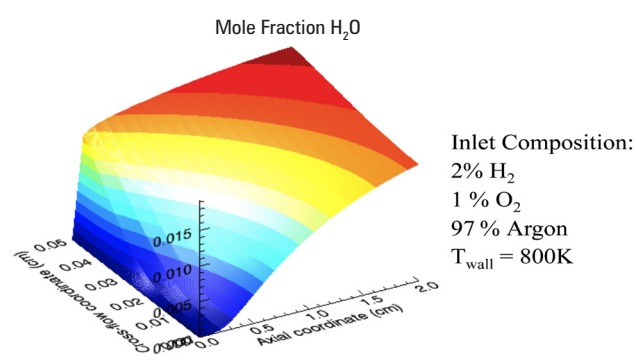

FIGURE 4. Water Distribution in Reactor When Wall Reaction Present

Results

Reactor Simulations

It is necessary to have some understanding of the fluid and thermodynamic states within the reactor. Since the reactor is very small it is impractical to carry out direct measurements within it. CFD was used to model the flow through the inlet system and reactor. The CFD results can be compared with flow rate measurements and with calibration kinetic measurements. Figure 3A shows the pressure distribution through the system when the inlet pressure is 2 atm. Figure 3B shows velocity profiles within the reactor. Temperature and pressure distributions are also calculated. Knowing the fluid and thermodynamic states within the reactor, one can also perform kinetic calculations. Figure 4 shows an example CHEMKIN simulation of the reactor flow assuming a nickel wall material. The inlet flow consisted of 2% H_2, 1% O_2 and the remainder the argon carrier gas. The Princeton gas phase and the Deutschmann surface mechanisms were used in the simulation.

Experimental Results

Experiments have been run with stainless steel, nickel and Inconel. Figure 5 shows the IR calibration spectra for runs of pure argon and argon seeded with D_2. The spectra clearly illustrate the necessity to account for background amounts of water vapor, which is why D_2 has been substituted for H_2. Figure 6 shows a set of IR D_2O (v_2 bending mode) spectra for a series of runs on nickel at different temperatures. As the wall temperature is increased, increasing percentages of D_2 are oxidized to D_2O.

The IR spectra are measured using the Fourier transform infrared technique. The instrument outputs spectra as optical density (OD). Given the OD, an estimate of the thickness of the matrix and the spectral properties of the absorber, it is possible to infer the concentration on the matrix. Knowing the total quantity of gas deposited, an estimate of conversion amount can be made. Equation 1 is used to determine the number of absorbers under an IR band in the units of molecules/cm^3, where z is the pathlength (cm), A the integrated infrared intensity for the molecule (km/mol), N_A is Avogadro's number, and the integral represents the total integrated area for a given vibrational mode. The ln(10) is needed to convert the reported optical

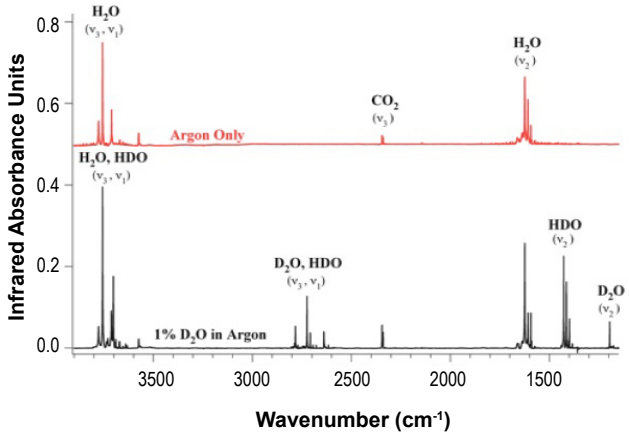

FIGURE 5. D_2O Calibration vs. Argon Only

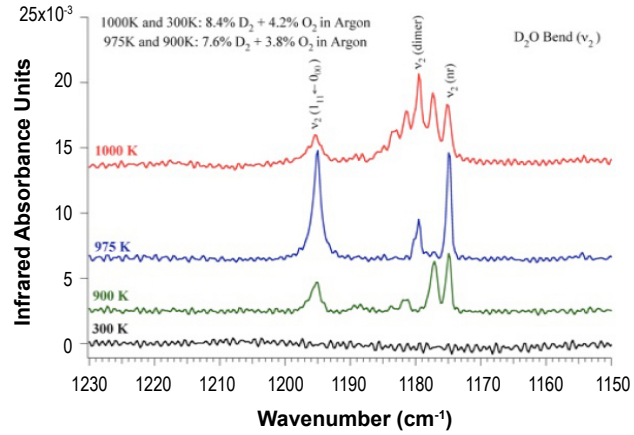

FIGURE 6. Nickel Results (D_2O v_2 Bend)

density, OD(v), from log base 10 to natural logarithm, used in the calculation of A.

$$n = \frac{N_A \ln(10)}{zA(10^5)} \int_{IR\ band} OD(\upsilon)d\upsilon$$

For the results shown in Figure 6, a 1% to 9% conversion of D_2 and O_2 to D_2O occurs in the Ni reactor.

Similar results are available for Inconel although conversion rates are somewhat less than for nickel, as expected. Inconel experiments are still being conducted.

Conclusions and Future Directions

The conclusion that gas phase reactions are not the cause of observed discrepancies between experiments and computation has led to exploration of catalytic wall reactions. Task II experiments are continuing using the high-temperature micro nozzle flow reactor facility. CFD simulations have been developed to assist in data interpretation. Results to date have demonstrated that nickel and Inconel do have a catalytic effect for hydrogen oxidation and that the nickel results are roughly predicted using an existing surface reaction mechanism.

During the remaining reporting period, additional IR runs on Inconel will be conducted. In addition, experiments at the DOE ALS at the Lawrence Berkeley National Laboratory, where the PIMS instrument will allow detection of all species of interest and performance of a complete fuel balance, will be conducted.

FY 2010 Publications/Presentations

1. "High Pressure Kinetics of Syngas and Nearly Pure Hydrogen Fuels," Talk presented at the UTSR Workshop, October 27–29, 2009.

2. "High Pressure Kinetics of Syngas and Nearly Pure Hydrogen Fuels," Semi-annual report, November 15, 2009.

3. Kimberly Jasch, G. Barney Ellison, and John Daily, "Study of Nickel Catalyzed Wall Reactions in the Combustion of Hydrogen-Rich Syngas," Spring Technical Meeting, Western States Section of the Combustion Institute, University of Colorado at Boulder, March 22–23, 2010.

4. Qi Guan, John W. Daily, and G. Barney Ellison, "CFD Simulation of Compressible Reacting Flow in a Hyperthermal Tubular Reactor," Spring Technical Meeting, Western States Section of the Combustion Institute, University of Colorado at Boulder, March 22–23, 2010.

IV. UNIVERSITY TURBINE SYSTEMS RESEARCH

C. Materials

IV.C.1 Degradation of Thermal Barrier Coatings from Deposits and Its Mitigation

Prof. Nitin P. Padture
The Ohio State University
2041 College Road
Watts Hall, Room 480
Columbus, OH 43210
Phone: (614) 247-8114; Fax: (614) 292-5241
E-mail: padture.1@osu.edu

DOE Project Manager: Briggs White
Phone: (304) 285-5437
E-mail: Briggs.White@netl.doe.gov

Contract Number: NT0006552

Start Date: October 1, 2008
End Date: September 30, 2011

FY 2010 Objectives

- Identify alternate materials for thermal barrier coatings (TBCs) that are resistant to degradation from molten particulate impurities such as fly ash.
- Use air plasma spray (APS) method to fabricate TBCs of new compositions and microstructures, and study interactions between the new TBCs and molten fly ash particulates at high temperatures in isothermal and thermal-gradient situations, with and without the presence of water vapor.
- Understand the mechanisms by which mitigation of deposit-induced degradation occurs in the new TBCs.

Accomplishments

- Alternate TBC material identified as gadolinium zirconate or $Gd_2Zr_2O_7$ (GZO), and isothermal testing shows greatly superior resistance to degradation from molten fly ash.
- A thermal gradient rig was constructed at The Ohio State University, and initial tests show GZO to have enhanced durability over conventional TBCs of 7 wt% yttria-stabilized zirconia (7YSZ) in the presence of molten fly ash.
- A water vapor furnace is being constructed at The Ohio State University to study the effects of water vapor on TBCs in the presence of molten fly ash.

Introduction

Integrated gas combined cycle (IGCC) turbine engines rely on fuel flexibility, where syngas is being used in place of natural gas. However, syngas carries the risk of having particulate impurities such as fly ash. Ingestion of impurity particulates into turbine engines can lead to particulate melting and deposition on ceramic TBCs that protect and insulate metallic components. These molten deposits can cause significant damage to the TBCs, leading to loss of strain tolerance and spallation, with catastrophic consequences. In aircraft engines, ingestion of airborne sand (calcium-magnesium-aluminosilicate or CMAS) is of great concern. In recent years, development of TBCs made of alternate ceramics has effectively mitigated these effects in aero engines, including our own research in this area [1]. In this project some of those strategies are used to design TBCs for mitigation of attack by molten fly ash, a possible particulate impurity in syngas, for IGCC engines.

The interaction of fly ash deposits with conventional yttria-stabilized zirconia TBCs has been studied in this project. Detailed characterization and analysis will be employed to understand the mechanisms of the interaction. The results of this analysis has led to the selection of an alternative TBC material, gadolinium zirconate, to mitigate the detrimental effects of fly ash on the TBCs. To better understand how the coatings will perform in service, testing of this material has been performed in both isothermal and thermal gradient conditions [2].

Approach

Several fly ash samples were identified and their chemical composition analyzed. All of the ashes analyzed are rich in silicon, calcium, aluminum, and iron. Of the materials surveyed, a representative fly ash, lignite, was chosen based on chemical composition and estimated viscosity at operating temperature. This fly ash was applied to TBCs of both 7YSZ and GZO, and the samples were isothermally heat treated. After the heat treatment, all samples were carefully characterized by a combination of scanning electron microscopy (SEM) with energy dispersive spectroscopy (EDS) mapping, transmission electron microscopy (TEM), and X-ray diffraction.

In-service coatings experience a significant thermal gradient, and understanding the mechanisms of degradation due to molten ash in such an environment is a crucial component of this work. TBC samples with applied ash were heat treated in a thermal gradient burner rig constructed at Ohio State. In the burner rig, samples experience a thermal gradient of approximately 100-200°C, simulating actual engine conditions. Results from these initial tests are presented.

Results

In previous reporting, we have shown that isothermally heat-treated lignite-coated 7YSZ TBCs are completely destroyed. The TBC ingest all of the ash and large voids from throughout the thickness of the coating. This is illustrated in Figure 1, a cross-sectional SEM image and corresponding EDS maps from Si and Ca.

GZO was selected as an alternative top-coat material. Air plasma sprayed coatings of GZO were treated with the same amount of lignite fly ash and heat treated under the same conditions. The SEM and EDS mapping of this sample can be seen in Figure 2. A layer of fly ash remains on top of the coating, showing that all of the ash was not ingested into the coating. A reaction zone of ~50 µm is clearly observed under which, no ash components can be found, effectively arresting the advancing front of molten ash. The remaining TBC thickness under the reaction zone is between 100 and 150 µm of the original 200 µm thick coating.

Characterization of the reaction zone between GZO and fly ash in the TEM has been preformed. Figure 3 shows the area in which a TEM foil was cut using the dual-beam focused ion beam (FIB) as well as a preliminary TEM image of the foil. Analysis of the phases present in the reaction zone show the presence of an apitite phase, presumably $Ca_2Gd_2(SiO_4)_6O_2$. Figure 4 shows the TEM foil in scanning dark field mode and a selected area diffraction pattern of the phase marked with an A. This apitite phase plays a pivotal role in arresting the molten ash. The formation of this apitite phase has previously been shown to arrest penetrating CMAS glass in GZO TBCs [3].

From EDS chemical analysis, the remaining light colored regions in Figure 4 are zirconium-rich, with significant amounts of gadolinium and calcium. The dark region is a crystalline phase consisting of aluminum, iron, silicon, and calcium. The exact mechanism of the arrest is currently being formulated.

With an understanding of the mechanisms occurring in isothermal tests, thermal gradient testing has begun. As previously mentioned, the construction of a thermal gradient burner rig to more accurately simulate the thermal profile of in service parts has

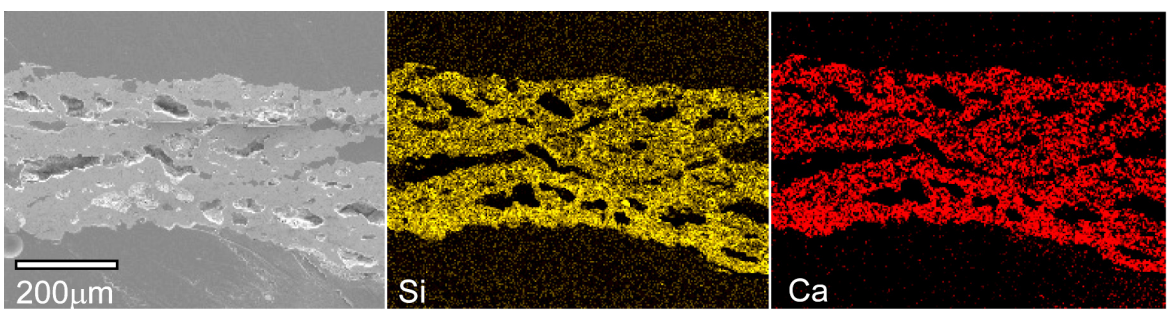

FIGURE 1. SEM image and elemental mapping on cross sectional samples of 7YSZ TBC treated with lignite at 1,200°C for 24 hrs in air, clearly showing that Si and Ca are diffusing through the entire TBC.

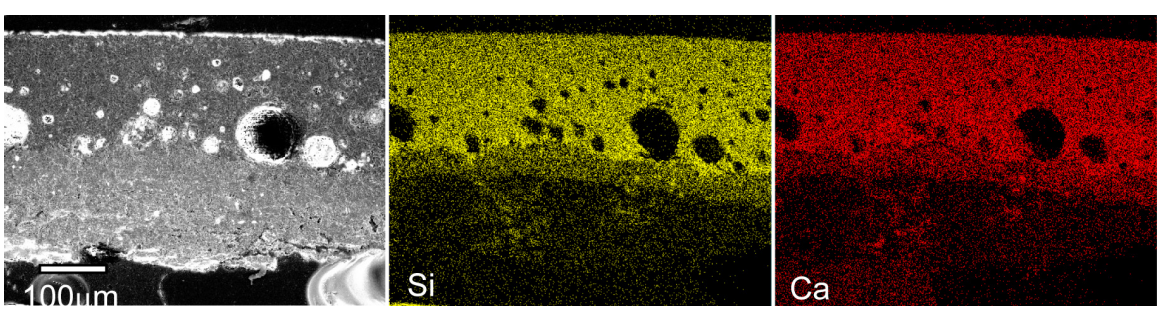

FIGURE 2. SEM image and elemental mapping on cross sectional samples of GZO TBC treated with lignite at 1,200°C for 24 hrs in air. A dense reaction zone has arrested the molten fly ash, preventing further penetration.

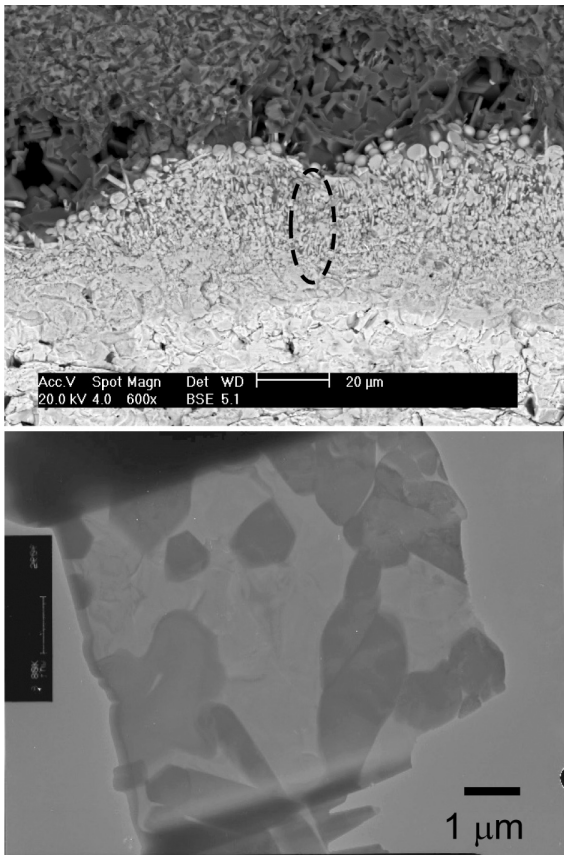

FIGURE 3. (Top) Higher magnification SEM image of reaction zone between lignite fly ash and GZO. The dashed circle indicates where a TEM foil was extracted with a dual beam FIB. (Bottom) Bright field TEM image of foil.

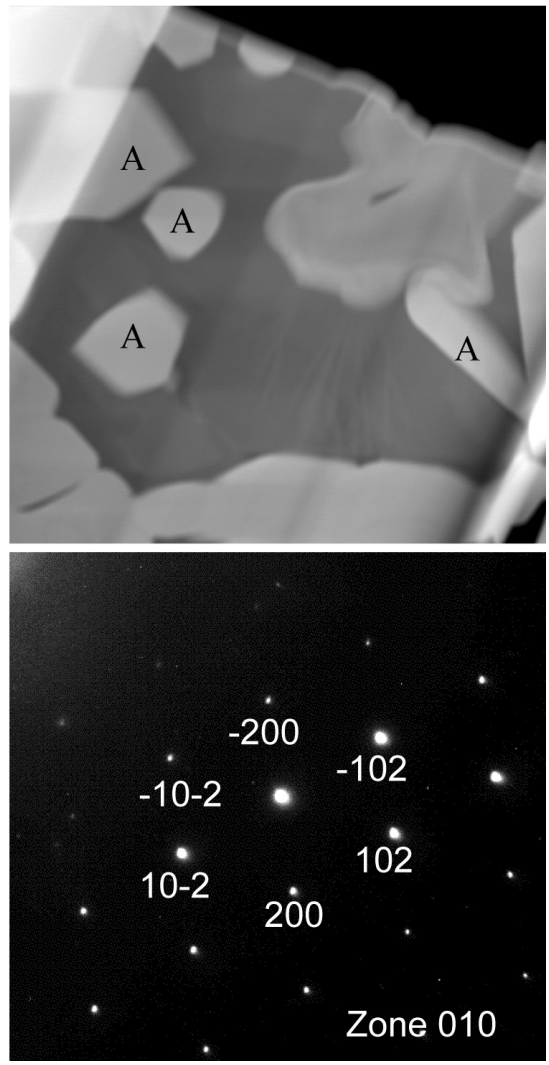

FIGURE 4. (Top) Dark field TEM of the reaction zone between GZO and lignite fly ash and (Bottom) a selected area diffraction pattern from one of the grains labeled A.

recently been completed. In the near future, the rig will also have the added capability of spraying a water/particulate mixture onto samples during thermal cycling.

Initial gradient testing of 7YSZ and GZO has been performed on ash-coated TBCs. Both materials received similar amounts of lignite fly ash, which was baked onto ensure adhesion during testing. The samples underwent thermal cycling, where one cycle consisted of heating for five-minutes, then cooling for two minutes. During the hot portion of the cycle, the front surface of the TBC was held at 1200°C and the back was actively cooled with forced air. After the five minutes of heating, the sample was actively cooled on both front and back for two minutes.

Failure of the 7YSZ sample occurred in four cycles. After the first cycle, degradation from the fly ash resulting in localized spallation over small regions of the surface. Each progressive cycle caused additional spallation. After four cycles, over 50% of the surface had spalled off and exposed the underlying metal bond coat.

In the GZO, failure occurred after 52 cycles, however the mechanism of failure was quite different. After the first cycle, the majority of the fly ash spalled off, taking a portion of the TBC top-coat with it. However, significant amounts of the top-coat remained, and the cycling continued as if the ash was never present. Additional testing is in progress to fully understand and characterize the process.

The testing of TBCs in the presence of water vapor is also significant. The facilities to perform such tests are currently under construction at Ohio State. This equipment will allow samples to be heated up to 1,300°C with high gas/liquid flow rates to simulate another aspect of the environment present in IGCC engines.

Conclusions and Future Directions

Progress towards the overall goal of understanding the mechanisms of degradation due to impurity particulate matter has been made. An alternative material, GZO, has been selected and initial testing illustrates far superior resistance to degradation from molten ash.

In the up-coming year, thermal gradient testing and water vapor testing will be conducted to further examine the mitigation mechanisms and estimate coating lifetime. Finally, all development will be transferred to original equipment manufacturers for additional development.

Patents Issued

1. M. Gell, X. Ma, E.H. Jordan, N.P. Padture, L. Xie, T.D. Xiao, and A. DeCramine, "Coatings, Materials, Articles, and Methods of Making Thereof," **United States Patent,** No. 7,563,503 (2009).

FY 2010 Publications/Presentations

Publication

1. J.M. Drexler, A. Aygun, D. Li, R. Vaßen, T. Steinke, N.P. Padture, "Thermal-Gradient Testing of Thermal Barrier Coatings under Simultaneous Attack by Molten Glassy Deposits and Its Mitigation," Surface & Coatings Technology, **204**, 2683-2688 (2010).

Invited Presentations

1. N.P. Padture, "Novel Concepts in Ceramic Thermal Barrier Coatings," EUROMAT'09, Glasgow, United Kingdom, September 2009.

2. N.P. Padture, "Degradation of Thermal Barrier Coatings from Deposits and Its Mitigation," DOE NETL Review Meeting, Orlando, Florida, October 2009.

3. N.P. Padture, "Novel Concepts in Advanced Structural Ceramics: Thermal Barrier Coatings and Multifunctional Nanocomposites," Instituto de Ceramica y Vidrio, Madrid, Spain, March 2010.

4. N.P. Padture, "Novel Thermal Barrier Coatings," International Conference on Metallurgical Coatings and Thin Films (ICMCTF), San Diego, California, April 2010.

References

1. A. Aygun, A.L. Vasiliev, N.P. Padture and X. Ma, "Novel Thermal Barrier Coatings That Are Resistant to High-Temperature Attack by Glassy Deposits," Acta Mater., **55**, 6734-45 (2007).

2. A.G. Evans and J.W. Hutchinson, "The Mechanics of Coating Delamination in Thermal Gradients," Surf. Coat. Technol., **201**, 7905-16 (2007).

3. S. Kramer, J. Yang, and C.G. Levi, "Infiltration-Inhibiting Reaction of Gadolinium Zirconate Thermal Barrier Coatings with CMAS Melts," J. Am. Ceram. Soc., **91** [2], 576-583 (2008).

IV.C.2 Evaluating Coatings for Current and Future Service

Associate Prof. Ted Bennett
University of California, Santa Barbara
Department of Mechanical Engineering
Santa Barbara, CA 93106
Phone: (805) 893-8115; Fax: (805) 893-8651
E-mail: bennett@engineering.ucsb.edu

DOE Project Manager: Mark Freeman
Phone: (412) 386-6094
E-mail: Mark.Freeman@netl.doe.gov

UTSR Manager of Research: Richard Wenglarz
Phone: (864) 656-2267
E-mail: RWNGLRZ@exchange.clemson.edu

Contract Number: 41431/UTSR 07-01-SR125

Start Date: October 1, 2007
End Date: September 30, 2010

FY 2010 Objectives

- Provide quantitative nondestructive measurements of the thermal protection offered by coatings on servable engine parts.
- Understand how individual elements of service related change effects the thermal protection provided by a coating.
- Monitor the complex physical changes that precede coating failure.

Accomplishments

- Investigated impact of calcium-magnesium-alumino-silicate (CMAS) infiltration into the coating on thermal performance.
- Investigated the relationship between coating density and thermal conductivity on infiltrated coatings.
- Investigated changes in coating properties with effective medium theory.

Introduction

Among the mechanisms limiting the durability of thermal barrier coatings (TBCs) [1] identified to date, one that has generated considerable concern is the infiltration of molten CMAS deposits [2-4]. The net effect is the crystallization of the molten material within the pore structure of the TBC degrades its in-plane compliance and increases the potential for delamination upon thermal cycling [5]. Because silicate deposits can melt at temperatures of ~1,200°C or even lower [2], which are on the same order as the surface temperature of TBCs in current technology, CMAS infiltration becomes a fundamental barrier to further increases in turbine inlet gas temperature, and hence in engine efficiency. In addition to degrading the in-plane compliance of the coating, the penetration of CMAS can attack chemically the insulating oxide, inducing de-stabilization of the t' phase [2,6,7] desirable for toughness. Moreover, the thermal insulation ability of the coating is reduced as the coating porosity is filled with solid phases [8], resulting in higher temperatures at the interface with the metallic substrate, and accelerated oxidation rates that can activate other modes of failure such as rumpling [9,10].

Proper characterization of the thermal behavior of an infiltrated TBC is essential in developing and validating models to predict the onset of delamination and the associated fail-safe condition [5]. A corollary benefit is a better understanding of the effect of CMAS on the overall heat transport through the coating system and temperatures at critical interfaces, notably those influencing the growth kinetics of the thermally grown oxide [8]. Photon transport through infiltrated coatings has been investigated previously [11]. That study demonstrated that CMAS infiltration caused an increase in radiation transport through the coating in the spectral range of 0.5-2.5 microns. The large increase in transmission, coupled with the higher gas temperatures in advanced engines where CMAS may be a problem, suggests that radiative heat transport can be significant for infiltrated coatings in an operating engine. The present report addresses the complementary mechanism of phonon transport through a CMAS impregnated system. The results from both studies can then provide a better overall description of coating thermal performance after CMAS penetration.

Approach

Phase of photothermal emission analysis (PopTea) [12], differential scanning calorimetry (DSC) and density measurements are used in this study to determine the thermal properties of a typical TBC deposited by air-plasma spray (APS) before and after CMAS infiltration. Because PopTea is relatively new, and is the primary method used in this study to measure thermal transport properties (conductivity and diffusivity), a brief overview the technique is given.

The principle of PopTea is to determine coating thermal properties by interrogating the phase of thermal emission from the coating established during modulated heating, as illustrated in Figure 1. The coating is heated with a CO_2 laser (10.6 µm and spot size of 6 mm) and thermal emission is measured with an indium antimonide detector in the mid infrared (5 µm). PopTea measurements are made at 70°C, as controlled by a resistively heated stage. At this temperature there is no risk of inducing delaminations within a TBC or changing the coating thermal properties. Since temperature excursions within the coating caused by modulated heating are small, heat transfer is dominated by conduction and the measurement is not influenced by radiative heat transfer through the coating. An analytic model has been developed to calculate the transient phase of thermal emission from the TBC as a function of unknown coating properties and known geometric parameters [12]. This model is used to evaluate candidate values of the coating thermal properties from experimental measurements. A single measurement consists of recording the phase of thermal emission as a function of laser frequency. The range of laser frequencies is selected to achieve a wide range of thermal penetration depths, which allows the coating properties to be uniquely determined.

A dense CMAS pellet was used for infiltration of the TBC. The pellet was formed by pressing a powder, with composition similar to CMAS seen in engines, into a flat disc and melting it on platinum foil. After cooling, the top side was polished flat to produce 80 µm thick CMAS disc of 1 cm diameter. To infiltrate the coating, the amorphous CMAS pellet was placed at the center of the coupon and heated uniformly in a temperature controlled furnace to 1,300°C at 10°C/min followed by immediate cooling at 10°C/min to 1,000°C. The TBC sample used for CMAS infiltration was a 7 wt% yttria-stabilized zirconia (7YSZ) coating deposited by air plasma spraying on a Rene 80 nickel-based superalloy. The coating thickness was 300 µm.

Results

Before infiltration, the dense amorphous CMAS pellet was thermally characterized. Since PopTea measurements require a contrast in thermal properties between a coating material and substrate material, the pellet was bonded with colloidal silver liquid to a Ni-base superalloy substrate (IN738). The thermal conductivity and volumetric heat capacity of the CMAS material was determined from PopTea measurements. Additionally, independent measurements of the specific heat by DSC and density using Archimedes principle were made for the CMAS material. The product of these latter two measurements yields a volumetric heat capacity of the CMAS pellet that is 2.2×10^6 J/m^3/K. In comparison, the PopTea measurement yielded a value of 2.0×10^6 J/m^3/K. Therefore, the two independent results are within a 10% agreement. Based on the PopTea and DSC measurements, the dense CMAS material was determined to have a thermal conductivity of $k_{CMAS} = 0.79$ W/m/K and density of $\rho_{CMAS} = 2225$ kg/m^3.

Measurements were made on the APS coating for three different conditions shown in Figure 2. The first measurement (1) was made before infiltration to acquire the baseline thermal properties needed for a pre/post infiltration comparison, and to determine the initial coating density and corresponding pore volume fraction. The coating was then infiltrated locally with CMAS in a high-temperature furnace. After infiltration, a second measurement (2) was made on

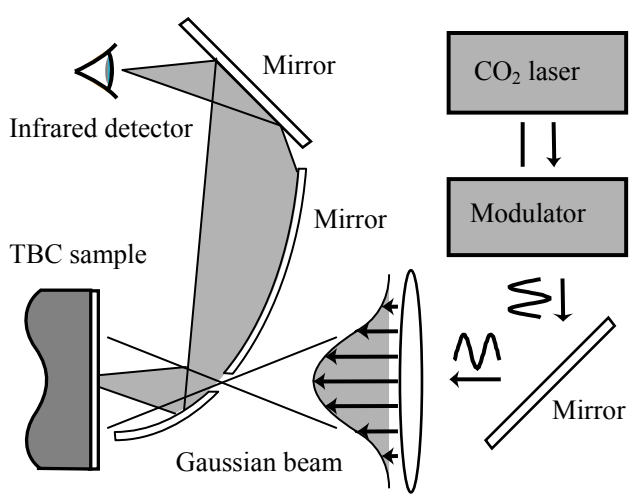

FIGURE 1. Schematic of PopTea Measurement Tool

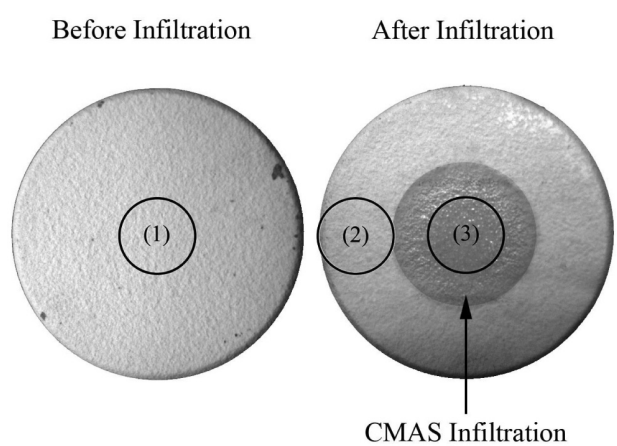

FIGURE 2. Top view of TBC before and after CMAS infiltration. Locations of PopTea measurements are highlighted. (1) Baseline, before infiltration; (2) annealed coating, after infiltration; (3) infiltrated coating, after infiltration.

an uninfiltrated area of the coating to assess possible changes in thermal properties from the as-deposited condition due to temperature effects alone. The final measurement (3) was made on an area of the coating experiencing the full CMAS infiltration.

The raw phase of thermal emission, as a function of heating frequency, collected for the PopTea measurements, are plotted in Figure 3 for the three different measurements made. Virtually no change is seen in the raw data between measurements made on the uninfiltrated TBC before and after the furnace exposure (measurements 1 and 2). In contrast, measurement (3) made on the region of the TBC infiltrated by CMAS during the furnace exposure shows a marked change from the preinfiltration condition. The change seen in the raw phase of emission measurements caused by CMAS infiltration is explained by significant changes in the coating thermal properties.

PopTea measurements of the thermal properties of the TBC for the as-deposited and CMAS infiltrated conditions are summarized in Table 1. By comparing the thermal properties between measurements (1) and (2) (i.e., coating properties before and after heat treatment), it is seen that there is no change. This shows that the high temperature treatment used for infiltration does not alter the coating's thermal properties. In contrast, there is a large change in thermal properties caused by the CMAS infiltration, as seen in measurement (3). The thermal conductivity experiences the largest change: from an initial conductivity of 0.9 W/m/K, CMAS infiltration causes the coating conductivity to increase by ~110%. The dramatic rise in thermal conductivity contrasts greatly with the more modest change in the volumetric heat capacity of the coating, which experiences an increase of 18%, with CMAS infiltration.

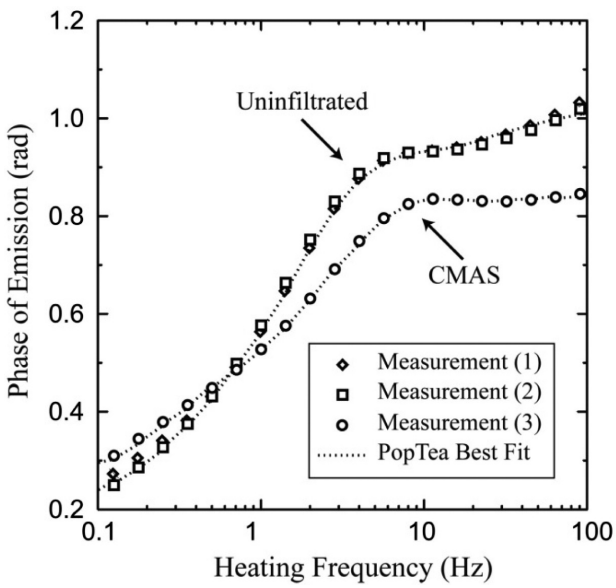

FIGURE 3. Phase of emission data for the three measurement locations in Figure 2, and corresponding PopTea fits.

TABLE 1. PopTea Measurements Made on a TBC

	Measurement (1) *Baseline*	Measurement (2) *Annealed 1300°C*	Measurement (3) *Infiltrated*
α (m^2/s)	4.46 x 10^{-7}	4.54 x 10^{-7}	8.46 x 10^{-7}
k (W/m/K)	0.91	0.88	2.09
ρC_p (J/m^3/K)	2.04 x 10^6	1.94 x 10^6	2.47 x 10^6
υ_{coat}	27%	31%	

Due to the complexity of coating morphology, predicting the thermal conductivity of a coating from first principles is difficult [13]. Two classical and relatively simple approaches, developed by Maxwell and Rayleigh are employed in this report to estimate the thermal conductivity of a CMAS infiltrated coating. In Maxwell's analysis [14], inclusions are considered to be spherical and non-interacting (i.e. inclusions are sufficiently separated such that heat transfer in the proximity of one inclusion does not influence another). Furthermore, the pore distribution within the coating is assumed to be random. For this system, the effective conductivity (k_{infilt}) determined by Maxwell's model is given by:

$$k_{\text{infilt}} = k_{7YSZ}\left(1+\frac{3\upsilon_{coat}}{\frac{\gamma+2}{\gamma-1}-\upsilon_{coat}}\right) \quad (1)$$

where υ_{coat} is the pore volume fraction, which is assumed to be filled with CMAS after infiltration, and $\gamma = k_{CMAS}/k_{7YSZ}$ is the ratio of conductivity between amorphous CMAS and bulk 7YSZ. Using equation (1), with $\gamma = 0.79/2.5 = 0.32$, to calculate the conductivity of the infiltrated coating yields, k_{infilt} (Maxwell) = 1.95 W/m/K. This calculated thermal conductivity is within 10% of the measured conductivity for the infiltrated coating in Table 1 (measurement 3).

Despite the relatively small difference between Maxwell's result and the PopTea measurement, closer agreement can be obtained by using an effective model developed by Rayleigh [15]. In his cylindrical model, Rayleigh assumes pores of cylindrical shape are situated on the corners of a square lattice. For this system, the effective thermal conductivity along the axis of the pores is determined from Rayleigh's model to be:

$$k_{\text{infilt}} = k_{7YSZ}\left(1+\upsilon_{coat}(\gamma-1)\right) \quad (2)$$

Using equation (2) gives an effective conductivity of k_{infilt} (Rayleigh)=2.05 W/m/K, which is still slightly

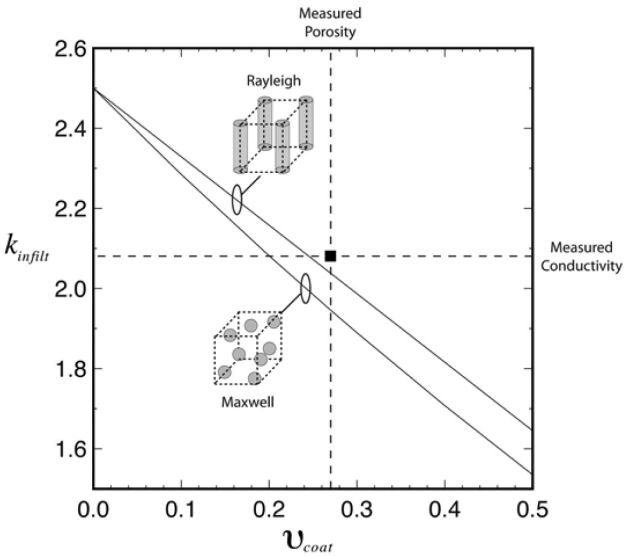

FIGURE 4. Plot of the effective thermal conductivity as a function of porosity for Maxwell and Rayleigh effective media models, and contrasted with measured value of conductivity for the fully infiltrated coating.

lower than the measured value of 2.09 W/m/K but in better agreement than Maxwell's model.

The effective thermal conductivity k_{infilt} is plotted in Figure 4 as a function of initial coating porosity for the two different effective media models of Maxwell and Rayleigh. The fact that the cylindrical model more closely describes the measured thermal conductivity suggests that the CMAS vertical connectivity is an important characteristic of the infiltrated system. As CMAS seeps through the coating porosity it is reasonable to assume that there is a vertical connectivity established throughout the coating thickness, as opposed to the CMAS conglomerating into isolated inclusions.

Conclusions and Future Directions

In this report, an APS coating attached to a superalloy substrate was fully infiltrated with CMAS and the thermal properties of the coating system were studied. Results showed that the largest change caused by infiltration was the thermal conductivity, which increased by more than 100%. Measured changes in thermal conductivity and density compared well to theoretical calculations, which assumed that the initial measured pore volume fraction of the coating was completely infiltrated with CMAS. Demonstrating the ability to measure changes in thermal properties of an infiltrated coating is the initial step for quantitative studies on real TBC systems experiencing CMAS attack. Further investigation is needed to study the change in thermal properties of partially infiltrated coatings, which can arise when CMAS is introduced to the system in the presents of thermal gradients. This situation gives rise to added complexity for the PopTea measurement, since the coating becomes a layered system with an unknown extent of CMAS infiltration.

FY 2010 Publications/Presentations

1. Tyler Kakuda, Ted Bennett, Andi Limarga, Anirudha Vaidya, and Anand Kulkarni, "Non-Destructive Thermal Property Measurements of an APS TBC on an Intact Turbine Blade," Surface and Coatings Technology, in press (2010).

2. Tyler R. Kakuda, Carlos G. Levi, and Ted D. Bennett, "The Thermal Behavior of CMAS Infiltrated Thermal Barrier Coatings," In preparation (2010).

3. Tyler R. Kakuda, Andi M. Limarga, Ted D. Bennett and David R. Clarke, "Evolution of Thermal Properties of EB-PVD 7YSZ Thermal Barrier Coatings with Thermal Cycling," Acta Materialia 57 (2009) 2583–2591.

4. Tyler Kakuda and Ted D. Bennett, "The Nondestructive Measurement of Thermal Barrier Coatings Thermal Properties," International Society of Automation EXPO 2009 Technical Conference, Houston, Texas.

References

1. A.G. Evans, D.R. Mumm, J.W. Hutchinson, G.H. Meier, and F.S. Pettit, "Mechanisms Controlling the Durability of Thermal Barrier Coatings," *Progress in Materials Science,* 46 (5) 505-553 (2001).

2. M.P. Borom, C.A. Johnson, and L.A. Peluso, "Role of Environmental Deposits and Operating Surface Temperature in Spallation of Air Plasma Sprayed Thermal Barrier Coatings," *Surface & Coatings Technology*, 86 (1) 116-126 (1996).

3. C. Mercer, S. Faulhaber, A.G. Evans, and R. Darolia, "A Delamination Mechanism for Thermal Barrier Coatings Subject to Calcium-Magnesium-Alumino-Silicate (CMAS) Infiltration," *Acta Materialia*, 53 (4) 1029-1039 (2005).

4. S. Krämer, S. Faulhaber, M. Chambers, D.R. Clarke, C.G. Levi, J.W. Hutchinson, and A.G. Evans, "Mechanisms of Cracking and Delamination within Thermal Barrier Systems in Aero-Engines Subject to Calcium-Magnesium-Alumino-Silicate (CMAS) Penetration," *Materials Science and Engineering A*, 490 26-35 (2008).

5. A.G. Evans and J.W. Hutchinson, "The Mechanics of Coating Delamination in Thermal Gradients," *Surface & Coatings Technology*, 201 (18), 7905-7916 (2007).

6. D.J. de Wet, R. Taylor, and F.H. Stott, "Corrosion Mechanisms of ZrO_2-Y_2O_3 Thermal Barrier Coatings in the Presence of Molten Middle-East Sand," *Journal de Physique IV*, 3 (C9) 655-663 (1993).

7. S. Krämer, J.Y. Yang, C.A. Johnson, and C.G. Levi, "Thermochemical Interactions of Thermal Barrier Coatings with Molten CaO-MgO-Al_2O_3-SiO_2 (CMAS)

Deposits," *Journal of the American Ceramic Society*, 89 (10) 3167-3175 (2006).

8. S. Kramer, J. Yang, and C.G. Levi, "Infiltration-Inhibiting Reaction of Gadolinium Zirconate Thermal Barrier Coatings with CMAS Melts," *Journal of the American Ceramic Society*, 91 (2) 576-583 (2008).

9. D.R. Mumm, A.G. Evans, and I.T. Spitsberg, "Characterization of a Cyclic Displacement Instability for a Thermally Grown Oxide in a Thermal Barrier System," *Acta Materialia,* 49 (12) 2329-2340 (2001).

10. V.K. Tolpygo and D.R. Clarke, "On the Rumpling Mechanism in Nickel-Aluminide Coatings. Part I: an Experimental Assessment," *Acta Materialia,* 52 5115-5127 (2004), also "Part II: Characterization of Surface Undulations and Bond Coat Swelling," *Acta Materialia*, 52 5129-5141 (2004).

11. L. Li and D.R. Clarke, "Effect of CMAS Infiltration on Radiative Transport Through an EB-PVD Thermal Barrier Coating," *International Journal of Applied Ceramic Technology*, 5 (3) 278-288 (2008).

12. T.D. Bennett, T.R. Kakuda, and A. Kulkarni, "Front Surface Thermal Property Measurements of Air Plasma Spray Coatings," *Journal of Applied Physics*, 105 (8) (2009).

13. F.C. Chen, C.L. Choy, and K. Young, "Theory of the Thermal Conductivity of Infiltrated Materials," *Journal of Physics*, D, Applied physics, 10 (4) 571-586 (1977).

14. J.C. Maxwell, A Treatise on Electricity and Magnetism, Clarendon Press, Oxford (1892), pp. 194–216.

15. Lord Rayleigh, Phil. Mag., 34, 481 (1892).

IV.C.3 Materials for Oxy-Fuel Turbomachine Conditions

Professor Gerald H. Meier (Primary Contact),
Professor Frederick S. Pettit
Department of Mechanical Engineering and Materials Science
848 Benedum Hall
University of Pittsburgh
Pittsburgh, PA 15261
Phone: (412) 624-9730
E-mail: ghmeier@pitt.edu; pettitfs@pitt.edu

DOE Project Manager: Mark Freeman
Phone: (412) 386-6094
E-mail: Mark.Freeman@netl.doe.gov

UTSR Manager of Research: Richard Wenglarz
Phone: (864) 656-2267
E-mail: RWNGLRZ@exchange.clemson.edu

Contract Number: 41431/UTSR 06-01-SR124

Start Date: July 15, 2007
End Date: September 30, 2010

FY 2010 Objectives

The overall objective of this investigation is to evaluate the durability of turbine materials at the temperatures and oxygen pressures typical of those in the high steam and CO_2 levels expected in coal-based oxy-fuel systems. Specific objectives include:

- Evaluating the performance of candidate alloys and coatings in environments starting with 85% steam and 15% CO_2 (by volume) and then for gases containing up to 5% O_2, which may represent excess oxygen needed to assure complete oxy-fuel combustion.
- Advancing the existing knowledge of how steam (water vapor) affects the selective oxidation of high temperature alloys.
- Investigate the effects of carbon and hydrogen on the oxidation of alloys exposed to H_2O-CO_2 mixtures.
- Examine the effects of steam and CO_2 gas mixtures on the degradation of yttria-stabilized zirconia thermal barrier coatings (TBCs).

Accomplishments

This project is approaching the end of the third year and has received a two-month no-cost extension. Accomplishments since the initiation of this project are as follows:

- The alloys and coatings to be studied have been obtained.
- An apparatus has been constructed whereby cyclic oxidation can be performed at temperatures from 700°C to 1,100°C in gas mixtures containing 85% H_2O-15% CO_2.
- Data in the literature have been tabulated for the alloys and coatings to be used in this project for exposure conditions involving steam and CO_2.
- It has been documented that water vapor affects selective oxidation of aluminum in alloys and that oxidation in CO_2 can cause more severe degradation of some alloys compared to pure air.

The general conclusion from all the results are that alloys which are "good chromia- or alumina-formers" in air will also be highly resistant in oxyfuel environments. Alloys which are "marginal chromia- or alumina-formers" in air will undergo severe degradation in the oxyfuel environments.

Introduction

In order for coal-based oxy-fuel systems to be used, it is necessary to investigate the effects of combustion gases containing 85% steam and 15% CO_2 on the degradation of gas turbine alloys and coatings at temperatures between 700°C (1,292°F) and 1,100°C (2,012°F). The upper temperature limit has been selected since the adverse effects produced by these gaseous species may be more obvious at the higher temperatures. The experimental approach for this investigation consists of exposing relevant alloys and coatings to controlled gas mixtures containing H_2O, CO_2, and O_2 at temperatures of interest. The presence of oxygen in some of the gas mixtures is necessary because when oxygen is added to the gas mixture of H_2O and CO_2, the attack may or may not be as severe as when it is absent. The degradation of the exposed specimens is being documented using weight change versus time measurements, X-ray diffraction, scanning electron microscopy, and optical metallography.

Approach

To achieve the project objectives the alloys René N5, GTD 111 and IN 738 as well as these alloys with a platinum-modified aluminide and a NiCoCrAlY coating are being exposed to gas mixtures containing 85% H_2O-15% CO_2 and 85% H_2O-10% CO_2-5% O_2 at temperatures between 700°C and 1,100°C. The

exposed specimens are being examined using optical metallography, scanning electron microscopy, and X-ray diffraction to document the attack of these alloys. In the final year of this project, the performance of TBCs exposed to the conditions described above is being studied.

Results

Castings of the superalloys IN 738, GTD 111 and René N5 have been obtained. Coupons (15 x 10 x 3 mm) of René N5 were coated with a platinum-modified diffusion aluminide coating. A NiCoCrAlY (Ni-22.5Co-16.5Cr-13.5Al-0.5Y wt%) coating was also to be exposed to the gas mixtures, however, it is difficult to deposit this coating on small coupons. Therefore the behavior of the NiCoCrAlY coating was examined using bulk specimens of this alloy that were prepared by casting and annealing.

A cyclic oxidation apparatus was constructed to obtain gas mixtures containing 85% H_2O and 15% CO_2. At one end of a reaction tube water is added to a gas stream of CO_2 using a peristaltic pump and sprayed into quartz wool at 200 to 300°C where it vaporizes. The specimen is suspended from a rod that is cycled into and from the furnace hot zone. Calculations indicated that an 85% H_2O- 15% CO_2 gas mixture could be obtained with a water flow rate of 0.76 cm^3/min and a CO_2 gas flow rate of 182.3 cm^3/min. Measurements using this apparatus have confirmed these flow conditions. A fused silica reaction tube is used at low temperature (700°C) and a mullite tube is used at higher temperatures (900 and 1,100°C).

Results have been obtained for oxidation of the alloys of interest in this project at 700, 900 and 1,100°C in dry air and an 85% H_2O-15% CO_2 gas mixture.

700°C

The alloys René N5, IN 738, and N5 with platinum modified aluminide coating have been exposed in both atmospheres at 700°C. Weight change versus time data for these experiments are presented in Figure 1. The weight changes are small and it appears that the weight changes are slightly greater for René N5 and IN 738 in the 85% H_2O-15% CO_2 gas mixture compared to air. However, metallographic cross-sections of these exposed specimens did not indicate that more attack had occurred in the 85% H_2O-15% CO_2 gas mixture.

900°C

The results that have been obtained for oxidation at 900°C in 85% H_2O-15% CO_2 show that no severe attack has been observed for René N5, IN 738, GTD 111, and the platinum aluminide coating

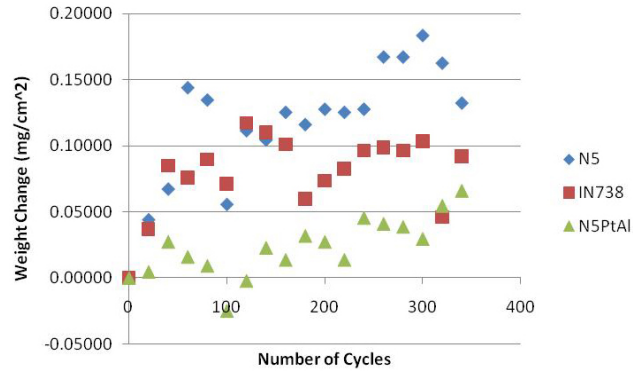

FIGURE 1. Weight change versus cycles for alloys exposed at 700°C to an 85% H_2O-15% CO_2 gas mixture (one cycle is 45 minutes at 700°C, 15 minutes in the cool zone of the furnace).

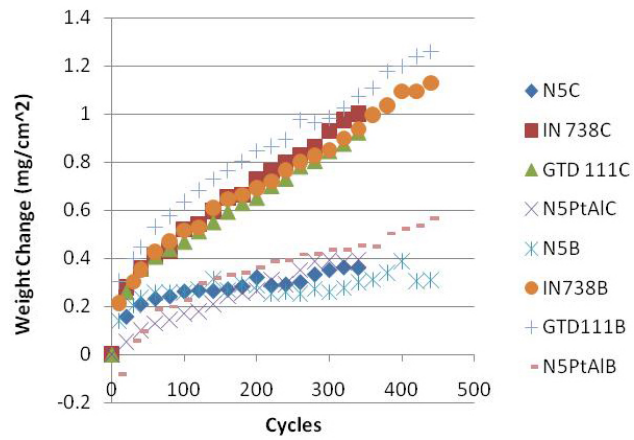

FIGURE 2. Weight change versus time measurements for some alloys and coatings for exposure at 900°C in an 85% H_2O-15% CO_2 gas mixture. Each cycle consists of 45 minutes at 900°C and 15 minutes in the cool zone of the furnace.

(Figure 2). Protective oxide scales were formed on all of the alloys and the coating. In this gas mixture it may be required to consume oxygen at a rapid rate before the carbon and hydrogen in these gas mixtures enter into the corrosion process.

In addition, some new alloys, namely Ni-8Cr-6Al, Fe-10Cr, and Fe-13.5Cr have been included. These three alloys form alumina and chromia external scales during oxidation, but exhibit substantial transient oxidation before the alumina or chromia scales are continuous over the specimens' surfaces. Consequently, these alloys may be more susceptible to oxidation when subjected to the 85% H_2O-15% CO_2 gas mixture. The cyclic oxidation data for these alloys exposed at 900°C to air and to 85% H_2O-15% CO_2 are presented in Figure 3. The Ni-8Cr-6Al alloy formed alumina scales in both air and the 85% H_2O-15% CO_2 gas mixture. The Fe-10Cr alloy was severely attacked

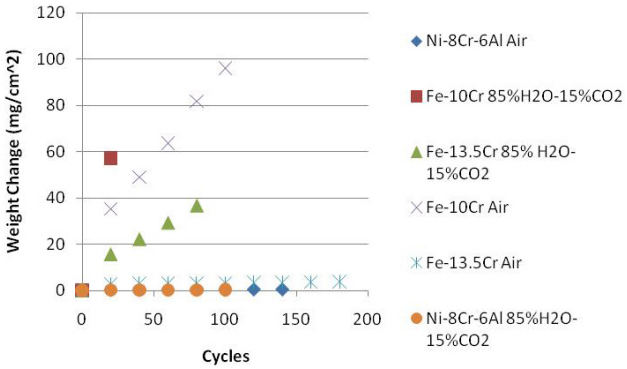

FIGURE 3. Cyclic oxidation data for alloys that have extended transient oxidation stages at 900°C in air and in 85% H_2O-15% CO_2.

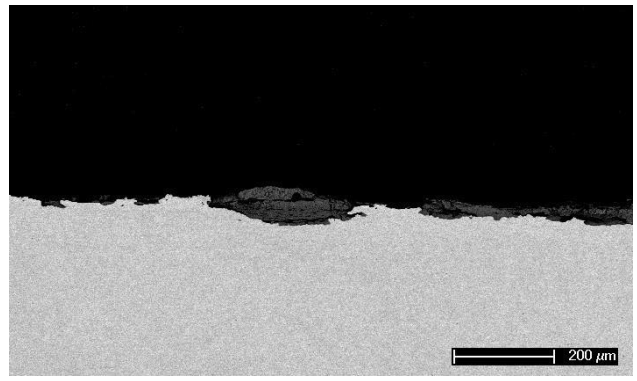

FIGURE 4. Scanning electron micrographs of the Fe-13.5Cr alloy after 190 hours of cyclic oxidation at 900°C in air. A protective oxide scale of chromium oxide has been formed.

in both gases where an external scale of iron oxides with an internal scale containing chromium developed. The Fe-13.5Cr alloy had larger weight gains in the gas mixture than in air. Furthermore, a continuous scale of chromia was formed on this alloy when exposed to air, Figure 4, whereas much thicker scales containing iron oxides were formed when this alloy was exposed in the 85% H_2O-15% CO_2 gas mixture, Figure 5. These results indicate that the 85% H_2O-15% CO_2 gas mixture will adversely affect the oxidation behavior of those alloys that undergo substantial transient oxidation prior to developing protective scales via selective oxidation.

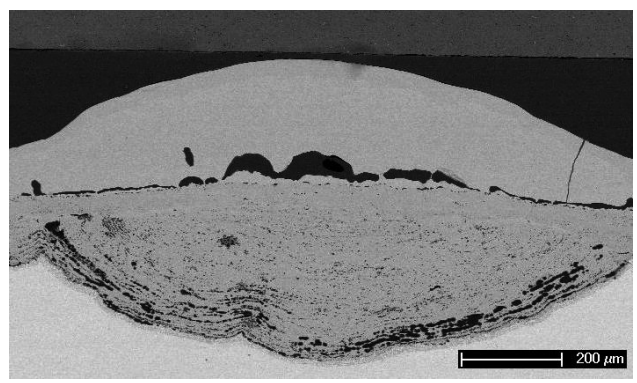

FIGURE 5. Scanning electron micrograph of Fe-13.5Cr alloy after 80 hours of cyclic exposure at 900°C in an 85% H_2O-15% CO_2 gas mixture.

1,100°C

The alloys René N5, IN 738, and aluminized N5 were exposed at 1,100°C in air and 85% H_2O-15% CO_2. The weight change data are presented in Figure 6. These data indicate that protective, adherent scales have been formed on René N5 and aluminized N5 in both atmospheres, but some oxide cracking and spalling may occur on IN 738. Such conclusions are confirmed by metallographic cross-sections. For René N5 there are some internal nitrides in the air specimen which are absent in the nitrogen-free 85% H_2O-15% CO_2 environment. The cross-sectional micrographs for IN 738 oxidized at 1,100°C are presented in Figure 7 for oxidation in air and Figure 8 for oxidation in 85% H_2O-15% CO_2. The selective oxidation process was disrupted in the 85% H_2O-15% CO_2 environment. In Figure 8 there are internal oxides rich in chromium, but no continuous scale was formed, leading to thick oxides rich in nickel. The nickel rich oxides are cracked and not adherent to the alloy, but have been retained through the 80 cycles of oxidation. The IN 738 oxidized in air shows internal nitrides as well as continuous or nearly continuous aluminum and chromium-rich scale. Above this scale are some nickel rich oxides and evidence of spallation

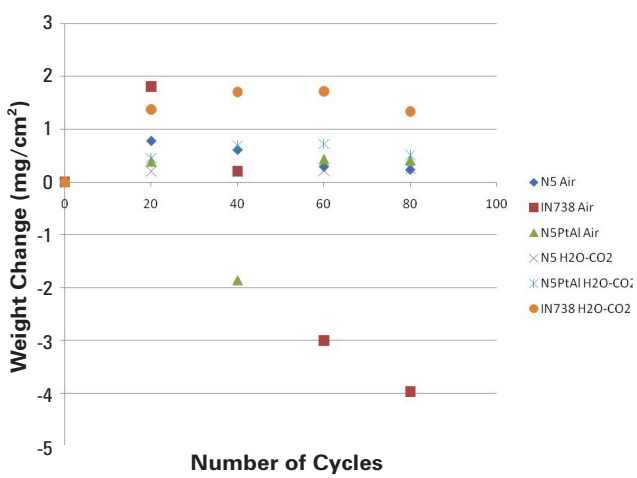

FIGURE 6. Weight change versus cycles for alloys exposed at 1,100°C in air and an 85% H_2O-15% CO_2 gas mixture (one cycle is 45 minutes at 1,100°C, 15 minutes in the cool zone of the furnace).

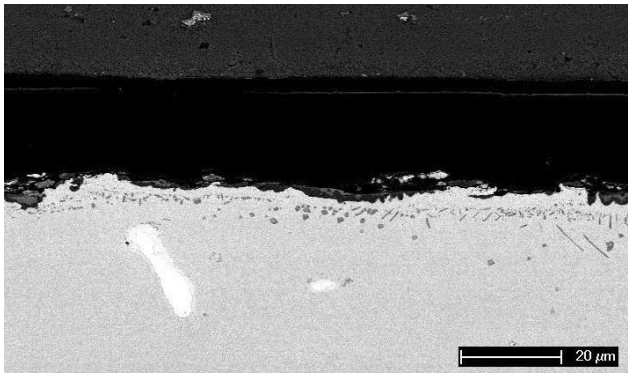

FIGURE 7. Cross-sectional scanning electron micrograph of IN 738 cyclically oxidized in air at 1,100°C for 80 cycles.

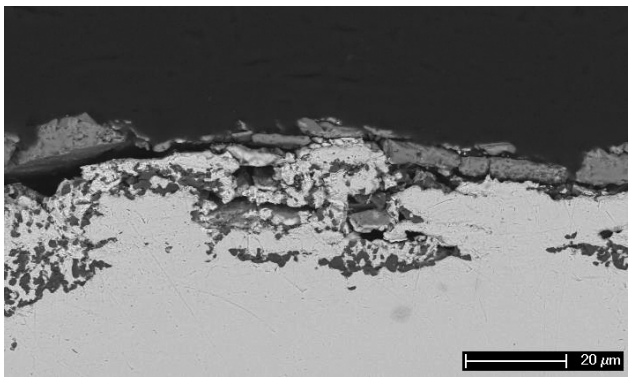

FIGURE 8. Cross-sectional scanning electron micrograph of IN 738 cyclically oxidized in 85% H_2O-15% CO_2 at 1,100°C for 80 cycles.

which explains the overall weight loss for this alloy (Figure 6).

Conclusions and Future Directions

The alloys René N5, IN 738, and aluminized N5 have been exposed at 700°C to air and an 85% H_2O-15% CO_2 gas mixture. A significant difference between the oxidation behaviors of these alloys in the two gas environments was not evident.

There was no indication of severe attack other than what is considered normal oxidation when the alloys René N5, IN 738, GTD 111, as well as a platinum aluminide coating on René N5 and a bulk NiCoCrAlY coating were exposed to an 85% H_2O-15% CO_2 gas mixture at 900°C for about 500 cycles (45 minutes hot, 15 minutes cool). The alloys Ni-8Cr-6Al, Fe-13.5Cr, and Fe-10Cr were also exposed to the same conditions and the Fe-13.5Cr alloy exhibited normal oxidation in air but accelerated attack in the 85% H_2O-15% CO_2 gas mixture. It is believed that such results show the 85% H_2O-15% CO_2 gas mixture can cause increased oxidation, but only for those alloys that exhibit extensive transient oxidation with excessive oxygen consumption.

Exposures at 1,100°C resulted in protective alumina formation on René N5 and the Pt-aluminide coating in both atmospheres. However, the H_2O/CO_2 atmosphere disrupted the selective oxidation process of the chromia-forming alloy IN 738.

The general conclusion from all the results are that alloys which are "good chromia- or alumina-formers" in air will also be highly resistant in oxyfuel environments. Alloys which are "marginal chromia- or alumina-formers" in air will undergo severe degradation in the oxyfuel environments.

The experiments which will be conducted during the remaining months of this project will be focused on:

1. The effect of excess oxygen on the degradation processes at 1,100°C.
2. The degradation of thermal barrier coated superalloys in oxyfuel environments.

FY 2010 Publications/Presentations

1. Poster Paper-Materials for Oxy-Fuel Turbomachine Conditions, F.S. Pettit, G.H. Meier, and E.J. Magee, Gordon Research Conference on High Temperature Corrosion, New London, New Hampshire, July 27–31, 2009.

2. G.H. Meier, "Materials for Oxy-Fuel Turbomachine Conditions," UTSR Peer Review Workshop, Orlando, Florida, October, 28, 2009.

IV.C.4 Hafnia-Based Nanostructured Thermal Barrier Coatings for Application in Advanced Turbine Technology

Chintalapalle V. Ramana (Primary Contact), Ahsan R. Choudhuri
University of Texas at El Paso
500 W University Avenue
El Paso, TX 79968
Phone: (915) 747-8690; Fax: (915) 747-5019
E-mail: rvchintalapalle@utep.edu

DOE Project Manager: Briggs White
Phone: (304) 285-5437
E-mail: Briggs.White@netl.doe.gov

Contract Number: FE0000765

Start Date: October 1, 2009
End Date: September 30, 2012

FY 2010 Objectives

- Fabricate hafnia-based nanostructured coatings with Y_2O_3, Gd_2O_3, ZrO_2 as stabilizers.
- Optimize the conditions to produce coatings with stable microstructure.
- Demonstrate the high temperature stable form of cubic crystal structure with columnar interface morphology.
- Understand the substrate-coating structure and stability.

Accomplishments

- Fabricated the yttria-stabilized hafnia (YSH) coatings under various growth conditions and onto various substrate materials.
- Evaluated the microstructure of the coatings.
- Stabilization of the cubic phase and columnar structure of the YSH coatings demonstrated.
- Found that the composition of the YSH coating is critical to obtain the specific phase and microstructure for thermal barrier coating (TBC) applications.

Introduction

TBCs are critical for future gas turbines of advanced coal-based power generation systems. Future generation gas turbine engines should tolerate fuel compositions ranging from natural gas to a broad range of syngas with high hydrogen contents which require TBCs with a surface temperature tolerance much higher than the current standard materials. A near- and mid-term target is to develop TBC architecture with a 1,300°C surface temperature tolerance for a minimum operating time of 8,000 hours [1]. The goal of the research is to investigate nanostructured TBCs to ensure a minimum 1,300°C surface temperature tolerance for long-duration operations.

A place to look for alternative, next-generation TBC materials with superior properties is among fluorite structure oxides [2], where HfO_2 and ZrO_2 are the most suitable candidates. The melting point of HfO_2 is higher than ZrO_2 and YSH has a durability to a temperature of 1,400°C (1,200°C for current standard). From this viewpoint, it is quite important to understand the science and engineering of HfO_2-based TBCs. The goal of the project is to develop nanostructured HfO_2-based coatings, namely Y_2O_3-stabilized HfO_2 (YSH), Gd_2O_3-stabilized HfO_2 (GSH) and Y_2O_3-stabilized ZrO_2-HfO_2 (YSZH) for TBCs of advanced hydrogen turbines. The proposed project work will engineer nanostructured HfO_2-based coatings, namely YSH, GSH and YSZH, for TBC applications.

Approach

The approach is to systematically vary the growth conditions and target/ingot materials to study their influence on the coatings' phase, microstructure, mechanical, thermal, chemical properties, and performance. *We will derive qualitative and quantitative models for failure mechanisms, life time and performance of the nanostructured YSH, GSH, and YSZH ceramic TBCs from all these studies*. The models will be used to predict pathways to further improve the coatings microstructure (at the reduced nano-dimensionality), properties and ultimately the performance. The central theme of the microstructure evaluation and various characterizations is to provide feedback to fabrications so as produce materials with superior stability, high temperature tolerance, thermal durability and reliable sensitivity.

The specific approach in this project is to provide a large number of interconnected surface nano-grains while maintaining the columnar structure. This will lead to a large interfacial thermal resistance and extremely low thermal conductivity. There are several types of material structure improvements that will also be specifically addressed; morphology/geometric

uniformity, crystal structure and phase, microstructure quality (nano-grain or nano-particle distribution, boundaries and linear defect densities), doping profiles (point defects) and material composition. In addition, fundamental thermo-mechanical and thermo-chemical properties and performance will be measured and correlated to the microstructure. The thermal conductivity and size-dependent surface reactivity of the ceramic coatings will be measured. Finally, laboratory experiments using accelerated test environments will be used to investigate the relative importance of various thermo-mechanical and thermo-chemical failure modes of TBCs. Effects of thermal stress cycling, oxidation degradation and their complex interaction on TBC failures will be evaluated using static and cyclic experimental matrix of syngas combustor rig. The parametric relation between turbine environments of high hydrogen content fuels and thermo-mechanical cracking in the ceramic layer will be developed.

Results

The YSH target was stabilized by 7.5% Y_2O_3. The YSH and YSHZ targets were prepared in the laboratory by using cold-pressing followed by solid state reaction and sintering. For the YSHZ target, 7.5% Y_2O_3 and a 1:1 ratio of HfO_2 and ZrO_2 powder were mixed along with a small amount of poly vinyl alcohol binder and subjected to very high pressure compression to form a pellet of 2” diameter and 0.125” thickness. Then the pellets were exposed to thermal treatment at 1,050°C for 12 hrs for solid state reaction and sintering. Copper backing plates were fixed to the bottom of the prepared pellets by using epoxy glue to get the stable target ready to be used for TBC deposition. The coatings fabricated exhibit more or less constant thickness on all the substrates (Figure 1).

Structural characterization of the fabricated TBC was performed by using X-ray diffraction (XRD). The XRD patterns indicate the cubic crystal structure of the YSH TBC. The TBCs grown on four different types of substrates show the similar crystal structure of the stabilized cubic phase. The variation in deposition temperature shows no significant changes in crystallographic structure of the TBC on any of the substrates. The crystal strain analysis is currently in progress. The XRD patterns of the YSH coatings grown on Ni-super alloy substrates are shown in Figure 2.

Conclusions and Future Directions

The results are encouraging and the composition to obtain the specific YSH TBCs is optimized. Future work will focus on thermal cycling behavior, stability of the phase and microstructure, thermo-mechanical and thermo-chemical properties evaluation of the coatings. Efforts will be directed to other compositions based on GSH and a comparative study of all the TBC compositions will be obtained.

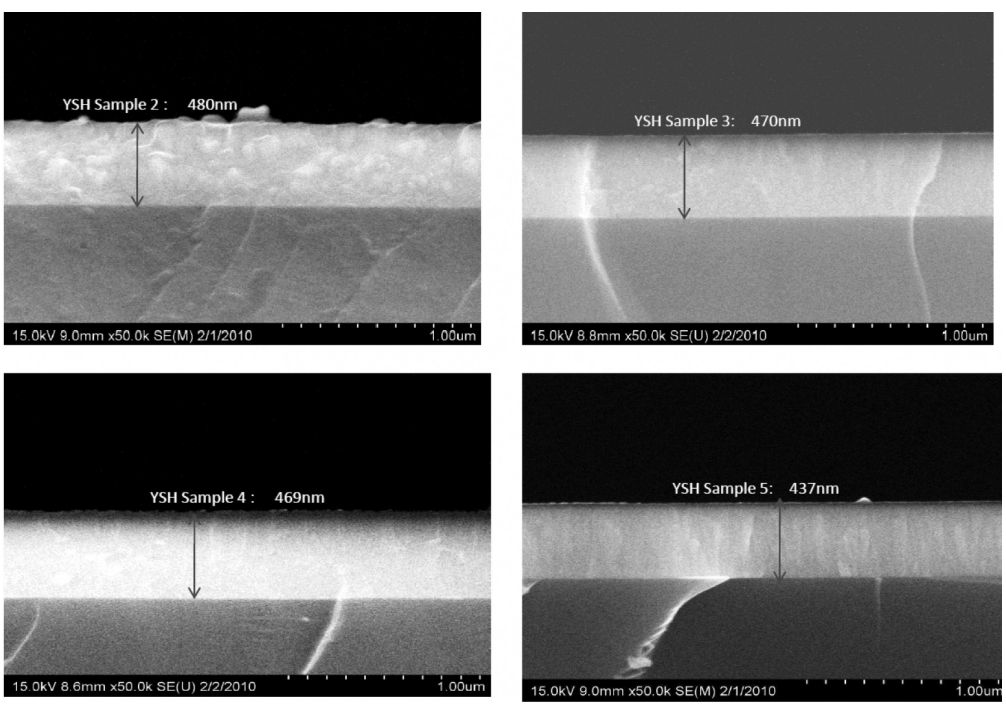

FIGURE 1. Interface analysis of the YSH coatings grown on various substrate materials.

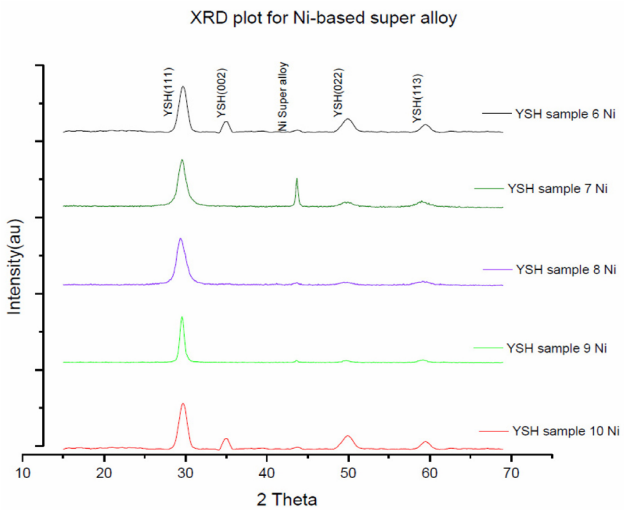

FIGURE 2. X-ray diffraction patterns of YSH coatings grown on Ni-super alloys. It can be seen that the effect of in situ temperature during growth is not very significant.

FY 2010 Publications/Presentations

1. N.A. Mohammad, A.R. Choudhuri and C.V. Ramana, "Microstructure analysis of yttria stabilized hafnia coatings," High-Temperature Coatings Symposium, AVS International Symposium, November, 2010 (accepted for oral presentation).

2. A comparative study of the growth and microstructure of yttria stabilized hafnia coatings, Manuscript in preparation (to be submitted).

References

1. DOE Funding Opportunity Number: DE-FOA-0000031, CFDA Number: 81.089 Fossil Energy Research and Development.

2. (a) D.R. Clarke and S.R. Phillpot, "Thermal barrier coating materials," *Mater. Today*, 2005, **8**(6), 22–29, (b) A.G. Evans, D.R. Mumm, J.W. Hutchinson, G.H. Meier, and F.S. Pettit, "Mechanisms controlling the durability of thermal barrier coatings," *Prog. Mater. Sci.,* 2001, **46**, 505-553.

V. SMALL BUSINESS INNOVATION RESEARCH

A. Alloys

V.A.1 Computational Design of Oxidation and Creep-Resistant Niobium Superalloys for High Temperature Turbine Applications

Dr. Abhijeet Misra
QuesTek Innovations LLC
1820 Ridge Avenue
Evanston, IL 60201
Phone: (847) 425-8233; Fax: (847) 328-5855
E-mail: amisra@questek.com

DOE Project Manager: Robin Ames
Phone: (304) 285-5436
E-mail: Robin.Ames@netl.doe.gov

Contract Number: SC0002475

Start Date: August 12, 2009
End Date: May 11, 2010

FY 2010 Objectives

- Establish design requirements for niobium superalloys.
- Develop alloy passivation strategy.
- Design proof-of-concept alloys to demonstrate Phase I concept feasibility.
- Fabricate laboratory-scale alloys.
- Process and temper optimization of alloys.
- Property evaluation: oxidation and strength.

Accomplishments

Model Nb-based alloys that achieve:

- High temperature capability >1,200°C.
- Enhanced oxidation resistance at 1,100-1,300°C – alloys with nearly an order of magnitude slower rate of oxidation compared to commercial Nb-based alloys.
- Oxidation rate trending towards commercial Ni-base superalloys.
- Microstructure close to 100% body centered cubic (BCC) – this is critical to achieving enhanced ductility.

Introduction

Rising natural gas prices, concerns about CO_2 and NO_x emissions, and a desire to efficiently utilize coal resources have increased interest in integrated gasification combined cycle (IGCC) and other advanced power plant technologies that promise to be environmentally friendly, emit lower levels of pollutants, and have efficiencies significantly better than what can be currently achieved. By using sophisticated cooling and coating technology current gas turbines are able to limit the metal temperature of the nickel-based superalloy turbine blades to around 1,100°C, while accommodating inlet firing temperatures of around 1,427°C. However, in order to meet long-term Turbine Program and IGCC/Hydrogen Program goals, targeting efficiencies greater than 50%, inlet temperatures need to be raised to higher than 1,500°C. This corresponds to metal surface temperatures beyond the capability for Ni-based superalloys, as they start melting at ~1,250°C [1]. Thus, there is a need for a new class of superalloys that can operate at temperatures beyond 1,250°C while retaining sufficient strength, creep-resistance, fatigue-load-resistance, and other properties.

In the Phase I Small Business Innovation Research (SBIR) project, QuesTek demonstrated the feasibility of achieving oxidation resistance and a ductile microstructure in Nb-based alloys. Under the proposed Phase II SBIR project, QuesTek will focus on further design optimization based on the identified Phase I concept space, scale up into larger scale ingots, property demonstration and coating process selection of the designed alloy, culminating in burner-rig tests to demonstrate coated system performance and integrity. The end result of the Phase II project will be an oxidation and creep-resistant Nb superalloy system for high temperature turbine applications at 1,300°C and above. At the end of the Phase II project, QuesTek anticipates generating the alloy property data needed in order to initiate a Phase III component level fabrication and qualification project. The alloy development project will involve a leading manufacturer of land-based gas turbines for IGCC power plants, and global world-leaders in refractory metal products, to ensure a commercialization path for the technology developed under this SBIR project.

Approach

The refractory metal niobium has a melting temperature of 2,467°C, is inherently ductile, and also has a low density, thus making it an attractive candidate for replacement of nickel. However, Nb has poor oxidation resistance and only moderate strength at high temperatures. This SBIR Phase II project will build upon the promising Phase I results to implement a systems-based approach to design precipitation-

strengthened Nb-based alloys that exploit coarsening-resistant multicomponent phases, providing creep strength and oxidation resistance at 1,300°C and above. A microstructural concept analogous to γ'-Ni_3Al strengthened Ni-based superalloys will be explored, where the nanoscale coherent precipitates within a ductile Nb matrix, will act both as the strengthening phase and as a source of reactive elements for the protective oxide. The design and development project will leverage QuesTek's state-of-the-art computational design tools within a *Materials by Design*® framework.

Results

The systems-design chart shown in Figure 1 is one of the critical steps of the *Materials by Design*® approach and provides detailed process parameters and intrinsic features (e.g., composition) that could potentially be altered to achieve desired property and performance objectives. QuesTek utilized the aforementioned approach to shortlist the candidate alloy compositions. To achieve superior oxidation resistance, QuesTek leveraged the information available on Ni-base superalloys. Ni-base superalloys overcome the issue of oxidation resistance by forming protective oxide coating such as Cr_2O_3 or Al_2O_3 in an oxidizing environment. On the other hand, Nb-based alloys form porous and non-protective oxide layer demonstrating linear growth kinetics. Promoting formation of protective oxide layer with parabolic growth kinetics in Nb-based alloys was the technical challenge addressed in this SBIR project.

To promote formation of protective oxide layer, the alloy must preferentially oxidize externally to the metal surface, i.e., by diffusion of reactive metal species to the metal/oxide interface. We utilized the mathematical relationship developed by Wahl [2], based on the classical treatment by Wagner [3], to describe the potency for formation of an external scale in a two-phase alloy system. It is important to note that while assessing the candidate alloy composition and process routes, QuesTek attempted to achieve better mechanical properties concurrently with enhanced oxidation resistance. Several oxidation concepts were examined and investigated.

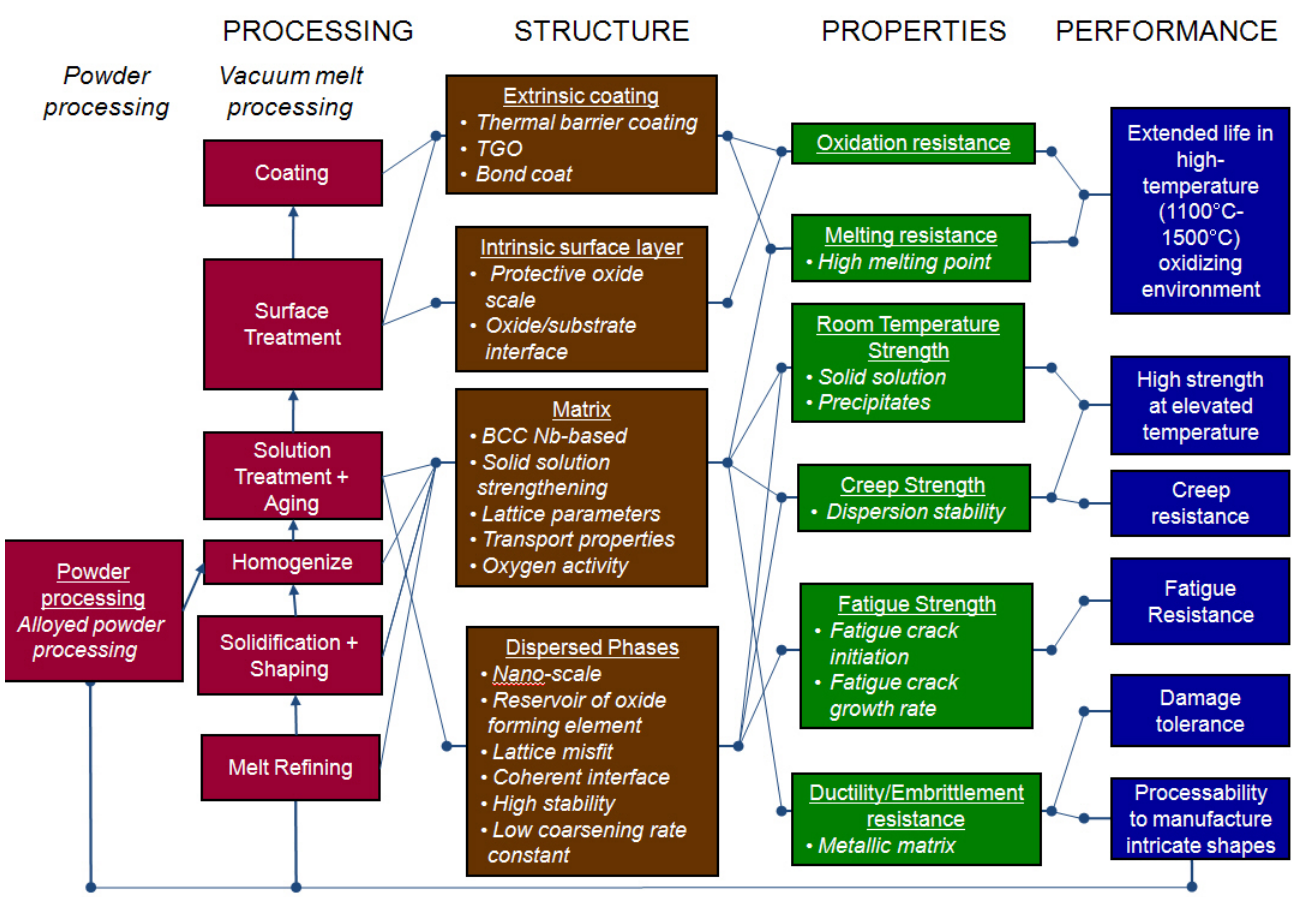

FIGURE 1. Systems-Design Chart for Oxidation and Creep Resistant Nb-Based Superalloys

Button alloys were produced using QuesTek's laboratory-scale arc melter. A total of four buttons, approximately 15 g for each of QuesTek's concepts were melted. A baseline sample of a Ni-based superalloy was also fabricated on a button-scale, and commercial Nb-based alloys were obtained for evaluation and comparison purposes.

Oxidation testing was performed at QuesTek and Northwestern University. Samples were cut from all four QuesTek concepts and from the commercial Nb alloys. The samples were carefully sectioned from each button to provide a measureable shape. The dimensions of each sample were measured and the samples were weighed. Subsequently, the samples were exposed to air at 1,100°C, 1,200°C, and 1,300°C for a period of five hours, and weight measurements were taken at the end of the test. The results of the oxidation tests and images of the resulting sample after exposure to oxidizing environment are shown in Figure 2. QuesTek concept #1 showed nearly an order of magnitude better behavior than commercial Nb-based alloys, and higher temperature capability than Ni-based alloys.

Conclusions and Future Directions

In summary, QuesTek was successful in designing novel Nb-based alloy concepts with better oxidation resistance and mechanical properties compared to commercial Nb-alloys. The QuesTek designed Nb-alloy concept demonstrated an order of magnitude slower oxidation rate compared to commercial Nb-alloys. Furthermore, the oxidation rate was observed to trend towards that of commercial Ni-base superalloys at high temperatures. QuesTek Nb-alloys showed superior high temperature operating capabilities (>1,200°C) and the microstructure was almost entirely BCC, critical to achieving enhanced ductility and toughness. Furthermore, initial characterization of mechanical properties revealed superior strength compared to commercial Ni-base superalloys.

To complete the alloy development in the two year Phase II project, QuesTek plans to collaborate with key stakeholders, including engineers from the DOE, original equipment manufacturers, and refractory alloy producers to define specific property goals and processing constraints; design alloys based on the promising Phase I concept to achieve oxidation resistance, while still maintaining room temperature strength and ductility; and produce and characterize these alloy designs both as sub-scale (~5 lb) alloy buttons, as well as intermediate-scale (~100 lb) heats. Initial coating selection and trials will also be conducted on the substrate alloy composition to demonstrate the coated system performance and integrity.

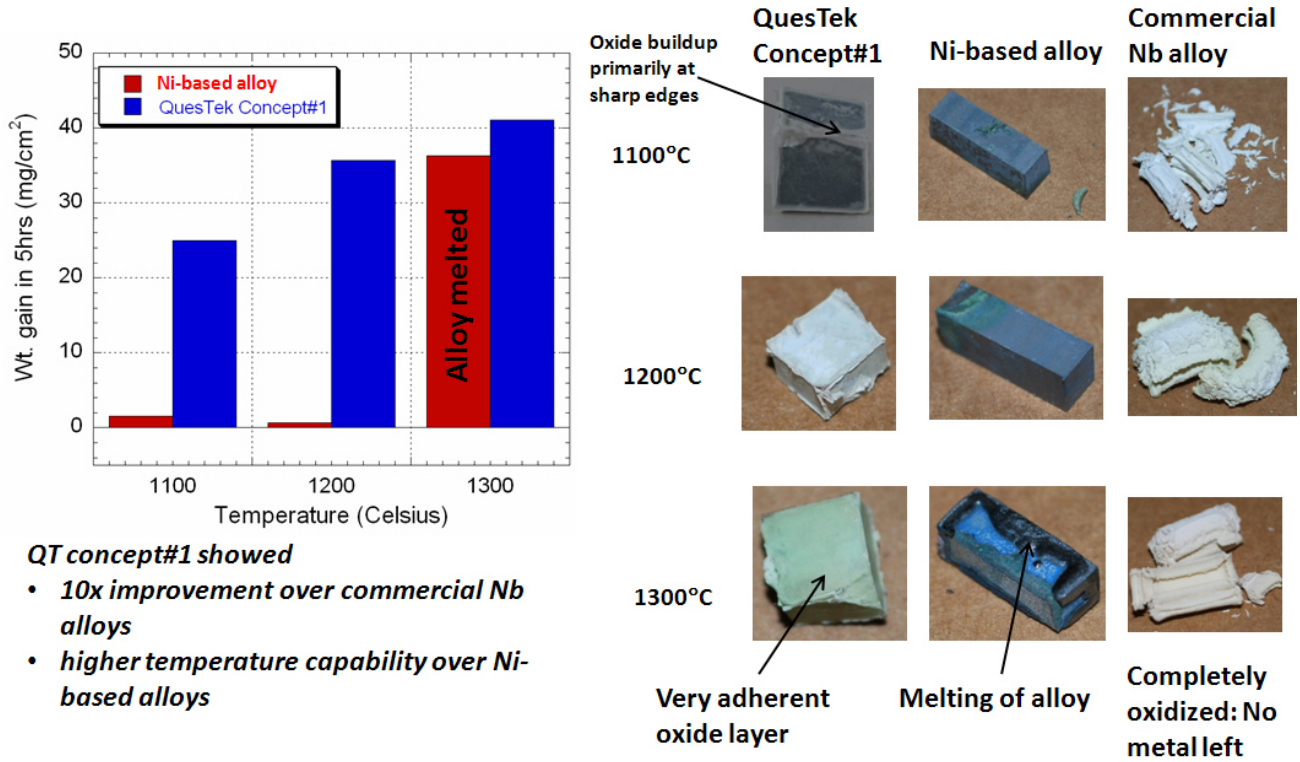

FIGURE 2. Comparison of QT Concept#, a Ni-Based Superalloy, and a Commercial Nb Alloy Samples after Thermal Exposure

At the end of the Phase II project, QuesTek anticipates generating all alloy property data that is needed in order to initiate a Phase III component level fabrication and qualification project.

References

1. B.P. Bewlay, M.R. Jackson, J.-C. Zhao, and P.R. Subramanian, *Met. & Mat. Trans. A*, vol. 34A, pp. 2043-2052 (2003).

2. G. Wahl, *Thin Solid Films*, vol. 107, pp. 417-426 (1983).

3. C. Wagner, *Z. Elektrochemie*, vol. 63, pp. 772-782 (1959).

V. SMALL BUSINESS INNOVATION RESEARCH

B. Innovative Cooling Concepts

V.B.1 Vaporization Cooling for IGCC Turbines

Dr. David Stickler (Primary Contact),
Dr. Kurt Annen
Aerodyne Research, Inc.
45 Manning Road
Billerica, MA 01821
Phone: (978) 663-9500; Fax: (978) 663-4918
E-mail: dstickler@aerodyne.com

DOE Project Manager: Robin Ames
Phone: (304) 285-5436
E-mail: Robin.Ames@netl.doe.gov

Subcontractor:
Thermacore, Inc., Lancaster, PA

Contract Number: SC0003591

Start Date: December 7, 2009
End Date: August 6, 2010

FY 2010 Objectives

- Identify low risk applications of Vaporization-Condensation Cycle (VCC) technology to gas turbine components that offer near-term improvements in component life and reliability, while being critical path components for efficiency gains in the long-term.
- Show feasibility of applying VCC cooling to the identified components.
- Develop performance estimates for gas turbines using VCC cooled components in comparison to baseline air-cooled components.

Accomplishments

- Identified high pressure compressor disc and turbine nozzles as low risk applications of VCC cooling that can be implemented in the near-term while providing a path to long-term efficiency improvements.
- Demonstrated feasibility of VCC-cooled compressor discs by detailed analysis of thermal and mechanical stresses that showed less than 10% increase in average stress due to VCC vapor/liquid transport passages.
- Developed a detailed design for implementing VCC cooling in compressor discs.
- Developed a VCC design for turbine nozzles that resolves problems previously encountered in incorporating heat pipes in nozzles.
- Showed a 7% efficiency gain from VCC cooling implementation in turbine blades alone, and nearly a 20% efficiency gain from complete implementation of VCC cooling in turbine systems.

Introduction

Gas turbine cycle efficiency is fundamentally limited by material temperature constraints imposed on achievable operating conditions. This limitation impacts fuel consumption, and consequently both power generation cost and emissions. Two component level constraints are dominant: compressor component temperature, which limits the cycle pressure ratio; and turbine component temperature, which directly impacts peak gas path temperature and thence theoretical thermodynamic efficiency. This project will substantially reduce these constraints by using a novel type of internal cooling called VCC for rotating turbine and compressor components. Static component cooling was addressed using relatively conventional high performance heat pipes. In this project, components of gas turbine systems were assessed for suitability for a first generation demonstration of VCC cooling in an integrated gasification combined cycle (IGCC) power application. This was achieved by assessing component level development priority and component requirements, developing conceptual level component designs, and evaluating VCC technology integration in a turbine system. Time scale for initial system application, cost, and initial user acceptance were considered in this review. While high cycle efficiency is the long-term payoff goal, user community acceptance and manufacturer commitment are expected to require a low risk approach.

Extensive research and preliminary demonstration of VCC cooling has been performed for aeropropulsion applications over the past decade, focused on turbine blade applications. A VCC cooled turbine blade design is shown in Figure 1, to illustrate the concept in that application. The results show both technical feasibility and substantial potential benefit [1-3]. As shown in Figure 2, extensive VCC cooling of turbine components has the potential to provide the next major step in gas turbine efficiency improvement. It can be used to increase both the cycle pressure ratio and peak gas temperature, while minimizing or eliminating negative performance and physical effects associated with air cooling. The overall benefit of increased cycle pressure ratio and temperature is a substantial increase in thermal efficiency, corresponding to decreased fuel consumption and pollutant emissions.

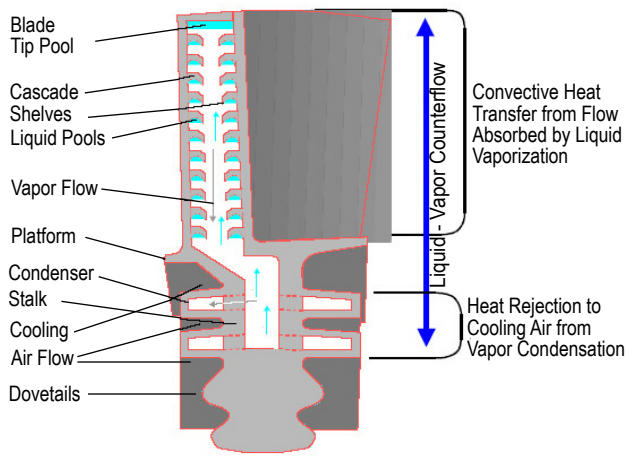

FIGURE 1. Functional Schematic of Flow in Vaporization Cooled Blade

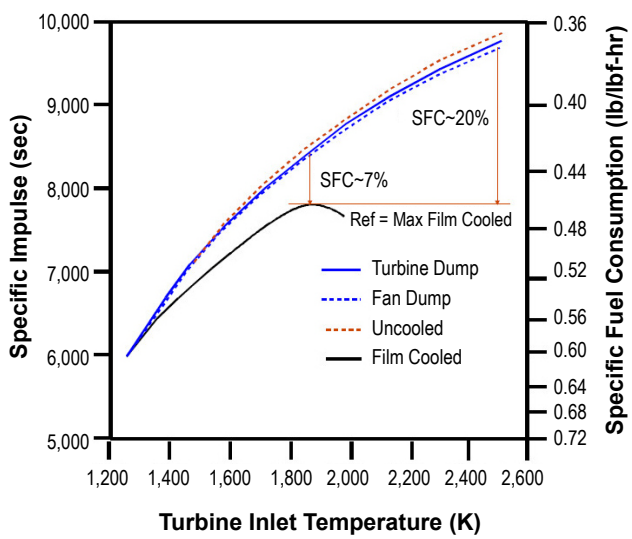

FIGURE 2. VCC Cooling Impact on Aircraft Gas Turbine Efficiency

Approach

The overall approach is focused on moving the advanced cooling technology to a level attractive to engine manufacturers, for development and integration into gas turbine engines. This requires a combination of technology demonstration, engine integration design, and performance impact prediction, together with ongoing interaction with the engine community. The overall goal of this three-phase project is to provide a combination of basic hardware demonstration and support analysis as a basis for subsequent engine-level component development by industry. It is anticipated that first generation engine application will be in high performance engines for Department of Defense (DOD) applications. The DOD motivation and payoff for propulsion system improvement is high, funding for hardware development can be obtained, and the risk tolerance is relatively high. Application in the commercial stationary power sector is expected to follow, after demonstration and risk reduction development in DOD applications.

Results

A wide range of gas turbine components was identified that can be cooled using the VCC approach. Together, they allow a substantial increase in cycle efficiency, and a corresponding decrease in fuel consumption and emissions. In addition to components currently cooled, such as combustor liners, nozzles, turbine blades and stators, it is also possible to cool other rotating components, notably compressor and turbine discs. Cooling was assessed at the component level, with impacts on efficiency, reliability and maintenance balanced against development time, cost and risk. While improved hot section components provide relatively near-term efficiency gains, they also imply higher technological risk and development time. High pressure compressor disc and turbine nozzles were identified as low risk applications of VCC cooling that can be implemented in the near-term while providing a path to long-term efficiency improvements.

Design studies of these two components were pursued to explore the feasibility of implementation in IGCC turbines. VCC application to a compressor disc functions primarily to force uniform disc temperature, with limited net heat rejection [4]. However, for simplicity, this process is referred to as cooling. A baseline VCC-cooled compressor disc was designed based on the geometry and constraints of a conventional high pressure stage disc. This included heat load calculations and analysis of internal fluid transport to define flow passage and structural requirements. Multiple internal coolants were assessed, in terms of their thermal and transport characteristics. Prior work on high temperature components had identified potassium as the optimum fluid, but the lower operating temperature range of compressor and turbine discs resulted in water being selected as working fluid. This disc cooling has two overall effects: it forces a near-uniform disc temperature, both steady state and transient; and decreases rim temperature for a given flow environment. Figure 3 shows a wedge section of the predicted cooled disc temperature distribution. This is a worst case, in which the rim is cooled by conduction only. This results in much lower thermal stress load, particularly during engine transients, which allows longer disc life. The second enables turbine operation at higher peak compression ratio, which in turn supports increased cycle efficiency. Detailed thermal and mechanical stresses were also modeled, based on the overall disc geometry, dynamic load and a

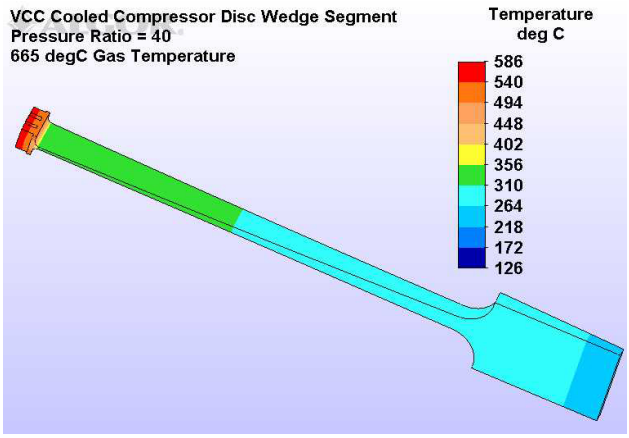

FIGURE 3. Temperature Distribution in VCC Cooled Compressor Disc Segment

preliminary layout of flow passages required for liquid and vapor flow and distribution in the disc. Figure 4 shows detailed stress distribution (note that edge and corner stresses are artifacts of the boundary conditions imposed). The net result of disc cooling combined with local stress concentrations forced by flow passages is an overall decrease in stress load. Identified design changes are expected to further decrease local stress loads. Consequently, a cooled compressor disc appears both technically feasible and economically attractive. The same technology can also be applied to turbine discs, with similar benefits.

A new VCC design was also developed for turbine nozzles. As static components, the dynamic transport mechanism used in disc and blade cooling is not applicable, but high performance alkali metal heat pipes are. Prior work on nozzle cooling using heat pipes treated the entire nozzle structure as a single heat pipe structure [5]. While this provided excellent thermal control and eliminated conventional film cooling, it also was subject to failure due to local structural cracking. A new approach was developed in which multiple independent heat pipes are embedded in the nozzle structure, separating thermal transport from the structural support and aerodynamic contour.

The impact of advanced cooling on overall gas turbine efficiency has been analyzed using tools developed for aeropropulsion systems. The results are indicative of trends and approximate efficiency differences in stationary power turbines. Calculations showed a 7% efficiency gain from VCC cooling implementation in turbine blades alone, and nearly a 20% efficiency gain from complete implementation of VCC cooling in turbine systems. The latter includes the impact of compressor disc cooling on cycle pressure ratio as well as elimination of bleed air losses in turbine cooling.

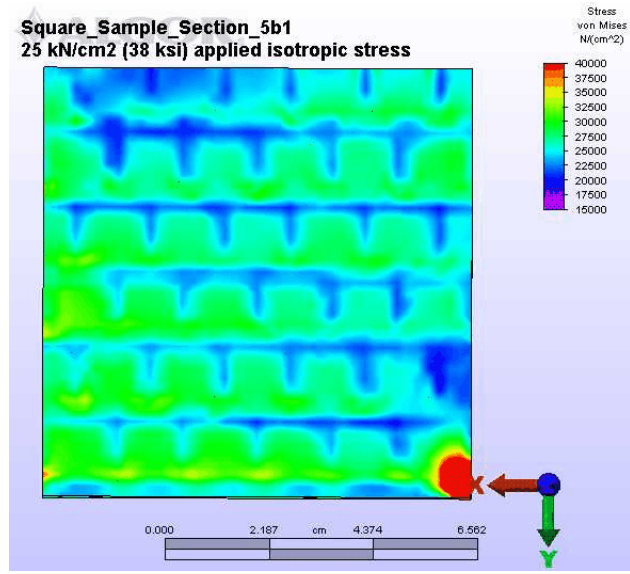

FIGURE 4. Von Mises Stress Results for Square Segment of Vaporization-Cooled Disc

Conclusions and Future Directions

The key result of work completed in Fiscal Year 2010 is that there is potential for significant improvement in turbine efficiency in IGCC power systems, as well as in a other stationary power applications, using advanced turbine cooling based on component level vaporization–condensation heat transfer. That cooling technology has been extensively studied in the past for application to gas turbine blades and compressor discs. Assessment of VCC component integration in IGCC turbines identified compressor discs and turbine nozzles and vanes as leading near-term candidates. They provide relatively low risk, useful payoff to the user community, and are critical path components for future high performance power systems. Conceptual design of these components and detailed thermal and stress analysis of a full-scale compressor disc, showed technical feasibility.

Future work is focused on component level development to enable application in engines. Ongoing development will be reviewed and critiqued in an informal interaction with a major gas turbine manufacturer, which has interest in application of these technologies to aircraft propulsion systems. That path is perceived as effective in dealing with first generation engine application, and minimizes risk perceived in the stationary power community. The first step planned is compressor disc and nozzle component fabrication and cooling function demonstration in laboratory test rigs. That will be followed by component design and analysis and fabrication for testing in more realistic environments using turbine rigs.

FY 2010 Publications/Presentations

1. Presentation to DOE Program Manager and NETL Staff, March 3, 2010.

References

1. J.L. Kerrebrock and D.B. Stickler, "Vaporization Cooling of Gas Turbines, The Return Flow Cascade," ASME Paper No. 98-GT-177.

2. J. Townsend, J. Kerrebrock, and D. Stickler, "Experimental Evaluation of a Turbine Blade with Potassium Evaporative Cooling," AIAA Paper No 2004-3571, Presented at the 40th AIAA/ASME/SAE/ASEE Joint Propulsion Conference and Exhibit, Fort Lauderdale, Florida, July 11-14, 2004.

3. "Vaporization Cooled Turbine Demonstration," Phase I Final Report, Contract Number HR0011-05-C-0132, February 2008.

4. "High Performance Compressor Cooling," Final Report, Contract NAS3-01036, August 2001.

5. "Heat Pipe Cooling of IHPTET Phase III Turboshaft Engine Components," Final Report, U.S. Army Contract DAAH10-98-C-0002.

V.B.2 High Temperature Capability and Innovative Cooling with a Spar and Shell Turbine Blade

James P. Downs
Florida Turbine Technologies, Inc.
1701 Military Trail, Suite 110
Jupiter, FL 33458-7887
Phone: (561) 427-6250; Fax: (561) 427-6190
E-mail: jdowns@fttinc.com

DOE Project Manager: Robin Ames
Phone: (304) 285-0978
E-mail: Robin.Ames@netl.doe.gov

Contract Number: 84668

Start Date: June 20, 2007
End Date: August 14, 2010

FY 2010 Objectives

- Develop detailed mechanical design concept that can be manufactured for test within a follow-on project.
- Identify materials best optimized to the Spar-Shell turbine blade for use in specific environments.
- Define cooling system features required to produce high thermal efficiency.
- Identify manufacturing and fabrication requirements.
- Evaluate benefits and costs of this system.

Accomplishments

- Florida Turbine Technologies is nearing completion of the detailed design of a rotating Spar-Shell turbine blade.
- The feasibility of the mechanical design, cooling and structural aspects of this design are supported by engineering calculations and analysis.
- Manufacture and assembly of the Spar-Shell blade has been verified with the construction of prototype models.

Introduction

Current gas turbine systems already operate at temperature and pressure levels that are sufficiently high to require the use of advanced materials and cooling of the turbine components. The use of cooling in the turbine, although permitting turbine components to operate within an environment of high temperature and pressure, causes an efficiency debit to the turbine subsystem and overall power plant. Technology advances within the turbine systems therefore represent an excelled avenue for improving the overall power plant efficiency. In particular, technologies that permit turbines to operate at increased temperatures and pressures are desired to achieve the specific performance goals. Advances of both the materials and cooling systems are clearly required to extend the envelope for improved performance and efficiency in the future systems.

To meet future power generation needs, Florida Turbine Technologies, Inc. (FTT) is developing an innovative design approach to provide highly durable turbine components that increase efficiency by requiring the lowest cooling flow possible. The proposed gas turbine rotating blade design is constructed of an internal structurally supporting member (spar) and a separate external covering (shell) to provide the aerodynamic envelope. The so-called Spar-Shell system enables the use of advanced, high temperature materials that are not available based on current design philosophies and manufacturing approaches. In addition to providing higher temperature capabilities, features of this system resolve another well-known technical barrier which causes current turbine components to fail by cracking due to thermally-induced stresses. This barrier limits the capabilities of today's turbine components, particularly at the interface between the main airfoil body and the platform/attachment structure. Further, this architecture facilitates the cooling system to be optimized to the smallest possible cooling flow required by enabling the use of practical and robust near-wall cooling features while minimizing the plugging risk of systems such as those associated with effusion and other porous media schemes. With this project, FTT has laid out a comprehensive plan for the design and development of this concept. Further, FTT has the full support and backing of a primary original equipment manufacturer, namely Siemens Energy with the expressed commitment to evaluate the design within the Siemens design review process and to test development hardware in an engine to permit design verification and validation data to be acquired.

Approach

FTT has proposed the development of a rotating Spar-Shell turbine blade system to realize the

future turbine system goals of reduced cooling flow consumption and increased efficiency. Development of the proposed Spar-Shell turbine component system offers several advantages relative to the current state-of-the-art. To realize these goals, several objectives, as delineated in the following paragraphs, must be pursued.

FTT recognizes the limitations of current turbine material and cooling systems and has been actively investigating alternatives to resolve the major issues. As a result, development of the Spar-Shell system has progressed to the point where detailed analytical and empirical verification was needed as a prerequisite to verification of the design concept in a test engine. One example of such a component is described in U.S Patent #7080971, "Cooled Turbine Spar-Shell Blade Construction" by Wilson and Brown (Figure 1). Development of the Spar-Shell system has proceeded beyond the fundamental details described in this patent, namely with respect to shell loading and attachment. As shown, this design approach utilizes an internal spar which is surrounded by an external shell. This fabrication approach has several advantages relative to the current state-of-the-art monolithic cast structures. First, the internal spar represents the primary framework of this concept. Since the shell protects this member from the hot working fluid passing around the airfoil, it can be maintained at a relatively low temperature very near that of the coolant. The spar material can therefore be optimized for very high strength at a moderate temperature level. Second, since the shell is structurally isolated from the spar, its' material can be selected on the basis of high temperature capability.

Thermally-induced stresses are a primary driver and limiter of existing cooled turbine components. The Spar-Shell turbine blade construction serves to mitigate the associated effects on low cycle fatigue and thermal-mechanical-fatigue distress through both thermal and mechanical isolation of the spar and shell. Further, other desirable thermal attributes, such as the ability to support high temperature and heat flux, can be considered as primary drivers in the shell material selection.

Results

Design and analysis of the Spar-Shell technology have been performed to support the feasibility of the concept. From a cooling perspective, the Spar-Shell blade may take many possible forms. However, to improve the performance of the cooling system while reducing the amount of cooling flow requires that the efficiency of the internal convection cooling system be increased while film cooling benefits are reduced with the reduction of overall cooling flow. To this end, a conceptual cooling circuitry has been defined to provide the required heat transfer characteristics. In addition, structural analyses have been performed within finite element models (Figure 2) to verify the basic structural and vibration characteristics. Results from these analyses support the feasibility of the design and indicate the need for continued research to refine and optimize the design.

During the course of this project, a prototype model of one possible representation of the Spar-Shell system was developed and constructed using a three-dimensional printing process. The geometry selected

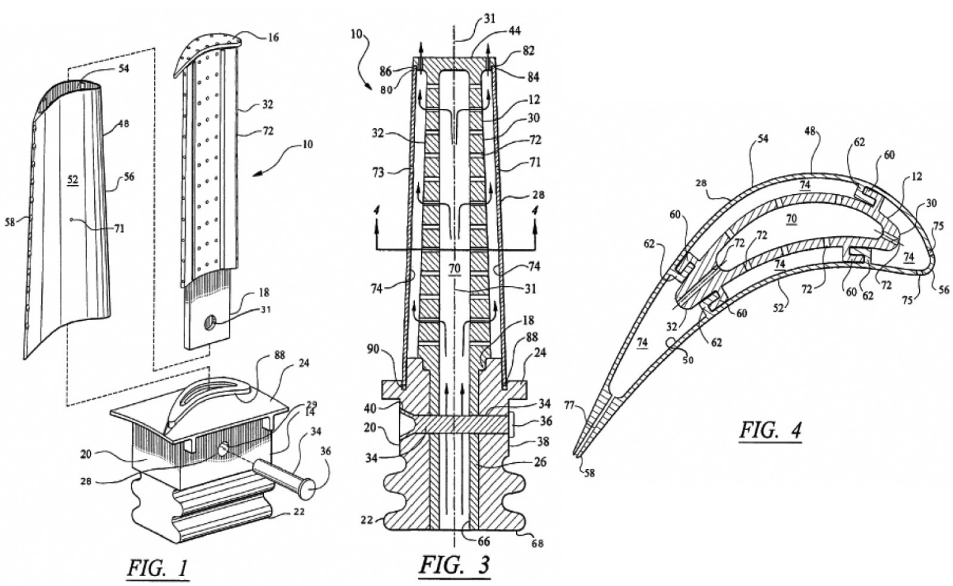

FIGURE 1. U.S. Patent #7080971, "Cooled Turbine Spar Shell Blade Construction"

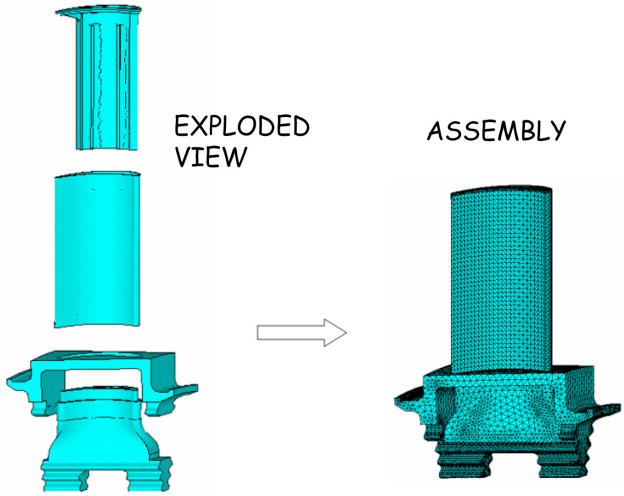

FIGURE 2. Analytical Model/Finite Element Mesh

for this demonstration was based on a spar which supports the shell from the tip of the airfoil. In this construction, the spar must be inserted through the shell from the tip of the airfoil with a mechanical joint used to fix the spar to an attachment and platform structure. For the purposes of this initial development, an airfoil having constant cross-sectional area was assumed and wall thickness was set constant from the root of the airfoil to the tip. The shell includes separate leading edge and trailing edge cooling cavities as might be employed with impingement-style cooling systems and four L-shaped hooks were modelled to provide support of the shell from the spar. The entire system was modelled in the Pro/ENGINEER computer-aided design system, and a physical model was constructed from this geometry definition (Figure 3).

Conclusions and Future Directions

Results from conceptual design work performed during the initial Phase I Small Business Innovation Research (SBIR) grant supported continued development of the technology and FTT was selected for a Phase II SBIR award to define a detailed design of a Spar-Shell turbine component. Work on the Phase II project has produced a viable design concept which continues to be developed within the detailed design phase.

Beyond the Phase II SBIR, development and optimization of the design approach and fabrication of test articles will continue with support from a Phase II supplement, Phase III SBIR or other funding source. The development project plan culminates in a prototype demonstration of the technology. To facilitate this demonstration, a test in an actual industrial gas turbine engine is proposed to:

- verify the feasibility of the spar-shell concept;
- demonstrate thermally free platforms;
- demonstrate thin-wall structures;
- demonstrate increased manufacturing yields and lower cost with single crystal;
- evaluate advanced airfoil cooling;
- evaluate advanced platform cooling;

FIGURE 3. Spar-Shell Prototype Model

- test advanced materials;
- evaluate advanced thermal barrier coatings; and
- evaluate fabricated blade and high speed machining capabilities.

To perform this demonstration, FTT has the expressed commitment of Siemens Energy to test approved engine hardware in their full engine test bed. To be approved for demonstration, the prototype hardware must pass all engineering and design review requirements. This type of test permits the construction of a so-called rainbow wheel where a mix of turbine blade configurations, materials and technologies may be installed in a single turbine rotor and be evaluated in a single engine test.

V.B.3 Development of Innovative Cooling Approaches for Robust Design

James P. Downs
Florida Turbine Technologies, Inc. (FTT)
1701 Military Trail, Suite 110
Jupiter, FL 33458-7887
Phone: (561) 427-6250; Fax: (561) 427-6190
E-mail: jdowns@fttinc.com

DOE Project Manager: Robin Ames
Phone: (304) 285-0978
E-mail: Robin.Ames@netl.doe.gov

Contract Number: SC0002713

Start Date: July 20, 2009
End Date: August 31, 2010

FY 2010 Objectives

- Perform a conceptual design of a Spar-Shell turbine vane.
- Define preliminary verification test plans for a Spar-Shell turbine vane.
- Define the plan for detailed design of equipment in a follow-on Phase II Small Business Innovation Research (SBIR) project.

Accomplishments

Florida Turbine Technologies is nearing completion of the conceptual design for a stationary Spar-Shell turbine vane.

Introduction

Since the invention of the gas turbine, many technological advancements have been introduced throughout the machine to increase the power, performance and overall efficiency. Many of these advancements have improved the efficiency of specific components, but the most significant improvements have been realized with the development of technologies that permit temperature and pressure of the turbine working fluid to be increased. To this end, turbine cooling represents an enabling technology that has propelled gas turbines to the forefront as a competitive means of producing power in the modern marketplace. Future turbine systems must permit additional, incremental increases of operating parameters to advance the state-of-the-art. These increases will permit even higher levels of power and efficiency to be achieved.

Despite the use of cooling methods, modern turbines are subject to distress from repeated long-term exposure to an extremely deleterious environment. Information available in literature shows that turbine and other hot section related issues are reported to cause 53% of failures in gas turbines smaller than 170 MW. Larger turbines are reported to be subject to a higher percentage of compressor-related issues, but combined hot section (combustor and turbine) issues still account for over 50% of failures.

Approach

To meet the needs of future turbomachinery systems, FTT is developing innovative cooling approaches for robust design. These approaches are needed to provide durable turbines while realizing the future turbine system goals of reduced cooling flow consumption and increased efficiency. Development of these approaches offer several advantages relative to the current state-of-the-art. To provide robust designs, cooling approaches must be developed to make turbine hardware capable of performing without failure over a wide range of operating conditions. To realize these goals, several objectives, as delineated in the following paragraphs, must be pursued.

To provide more than a small improvement to overall turbine system capabilities, FTT understands that future turbine systems must be designed around the requirements for reduced cooling flow (increased performance) while continuing to provide high levels of durability in a part that is readily manufactured. Specifically, the flow path heat transfer properties of future turbines will be highly dependant on the thermodynamic transport properties of the specific working fluid(s), and will also be highly dependant on cycle performance characteristics (i.e., pressure level). For future clean energy industrial gas turbine applications, working fluid compositions having reduced nitrogen content and increased fractions of water (steam) and/or carbon dioxide are expected with the combustion of coal-derived syngas and high hydrogen fuels derived from syngas with oxygen separated from air.

FTT recognizes the limitations of current turbine material and cooling systems and has been actively investigating alternatives to resolve the major issues. Under this SBIR project FTT is investigating alternative solutions to these problems such that the part can still be robust, but without the need to use excessive quantities of cooling air. To give an example, consider

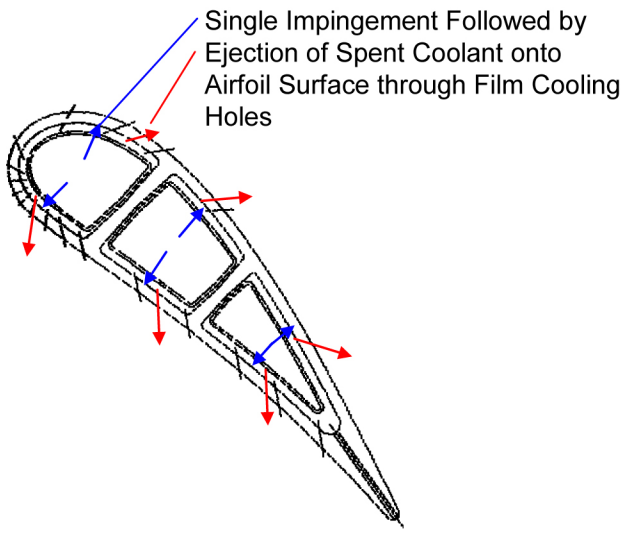

FIGURE 1. Current State-of-the-Art First Stage Turbine Vane Uses Single Impingement

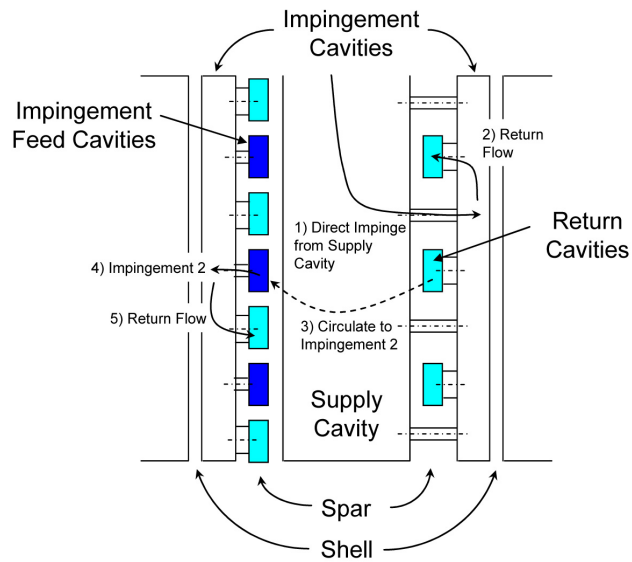

FIGURE 2. FTT Invention Disclosure F650R, Cooled Turbine Vane

a first stage turbine vane shown in Figure 1 which is typically cooled by the three methods: internal cooling by convection heat transfer, ejection of spent coolant to provide a film cooling effect, and the use of a thermal barrier coating (TBC) as a layer of thermal protection. These components are cooled by internal convection heat transfer; typically accomplished by impingement of cooling air onto the internal surfaces of the component. To facilitate this mechanism, tubes containing a myriad of holes are inserted into the component. Coolant is allowed to flow into the tubes and impingement jets are formed as the coolant exits through the myriad of holes. Once the coolant has accomplished the internal cooling by convection heat transfer, it is allowed to enter film cooling holes where it is ejected from the part to form a film cooling effect. In the meantime, the TBC reduces the heat load from the part and further protects it from the hot gases flowing around it.

To improve internal convection heat transfer under these circumstances, FTT is developing an innovative cooling system based on the use of a sequential impingement cooling scheme. This design approach facilitates simultaneous optimization of the structural, cooling, and materials systems. Although the basic concept of sequential impingement is not new, its utilization in a cooled Spar-Shell turbine airfoil as described in the following paragraphs is considered to be novel. A schematic representation of such a system is illustrated in Figure 2. As shown in this figure, coolant flow enters a supply cavity located centrally within the airfoil. The coolant first passes through impingement cooling holes from the supply cavity to impinge directly on a defined heat transfer surface. Second, this flow is collected in return cavities located within the inner structure to be circulated to another region of the part where it again passes through holes to impinge on a second heat transfer surface of interest. The process can be repeated several times within the range of allowable pressure conditions for the coolant. Ideally, the first impingement regions would be the surfaces adjoining high gas path pressures, such as the leading edge and forward pressure side surfaces. Secondary impingement could be directed at surfaces adjacent to lower gas path pressure regions, such as the aft pressure side and suction side of the airfoil. Using this system, cooling flow could be leveraged by impinging on separate heat transfer surfaces in a sequential fashion. Further, this approach might be useful to reduce or eliminate the effects of impingement heat transfer degradation due to cross flow, which are prevalent in existing impingement cooling designs.

Results

An intensive search of intellectual property (IP) was performed to identify and characterize the historical records. As mentioned previously, the concept of sequential impingement is not new, and the results from the IP search revealed several examples within the patent databases. However, all of the concepts identified by the search differ from the FTT approach in some manner.

During the Phase I SBIR project, the mechanical configuration was developed to the extent needed to demonstrate feasibility. To this end, a three-dimensional representation of the geometry has been developed. An overview of this geometry is illustrated in Figure 3. As shown, the arrangement consists of an internal spar and an external shell. The shell is

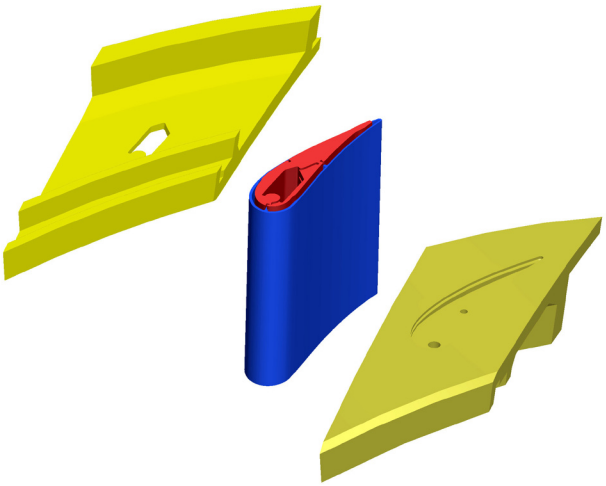

FIGURE 3. Concept Design Configuration

supported by the spar using an attachment system. The shell is a relatively simple geometry that may be represented by an extruded section which could be fabricated by a variety of means. One fabrication approach for the shell would be by cutting from a block of material using the electrical discharge machining wire slicing method. The spar represents the structural backbone of the system and this article provides all of the coolant flow routing through the system. In one construction approach, the spar is constructed of a number of layers to provide the local impingement of flow to specified regions of the airfoil and also to collect and return these flows to be routed to other regions of the airfoil for impingement onto other regions of the airfoil.

To understand the benefits of a sequential impingement cooling system in a first stage turbine vane, a comparison was made of the typical design practice with the proposed approach. In today's "state-of-the-art" vane, the impingement ratio is limited by the magnitude of static pressure on the leading edge of the airfoil. This is especially important where the cooling holes are present. The impingement pressure ratio is an important contributor to the overall cooling effectiveness because increased impingement ratios are known to promote higher rates of convection heat transfer. Conversely, in the sequential-impingement approach multiple levels of post impingement pressure can be used to optimize the system for high impingement heat transfer. To improve the cooling effectiveness, the goal is to increase the heat transfer for a given quantity of cooling flow. In the studies performed during the Phase I project, the results from calculations based on these examples indicate the heat transfer can be increased by 280% for a given cooling flow.

Conclusions and Future Directions

Results from conceptual design work performed during the initial Phase I SBIR project support continued development of the technology and FTT has submitted a proposal for a Phase II follow-on project to continue the work into the detailed design phase. Beyond the Phase II SBIR, development would continue to demonstrate and validate the technology with the ultimate goal to produce a commercial product or to license the technology.

To perform this demonstration, FTT has the expressed commitment of Siemens Energy to test approved engine hardware in their full engine test bed. To be approved for demonstration, the prototype hardware must pass all engineering and design review requirements. This type of test permits the construction of a so-called rainbow wheel where a mix of turbine blade configurations, materials and technologies may be installed in a single turbine rotor and be evaluated in a single engine test.

V.B.4 Industrial Gas Turbine Cores Produced with Advanced Cooling Features

Michael Appleby
Mikro Systems, Inc.
1180 Seminole Trail, Suite 220
Charlottesville, VA 22901
Phone: (434) 244-2480; Fax: (434) 244-6485
E-mail: appleby@mikrosystems.com

DOE Project Manager: Maria Reidpath
Phone: (304) 285-4140
E-mail: Maria.Reidpath@netl.doe.gov

Contract Number: SC0001359

Start Date: August 12, 2009
End Date: May 11, 2010

FY 2010 Objectives

Demonstrate that Mikro's TOMO™ technology can produce advanced turbine blade cooling features significantly faster and cheaper than current production methods. To accomplish this, Phase I had the following specific objectives:

- Produce three trailing edge designs with advanced cooling features,
- Produce ceramic core samples of each design suitable for directional solidification (DS) or single crystal (SX) foundry casting,
- Characterize the ceramic core samples, and
- Conduct initial foundry casting trials using the new designs.

Accomplishments

- Completed three trailing edge designs incorporating advanced cooling feature designs provided by Siemens Energy.
- Produced master tooling and production tooling for ceramic core samples.
- Produced eight ceramic core samples incorporating the advanced cooling designs.
- Characterized ceramic core samples dimensionally.
- Conducted DS foundry casting tests at Alcoa Howmet using Mikro-produced ceramic core samples. Eight parts were cast (four each of two designs). Results showed excellent casting of most cooling features demonstrating conclusively that Mikro's ceramic cores are fully compatible with the DS casting process and providing initial feedback on the capabilities and limitations of the casting process in defining advanced cooling features.
- Characterized the cast samples.

All Phase I objectives were met, including the initial foundry test. During this nine-month $100,000 project Mikro designed, tooled and produced ceramic core samples embodying three revolutionary cooling designs that have never been produced. In addition, we conducted initial foundry casting trials using the designs. All of this was accomplished in a fraction of the time and cost of conventional techniques. Mikro demonstrated that the TOMO™ process can lead to revolutionary new turbine cooling designs, which can be developed faster and at significantly lower cost than current techniques allow.

Introduction

Turbine blade and vane survivability at higher operating temperatures is the key to improving turbine engine performance. Innovative cooling approaches are a critical enabling technology to meet this need. This project addressed two important aspects of the problem. First is the need to increase core manufacturing process capability (quality and reliability) to enable advanced cooling features to be incorporated in future turbines. Second is the need to rapidly and economically produce tools and prototype hardware whereby advanced designs can be empirically tested and optimized.

Approach

Mikro Systems applied its patented Tomo Lithographic Molding process (TOMO™) to the manufacture of advanced turbine blades for use in integrated gasification combined cycle power plants. In order to improve heat transfer and lower cooling air requirements, the advanced blade designs will require more complex internal cooling passages than can be produced using current investment casting techniques.

During Phase I, Mikro demonstrated the ability to produce the trailing edge portion of the blade to incorporate advanced cooling features that currently are not manufacturable. Verification was was done by producing "foundry ready" trailing edge core samples representing three unique advanced cooling designs using TOMO™ technology. In addition, Mikro

conducted DS foundry casting tests at Alcoa Howmet using Mikro-produced ceramic core samples.

Results

Design Trailing Edge Cores. An existing commercial blade was provided by Siemens Energy to use as a baseline during the design process. While the subject cores had the same outside dimensions and shape as the cores used to produce the baseline blade, they incorporated advanced cooling features designed for the trailing edge portion. The advantages of using a baseline blade were clear:

- Mikro Systems had already produced ceramic cores for this blade, which had been evaluated through an entire DS foundry trial.
- Using an existing blade provided a benchmark for cooling performance and blade production in a possible later phase.
- Significant cost savings were realized by using existing core tooling.
- Additional cost savings may be realized in a later phase by using existing foundry tools to support more extensive casting trials.

The first step of the design process was a meeting of the Siemens designers and the Mikro engineers. The purpose was to familiarize the designers with the capabilities of the TOMO™ process. Specifically the discussion centered on how TOMO™ could enable new, previously unmanufacturable, trailing edge cooling features. Mikro demonstrated how specific core geometries could be made using TOMO™ technology that could not be produced using current core manufacturing techniques, thereby overcoming current cooling design limitations.

Based on this meeting, Siemens developed an advanced trailing edge design. The design represents a radical departure from current core designs.

To demonstrate the manufacturability of turbine blades using this type of design, it was ultimately necessary to show: 1) that ceramic cores can be produced with these features, and 2) that those cores can be used to cast turbine blades incorporating the cooling features. After reviewing the Siemens design, Mikro was confident that most of the advanced cooling features (micro-fins, hour-glass walls etc.) could be produced in a ceramic core using our TOMO™ process. However, considering that no blade design like this had ever been produced, Mikro was not certain whether these features were beyond the capability of the DS or SX investment casting processes for turbine blades.

To answer the critical fabrication questions, Mikro translated the Siemens design concept into five different core designs, three of which were intended to verify Mikro's ceramic core capabilities for advanced trailing edges and two to verify foundry casting capabilities.

Foundry Test Cores. The foundry test cores were designed to allow a range of experiments (DOE) to evaluate the ability of standard investment casting processes to incorporate the advanced cooling features. As will be described, by analyzing a number of cast cores with increasingly fine features, we were able to determine if, and at what point, specific features became uncastable.

All projects tasks related to the core design were successful. A radical new design concept was developed and cores were designed to allow thorough evaluation of both core and casting capability of these advanced design features. No problems were encountered and all tasks were completed on time and within our estimated budget.

Support Tooling. Additional process tooling was designed and produced for core production, including:

- Core casting molds, which required a machined fixture for mold production.
- A green-state setting tool used for trailing edge thermo-forming.
- A setting fixture used to maintain the dimensional shape of the trailing edge cores during high-temperature ceramic sintering.

No problems were encountered and all tasks related to the production of core tooling during were completed on time and within the estimated budget.

Produce Phase I Cores. All cores were produced using a ceramic material system that is fully foundry-compatible for DS (or SX) casting. Using the tooling produced in this project, the five core designs were produced from our ceramic casting and sintering process. Small lots (minimum of three) of four of the designs were successfully produced without any problems. The resulting cores were of excellent quality. However, problems were encountered with the casting fixture of the most complicated design. A solution was identified, but unfortunately, at that point, we did not have enough time remaining to redesign and re-make the fixture. We understand the problem, we are confident that we can produce this last design, and we intend to demonstrate this in a later phase.

Cores with four of the five designs were successfully cast, fired, and sintered. Master tooling was produced for the final design was produced but cores could not be cast due to fixture design issue. Overall, we feel 85-90% of the objectives of this task were completed on time and within the estimated budget.

Foundry Test. In this task, Alcoa Howmet Research Center (AHRC) was contracted to conduct foundry tests on eight cores. The objective was to use cores supplied by Mikro for a DS casting evaluation of the cores using 247LC alloy. To accomplish this, AHRC performed the following operations:

1. Measured the TOMO™ cores by means of coordinate measuring machine (CMM).
2. X-rayed the TOMO™ cores and reported the results.
3. Wrapped pattern wax around the cores (four each of two core configurations).
4. Assembled the wax patterns into one, 1 x 8 case size mold.
5. Invested the mold with the Howmet Monoshell system.
6. Evaluated the core after dewax and firing, and reported the results.
7. DS cast the mold in 247LC alloy using the standard Howmet DS foundry technology.
8. Post casting processing including knocking out, cutoff, and abrasive blast cleaning and belting.
9. Core removal on the cast parts (leached).
10. X-ray inspection on all parts.
11. Sectioning of all cast parts to examine core reaction.
12. CMM operations on all castings of the internals of the sectioned castings.
13. Delivered eight cast parts, all of which were sectioned in the as-cast condition including the alloy heat cert chemistry, X-ray film, and summary report.

Eight parts were cast (four each of each core design). The results showed excellent casting of most features. After discussions with Alcoa Howmet and Siemens, we believe that a different casting technique known as Intri-casting would be more successful. We intend to explore this further a later phase. The characterization results demonstrated conclusively that Mikro's ceramic cores are fully compatible with the DS casting process and provided initial feedback on the capabilities and limitations of the casting process. All major objectives of this task were accomplished within the estimated time and budget constraints.

Characterize Trailing Edge Cores. All cores were dimensionally characterized at Mikro in the "green" state prior to sintering using mechanical and optical metrology methods. Per the proposal, sintered cores were to be characterized using Digital Shape Sampling and Processing which compares the ceramic cores directly to the solid computer-aided design model. As a cost saving measure, and with DOE approval, the sintered cores were characterized in-house with the same inspection methods used to inspect the green cores. In addition, critical ceramic material properties were tested during the project.

Summary Evaluation of Objectives and Estimate of Technical Feasibility

All major objectives were achieved including the added foundry testing. Technical feasibility was demonstrated by:

1. Radical design: Producing tooling and trailing edge cores embodying revolutionary cooling features that have never been produced before.
2. Reduced time: Five different designs were produced and two were foundry tested within nine months – a fraction of the time it would take with conventional techniques.
3. Reduced cost: Five different core designs were tooled and produced, and two core designs were foundry tested for $100,000 – a fraction of the cost using conventional techniques.

Conclusions and Future Directions

We believe this project demonstrates that the TOMO™ process can lead to revolutionary new turbine cooling designs that can be developed and tested in a fraction of the time using current techniques and at significantly lower cost (better, faster, and cheaper).

Mikro has submitted a proposal for a Phase II Small Business Innovation Research to continue this project. During Phase II we will expand the scope of our investigation and produce full-scale turbine blades with internal cooling passages that are beyond the current state-of-the-art. In support of blade design and production, heat transfer experiments will be conducted and the advanced designs will be modeled and tested with computational fluid dynamics (CFD) software.

Our primary Phase II objectives will be:

- Produce a full-scale advanced turbine blade design and two design variants.
- Perform CFD testing and analysis of the turbine blades.
- Perform bench level heat transfer testing.
- Produce a minimum of three full-scale blades of each design.
- Test the blades using bench level protocols.
- Demonstrate a two-thirds reduction in the overall design-to-production cycle for an advanced turbine blade.

V.B.5 Transpiration-Cooled Turbine Components for High Temperature IGCC Turbines

Timothy R. Stewart
Ultramet
12173 Montague Street
Pacoima, CA 91331
Phone: (818) 899-0236; Fax: (818) 890-1946
E-mail: tim.stewart@ultramet.com

DOE Project Manager: Maria Reidpath
Phone: (304) 285-4140
E-mail: Maria.Reidpath@netl.doe.gov

Subcontractors:
- Pratt & Whitney Rocketdyne, Canoga Park, CA
- Plasma Technology, Torrance, CA

Contract Number: SC0002484

Start Date: July 20, 2009
End Date: April 20, 2010

FY 2010 Objectives

- In conjunction with Pratt & Whitney Rocketdyne (PWR; Canoga Park, California), select an integrated gasification combined cycle (IGCC) gas turbine and turbine component to be modeled and manufactured in the Phase I project.
- Demonstrate the capability to manufacture open-cell foam structures in the shape of a turbine vane using the selected material system.
- Apply, via plasma spray, a porous airfoil skin to the molybdenum open-cell foam airfoil core.
- Assess key flow behavior characteristics of the transpiration-cooled material system for the PWR transpiration-cooled model to assess feasibility of the concept.
- Conclude system design and evaluation and transpiration-cooled modeling performed by PWR.

Accomplishments

- Phase I development successfully demonstrated that a complex two-dimensional vane shape using molybdenum open-cell foam and porous molybdenum skin could be manufactured. Molybdenum was used in Phase I because it offered ease of manufacturing that facilitated both manufacturing and modeling studies as well as the time and budget scope of the project.
- Foam core geometry was easily manufactured to tight tolerances given ease of machinability of the open-cell reticulated vitreous carbon (RVC) foam.
- Plasma sprayed porous coatings containing 8–10% porosity evenly distributed throughout were uniformly applied.
- Pressure drop data were fairly uniform across samples and were shown by PWR analysis to be close to data collected in past transpiration-cooled projects.
- Two molybdenum foam blades were then coated with 0.040" of porous molybdenum. The coated blades were then machined to a final length of 2.0" and saved as demonstration pieces.
- PWR produced a turbine vane airfoil design was that was based on a Siemens power generation turbine, SGT6-5000F, with a power generating capacity of 200 MW_e.
- PWR transpiration code was modified and used to show that the Ultramet material system can be supplied with adequate coolant to efficiently cool a vane in the advanced turbine environment.

Introduction

Power plants using coal gasification, combined cycles, or oxy-fuel cycles are targeting a goal of ≥50% efficiency. Efficient and cost-effective IGCC turbines are directly related to the development of gas turbines with higher firing temperatures and pressure ratios. The key to the successful evolution of gas turbine systems is a strong technology base focused on two critical areas: the introduction of new materials and the usage of transpiration cooling for turbine vane cooling. Using advanced cooling technologies in power turbines has been found to introduce the potential for significantly increased firing temperature without the losses associated with increased cooling air extraction.

In the Phase I project, a low-cost and short lead time process was developed in conjunction with PWR to produce high temperature transpiration-cooled turbine vanes for use as a first-stage nozzle vane in an advanced PWR IGCC turbine engine. IGCC power generation is a cleaner alternative to traditional combustion power plants. Part of this cycle uses a gas turbine to generate electricity by burning syngas produced by the gasifier. New gas turbines in these systems are continuously being pushed to higher

operating efficiencies. The transpiration-cooled vane design demonstrated in Phase I, in which coolant features are integral to the material fabrication, offers the potential to simultaneously lower fabrication costs and increase maximum operating temperature thus meeting the higher operating efficiencies that are desired by the DOE for coal gasification power turbines.

Approach

In Phase I, a transpiration-cooled high temperature first-stage nozzle vane was developed. The core of the vane was formed using structural open-cell foam that defines the interior cooling path, adds structural stiffness and strength, and functions as a template for application of an outer skin with fine, uniform porosity for flow of the transpiration coolant.

A subscale vane was designed based on a current turbine engine selected by PWR, and PWR developed a transpiration cooling model that was based on the foam core porous skin material system. Component specimens were fabricated using a molybdenum foam core with a porous molybdenum skin, and pressure drop data were generated by flowing gas through the foam and porous skin to identify the permeability of the skin and provide crucial data for the transpiration model. Phase I modeling was performed to assess the vane's cooling efficiency and overall efficiency of IGCC engines that could be realized through use of the Phase I transpiration-cooled foam core vane design.

Results

PWR previously worked with Siemens on several versions of a power generation turbine. PWR research showed that the highest performance gas turbine offered by Siemens for power generation is the SGT6-5000F, with a power generating capacity of 200 MW_e and a compression ratio of 17:1. The next generation of these gas turbines is expected to push 20:1 compression ratio, so this was chosen as an arbitrary point on which to base the vane geometry analysis.

The following input parameters for the turbine system were assumed:

- 200 MW_e gas turbine size
- 20:1 pressure ratio (20 atmospheres, maximum pressure)
- Natural gas + oxygen (with CO_2 diluent) combustion (natural gas is close in composition to syngas)
- Maximum hot gas temperature of 3,140°F
- 12-stage power turbine
- Constant two-dimensional vane cross-section (eases manufacture for this proof-of-concept)

Based on the input parameters for this turbine engine, a vane profile was designed by PWR.

The material system for the Phase I project was a molybdenum open-cell foam core with a molybdenum porous plasma sprayed airfoil skin. Although molybdenum is not inherently resistant to a high temperature oxidizing environment, it was selected to establish Phase I feasibility because of its use in Ultramet's previous transpiration-cooled rocket engine development. In the interest of demonstrating that the vane concept could be designed, modeled, and fabricated in the Phase I project, molybdenum, a material with an established legacy, was used. This allowed a more straightforward approach in design and modeling for PWR because material properties for the foam, facesheet, and foam/facesheet composite sandwich structure were already recorded, thus allowing more time for design and analysis and less on new material property data collection.

The foam core was manufactured by producing RVC foam through resin impregnation and pyrolysis of commercially available polyurethane foam. RVC foam is easily machined, and at this stage the vane shapes were produced. The RVC foam vanes were then uniformly infiltrated with molybdenum to 20 vol% dense (80 vol% porous) via chemical vapor infiltration. In this process a uniform molybdenum coating is applied around each ligament through the entire structure, as shown in Figure 1. After foam infiltration with molybdenum, the final step of applying the porous molybdenum facesheet was performed.

Thermal sprayed molybdenum coatings were applied by Plasma Technology (Torrance, CA) to two molybdenum foam turbine vanes. The target thickness of the coating applied to all foam components was 0.040", in accordance with the defined thickness for the turbine vane airfoil skin. Cold flow test molybdenum foam buttons were coated first, and permeability was measured to confirm the data correlated well with data previously generated. Once the permeability was confirmed, Plasma Technology plasma sprayed the molybdenum foam turbine vanes with a 0.040" molybdenum facesheet.

Figure 2 shows the vane component cut to final length. As desired the thickness of the coating was determined to be uniform (±10%) around the perimeter.

Figure 3 illustrates two problems associated with this processing method that were beyond the scope of the Phase I project to address but would be addressed in Phase II. First is the surface roughness, which is not desirable for a vane component with subsonic flow passing over its surface within an IGCC turbine engine. To achieve a smooth airfoil surface, the coating will have to be machined after processing. Second is the sharp trailing edge of the vane. As shown, the

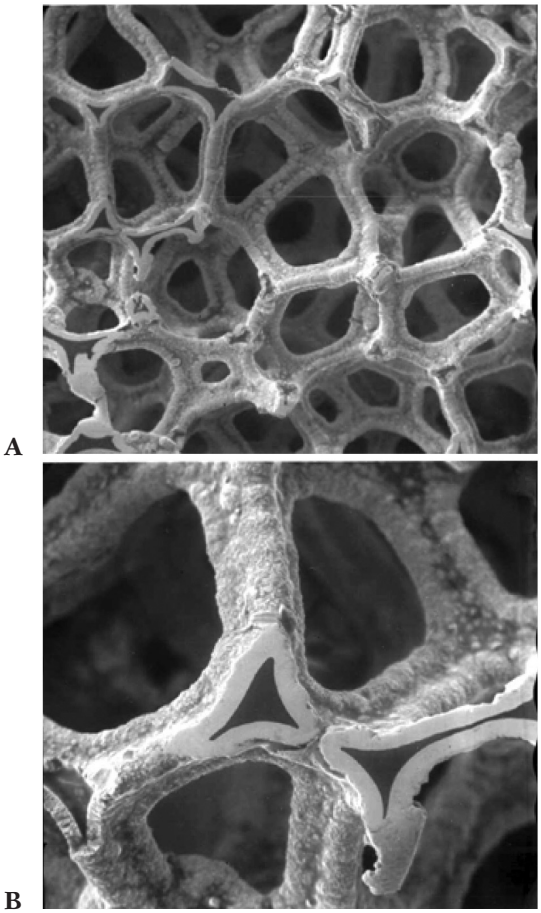

FIGURE 1. Micrographs of 80 ppi Molybdenum Foam

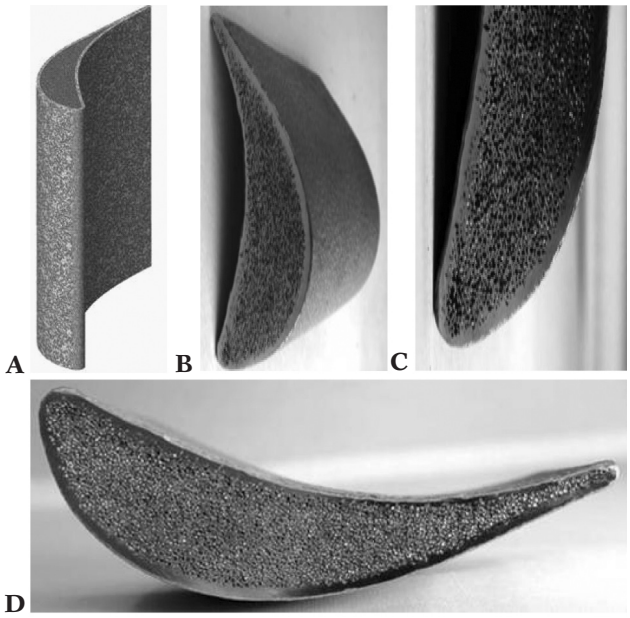

FIGURE 2. Computer-aided Design Rendering (A) and Final Molybdenum Foam Vane (B-D) Coated with Porous Molybdenum Skin after Being Cut to 2.0" Depth (3.0" Chord Length)

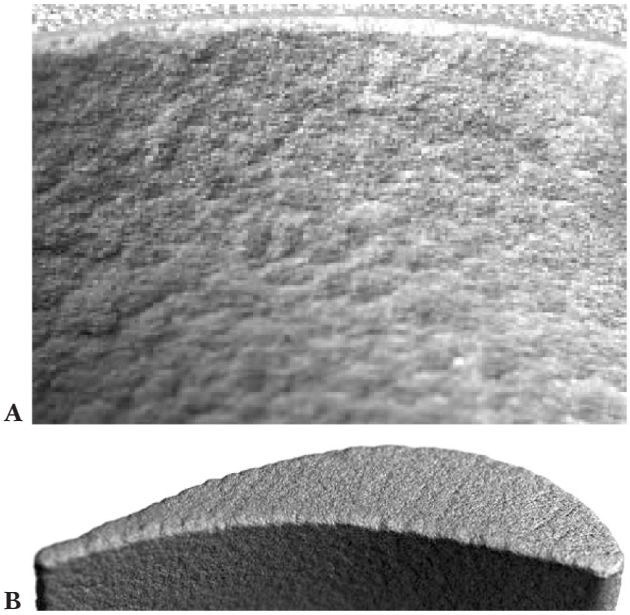

FIGURE 3. Roughness of As-Deposited Surface (A) and Increase in Trailing Edge Radius (B)

plasma spray process rounded the sharp trailing edge of the foam core as more coating was applied. This development is not considered negative, because the machining required to smooth the surface roughness of the coating can also be used to quickly and effectively create the desired sharp trailing edge.

Cross-sectional analysis was performed on pieces cut off the ends of the turbine vane demonstration articles. The molybdenum skin coating applied to the molybdenum foam is shown in Figure 4. As can be seen the molybdenum coating exhibits well-distributed porosity across the thickness. Along with even distribution, the porosity is interconnected, and these two characteristics are essential to the effectiveness of this transpiration cooling concept.

To vary the level of transpiration cooling provided by the plasma spray coating, the thickness can be varied (i.e., a thicker coating for less permeability and vice versa). In this way, the coolant can be directed to flow at a greater rate in areas that require more cooling by making the sprayed coating thinner in those areas.

The PWR modeling showed that a transpiration-cooled turbine vane is an attractive and promising solution to enable higher temperature and higher efficiency IGCC turbines. A notional, higher performance future turbine environment with higher pressure and temperature than the state-of-the-art was defined. A turbine vane airfoil design was produced that is applicable for this environment. The PWR X-Cool transpiration code was modified and used to show that the Ultramet material system (consisting of

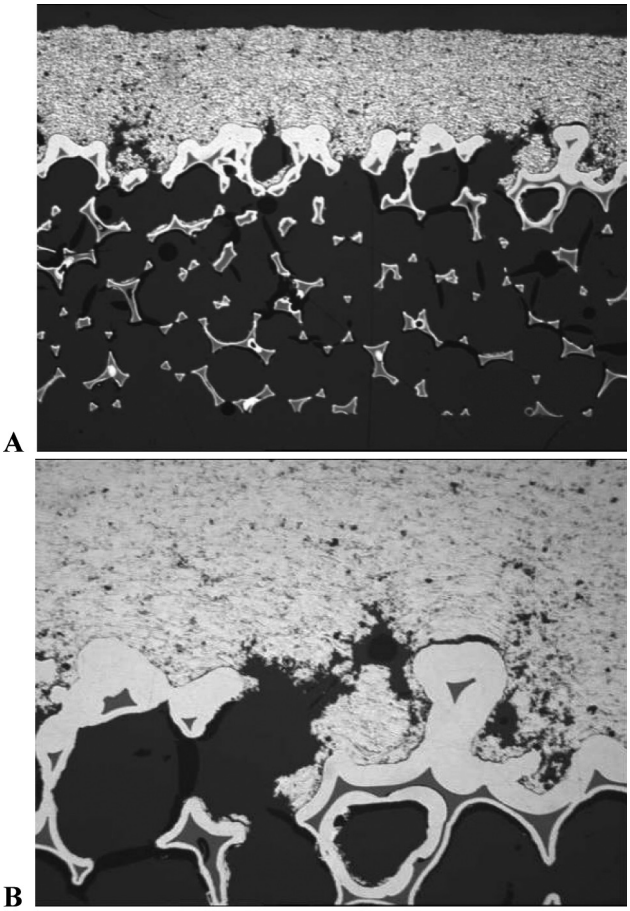

FIGURE 4. Optical Micrographs of Plasma Sprayed Molybdenum Coating Applied to Molybdenum Foam Vane: A, 20×; B, 50×

a thermal sprayed porous skin on a refractory foam substrate) can be supplied with adequate coolant to efficiently cool a vane in the advanced turbine environment. Surface roughness improvement of the thermal sprayed skin will be beneficial as part of Phase II development to minimize the heat flux and the necessary coolant flow to maximize vane efficiency.

Permeability test development specimens, representing the desired foam/porous skin structure, were fabricated and subjected to air flow testing to compare data with those generated in previous work and to support modeling at PWR. By using the measured permeability of the disk samples, the transpiration flow performance of the skin was evaluated for the hot gas transpiration environment. Even though the average permeability was slightly higher than the target, the permeability estimated for transpiration cooling of a vane in a notional advanced turbine environment is even greater. To increase permeability, either a thinner or a more permeable skin is required, both of which are feasible through continued optimization of the thermal spray deposition process.

Conclusions and Future Directions

The goal of Phase I, to establish the feasibility of a transpiration-cooled foam core vane for high temperature/high efficiency IGCC turbines, was clearly established. The results of PWR analysis suggested that relatively minor modifications to the porous skin applied to the foam core in Phase I will yield the thermal behavior required for a high performance vane, and initial development performed at Ultramet supports manufacturability of the structural foam/porous skin design in a vane shape. The Phase I project was concluded in Fiscal Year 2010. Based on the Phase I success and the positive material and modeling development, a Phase II Small Business Innovation Research proposal has been submitted to the DOE.

V. SMALL BUSINESS INNOVATION RESEARCH

C. Manufacturing

V.C.1 Application of Advanced Refractory Metals in Revolutionary Turbine Airfoils

John W. Appleby
Florida Turbine Technologies, Inc. (FTT)
1701 Military Trail, Suite 110
Jupiter, FL 33458-7101
Phone: (561) 427-6470; Fax: (561) 427-6470
E-mail: jappleby@fttinc.com

DOE Project Manager: Robin Ames
Phone: (304) 285-0978
E-mail: Robin.Ames@netl.doe.gov

Contract Number: 85390

Start Date: July 20, 2009
End Date: July 31, 2010

FY 2010 Objectives

- Perform refractory material system survey to determine applicability as gas turbine materials.
- Perform conceptual design and analysis of a refractory metal airfoil shell.
- Perform experimental assessment of refractory metal systems.

Accomplishments

- Florida Turbine Technologies has performed a survey of refractory material systems physical and mechanical properties for incorporation into a design analysis system.
- Environmental stability assessment has been performed using static oxidation testing.
- Conceptual design study performed using refractory metal shell in a spar-shell turbine airfoil construction.
- Subscale shell test article fabricated from refractory metal.

Introduction

Future turbine systems require increased efficiency and fuel flexibility to address problems arising from increased global energy usage and emissions. One approach to improve the efficiency is by increasing the turbine inlet temperature and pressure. These efforts can be undermined, however, as parasitic losses are increased by the additional cooling flow necessary to maintain components at acceptable operating temperatures. The combustion of alternative fuels, including gasified coal, hydrogen and biomass, raises the H_2O content in the working fluid, increasing the heat flux on the components. Contaminants within some of these fuels are also known to cause corrosion damage to substrate materials. The challenge in the design of future turbine systems burning alternative fuels and firing at higher temperatures is, therefore, to retain durable and reliable operation, while reducing cooling flow levels to achieve the improvements in efficiency.

Today's turbine components are typically produced as monolithic castings of high-strength nickel or cobalt-based alloys. The investment casting process allows the formation of passages within a component for cooling. Convective cooling of the inside wall, discharged as film to reduce the boundary layer temperature, and use of thermal-barrier coatings permit the gas-path fluid to be substantially higher temperature than the material capability. The crystalline structure of the cast material is controlled to specific grain boundary structure and orientation; equiaxed, directionally solidified, and single crystal morphologies are tailored such that the resulting component exhibits an acceptable blend of high-temperature strength, corrosion resistance, and low cost.

FTT is developing, in a parallel project, a spar-shell turbine component system to realize the future turbine system goals of reduced cooling flow consumption and increased efficiency. Development of the spar-shell turbine component system offers several advantages relative to the current state-of-the-art.

The concept of a spar-shell turbine component is not new. One example of such a component is described in U.S. Patent #7080971, "Cooled Turbine Spar Shell Blade Construction" by Wilson and Brown. Although development of the spar-shell system has proceeded beyond this patent, namely with respect to attachment features and shell loading, the art reproduced in Figure 1 illustrates the salient elements of this design approach. As shown, the spar-shell design utilizes an internal spar which is surrounded by an external shell. This fabrication approach has several advantages relative to the current state-of-the-art monolithic cast structures. First, the internal spar represents the primary framework of this concept. Since this member is thermally protected by the shell from the hot working fluid passing around the airfoil,

it can be maintained at a relatively low temperature very near that of the coolant. The spar material can therefore be optimized for very high strength at a moderate operating temperature level. Second, since the shell is structurally isolated from the spar, its material can be selected on the basis of high temperature capability. Thermally induced stresses are a primary driver and limiter of existing cooled turbine components. This design approach serves to mitigate the associated effects on low cycle fatigue and thermal-mechanical fatigue distress through both thermal and mechanical isolation of the spar and shell. Further, other desirable thermal attributes, such as the ability to support high temperature and heat flux, can be considered as primary drivers in the shell material selection.

The application of refractory metals in the gas turbine industry is not entirely new, but use has been mostly limited as trace additions to nickel, cobalt, and iron base alloys for strengthening and improving wear resistance. Use in the pure form or as base-metal alloys in the fabrication of airfoil components, however, presents a number of challenges. While they offer extraordinary heat resistance, they are also highly susceptible to oxidation in a flowing air environment, and will require reliable environmental protective coatings. Another consideration is that due to their high melting temperature, conventional investment casting of components is not possible, and that joining processes must be in an inert atmosphere.

Approach

Successful application of refractory materials in future gas turbine components requires a revolutionary approach to the component design, integrated with advanced environmental protective coatings for the refractory metal substrate.

Between the conventional and refractory metals, notable differences are seen in melting point, elevated temperature strength, thermal expansion and thermal conductivity. Components constructed of a high-temperature material then can operate within a gas temperature environment below the material melting point. These parts will have reduced risk in the event of local failure or breakdown of the cooling system or thermally-protective coatings. Materials having greater strength at temperature can be utilized to either carry higher mechanical loads or to reduce the degree of plastic deformation that typically contributes to reduced fatigue life. Lower thermal expansion is of benefit because it results in less thermal stress, thus greater strength margins and fatigue life. Higher thermal conductivity has a similar benefit, reducing thermal gradients that are a normal consequence of cooling by internal convection.

Under this project, FTT will identify potential refractory materials and determine their applicability as gas turbine material candidates. As depicted in Figure 2, this approach follows the *revolutionary* path, making use of very high temperature capability

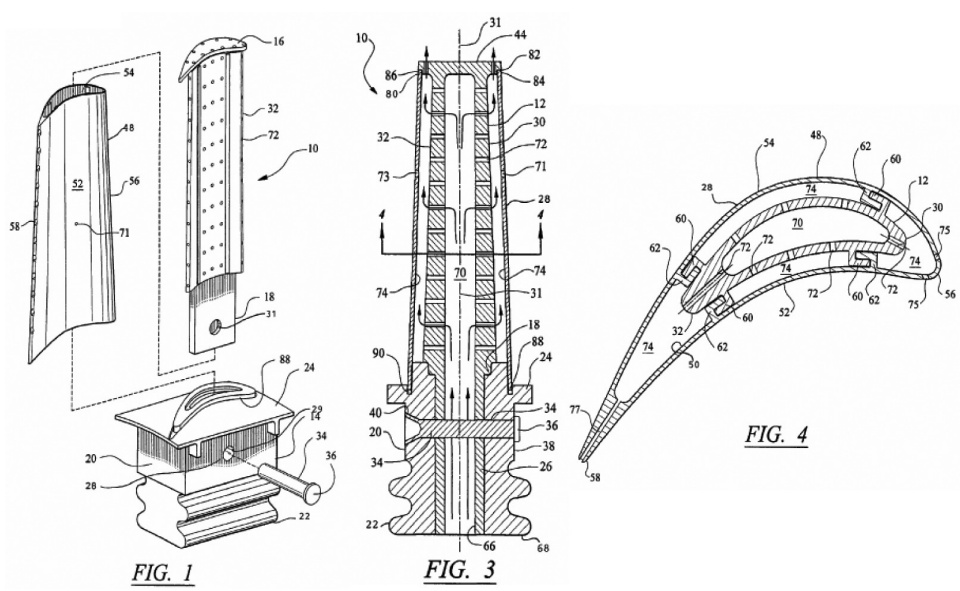

FIGURE 1. U.S. Patent #7080971, "Cooled Turbine Spar Shell Blade Construction"

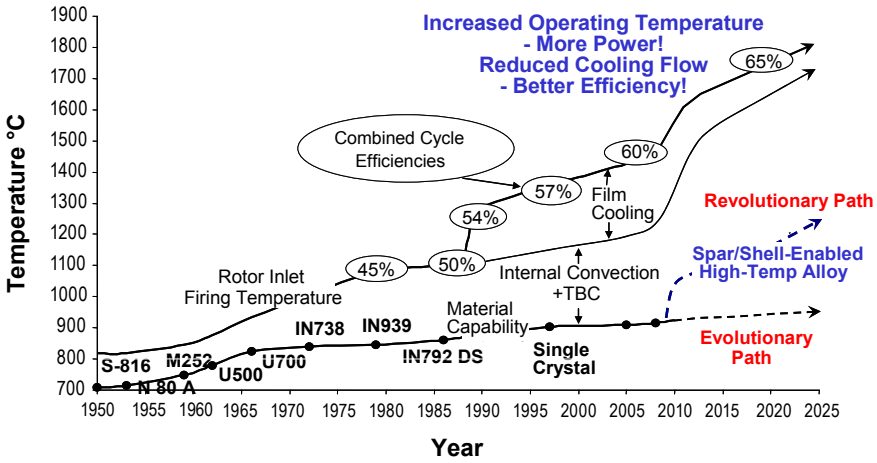

Data up to 1992 based on graph published by Schilke et.al.

FIGURE 2. Refractory Metals Enable Efficiency Improvements with Revolutionary Turbine Airfoils

refractory metals, enabled for gas turbine application by advanced coating systems and innovations in component design, as opposed to the evolutionary path of seeking incremental improvements in conventional materials.

Results

A survey of refractory materials and requirements for environmental protection was performed. This information was integrated into FTT's design analysis system, and a conceptual design was performed using refractory materials in the current spar-shell component design.

Candidate material systems that were commercially available were purchased and processed into laboratory test specimens for evaluation in static and cyclic oxidation studies. Specimens were provided to two coating suppliers for application of environmentally-protective coatings.

Uncoated and coated refractory material specimens were evaluated by static oxidation testing to evaluate coating life and temperature capability of the uncoated system. The evaluation clearly showed that environmentally-protective coatings are required for temperatures below that of engine operation. Environmentally protective coatings performed well up to current engine operating conditions; the extent of FTT's current testing capabilities. Complimentary to this project, FTT has purchased higher capability static furnaces to extend the evaluation to future engine requirements. The new furnace is now being installed.

A subscale shell fabricated from a refractory alloy was fabricated to a representative spar-shell design developed under the complimentary FTT design project as modeled in the Pro/ENGINEER computer-aided design system. The geometry selected for this demonstration was based on a spar which supports the shell from the tip of the airfoil. In this construction, the spar must be inserted through the shell from the tip of the airfoil with a mechanical joint used to fix the spar to an attachment and platform structure. For the purposes of this initial development, an airfoil having constant cross-sectional area was assumed and wall thickness was assumed to be constant from the root of the airfoil to the tip. A photograph of the wire-sliced by electrical-discharge-machining solid airfoil cross-section is shown in Figure 3. Internal geometry was subsequently created in this specimen using the same machining process.

Conclusions and Future Directions

Results from conceptual design analysis and environmental testing work performed during this Phase I Small Business Innovative Research (SBIR) project supports continued development of the technology. FTT has submitted a Phase II SBIR proposal to perform a more extensive materials characterization study, perform environmental and damage tolerant coating evaluation, and support the detailed design of a spar-shell turbine component using refractory materials and advanced nickel intermetallics.

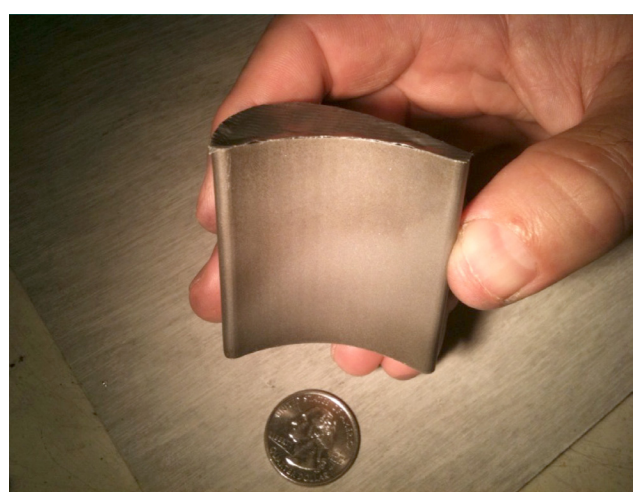

FIGURE 3. Spar-Shell Subscale Test Article with Refractory Material Shell

Beyond the Phase II SBIR, development would consist of fabrication of test articles based on a Phase III SBIR or other funding source. The development project plan culminates in a prototype demonstration of the technology. To facilitate this demonstration, a test in an actual industrial gas turbine engine is proposed to:

- verify the feasibility of the spar-shell concept;
- demonstrate thermally free platforms;
- demonstrate thin-wall structures;
- demonstrate increased manufacturing yields and lower cost with single crystal;
- evaluate advanced airfoil cooling;
- evaluate advanced platform cooling;
- test advanced materials;
- evaluate refractory materials and advanced thermal barrier coatings; and
- evaluate fabricated blade and high speed machining capabilities.

To perform this demonstration, FTT has the expressed commitment of Siemens Energy to test approved engine hardware in their full engine test bed. To be approved for demonstration, the prototype hardware must pass all engineering and design review requirements. This type of test permits the construction of a so-called rainbow wheel where a mix of turbine airfoil configurations, materials and technologies may be installed in a single turbine wheel and be evaluated in a single engine test.

V.C.2 Spar-Shell Cooling Technology Verification and Manufacturing Development

James P. Downs
Florida Turbine Technologies, Inc.
1701 Military Trail, Suite 110
Jupiter, FL 33458-7887
Phone: (561) 427-6250; Fax: (561) 427-6190
E-mail: jdowns@fttinc.com

DOE Project Manager: Robin Ames
Phone: (304) 285-0978
E-mail: Robin.Ames@netl.doe.gov

Contract Number: SC0003574

Start Date: December 7, 2009
End Date: June 6, 2010

FY 2010 Objectives

- Define Spar-Shell risks.
- Develop test strategy.
- Define validation test concepts.

Accomplishments

- Technical risks associated with the Spar-Shell turbine blade have been identified within the context of a full failure modes and effects analysis (FMEA). Results from this task have been used to define mitigation test plans.
- A test strategy has been defined to mitigate the risks defined within the FMEA activity. The defined strategy addresses the significant risk items and formulates an approach to reduce the overall risk through successful validation/verification testing.
- Mitigation tests have been defined in detail including associated test requirements, execution plans and procedures, schedule and estimated costs. These plans will be used to perform the actual validation/verification testing within a follow-on American Recovery and Reinvestment Act Phase II Small Business Innovation Research (SBIR) project.

Introduction

The efficiency of future power production facilities must be increased to address well-known problems of increasing global energy usage and emissions from the combustion of carbon-based fuels. These emissions, carbon dioxide in particular, are increasingly accepted as a significant cause and contributor to global warming. More and more, initiatives to reduce carbon dioxide emissions are being legislated throughout the world. Technology advances within the turbine systems represents an excelled avenue for improving the overall power plant efficiency. In particular, technologies that permit turbines to operate at increased temperatures and pressures are desired to achieve the specific performance goals. Current gas turbine systems already operate at temperature and pressure levels that are sufficiently high to require the use of advanced materials systems and cooling of the turbine components. The use of cooling in the turbine, although permitting turbine components to operate within an environment of high temperature and pressure, causes an efficiency debit to the turbine subsystem and overall power plant. This is a direct result of the needs to compress the coolant to the working pressure of the turbine, and the fact that heat cannot be added to the coolant to provide useful work through expansion in the turbine. Advances of both the materials and cooling systems are clearly required to extend the envelope for improved performance and efficiency in the future systems.

To meet future power generation needs, Florida Turbine Technologies, Inc. (FTT) is developing innovative design approaches to provide highly durable turbine components that require the lowest cooling flow possible. The Spar-Shell turbine blade system enables the use of advanced, high-temperature materials that are not available based on current design philosophies and manufacturing approaches. This SBIR project is focused on verifying and validating this technology and developing the manufacturing techniques that will be required to produce the unique hardware. In addition to providing higher temperature capabilities, features of this system resolve the well-known technical barrier, thermal-mechanical-fatigue. This barrier limits heat flux levels and cyclic life of today's turbine components, particularly at the interface between the main airfoil body and the platform/attachment structure. Further, this architecture facilitates the cooling system to be

optimized to the smallest possible cooling flow by enabling the use of practical and robust near-wall cooling features while minimizing the plugging risk of systems such as those associated with effusion and other porous hole schemes. With this project, FTT has laid out a comprehensive plan for the initial validation of the design and development of manufacturing techniques required to produce hardware. Further, FTT has the full support and backing of a primary original equipment manufacturer, namely Siemens Energy, Inc. with the expressed commitment to evaluate the design within the Siemens Energy, Inc. design review process. Further, upon successful completion of this work, Siemens proposes to demonstrate and evaluate development hardware in a full-scale engine test.

Approach

Spar-Shell Airfoil technology is a transformative approach to turbine airfoil design which leads to a step-change improvement in turbine performance levels and enables the use in industrial gas turbine power plants that use alternative fuels such as gasified coal, hydrogen, and biomass. Over the past several decades, advances in cooling systems and coatings applied to nickel-based "superalloys" have incrementally improved turbine efficiencies and increased power output. Future turbine components, however, will be subjected to increasing levels of heat flux as a result of increased temperature and pressure operating environments. Further, the working fluids of advanced hydrogen, oxy-fuel and alternative fuel applications will have a higher H_2O content relative to conventional power cycles. The combination of these conditions will aggravate thermal-mechanical-fatigue and creep rupture failure mechanisms in current technology turbine components. This problem demands a new approach to turbine airfoil design. FTT's Spar-Shell turbine components are an innovative and game-changing approach to this challenge. The Spar-Shell turbine components will enable future high heat flux applications and improved cycle performance for both future and existing gas turbine power plants.

Public benefits resulting from Spar-Shell cooling technology verification and manufacturing development include the more efficient use of available global resources. As such, worldwide energy inventories can be utilized to better meet current demands and/or to preserve the existing resources for future use. An additional public benefit associated with the use of the proposed new technologies is the reduction of harmful emissions. This results from the fact that improved efficiency requires less fuel to be burned to produce the desired output. Use of the proposed Spar-Shell turbine components is not restricted to current natural gas and oil burning systems. In fact, the proposed technologies are particularly well-suited to technologies that are envisioned for the future. In particular, current Department of Energy (DOE) initiatives to develop energy systems based on the use of abundant national resources, namely coal, makes these technologies particularly attractive for proposed clean-burning power plants fired with coal-based syngas and/or high hydrogen fuels derived from coal.

Work performed under this program is leveraging previous, ongoing, and anticipated research and development funding in this area. This DOE project bridges the gap between initial concept development and commercialization of the technology through full-scale production. Successful completion of the validation test phase of this important project, and ensuring that the technology is ready for full-scale engine testing and commercial application are critical to meeting the goals as set forth within the Fossil Energy (FE) turbine program. This project is incorporating "lessons learned" from predecessor Spar-Shell SBIR effort(s) to finalize the blade and vane designs, fabricate hardware, and provide validation testing to move the technology toward production readiness. The work being performed under this DOE project is targeted to transition the Technology Readiness Level (TRL) from TRL-3 (the level anticipated at the conclusion of the concept designs) to TRL-7 at the end of this project by performing required design verification and validation testing and performing the manufacturing development needed to produce hardware in large-scale quantities. The following paragraphs express the extent to which the project goals were accomplished within the Phase I project.

To better understand the risks associated with the Spar-Shell turbine blade, a full FMEA was completed. The FMEA is a rigorous approach used to define and evaluate all of the possible risks associated with a desired function, in this case a Spar-Shell blade producing shaft power within the engine. To accomplish this, the potential consequences of all of the risk items are considered within the ranking process. For the Spar-Shell design, the entire assembly was broken into 15 distinct regions or interfaces to be considered for possible areas of risk for the Spar-Shell blade system to fail to provide the desired function. For each of the 15 possible risk locations, all of the possible failure modes and the worst case failure mode effects were listed and ranked.

The three rankings that are given to each failure mode are: 1) the likelihood of occurrence of a particular event; 2) the consequence of the potential failure if it occurs; and 3) the detectability that the failure could be identified, preventing the potential consequence. Each of these items is given a value from 1 to 10, with 1 being the lowest likelihood, smallest consequence, or the best chance of detectability

and 10 being the worst case with certain failure event occurring, worst possible consequence and no detectability. Then the values of likelihood, consequence and detectability are all multiplied to give the overall Risk Priority Number, RPN. This risk priority number was used to rate all of the risks and to categorize them into groups consisting of low, medium and high risk. This methodology is shown in Figure 1.

With all of the risks ranked, the risk mitigation plan is created. The prioritization of the risk mitigations are scheduled to reduce the level of risk to the appropriate level as the Spar-Shell project moves from the conceptual design to full engine testing. This insures that the technology readiness level is appropriate for the next step level of investment and effort. The steps that need to be considered include:

- Design and Analysis
- Manufacturing Trials
- Functional Tolerances (i.e.: Flow)
- Component Validation
- System Calibration
- Engine Validation
- Engine Monitoring

These functional steps are used to guide how the tasks should be approached along the design process. With consideration also being given to the risk of each failure mode as advancement toward the next step is being completed. This also leads the Spar-Shell design to a gradual reduction of risk/failure as the project continues from design and analysis, all the way to full-scale engine test and monitoring. The goal of the FMEA at each step will be to reduce the risk to acceptable levels before continuing on to the next step.

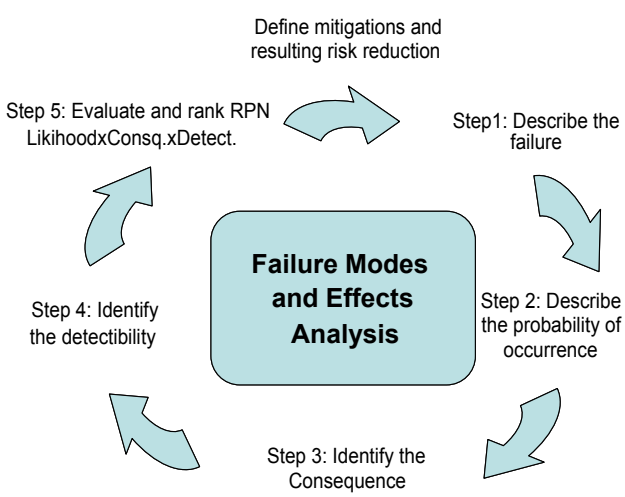

FIGURE 1. FMEA Process and Methodology

Results

During the FMEA activity, there were 70 potential risks identified within the 15 potential risk locations for the Spar-Shell blade design. After identifying the 15 locations and the potential risk associated with each location, the potential failure mode and the worst case effect of each potential failure mode was identified. The rankings of the likelihood of occurrence, the consequence of the potential failure, and the detectability that the failure occurs were now tabulated to come up with the risk priority numbers. These values were then associated into categories of high, medium, and low risk for each location to facilitate risk ranking definition of mitigation test plans.

The data indicates the areas of the design where further design and test activity should be focused to balance and reduce the risk level. The team identified multiple test rigs to mitigate or lower the risk to a sufficient level to move on to the next step. Then these test rigs were tabulated and sorted to determine how many of each of the high, medium and low risks would be treated by the identified test types.

During the Phase I project, an initial manufacturing assessment was performed to determine the feasibility of producing Spar-Shell components using existing machining methods. To accomplish this task, a spar and shell were machined from 410 steel stock using the well-known non-conventional electrical discharge machining (EDM) by wire method. 410 steel was selected for this study because: 1) it is available; 2) it is dimensionally stable; and 3) its EDM machining characteristics and room temperature strength are similar to the nickel-based superalloys used in gas turbine components today. The geometry produced in this trial was derived from the ongoing Phase II SBIR project titled: High Temperature Capability and Innovative Cooling with a Spar-Shell Turbine Blade (DE-FG02-07ER84668). This geometry contains a light weight external shell having integral hooks, and a separate internal supporting spar having mating hooks. This trial was successful and the results are shown in Figure 2. Dimensional accuracy of these parts was verified using the white-light scanning technique with results indicating this trial produced parts having good surface finish and acceptable manufacturing tolerances that permitted the two pieces to be assembled after machining.

Conclusions and Future Directions

This Spar-Shell Cooling Technology Verification and Manufacturing Development project is one part of a well-integrated plan to develop Spar-Shell turbine components. Figure 3 shows the key elements in the overall technology development roadmap. As shown, the roadmap represents a systematic approach to

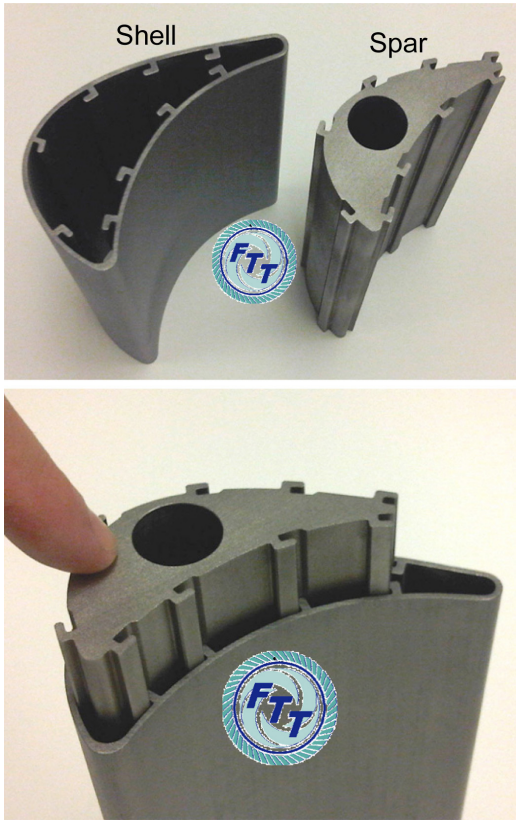

FIGURE 2. Spar-Shell Manufacturing Feasibility Demonstration

product development, progressing from a TRL of 2 (conception) through 8 (production-ready) utilizing various funding sources as appropriate. One of the key elements includes the development of a Spar-Shell rotating turbine blade which is currently supported by a DOE-funded Phase II SBIR project[1]. Additional SBIR Phase I activities are currently in place to:

a. Design a static Spar-Shell turbine vane (DE-SC0002713).
b. Provide for Spar-Shell technology and associated advanced materials validation and demonstration through rig and full-scale engine tests per the subject Phase I and proposed Phase II follow-on projects.
c. Identify and develop next-generation materials that are enabled by Spar-Shell technologies to realize the full technology potential (DE-SC0002450).

Finally, in support of DE-SC0002450, Oak Ridge National Laboratory is currently on contract to provide materials development and characterization testing for the next-generation materials under investigation in c) above.

While the Phase I SBIR project defined the potential risks, risk mitigation plans and initial validation test requirements, the primary technical objective of the work proposed for a Phase II follow-on

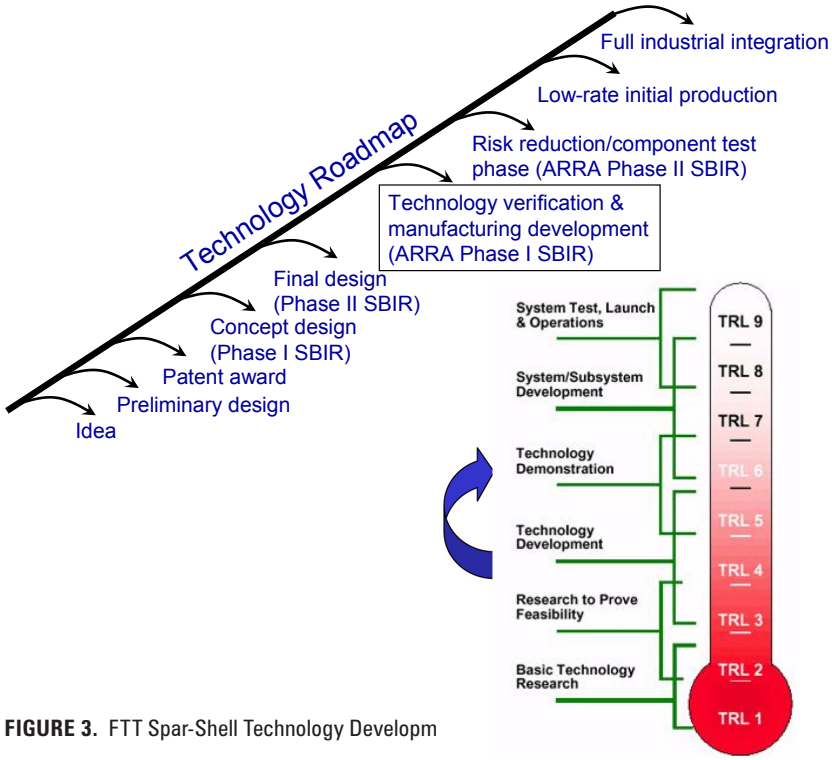

FIGURE 3. FTT Spar-Shell Technology Developm

[1] DE-FG02-07ER84668, High Temperature Capability and Innovative Cooling with Spar-Shell Turbine Components

project will be to carry out the plans as laid during the Phase I project to validate the technology and clear the hurdles to begin the transition to commercialization of Spar-Shell turbine component products. A key objective of the overall Spar-Shell development project is to permit the hot section components to operate within the limitations of their material capabilities while requiring a minimum quantity or flow rate of cooling air flow. This requires the development and validation of Spar-Shell systems to maximize the efficiency.

V.C.3 Advanced Laser Machining Techniques for Cooling Holes in Gas Turbines

Dr. John Steinbeck (Primary Contact),
Dr. Frederick Lauten
Physical Sciences Inc.
20 New England Business Center
Andover, MA 01810
Phone: (978) 738-8148; Fax: (978) 689-3232
E-mail: steinbeck@psicorp.com

DOE Project Manager: Robin Ames
Phone: (304) 285-5436
E-mail: Robin.Ames@netl.doe.gov

Contract Number: SC0003400

Start Date: December 7, 2009
End Date: September 30, 2010

FY 2010 Objectives

- Design, build and demonstrate a module that can be attached to a commercial laser cutting head and deliver more than 50% of the output laser energy to the surface of a work piece through a low pressure stream of water.
- Demonstrate that 0.020" holes can be successfully drilled into 0.050" thick Inconel 718 sheet using a water-guided laser in less than 3 sec at elevation angles to 20° from the work piece surface.
- Demonstrate the airflow through 10 cooling hole arrays drilled using water-guided laser drilling varies by less than ±5%.
- Show that the microstructure of the walls of the holes contains no microcracks and that debris generated by the drilling process is not deposited on the walls of the holes or forms a ridge on either the entry or exit holes.
- Develop an improved module design that can be used to improve airflow uniformity to better than ±2% and can be mounted on a commercial laser machining system.

Accomplishments

- Designed, built and tested a water guiding laser drilling module for a commercial pulsed Nd:YaG laser cutting head.
- Successfully used water-guided laser drilling to drill 0.018" diameter holes at elevations to 40° in 0.005" stainless steel.
- Successfully used water-guided laser drilling to drill 0.18" diameter through holes in 0.050" Inconel 718 substrates at normal incidence and at 45° elevation.
- Successfully demonstrated hole drilling in 0.050" Inconel 718 at rates exceeding 3 sec/hole.
- Successfully adapted the water guiding laser drilling head to a YLR-1000-SM fiber laser cutting system.

Introduction

The generation of a boundary layer to protect gas turbine components from hot combustion gases is critical to enable combustion gas temperatures to approach or exceed the melting temperature of the alloys used in gas turbine systems. The air used to create the boundary layer is supplied through cooling holes drilled into individual turbine components. Current methods for drilling cooling holes balance the cost of drilling with the air flow performance of the cooling holes. These methods currently produce cooling holes with air flow variations of ±10% so that more than the minimum number of cooling holes must be drilled into components to ensure that the gas turbine can meet its operational specifications. Physical Sciences Inc. (PSI) is developing a reliable low cost water-guided laser drilling process for drilling the tens of thousands of holes needed in gas turbine systems. The process will improve air flow variations to less than ±2% enabling air previously needed for boundary layer cooling to be redirected through the flow path to increase the fuel efficiency of turbine systems.

PSI's water-guided laser drilling technology can be integrated onto existing laser machining platforms to enable rapid transition to gas turbine manufacturing. The method is applicable to all high temperature alloys used in gas turbine systems. Hole size may be adjusted by changing the size of the water stream for percussion (stationary) drilling or by adjusting the path of the beam for trepanning (circumscribed drilling).

Approach

Water-guided laser drilling uses a high pressure stream of water as an optical waveguide to direct a high energy laser beam to the work piece to be drilled. A schematic is shown in Figure 1. The diameter of the

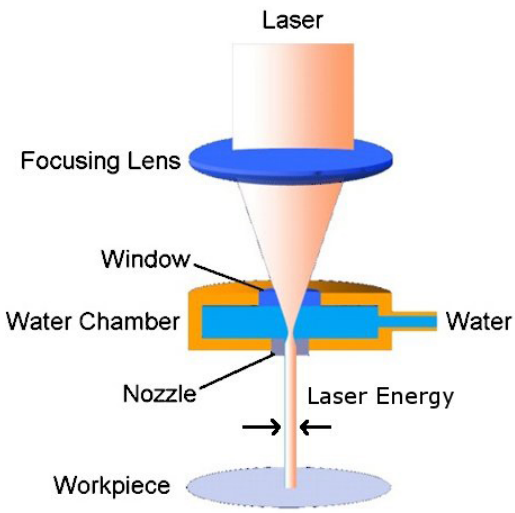

FIGURE 1. Schematic of the water-guided laser drilling system. The module comprises the water chamber, window and nozzle assembly.

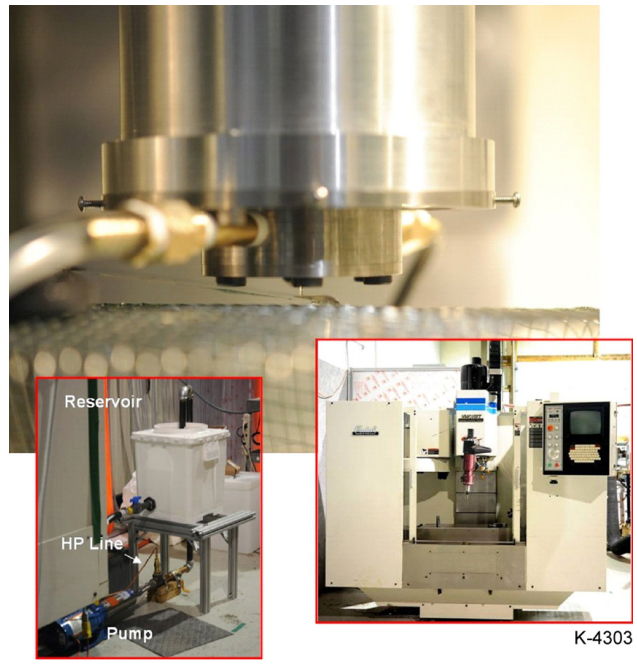

FIGURE 2. Water-guided laser drilling system built at PSI. The water-guided laser drilling head is mounted on a Fadal 15 XCT machining system. Water is supplied to the head by a separate pumping and degassing system.

water stream defines the diameter of the hole since all of the laser energy will be contained within the stream. The diameter of the water stream can be maintained for distances exceeding 100 mm, making the water guided laser drilling technique less sensitive to the absolute position of the work piece from the laser cutting head than laser drilling techniques that use lenses to focus the drilling laser. The high pressure water stream will be more effective than high pressure gas for purging debris from the hole **thereby reducing or eliminating the need for post drilling deburring**. In addition, water-guided laser drilling will impede over-drilling when drilling cooling holes in blades and vanes where the surface being drilled will be close to the backside of the part.

Results

During the Phase I project PSI successfully designed, built and tested a water-guided laser drilling head that was fitted to PSI's prototype in-house laser machining system as shown in Figure 2. The system uses a JK702H Nd:YaG laser for machining/drilling operations. We successfully demonstrated water-guided laser drilling processes using this system on stainless steel and Inconel 718 and have designed a second generation water-guided laser drilling head to overcome deficiencies in our Phase I design.

We successfully used the water guiding laser head to drill holes in 0.050" Inconel 718 alloy at rates exceeding 3 sec/hole at normal incidence. An example of a successfully drilled hole is shown in Figure 3. The entry and exit sides of the hole show little recast material about their periphery compared to drilling

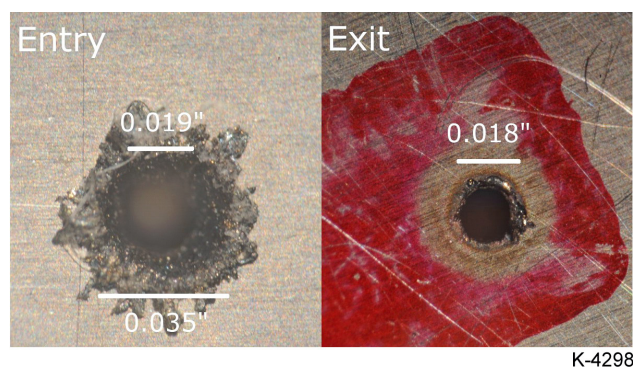

FIGURE 3. Successful hole drilling through 0.050" Inconel 718. Holes are drilled at rates exceeding 3 sec/hole.

processes using similar power density pulsed lasers and gas purging. Reduction of recast debris on the drilled hole is the primary goal for improving the predictability of cooling air flow through the cooling holes in a gas turbine system. Reduction of the recast can eliminate post drilling deburring processes that have been identified as an important contributor to air flow variation.

During the Phase I project we also successfully coupled the water-guided laser drilling head to a YLR-1000-SM fiber laser system. This single mode laser can be focused to spot diameters of 0.002" that will enable improved coupling of the laser to the water

stream and potentially reduce the amount of laser energy required to drill holes in high temperature alloys using trepanning techniques. We successfully coupled the fiber laser into water streams with a diameter as small as 0.010" and showed that drilling processes are possible. Limitations in the optical system of the prototype water guided laser drilling head prevented drilling through 0.050" Inconel 718 material. We are currently implementing improvements to our design to over come this limitation.

Conclusions and Future Directions

PSI continues to develop the water-guided laser drilling process by improving the hardware design. We will develop a second generation water-guided laser drilling head during Phase II that will improve the coupling between the laser and the water stream. An illustration of the concept head is shown in Figure 4. The improved coupling will increase the rate at which holes can be drilled as well as expand the process envelope to reduce the debris remaining in and around the drilled holes.

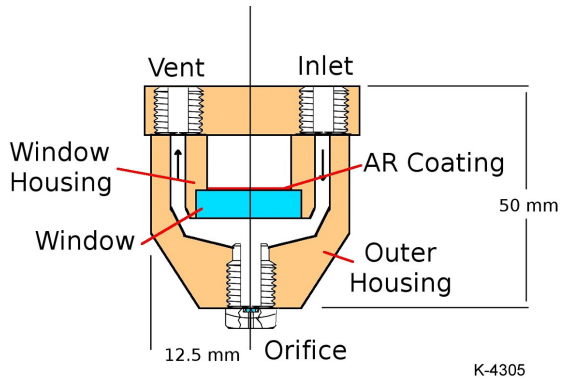

FIGURE 4. Next generation water-guided laser drilling head concept. Compact design and improved optical path will increase the process envelope.

The Phase II plan also includes tasks to develop plans to transition the water-guided laser drilling process to a commercial laser drilling system. Water-guided laser drilling trials on turbine components will be performed during Phase III.

V. SMALL BUSINESS INNOVATION RESEARCH

D. Thermal Barrier Coatings

V.D.1 Novel Coating Methods for Unique TBC/Bond Coat Architectures for Elevated Temperature Operation

D.D. Hass (Primary Contact), B. Gogia
Directed Vapor Technologies
2 Boar's Head Lane
Charlottesville, VA 22903
Phone: (434) 977-1405; Fax: (434) 977-1482
E-mail: derekh@directedvapor.com

DOE Project Manager: Mark Freeman
Phone: (412) 386-6094
E-mail: Mark.Freeman@netl.doe.gov

Subcontractors:
- Brian Gleeson, University of Pittsburgh, Pittsburgh, PA
- Andrew Nix, University of West Virginia, Morgantown, WV

Contract Number: SC0002495

Start Date: July 20, 2009
End Date: April 19, 2010

FY 2010 Objectives

- Demonstrate the deposition of the chosen high temperature thermal barrier coating (TBC) system using appropriate processing approaches.
- Characterization and performance analysis of TBC system in a simulated combustion environment.

Accomplishments

- TBC systems consisting of a dense, directed vapor deposition (DVD) deposited, γ/γ'-based bond coat and a bi-layered 7 mol% yttria-stabilized zirconia (7YSZ)/multi-component hafnia top coat were successfully created having the desired coating microstructure and composition.
- DVD deposited TBC systems were successful tested in a jet engine thermal shock (JETS) thermal gradient test (surface temperature = 1,400°C).
- A TBC system consisting of a DVD γ/γ' bond coat and a DVD 7YSZ layer was tested in cyclic oxidation at 1,150°C for 500 hours without any failure.
- Thermal conductivity testing of the DVD multi-component hafnia top coat was performed in a laser-based testing rig at the National Aeronautics and Space Administration (NASA) (collaboration: Dongming Zhu at NASA) indicating a thermal conductivity of 0.8 W/m-K. This value is similar to conventionally applied TBCs in use on land-based turbine components.

Introduction

Concerns over the use of domestic energy supplies and the desire to reduce CO_2 emissions have driven increased interest in the use of alternative fuels (such as coal "syngas"), as well as interest in alternative engine cycles. This has led to the increased use of an integrated gasification combined cycle, or IGCC, which turns coal into synthesis gas and then removes impurities from the coal gas before it is combusted. The result is lower emissions of sulfur dioxide, particulates and mercury and improved efficiency compared to conventional pulverized coal as well as good energy efficiencies (typically ranging from 35 to 45%). Long-term DOE Turbine Program goals, however, are targeting efficiencies greater than 50%, with the largest efficiency gains believed to be achievable by increasing the engine inlet temperatures (perhaps as high as 1,500°C (2,732°F) [1]. These temperatures are anticipated to drive the need for significant advances in the methodologies used to operate turbine engines at highly elevated temperatures.

Key areas for the management of the thermal load on IGCC turbine components are the development of advanced turbine engine materials, turbine component cooling concepts and high-temperature coatings. This may include the development of higher temperature alloys or ceramic materials, the incorporation of directionally solidified and single crystal turbine blades, the making of airfoil components with internal cooling conduits to allow injected compressor discharge air to decrease the component temperature and the use of TBCs to provide thermal protection. Most of these approaches, however, have limitations. For example, the use of cooling air reduces engine efficiency, directionally solidified and single crystal blades are difficult to manufacture for large industrial gas turbine (IGT) blades and the development of higher temperature replacement materials for the nickel-based superalloy components is both costly and challenging. Of the alternate strategies for higher engine inlet temperatures, the highest potential near-term gain is from exploiting the insulating abilities of TBCs [2]. Thus, the development of highly durable TBC materials and architectures that can withstand high thermal

loads is of critical importance to advanced power generation system designs.

Approach

For advanced IGCC applications, TBC systems must also survive higher temperature exposures of the top and bond coats, as well as, the unpredictable TBC loss at airfoil leading edges due to erosion from engine contaminants. In these engines, complex gaseous environments are also created during the conversion of fossil fuels that result in both oxidizing, sulfidizing and water vapor containing conditions. The multi-oxidant process environments are often non-equilibrium and can vary in degree of aggressiveness. Thus, TBCs used in these situations must be resistant to an oxidizing-sulfidizing environment. In addition, TBCs in IGCC turbines can also experience deposition of contaminants (primarily Fe_2O_3) which penetrate into the TBC porosity and degrade TBC performance. To achieve the desired performance in these operating environments will require improvements to the current TBC materials and architectures. Key attributes required include:

1. Reduced substrate/coating interaction.
2. Higher temperature capability of TBC bond coat (reduced thermally grown oxide growth rate).
3. Improved thermal protection.
4. Reduced susceptibility to sintering, phase de-stabilization and creep.
5. Resistance to environmental effects (hot corrosion and erosion resistance).

Our approach to resolving the above issues for IGCC TBCs is to develop novel TBC processing approaches that enable the creation of TBC systems consisting of advanced materials and architectures for use on nickel-based superalloy components.

Results

Work during the Phase I Small Business Innovation Research project has sought to develop advanced TBCs having enhanced temperature capability and durability in an IGCC environment. Novel coating materials, unique coating architectures and the advanced processing approaches required for their application have been used to meet these goals. Coatings in this work were deposited using a high rate DVD approach (Figure 1). DVD provides the technical basis for a flexible, high quality coating process capable of atomistically depositing dense or porous, compositionally controlled coatings onto line-of-sight ***and*** non line-of-sight regions of engine components. Unlike other physical vapor deposition approaches, DVD is specifically designed to enable the transport of vapor atoms from a source to a substrate to be highly controlled. To achieve this, DVD technology utilizes a trans-sonic gas jet to direct and transport a thermally evaporated vapor cloud onto a component. Typical operating pressures are in the 1 to 50 Pa range requiring that only fast and inexpensive mechanical pumping need be used resulting in short (several minutes) chamber pump-down times. In this processing regime, collisions between the vapor atoms and the gas jet create a mechanism for controlling vapor transport. This enables several unique capabilities including, high rate deposition, non line-of-sight deposition and controlled intermixing during multiple source evaporation.

The results to date have indicated that the chosen processing techniques used to apply the novel coating compositions and architectures are effective at creating durable TBC systems which have enhanced

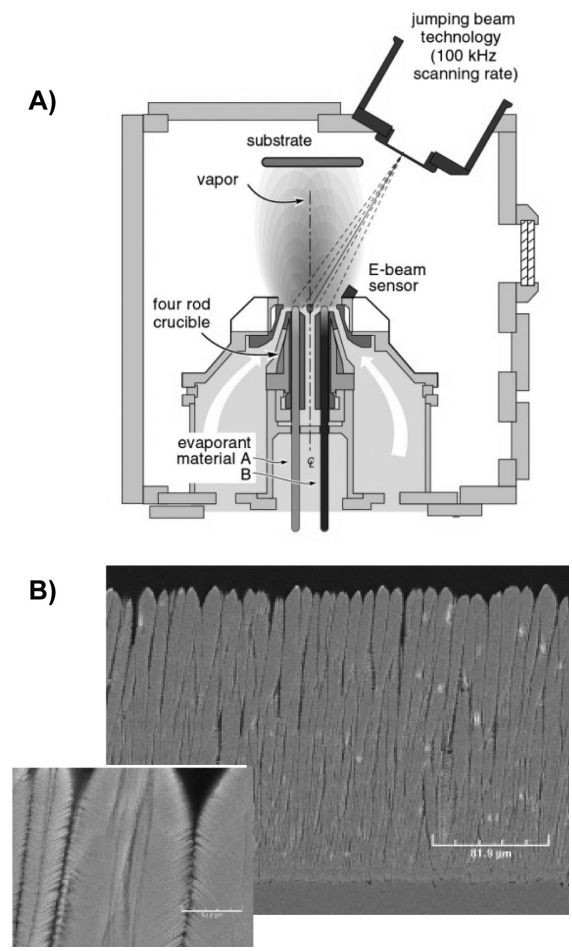

FIGURE 1. A) Schematic illustration of the DVD system. Shown is the use of multi-source evaporation to deposited alloy compositions. B) Scanning electron microscopy (SEM) cross-sectional images of a multi-component YSZ coating deposited using the directed vapor deposition approach. The coating has a strain tolerant columnar microstructure with finer intra-columnar porosity aligned nearly parallel to the heat conduction path.

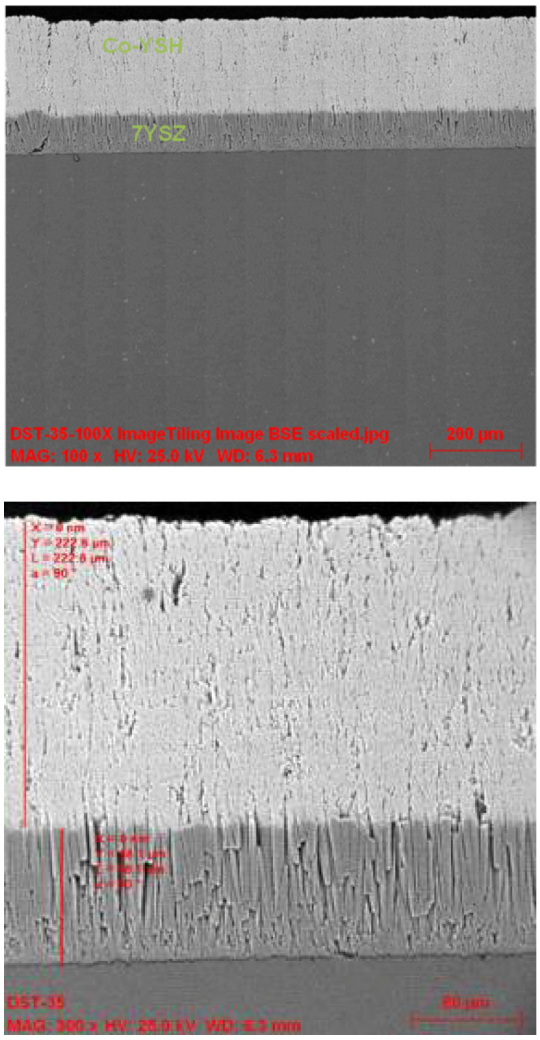

FIGURE 2. SEM images showing the microstructure of a bi-layered top coat having an initial layer of 7YSZ and a secondary layer of multi-component hafnia. The entire top coat was deposited in a single processing sequence.

temperature capability and thermal protection. Key results include:

1. The creation of TBC systems consisting of a dense, DVD γ/γ' bond coat and a bi-layered 7YSZ/co-doped hafnia top coat (Figure 2). The hafnia-based TBC top coat compositions have excellent high temperature capability [3].
2. The successful testing of the DVD TBC systems in a JETS thermal gradient test (surface temperature = 1,400°C), Figure 3, demonstrates the effectiveness of such systems when exposed to high temperatures and thermal gradients. Coatings in this test were exposed to a surface temperature of 1,400°C for 20 seconds with the backside of the substrate held at 700°C. A total of 2,000 cycles were completed before the test was interrupted. No signs of coating damage were observed.

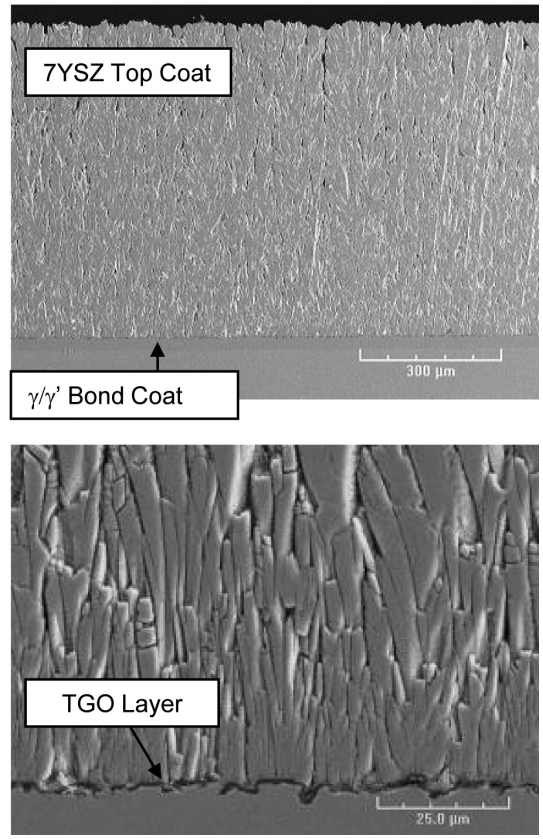

FIGURE 3. SEM images showing a 25 mil thick, 7YSZ top coat and γ/γ' bond coat following 2,000 cycles (20 sec in duration) in a thermal gradient JETS test. The surface temperature was 1,400°C and the substrate backside was 700°C.

3. Demonstration of a TBC system consisting of a DVD γ/γ' bond coat and a DVD 7YSZ layer. A 500 hr cyclic exposure at 1,150°C was administered without any failure. The planar, well adhered alumina oxide scale is observed to form on the DVD bond coat which promotes top coat adhesion and resistance to coating spallation during cyclic exposure. The thickness of the oxide scale following the 500 hr exposure was similar to that observed on bulk coating alloy experiments indicating the effectiveness of the deposition process in obtaining the desired coating chemistry.
4. Thermal conductivity testing of the DVD co-doped hafnia top coat in a laser-based testing rig which demonstrated a low thermal conductivity of 0.8 W/m-K, Figure 4. The thermal conductivity compares well with existing TBC materials used in land-based turbine applications. The measured thermal conductivity remained constant during 12 hrs of testing at 1,450°C indicating good resistance to sintering induced microstructural modifications.

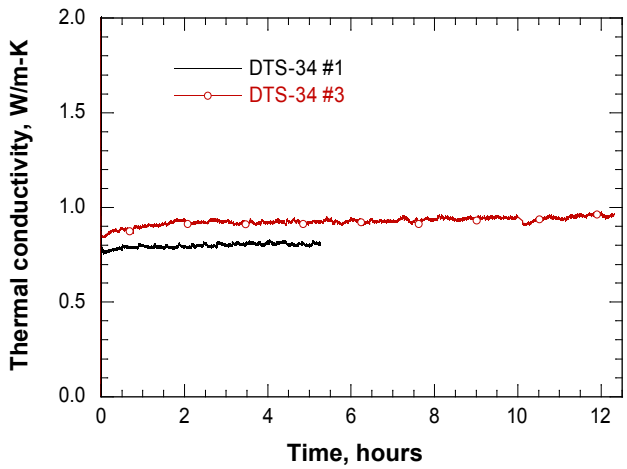

FIGURE 4. Plots showing the thermal conductivity of DVD deposited, multi-component hafnia top coats as a function of exposure time ($T_{surface}$ = 1,450°C) in a NASA laser rig test. The thermal conductivity was 0.8 W/m-K for sample DTS-34 #1 and 0.9 W/m-K for sample DTS-34 #3. The lack of change in the thermal conductivity with time is evidence of the good sintering resistance of the chosen material and the good durability of the TBC (crack formation within the TBC will alter the thermal conductivity).

Conclusions and Future Directions

Work during the Phase I project demonstrated the feasibility of effectively depositing advanced TBC systems needed for use in high-temperature IGCC environments. Based on these results, a Phase II proposal has been submitted in which the following work is planned:

1. Optimization of the processing approaches used to create the compositionally and architecturally advanced TBC systems.
2. Demonstrate the deposition of the chosen high-temperature TBC system using appropriate processing approaches.
3. Characterization and performance analysis of TBC system in a simulated combustion environment.
4. TBC application onto IGT component.
5. Identify commercialization pathways for the develop TBC technology.

FY 2010 Publications/Presentations

1. D.D. Hass, S. Eustis and B. Gogia, "Novel Processing Approaches for Advancecd Thermal / Environmental Barrier Coatings," Aeromat 2010, Bellevue, Washington, June 2010.

References

1. W.P. Parks, W.Y. Lee, and I.G. Wright. Final Report for U.S. Government contract DE-AC05-84OR21400.

2. A. Maricocchi, A. Bartz, and D. Wortman, *Proceedings of the Thermal Barrier Coatings Workshop*, NASA CP 3312 (1995), P. 17.

3. D. Zhu et al., NASA/TM – 2005-213444.

V.D.2 FARADAYIC ElectroPhoretic Deposition of YSZ for Use in Thermal Barrier Coatings

Heather McCrabb (Primary Contact),
Joseph Kell
Faraday Technology, Inc.
315 Huls Drive
Clayton, OH 45315
Phone: (937) 836-7749; Fax: (937) 836-9498
E-mail: heathermccrabb@faradaytechnology.com

DOE Project Manager: Mark Freeman
Phone: (412) 386-6094
E-mail: Mark.Freeman@netl.doe.gov

Subcontractor:
University of Dayton Research Institute, Dayton, OH

Contract Number: 84202

Start Date: June 27, 2005
End Date: August 6, 2010

FY 2010 Objectives

- Optimization and validation of the FARADAYIC Electrophoretic Deposition (EPD) process for deposition of thermal barrier coatings (TBCs) with the appropriate microstructures to prevent coating failure during standard and accelerated turbine engine operation in natural and syngas environments.
- Development and validation of a post-deposition thermal treatment for the EPD coatings to preserve the necessary microstructure to maintain coating durability and reliability during operation.
- Qualification of coating durability and reliability through appropriate tests of merit, e.g. thermal stability, thermal cycling, thermal conductivity, etc.

Accomplishments

- Demonstrated that the FARADAYIC EPD process can reduce surface roughness and hydrolysis related coating defects observed during conventional EPD.
- Post processing of the coatings deposited by the FARADAYIC EPD process are porous and laminar and do not show a change in phase, remaining in the tetragonal state.
- Long-term thermal cycling data showed that the FARADAYIC EPD process can produce coatings that survive in excess of 300 cycles on bond-coated Haynes 230 substrate with cycles consisting of: room temperature → 1,100°C (1 hour hold) → room temperature (15 minutes, forced air) → repeat.
- Cross-sections of samples showed that samples produced with lower duty cycles exhibited less hydrolysis-related defects and smoother, more uniform surfaces.
- Demonstrated that FARADAYIC EPD process does not significantly reduce cooling hole diameter during TBC deposition.
- Executed a contract with an interested party to conduct component testing in a simulated turbine environment.
- Designed and began construction of a deposition cell for components for a simulated turbine environment.

Introduction

The design and manufacturing of gas turbine engines is challenging from both an engineering and material science standpoint due to the engine's high rotational speeds and high operating temperatures. Component failure stems from several sources including corrosion due to hot gases contaminated with chloride and sulfate, oxidation in an enriched oxygen environment, mechanical wear and erosion. Additionally, the components experience extreme temperatures, constant thermal cycling and thermal shock. Turbine blades are especially susceptible to damage, requiring routine maintenance for repairs, refurbishing or replacement. TBCs are employed to protect the turbine engine components. These coating systems provide thermal, oxidation and mechanical protection, reduce thermal gradients and lower the metal substrate surface temperature, extending the life of the engine components.

Faraday is developing a new manufacturing process, the FARADAYIC EPD process, for TBC deposition of yttria-stabilized zirconia (YSZ) onto gas turbine components. It should be noted that EPD can deposit any material that can be manufactured in submicron powder form, thus it is not restricted to YSZ and would be suitable for new TBC material sets that have lower thermal conductivity necessary for increased turbine operating temperatures. The FARADAYIC EPD process combines conventional EPD with pulsed electric fields to induce migration

of charged particles in a suspension to uniformly deposit the TBCs onto the gas turbine components. It is a non-line-of-sight process, making it suitable for coating complex shaped components with a TBC of controllable thickness and a microstructure that is sufficiently strain tolerant to survive in the turbine environment.

Approach

Conventional EPD is similar to electrolytic deposition except that the deposited particles do not undergo a valence change during deposition. Conventional EPD involves charging the particles in suspension, applying a direct current electric field induced migration of the particles toward the oppositely charged component to be coated and deposition and adherence of the particles onto the component. Conventional EPD has the benefits of fast deposition rates, non-line-of-sight deposition, simple deposition equipment, low levels of contamination and reduction of waste relative to dipping or spraying processes.

The FARADAYIC EPD process combines conventional EPD with pulsed electric fields to induce migration of charged particles in a suspension to uniformly deposit the TBCs onto the gas turbine components. Figure 1 shows a schematic drawing of a FARADAYIC pulse reverse electric field used to electrically mediate the applied electric field during the FARADAYIC EPD process.

The application of a coating using conventional or FARADAYIC EPD results in a loosely bonded layer of coating particles defined as a green coating. A post-processing thermal treatment is required to transform the green coating into its final form. Since the green coating has limited strength, the post-processing methods must be controlled from several aspects, including care in handling, exposure to contaminants, and elapsed time between operations. The approach for the post-processing of EPD coatings is to establish the requirements for a coating system in terms of thickness, grain morphology, thermal properties and bond strength to the substrate. There are a variety of post-processing methods that are applicable to EPD methods; for TBCs, Faraday is investigating thermal sintering as well as alternative techniques such as directional heating, microwave and infrared sintering. The priorities for a post-deposition process are as follows:

- Establishment of a quality bond between the coating layer and the bond coated substrate material.
- Diffusion, densification, and consolidation to the required percent theoretical density.
- Preservation of the coating and substrate microstructures.
- Control of the dimensional thickness.

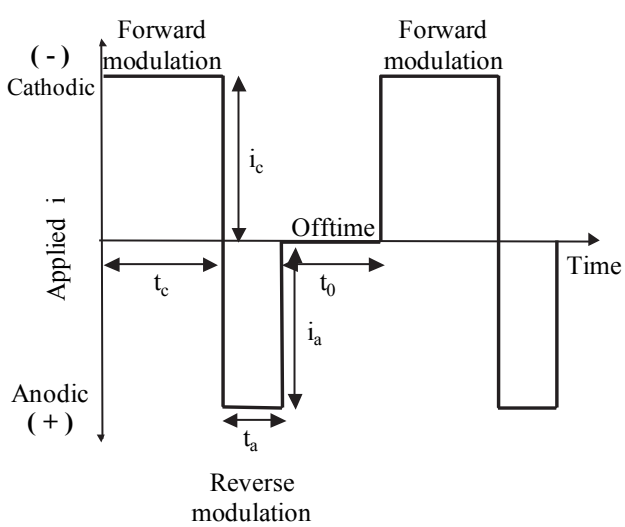

FIGURE 1. FARADAYIC Electric Field

Results

Faraday is performing deposition experiments with bond coated IN939 and Haynes 230 button samples supplied by Siemens Power Generation, Inc. in Orlando, Florida. The substrate alloys are formulations currently used in the turbine engines and the bond coat is sufficiently rough enough to enable the adhesion of the YSZ particle applied using EPD. A benchtop EPD system that includes an EPD deposition cell, a TEGAM arbitrary waveform generator, a Kepco bipolar power supply/amplifier, a Sears multimeter, and a Fluke oscilloscope was assembled for the deposition experiments.

Coatings were deposited from a suspension of YSZ particles suspended in ethanol. Organic dispersants and binders were used to charge the particles and enhance the green coating adhesion. Scanning electron microscopy (SEM) analysis of a cross-section of the green coating suggests that the microstructure is porous and laminar with intermittent microcracks that should provide a low thermal conductivity (Figure 2). The currently optimized EPD coatings are ~110 µm thick and the coating porosity is estimated at ~40% (yielding an approximate density of 60% of the theoretical density of YSZ).

Faraday has also continued to develop the post deposition thermal treatment process to consolidate the EPD green coatings and increase the mechanical integrity of the coating. The thermal post deposition treatment includes an integrated binder burnout step and sintering step. Differential scanning calorimetry and gravimetric analysis were used to determine the

temperature at which the binders can be successfully removed from the coating before sintering. Energy dispersive X-ray spectroscopy (EDS) was used to confirm the organics were removed (binders and dispersants) from the coating prior to sintering. Faraday has made the following conclusions about the post-deposition thermal treatment based on the experiments that have been conducted:

- Mud cracks, which are known to be related to the drying step, seem to be associated with relative maximum peaks in the underlying bond coat, likely meaning that smoother bond coats may help minimize or eliminate the mud cracks (see Figure 2).
- Hardness testing of sintered samples has shown that the samples continue to sinter at 1,092°C, indicating that the post-processing plays a significant role in the mechanical properties of the sample.
- X-ray diffraction studies showed that no detrimental monoclinic phase changes resulted from the EPD process or sintering (see Figure 3).

SEM/EDS was performed to examine the bond coat and substrate interfacial region subsequent to the post-deposition thermal treatment. EDS was performed on a sample deposited using a waveform that consisted of a medium γ and low frequency to analyze the bond coat/TBC interface region. Figure 3 shows the region of the sample that was investigated.

It appears from both the picture and the trace in Figure 3 that the thermally grown oxide (TGO) that forms between the bond coat and TBC consists of two distinct phases, an aluminum/zirconium-rich oxide phase and an aluminum-rich oxide phase. This may be due to TGO growth into the TBC due to the high porosity of the TBC and may be potentially advantageous for increasing coating adhesion, although further tests will need to be done to confirm this theory. The TGO is approximately 2 microns thick, with each phase being approximately 1 micron thick. As expected, nickel does not have a significant presence within the TGO and the oxide content decreases rapidly within the bond coat.

Advanced thermal cycling data showed that the FARADAYIC EPD process can produce coatings that survive in excess of 300 cycles on bond-coated Haynes 230 substrate with cycles consisting of: room temperature → 1,100°C (1 hour hold) → room temperature (15 minutes, forced air) → repeat (Figure 4). Additionally, preliminary experiments have shown that the FARADAYIC EPD process can be used to deposit TBCs onto turbine components that contain cooling holes with diameters as small as 396 µm without significantly reducing the original diameter

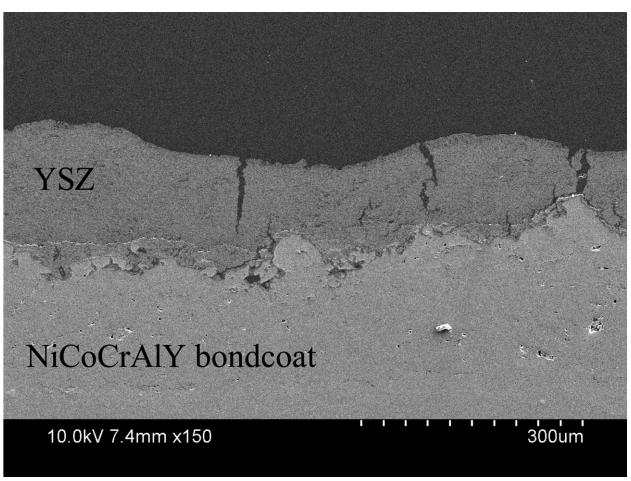

FIGURE 2. Cross-sectional image from a low duty cycle sample. Vertical cracks are mud-cracking effects due to drying.

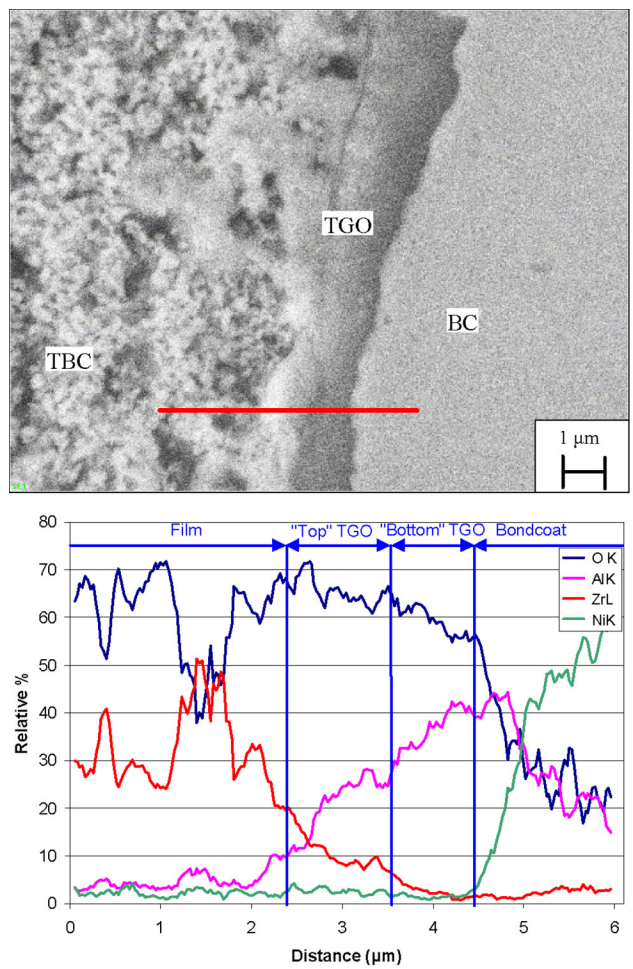

FIGURE 3. Top - region investigated in the SEM/EDS investigation. Horizontal line depicts region scanned to determine compositions of layers and the diffusion of species throughout the TBC, TGO, and bond coat. Bottom - linear scan showing major constituents of the various layers. The TGO contains two distinct regions (also evident in the picture).

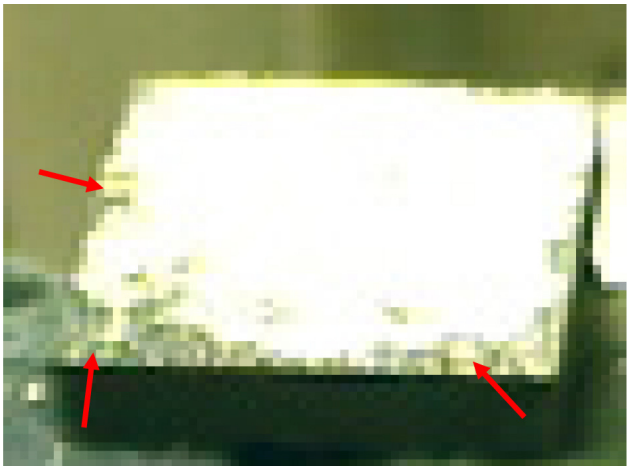

FIGURE 4. Photographs of a Haynes 230 sample after undergoing thermal cycling. Red arrows show areas of rubbing that occurred between samples due to differences in thermal expansion coefficients with the holder.

of the cooling hole. Turbines could benefit from being able to use conventional machining techniques to manufacture cooling holes prior to TBC deposition as opposed to using costly laser drilling to manufacture the cooling holes after TBC deposition.

Conclusions and Future Directions

In addition to the completed activities described previously, several activities are ongoing:

- Continued optimization of the FARADAYIC EPD processing parameters, including peak voltage, total deposition time, and pulsed-reverse parameters.
- Further exploration of post-deposition thermal processing parameters, more specifically processes that preferentially heat the TBC so as not to damage the substrate.
- Further analysis of coating properties as they relate to the various processing parameters, most notably the pulse reverse parameters, including thickness, roughness, uniformity, and hardness.
- Conclusive determination of the coating thermal conductivity.
- Further analysis of the coating properties through thermal stability and thermal cycling tests, especially as they relate to end use conditions.

FY 2010 Publications/Presentations

1. J.W. Kell and H.A. McCrabb, *Faradayic Electrophoretic Deposition of Thermal Barrier Coatings*, Oral Presentation at the 34th International Conference on Advanced Ceramics and Composites (ICACC 2010), Daytona Beach, Florida, USA, The American Ceramics Society, January 2010.

2. J.W. Kell and H.A. McCrabb, *The Faradayic EPD Process for Use in Depositing Thermal Barrier Coatings*, Poster Presentation at ICACC 2010, Daytona Beach, Florida, USA, The American Ceramics Society, January 2010.

3. J.W. Kell, H.A. McCrabb, and B. Kumar, *Faradayic Process for Electrophoretic Deposition of Thermal Barrier Coatings for Use in Gas Turbine Engines*, Oral Presentation at the Ultrasupercritical Steering Committee (USC) Meeting of the Electrical Power Research Institute (EPRI), Chicago, Illinois, USA, December 2009.

4. J.W. Kell, H.A. McCrabb, and S. Snyder, *FARADAYIC Electrophoretic Deposition of Thermal Barrier Coatings*, Poster Presentation at the University Turbine Systems Research (UTSR) Workshop VII, Orlando, Florida, USA, The National Energy Technology Laboratory (NETL), October 2009.

5. J.W. Kell and H.A. McCrabb, *Faradayic Electrophoretic Deposition of Thermal Barrier Coatings*, Oral Presentation at the Materials Science and Technology 2009 Conference and Exhibition (MS&T'09), Pittsburgh, Pennsylvania, USA, October 2009.

6. J.W. Kell and H.A. McCrabb, *FARADAYIC Electrophoretic Deposition of Thermal Barrier Coatings*, Oral Presentation at the Materials Science and Technology 2009 Conference and Exhibition (MS&T'09), Pittsburgh, Pennsylvania, USA, October 2009.

V.D.3 Functionally Graded Laminated Metal-Ceramic Thermal Barrier Systems by Low-Cost Electrochemical Processing

John D. Whitaker, Ph.D.
Modumetal, Inc.
1443 N. Northlake Way
Seattle, WA 98103
Phone: (877) 632-4242; Fax: (206) 770-7338
E-mail: john.whitaker@modumetal.com

DOE Project Manager: Mark Freeman
Phone: (412) 386-6094
E-mail: Mark.Freeman@netl.doe.gov

Contract Number: SC0001223

Start Date: July 20, 2009
End Date: April 19, 2010

FY 2010 Objectives

- Demonstrate functional gradation and lamination of both material/chemistry and porosity.
- Demonstrate reduced coefficient of thermal expansion and improved oxidation resistance in $Ni_3Al/Ni\text{-}Al_2O_3$ bond coats.
- Demonstrate top coat thermal conductivities below 0.7 W/mK.
- Demonstrate improved cyclic oxidation performance over a commercial thermal barrier coating (TBC) system.

Accomplishments

- Demonstrated lamination of top coat (TC) and bond coat (BC) chemistry (YSZ/Al_2O_3 and $Ni/NiAl\text{-}Al_2O_3$, respectively).
- Demonstrated functional gradation of TC from Al_2O_3 to yttria-stabilized zirconia (YSZ).
- Demonstrated the ability to grow metal coatings with tailorable porosities ranging from fully dense to ~60% porosity.
- Demonstrated the ability to deposit $NiAl/Al_2O_3$ composite BC alloys ranging from 0 to 90% nickel.

Introduction

Gas turbines achieve higher efficiencies at higher operating temperatures. Increasing the combustion temperature therefore reduces both fuel consumption and emissions, but places additional thermal stress on turbine materials. Advanced turbines already operate at or above the melting point of the blade materials, a feat made possible through a combination of internal cooling channels and insulating TBCs. TBCs contain a ceramic TC which differs substantially in properties compared to the blade metal. In particular, differences in expansion and contraction upon heat-up and cool-down of the turbine can result in coating cracking and spallation. Additionally, TBC ceramics are typically based on YSZ, through which oxygen can easily pass. The resulting hot oxygen-containing atmosphere oxidizes the underlying metal which, anticipating this, is coated with an aluminum-rich alloy coating called a BC; the BC forms an oxygen-impermeable alumina film upon oxidation, thereby slowing further metal oxidation. Ultimately, this thermally grown oxide (TGO) grows to a critical thickness, depleting the underlying BC alloy of aluminum and destabilizing the TBC system.

This project investigated a new route for producing both BC and TCs with chemistries and microstructures that would both increase TBC life and improve their insulation efficacy. This in turn is anticipated to enable higher operating temperatures and prolong the time between turbine blade recoating.

Approach

Modumetal's approach involves leveraging both a) micro- and nanolamination, and b) functional gradation to improve TBC performance. Micro- and nanolamination are a demonstrated route to improving a materials' resistance to fracture and fatigue, as well as enhancing thermal insulation efficacy, and is therefore a promising route to enhancing the performance of TBC systems. Functional gradation, or the gradual transition between two materials, is a further route to improving TBC performance by reducing material property mismatch stresses that would occur at a single, discrete interface (as opposed to the tens to thousands of interfaces in a laminated TBC).

Existing TBC application processes such as thermal spray are not readily suited to producing laminated or functionally graded coating architectures. This project will assess Modumetal's low-temperature electrochemical processes' ability to achieve both laminated and functionally graded top coats and bond coats over a wide variety of compositions.

Results

The technical objectives for Phase I had two primary purposes: 1) confirm our ability to produce a suite of microstructures in both the BC and TC, and 2) demonstrate the properties of these architectures in both fundamental thermal property tests and cyclic oxidation testing.

We succeeded in meeting the majority of objectives regarding microstructure, especially regarding ceramic TCs. We developed processes for producing stout green ceramic coatings of YSZ, Al_2O_3, laminates, and functionally graded hybrids. Regarding BCs, we successfully demonstrated the ability to produce deposits ranging from nearly pure nickel to pure aluminum using ionic liquids, and to alternate between these compositions to produce thin nanolaminated deposits with wavelengths down to ~500 nm.

Achieving the above required more effort than anticipated, however, and as a result, several objectives remain unfulfilled. These are: 1) quantifying the amount of alumina nanoparticles occluded in BC samples as a function of plating parameters, 2) validating our ability to control porosity during TC deposition, and 3) measuring both fundamental thermal properties and cyclic oxidation resistance of the resulting architectures. Before the latter objective can be met, several challenges must be addressed, and will compose a portion of the Phase II research. These are 1) slow rates of deposition of nickel-rich NiAl alloys, and 2) shrinkage (and associated cracking) during top coat heat treatment.

Partially counteracting obstacles and unrealized objectives, however, are four results that were unanticipated at the inception of Phase I. These are 1) our ability to produce deposits over nearly the entire Ni-Al composition range using ionic liquid electrolytes, 2) our ability to tailor the porosity of these alloys through control of deposition parameters, 3) the ability to produce ceramic laminates consisting of fully-dense layers separating vertically segmented layers, and 4) development of electrophoretically deposited coatings with wet green strengths (unsintered, as-deposited) sufficiently high to withstand extreme hydrodynamic fields without shearing off.

Bond Coats: Figure 1 (top) presents the energy dispersive X-ray composition data from deposits produced using Modumetal's BC deposition bath. Note that at low values of the controlled process parameter, nearly pure nickel is deposited, and by alternating between nickel-rich and aluminum-rich regions on the 'map', nanolaminates can be prepared as shown in Figure 1 (bottom). The laminates' morphology grew progressively more nodular as deposition proceeded, producing large 'trees' that were subsequently

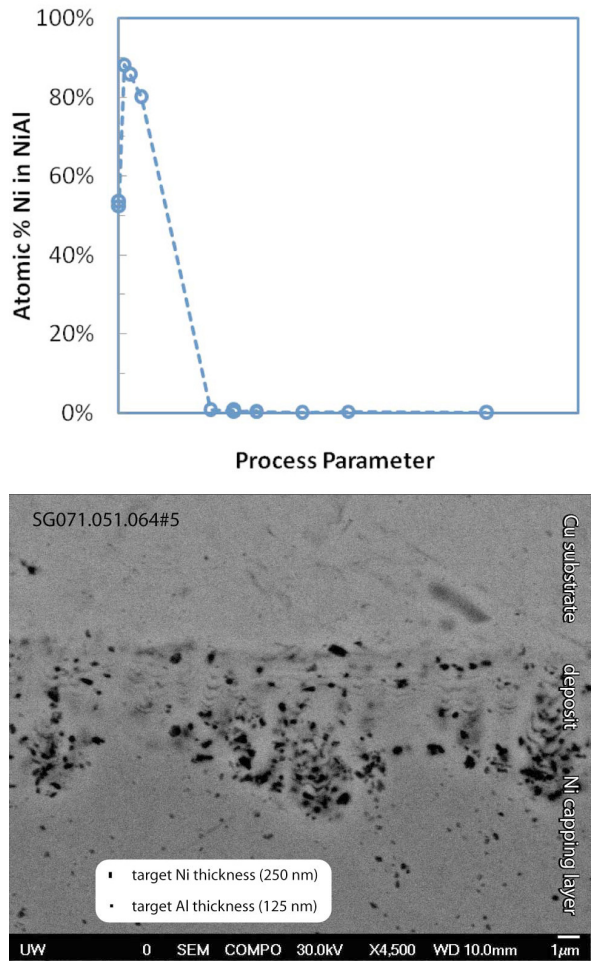

FIGURE 1. (top) Composition modulation mapping of nickel-aluminum alloys using an ionic liquid electrolyte. (bottom) Nanolaminate produced by alternating between nickel-rich and nickel-poor deposition conditions.

encapsulated in the capping nickel layer. Phase II will further investigate this phenomena.

Figure 2 shows an unexpected phenomenon which arose from this Small Business Innovation Research's research. Under certain processing conditions, variations in one process parameter had a dramatic effect on deposit porosity. Quantitative image analysis (using NIH's ImageJ) of the pore size distributions and porosities of these deposits are presented graphically below the micrographs. Note that at very low values of process parameter the deposit is smooth and nonporous (not shown).

Ceramic Top Coats: Modumetal's proprietary electrophoretic ceramic deposition bath, developed under this project, produced unsintered films with wet strengths superior to any of the multiple literature precedents tested in our laboratory. Deposits' wet strength was great enough to allow deposition onto

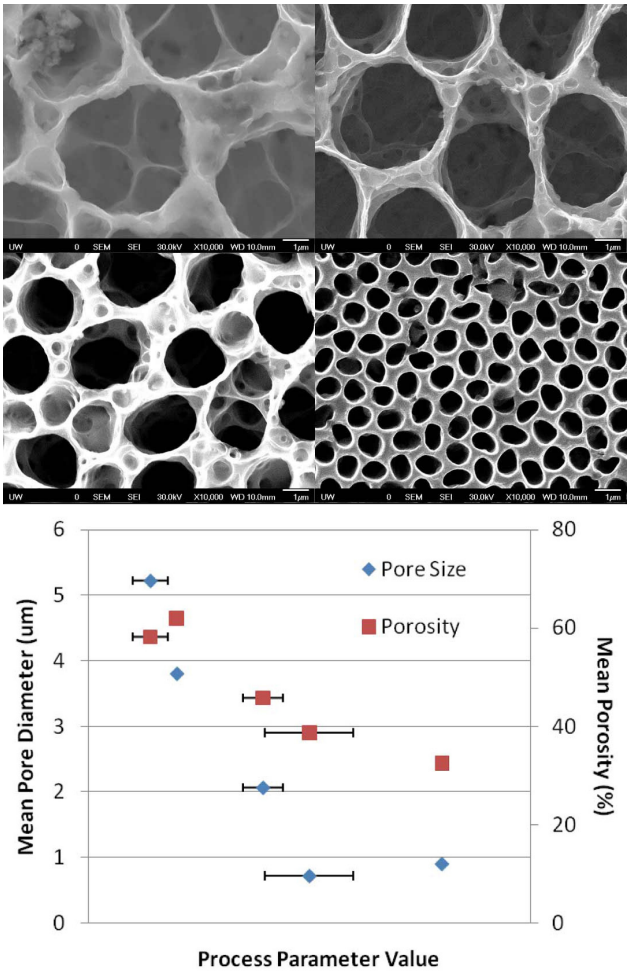

FIGURE 2. Bond coat porosity control. Variations in processing parameters allowed deposition of bond coat alloys ranging from fully dense (not shown) to up to 60% porosity.

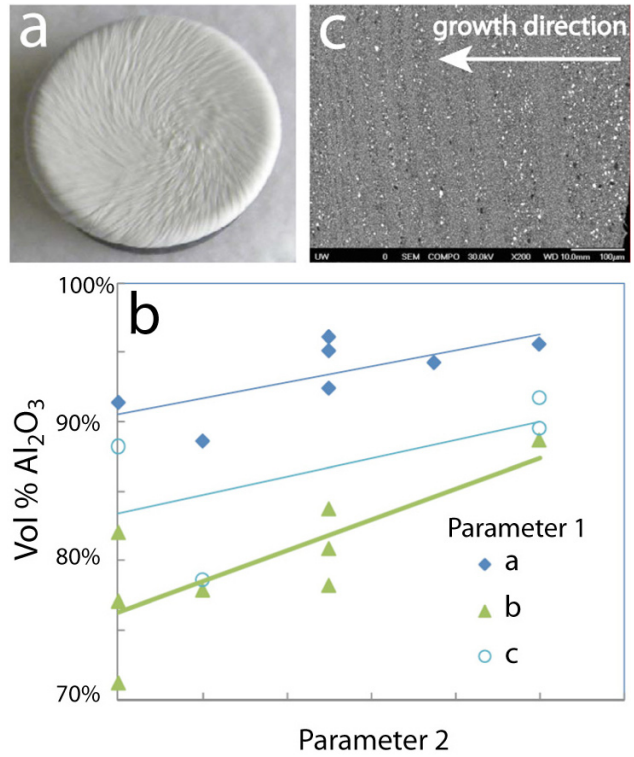

FIGURE 3. Electrophoretically deposited ceramic top coats. (a) Macrograph illustrating deposit morphology. Diameter of sample is ½". (b) Bath map illustrating dependence of ceramic composition on processing parameters. (c) Composition modulated ceramic composite produced in situ by alternating between different process parameters during deposition.

a rotating disc electrode spinning at 2,000 rpm. Figure 3a illustrates the typical appearance of deposits produced from this bath.

Figure 3b shows the bath map correlating alumina content in the deposit with process parameters for this down-selected bath. There is no strong correlation of alumina content and parameter 1, but a modest but fairly consistent correlation with parameter 2. This trend was subsequently used to create composition-modulated samples by alternating between high and low parameter values, an example of which is shown in Figure 3c.

During Phase I, in the interest of quickly attaining the maximum possible composition variations, a two-bath approach was adopted. In this approach, laminated samples were created by alternately immersing the sample (under applied voltage) in alumina-containing and YSZ-containing baths, each based on the same down-selected formulation cited above. Similarly, functionally graded samples were created by slowly mixing one bath with the other during deposition. Figure 4a and 4b shows examples of both laminated and functionally graded samples produced using this 'dual-bath' approach. Again, dark regions correspond to alumina, light regions to YSZ. Obtaining these microstructures was a key objective of the Phase I research. The laminated sample of Figure 4a was sintered to 1,500°C in air at the University of Washington's Materials Science & Engineering Department, resulting in fully dense YSZ layers separated by partially sintered, porous alumina. Stabilizing porosity by locating pores in alumina-rich regions is a plausible route to maintaining low thermal conductivity in the top coat by slowing densification.

Conclusions and Future Directions

We have demonstrated the ability to functionally grade and laminate composite TCs of YSZ and alumina, and have developed a new BC deposition route using ionic liquid electrolytes. Thin nanolaminated NiAl composites were demonstrated using this approach. Future work will be focused on

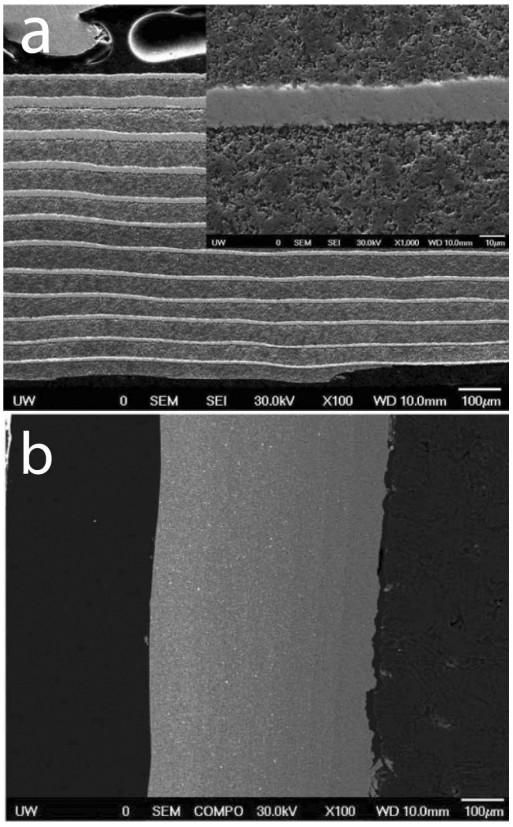

FIGURE 4. Laminated and functionally-graded TCs. (a) Laminated alumina-YSZ composite sintered to 1,500°C in air. (b) Green functionally-graded coating transitioning from pure alumina (at right) to a zirconia-rich Al_2O_3/YSZ mixture (at left).

structure-property correlation for both BCs and TCs, with the ultimate objective of qualification for use on land-based and aeroengine turbine blades.

V.D.4 Ultra High Temperature Environmentally Robust Nanocomposite Thermal Barrier Coatings for Nickel Super Alloy IGCC Turbine Components

Vince Baranauskas, Ph.D.
Director of Polymer Science and Engineering
NanoSonic, Inc.
1485 South Main Street
Blacksburg, VA 24060
Phone: (540) 953-1785; Fax: (540) 953-5022
E-mail: vince@nanosonic.com

DOE Project Manager: Mark Freeman
Phone: (412) 386-6094
E-mail: Mark.Freeman@netl.doe.gov

Contract Number: SC0002723

Start Date: July 20, 2009
Technical End Date: April 19, 2010
Final Report Due Date: July 18, 2010

FY 2010 Objectives

- **Technical Objective 1:** Synthesize ceramic yielding nanocomposite resins with tailored weight percentages of functionalized metal oxide nanoparticles.
- **Technical Objective 2:** Identify optimal thermal cycles for converting polysilazane nanoparticle resins to ceramic nanocomposite coatings with exceptional high temperature thermomechanical, corrosion/erosion resistance and thermal conductivities <0.7 W/mK.
- **Technical Objective 3:** Demonstrate enhanced corrosion/oxidation resistance, mechanical stability, and erosion durability imparted to nanocomposite coated nickel super alloy substrates.
- **Technical Objective 4:** Demonstrate ability to spray deposit down-selected nanocomposite resins onto large (>1 meter) nickel super alloy substrates using conventional high volume, low pressure (HVLP) spray deposition processes.

Accomplishments

Through Phase I DOE Small Business Innovation Research (SBIR) funding, NanoSonic has successfully demonstrated the thermal durability of its spray-deposited polymer-derived nanocomposite thermal barrier coating (TBC) technology up to the thermal limit of modern nickel superalloys of 1,200°C. To that end, researchers molecularly engineered over 100 coating formulations to identify a synergy of copolymer-nanoparticle compositions that anneal to high durability TBC nanocomposites that retain their desirable adhesive, impact, thermomechanical and abrasion durability after repeated cycling from room temperature to 1,200°C. Compared to competing line-of-sight electron beam-physical vapor deposited (EB-PVD) high temperature protective coatings, NanoSonic's polymer-derived nanocomposite coatings may be spray-deposited under ambient conditions using low-cost, conventional spray equipment and converted to mechanically robust, thermally insulative TBCs on a production basis with significantly reduced material and labor cost, as well as without hidden uncoated areas inherent to line of sight deposition techniques. In fact, it has been demonstrated that after 20 heating cycles from room temperature to 1,200°C for 1 hour, Inconel substrates coated with optimized polymer-derived nanocomposite formulations retain the following performance metrics:

- Adhesive rating of 5 A per ASTM D3359
- Impact durability per ASTM D5628-07
- Exceptional abrasion resistance (less than 0.05 weight percent loss after 1,000 wear cycles with a 250 g load)
- No coating spallation, cracking or delamination
- Less than 0.1 weight percent loss after soaking at 1,200°C for 12 hours
- Rapid spray deposition onto planar and curved 2' x 2' nickel alloy substrates using commonly employed facile high volume low pressure (HVLP) painting techniques used for aerospace topcoats

Compared to competing line-of-sight EB-PVD high-temperature protective coatings, NanoSonic's polymer-derived nanocomposite coatings may be spray deposited under ambient conditions using low-cost, conventional spray equipment and converted to mechanically robust, thermally insulative TBCs on a production basis with significantly reduced material and labor cost, as well as without hidden uncoated areas inherent to line-of-sight deposition techniques.

Introduction

NanoSonic has successfully demonstrated the thermal durability of its low-cost, spray-deposited nanocomposite TBC technology up to the thermal limit

of modern nickel superalloys of 1,200°C. Researchers molecularly engineered over 100 coating formulations to identify a synergy of copolymer-nanoparticle compositions that anneal to TBC nanocomposites that retain their desirable adhesive, impact, thermomechanical and abrasion durability after repeated cycling from room temperature to 1,200°C.

The maturation of the proposed nanocomposite TBCs may afford an integral element enabling integrated gasification combined cycle (IGCC) power plant efficiency gains beyond 50% and extended turbine component lifetimes; thus, a cleaner, more abundant energy supply may be realized with lower cost IGCC power plants. Additional public benefits include enhanced component lifetimes, increased operational temperatures and reduced maintenance costs for the aerospace, automotive, marine, and electronic industries.

Approach

NanoSonic has synthesized a family of ceramic yielding polymeric nanocomposites engineered to function as next generation TBCs for nickel super alloy IGCC components. **The potential technological advancements of the proposed nanocomposite coatings include their ease of fabrication, facile deposition processes, thermomechanical properties, gas barrier properties, low thermal conductivities and exceptional corrosion/erosion resistance.**

The matrix for the proposed nanocomposite coatings consists of silicon nitride (Si_3N_4) ceramics derived from innovative ceramic yielding hybrid copolymers. These unique copolymer materials may be converted to high performance silicon nitride ceramics upon thermal treatment and afford exceptional erosion, corrosion and oxidation resistance coatings for metallic substrates. Moreover, it is well-established that silicon nitride ceramics possess outstanding thermal shock resistance, high mechanical strength, creep resistance, low ceramic density, high fracture toughness, and chemical resistance. The efficient thermal transition of fluidic polysilazane resins to corrosion resistant coatings affords a simple and cost-effective route for coating large, irregularly shaped turbine nickel super alloy turbine components on a production basis.

In comparison to competing line-of-sight EB-PVD high-temperature protective coatings, NanoSonic's polymer-derived nanocomposite coatings may be spray-deposited under ambient conditions using low-cost, conventional spray equipment and converted to mechanically robust, thermally insulative TBCs on a production basis with significantly reduced material and labor cost, as well as without hidden uncoated areas inherent to line-of-sight deposition techniques.

Results

Through Phase I DOE SBIR funding, NanoSonic has successfully demonstrated the thermal durability of its spray-deposited polymer-derived nanocomposite TBC technology up to the thermal limit of modern nickel superalloys of 1,200°C. To that end, researchers molecularly engineered over 100 coating formulations to identify a synergy of copolymer-nanoparticle compositions that anneal to high durability TBC nanocomposites that retain their desirable adhesive, impact, thermomechanical and abrasion durability after repeated cycling from room temperature to 1,200°C. In fact, it has been demonstrated that after 20 heating cycles from room temperature to 1,200°C for 1 hour, Inconel substrates coated with optimized polymer-derived nanocomposite formulations retain the following performance metrics:

- Adhesive rating of 5 A per ASTM D3359 (Figure 1)
- Impact durability per ASTM D5628-07
- Exceptional abrasion resistance (less than 0.05 weight percent loss after 1,000 wear cycles with a 250 g load)
- No coating spallation, cracking or delamination
- Less than 0.1 weight percent loss after soaking at 1,200°C for 12 hours

Building from these promising findings, NanoSonic has established a collaborative partnership with Dr. Choudhuri's group of the University of Texas

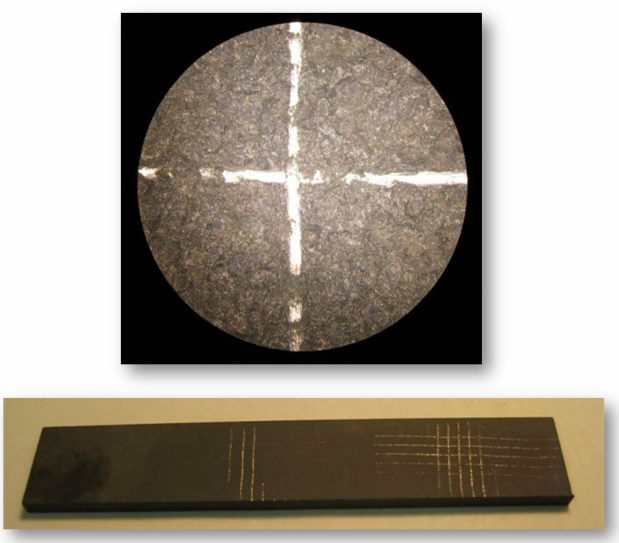

FIGURE 1. Image of nanocomposite-coated nickel super alloy coupon after ASTM D3359 adhesion testing. The above coupon was rapidly heated (>200°C/min) to 1,200°C for 12 hours (thermal limit of Inconel super alloy) and cooled to room temperature prior to adhesion testing. As shown above, the nanocomposite coating achieved the highest adhesive rating of 5 A, as zero evidence of coating failure or delamination within the areas of introduced deformation was observed.

at El Paso (UTEP) to evaluate and optimize the performance of down-selected nanocomposite TBCs within simulated turbines (combustor, inlet and outlet) with operational environments up to 1,500°C alongside currently employed yttria-stabilized zirconia (YSZ) TBCs provided by Oak Ridge National Laboratory. In that vein, during the Phase II project UTEP and NanoSonic will work to:

1. Develop an accelerated testing model for nanocomposite-coated nickel super alloys within syngas turbine environments employing DOE specified gas compositions, pressures and temperatures.
2. Setup experimental facilities to test samples based on the accelerated test models and compare down-selected nanocomposite TBCs with currently employed YSZ TBCs within each turbine environment up to 1,500°C.
3. Optimize and down-select polymer-derived nanocomposite TBCs that outperform YSZ TBCs.

Of particular interest for near-term integration pathways as high-temperature TBCs within syngas, hydrogen-fired, and oxy-fuel turbine components, NanoSonic has tailored the viscosity, processing, and cure kinetics of Phase I down-selected nanocomposite coatings for rapid, room temperature spray deposition onto IGCC coal-fire turbine components using commonly employed facile HVLP painting techniques used for aerospace topcoats (Figure 2).

This efficient, low-cost deposition process will afford a considerable cost saving advantage over costly line-of-sight vacuum deposited high-temperature protective coatings, as commercially available spray equipment may be employed to rapidly coat large area planar and curved turbine components on a production basis.

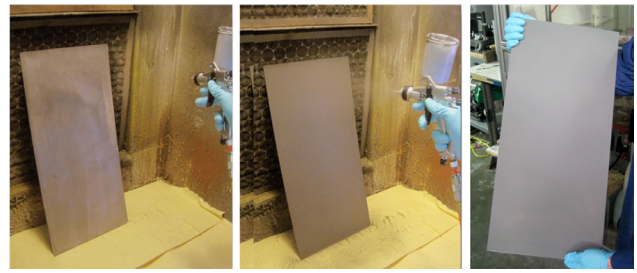

FIGURE 2. HVLP spray deposition of NanoSonic's Phase I optimized nanocomposite TBC for IGCC turbines. The above coating was deposited using commercial spray equipment and rapidly gelled at room temperature to a tack free coating in 15 minues. Upon heating to elevated temperatures within turbine environments, the nanocomposite will gracefully transition to a dense, strongly adhered ceramic nanocomposite coating with currently demonstrated durability in excess of 1,200°C

Through a related effort, NanoSonic has been awarded a U.S. Navy commercialization pilot program (CPP) to establish the equipment necessary for producing 100,000 to 1,000,000 lbs of related high-temperature nanocomposite materials. This successful transition from lab to pilot-scale manufacturing provides an exemplary maturation pathway for the proposed polymer-derived nanocomposite TBCs (Figure 3).

The primary objectives of a potential Phase II SBIR project are to empirically demonstrate the utility of NanoSonic's nanocomposite TBCs within simulated IGCC turbine environments up to 1,500°C and establish Phase III integration pathways for optimized TBCs within syngas, hydrogen-fired and oxy-fuel turbines. To meet this challenge, NanoSonic has teamed up with the Center for Space Exploration and Technology Research at UTEP to develop and execute an extensive test plan achievable through Phase II funding. This collaborative partnership will

FIGURE 3. Through a U.S. Navy CPP, NanoSonic has set up a pilot-scale manufacturing process currently capable of producing >2,000 lbs/day of similar high-temperature nanocomposite resins. This established infrastructure provides an exemplary scale-up pathway.

qualify NanoSonic's TBCs for combustor, inlet, and exhaust components using 2010 and 2015 DOE Fossil Energy (FE) coal program goals (Table 1). Throughout testing, NanoSonic's coatings will be continuously evaluated against currently employed YSZ TBCs to empirically validate, as well as qualify, their near-term utility within IGCC turbines at DOE targeted gas compositions, temperatures, and pressures.

Compared to competing line-of-sight EB-PVD high-temperature protective coatings, NanoSonic's polymer-derived nanocomposite coatings may be spray-deposited under ambient conditions using low-cost, conventional spray equipment and converted to mechanically robust, thermally insulative TBCs on a production basis with significantly reduced material and labor cost, as well as without hidden uncoated areas inherent to line-of-sight deposition techniques (Figure 4).

In addition to cost savings from a drastically simplified deposition process, NanoSonic's pioneering high-temperature nanocomposite coatings may further enhance the operating efficiencies of IGCC gas turbines by enabling nickel super alloy components operational utility at higher temperatures (1,500°C) for sustained periods of operation (>8,000 hours). Sustained utility for nickel super alloy will be imparted through the deposition of tailored nanocomposites engineered for thermal conductivities <0.5 W/mK, thermal stabilities >1,200°C, coefficient of thermal expansion compatibility with super alloy substrates and exceptional adhesion without the use of bond coat materials. **The potential technological advancements of the proposed nanocomposite coatings include their ease of fabrication, facile deposition processes, thermomechanical properties, gas barrier properties,**

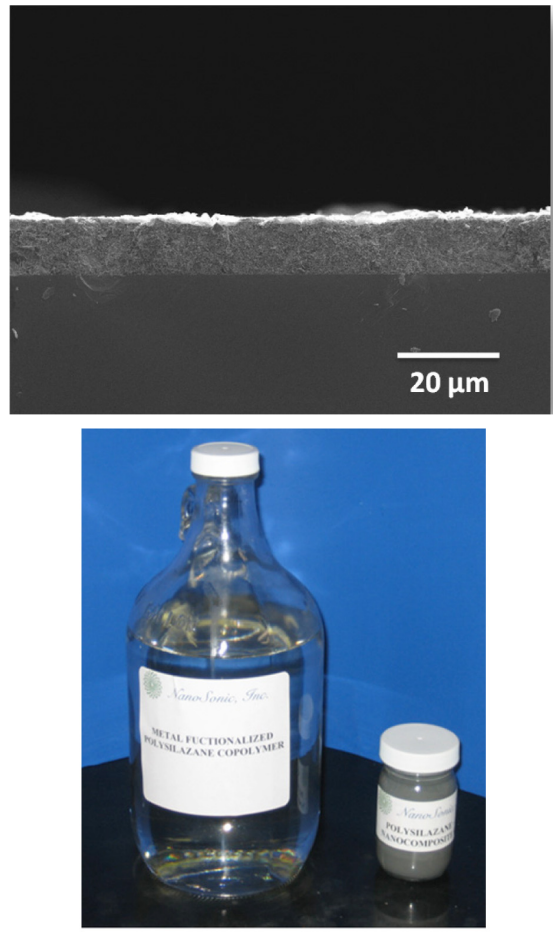

FIGURE 4. NanoSonic's polymer-derived ceramic nanocomposite resins may be spray-deposited using conventional HVLP equipment and annealed to provided high temperature IGCC TBCs with currently demonstrated operational durability at 1,200°C (the thermal limit of the current generation of nickel super alloy substrates).

TABLE 1. DOE FE coal program targets that will employed for the qualification of NanoSonic's nanocomposite TBCs with team partner UTEP during the Phase II effort.

	Syngas Turbine 2010	Hydrogen-Fired Turbine 2015	Oxy-Fuel Turbine 2010	Oxy-Fuel Turbine 2015
Combustor Exhaust Temp, °C (°F)	~1480+ (~2700+)	~1480+ (~2700+)		
Turbine Inlet Temp, °C (°F)	~1370 (~2500)	~1425 (~2600)	~620 (~1150)	~760 (~1400) (HP) ~1760 (~3200) (IP)
Turbine Exhaust Temp, °C (°F)	~595 (~1100)	~595 (~1100)		
Turbine Inlet Pressure, psig	~265	~300	~450	~1500 (HP) ~625 (IP)
Combustor Exhaust Composition, %	CO_2 (9.27) H_2O (8.5) N_2 (72.8) Ar (0.8) O_2 (8.6)	CO_2 (1.4) H_2O (17.3) N_2 (72.2) Ar (0.9) O_2 (8.2)	H_2O (82) CO_2 (17) O_2 (0.1) N_2 (1.1) Ar (1)	H_2O (75-90) CO_2 (25-10) O_2, N_2, Ar (1.7)

R.A.Dennis, "FE Research Direction – Thermal Barrier Coatings and Health Monitoring Techniques," Workshop on Advanced Coating Materials and Technology for Extreme Environments, Pennsylvania State University, State College, PA, September 12 - 13, 2006

low thermal conductivities and exceptional corrosion/erosion resistance.

Conclusions and Future Directions

NanoSonic has successfully demonstrated the thermal durability of its low-cost, spray-deposited nanocomposite TBC technology up to the thermal limit of modern nickel superalloys of 1,200°C. Researchers molecularly engineered over 100 coating formulations to identify a synergy of copolymer-nanoparticle compositions that anneal to TBC nanocomposites that retain their desirable adhesive, impact, thermomechanical and abrasion durability after repeated cycling from room temperature to 1,200°C.

NanoSonic and UTEP team members will work to build from Phase I accomplishments and optimize/validate the ability of promising nanocomposite TBCs to provide superior performance over currently employed YSZ coating technologies. The principal objective of the proposed Phase II SBIR project will be empirically demonstrating optimized nanocomposite TBCs provide enhanced thermal/corrosion protection over currently employed YSZ coatings within current and future IGCC turbine environments employing DOE specified gas compositions, pressures, and temperatures. In that vein, NanoSonic and Dr. Choudhuri's group will develop an accelerated testing model for quickly assessing the performance of candidate nanocomposite TBCs against currently employed YSZ TBCs on nickel super alloy substrates within the aforementioned testing environments. The EB-PVD YSZ samples will integrate currently employed bond coats and be prepared by Oak Ridge National Laboratory while NanoSonic will HVLP spray deposit Phase II nanocomposite TBCs with and without existing TBC metal oxide bondcoats on CMSX-4 substrates.

Upon qualification, NanoSonic will develop heat transfer prediction capabilities for modeling heat transfer mechanisms due to conduction, convection and emission within inlet, outlet, and combustor components of IGCC coal-fired turbines. Down-selected coating compositions will be further improved and provided to team partner UTEP for additional qualification within simulated turbine environments. During the final segment of the Phase II effort, NanoSonic will transition optimized nanocomposite resin precursors to 55-gallon batch production quantities and work to distribute these materials to DOE specified IGCC coal turbine manufacturers to facilitate near-term Phase III commercialization success.

V.D.5 High Temperature Bond and Thermal Barrier Coatings

Tim McKechnie
Plasma Processes, Inc. (PPI)
4914 Moores Mill Road
Huntsville, AL 35811
Phone: (256) 851-7653 x103
E-mail: timmck@plasmaPros.com

DOE Project Manager: Mark Freeman
Phone: (412) 386-6094
E-mail: Mark.Freeman@netl.doe.gov

Contract Number: SC0001601

Start Date: July 20, 2009
End Date: April 19, 2010

FY 2010 Objectives

The SBIR Phase 1 objective is to demonstrate a bond and thermal barrier coating (TBC) system for superalloys used in IGCC turbines that can function with a 1,300°C TBC surface temperature capability.

- Demonstrate a stable oxidation and corrosion-resistant coating based on iridium.
- Eliminate/minimize loss of iridium coating to the superalloy with thin diffusion barrier of rhenium.
- Demonstrate formation of thick, stable thermal grown oxide based on the conversion of hafnium to hafnium oxide.
- Manipulate the structure of TBC via a new very low pressure plasma spray (VLPPS) process and chemistry changes.
- Test new system for stability and oxidation resistance.
- Analyze results with gas turbine manufacturer, GE.
- Report and make recommendations.

Accomplishments

- A complex new environmental barrier coating (EBC)/TBC system has been formed on superalloys. The coating system is comprised of four layers (Figure 1):
  - Rhenium (a diffusion barrier between superalloy and EBC)
  - Iridium (EBC)
  - HfO_2 thermally grown oxide (TGO) (formed from Hf layer)
  - ZrO_2-$8Y_2O_3$ (TBC)
- Due to electrochemical reaction with rhenium electrolyte, Inconel 738LC (low carbon) also required a nickel barrier coating.
- In thermal exposure and cycle testing, the following were observed:
  - Bare iridium volatilized.
  - Hf/HfO_2 TGO slowed iridium volatilization to a minimum.
  - HfO_2 TGO separated with zirconia TBC from iridium (or the remaining Ir-Hf compound).

Introduction

State-of-the-art integrated gasification combined cycle power plants utilize single crystal turbine blades protected from hot gas by TBCs. Current TBCs consist of either a MCrAlY or PtAl bond coating that serves as the EBC and a yttria-stabilized zirconia (YSZ) TBC. Higher use temperatures lead to early failure of the coating system primarily due to TGO thickening and depletion of the bond coating of aluminum. Lowering the thermal conductivity of the YSZ or alternative ceramic will help, but the weak point will always be the non-stable bond coating.

Approach

A revolutionary approach to enable higher turbine inlet temperatures is to replace the current bond coatings with a much higher temperature system. For high-temperature oxidation and corrosion resistance, the best coating is iridium, a platinum group metal that typically costs a third of platinum but has a melting point of 2,454°C. To increase long-term bonding to

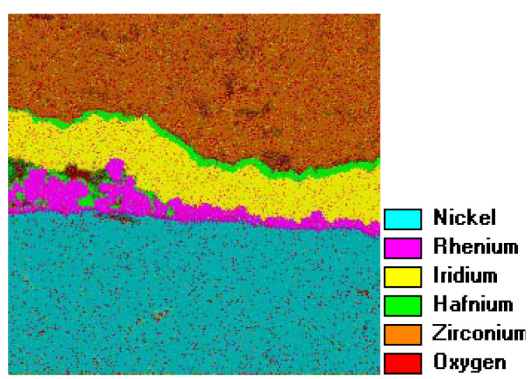

FIGURE 1. X-ray map of a coating system before thermal cycling.

the TBC, a TGO of hafnium oxide or aluminide is being employed. Both materials can be deposited by electroforming using a new technique, EL-Form™ electrodeposition. To increase the long life capabilities (i.e., >8,000 hours) of the coating system, a thin diffusion barrier of rhenium can be applied to the superalloy turbine components.

Results

Two techniques are commonly used to deposit YSZ: electron beam physical vapor deposition (EB-PVD) and air plasma spray (APS). The EB-PVD technique produces a dense columnar structure which has been shown to be more strain tolerant due to vertical column structure. The APS coatings include high levels of porosity (typically 10-20%) which provide a more insulating, lower thermal conductivity barrier. A new technique, VLPPS, is being developed to deposit YSZ. With the VLPPS process, columnar deposits can be made which can include micro-porosity. Therefore the process combines the strain tolerance of EB-PVD with the lower thermal conductivity of APS YSZ and pyrochlores for lower thermal conductivity and better phase stability [1]. A schematic of the material system is shown in Figure 2.

Oxidation and Corrosion Barrier: Iridium

Iridium is an excellent high temperature protective coating that is stable at the required temperature for IGCC while offering protection of nickel-based superalloys. Iridium has excellent oxidation resistance as well as the lowest oxygen permeability for metals. Iridium does not react with water or carbon containing atmospheres and has the best resistance to molten salts. Because of its compatibility with oxides, iridium is widely used as a container for single crystal production. Additionally, iridium has excellent strain capability at all temperatures. Iridium oxidation and corrosion barriers have been used in applications from 1,600°C to 2,000°C on rocket engines. Multiple satellites currently use iridium lined rhenium thrusters (Figure 3).

TGO: Hafnium Oxide and Platinum-Iridium-Hafnium-Aluminide

Platinum and modified nickel aluminide usually form spinel type phases. As a result of internal oxidation, thermally-grown α-Al_2O_3 is formed, replacing the spinel phases. After long thermal exposure and inward diffusion of Al into the substrate, aluminum is depleted, and the bond coat finally degrades. Recent research shows that partial substitution of iridium for platinum and the addition of hafnium are beneficial for both wet and dry air oxidation resistance of nickel aluminide [2]. Iridium-hafnium alloys and intermetallics [3] have demonstrated high oxidation resistance with hafnium content more than 65%. Kamiya and Muracami reported that Ir-Hf coated and aluminized specimens showed better adhesion to YSZ TBCs and longer spallation life than Pt coated and aluminized specimens [4]. Iridium coated with hafnium after completing 1,300°C for 3 hours exposure shows formation of a stable hafnium oxide TGO (Figure 4).

Improved TBC

VLPPS is a novel concept that has only recently begun to find applications in industry during which coatings are formed via deposition of ceramic or metallic material in the form of powder or from the vapor phase onto a substrate at low pressures (1-20 torr). The unique features of VLPPS deposition from the vapor phase include large deposition footprint (8-16" diameter), rapid deposition rates (10 microns/min/m^2), and the ability to coat blind surfaces (any

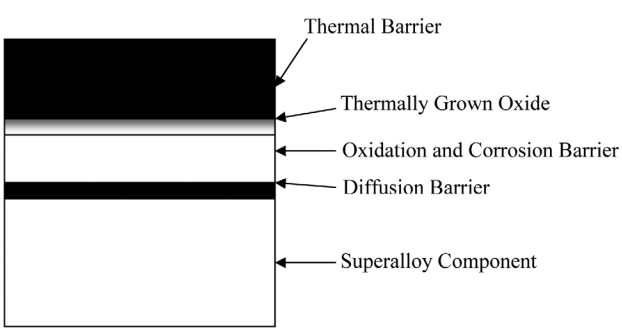

FIGURE 2. High temperature thermal protection architecture of Phase I, in Phase II the diffusion barrier will be eliminated to simplify the system.

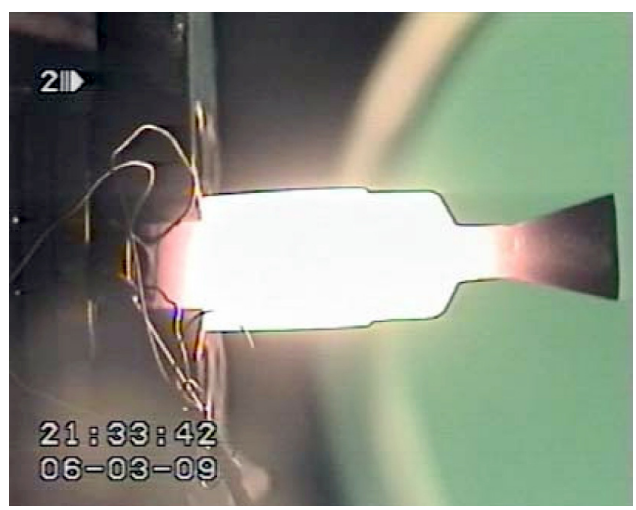

FIGURE 3. Iridium lined rocket nozzles being tested at 1,650°C with oxidizing propellants.

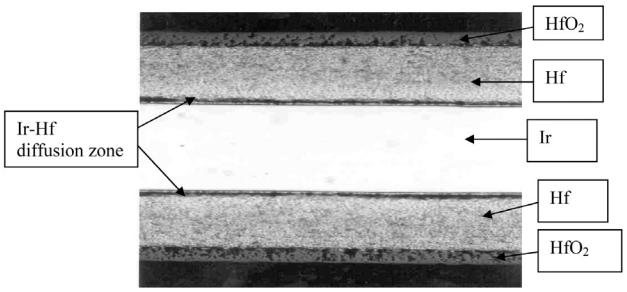

FIGURE 4. Microstructure of hafnium deposited on iridium at PPI after exposure to 1,300°C air for 3 hours. Note the dense thermal oxide film formed.

surface that is not in-line with the direction of coating deposition, i.e. not line-of-sight) to produce high purity coatings [5,6]. In work performed by PPI for DOE's nuclear fusion program, nanoporous metals have been deposited.

Conclusions and Future Directions

The following recommendations are made:

- Stabilize TGO with alloying additions.
- Make strain tolerant, columnar zirconia.
- Modify Ir electrolyte to enable direct coating of turbine alloys.
- Simplify coating system by eliminating diffusion barrier of rhenium.
- Test developed system in turbine conditions with gas turbine manufacturers.

References

1. M.D. Hill, "Effective Barrier," *Ceramic Industry*, 9/2003.

2. R. Kartono and D.J. Yung, "Effectiveness of platinum and iridium in improving the resistance of Ni-Al to thermal cycling in air steam mixture," *Material and Corrosion*, vol. 59, issue 6, pp. 455-462, 2008.

3. K.N. Lee and W.L. Worrell, "The oxidation of iridium-hafnium and iridium-hafnium intermetallics at temperatures above 1550°C," *Oxidation of Metals*, vol. 32, nos. 5/6, 1989.

4. K. Koichiro, M. Hideyuki, "Characterization of an Ir-Hf alloy as a bond coat material," *Nippon Kinzoku Gakkaishi*, 2005, vol. 69, N1, pp. 73-79.

5. M. Gindrat, A. Refke, and R. Damani, "APS-triplex and LPPS-thin film as advanced plasma spraying technologies for industrialization of SOFC components," *Proceedings of International Thermal Spray Conference 2008*, DVS-Verlag GmbH, Dusseldorf, Germany, 2008.

6. C. Verdy, C. Zhang, D. Sokolov, H. Liao, D. Klein, and C. Coddet, Belforf/F, "Gas-tight coatings produced by very low pressure plasma spraying," *Proceedings of International Thermal Spray Conference 2008*, DVS-Verlag GmbH, Dusseldorf, Germany, 2008.

V.D.6 Novel Thermally-Sprayed Architectures for High Temperature Thermal Barrier Coating Systems

Dr. Satish Dixit (Primary Contact),
Michael Chin, Rashmi Dixit
Plasma Technology Inc.
1754 Crenshaw Blvd.
Torrance, CA 90501
Phone: (310) 320-3373; Fax: (310) 533-1677
E-mail: sdixit@ptise.com

DOE Project Manager: Mark Freeman
Phone: (412) 386-6094
E-mail: Mark.Freeman@netl.doe.gov

Subcontractor:
Prof. Sanjay Sampath
Center for Thermal Spray Research (CTSR)
Stony Brook University, Stony Brook, NY

Contract Number: SC0001422

Start Date: July 20, 2009
End Date: April 19, 2010

FY 2010 Objectives

- Develop thermally-sprayed multilayer thermal barrier coatings (TBCs) for integrated gasification combined cycle (IGCC) turbines by specifically addressing two factors: top coat architecture (multilayer or co-doped multicomponent) and top coat material composition (zirconates and yttria-stabilized zirconia [YSZ]). The top coat material selection is based on extending the proven work in the literature with the emphasis on multilayer design for multifunctional performance.
- Investigate the role of the bond coat using current CoNiCrAlY base alloys and high velocity oxy fuel (HVOF) deposition with proven capabilities in gas turbines.
- Evaluate the coating architecture for its physical properties such as thermal conductivity, internal stress, thermal cyclic behavior, erosion and impact resistance etc. relevant to IGCC environment.

Accomplishments

- Through past and current collaborations between Stony Brook Center for Thermal Spray Research and Dr. Robert Vassen of Julich Research Center as well as Prof. Carlos Levi of University of California, Santa Barbara, assessment of the various new generations of TBC materials with potential applicability in IGCC environments was conducted.
- Completed initial screening tests on novel multilayer film cooling configurations, achieving a 20% increase in film effectiveness.
- Process-microstructure relationships for plasma-sprayed YSZ and novel zirconates, such as, gadolinium zirconate ($Gd_2Zr_2O_7$) with a pyrochlore structure were investigated using plasma spray while in situ diagnostics using the concept of process maps was conducted.
- In addition to $Gd_2Zr_2O_7$, other new materials such as $La_2Zr_2O_7$ and co-doped zirconates along with YSZ were also investigated. The new materials had significant reduction in thermal conductivity at both ambient and elevated temperatures.
- $Gd_2Zr_2O_7$ shows phase stability after exposure at 1,125°C in 90% water vapor.
- Also, the co-doped YSZ-zirconate material provided similar superior erosion resistance as the YSZ material while the Gd and La zirconates were expectedly poorer in erosion resistance.

Introduction

TBCs are multilayer systems designed to provide thermal and oxidation protection for nickel-superalloy components in gas turbine engines used both in propulsion and power generation. Typical TBC systems consist of a MCrAlY (M = Ni, Co, and/or Fe) bond coat and a YSZ top coat. With its low thermal conductivity, the YSZ top coat is primarily responsible for shielding the metallic component from high gas temperatures. The MCrAlY bond coat's primary role is to enhance the adhesion of the ceramic top coat with the underlying metal component. The bond coat also serves to provide some oxidation protection for the nickel-superalloy substrate. This multifunctional coating system allows for increased gas turbine performance and efficiency, as well as life-extension of expensive superalloy thermo-structural components. TBCs are vital to the economic and efficient operation of modern day energy systems and as such are a subject of intensive scientific and technological research.

TBCs are widely applied in natural gas-based turbines system, notably the large "frame" systems. In recent years, there has been an interest in expanding the application of gas turbines to alternative fuels notably coal-based syngas and/or hydrogen derived

from the gas. New opportunities have emerged through the DOE IGCC power systems programs aimed at developing modifications to traditional gas turbine materials and processes to accommodate coal-derived gas fuel. The role of TBCs in IGCC power plants is to allow for higher turbine inlet temperatures in an effort to increase the overall efficiency of the system [1,2]. Improvements in TBC phase stability, long-term thermo-mechanical properties, and resistance to environmental degradation must be made in order for higher efficiencies in IGCC power plants to be realized [3]. Of particular importance is that these requirements must be concurrently considered in a multifunctional materials theme as no singular material may meet all of the requirements.

Approach

A multipronged approach was developed during Phase I to concurrently address the challenges in implementation of TBCs for an IGCC environment. This included identification and selection of candidate oxide materials (such as Gd and La zirconates and their co-doped combinations with YSZ) suitable to meet the multifunctional requirements of the ceramic, development of a novel coating design (co-doped and multilayer combinations) and processing strategies based on a multilayer architecture and preliminary evaluation on performance in relevant environments.

Results

The major tasks of the Phase I project were:

- Identification of the materials and processing techniques; and
- Design and evaluation of the multilayer and/or co-doped coating configurations.

Based on the above, following experimental results are reported.

Optimization of the Architecture of Individual Thermally-Sprayed YSZ Layers

By investigating process-microstructure relationships for plasma-sprayed YSZ and novel zirconates, process conditions to produce the distinct layers in the multi-layer coating as illustrated in the architecture design in Figure 1 were optimized.

Gadolinium zirconate ($Gd_2Zr_2O_7$) and lanthanum zirconate ($La_2Zr_2O_3$) with a pyrochlore structure were processed using plasma spray while in situ diagnostics were being conducted. The concept of 1st and 2nd order process maps (Figure 2) was adapted for the zirconate work [4]. As can be seen in Figure 2, significant differences in the in-flight particle temperature

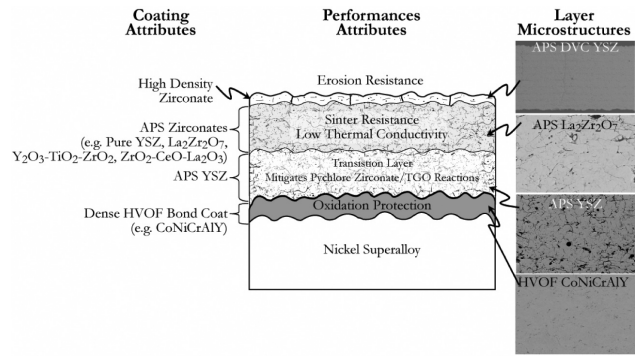

FIGURE 1. Coating Architecture Schematic

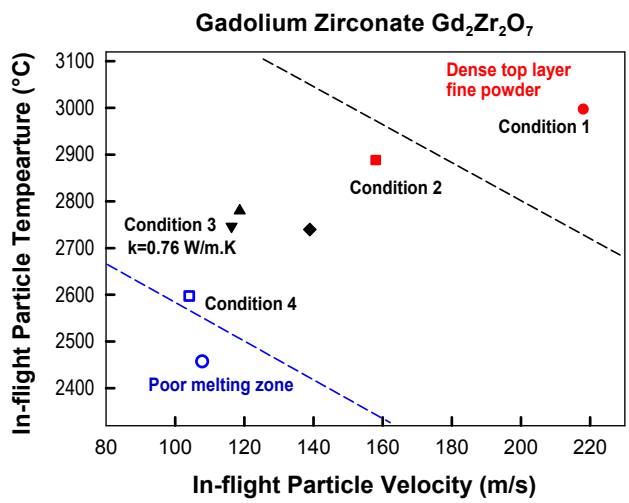

FIGURE 2. Process Optimization and Mapping of Plasma-Sprayed $Gd_2Zr_2O_7$

and velocity can be achieved by changing plasma conditions, and as such the coating microstructure and properties can be tailored.

From the process map in Figure 2, the condition giving the maximum in-flight temperature and velocity was used to deposit dense top-layer. The condition with the lowest temperature had very poor melting and deposition efficiency. For the other four conditions, individual coatings were produced and room temperature thermal conductivity was measured on free-standing samples (Figure 3). Condition 3 achieved the lowest coating thermal conductivity (~0.76 W/mK) among the four conditions.

In addition to $Gd_2Zr_2O_7$, other new materials such as $La_2Zr_2O_7$ and co-doped zirconates along with YSZ were also been processed. The new materials had significant reduction in thermal conductivity at both ambient and elevated temperatures.

Coating thermal conductivity was measured as a function of heat treatment time to determine

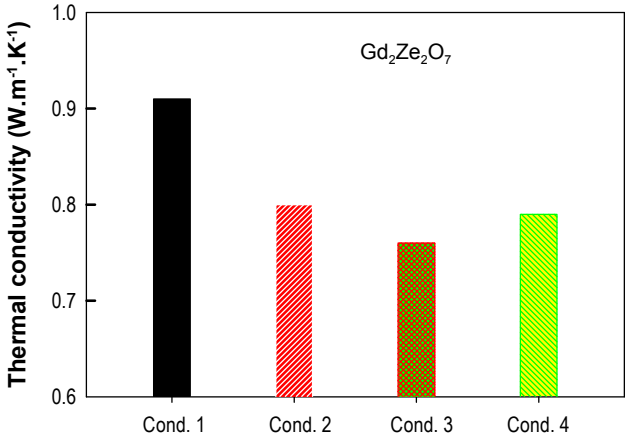

FIGURE 3. Thermal Conductivity of Various $Gd_2Zr_2O_7$ Coatings

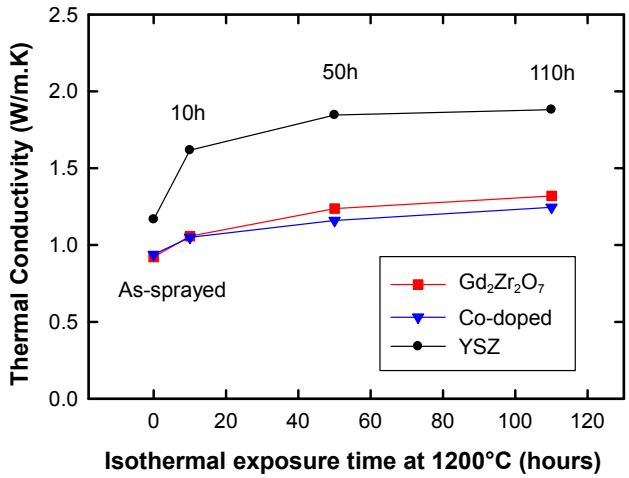

FIGURE 4. Sintering Effect on Thermal Conductivity of Various Plasma-Sprayed Coating Materials

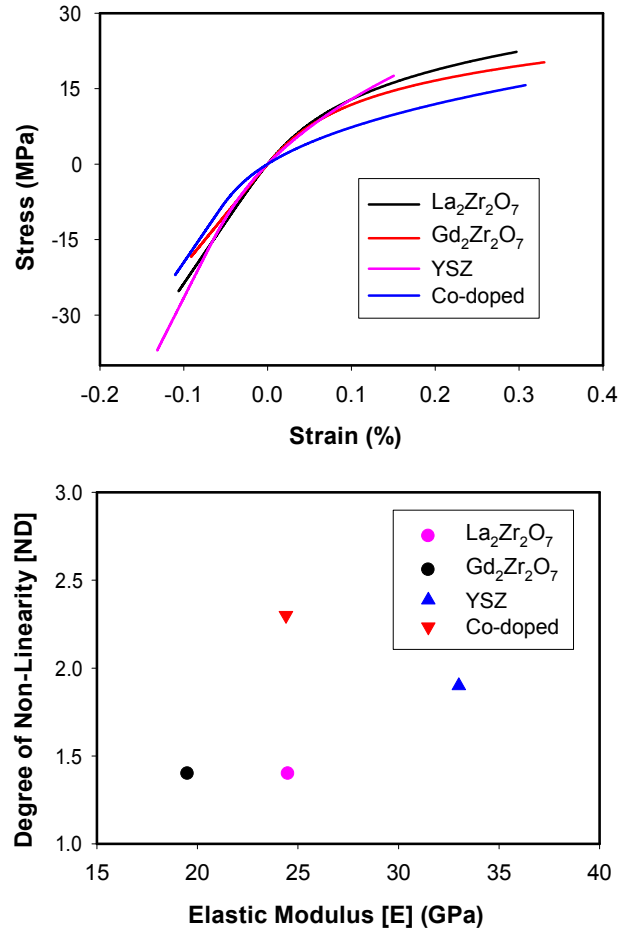

FIGURE 5. (Top) Non-Linear Elastic Properties for Various Novel TBC Materials (Bottom) Double-Layer TBC Thermal Imaging Result

the efficacy of the structures to mitigate sintering (Figure 4). Gd_2Zr_2O7 and co-doped coating showed better sintering resistance at 1,200°C.

Multilayer TBCs on substrates were also characterized by the in situ coating property (ICP) sensor [5]. This advanced capability was developed in recent years at Stony Brook University and allows full field stress-strain measurements of TBCs on metallic substrates to assess their compliance. Figure 5 shows the non-linear stress-strain curves for the various ceramic coatings obtained through the curvature technique. The results suggest that the zirconates are generally lower in elastic modulus for similar spray parameters compared to both YSZ and co-doped YSZ possibly due to lower toughness and associated microcracking.

IGCC Corrosion Testing

High water vapor environmental exposure. X-ray diffraction (XRD) was performed on the top surface of thermally exposed samples at atmosphere and water vapor conditions in a controlled-atmosphere furnace containing elevated moisture content to simulate the IGCC gas turbine environment when clean syngas is being used. $Gd_2Zr_2O_7$ shows phase stability after exposure at 1,125°C in 90% water vapor (Figure 6).

Evaluation of the degradation of multi-layer TBCs in IGCC environment. Prior to aggressive testing, understanding of single-layer TBC baseline performance of the new materials was required. This includes both solid particle erosion testing as well as gradient exposure testing in a traditional burner rig. Figure 7 shows erosion results on YSZ, co-doped YSZ and zirconate ceramics applied to similar densities via plasma spray. The results indicate that the co-doped material provides similar superior erosion resistance as the YSZ material while the zirconates were expectedly

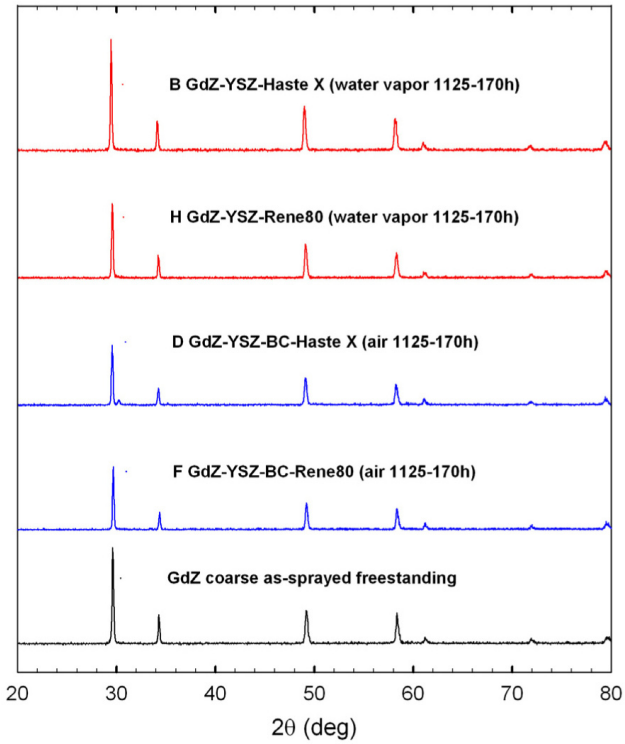

FIGURE 6. XRD Results on Thermally Exposed YSZ and Multilayer $Gd_2Zr_2O_7$/YSZ Structure Showing the Phase Stability of $Gd_2Zr_2O_7$

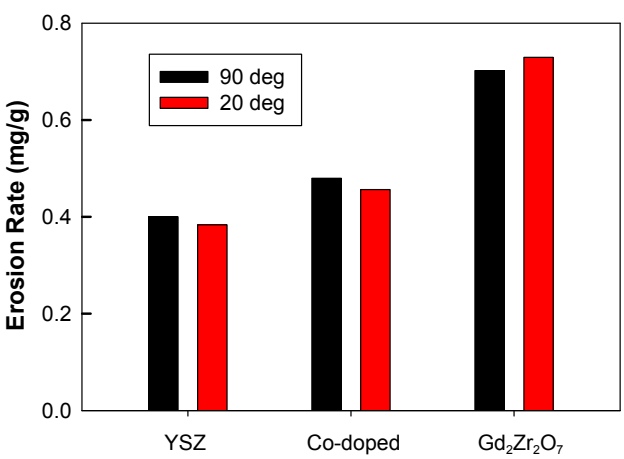

FIGURE 7. Erosion Rates for Various Coatings Measured at 20° and 90°

poorer in erosion resistance. New strategies are envisaged to improve the erosion resistance through modification of microstructure and stresses.

Conclusions and Future Directions

During Phase I of this Small Business Technology Transfer project, thermally-sprayed TBCs were developed for IGCC gas turbines by specifically addressing two factors: top coat architecture and top coat material composition. Significant progress has been made throughout the course of the Phase I project as described above. The top coat material selection was based on extending the proven work in the literature and at CTSR with the emphasis on multilayer design for multifunctional performance. Thermal imaging has been tested before IGCC environmental test, and will be conducted in Phase II after thermal exposures. Phase II will build upon the initial work and will include the investigation of bond coat alloys and evaluate TBC system performance in IGCC gas turbine atmospheres. The principle area of reassessment is the definition of the ash testing and as well as gradient testing. Our conversations with original equipment manufacturers have suggested that it is important to initially demonstrate viability of the novel ceramics in traditional turbine environments prior to pursuing new environments. Overall, the Phase I project has met or exceeded all of the stated objectives.

Special Recognitions & Awards/Patents Issued

1. CTSR publication "Sensing Control and In situ Measurement of Coating Properties: An Integrated Approach toward Establishing Process-Property Correlations" was selected as the best paper for JTST Vol. 18, 2009. The contributors include Prof. Sampath, Dr. Vasu Srinivasan, Dr. Alfredo Valarezo, Dr. Anirudha Vaidya and Dr. Tilo Streibl.

References

1. O. Maurstad, *An Overview of Coal Based Integrated Gasification Combine Cycle (IGCC) Technology* (MIT: Laboratory for Energy and the Environment, 2005).

2. I. Wright and T. Gibbons, "Recent Developments in Gas Turbine Materials and Technology and Their Implications for Syngas Firing," *International Journal of Hydrogen Energy* **32**, 3610-3621 (2007).

3. R. Vassen, F. Traeger, and D. Stover, "Correlation between Spraying Conditions and Microcrack Density and Their Influence on Thermal Cycling Life of Thermal Barrier Coatings," *Journal of Thermal Spray Technology* **13**, 396-404 (2004).

4. A. Vaidya et al., "Process Maps for Plasma Spraying of Yttria-Stabilized Zirconia: An Integrated Approach to Design, Optimization and Reliability," *Materials Science and Engineering: A* **497**, 239-253 (2008).

5. J. Matejicek, S. Sampath, P.C. Brand, and H.J. Prask, "Quenching, Thermal and Residual Stress in Plasma Sprayed Deposits: NiCrAlY and YSZ Coatings," *Acta Materialia* **47**, 607.153 (1999).

VI. Acronyms and Abbreviations

°	Degree
°C	Degree(s) Celsius
°F	Degree(s) Fahrenheit
&	And
@	At
Δ	Change (delta)
ϕ	Equivalence ratio
λ	Conductivity
μm	Micrometer(s), micron(s)
#	Number
%	Percent
~	Approximately
<	Less than
>	Greater than
2D	Two dimensional
3D	Three dimensional
7YSZ	7 wt% yttria-stabilized zirconia
8YSZ	8 wt% yttria-stabilized zirconia
A&M	Agricultural and Mechanical
A&WMA	Air and Waste Management Association
AC	Alternating current
AHRC	Alcoa Howmet Research Center
AIAA	American Institute of Aeronautics and Astronautics
AJTEC	ASME-JSME Thermal Engineering Joint Conference
Al	Aluminum
ALS	Advanced Light Source
Am.	American
ANOVA	Analysis of variance
ANSYS	An engineering simulation and modeling company
APS	Air plasma spray
Ar	Argon
ASME	American Society of Mechanical Engineers
ASTM	American Society for Testing and Materials
ATI	Associazione Termotecnica Italiana
atm	Atmosphere(s)
ATP	Advanced Turbine Program
AVS	American Vacuum Society
BC	Bond coat
BCC	Body centered cubic
B.R.	Blowing ratio
BSE	Back-scatter electron
BYU	Brigham Young University
C	Carbon
C	Celsius
C	Spacing
Ca	Calcium
CA	California
CC	Combined cycle
CCS	Carbon capture and storage
C/D	Spacing to diameter ratio
CEAS	Council of European Aerospace Societies
Ceram.	Ceramics
CES	Clean Energy Systems
CFD	Computational fluid dynamics
CFM56	A nozzle guide vane
CFX	A general purpose computational fluid dynamics software suite
CH_4	Methane
C_2H_6	Ethane
C_2H_4	Ethylene
Chem.	Chemical
cm	Centimeter(s)
cm^2	Square centimeter(s)
CM247LC	An alloy provided by Siemens Power Systems
cm^3	Cubic centimeter(s)
cm^3/min	Cubic centimeter(s) per minute
CMAS	Calcium-magnesium-alumina-silicate
CMM	Coordinate measuring machine
CMSX	A nickel-based alloy
CMSX-4	A nickel-based alloy
Co	Cobalt
CO	Carbon monoxide
CO	Colorado
CO_2	Carbon dioxide
Cr	Chromium
CRC	Chemical Rubber Company
CT	Connecticut
CTE	Coefficient of thermal expansion
CTSR	Center for Thermal Spray Research
CU	University of Colorado at Boulder
D	Deuterium
DBC	Diffusion barrier coating

D.C.	District of Columbia
DETE	Discrete error transport equation
DLN	Dry low NOx
DMS	Dynamic multi-scale
D_2O	Deuterium oxide (heavy water)
DOD	U.S. Department of Defense
DoE	Design of experiments
DOE	U.S. Department of Energy
Dr.	Doctor
DS	Directional solidification
DSC	Differential scanning calorimetry
DVC	Dense vertically cracked
DVD	Directed vapor deposition
EBC	Environmental barrier coating
EBPVD, EB-PVD	Electron beam physical vapor deposition
ECY	A cobalt-based alloy
ECY768	A cobalt-based alloy
ed.	Editor
EDM	Electrical discharge machining
EDS	Energy dispersive spectroscopy
eds.	Editors
EEE	Energy Efficient Engine
e.g.	*Exempli gratia*: for example
EGR	Exhaust gas recycle
EISG	Energy Innovations Small Grant
Eng.	Engineering
EPD	Electrophoretic deposition
EPMA	Electron microprobe analysis
EPRI	Electric Power Research Institute
et al.	*Et Alii*: and others
F	Fahrenheit
Fe	Iron
FE	Fossil Energy (Office of the U.S. Department of Energy)
FEA	Finite element analysis
FIG.	Figure
FL	Florida
FLUENT	A computational fluid dynamics code
FMEA	Failure modes and effects analysis
FOD	Foreign object damage
FTT	Florida Turbine Technologies
FY	Fiscal year
g	Gram(s)
GA	Georgia
Gd	Gadolinium
GE	General Electric
GIM	General instability model
GPa	Gigapascal(s)
GRC	Glenn Research Center
GSA	General Services Administration
GSH	Gadolinia-stabilized hafnia
GT	Gas turbine
GTD	General Electric proprietary nickel-base superalloy
GTI	Gas Technology Institute
GZO	Gadolinium zirconate
h	Hour(s)
H	Height
H	Hydrogen
H_2	Diatomic hydrogen
HA188	A cobalt based alloy
H/D	Height to diameter ratio
He	Helium
Hf	Hafnium
HfO_2	Hafnia
HHC	High hydrogen content
HHF	High-hydrogen fuel
H_2O	Water
H_2O/N_2	Water/nitrogen
H_2O/CO_2	Water/carbon dioxide
HP	High pressure
HP-LD	High-purity, low-density
HPLFR	High-pressure laminar flow reactor
HPT/IPT	High pressure turbine/intermediate pressure turbine
hrs, hrs.	Hours
HVLP	High volume low pressure
HVOF	High velocity oxygen fuel
Hz	Hertz
IA	Iowa
ICACC	International Conference and Exposition on Advanced Ceramics and Composites
ICEPAG	International Colloquium on Environmentally Preferred Advanced Power Generation
ICMCTF	International Conference on Metallurgical Coatings and Thin Films
i.e.	*id est*: that is
IGCC	Integrated gasification combined cycle
IGT	Industrial gas turbine
IGTI	International Gas Turbine Institute
IHPTET	Integrated High Performance Turbine Engine Technology

IL	Illinois
IN	Indiana
IN718	A nickel-based alloy (Inconel 718)
IN738	A nickel-based alloy (Inconel 738)
IN939	A nickel-based alloy (Inconel 939)
Inc.	Incorporated
Int.	International
IP	Intermediate pressure
IPT	Intermediate pressure turbine
Ir	Iridium
IR	Infrared
ISTP	International Symposium on Transport Phenomena
J.	Journal
J79	A gas turbine combustor
JETS	Jet engine thermal shock
JSME	Japan Society of Mechanical Engineers
K	Conductivity
K	Kelvin
kg	Kilogram(s)
Kin.	Kinetics
kN	Kilonewton(s)
KPP	Kimberlina Power Plant
ksi	Kilopound(s) per square inch
kW	Kilowatt(s)
La	Lanthanum
lb	Pound(s)
lbf	Pound(s)-force
LBNL	Lawrence Berkeley National Laboratory
LCF	Low cycle fatigue
LE	Leading edge
LES	Large eddy simulation
LHV	Lower heating value
LLC	Limited liability company
LPPS	Low-pressure plasma-sprayed
LPT	Low-pressure turbine
LSI	Low-swirl injector
m	Meter(s)
MA	Massachusetts
Mag.	Magazine
MarM509	A cobalt-based alloy
Mat.	Materials
Mater.	Materials
MB/MS	Molecular beam/mass spectrometry
MCrAlY	M-chromium-aluminum-yttrium alloy, where M is one of several different metals
Met.	Metallurgical
mg	Milligram(s)
Mg	Magnesium
min	Minute(s)
MIS	Matrix isolation spectroscopy
MIT	Massachusetts Institute of Technology
mK	Milli-Kelvin(s)
mm	Millimeter(s)
mm^2	Square millimeter(s)
MM509	MarM509, A cobalt-based alloy
Mod	Model
mol	Molecule
mol	Mole
MPa	Megapascal(s)
MPU	Multiple-partial unloading
m/s	Meter(s) per second
MS	Mail stop
MS&T	Materials Science and Technology
mW	Milliwatt(s)
MW	Megawatt(s)
MW_e	Megawatt(s) electric
MW_{th}	Megawatt(s) thermal
N	Nitrogen
N_2	Diatomic nitrogen
N5	A nickel-based alloy
N6	A nickel-based alloy
NAS	National Academy of Science
NASA	National Aeronautics and Space Administration
Nb	Niobium
Nd	Neodymium
NDE	Non-destructive evaluation
NETL	National Energy Technology Laboratory
NG	Natural gas
NGV	Nozzle guide vane
Ni	Nickel
NiAl	Nickel aluminum
NIST	National Institute for Standards and Technology
NJ	New Jersey
No.	Number
NOx	Oxides of nitrogen
NY	New York
O	Oxygen
O_2	Diatomic oxygen
OD	Optical density

ODS	Oxide dispersion strengthened
OEM	Original equipment manufacturer
O-F	Oxy-fuel
O-FRH	Oxy-fuel reheat
OFT	Oxy-fuel turbine
OH	Ohio
OR	Oregon
ORNL	Oak Ridge National Laboratory
OSU	Ohio State University
p.	Page
P	Pressure
PA	Pennsylvania
PCI	Precision Combustion, Inc.
Ph.D.	Doctor of Philosophy
Phil.	Philosophy
Phys.	Physics
PIMS	Photoionization mass spectrometry
PIV	Particle image velocimetry
P.O.	Post office
pp.	Pages
PPI	Plasma Processes, Inc.
ppm	Part(s) per million
ppmv	Part(s) per million by volume
Prog.	Progress
psi	Pound(s) per square inch
PSI	Physical Sciences Inc.
Pt	Platinum
Pts	Points
PVC	Polyvinyl chloride
PWA1483SX	An alloy provided by Siemens Power Systems
PWR	Pratt and Whitney Rocketdyne
Q1	First quarter
RANS	Reynolds-averaged Navier-Stokes
RCH	Rich catalytic hydrogen
RCL®	Rich catalytic lean-burn
RCM	Rapid compression machine
RCV	Reticulated vitreous carbon
Rd.	Road
R&D	Research and development
RD&D	Research, development, and demonstration
REFPROP	Reference Fluid Thermodynamic and Transport Properties Database
René N5	A nickel-based alloy
RMS	Root mean square
rpm	Revolution(s) per second
RPN	Risk priority number
Rq	Roughness
RSM	Reynolds stress model
RUA	Regional University Alliance
s	Second(s)
S	Speed
SAE	Society of Automotive Engineers
SBIR	Small Business Innovation Research
Sci.	Science
sec	Second(s)
SEM	Scanning electron microscopy
SGT	Siemens Gas Turbine
Si	Silicon
SimVal	Simulation and Validation
Soc.	Society
SOTA	State of the art
SRZ	Secondary reaction zone
SS	Suction side
SST k-ω	Shear stress transport turbulence model
S_T	Flame speed
SW	Southwest
SX	Single crystal
T	Temperature
T91	A ferritic steel
T92	A ferritic steel
TADF	Turbine Accelerated Deposition Facility
TBC	Thermal barrier coating
TC	Top coat
Technol.	Technology
TEM	Transmission electron microscope
Tg	Gas temperature
TGO	Thermally grown oxide
Ti	Titanium
TIT	Turbine inlet temperature
Tm	Temperature at melting point
TMS	The Minerals, Metals and Materials Society
TMS-82	A nickel-based alloy
TN	Tennessee
TPFL	Turbomachinery performance and flow
TP-S1N	Transition piece to stage 1 nozzle
Trans.	Transactions
TRL	Technology readiness level
TSP	Thermal scaling parameter
TuRFR	Turbine reacting flow rig
TX	Texas

U520	A nickel-based alloy
UCI	University of California, Irvine
UCSB	University of California, Santa Barbara
UES	(unsure what this stands for - it is a science and technology company based in Dayton, OH)
UIT	Unione Italiana di Termofluidodinamica
UK	United Kingdom
um	Micron(s)
URANS	Unsteady Reynolds-averaged Navier-Stokes
U.S.	United States
USA	United States of America
USC	Ultrasupercritical Steering Committee
UT	University of Texas at Austin
UT	Utah
UTSR	University Turbine Systems Research
v.	Volume
V	Vector
VA	Virginia
Vac.	Vacuum
VCC	Vaporization-condensation cycle
VLPPS	Very low pressure plasma spray
Vol., vol.	Volume
vol%	Volume percent
vs.	Versus
W	Watt(s)
W	Width
w/	with
W/m/K	Watt(s) per meter per Kelvin
WPC	Westinghouse Plasma Corporation
WV	West Virginia
x, X	Times
X-45	A cobalt-based alloy
Y	Yttrium
Y_2O_3	Yttria
YSH	Yttria-stabilized hafnia
YSZ	Yttria-stabilized zirconia
YSZH	Yttria-stabilized ZrO_2-HfO_2
Zr	Zirconium
ZrO_2	Zirconia

VII. Primary Contact Index

A

Alvin, Mary Anne 34, 92, 99
Anderson, Reed 21
Appleby, John. 203
Appleby, Michael. 194

B

Baranauskas, Vince 229
Bennett, Ted. 163
Bischoff, Ronald 45
Bogard, David 126
Bons, Jeffrey. 117

C

Casleton, Kent 58
Cheng, Robert 54

D

Daily, John 152
Dixit, Satish 237
Downs, James 187, 191, 207

E

Etemad, Shahrokh 72, 75

F

Fadok, Joseph 25

H

Harvey, Allan 63
Hass, D.D. 217
Hawk, Jeffrey 88
Holcomb, Gordon 85
Horazak, Dennis 110

J

Ju, Yiguang. 78

L

Lieuwen, Tim. 50

M

Mansour, Adel 67
McCrabb, Heather. 221
McDonell, Vincent 148
McKechnie, Tim 234
Meier, Gerald. 168
Misra, Abhijeet 177

P

Padture, Nitin 159
Pint, Bruce 105

R

Ramana, Chintalapalle. 172

S

Santavicca, Dom 144
Santoro, Robert 140
Schobeiri, Meinhard 121
Seitzman, Jerry 137
Shih, Tom. 31
Steinbeck, John 212
Stewart, Timothy. 197
Stickler, David 183

T

Tafti, Danesh 131

W

Whitaker, John 225

VIII. Organization Index

A

Aerodyne Research, Inc. 183

C

Clean Energy Systems, Inc. 45

D

Directed Vapor Technologies. 217

F

Faraday Technology, Inc. 221

Florida Turbine Technologies, Inc. 187, 191, 203, 207

G

GE Energy 21

Georgia Institute of Technology 50, 137

L

Lawrence Berkeley National Laboratory 54

M

Mikro Systems, Inc. 194

Modumetal, Inc. 225

N

NanoSonic, Inc.. 229

National Energy Technology Laboratory 34, 58, 85, 88, 92, 99

National Institute of Standards and Technology. . . . 63

O

Oak Ridge National Laboratory 105

Ohio State University (The). 117, 159

P

Parker Hannifin 67

Pennsylvania State University (The). 140, 144

Physical Sciences Inc.. 212

Plasma Processes, Inc. 234

Plasma Technology Inc. 237

Precision Combustion, Inc. 72, 75

Princeton University. 78

Purdue University 31

Q

QuesTek Innovations LLC 177

S

Siemens Energy, Inc.. . . . . 25, 110

T

Texas A&M University 121

U

Ultramet 197

University of California, Irvine 148

University of California, Santa Barbara 163

University of Colorado at Boulder 152

University of Pittsburgh 168

University of Texas at Austin 126

University of Texas at El Paso 172

V

Virginia Polytechnic Institute and State University 131

IX. Contract Number Index

0004000.5.610.243.001 . . . . . 34, 92, 99
05054 144
41431/UTSR 06-01-SR124 168
41431/UTSR 07-01-SR122 137
41431/UTSR 07-01-SR123 131
41431/UTSR 07-01-SR125 163
41431/UTSR 07-01-SR126 152
41431/UTSR 07-01-SR127 126
42643 21
42644 25
42645 45
42646 110
42647 75
42648 67
42716 78
42957 63
43069 50
84202 221
84668 187
85015 72
85390 203
678403 54
10220623 6926 58
AL05205018 31
FE0000753 121
FE0000765 172
FEAA070 105
FY10.MSE.1610243.682 85
FY10.MSE.1610243.683 88
NT0000752 140
NT0005055 117
NT0006551 148
NT0006552 159
SC0001223 225
SC0001359 194
SC0001422 237
SC0001601 234
SC0002475 177
SC0002484 197
SC0002495 217
SC0002713 191
SC0002723 229
SC0003400 212
SC0003574 207
SC0003591 183

NATIONAL ENERGY TECHNOLOGY LABORATORY

1450 Queen Avenue SW
Albany, OR 97321-2198
541-967-5892

2175 University Avenue South
Suite 201
Fairbanks, AK 99709
907-452-2559

3610 Collins Ferry Road
P.O. Box 880
Morgantown, WV 26507-0880
304-285-4764

626 Cochrans Mill Road
P.O. Box 10940
Pittsburgh, PA 15236-0940
412-386-4687

13131 Dairy Ashford, Suite 225
Sugar Land, TX 77478
281-494-2516

Richard A. Dennis
Technology Manager, Turbines
304-285-4515
richard.dennis@netl.doe.gov

Visit the NETL website at:
www.netl.doe.gov

Customer Service:
1-800-553-7681

U.S. DEPARTMENT OF ENERGY

DOE/NETL-2010/1437

October 2010